ELSEVIER

World Journal of Gastroenterology®

Supported by NSFC 2005-2006

Volume 11 Number 2
January 14, 2005

National Journal Award

Contents

REVIEW

155 Carbonic anhydrases in normal gastrointestinal tract and gastrointestinal tumours
Kivelä AJ, Kivelä J, Saarnio J, Parkkila S

LIVER CANCER

164 Desensitization of T lymphocyte function by CXCR3 ligands in human hepatocellular carcinoma
Liu YQ, Poon RT, Hughes J, Li QY, Yu WC, Fan ST

171 Do the expressions of gap junction gene connexin messenger RNA in noncancerous liver remnants of patients with hepatocellular carcinoma correlate with postoperative recurrences?
Sheen IS, Jeng KS, Shih SC, Kao CR, Wang PC, Chen CZ , Chang WH, Wang HY, Shyung LR

176 Clinicopathological and prognostic implications of endoglin (CD105) expression in hepatocellular carcinoma and its adjacent non-tumorous liver
Ho JW, Poon RT, Sun CK, Xue WC, Fan ST

182 Construction of recombinant eukaryotic expression plasmid containing murine CD40 ligand gene and its expression in H22 cells
Jiang YF, He Y, Gong GZ, Chen J, Yang CY, Xu Y

187 Clinical significance of the expression of isoform 165 vascular endothelial growth factor mRNA in noncancerous liver remnants of patients with hepatocellular carcinoma
Sheen IS, Jeng KS, Shih SC, Kao CR, Chang WH, Wang HY, Wang PC, Wang TE, Shyung LR, Chen CZ

193 Survivin antisense compound inhibits proliferation and promotes apoptosis in liver cancer cells
Dai DJ, Lu CD, Lai RY, Guo JM, Meng H, Chen WS, Gu J

200 Detection of hypervascular hepatocellular carcinoma: Comparison of multi-detector CT with digital subtraction angiography and Lipiodol CT
Zheng XH, Guan YS, Zhou XP, Huang J, Sun L, Li X, Liu Y

204 Specific COX-2 inhibitor NS398 induces apoptosis in human liver cancer cell line HepG2 through BCL-2
Huang DS, Shen KZ, Wei JF, Liang TB, Zheng SS, Xie HY

208 Prediction of HLA-A2-restricted CTL epitope specific to HCC by SYFPEITHI combined with polynomial method
Dong HL, Sui YF

212 Adhesion of different cell cycle human hepatoma cells to endothelial cells and roles of integrin β_1
Song GB, Qin J, Luo Q, Shen XD, Yan RB, Cai SX

216 Effects of thalidomide on angiogenesis and tumor growth and metastasis of human hepatocellular carcinoma in nude mice
Zhang ZL, Liu ZS, Sun Q

World Journal of Gastroenterology®
Volume 11 **Number** 2 **January** 14, 2005

Contents

LIVER CANCER

221 TIP30 regulates apoptosis-related genes in its apoptotic signal transduction pathway
Shi M, Zhang X, Wang P, Zhang HW, Zhang BH, Wu MC

228 Expression of fragile histidine triad in primary hepatocellular carcinoma and its relation with cell proliferation and apoptosis
Nan KJ, Ruan ZP, Jing Z, Qin HX, Wang HY, Guo H, Xu R

BASIC RESEARCH

232 Prostacyclin inhibition by indomethacin aggravates hepatic damage and encephalopathy in rats with thioacetamide-induced fulminant hepatic failure
Chu CJ, Hsiao CC, Wang TF, Chan CY, Lee FY, Chang FY, Chen YC, Huang HC, Wang SS, Lee SD

237 Increase in neurokinin-1 receptor-mediated colonic motor response in a rat model of irritable bowel syndrome
La JH, Kim TW, Sung TS, Kim HJ, Kim JY, Yang IS

242 Screening of stimulatory effects of dietary risk factors on mouse intestinal cell kinetics
Shivshankar P, Devi SCS

249 Expression of sialyl Lewis^a relates to poor prognosis in cholangiocarcinoma
Juntavee A, Sripa B, Pugkhem A, Khuntikeo N, Wongkham S

CLINICAL RESEARCH

255 Clinical usefulness of biochemical markers of liver fibrosis in patients with nonalcoholic fatty liver disease
Sakugawa H, Nakayoshi T, Kobashigawa K, Yamashiro T, Maeshiro T, Miyagi S, Shiroma J, Toyama A, Nakayoshi T, Kinjo F, Saito A

260 Giant malignant gastrointestinal stromal tumors: Recurrence and effects of treatment with STI-571
Chen TW, Liu HD, Shyu RY, Yu JC, Shih ML, Chang TM, Hsieh CB

BRIEF REPORTS

264 Mitochondrial DNA sequence analysis of two mouse hepatocarcinoma cell lines
Dai JG, Lei X, Min JX, Zhang GQ, Wei H

268 Effects of oxymatrine on experimental hepatic fibrosis and its mechanism *in vivo*
Shi GF, Li Q

272 Polymorphism of glutathione S-transferase mu 1 and theta 1 genes and hepatocellular carcinoma in southern Guangxi, China
Deng ZL, Wei YP, Ma Y

275 Polymerase chain reaction-single strand conformational polymorphism analysis of rearranged during transfection proto-oncogene in Chinese familial hirschsprung's disease
Guan T, Li JC, Li MJ, Tou JF

280 Anticancer activity of resveratrol on implanted human primary gastric carcinoma cells in nude mice
Zhou HB, Chen JJ, Wang WX, Cai JT, Du Q

285 Loss of heterozygosity on 10q23.3 and mutation of tumor suppressor gene PTEN in gastric cancer and precancerous lesions
Li YL, Tian Z, Wu DY, Fu BY, Xin Y

World Journal of Gastroenterology®
Volume 11 **Number** 2 **January** 14, 2005

Contents

BRIEF REPORTS	**289**	Homozygosity for Pro of p53 Arg72Pro as a potential risk factor for hepatocellular carcinoma in Chinese population *Zhu ZZ, Cong WM, Liu SF, Dong H, Zhu GS, Wu MC*
	293	Mechanism of benign biliary stricture: A morphological and immunohistochemical study *Geng ZM, Yao YM, Liu QG, Niu XJ, Liu XG*
	296	Heart-shaped anastomosis for Hirschsprung's disease: Operative technique and long-term follow-up *Wang G, Sun XY, Wei MF, Weng YZ*
	299	Incidence of HBV variants with a mutation at nt551 among hepatitis B patients in Nanjing and its neighbourhood *Ma CL, Fang DX,Yao K, Li FQ, Jin HY, Li SQ, Tan WG*
CASE REPORTS	**303**	Acute hepatitis induced by an Aloe vera preparation: A case report *Rabe C, Musch A, Schirmacher P, Kruis W, Hoffmann R*
	305	Gallbladder polyp as a manifestation of hemobilia caused by arterial-portal fistula after percutaneous liver biopsy: A case report *Lin CL, Chang JJ, Lee TS, Lui KW, Yen CL*
ACKNOWLEDGEMENTS	**308**	Acknowledgements to reviewers for this issue
APPENDIX	**1A**	Meetings
	2A	Instructions to authors
	4A	*World Journal of Gastroenterology* standard of quantities and units
FLYLEAF	I-V	Editorial Board
INSIDE FRONT COVER		ISI journal citation reports 2003-GASTROENTEROLOGY AND HEPATOLOGY
INSIDE BACK COVER		E-journal of *World Journal of Gastroenterology*

Editorial Coordinator for this issue: Michelle Gabbe, PhD

World Journal of Gastroenterology®
World J Gastroenterol
Weekly
Founded with a name of *China National Journal of New Gastroenterology* on 1st October, 1995
Renamed as *World Journal of Gastroenterology* on January 25, 1998
Publication date January 14, 2005
President and Editor-in-Chief
Lian-Sheng Ma
Editor-in-Chief
Bo-Rong Pan
Managing Director
Jing-Yun Ma
Associate Managing Editor
Jian-Zhong Zhang, Shi-Yu Guo
Typesetter Meng Li
Proofreaders Hong Li, Wu-Zhou Li

Edited by Editorial Board of *World Journal of Gastroenterology*, PO Box 2345, Beijing 100023, China
Published jointly by The WJG Press and Elsevier Inc. For inquiries regarding distribution of the material in China, please contact The WJG Press; for inquiries regarding distribution elsewhere, please contact Elsevier Inc.
Subscriptions
Domestic Local Post Offices Code No. BM 82-261
Foreign Elsevier (Singapore) Pte Ltd, 3 Killiney Road #08-01, Winsland House I, Singapore 239519
Telephone: +65-6349 0200 **Fax:** +65-6733 1817
E-mail: r.garcia@elsevier.com
http://asia.elsevierhealth.com
Personal Price: USD700.00
Institutional Price: USD1 500.00
Online Submissions
http://www.wjgnet.com/wjg/index.jsp
Telephone: +86-(0)10-85381901 **Fax:** +86-(0)10-85381893
E-mail: wjg@wjgnet.com **http:** //www.wjgnet.com

Indexed and Abstracted in: *Index Medicus*, MEDLINE, PubMed, Chemical Abstracts, EMBASE, Abstracts Journals, *Nature Clinical Practice Gastroenterology* and *Hepatology,* CAB Abstracts and Global Health. **ISI JCR 2000-2003:** IF = 0.993, 1.445, 2.532 and 3.318 respectively. A total of 687 articles published in WJG were cited by 389 ISI/SCI-covered journals distributed in 39 countries during January 1998 - March 2004. Supported by the National Natural Science Foundation of China, No. 30224801; Certificate of the 100 Outstanding Academic Journals of China 2002, National Journal Award, Journal of the Statistic Source of Papers on Science and Technology of China and Key Journals of China Science and Technology.

ISSN 1007-9327 CN 14-1219/R

World Journal of Gastroenterology®

Editorial Board

2004-2006

Published by The WJG Press and Elsevier Inc., PO Box 2345, Beijing 100023, China
Fax: +86-(0)10-85381893 E-mail: wjg@wjgnet.com http://www.wjgnet.com

Bulgaria
Zahariy Alexandrov Krastev, *Sofia*

Canada
Wang-Xue Chen, *Ottawa*
Richard N Fedorak, *Edmonton*
Hugh James Freeman, *Vancouver*
Samuel S Lee, *Calgary*
Philip Martin Sherman, *Toronto*
Alan BR Thomson, *Edmonton*
Eric M Yoshida, *Vancouver*

China
Francis KL Chan, *Hong Kong*
Xiao-Ping Chen, *Wuhan*
Jun Cheng, *Beijing*
Chi-Hin Cho, *Hong Kong*
Zong-Jie Cui, *Beijing*
Da-Jun Deng, *Beijing*
Er-Dan Dong, *Beijing*
Sheung-Tat Fan, *Hong Kong*
Xue-Gong Fan, *Changsha*
Jin Gu, *Beijing*
De-Wu Han, *Taiyuan*
Shao-Heng He, *Shantou*
Fu-Lian Hu, *Beijing*
Wayne HC Hu, *Hong Kong*
Ching Lung Lai, *Hong Kong*
Kam Chuen Lai, *Hong Kong*
Wai-Keung Leung, *Hong Kong*
Zhi-Hua Liu, *Beijing*
Ai- Ping Lu, *Beijing*
Jing-Yun Ma, *Beijing*
Lun-Xiu Qin, *Shanghai*
Yu-Gang Song, *Guangzhou*
Peng Shang, *Xi'an*
Qin Su, *Beijing*
Yuan Wang, *Shanghai*
Benjamin Wong, *Hong Kong*
Wai-Man Wong, *Hong Kong*
Hong Xiao, *Shanghai*
Dong-Liang Yang, *Wuhan*
Xue-Biao Yao, *Hefei*
Yuan Yuan, *Shenyang*
Man-Fung Yuen, *Hong Kong*
Jian-Zhong Zhang, *Beijing*
Zhi-Rong Zhang, *Chengdu*
Xiao-Hang Zhao, *Beijing*
Shu Zheng, *Hangzhou*

Costa Rica
Edgar M Izquierdo, *San José*

Croatia
Marko Duvnjak, *Zagreb*

Denmark
Flemming Burcharth, *Herlev*
Peter Bytzer, *Copenhagen*
Hans Gregersen, *Aalborg*
Jens H Henriksen, *Hvidovre*
Fin Stolze Larsen, *Copenhagen*
Søren Møller, *Hvidovre*

Egypt
Abdel-Rahman El-Zayadi, *Giza*

Finland
Pentti Sipponen, *Espoo*

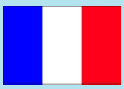

France
Charles Paul Balabaud, *Bordeaux*
Jacques Belghiti, *Clichy*
Pierre Brissot, *Rennes*
Franck Carbonnel, *Besancon*
Bruno Clément, *Rennes*
Jacques Cosnes, *Paris*
Francoise Degos, *Clichy*
Francoise Lunel Fabian, *Angers*
Gérard Feldmann, *Paris*
Jean Fioramonti, *Toulouse*
Rene Lambert, *Lyon*
Didier Lebrec, *Clichy*
Francis Mégraud, *Bordeaux*
Richard Moreau, *Clichy*
Jose Sahel, *Marseille*
Jean-Yves Scoazec, *Lyon*
Jean-Pierre Henri Zarski, *Grenoble*

Germany
HD Allescher, *Garmisch-Partenkirchen*
Rudolf Arnold, *Marburg*
Hubert Blum, *Freiburg*
Peter Born, *Muchen*
Heinz J Buhr, *Berlin*
Haussinger Dieter, *Düsseldorf*
Dietrich CF, *Bad Mergentheim*
Wolfram W Domschke, *Muenster*
Ulrich Robert Fölsch, *Kiel*
Peter R Galle, *Mainz*
Burkhard Göke, *Munich*
Axel M Gressner, *Aachen*
Eckhart Georg Hahn, *Erlangen*
Werner Hohenberger, *Erlangen*
RG Jakobs, *Ludwigshafen*
Joachim Labenz, *Siegen*
Ansgar W Lohse, *Hamburg*
Peter Malfertheiner, *Magdeburg*
Andrea Dinah May, *Wiesbaden*
Stephan Miehlke, *Dresden*
Gustav Paumgartner, *Munich*
Ulrich Ks Peitz, *Magdeburg*
Giuliano Ramadori, *Göttingen*
Tilman Sauerbruch, *Bonn*
Hans Seifert, *Oldenburg*
J Ruediger Siewert, *Munich*
Manfred V Singer, *Mannheim*
Jurgen M Stein, *Frankfurt*
Manfred Stolte, *Bayreuth*
Wolfgang R Stremmel, *Heidelberg*
Hans Ludger Tillmann, *Leipzig*
Siegfried Wagner, *Deggendorf*
Bertram Wiedenmann, *Berlin*

Greece
Arvanitakis C, *Thessaloniki*
Elias A Kouroumalis, *Heraklion*

Hungary
Simon A László, *Szekszárd*
János Papp, *Budapest*

Iceland
Hallgrimur Gudjonsson, *Reykjavik*

India
Sujit Kumar Bhattacharya, *Kolkata*
Chawla YK, *Chandigarh*
Radha Dhiman K, *Chandigarh*
Sri Prakash Misra, *Allahabad*
Kartar Singh, *Lucknow*

Iran
Reza Malekzadeh, *Tehran*

Israel
Abraham Rami Eliakim, *Haifa*
Yaron Niv, *Pardesia*

Italy
Giovanni Addolorato, *Roma*
Alfredo Alberti, *Padova*
Annese V, *San Giovanni Rotondo*
Giovanni Barbara, *Bologna*
Gabrio Bassotti, *Perugia*
Franco Bazzoli, *Bologna*
Adolfo Francesco Attili, *Roma*
Antomio Benedetti, *Ancona*
Giovanni Cammarota, *Roma*
Antonino Cavallari, *Bologna*
Dario Conte, *Milano*
Gino Roberto Corazza, *Pavia*
Guido Costamagua, *Roma*
Antonio Craxi, *Palermo*
Fabio Farinati, *Padua*
Giovanni Gasbarrini, *Roma*
Paolo Gentilini, *Florence*
Edoardo G Giannini, *Genoa*

Paolo Gionchetti, *Bologna*
Roberto De Giorgio, Bologna
Mario Guslandi, *Milano*
Giovanni Maconi, *Milan*
Giulio Marchesini, *Bologna*
Giuseppe Montalto, *Palermo*
Luisi Pagliaro, *Palermo*
Fabrizio R Parente, *Milan*
Perri F, *San Giovanni Rotondo*
Raffaele Pezzilli, *Bologna*
Pilotto A, *San Giovanni Rotondo*
Massimo Pinzani, *Firenze*
Gabriele Bianchi Porro, *Milano*
Piero Portincasa, *Bari*
Giacomo Laffi, *Firenze*
Enrico Roda, *Bologna*
Massimo Rugge, *Padova*
Vincenzo Savarino, *Genova*
Vincenzo Stanghellini, *Bologna*
Calogero Surrenti, *Florence*
Roberto Testa, *Genoa*
Dino Vaira, *Bologna*

Japan

Kyoichi Adachi, *Izumo*
Takashi Aikou, *Kagoshima*
Taiji Akamatsu, *Matsumoto*
Takafumi Ando, *Nagoya*
Akira Andoh, *Otsu*
Taku Aoki, *Tokyo*
Masahiro Arai, *Tokyo*
Tetsuo Arakawa, *Osaka*
Yasuji Arase, *Tokyo*
Masahiro Asaka, *Sapporo*
Hitoshi Asakura, *Tokyo*
Yutaka Atomi, *Tokyo*
Takeshi Azuma, *Fukui*
Nobuyuki Enomoto, *Yamanashi*
Kazuma Fujimoto, *Saga*
Toshio Fujioka, *Oita*
Yoshihide Fujiyama, *Otsu*
Hiroyuki Hanai, *Hamamatsu*
Kazuhiro Hanazaki, *Nagano*
Naohiko Harada, *Fukuoka*
Makoto Hashizume, *Fukuoka,*
Tetsuo Hayakawa, *Nagoya*
Kazuhide Higuchi, *Osaka*
Ichiro Hirata, *Osaka*
Keiji Hirata, *Kitakyushu*
Takafumi Ichida, *Shizuoka*
Kenji Ikeda, *Tokyo*
Kohzoh Imai, *Sapporo*
Fumio Imazeki, *Chiba*
Masayasu Inoue, *Osaka*
Hiromi Ishibashi, *Nagasaki*
Shunji Ishihara, *Izumo*
Toru Ishikawa, *Niigata*
Kei Ito, *Sendai*
Masayoshi Ito, *Tokyo*
Hiroaki Itoh, *Akita*
Hiroshi Kaneko, *Aichi-Gun*
Shuichi Kaneko, *Kanazawa*
Takashi Kanematsu, *Nagasaki*
Junji Kato, *Sapporo*
Mototsugu Kato, *Sapporo*
Shinzo Kato, *Tokyo*
Sunao Kawano, *Osaka*
Yoshikazu Kinoshita, *Izumo*
Masaki Kitajima, *Tokyo*
Tsuneo Kitamura, *Chiba*
Seigo Kitano, *Oita*
Hironori Koga, *Kurume*
Satoshi Kondo, *Sapporo*
Shoji Kubo, *Osaka*
Shigeki Kuriyama, *Kagawa*
Masato Kusunoki, *Mie*
Takashi Maeda, *Fukuoka*
Shin Maeda, *Tokyo*
Osamu Matsui, *Kanazawa*
Yasushi Matsuzaki, *Tsukuba*
Hiroto Miwa, *Hyogo*
Masashi Mizokami, *Nagoya*
Motowo Mizuno, *Hiroshima*
Morito Monden, *Suita*
Hisataka S Moriwaki, *Gifu*
Yoshiharu Motoo, *Kanazawa*
Akihiro Munakata, *Hirosaki*
Kazunari Murakami, *Oita*
Kunihiko Murase, *Tusima*
Masato Nagino, *Nagoya*
Yujl Naito, *Kyoto*
Hisato Nakajima, *Tokyo*
Hiroki Nakamura, *Yamaguchi*
Shotaro Nakamura, *Fukuoka*
Akimasa Nakao, *Nagoya*
Mikio Nishioka, *Niihama*
Susumu Ohmada, *Maebashi*
Masayuki Ohta, *Oita*
Tetsuo Ohta, *Kanazawa*
Susumu Okabe, *Kyoto*
Katsuhisa Omagari, *Nagasaki*
Saburo Onishi, *Nankoku*
Morikazu Onji, *Ehime*
Hiromitsu Saisho, *Chiba*
Hidetsugu Saito, *Tokyo*
Takafumi Saito, *Yamagata*
Isao Sakaida, *Yamaguchi*
Michiie Sakamoto, *Tokyo*
Iwao Sasaki, *Sendai*
Motoko Sasaki, *Kanazawa*
Chifumi Sato, *Tokyo*
Shuichi Seki, *Osaka*
Hiroshi Shimada, *Yokohama*
Mitsuo Shimada, *Tokushima*
Hiroaki Shimizu, *Chiba*
Tooru Shimosegawa, *Sendai*
Tadashi Shimoyama, *Hirosaki*
Ken Shirabe, *Iizuka City*
Yoshio Shirai, *Niigata*
Katsuya Shiraki, *Mie*
Yasushi Shiratori, *Okayama*
Yasuhiko Sugawara, *Tokyo*
Toshiro Sugiyama, *Toyama*
Kazuyuki Suzuki, *Morioka*
Hidekazu Suzuki, *Tokyo*
Tadatoshi Takayama, *Tokyo*
Tadashi Takeda, *Osaka*
Koji Takeuchi, *Kyoto*
Kiichi Tamada, *Tochigi*
Akira Tanaka, *Kyoto*
Eiji Tanaka, *Matsumoto*
Noriaki Tanaka, *Okayama*
Shinji Tanaka, *Hiroshima*
Kyuichi Tanikawa, *Kurume*
Tadashi Terada, *Shizuoka*
Akira Terano, *Shimotsugagun*
Kazunari Tominaga, *Osaka*
Hidenori Toyoda, *Ogaki*
Akihito Tsubota, *Chiba*
Shingo Tsuji, *Osaka*
Takato Ueno, *Kurume*
Shinichi Wada, *Tochigi*
Hiroyuki Watanabe, *Kanazawa*
Sumio Watanabe, *Akita*
Toshio Watanabe, *Osaka*
Yuji Watanabe, *Ehime*
Chun-Yang Wen, *Nagasaki*
Koji Yamaguchi, *Fukuoka*
Takayuki Yamamoto, *Yokkaichi*
Takashi Yao, *Fukuoka*
Hiroshi Yoshida, *Tokyo*
Masashi Yoshida, *Tokyo*
Norimasa Yoshida, *Kyoto*
Kentaro Yoshika, *Toyoake*
Masahide Yoshikawa, *Kashihara*

Lithuania

Sasa Markovic, *Japljeva*

Macedonia

Vladimir Cirko Serafimoski, *Skopje*

Malaysia

Andrew Seng Boon Chua, *Ipoh*
Jayaram Menon, *Sabah*
Khean-Lee Goh, *Kuala Lumpur*

Monaco

Patrick Rampal, *Monaco*

Netherlands

Louis MA Akkermans, *Utrecht*
Karel Van Erpecum, *Utrecht*
Albert K Groen, *Amsterdam*
Dirk Joan Gouma, *Amsterdam*
Jan BMJ Jansen, *Nijmegen*
Evan Anthony Jones, *Abcoude*
Ernst Johan Kuipers, *Rotterdam*
Chris JJ Mulder, *Amsterdam*
Michael Müller, *Wageningen*

Pena AS, *Amsterdam*
Andreas Smout, *Utrecht*
RW Stockbrugger, *Maastricht*
GP Vanberge-Henegouwen, *Utrecht*

New Zealand
Ian David Wallace, *Auckland*

Norway
Trond Berg, *Oslo*
Helge Lyder Waldum, *Trondheim*

Pakistan
Muhammad S Khokhar, *Lahore*

Philippines
Eulenia Rasco Nolasco, *Manila*

Poland
Tomasz Brzozowski, *Cracow*
Andrzej Nowak, *Katowice*

Portugal
Miguel Carneiro De Moura, *Lisbon*

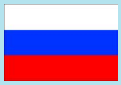

Russia
Vladimir T Ivashkin, *Moscow*
Leonid Lazebnik, *Moscow*
Vasiliy I Reshetnyak, *Moscow*

Singapore
Bow Ho, *Kent Ridge*
Francis Seow-Choen, *Singapore*

Slovakia
Anton Vavrecka, *Bratislava*

South Africa
Michael C Kew, *Parktown*

South Korea
Jin-Hong Kim, *Suwon*
Myung-Hwan Kim, *Seoul*
Yun-Soo Kim, *Seoul*
Yung-Il Min, *Seoul*
Jae-Gahb Park, *Seoul*
Dong Wan Seo, *Seoul*

Spain
Abraldes JG, *Barcelona*
Fernando Azpiroz, *Barcelona*
Ramon Bataller, *Barcelona*
Josep M Bordas, *Barcelona*
Maria Buti, *Barcelon*
Xavier Calvet, *Sabadell*
Antoni Castells, *Barcelona*
Manuel Daz-Rubio, *Madrid*
Juan C Garcia-Pagán, *Barcelona*
Genover JB, *Barcelona*
Javier P Gisbert, *Madrid*
Jaime Guardia, *Barcelona*
Angel Lanas, *Zaragoza*
Ricardo Moreno-Otero, *Madrid*
Julian Panes, *Barcelona*
Miguel Perez-Mateo, *Alicante*
Josep M Pique, *Barcelona*
Jesus Prieto, *Pamplona*
Luis Rodrigo, *Oviedo*

Sri Lanka
Janaka De Silva, *Ragama*

Swaziland
Gerd Kullak-Ublick, *Zurich*

Sweden
Lars Christer Olbe, *Molndal*
Curt Einarsson, *Huddinge*
Lars R Lundell, *Stockholm*
Xiao-Feng Sun, *Linkoping*

Switzerland
Christoph Beglinger, *Basel*
Michael W Fried, *Zurich*
Bruno Stieger, *Zurich*
Arthur Zimmermann, *Berne*

Turkey
Yusuf Bayraktar, *Ankara*
Figen Gurakan, *Ankara*
Cihan Yurdaydin, *Ankara*

United Kingdom
Axon ATR, *Leeds*
Paul Jonathan Ciclitira, *London*
Amar Paul Dhillon, *London*
Stuarts Forbes
Subrata Ghosh, *London*
Brian T Johnston, *Belfast*
David EJ Jones, *Newcastle*
Michael A Kamm, *Harrow*
Hong-Xiang Liu, Cambridge
Giorgina Mieli-Vergani, *London*
Nikolai V Naoumov, *London*
John P Neoptolemos, *Liverpool*
James Neuberger, *Birmingham*
Colm Antoine O'Morain, *Dublin*
Simon D Taylor-Robinson, *London*
Frank Ivor Tovey, *Basingstoke*
Min Zhao, *Foresterhill*

United States
Firas H Ac-Kawas, *Washington*
Gianfranco D Alpini, *Temple*
Paul Angulo, *Rochester*
Jamie S Barkin, *Miami Beach*
Todd Baron, *Rochester*
Kim Elaine Barrett, *San Diego*
Jennifer D Black, *Buffalo*
Xu Cao, *Birmingham*
David L Carr-Locke, *Boston*
Marc F Catalano, *Milwaukee*
Xian-Ming Chen, *Rochester*
James M Church, *Cleveland*
Vincent Coghlan, *Beaverton*
James R Connor, *Hershey*
Pelayo Correa, *New Orleans*
John Cuppoletti, *Cincinnati*
Peter V Danenberg, *Los Angeles*
Kiron Moy Das, *New Brunswick*
Hala El-Zimaity, *Houston*
Ronnie Fass, *Tucson*
Emma E Furth, *Pennsylvania*
John Geibel, *New Haven*
Graham DY, *Houston*
Joel S Greenberger, *Pittsburgh*
Anna S Gukovskaya, *Los Angeles*
Gavin Harewood, *Rochester*
Atif Iqbal, *Omaha*
Hajime Isomoto, *Rochester*
Dennis M Jensen, *Los Angeles*
Leonard R Johnson, *Memphis*
Peter James Kahrilas, *Chicago*
Anthony Nicholas Kalloo, *Baltimore*
Neil Kaplowitz, *Los Angeles*
Emmet B Keeffe, *Palo Alto*
Joseph B Kirsner, *Chicago*
Burton I Korelitz, *New York*
Robert J Korst, *New York*
Richard A Kozarek, *Seattle*
Shiu-Ming Kuo, *Buffalo*
Frederick H Leibach, *Augusta*
Andreas Leodolter, *La Jolla*
Ming Li, *New Orleans*
Lenard M Lichtenberger, *Houston*
Gary R Lichtenstein, *Philadelphia*
Josep M Llovet, *New York*
Martin Lipkin, *New York*

Manuscript reviewers of *World Journal of Gastroenterology*

PO Box 2345, Beijing 100023, China
Fax: +86-10-85381893
E-mail: wjg@wjgnet.com www.wjgnet.com

ELSEVIER

World J Gastroenterol 2005;11(2):155-163
World Journal of Gastroenterology ISSN 1007-9327

• REVIEW •

Carbonic anhydrases in normal gastrointestinal tract and gastrointestinal tumours

Antti J. Kivelä, Jyrki Kivelä, Juha Saarnio, Seppo Parkkila

Antti J. Kivelä, Department of Anatomy and Cell Biology, University of Oulu, Finland
Antti J. Kivelä, Seppo Parkkila, Institute of Medical Technology, University of Tampere and Tampere University Hospital, Finland
Jyrki Kivelä, Institute of Dentistry, University of Helsinki, Finland
Jyrki Kivelä, Research Institute of Military Medicine, Central Military Hospital, Helsinki, Finland
Juha Saarnio, Department of Surgery, University of Oulu, Finland
Seppo Parkkila, Department of Clinical Chemistry, University of Oulu, Finland
Supported by the Grants from Sigrid Juselius Foundation, The Academy of Finland (SP), Finnish Cultural Foundation and Finnish Dental Society (JK)
Correspondence to: Antti J. Kivelä, Institute of Medical Technology, University of Tampere, Biokatu 6, FIN-33520 Tampere, Finland. antti.j.kivela@fimnet.fi
Telephone: +358-50-3247762 **Fax:** +358-3-2158597
Received: 2004-03-27 **Accepted:** 2004-05-13

Abstract

Carbonic anhydrases (CAs) catalyse the hydration of CO_2 to bicarbonate at physiological pH. This chemical interconversion is crucial since HCO_3^- is the substrate for several biosynthetic reactions. This review is focused on the distribution and role of CA isoenzymes in both normal and pathological gastrointestinal (GI) tract tissues. It has been known for many years that CAs are widely present in the GI tract and play important roles in several physiological functions such as production of saliva, gastric acid, bile, and pancreatic juice as well as in absorption of salt and water in intestine. New information suggests that these enzymes participate in several processes that were not envisioned earlier. Especially, the recent reports on plasma membrane-bound isoenzymes IX and XII have raised considerable interest since they were reported to participate in cancer invasion and spread. They are induced by tumour hypoxia and may also play a role in von Hippel-Lindau (VHL)-mediated carcinogenesis.

Key words: Gastrointestinal tract; Gastrointestinal tumour; Carbonic anhydrases

Kivelä AJ, Kivelä J, Saarnio J, Parkkila S. Carbonic anhydrases in normal gastrointestinal tract and gastrointestinal tumours. *World J Gastroenterol* 2005; 11(2): 155-163
http://www.wjgnet.com/1007-9327/11/155.asp

CARBONIC ANHYDRASES - GENERAL ASPECTS

Carbonic anhydrases are a group of zinc-containing metalloenzymes that catalyse the reversible hydration of carbon dioxide, $CO_2+H_2O <=> HCO_3^- + H^+$. Up to now, 12 enzymatically active alpha carbonic anhydrases have been identified and characterized in mammals including 5 cytoplasmic (CA I, CA II, CA III, CA VII, and CA XIII), 2 mitochondrial (CA VA and CA VB), 1 secreted (CA VI), and 4 membrane-associated (CA IV, CA IX, CA XII, and CA XIV) forms.

CAs are virtually ubiquitous in living systems, having varied functions in animal, plant and bacterial cells. The great diversity in both cellular distribution (Figure 1) and biological functions is remarkable and the catalytic activity of CAs, found in almost all organisms, is extremely high, placing the high-activity isoenzymes among the most efficient enzymes known[1]. In addition to its role in the regulation of pH homeostasis, CA activity facilitates biosynthetic processes, which involve an early carboxylation step requiring bicarbonate. These processes include gluconeogenesis and synthesis of certain amino acids (pyruvate carboxylase), lipogenesis (pyruvate carboxylase and acetyl CoA carboxylase), ureagenesis (carbamyl phosphate synthetase I), and pyrimide synthesis (carbamyl phosphate synthetase II)[2].

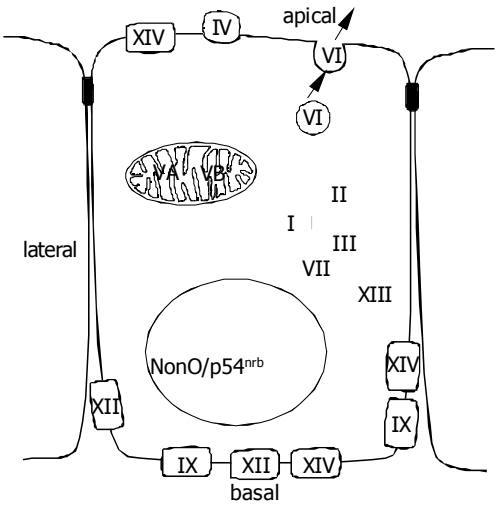

Figure 1 Subcellular localization of active CA isoenzymes and a novel nonclassical form of CA (nonO/p54^{nrb}).

Carbonic anhydrase isoenzymes

CA I is a well characterized cytoplasmic low-activity isoenzyme with a molecular weight of about 30 kDa[3,4]. It is one of the most abundant proteins in mammalian red cells[5,6]. Interestingly, it is not expressed in red cells of certain species, e.g., ruminants and felids, and no haematological abnormalities have emerged in its absence as the result of a mutation. Thus, the assignment of the physiological role of CA I is problematic[7-9].

CA II is the most widely distributed member of the CA family, being present in virtually every human tissue or organ[9]. The gene for human CA II is 17 kb long and located on chromosome 8, like those for CA I and III[1,10]. The high-active, cytoplasmic isoenzyme CA II has a turnover number of $1.3\text{-}1.9\times10^6$ /s under physiological conditions, and thus it is one of the most efficient enzymes known[11-13]. CA II participates in the control of bone resorption. Osteopetrosis, involving renal acidosis and cerebral calcification, is a human recessive inherited syndrome with a deficiency of CA II as a primary defect[14-17]. Even though CA II is the most abundant isoenzyme in the alimentary tract, no gastrointestinal symptoms have been associated with CA II-deficient patients.

Hormonally regulated cytoplasmic CA III has very low CA catalytic activity. On the other hand, it seems to protect from hydrogen peroxide-induced apoptosis and induce cell proliferation, whereas CA II does not have these effects[18]. These results suggest that CA III may provide protection against oxidative damage, and the lower levels of free radicals in cells overexpressing CA III may also affect growth signalling pathways.

To date four membrane-associated CA isoenzymes have been identified. CA IV is a glycosylphosphatidylinositol-anchored enzyme being expressed in the apical plasma membrane of epithelial cells (Figures 1, 2). The gene for CA IV is located on chromosome 17[19,20] and the molecular weight of the human protein is 35 kDa[21]. Human CA IV is present in the subepithelial capillary endothelium in all segments of the gastrointestinal canal as well as in epithelial cells of colon and gallbladder[22,23].

CA V is a low-activity isoenzyme located in the mitochondrial matrix[24]. cDNA for human mitochondrial CA V was originally cloned from a human liver cDNA library, and its gene was localized to chromosome 16[24]. Recently, two laboratories independently characterized another mitochondrial CA and thereafter the two isoenzymes have been termed CA VA and CA VB[25,26]. The expression of human *CA5A* mRNA has been demonstrated only in liver[26]. In the alimentary tract, *CA5B* mRNA has been shown in pancreas and salivary glands by reverse transcription-PCR (RT-PCR)[26].

CA VI is to date the only known secretory isoenzyme of the CA gene family. This isoenzyme with a molecular weight of 39-46 kDa has several properties that distinguish it from the well-characterized cytoplasmic isoenzymes[27-33]. On the other hand, the catalytic domain of CA VI is highly homologous to four other "extracellular" CAs (CA IV, CA IX, CA XII, and CA XIV), which are in fact transmembrane proteins with an extracellularly exposed CA domain[34,35].

CA VII is a cytoplasmic isoenzyme, the gene of which has been isolated from a human genomic library[9,36]. The gene is about 10 kb long and located on chromosome 16, and the predicted amino acid sequence of CA VII has shown that it is the most highly conserved isoenzyme in mammals[37]. Recombinant CA VII has shown high enzyme activity, but the expression of the protein in tissues has not yet been described[38]. Its mRNA has been detected in the human salivary gland[36], rat and mouse lung[39] and mouse brain neurons[37,40].

CA IX was first recognized as a novel tumour-associated antigen, MN, in several human carcinomas and normal gastric mucosae[41,42]. When the full-length cDNA for MN protein was cloned, it was found to contain a central part with sequence homology to the CAs[42,43], on which basis the MN protein was named CA IX[44]. Human *CA9* gene has been mapped to chromosome 17[45]. CA IX is a glycoprotein of 54 and 58 kDa mass expressed at the basolateral plasma membrane of epithelial cells (Figure 1) and, in some cases, also in nuclei[46]. The mature CA IX molecule consists of a proteoglycan-like domain, CA domain, transmembrane segment, and a short intracellular tail (Figure 2)[42].

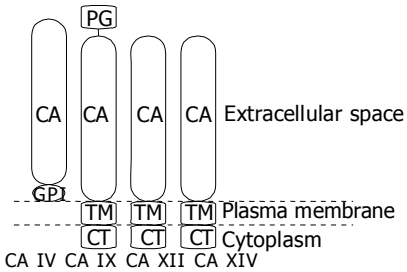

Figure 2 Topography of membrane-associated CA isoenzymes. CA: carbonic anhydrase domain, GPI: glycosylphosphatidylinositol link, TM: transmembrane part, CT: cytoplasmic C-terminal tail, PG: proteoglycan domain.

Table 1 Immunohistochemical distribution of CAs in human alimentary tract

Isoenzyme	Molecular weight (ku)	Positive cell types	Main references
CA I	30	Epithelial cells of	[5,60,61,86]
		oesophagus	
		jejunum	
		ileum	
		colon	
		Subepithelial capillary endothelium	
		α-cells of Langerhans islets	
CA II	30	Epithelial cells of	[5, 60,64,75,86]
		salivary glands	
		oesophagus	
		stomach	
		duodenum	
		jejunum	
		ileum	
		caecum	
		colon	
		rectum	
		biliary tract	
		pancreatic duct	
		Brunner's glands	
		Hepatocytes	
CA III	30	Epithelial cells of oesophagus	[74, 86]
		Hepatocytes	
CA IV	35	Epithelial cells of	[22, 23, 61, 86]
		oesophagus	
		duodenum	
		colon	
		rectum	
		biliary tract	
		Subepithelial capillary endothelium	
CA V	30	Hepatocytes	[14, 24,79]
		β-cells of Langerhans islets	
CA VI	42	Epithelial cells of	[62, 64]
		salivary glands	
		von Ebner's glands	
CA VII			
CA IX	54/58	Epithelial cells of	[61,78,88,117]
		salivary glands	
		oesophagus	
		stomach	
		duodenum	
		jejunum	
		ileum	
		colon	
		rectum	
		biliary tract	
		pancreatic duct	
CA XII	44	Epithelial cells of	[117]
		salivary glands	
		stomach	
		colon	
		pancreatic acini	
CA XIII	30	Epithelial cells of	[52]
		salivary glands	
		intestine	
		colon	
CA XIV	37.5		

Expression of *CA9* gene is subject to complex regulation both via promoter/enhancer elements at the level of transcription initiation[47] and via VHL tumour suppressor protein, possibly at the level of transcription elongation[45,48]. CA IX has been linked to oncogenesis, and its overexpression has been observed in malignant tumour cells. CA IX expression was found to be regulated by cell density in HeLa cells and to correlate with tumourigenicity in HeLa cell/fibroblast cell hybrids[49]. Moreover, transfection of NIH3T3 fibroblasts with CA IX caused changes in both morphology and growth parameters that were indicative of transformation[42].

Another active transmembrane CA isoenzyme is CA XII. *CA12* gene has been mapped to chromosome 15[50]. The cDNA sequence predicts a 354-amino acid polypeptide with a molecular mass of 39 448 Da[45,50]. The amino acid sequence includes a 29-amino acid signal peptide, 261-amino acid CA domain, an additional short extracellular segment, a 26-amino acid hydrophobic transmembrane domain, and a 29-amino acid C-terminal cytoplasmic tail containing two potential phosphorylation sites. The extracellular CA domain has three zinc-binding histidine residues found in active CAs and two potential sites for asparagine glycosylation[50]. It has a sequence identity of 30-42% to other CAs. The reported molecular weight of CA XII produced in transfected COS cells is 43-44 kDa. It is reduced to 39 kDa by PNGase F digestion, which is consistent with the removal of two oligosaccharide chains[50]. Recombinant CA XII protein is an active isoenzyme and its catalytic properties are similar to those of the high-activity membrane-associated CA IV[51].

Recent analyses of human and mouse databases provided evidence that human and mouse genomes contain genes for still another cytosolic CA isoenzyme named CA XIII. It is a globular molecule with high structural similarity to CAs I, II, and III[52]. Recombinant mouse CA XIII has catalytic activity similar to those of mitochondrial CA V and cytosolic CA I. Immunohistochemical staining and RT-PCR have shown a unique and widespread distribution pattern for CA XIII protein and mRNA compared to the other cytosolic CA isoenzymes. It is present in several gastrointestinal organs including salivary glands, small and large intestine.

CA XIV is a recently described transmembrane isoenzyme[35], consisting of a putative amino-terminal signal sequence, a CA domain with high homology with other extracellular CAs, a transmembrane domain and a short intracellular C-terminal tail. A cDNA coding for human CA XIV has been reported and the *CA14* gene has been mapped to chromosome 1q21[53]. The Northern blot method showed *CA14* mRNA expression in human heart, brain, liver and skeletal muscle. RT-PCR analysis pointed to an intense signal in the normal human liver and spinal cord. RNA dot blot analysis showed weak signals in the small intestine, colon, kidney, and urinary bladder[53]. By immunohistochemistry, CA XIV protein has been demonstrated in the mouse brain, liver, and kidney[54-56]. In the brain, high signal has been detected in the neuronal membranes and axons[54]. In the liver, CA XIV is confined to the plasma membrane of hepatocytes[55]. Interestingly, it is located in both the apical and basolateral membranes. In contrast, the other transmembrane isoenzymes, CA IX and XII, are clearly restricted to the basolateral membranes. The location in apical and basolateral membrane domains has been described for CA XIV also in the kidney, where the enzyme is expressed in the proximal tubules and thin descending limb of Henle[56].

In addition to the members of the classical CA gene family, a 66-kDa polypeptide was recently purified from several rat tissues on CA inhibitor affinity chromatography[57]. Its amino acid sequence has revealed that it represents the previously cloned and characterized nuclear protein, nonO/p54^{nrb}, a non-POU (Pit-Oct-Unc) domain-containing octamer-binding protein, which is homologous to the nuclear 54 kDa RNA-binding protein[58,59]. CA activity of nonO is interesting because no other classes of mammalian proteins except CAs have been shown to bind specifically to CA inhibitor affinity chromatography matrix and to contain CA catalytic activity. CA catalytic activity in nonO could explain at least part of the nuclear CA activity seen in histochemical CA staining[57]. It also suggests that CA activity is an important factor in transcriptional regulation, which would be a novel function for CA.

CARBONIC ANHYDRASES IN THE GASTROINTESTINAL TRACT

Carbonic anhydrases are evolutionarily ancient enzymes, which can be found along the entire GI tract, from the mouth and salivary glands to the rectum (Table 1)[60-62]. However, there is a considerable heterogeneity between different organs with respect to CA enzymatic activity, isoenzyme content, and their cellular localization. It is also notable that CAs of the GI tract can serve several functions such as regulation of acid-base homeostasis, salt absorption and cell volume[63].

Major digestive glands

Three CA isoenzymes, CAs II, VI, and XIIII, are known to be expressed in the mammalian salivary glands[52,64]. A study by Leinonen *et al*[65] showed that salivary CA VI was associated with the enamel pellicle, a thin layer of proteins covering the dental enamel. It has also been detected in the gastric mucus, but the failure to find any expression of it in the gastric epithelial cells[60] implies that gastric CA VI must be of salivary origin. CAs II, VI, and XIII may together form a complementary system regulating the acid-base balance in the mouth and upper alimentary tract[63,64,66,67]. CAs II and XIII in the salivary glands may supply the saliva with HCO_3- and the CA VI secreted into the saliva would then accelerate the removal of bacterially produced acid from the local microenvironment of the tooth surface in the form of CO_2. This hypothetical model of CA VI functions is supported by Kivelä *et al*[68], who showed that low salivary CA VI concentrations were associated with increased caries prevalence, particularly in subjects with neglected oral hygiene. In the gastric mucus, CA VI may contribute to the maintenance of pH gradient on the surface epithelial cells by catalyzing the conversion of bicarbonate produced by these cells and protons of the gastric juice to water and carbon dioxide.

Recent studies have shown that CA VI is also present in human and rat milk[69]. The high concentration of CA VI in colostrum suggests that it may play an important developmental role in the morphogenesis of the gastrointestinal canal during the early postnatal period.

There are two other findings pointing to novel physiological roles for CA VI. First, gustin, a salivary factor involved in taste perception, was shown to be identical to CA VI[70], and second, identification of a novel stress-inducible intracellular form of CA VI (type B) suggests that the enzyme could also participate in intracellular pH changes induced by stress, including apoptosis[71].

Compared with other secretory organs, the mammalian liver contains relatively low levels of total CA activity. A basic physiological function of CA II in the liver is to produce HCO_3^- for the alkalization of the bile[72]. The mammalian liver expresses high levels of mitochondrial CA V[14,24,26], which has been implicated in two metabolic processes: ureagenesis and gluconeogenesis, supplying bicarbonate for the first urea cycle enzyme, carbamyl phosphate synthetase I in ureagenesis and for pyruvate carboxylase in gluconeogenesis[73].

The presence of low activity, hormonally regulated CA III in hepatocytes[74,75] has aroused interest in its specific function. Cabiscol and Levine[76] have demonstrated that it functions in

an oxidizing environment and that it is the most oxidatively modified protein in the liver known so far. These and other results[18] suggest that CA III may provide protection against oxidative damage and CA III may serve as a useful marker protein to investigate the *in vivo* mechanisms, which contribute to oxidative damage in the liver.

In addition to CA II, CA III, and CA VA, hepatocytes contain CA XIV[55]. Positive signal for CA XIV was detected in both domains of the plasma membrane, i.e., basolateral and apical (canalicular), but the apical membrane was more strongly labelled by immunohistochemical staining[55]. CA XIV is the only membrane-bound CA isoform which most probably regulates pH and ion transport between hepatocytes, bile canaliculi and hepatic sinusoids. CA II is expressed in epithelial cells of the hepatic bile ducts and gallbladder[60,77]. Immunohistochemical studies have also shown that two membrane associated CA isoenzymes, CA IV and CA IX, are expressed in the biliary epithelial cells, whereas hepatocytes are negative[23,78]. It is notable that both isoenzymes show high expression in the human gallbladder - CA IV at the apical and CA IX at the basolateral plasma membrane. Based on the localization, CAs might be involved in acidification and concentration of bile, even though the exact functional mechanisms have not been described.

Pancreas contains two morphologically and functionally different elements: endocrine and exocrine compartments. CA I is expressed in α-cells of the endocrine Langerhans islets[60]. However, the physiological role of CA I in α-cell function has remained unclear. CA V is another isoenzyme described in the endocrine pancreas where its expression is solely confined to β-cells[79]. The suggestion that CA V may have a role in the regulation of insulin secretion was based on its cellular distribution and the observation that the CA inhibitor acetazolamide inhibited glucose-stimulated insulin secretion[79].

In the exocrine pancreas, immunohistochemical staining has shown an intense positive signal for CA II in epithelial duct cells[80-82], where its role has been linked to secretion of bicarbonate into the pancreatic juice[72]. In addition to CA II, both CA IX and XII have been detected in the pancreatic epithelium, the expression being confined to the basolateral plasma membranes of acinar and ductal cells[83]. The mechanisms involved in the pancreatic duct cell ion transport have been recently reviewed by Ishiguro *et al*[84]. They presented a model where the basolateral plasma membrane contained Na^+-HCO_3^- cotransporter and Cl^-/HCO_3^- exchanger. The bicarbonate secretion across the apical plasma membrane was proposed to occur by exchange for Cl^- ions on Cl^-/HCO_3^- exchanger working in parallel with the cystic fibrosis transmembrane conductance regulator (CFTR) Cl^- channel. Solving the question of how different CAs can function in pancreatic duct and acinar cells will be a challenging task, not least technically. The knockout mouse models will hopefully provide invaluable information on the role of each isoenzyme. It is noteworthy, however, that recent studies on CA IX-deficient mice did not reveal any obvious pancreatic phenotype[85].

Gastrointestinal canal

Squamous epithelial cells of the human oesophagus express several CA isoenzymes. The cytoplasmic low-activity isoenzymes CAs I and III are confined to the basal cell layer, where they have been suggested to facilitate the efflux of CO_2 and H_2O from metabolically active basal cells to capillaries of lamina propria[86]. CA II has been located in the suprabasal cell layers, where it may contribute to HCO_3^- secretion[60,86]. The presence of this high-activity isoenzyme in the oesophagus is physiologically important, because endogenous HCO_3^- secretion is capable of raising the pH of the gastro-oesophageal reflux-derived residual acid from 2.5 almost to neutrality[87]. The immunohistochemical evidence for the presence of CA II in the human oesophagus is thus in accordance with the biochemical evidence that the oesophagus disposes of an endogenous mechanism for protecting the mucosa against acidity, but suggests that the stratified oesophageal epithelium rather than the submucous glands is responsible for HCO_3^- secretion.

In addition to cytoplasmic isoenzymes, two membrane-associated CAs are expressed in the oesophageal epithelium. Immunohistochemical studies have revealed a positive signal for the membrane-linked CA IV in suprabasal cell layers[86]. Similarly, weak immunostaining for CA IX has been found in the basal layer of the oesophageal epithelium[88].

Immunohistochemical techniques have revealed cytosolic CA II in parietal cells of the gastric glands, where it regulates the acidity of the gastric juice by proton secretion[5,60,63,81]. On the other hand, in gastric surface epithelial cells CA II is involved in the secretion of mucus and HCO_3^- to form a bicarbonate containing mucous gel layer covering the epithelium and protecting it from digestion. This gastroduodenal HCO_3^- secreted by the surface epithelial cells neutralizes the gastric acid[89].

Membrane-associated CA IX is another major CA isoenzyme expressed in gastric epithelium. Both parietal and surface epithelial cells contain CA IX at the basolateral plasma membrane[78]. Evolutionary conservation in vertebrates and the abundant expression of CA IX in normal human gastric mucosa have indicated its physiological importance. CA IX may participate in physiological processes via the activity of its CA-like domain. On the other hand, basolateral localization of CA IX suggests its possible involvement in intercellular communication and/or cell proliferation. Recent study on CA IX knockout mice demonstrated that this enzyme deficiency could result in a clear gastric phenotype[85]. These mice showed gastric hyperplasia and numerous cysts in gastric mucosa. The number of proliferative cells in gastric mucosa was increased, whereas the indices of gastric secretion showed normal values.

In the small intestine, CA I has been found in cryptal enterocytes[61] and CA II in surface epithelial cells[60]. High expression of CA IX has been reported in the epithelium of intestinal mucosa, where CA IX is confined to the basolateral cell surface of enterocytes and the cellular distribution is restricted to the proliferative cryptal enterocytes[61,78]. Interestingly, its regional expression is distinctive compared with other CAs, being most intense in the duodenum and jejunum and decreasing distally to only weak and sporadic expression in the distal large intestine[61].

It is known that cytosolic CAs I, II, and XIII are expressed in non-goblet epithelial cells of the mammalian colon[5,52,60,61], in which these isoenzymes may participate in the regulation of electroneutral NaCl reabsorption via the synchronous operation of apical Na^+-H^+ and Cl^--HCO_3^- exchange[90]. In addition to cytosolic CAs I, II, and XIII, and mitochondrial CA V, intestinal enterocytes express at least four membrane-associated isoenzymes, CA IV[22], CA IX[61,78], CA XII[91], and CA XIV[55]. In the colon, CA IX is restricted to the colonic glands[61]. CA XII is highly expressed in the caecum, ascending colon, transverse colon, descending colon, sigmoid colon, and rectum. The expression is confined to the basolateral plasma membranes in enterocytes and is most prominent in the surface epithelial cuff region of the large intestine[91].

The new evidence that at least eight enzymatically active CA isoenzymes (CAs I, II, IV, V, IX, XII, XIII, and XIV) are expressed in the mammalian large intestine indicates the complexity of the physiological processes occurring in the GI tract. In addition, CA isoenzymes are differentially expressed along the intestinal segments and also between cryptal and villal enterocytes. Finally, it is a matter of debate whether the

regulatory mechanisms could be different depending on the species studied. Even though some of these isoenzymes have heretofore been demonstrated only in rodents or humans, it is conceivable that general transport and pH regulation mechanisms are qualitatively similar in various species[92,93].

CA function is ultimately linked to certain transport proteins in both apical and basolateral cell membranes. In a recent article, Kunzelmann and Mall[94] have thoroughly reviewed these ion transport mechanisms in both colonic absorption and secretion. Identification of various ion transport proteins in the colon has made it possible to build schematic models for ion movement in different segments of the colon. Figure 3 represents a model for colonic ion and water transport that incorporates current knowledge regarding membrane transport processes[92,94-97]. It is important to emphasize that it is still a matter of discussion whether some of the proposed ion transport proteins are functional in the human colon. The absorption of NaCl can be electrogenic or electroneutral depending on the site of the process. In the proximal colon the absorption is primarily due to an electroneutral process via parallel luminal Na^+/H^+ and Cl^-/HCO_3^- exchange[98]. Electroneutral luminal Na^+ uptake is driven by the basolateral Na^+-K^+-ATPase lowering intracellular Na^+ concentration. Na^+ and Cl^- transport is coupled via changes in intracellular pH and Cl^- concentration[99]. Electroneutral NaCl absorption is also stimulated by short-chain fatty acids (SCFA), which are produced by colonic bacteria. The absorbed SCFA can stimulate apical Na^+/H^+ and Cl^-/HCO_3^- exchangers, thus having a significant impact also on the regulation of colonic fluid balance and luminal as well as cytosolic pH[94]. The electrogenic absorption of NaCl mainly occurs in the distal colon via the luminal epithelial Na^+ channels (ENaC) and transcellular/paracellular absorption of Cl^-[100].

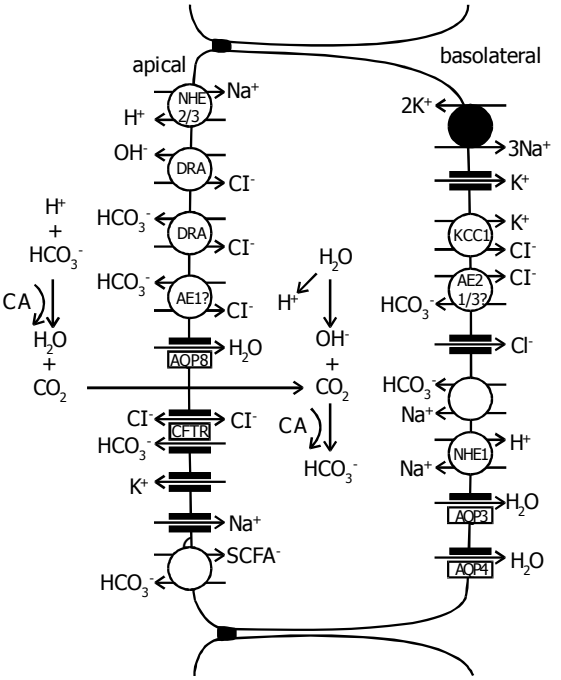

Figure 3 Schematic model of the cellular absorption and secretion of electrolytes and water in mammalian colon. Examples of ion transport mechanisms were demonstrated in a single enterocyte. Na^+/H^+ exchangers types 1, 2, and 3 (NHE1/2/3), proteins downregulated in adenoma (DRA), anion exchangers types 1, 2, and 3 (AE1/2/3), aquaporins 3, 4, and 8 (AQP3/4/8), cystic fibrosis transmembrane conductance regulator (CFTR), short-chain fatty acids ($SCFA^-$), KCl cotransporter (KCC1), carbonic anhydrase (CA).[92,94-97]

The participation of colonic CA in the electroneutral NaCl reabsorption is well established. Studies with acetazolamide suggest that CA activity is involved in the absorption of NaCl via the synchronous operation of apical Na^+/H^+ and Cl^-/HCO_3^- exchange processes. CAs are also shown to participate in the alkalization of the luminal contents by generating HCO_3^- for apical Cl^-/HCO_3^- exchange[101]. Recent exciting results from Casey's laboratory have indicated that CAs can physically and functionally associate with Cl^-/HCO_3^- (AE1) and Na^+/H^+ exchangers[102-104]. So far, CA IV is the only membrane-bound CA isoenzyme known to interact with AE1 protein[103]. It would be tempting to hypothesize that CAs IX, XII, and XIV could also drive ion exchange across the plasma membrane via direct links with transport proteins. The locations of membrane-associated isoenzymes CAs IV, IX, XII, and XIV in the surface epithelium of the colon, place them in a strategic position for the regulation of luminal and extracellular acid-base homeostasis and microclimate[22,55,61,91].

The net movement of water in colon is driven osmotically. Water is transported via both paracellular and transepithelial routes[105]. Although the proteins involved in NaCl absorption have been studied for decades, the exact molecular mechanisms of water absorption have remained largely unresolved. Recently, new information on water channel proteins, aquaporins (AQP), has opened new avenues to explore this understudied area of physiology. From different isoforms of AQPs, at least AQP3, AQP4, and AQP8 are expressed in colonic epithelial cells[106-109]. AQP3 and AQP4 are expressed at the basolateral plasma membrane like CA XII. AQP8 is confined to the apical plasma membrane like CA IV and CA XIV. Interestingly, Nakhoul *et al*[110] have shown that in *Xenopus* oocytes CO_2 flux can be mediated by AQP1, and therefore, AQPs could act as a gas channel even though CO_2 has earlier been believed to diffuse freely across the cell membranes. Despite that there is no experimental evidence yet available, one could speculate that AQPs would be an interesting target when searching protein interactions of membrane-bound CAs. By analogy to ion exchangers, AQPs are typically expressed in tissues expressing high levels of CAs such as colon, liver, pancreas, kidney, salivary gland, and stomach tissues[111].

CARBONIC ANHYDRASES IN NEOPLASTIC GASTROINTESTINAL TISSUES

To date, CA expression has been studied most extensively in colorectal tumors[91,112,113]. Scattered reports have also been published on hepatobiliary[114], pancreatic[83,115], esophageal[88], and gastric tumours[116]. In view of the recent experimental data, it appears inevitable that some CA isoenzymes may play a role in carcinogenic processes such as uncontrolled cell proliferation and malignant cell invasion. Studies have shown an important causal link between hypoxia, extracellular acidification, and induction or enhanced expression of these enzymes in human tumours[117]. A first direct link has been obtained by the discovery that isoenzymes CA IX and XII are down-regulated by wild-type VHL tumour suppressor protein, and a mutation in *VHL* gene can lead to overexpression of these enzymes[45].

CA IX is a predominant isoenzyme in various tumours including those arising from the GI tract. It has been demonstrated that CA IX is expressed in proliferating enterocytes of the normal human colon and its expression is increased in most adenomas and primary colorectal carcinomas[61,113]. The co-occurrence of CA IX and Ki-67 at the site of rapid cell proliferation indicates that CA IX could be used as a biomarker of increased cell proliferation in colorectal mucosa. Furthermore, its high expression in premalignant lesions such as adenomas suggests

that it might be an especially useful biomarker in early stages of adenoma-carcinoma sequence.

Recent results have demonstrated that in colorectal tumours the expression of CA XII is up-regulated in the deep parts of the mucosa where it is weakly expressed[91]. In contrast, CAs I and II have shown maximal immunoreactions in normal colorectal mucosa, and the reactions decline in adenomas and carcinomas[118]. The reciprocal changes in the expression of soluble cytoplasmic isoenzymes (CAs I and II) and membrane-associated forms (CAs IX and XII) observed in colorectal tumours are probably due to different mechanisms. Loss of expression of the closely linked *CA1* and *2* genes could result from loss of alleles specifying these genes. As a second option, the down-regulation of CAs I and II could also result from reduced levels of a common transcription factor. The latter is supported by a recent finding that a reduced expression of CA II in colorectal cancer is due to disruption of β-catenin/TCF-4 activity[119].

Up-regulation of CAs IX and XII could also be explained by two different mechanisms. First, contribution of microenvironmental stress to development of tumour phenotype has become an increasingly accepted explanation. Indeed, Wykoff *et al*[120] have demonstrated a close connection between tumour hypoxia and the expression of CAs IX and XII. They showed that up-regulation of CA IX occurred at the level of transcriptional activation via HIF-1 transcriptional complex, the critical mediator of hypoxic responses. The transcriptional complex hypoxia-inducible factor-1 (HIF-1) has emerged as an important mediator of gene expression patterns in tumours[121]. HIF-1 is regulated by ubiquitin-mediated proteolysis and targeted for destruction by the pVHL in normoxia and stabilized under hypoxia[122]. Both *CA9* and *CA12* are strongly induced by hypoxia in a range of tumour cell lines. They define a new class of HIF-1-responsive genes, the activation of which has implications for the understanding of hypoxic tumour metabolism and which may provide endogenous markers for tumour hypoxia[120].

Second, overexpression of CAs IX and XII has been associated with the loss of expression of the *VHL* tumour suppressor gene. In 1998, Ivanov and his group[45] used renal cell carcinoma cell lines stably transfected with wild-type VHL-expressing transgenes to discover genes involved in VHL-mediated carcinogenesis. The involvement of CAs IX and XII was indirectly supported by the findings that normal von Hippel-Lindau protein down-regulated the expression of both CA IX and CA XII, while the mutations in the *VHL* gene found in renal cell carcinomas could lead to overexpression of these isoenzymes.

The *VHL* gene is a tumour suppressor gene. This means that its role in a normal cell is to stop uncontrolled growth and proliferation. If the gene is deleted or mutated, its inhibitory effect on cell growth can be consequently lost or diminished, which in combination with defects in other regulatory proteins, can lead to cancerous growth. VHL seems to act as a 'gatekeeper' to the multistep process of tumourigenesis. The molecular mechanisms by which the product of VHL (pVHL) modulates the expression of target genes are not well understood. The original hypothesis based on the discovery of elongin B bound to pVHL assumed that VHL could negatively regulate transcription elongation of target genes, *CA9* and *CA12*, by inhibiting the elongin function. Although this expectation has been confirmed *in vitro*, there is no compelling evidence to date that pVHL can exert the same effect *in vivo*[45,123,124].

Both CA IX and CA XII are transmembrane proteins with catalytic domain on the cell exterior, suggesting that they might participate in acid-base regulation of the extracellular space. There is substantial evidence that extracellular pH of human tumours is generally more acidic than that of normal tissues[125] and that this acidic pH may enhance both the migration and the invasive behaviour of some tumour cell types[126]. Ivanov *et al*[45] hypothesized that CA XII might be involved in tumour invasion by acidifying the extracellular milieu surrounding the cancer cells. This acidification would, in turn, contribute to the activation of enzymes involved in extracellular matrix degradation. This hypothesis is supported by more recent findings that acetazolamide, a potent inhibitor of CA activity, could reduce the invasive capacity of renal cancer cells[127]. Even more interesting from this point of view is the finding that a similar effect was described in a number of other malignant cell types including those derived from colorectal cancer[128].

The mechanism by which CA inhibitors affect tumour growth is not known at present, but several hypotheses have been proposed. These compounds might reduce the provision of bicarbonate for the synthesis of nucleotides and other cell components. On the other hand, CA inhibitors could prevent the acidification of extracellular milieu. A combination of several mechanisms is also possible. E7070, a member of recently reported class of antitumour sulfonamides, blocks cell cycle progression in the G1 phase. It has been suggested that E7070, possessing a free SO_2NH_2 moiety, probably acts as a strong CA inhibitor[129]. This compound demonstrates significant antitumour activity *both in vitro* and *in vivo* against different human tumours, e.g., human colon carcinoma. E7070 produces not only growth suppression but also reduction in tumour size. The clinical trials with E7070 may turn out to be successful, since CA inhibitor (acetazolamide) has already been shown to be beneficial in anticancer therapies in combination with cytotoxic agents[130].

REFERENCES

1 **Tashian RE**. The carbonic anhydrases: widening perspectives on their evolution, expression and function. *Bioessays* 1989; **10**: 186-192
2 **Chegwidden WR**, Dodgson SJ, Spencer IM. The roles of carbonic anhydrase in metabolism, cell growth and cancer in animals. *EXS* 2000: 343-363
3 **Bundy HF**. Carbonic anhydrase. *Comp Biochem Physiol B* 1977; **57**: 1-7
4 **Lindskog S**, Engberg P, Forsman C, Ibrahim SA, Jonsson BH, Simonsson I, Tibell L. Kinetics and mechanism of carbonic anhydrase isoenzymes. *Ann N Y Acad Sci* 1984; **429**: 61-75
5 **Lönnerholm G**, Selking Ö, Wistrand PJ. Amount and distribution of carbonic anhydrases CA I and CA II in the gastrointestinal tract. *Gastroenterology* 1985; **88**: 1151-1161
6 **Venta PJ**, Montgomery JC, Tashian RE. Molecular genetics of carbonic anhydrase isozymes. *Isozymes Curr Top Biol Med Res* 1987; **14**: 59-72
7 **Tashian RE**, Goodman M, Headings VE, Ward RH, DeSimone J. Genetic variation and evolution in the red cell carbonic anhydrase isozymes of macaque monkeys. *Biochem Genet* 1971; **5**: 183-200
8 **Tashian RE**, Kendall AG, Carter ND. Inherited variants of human red cell carbonic anhydrases. *Hemoglobin* 1980; **4**: 635-651
9 **Tashian RE**. Genetics of the mammalian carbonic anhydrases. *Adv Genet* 1992; **30**: 321-356
10 **Nakai H**, Byers MG, Venta PJ, Tashian RE, Shows TB. The gene for human carbonic anhydrase II (CA2) is located at chromosome 8q22. *Cytogenet Cell Genet* 1987; **44**: 234-235
11 **Khalifah RG**. The carbon dioxide hydration activity of carbonic anhydrase. I. Stop-flow kinetic studies on the native human isoenzymes B and C. *J Biol Chem* 1971; **246**: 2561-2573
12 **Sanyal G**, Maren TH. Thermodynamics of carbonic anhydrase catalysis. A comparison between human isoenzymes B and C. *J Biol Chem* 1981; **256**: 608-612
13 **Wistrand PJ**. The importance of carbonic anhydrase B and C for the unloading of CO2 by the human erythrocyte. *Acta Physiol Scand* 1981; **113**: 417-426
14 **Sly WS**, Hu PY. Human carbonic anhydrases and carbonic

anhydrase deficiencies. *Annu Rev Biochem* 1995; **64**: 375-401
15 **Sly WS**, Hewett-Emmett D, Whyte MP, Yu YS, Tashian RE. Carbonic anhydrase II deficiency identified as the primary defect in the autosomal recessive syndrome of osteopetrosis with renal tubular acidosis and cerebral calcification. *Proc Natl Acad Sci USA* 1983; **80**: 2752-2756
16 **Sly WS**, Whyte MP, Sundaram V, Tashian RE, Hewett-Emmett D, Guibaud P, Vainsel M, Baluarte HJ, Gruskin A, Al-Mosawi M. Carbonic anhydrase II deficiency in 12 families with the autosomal recessive syndrome of osteopetrosis with renal tubular acidosis and cerebral calcification. *N Engl J Med* 1985;**313**: 139-145
17 **Sly WS**, Hu PY. The carbonic anhydrase II deficiency syndrome: osteopetrosis with renal tubular acidosis and cerebral calcification. In: Scriver CR, Beaudet AL, Sly WS, Valle D, eds. The Molecular and Metabolic Bases of Inherited Disease. *New York: McGraw-Hill* 1995: 4113-4124
18 **Räisänen SR**, Lehenkari P, Tasanen M, Rahkila P, Härkönen PL, Väänänen HK. Carbonic anhydrase III protects cells from hydrogen peroxide-induced apoptosis. *FASEB J* 1999; **13**: 513-522
19 **Okuyama T**, Sato S, Zhu XL, Waheed A, Sly WS. Human carbonic anhydrase IV: cDNA cloning, sequence comparison, and expression in COS cell membranes. *Proc Natl Acad Sci USA* 1992; **89**: 1315-1319
20 **Okuyama T**, Batanian JR, Sly WS. Genomic organization and localization of gene for human carbonic anhydrase IV to chromosome 17q. *Genomics* 1993; **16**: 678-684
21 **Zhu XL**, Sly WS. Carbonic anhydrase IV from human lung. Purification, characterization, and comparison with membrane carbonic anhydrase from human kidney. *J Biol Chem* 1990; **265**: 8795-8801
22 **Fleming RE**, Parkkila S, Parkkila AK, Rajaniemi H, Waheed A, Sly WS. Carbonic anhydrase IV expression in rat and human gastrointestinal tract regional, cellular, and subcellular localization. *J Clin Invest* 1995; **96**: 2907-2913
23 **Parkkila S**, Parkkila AK, Juvonen T, Waheed A, Sly WS, Saarnio J, Kaunisto K, Kellokumpu S, Rajaniemi H. Membrane-bound carbonic anhydrase IV is expressed in the luminal plasma membrane of the human gallbladder epithelium. *Hepatology* 1996; **24**: 1104-1108
24 **Nagao Y**, Platero JS, Waheed A, Sly WS. Human mitochondrial carbonic anhydrase: cDNA cloning, expression, subcellular localization, and mapping to chromosome 16. *Proc Natl Acad Sci USA* 1993; **90**: 7623-7627
25 **Shah GN**, Hewett-Emmett D, Grubb JH, Migas MC, Fleming RE, Waheed A, Sly WS. Mitochondrial carbonic anhydrase CA VB: differences in tissue distribution and pattern of evolution from those of CA VA suggest distinct physiological roles. *Proc Natl Acad Sci USA* 2000; **97**: 1677-1682
26 **Fujikawa-Adachi K**, Nishimori I, Taguchi T, Onishi S. Human mitochondrial carbonic anhydrase VB. cDNA cloning, mRNA expression, subcellular localization, and mapping to chromosome x. *J Biol Chem* 1999; **274**: 21228-21233
27 **Kadoya Y**, Kuwahara H, Shimazaki M, Ogawa Y, Yagi T. Isolation of a novel carbonic anhydrase from human saliva and immunohistochemical demonstration of its related isozymes in salivary gland. *Osaka City Med J* 1987; **33**: 99-109
28 **Murakami H**, Sly WS. Purification and characterization of human salivary carbonic anhydrase. *J Biol Chem* 1987; **262**: 1382-1388
29 **Feldstein JB**, Silverman DN. Purification and characterization of carbonic anhydrase from the saliva of the rat. *J Biol Chem* 1984; **259**: 5447-5453
30 **Ogawa Y**, Chang CK, Kuwahara H, Hong SS, Toyosawa S, Yagi T. Immunoelectron microscopy of carbonic anhydrase isozyme VI in rat submandibular gland: comparison with isozymes I and II. *J Histochem Cytochem* 1992; **40**: 807-817
31 **Fernley RT**. Carbonic anhydrases secreted in the saliva. In: Dodgson SJ, Tashian RE, Gros G, Carter ND, eds. The Carbonic Anhydrases. Cellular physiology and molecular genetics. *New York: Plenum Press* 1991: 365-373
32 **Fernley RT**. Secreted carbonic anhydrases. In: Botré F, Gros G, Storey BT, eds. Carbonic anhydrase. From biochemistry and genetics to physiology and clinical medicine. *Weinheim: VCH Verlagsgesellschaft* 1991: 178-185
33 **Parkkila S**, Kaunisto K, Rajaniemi H. Location of the carbonic anhydrase isoenzymes VI and II in human salivary glands by immunohistochemistry. In: Botré F, Gros G, Storey BT, eds. Carbonic anhydrase. From Biochemistry and Genetics to Physiology and Clinical Medicine. *Weinheim: VCH Verlagsgesellschaft* 1991: 254-257
34 **Fujikawa-Adachi K**, Nishimori I, Sakamoto S, Morita M, Onishi S, Yonezawa S, Hollingsworth MA. Identification of carbonic anhydrase IV and VI mRNA expression in human pancreas and salivary glands. *Pancreas* 1999; **18**: 329-335
35 Mori K, Ogawa Y, Ebihara K, Tamura N, Tashiro K, Kuwahara T, Mukoyama M, Sugawara A, Ozaki S, Tanaka I, Nakao K. Isolation and characterization of CA XIV, a novel membrane-bound carbonic anhydrase from mouse kidney. *J Biol Chem* 1999; **274**: 15701-15705
36 **Montgomery JC**, Venta PJ, Eddy RL, Fukushima YS, Shows TB, Tashian RE. Characterization of the human gene for a newly discovered carbonic anhydrase, CA VII, and its localization to chromosome 16. *Genomics* 1991; **11**: 835-848
37 **Lakkis MM**, O'Shea KS, Tashian RE. Differential expression of the carbonic anhydrase genes for CA VII (Car7) and CA-RP VIII (Car8) in mouse brain. *J Histochem Cytochem* 1997; **45**: 657-662
38 **Earnhardt JN**, Qian M, Tu C, Lakkis MM, Bergenhem NC, Laipis PJ, Tashian RE, Silverman DN. The catalytic properties of murine carbonic anhydrase VII. *Biochemistry* 1998; **37**: 10837-10845
39 **Ling B**, Bergenhem NCH, Dodgson SJ, Forster RE, Tashian RE. Determination of mRNA levels for six carbonic anhydrase isozymes in rat lung. *Isozyme Bull* 1994; **28**: 32
40 **Lakkis MM**, Bergenhem NC, Tashian RE. Expression of mouse carbonic anhydrase VII in *E. coli* and demonstration of its CO_2 hydrase activity. *Biochem Biophys Res Commun* 1996; **226**: 268-272
41 **Liao SY**, Brewer C, Závada J, Pastorek J, Pastoreková S, Manetta A, Berman ML, DiSaia PJ, Stanbridge EJ. Identification of the MN antigen as a diagnostic biomarker of cervical intraepithelial squamous and glandular neoplasia and cervical carcinomas. *Am J Pathol* 1994; **145**: 598-609
42 **Pastorek J**, Pastoreková S, Callebaut I, Mornon JP, Zelník V, Opavský R, Zat'ovicová M, Liao S, Portetelle D, Stanbridge EJ. Cloning and characterization of MN, a human tumor-associated protein with a domain homologous to carbonic anhydrase and a putative helix-loop-helix DNA binding segment. *Oncogene* 1994; **9**: 2877-2888
43 **Opavský R**, Pastoreková S, Zelník V, Gibadulinová A, Stanbridge EJ, Závada J, Kettmann R, Pastorek J. Human MN/CA9 gene, a novel member of the carbonic anhydrase family: structure and exon to protein domain relationships. *Genomics* 1996; **33**: 480-487
44 **Hewett-Emmett D**, Tashian RE. Functional diversity, conservation, and convergence in the evolution of the alpha-, beta-, and gamma-carbonic anhydrase gene families. *Mol Phylogenet Evol* 1996; **5**: 50-77
45 **Ivanov SV**, Kuzmin I, Wei MH, Pack S, Geil L, Johnson BE, Stanbridge EJ, Lerman MI. Down-regulation of transmembrane carbonic anhydrases in renal cell carcinoma cell lines by wild-type von Hippel-Lindau transgenes. *Proc Natl Acad Sci USA* 1998; **95**: 12596-12601
46 **Pastoreková S**, Závadová Z, Kost'ál M, Babusikova O, Závada J. A novel quasi-viral agent, MaTu, is a two-component system. *Virology* 1992; **187**: 620-626
47 **Kaluz S**, Kaluzová M, Opavský R, Pastoreková S, Gibadulinová A, Dequiedt F, Kettmann R, Pastorek J. Transcriptional regulation of the MN/CA 9 gene coding for the tumor-associated carbonic anhydrase IX. Identification and characterization of a proximal silencer element. *J Biol Chem* 1999; **274**: 32588-32595
48 **Chen F,** Kishida T, Duh FM, Renbaum P, Orcutt ML, Schmidt L, Zbar B. Suppression of growth of renal carcinoma cells by the von Hippel-Lindau tumor suppressor gene. *Cancer Res* 1995; **55**: 4804-4807
49 **Závada J**, Závadová Z, Pastoreková S, Ciampor F, Pastorek J, Zelník V. Expression of MaTu-MN protein in human tumor cultures and in clinical specimens. *Int J Cancer* 1993; **54**: 268-274

50 **Türeci Ö,** Sahin U, Vollmar E, Siemer S, Göttert E, Seitz G, Parkkila AK, Shah GN, Grubb JH, Pfreundschuh M, Sly WS. Human carbonic anhydrase XII: cDNA cloning, expression, and chromosomal localization of a carbonic anhydrase gene that is overexpressed in some renal cell cancers. *Proc Natl Acad Sci USA* 1998; **95**: 7608-7613

51 **Ulmasov B**, Waheed A, Shah GN, Grubb JH, Sly WS, Tu C, Silverman DN. Purification and kinetic analysis of recombinant CA XII, a membrane carbonic anhydrase overexpressed in certain cancers. *Proc Natl Acad Sci USA* 2000; **97**: 14212-14217

52 **Lehtonen J**, Shen B, Vihinen M, Casini A, Scozzafava A, Supuran CT, Parkkila AK, Saarnio J, Kivelä AJ, Waheed A, Sly WS, Parkkila S. Characterization of CA XIII, a novel member of the carbonic anhydrase isozyme family. *J Biol Chem* 2004; 279: 2719-2727

53 **Fujikawa-Adachi K**, Nishimori I, Taguchi T, Onishi S. Human carbonic anhydrase XIV (CA14): cDNA cloning, mRNA expression, and mapping to chromosome 1. *Genomics* 1999; **61**: 74-81

54 **Parkkila S**, Parkkila AK, Rajaniemi H, Shah GN, Grubb JH, Waheed A, Sly WS. Expression of membrane-associated carbonic anhydrase XIV on neurons and axons in mouse and human brain. *Proc Natl Acad Sci USA* 2001; **98**: 1918-1923

55 **Parkkila S**, Kivelä AJ, Kaunisto K, Parkkila AK, Hakkola J, Rajaniemi H, Waheed A, Sly WS. The plasma membrane carbonic anhydrase in murine hepatocytes identified as isozyme XIV. *BMC Gastroenterol* 2002; **2**: 13

56 **Kaunisto K**, Parkkila S, Rajaniemi H, Waheed A, Grubb J, Sly WS. Carbonic anhydrase XIV: luminal expression suggests key role in renal acidification. *Kidney Int* 2002; **61**: 2111-2118

57 **Karhumaa P**, Parkkila S, Waheed A, Parkkila AK, Kaunisto K, Tucker PW, Huang CJ, Sly WS, Rajaniemi H. Nuclear NonO/p54(nrb) protein is a nonclassical carbonic anhydrase. *J Biol Chem* 2000; **275**: 16044-16049

58 **Yang YS**, Hanke JH, Carayannopoulos L, Craft CM, Capra JD, Tucker PW. NonO, a non-POU-domain-containing, octamer-binding protein, is the mammalian homolog of Drosophila nonAdiss. *Mol Cell Biol* 1993; **13**: 5593-5603

59 **Dong B**, Horowitz DS, Kobayashi R, Krainer AR. Purification and cDNA cloning of HeLa cell p54nrb, a nuclear protein with two RNA recognition motifs and extensive homology to human splicing factor PSF and Drosophila NONA/BJ6. *Nucleic Acids Res* 1993; **21**: 4085-4092

60 **Parkkila S**, Parkkila AK, Juvonen T, Rajaniemi H. Distribution of the carbonic anhydrase isoenzymes I, II, and VI in the human alimentary tract. *Gut* 1994; **35**: 646-650

61 **Saarnio J**, Parkkila S, Parkkila AK, Waheed A, Casey MC, Zhou XY, Pastoreková S, Pastorek J, Karttunen T, Haukipuro K, Kairaluoma MI, Sly WS. Immunohistochemistry of carbonic anhydrase isozyme IX (MN/CA IX) in human gut reveals polarized expression in the epithelial cells with the highest proliferative capacity. *J Histochem Cytochem* 1998; **46**: 497-504

62 **Leinonen J**, Parkkila S, Kaunisto K, Koivunen P, Rajaniemi H. Secretion of carbonic anhydrase isoenzyme VI (CA VI) from human and rat lingual serous von Ebner's glands. *J Histochem Cytochem* 2001; **49**: 657-662

63 **Parkkila S**, Parkkila AK. Carbonic anhydrase in the alimentary tract. Roles of the different isozymes and salivary factors in the maintenance of optimal conditions in the gastrointestinal canal. *Scand J Gastroenterol* 1996; **31**: 305-317

64 **Parkkila S**, Kaunisto K, Rajaniemi L, Kumpulainen T, Jokinen K, Rajaniemi H. Immunohistochemical localization of carbonic anhydrase isoenzymes VI, II, and I in human parotid and submandibular glands. *J Histochem Cytochem* 1990; **38**: 941-947

65 **Leinonen J**, Kivelä J, Parkkila S, Parkkila AK, Rajaniemi H. Salivary carbonic anhydrase isoenzyme VI is located in the human enamel pellicle. *Caries Res* 1999; **33**: 185-190

66 **Kivelä J**, Parkkila S, Parkkila AK, Leinonen J, Rajaniemi H. Salivary carbonic anhydrase isoenzyme VI. *J Physiol* 1999; **520** Pt 2: 315-320

67 **Parkkila S**, Parkkila AK, Lehtola J, Reinilä A, Södervik HJ, Rannisto M, Rajaniemi H. Salivary carbonic anhydrase protects gastroesophageal mucosa from acid injury. *Dig Dis Sci* 1997; **42**: 1013-1019

68 **Kivelä J**, Parkkila S, Parkkila AK, Rajaniemi H. A low concentration of carbonic anhydrase isoenzyme VI in whole saliva is associated with caries prevalence. *Caries Res* 1999; **33**: 178-184

69 **Karhumaa P**, Leinonen J, Parkkila S, Kaunisto K, Tapanainen J, Rajaniemi H. The identification of secreted carbonic anhydrase VI as a constitutive glycoprotein of human and rat milk. *Proc Natl Acad Sci USA* 2001; **98**: 11604-11608

70 **Thatcher BJ**, Doherty AE, Orvisky E, Martin BM, Henkin RI. Gustin from human parotid saliva is carbonic anhydrase VI. *Biochem Biophys Res Commun* 1998; **250**: 635-641

71 **Sok J**, Wang XZ, Batchvarova N, Kuroda M, Harding H, Ron D. CHOP-Dependent stress-inducible expression of a novel form of carbonic anhydrase VI. *Mol Cell Biol* 1999; **19**: 495-504

72 **Swenson ER**. Distribution and functions of carbonic anhydrase in the gastrointestinal tract. In: Dodgson SJ, Tashian RE, Gros G, Carter ND, eds. The Carbonic Anhydrases. Cellular Physiology and Molecular Genetics. *New York: Plenum Press* 1991: 265-287

73 **Dodgson SJ**. Liver mitochondrial carbonic anhydrase (CA V), gluconeogenesis, and ureagenesis in the hepatocyte. In: Dodgson SJ, Tashian RE, Gros G, Carter ND, eds. The Carbonic Anhydrases. Cellular Physiology and Molecular Genetics. *New York: Plenum Press* 1991: 297-306

74 **Jeffery S**, Edwards Y, Carter N. Distribution of CAIII in fetal and adult human tissue. *Biochem Genet* 1980; **18**: 843-849

75 **Carter N**, Wistrand PJ, Lönnerholm G. Carbonic anhydrase localization to perivenous hepatocytes. *Acta Physiol Scand* 1989; **135**: 163-167

76 **Cabiscol E**, Levine RL. Carbonic anhydrase III. Oxidative modification *in vivo* and loss of phosphatase activity during aging. *J Biol Chem* 1995; **270**: 14742-14747

77 **Juvonen T**, Parkkila S, Parkkila AK, Niemelä O, Lajunen LH, Kairaluoma MI, Perämäki P, Rajaniemi H. High-activity carbonic anhydrase isoenzyme (CA II) in human gallbladder epithelium. *J Histochem Cytochem* 1994; **42**: 1393-1397

78 **Pastoreková S**, Parkkila S, Parkkila AK, Opavský R, Zelník V, Saarnio J, Pastorek J. Carbonic anhydrase IX, MN/CA IX: analysis of stomach complementary DNA sequence and expression in human and rat alimentary tracts. *Gastroenterology* 1997; **112**: 398-408

79 **Parkkila AK**, Scarim AL, Parkkila S, Waheed A, Corbett JA, Sly WS. Expression of carbonic anhydrase V in pancreatic beta cells suggests role for mitochondrial carbonic anhydrase in insulin secretion. *J Biol Chem* 1998; **273**: 24620-24623

80 **Kumpulainen T**, Jalovaara P. Immunohistochemical localization of carbonic anhydrase isoenzymes in the human pancreas. *Gastroenterology* 1981; **80**: 796-799

81 **Kumpulainen T**. Immunohistochemical localization of human carbonic anhydrase isozymes. *Ann N Y Acad Sci* 1984; **429**: 359-368

82 **Spicer SS**, Sens MA, Tashian RE. Immunocytochemical demonstration of carbonic anhydrase in human epithelial cells. *J Histochem Cytochem* 1982; **30**: 864-873

83 **Kivelä AJ**, Parkkila S, Saarnio J, Karttunen TJ, Kivelä J, Parkkila AK, Pastoreková S, Pastorek J, Waheed A, Sly WS, Rajaniemi H. Expression of transmembrane carbonic anhydrase isoenzymes IX and XII in normal human pancreas and pancreatic tumours. *Histochem Cell Biol* 2000; **114**: 197-204

84 **Ishiguro H**, Naruse S, San Roman JI, Case M, Steward MC. Pancreatic ductal bicarbonate secretion: past, present and future. *JOP* 2001; **2**: 192-197

85 **Ortova Gut M**, Parkkila S, Vernerová Z, Rohde E, Závada J, Hocker M, Pastorek J, Karttunen T, Gibadulinová A, Závadová Z, Knobeloch KP, Wiedenmann B, Svoboda J, Horak I, Pastoreková S. Gastric hyperplasia in mice with targeted disruption of the carbonic anhydrase gene Car9. *Gastroenterology* 2002; **123**: 1889-1903

86 **Christie KN**, Thomson C, Xue L, Lucocq JM, Hopwood D. Carbonic anhydrase isoenzymes I, II, III, and IV are present in human esophageal epithelium. *J Histochem Cytochem* 1997; **45**: 35-40

87 **Meyers RL**, Orlando RC. *In vivo* bicarbonate secretion by human esophagus. *Gastroenterology* 1992; **103**: 1174-1178

88 **Turner JR**, Odze RD, Crum CP, Resnick MB. MN antigen expression in normal, preneoplastic, and neoplastic esophagus: a clinicopathological study of a new cancer-associated

biomarker. *Hum Pathol* 1997; **28**: 740-744
89 **Richardson CT**. Pathogenetic factors in peptic ulcer disease. *Am J Med* 1985; **79**: 1-7
90 **Charney AN**, Egnor RW. Membrane site of action of CO2 on colonic sodium absorption. *Am J Physiol* 1989; **256**: C584-C590
91 **Kivelä A**, Parkkila S, Saarnio J, Karttunen TJ, Kivelä J, Parkkila AK, Waheed A, Sly WS, Grubb JH, Shah G, Türeci Ö, Rajaniemi H. Expression of a novel transmembrane carbonic anhydrase isozyme XII in normal human gut and colorectal tumors. *Am J Pathol* 2000; **156**: 577-584
92 **Dawson DC**. Ion channels and colonic salt transport. *Annu Rev Physiol* 1991; **53**: 321-339
93 **Wills NK**. Apical membrane potassium and chloride permeabilities in surface cells of rabbit descending colon epithelium. *J Physiol* 1985; **358**: 433-445
94 **Kunzelmann K**, Mall M. Electrolyte transport in the mammalian colon: mechanisms and implications for disease. *Physiol Rev* 2002; **82**: 245-289
95 **Flemström G**, Isenberg JI. Gastroduodenal mucosal alkaline secretion and mucosal protection. *News Physiol Sci* 2001; **16**: 23-28
96 **Alrefai WA**, Tyagi S, Nazir TM, Barakat J, Anwar SS, Hadjiagapiou C, Bavishi D, Sahi J, Malik P, Goldstein J, Layden TJ, Ramaswamy K, Dudeja PK. Human intestinal anion exchanger isoforms: expression, distribution, and membrane localization. *Biochim Biophys Acta* 2001; **1511**: 17-27
97 **Seidler U**, Bachmann O, Jacob P, Christiani S, Blumenstein I, Rossmann H. Na^+/HCO_3^- cotransport in normal and cystic fibrosis intestine. *JOP* 2001; **2**: 247-256
98 **Rajendran VM**, Binder HJ. Characterization and molecular localization of anion transporters in colonic epithelial cells. *Ann N Y Acad Sci* 2000; **915**: 15-29
99 **Geibel JP**, Rajendran VM, Binder HJ. Na(+)-dependent fluid absorption in intact perfused rat colonic crypts. *Gastroenterology* 2001; **120**: 144-150
100 **Greger R**, Bleich M, Leipziger J, Ecke D, Mall M, Kunzelmann K. Regulation of ion transport in colonic crypts. *News Physiol Sci* 1997; **12**: 62-66
101 **Feldman GM**. $HCO3^-$ secretion by rat distal colon: effects of inhibitors and extracellular Na^+. *Gastroenterology* 1994; **107**: 329-338
102 **Sterling D**, Reithmeier RA, Casey JR. A transport metabolon. Functional interaction of carbonic anhydrase II and chloride/bicarbonate exchangers. *J Biol Chem* 2001; **276**: 47886-47894
103 **Sterling D**, Alvarez BV, Casey JR. The extracellular component of a transport metabolon. Extracellular loop 4 of the human AE1 Cl^-/HCO_3^- exchanger binds carbonic anhydrase IV. *J Biol Chem* 2002; **277**: 25239-25246
104 **Li X**, Alvarez B, Casey JR, Reithmeier RA, Fliegel L. Carbonic anhydrase II binds to and enhances activity of the Na^+/H^+ exchanger. *J Biol Chem* 2002; **277**: 36085-36091
105 **Spring KR**. Routes and mechanism of fluid transport by epithelia. *Annu Rev Physiol* 1998; **60**: 105-119
106 **Hasegawa H**, Lian SC, Finkbeiner WE, Verkman AS. Extrarenal tissue distribution of CHIP28 water channels by in situ hybridization and antibody staining. *Am J Physiol* 1994; **266**: C893-C903
107 **Ishibashi K**, Sasaki S, Saito F, Ikeuchi T, Marumo F. Structure and chromosomal localization of a human water channel (AQP3) gene. *Genomics* 1995; **27**: 352-354
108 **Frigeri A**, Gropper MA, Turck CW, Verkman AS. Immunolocalization of the mercurial-insensitive water channel and glycerol intrinsic protein in epithelial cell plasma membranes. *Proc Natl Acad Sci USA* 1995; **92**: 4328-4331
109 **Koyama Y**, Yamamoto T, Kondo D, Funaki H, Yaoita E, Kawasaki K, Sato N, Hatakeyama K, Kihara I. Molecular cloning of a new aquaporin from rat pancreas and liver. *J Biol Chem* 1997; **272**: 30329-30333
110 **Nakhoul NL**, Davis BA, Romero MF, Boron WF. Effect of expressing the water channel aquaporin-1 on the CO^2 permeability of Xenopus oocytes. *Am J Physiol* 1998; **274**: C543-C548
111 **Ma T**, Verkman AS. Aquaporin water channels in gastrointestinal physiology. *J Physiol* 1999; **517**(Pt 2): 317-326
112 **Mori M**, Staniunas RJ, Barnard GF, Jessup JM, Steele GD, Chen LB. The significance of carbonic anhydrase expression in human colorectal cancer. *Gastroenterology* 1993; **105**: 820-826
113 **Saarnio J**, Parkkila S, Parkkila AK, Haukipuro K, Pastoreková S, Pastorek J, Kairaluoma MI, Karttunen TJ. Immunohistochemical study of colorectal tumors for expression of a novel transmembrane carbonic anhydrase, MN/CA IX, with potential value as a marker of cell proliferation. *Am J Pathol* 1998; **153**: 279-285
114 **Saarnio J**, Parkkila S, Parkkila AK, Pastoreková S, Haukipuro K, Pastorek J, Juvonen T, Karttunen TJ. Transmembrane carbonic anhydrase, MN/CA IX, is a potential biomarker for biliary tumours. *J Hepatol* 2001; **35**: 643-649
115 **Parkkila S**, Parkkila AK, Juvonen T, Lehto VP, Rajaniemi H. Immunohistochemical demonstration of the carbonic anhydrase isoenzymes I and II in pancreatic tumours. *Histochem J* 1995; **27**: 133-138
116 **Leppilampi M**, Saarnio J, Karttunen TJ, Kivelä J, Pastoreková S, Pastorek J, Waheed A, Sly WS, Parkkila S. Carbonic anhydrase isozymes IX and XII in gastric tumors. *World J Gastroenterol* 2003; **9**: 1398-1403
117 **Ivanov S**, Liao SY, Ivanova A, Danilkovitch-Miagkova A, Tarasova N, Weirich G, Merrill MJ, Proescholdt MA, Oldfield EH, Lee J, Závada J, Waheed A, Sly W, Lerman MI, Stanbridge EJ. Expression of hypoxia-inducible cell-surface transmembrane carbonic anhydrases in human cancer. *Am J Pathol* 2001; **158**: 905-919
118 **Kivelä AJ**, Saarnio J, Karttunen TJ, Kivelä J, Parkkila AK, Pastoreková S, Pastorek J, Waheed A, Sly WS, Parkkila TS, Rajaniemi H. Differential expression of cytoplasmic carbonic anhydrases, CA I and II, and membrane-associated isozymes, CA IX and XII, in normal mucosa of large intestine and in colorectal tumors. *Dig Dis Sci* 2001; **46**: 2179-2186
119 **van de Wetering M**, Sancho E, Verweij C, de Lau W, Oving I, Hurlstone A, van der Horn K, Batlle E, Coudreuse D, Haramis AP, Tjon-Pon-Fong M, Moerer P, van den Born M, Soete G, Pals S, Eilers M, Medema R, Clevers H. The beta-catenin/TCF-4 complex imposes a crypt progenitor phenotype on colorectal cancer cells. *Cell* 2002; **111**: 241-250
120 **Wykoff CC**, Beasley NJ, Watson PH, Turner KJ, Pastorek J, Sibtain A, Wilson GD, Turley H, Talks KL, Maxwell PH, Pugh CW, Ratcliffe PJ, Harris AL. Hypoxia-inducible expression of tumor-associated carbonic anhydrases. *Cancer Res* 2000; **60**: 7075-7083
121 **Wenger RH**, Gassmann M. Oxygen(es) and the hypoxia-inducible factor-1. *Biol Chem* 1997; **378**: 609-616
122 **Maxwell PH**, Wiesener MS, Chang GW, Clifford SC, Vaux EC, Cockman ME, Wykoff CC, Pugh CW, Maher ER, Ratcliffe PJ. The tumour suppressor protein VHL targets hypoxia-inducible factors for oxygen-dependent proteolysis. *Nature* 1999; **399**: 271-275
123 **Duan DR**, Pause A, Burgess WH, Aso T, Chen DY, Garrett KP, Conaway RC, Conaway JW, Linehan WM, Klausner RD. Inhibition of transcription elongation by the VHL tumor suppressor protein. *Science* 1995; **269**: 1402-1406
124 **Zbar B**, Kaelin W, Maher E, Richard S. Third International Meeting on von Hippel-Lindau disease. *Cancer Res* 1999; **59**: 2251-2253
125 **Griffiths JR**. Are cancer cells acidic? *Br J Cancer* 1991; **64**: 425-427
126 **Martinez-Zaguilan R**, Seftor EA, Seftor RE, Chu YW, Gillies RJ, Hendrix MJ. Acidic pH enhances the invasive behavior of human melanoma cells. *Clin Exp Metastasis* 1996; **14**: 176-186
127 **Parkkila S**, Rajaniemi H, Parkkila AK, Kivelä J, Waheed A, Pastoreková S, Pastorek J, Sly WS. Carbonic anhydrase inhibitor suppresses invasion of renal cancer cells *in vitro*. *Proc Natl Acad Sci USA* 2000; **97**: 2220-2224
128 **Supuran CT,** Briganti F, Tilli S, Chegwidden WR, Scozzafava A. Carbonic anhydrase inhibitors: sulfonamides as antitumor agents? *Bioorg Med Chem* 2001; **9**: 703-714
129 **Casini A**, Scozzafava A, Mastrolorenzo A, Supuran LT. Sulfonamides and sulfonylated derivatives as anticancer agents. *Curr Cancer Drug Targets* 2002; **2**: 55-75
130 **Teicher BA**, Liu SD, Liu JT, Holden SA, Herman TS. A carbonic anhydrase inhibitor as a potential modulator of cancer therapies. *Anticancer Res* 1993; **13**: 1549-1556

Edited by Wang XL **Proofread by** Xu FM

PO Box 2345, Beijing 100023, China
Fax: +86-10-85381893
E-mail: wjg@wjgnet.com www.wjgnet.com

ELSEVIER

World J Gastroenterol 2005;11(2):164-170
World Journal of Gastroenterology ISSN 1007-9327

Desensitization of T lymphocyte function by CXCR3 ligands in human hepatocellular carcinoma

Yu-Qing Liu, Ronnie T. Poon, Jeremy Hughes, Qin-Yu Li, Wan-Ching Yu, Sheung-Tat Fan

Yu-Qing Liu, Ronnie T. Poon, Qin-Yu Li, Wan-Ching Yu, Sheung-Tat Fan, Centre for the Study of Liver Disease and Department of Surgery, The University of Hong Kong, Pokfulam, Hong Kong, China
Jeremy Hughes, Phagocyte Laboratory, MRC Centre for Inflammation Research, University of Edinburgh, Edinburgh, United Kingdom
Supported by the Sun C. Y. Research Foundation for Hepatobiliary and Pancreatic Surgery of the University of Hong Kong
Correspondence to: Dr. Ronnie T. Poon, Department of Surgery, University of Hong Kong, Queen Mary Hospital, 102 Pokfulam Road, Hong Kong, China. poontp@hkucc.hku.hk
Telephone: +86-852-28553641 **Fax:** +86-852-28175475
Received: 2004-04-04 **Accepted:** 2004-06-17

Abstract

AIM: Despite the presence of lymphocyte infiltration, human hepatocellular carcinoma (HCC) is typically a rapidly progressive disease. The mechanism of regulation of lymphocyte migration is poorly understood. In this study, we investigated various factors regulating T cell migration in HCC patients. We examined serum CXC chemokine levels in HCC patients and demonstrated the production of CXC chemokines by HCC cell lines. We determined the effect of both HCC patient serum and tumor cell conditioned supernatant upon lymphocyte expression of chemokine receptor CXCR3 as well as lymphocyte migration. Lastly, we examined the chemotactic responses of lymphocytes derived from HCC patients.

METHODS: The serum chemokines IP-10 (CXCL10) and Mig (CXCL9) levels were measured by cytometric bead array (CBA) and the tumor tissue IP-10 concentration was measured by ELISA. The surface expression of CXCR3 on lymphocytes was determined by flow cytometry. The migratory function of lymphocytes to the corresponding chemokines was assessed using an *in vitro* chemotactic assay. Phosphorylation of extracellular signal-regulated kinase (ERK) was determined by Western blot analysis.

RESULTS: Increased levels of IP-10 and Mig were detected in HCC patient serum and culture supernatants of HCC cell lines. The IP-10 concentration in the tumor was significantly higher than that in the non-involved adjacent liver tissues. HCC cell lines secreted functional chemokines that induced a CXCR3-specific chemotactic response of lymphocytes. Furthermore, tumor-cell-derived chemokines induced initial rapid phosphorylation of lymphocyte ERK followed by later inhibition of ERK phosphorylation. The culture of normal lymphocytes with HCC cell line supernatants or medium containing serum from HCC patients resulted in a significant reduction in the proportion of lymphocytes exhibiting surface expression of CXCR3. The reduction in T cell expression of CXCR3 resulted in reduced migration toward the ligand IP-10, and both $CD4^+$ and $CD8^+$ T cells from HCC patients exhibited diminished chemotactic responses to IP-10 *in vitro* compared to T cells from healthy control subjects.

CONCLUSION: This study demonstrates functional desensitization of the chemokine receptor CXCR3 in lymphocytes from HCC patients by CXCR3 ligands secreted by tumor cells. This may cause lymphocyte dysfunction and subsequently impaired immune defense against the tumor.

Key words: Hepatocellular carcinoma; CXCR3 ligands

Liu YQ, Poon RT, Hughes J, Li QY, Yu WC, Fan ST. Desensitization of T lymphocyte function by CXCR3 ligands in human hepatocellular carcinoma. *World J Gastroenterol* 2005; 11(2): 164-170
http://www.wjgnet.com/1007-9327/11/164.asp

INTRODUCTION

Hepatocellular carcinoma (HCC) is one of the most common cancers in the world. The prognosis of patients with HCC is generally poor because the cancer is characterized by a rapid growth rate and vascular invasion[1]. T-lymphocyte-mediated cellular immunity plays an important role in host defense against tumors. Indeed, the presence of a heavy lymphocyte infiltration is associated with low recurrence and high survival rates in a variety of cancers including HCC[2-7] with most of the infiltrating lymphocytes in HCC being $CD8^+$ or $CD4^+$ T cells[6]. Activated $CD8^+$ T cells constitute an essential arm of the immune system for controlling tumor growth[8], and stimulated $CD4^+$ T cells are critical for successful tumor eradication[9-11]. However, marked lymphocyte infiltration was only observed in 10-20% cases of HCC, and the number of tumor-infiltrating lymphocytes (TIL) in HCC is generally lower than that evident in other cancers[6]. Although the mechanism underlying the regulation of lymphocyte traffic in patients with HCC is not well characterized, it is likely to involve a process of regulated adhesion and migration that requires tethering, triggering, integrin-mediated adhesion and chemotactic factors[12]. The most important molecules involved in triggering and directing lymphocyte migration are chemokines[13]. Lymphocyte migratory pathways are tightly regulated by chemokine receptor expression and exposure to chemokines. Lymphocytes could only be recruited if they express the corresponding chemokine receptors[13].

Chemokines are 8- to 12-kDa, heparin-binding cytokines distinguished by the specificity of their chemotactic properties for target cells[14]. They can be divided into four groups: CC, CXC, C and CX3C, based on the arrangement of conserved cysteine residues[15]. The importance of chemokines in regulating lymphocyte trafficking is suggested by the large number of chemokines in each of the four chemokine subfamilies that have been demonstrated to influence lymphocyte behaviors *in vitro*[16,17]. IP-10 and Mig, members of the CXC chemokine family, induce potent lymphocyte chemotaxis following interaction with their receptor, CXCR3[18,19], and play an important role in various inflammatory diseases[20-25]. CXCR3 exerts an important role in the recruitment of lymphocytes to both normal

and diseased tissues[26-29]. However, the role of CXCR3 in the regulation of lymphocyte traffic in HCC remains unclear.

In this study, we examined the serum levels of chemokines IP-10 and Mig in HCC patients together with IP-10 levels in tumor and adjacent nontumor tissues. We also examined chemokine production by HCC cell lines and evaluated the interaction between these chemokines and their receptor CXCR3 in T lymphocytes. The role of these chemokines and their corresponding receptor in regulating T cell function in HCC were addressed in this study.

MATERIALS AND METHODS

Patients and samples

Fresh whole blood and serum samples were obtained from 35 patients (31 men, 4 women; median age 54 years, range 36-84 years) with a diagnosis of HCC. Fresh tumor and peritumor liver specimens were obtained from 32 patients who underwent liver resection for HCC. Fresh whole blood and serum samples were also obtained from 12 healthy controls (10 men, 2 women; median age 46 years, range 27-58 years). None of the patients had received immunosuppressive drugs or chemotherapy. This study was approved by the Ethics Committee of our institution and informed consent was given by the patients.

Preparation of lymphocytes

Peripheral blood lymphocytes (PBLs) were isolated by Ficoll-Hypaque density gradient separation and washed twice in PBS. Mononuclear cells were suspended in RPMI-1640 medium and incubated at 37 ℃ for 90 min in a 6-well plate. Non-adherent lymphocytes were then collected for flow cytometric analysis, chemotaxis assays and Western blot analysis.

Cell lines

The HCC cell line Hep3B was obtained from the American Type Culture Collection (ATCC, Rockville, MD, USA) and HuH 7 was provided by Dr H. Nakabayashi (Hokkaido University School of Medicine, Hokkaido, Japan). Immortalized human hepatocyte MIHA was provided by Dr Roy Chowdhury (Albert Einstein College of Medicine, New York, USA). Hep3B and HuH 7 were cultured in DMEM medium containing penicillin/streptomycin and L-glutamine supplemented with 10% FCS. MIHA was cultured in Waymouth's MB 752/1 medium (Gibco/BRL) supplemented with 10% FCS, penicillin/streptomycin and L-glutamine. Culture supernatants were collected from 3-d-old tumor cell cultures for further experiments.

Cytometric bead array (CBA) for chemokines

The concentrations of IP-10 and Mig in serum and cell culture supernatants were measured using the human chemokine CBA kit I (BD PharMingen, San Diego, CA, USA). In brief, 20 μL of mixed chemokine IP-10 and Mig capture beads was mixed with 20 μL of serum or culture supernatants and 20 μL of PE detection reagent and incubated for 3 h at room temperature. The beads were then washed with wash buffer and analyzed by FACS caliber (Becton Dickinson, San Jose, CA, USA).

Measurement of tumor and non-tumor IP-10 protein concentration

IP-10 of both tumor and adjacent nontumor tissue cytosolic samples was measured by the Quantikine human IP-10 ELISA kit (R&D Systems, Minneapolis, MN, USA). Protein fraction was obtained by homogenization of tissues in lysis buffer (1% Nonidet, 0.5% sodium deoxycholate, 0.1% SDS, 1 mmol/L PMSF and protease inhibitor cocktail at 1 tablet per 50 mL extraction solution). Homogenates were centrifuged at 20 000 g at 4 ℃ for 10 min and the supernatants were collected for assay of IP-10 levels.

Flow cytometry analysis

The following antibodies were used in this study: APC-conjugated anti-CD4, PerCP-conjugated anti-CD8, phycoerythrin-conjugated anti-CXCR3 and IgG isotype control (BD PharMingen, San Diego, CA, USA). Lymphocytes were incubated with the antibodies for 30 min at 4 ℃, and two-color or three-color flow cytometry was performed on an FACS caliber analyzer (Becton Dickinson, San Jose, CA, USA).

Chemotaxis assay

Lymphocyte chemotaxis assay was performed using 5.0-μm pore size Transwell inserts (Corning Costar, Cambridge, MA, USA). Six hundred mL of tumor culture supernatant, chemokine IP-10 (100 ng/mL) (PeproTech, London, UK) or medium alone were added to the lower Transwell chamber. A total of 5×10^5 PBL in 100 μL were added to the upper Transwell chamber containing 50 mL/L CO_2 and incubated for 3 h at 37 ℃. In some experiments, PBLs were incubated with blocking anti-CXCR3 monoclonal antibodies or isotype control antibody (R&D Systems, Minneapolis, MN, USA) for 1 h at room temperature before they were added to the upper chamber of the Transwell. Migrated cells were collected from the lower chamber after the lowerside of the filter was carefully washed. Cells were washed in flow cytometry buffer and then incubated for 30 min at 4 ℃ with APC-conjugated anti-CD4 and PerCP-conjugated anti-CD8. Cells were then washed and analyzed by flow cytometry with counting of viable cells for 1 min. Chemotaxis was quantified by dividing the number of CD4 or CD8 positive cells migrating in the presence of chemokines by the number of cells migrating toward the medium alone.

Assessment of chemokine receptor expression on normal PBLs pretreated with tumor conditioned medium or medium supplemented by serum derived from HCC patients

Hep3B and HuH-7 were seeded in 24-well plates and incubated in DMEM medium containing L-glutamine supplemented with 10% FCS for 3 d. The culture supernatants were aspirated and centrifuged. Freshly isolated normal PBLs from eight healthy control subjects were incubated with the conditioned supernatant for 20 h with 3-d MIHA culture medium serving as control. To determine the effect of the cell supernatants on the expression of CXCR3 by PBLs, surface CXCR3 expression was measured by flow cytometry. For the effect of the serum from HCC patients on lymphocyte CXCR3 expression, normal PBLs were incubated with either medium with 10% serum from HCC patients or 10% serum from healthy control subjects for 24 h. Normal PBLs cultured in the full medium with 10% FCS served as medium control. Surface expression of CXCR3 was measured by flow cytometry.

Western blot analysis

Normal PBLs were incubated for 10 min or overnight with cell culture supernatants or IP-10 at 37 ℃. The cells were collected, washed twice with PBS, and then lysed in lysis buffer (Cell signaling, Beverly, MA, USA) for 15 min at 4 ℃. The lysates were centrifuged at 12 000 g for 15 min at 4 ℃ and equal amounts of solubilized proteins were separated by SDS-PAGE, and then transferred to nitrocellulose membranes (Amersham Biosciences, Piscataway, NJ, USA). The membranes were blocked with TBST (20 mmol/L Tris, pH 7.6, 135 mmol/L NaCl, 0.1% Tween 20) containing 5% non-fat milk and immunoblotted with anti-phosphorylated ERK (1:000) (Cell ignaling, Beverly, MA, USA) for 18 h at 4 ℃, followed by detection using HRP-conjugated secondary antibody (Santa Cruz Biotechnology, Santa Cruz, CA, USA) for 1 h at room temperature. Immunoreactive protein

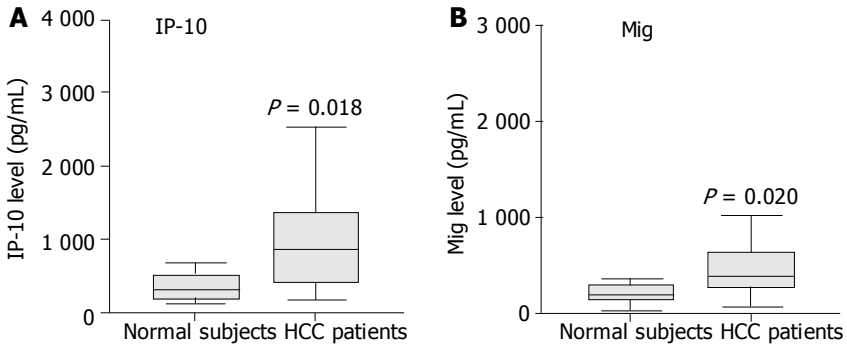

Figure 1 Assay of IP-10 and Mig in serum from 35 patients and 12 healthy controls by cytometric bead array analysis. Serum levels of IP-10 and Mig in patients with HCC were significantly higher than those of healthy controls. Data are presented as boxplots as medians and the 25th, 75th and 90th percentiles, $P<0.05$.

bands were visualized by the ECL system (Amersham Biosciences, Piscataway, NJ, USA).

Statistical analysis

Comparison of continuous variables between unpaired groups was performed using the Mann-Whitney U test. Wilcoxon's rank sum test was used for the analysis of difference between paired groups. Correlation between continuous variables was performed using the Spearmann's correlation coefficient (r). A P value less than 0.05 was defined as statistically significant. All statistical analyses were performed using the SPSS statistical software package (SPSS 10.0 for Windows, SPSS, Inc, Chicago, IL, USA).

RESULTS

Serum IP-10, Mig and tumor IP-10 levels in HCC patients

Serum IP-10 and Mig levels were significantly elevated in HCC patients compared with normal healthy subjects (Figure 1). In HCC patients, serum IP-10 level was significantly correlated with Mig level (correlation coefficient = 0.631, $P<0.0001$). Furthermore, analysis of tissue IP-10 levels indicated that tumor IP-10 level was significantly higher than that of the adjacent non-tumor tissues (Figure 2).

HCC tumor cell lines secreted functional chemokines

IP-10 and Mig were also detected in the supernatants of tumor cells Hep3B and HuH 7 whilst immortalized hepatocytes produced negligible levels, thereby providing further evidence that HCC tumor tissue might be a likely source of the elevated serum levels of chemokines in HCC patients (Figure 3). We tested the chemotactic effect of tumor cell supernatants upon normal PBLs. Both $CD4^+$ and $CD8^+$ T cells exhibited a significant chemotactic response to Hep3B supernatants but not to supernatants of the control liver cell line MIHA. This chemotactic response was demonstrated to be CXCR3 specific since pre-incubation of T cells with a function blocking anti-CXCR3 monoclonal antibody (mAb) significantly reduced both the $CD4^+$ and $CD8^+$ T cell chemotactic activity of the Hep3B supernatants compared to isotype control mAb (Figure 4).

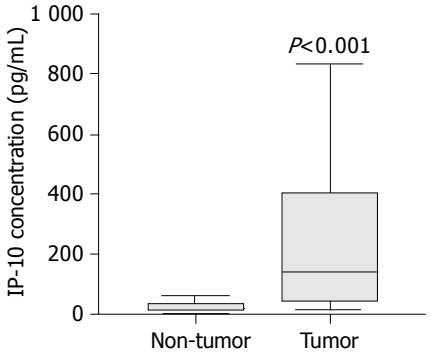

Figure 2 Boxplots show significant increase of tumor IP-10 level compared to that of non-tumor liver tissue. Data are presented as boxplots as medians and the 25th, 75th and 90th percentiles, $n = 32$, $P<0.001$.

We also studied the effect of tumor cell culture supernatants on the phosphorylation of ERK in normal PBLs. Stimulation of normal PBLs for 10 min with tumor cell supernatants but not immortalized liver cell supernatant induced the transient

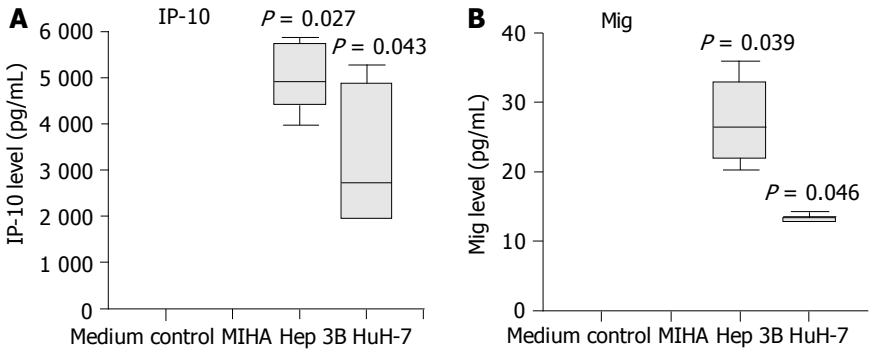

Figure 3 Secretion of IP-10 and Mig by HCC cell lines Hep3B and HuH-7, but not by control liver cell line MIHA. Three-day cell culture supernatants were collected and IP-10, Mig levels were quantified by cytometric bead array analysis. Significantly higher levels of IP-10 and Mig were detected in HCC cell line supernatants compared with those of control cell line MIHA. Data are presented as boxplots as medians and the 25th, 75th and 90th percentiles, $^aP<0.05$.

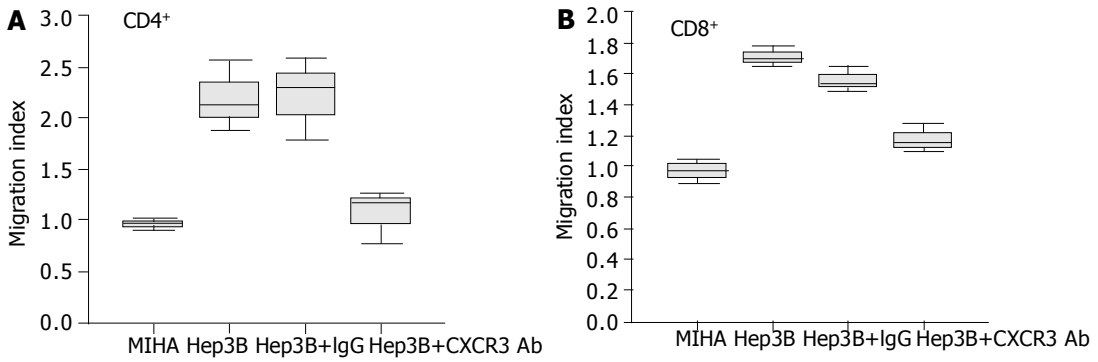

Figure 4 Secretion of chemotactic factors by Hep3B cells for lymphocytes from healthy subjects *in vitro*. The ability of culture supernatants from Hep3B cells to induce $CD4^+$ (A) and $CD8^+$ (B) T cell chemotaxis was tested by chemotactic experiments as described in Materials and Methods. To test the effect of blocking CXCR3 on the chemotactic response of lymphocytes to Hep3B culture supernatants, lymphocytes were pretreated with anti-CXCR3 monoclonal antibody or IgG control before the chemotaxis assay. Results are expressed as migration index, calculated as described in Materials and Methods.

phosphorylation of ERK. However, prolonged overnight stimulation of normal PBLs with tumor cell culture supernatants inhibited ERK phosphorylation. Cells stimulated with IP-10 at 100 nmol/L for 10 min or overnight were included as controls (Figure 5).

Proportion of CXCR3-expressing T lymphocytes was downregulated by tumor-conditioned medium and tumor patient serum

Following incubation with medium conditioned by the tumor cell lines Hep3B and HuH-7 for 20 h, the proportion of $CD4^+$ and $CD8^+$ T cells from normal healthy subjects that expressed the chemokine receptor CXCR3 was significantly reduced (Figures 6 A,B, $P<0.05$). However, such an effect was not observed following incubation with medium conditioned by the control cell line MIHA for 20 h (Figure 6). Furthermore, the proportion of $CD4^+$ and $CD8^+$ T cells from normal healthy subjects that expressed the chemokine receptor CXCR3 was significantly reduced following incubation with medium supplemented with 10% serum from HCC patients for 24 h (Figures 7 A,B, $P<0.05$). Such an effect was not observed following incubation with medium containing the serum of normal subjects for 24 h (Figure 7).

Migration of T lymphocytes toward chemokine IP-10 was reduced in HCC patients

To determine whether the reduced CXCR3 expression on lymphocytes was biologically significant, we examined the migration of T cells toward the corresponding chemokine ligands. As shown in Figure 8A, $CD4^+$ T cells from patients with HCC failed to display a significant migratory response to the CXCR3 ligand IP-10. In contrast, $CD4^+$ T cells from healthy controls exhibited a significant chemotactic response to IP-10 ($P<0.01$). Similar results were obtained when $CD8^+$ T cells derived from HCC cases were studied, but no significant migratory activity toward IP-10 was observed (Figure 8B). In contrast to HCC cases, $CD8^+$ T cells from normal controls displayed a significant chemotactic response to IP-10 (Figure 8B, $P<0.01$).

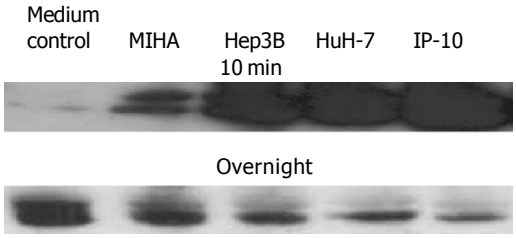

Figure 5 Early activation and later inhibition of ERK phosphorylation induced by tumor cell culture supernatants in lymphocytes from normal controls. A total of 5×10^6 freshly isolated lymphocytes were incubated with 500 μL of culture supernatants or IP-10 at 100 nmol/L in a 37 ℃ incubator for either 10 min or overnight. The cells were lysed and ERK phosphorylation was determined by Western blotting. The SDS-PAGE profile represents one experiment out of three.

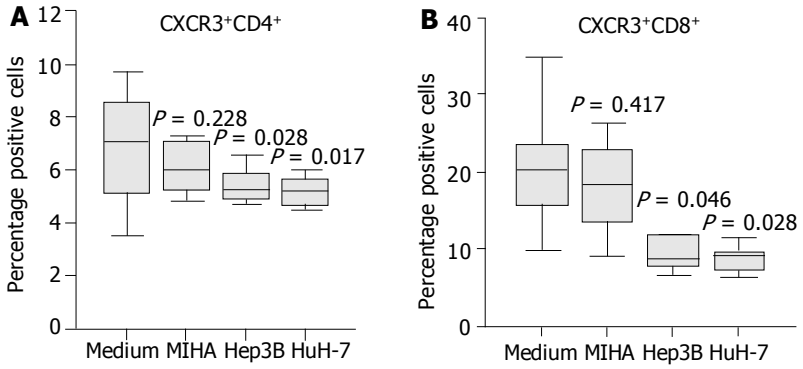

Figure 6 Expression of CXCR3 on normal $CD4^+$ or $CD8^+$ T cells incubated with unconditioned medium or medium conditioned with the tumor cell lines or a control cell line. Cell culture supernatants conditioned for 3 d by the HCC cell lines Hep3B, HuH-7 or the control cell line MIHA were collected. Freshly isolated normal PBLs were incubated in unconditioned or conditioned medium for 20 h and T cell expression of CXCR3 was assessed by flow cytometry. Diminished CXCR3 expression on $CD4^+$ T cells (A) and $CD8^+$ T cells (B) was observed following incubation in HCC cell line supernatants whilst the control cell line supernatant had no significant effect. Data represent the median and the 25th, 75th and 90th percentiles, $n = 8$, $^aP<0.05$ *vs* medium control.

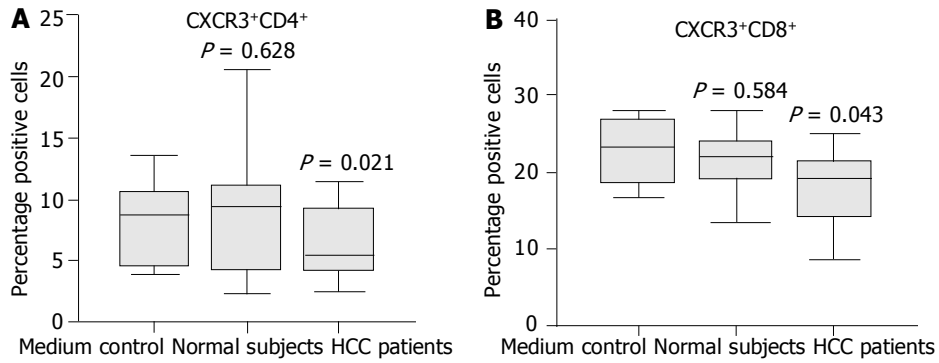

Figure 7 Expression of CXCR3 on normal $CD4^+$ or $CD8^+$ T cells incubated with medium supplemented with 10% serum from either HCC patients or normal subjects. Normal T cells cultured in the full medium with 10% FCS served as medium control. After 24 h, surface expression of CXCR3 on T cells was assessed by flow cytometry. Diminished CXCR3 expression on $CD4^+$ T cells (A) and $CD8^+$ T (B) cells was observed after incubation with HCC patient serum compared with normal serum. Data represent the median and the 25th, 75th and 90th percentiles, $n = 9$, $^aP<0.05$.

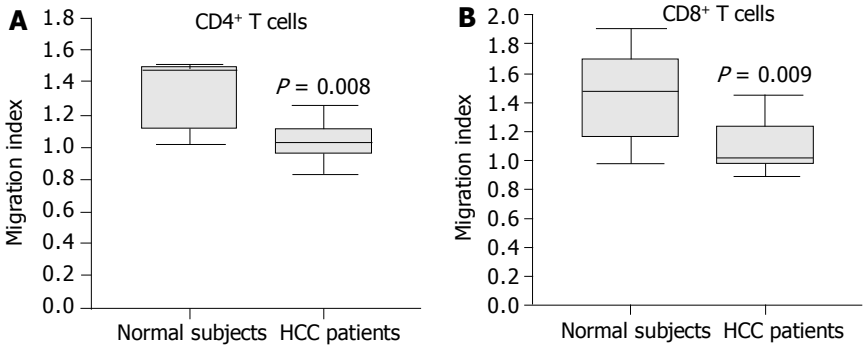

Figure 8 Chemotactic responsiveness of $CD4^+$ T cells and $CD8^+$T cells to IP-10. $CD4^+$ T cells and $CD8^+$T cells from HCC patients did not exhibit a significant chemotactic response toward IP-10 compared to $CD4^+$ T cells and $CD8^+$T cells from normal subjects. Results are expressed as migration index, calculated as described in Materials and Methods. Data are the median and the 25th, 75th and 90th percentiles, $n = 7$, $^aP<0.05$.

DISCUSSION

The low proportion of HCC exhibiting a significant lymphocyte infiltration compared with some other cancers is an intriguing phenomenon, and might well be related to the generally poor prognosis of HCC patients[6,7]. In this study, we attempted to elucidate the role of chemokines and chemokine receptors in the regulation of lymphocyte migration in HCC. We measured the serum levels of chemokines in HCC patients and compared them to normal control subjects. The serum levels of IP-10 and Mig were significantly elevated in HCC patients. Furthermore, serum IP-10 level was significantly positively correlated with serum Mig level in HCC cases. In addition, the IP-10 level in tumor tissues was significantly higher than that in noninvolved adjacent liver tissues. Lastly, analysis of cell culture supernatants indicated that HCC tumor cell lines secreted a significant amount of IP-10 and Mig that was functionally active in chemotactic assays.

The interaction between chemokines and chemokine receptors is a key determinant for the selectivity of local immunity. We therefore investigated whether tumor-cell-derived chemokines acted to direct lymphocyte movements. Our data indicated that the tumor cell line Hep3B secreted functional chemotactic factors for normal lymphocytes. Furthermore, function blocking monoclonal antibody to CXCR3 could partially inhibit lymphocyte chemotaxis, indicating the involvement of ligands to CXCR3. Treatment of lymphocytes with IP-10 resulted in rapid ERK phosphorylation, but the activation was transient and rapidly desensitized[30]. Interestingly, we found that exposure of normal lymphocytes to tumor cell culture supernatants resulted in rapid phosphorylation of tyrosine residues on ERK but inhibition of ERK activation after prolonged stimulation, an effect that may well be secondary to the presence of IP-10 in the tumor cell supernatant. It was previously documented that phosphorylation of ERK was linked to cell migration, adhesion, proliferation and survival[31,32]. Therefore, it is possible that sustained exposure of lymphocytes to IP-10 secreted by tumors might inhibit lymphocyte function. To investigate this hypothesis, we analyzed the chemokine receptor expression following incubation of normal PBLs with tumor cell conditioned medium. This treatment led to the reduction in the proportion of both $CD4^+$ and $CD8^+$ T cells with surface expression of CXCR3, thereby suggesting that HCC might secret factors that reduce chemokine receptor expression on PBLs. Previous work indicated that the chemokine receptor CXCR3 on PBLs could be modulated by internalization and desensitization following interaction with their chemokine ligands[33], and that chemokine receptors could be desensitized by either high levels of chemokines or prolonged exposure to chemokines[34]. We therefore speculated that the reduced surface expression of CXCR3 on normal PBLs after exposure to tumor-cell-conditioned medium might partially be due to the desensitization of lymphocytes by tumor-cell-derived chemokines. To further test this hypothesis, we also examined the effect of serum from either HCC patients or normal control subjects upon lymphocyte CXCR3 expression. Our data indicated that normal lymphocytes exhibited a reduced lymphocyte expression of CXCR3 after treatment with HCC patient serum compared to normal serum. These data resonate with the work by Kurt *et al*[35] who pointed out that T cells from naïve animals demonstrated a greater chemotactic response to tumor-derived chemokines

compared to T cells from tumor-bearing mice, suggesting the presence of chemokine receptor desensitization in the tumor bearing mice.

Undoubtedly, there is an inadequate induction of tumor immunity in HCC patients. Indeed, the function of peripheral blood dendritic cells was also decreased in this patient group[36]. We demonstrated that CXCR3 expression on PBLs from HCC patients was reduced compared to that of healthy control subjects[37]. Furthermore, we demonstrated that the reduced CXCR3 expression in HCC correlated with decreased migratory responses of $CD4^+$ and $CD8^+$ T cells toward chemokine IP-10. Chemokine receptor expression level is critically important in lymphocyte function[29], and our results therefore indicated that impaired migratory function of peripheral lymphocytes in HCC patients was due to decreased chemokine receptor expression. Despite the presence of lymphocyte recruitment likely mediated by CCR5, CCR6 and CXCR3[37], the levels of infiltrating lymphocytes might still be inadequate. Indeed, elevated levels of circulating CXCR3 ligands can act to induce peripheral desensitization of circulating T cells and this could limit further on-going lymphocyte recruitment. This may well underlie the somewhat paradoxical combination of chemokine production by HCC tumor tissue in the absence of marked lymphocytic infiltration of HCC.

In conclusion, this study demonstrated elevated serum levels of IP-10 and Mig in HCC patients as well as increased IP-10 concentration in tumor tissues compared to adjacent non-tumor tissues. These findings are associated with the reduced migratory function of peripheral blood T cells in HCC patients and our data suggest that this is likely to be a consequence of desensitization of the chemokine receptor CXCR3 by prolonged exposure to a high level of circulating CXCR3 ligands. T-cell based immunotherapy provides a great future potential for treatment of cancer including HCC[38]. The insufficient anti-tumor response in HCC patients may in part lie in the deficient expression of appropriate chemokine receptors by T cells. Chemokines are expressed by a range of tumors including HCC and may serve as suitable targets for directing specific T cells toward the tumor[39]. Chemokine receptors such as CCR5 play a critical role in T cell migration to cancer and subsequent induction of tumor regression[40]. However, the reduced expression of specific chemokine receptors on peripheral lymphocytes in HCC patients and the resultant loss of lymphocyte responsiveness to tumor-derived chemokines may partially 'blind' them to the presence of life threatening tumors. The clinical challenge is therefore to find novel approaches to augment the specific chemokine receptor expression of lymphocytes in HCC patients.

ACKNOWLEDGEMENTS

The authors thank Professor David Adams (Liver Research Laboratories, MRC Centre for Immune Regulation, The University of Birmingham) for his suggestion.

REFERENCES

1 **Tang ZY**. Hepatocellular carcinoma-cause, treatment and metastasis. *World J Gastroenterol* 2001; **7:** 445-454
2 **Watanabe H**, Enjoji M, Imai T. Gastric carcinoma with lymphoid stroma. Its morphologic characteristics and prognostic correlations. *Cancer* 1976; **38:** 232-243
3 **Svennevig JL**, Lunde OC, Holter J, Bjorgsvik D. Lymphoid infiltration and prognosis in colorectal carcinoma. *Br J Cancer* 1984; **49:** 375-377
4 **Shimokawara I**, Imamura M, Yamanaka N, Ishii Y, Kikuchi K. Identification of lymphocyte subpopulations in human breast cancer tissue and its significance: an immunoperoxidase study with anti-human T- and B-cell sera. *Cancer* 1982; **49:** 1456-1464
5 **Itoh K**, Platsoucas CD, Balch CM. Autologous tumor-specific cytotoxic T lymphocytes in the infiltrate of human metastatic melanomas. Activation by interleukin 2 and autologous tumor cells, and involvement of the T cell receptor. *J Exp Med* 1988; **168:** 1419-1441
6 **Wada Y**, Nakashima O, Kutami R, Yamamoto O, Kojiro M. Clinicopathological study on hepatocellular carcinoma with lymphocytic infiltration. *Hepatology* 1998; **27:** 407-414
7 **Ng IO**, Lai EC, Fan ST, Ng MM, So MK. Prognostic significance of pathologic features of hepatocellular carcinoma. A multivariate analysis of 278 patients. *Cancer* 1995; **76:** 2443-2448
8 **Shrikant P**, Mescher MF. Control of syngeneic tumor growth by activation of $CD8^+$ T cells: efficacy is limited by migration away from the site and induction of nonresponsiveness. *J Immunol* 1999; **162:** 2858-2866
9 **Hung K**, Hayashi R, Lafond-Walker A, Lowenstein C, Pardoll D, Levitsky H. The central role of CD4(+) T cells in the antitumor immune response. *J Exp Med* 1998; **188:** 2357-2368
10 **Overwijk WW**, Lee DS, Surman DR, Irvine KR, Touloukian CE, Chan CC, Carroll MW, Moss B, Rosenberg SA, Restifo NP. Vaccination with a recombinant vaccinia virus encoding a "self" antigen induces autoimmune vitiligo and tumor cell destruction in mice: requirement for CD4(+) T lymphocytes. *Proc Natl Acad Sci USA* 1999; **96:** 2982-2987
11 **Ossendorp F**, Toes RE, Offringa R, van der Burg SH, Melief CJ. Importance of CD4(+) T helper cell responses in tumor immunity. *Immunol Lett* 2000; **74:** 75-79
12 **Adams DH**, Shaw S. Leucocyte-endothelial interactions and regulation of leucocyte migration. *Lancet* 1994; **343:** 831-836
13 **Moser B**, Loetscher P. Lymphocyte traffic control by chemokines. *Nat Immunol* 2001; **2:** 123-128
14 **Baggiolini M**. Chemokines and leukocyte traffic. *Nature* 1998; **392:** 565-568
15 **Gale LM**, McColl SR. Chemokines: extracellular messengers for all occasions? *Bioessays* 1999; **21:** 17-28
16 **Hedrick JA**, Zlotnik A. Chemokines and lymphocyte biology *Curr Opin Immunol* 1996; **8:** 343-347
17 **Mackay CR**. Chemokine receptors and T cell chemotaxis. *J Exp Med* 1996; **184**: 799-802
18 **Liao F**, Rabin RL, Yannelli JR, Koniaris LG, Vanguri P, Farber JM. Human Mig chemokine: biochemical and functional characterization. *J Exp Med* 1995; **182:** 1301-1314
19 **Taub DD**, Longo DL, Murphy WJ. Human interferon-inducible protein-10 induces mononuclear cell infiltration in mice and promotes the migration of human T lymphocytes into the peripheral tissues and human peripheral blood lymphocytes-SCID mice. *Blood* 1996; **87:** 1423-1431
20 **Uguccioni M**, Gionchetti P, Robbiani DF, Rizzello F, Peruzzo S, Campieri M, Baggiolini M. Increased expression of IP-10, IL-8, MCP-1, and MCP-3 in ulcerative colitis. *Am J Pathol* 1999; **155:** 331-336
21 **Flier J**, Boorsma DM, van Beek PJ, Nieboer C, Stoof TJ, Willemze R, Tensen CP. Differential expression of CXCR3 targeting chemokines CXCL10, CXCL9, and CXCL11 in different types of skin inflammation. *J Pathol* 2001; **194:** 398-405
22 **Belperio JA**, Keane MP, Burdick MD, Lynch JP, Xue YY, Li K, Ross DJ, Strieter RM. Critical role for CXCR3 chemokine biology in the pathogenesis of bronchiolitis obliterans syndrome. *J Immunol* 2002; **169:** 1037-1049
23 **Narumi S**, Tominaga Y, Tamaru M, Shimai S, Okumura H, Nishioji K, Itoh Y, Okanoue T. Expression of IFN-inducible protein-10 in chronic hepatitis. *J Immunol* 1997; **158:** 5536-5544
24 **Nishioji K**, Okanoue T, Itoh Y, Narumi S, Sakamoto M, Nakamura H, Morita A, Kashima K. Increase of chemokine interferon-inducible protein-10 (IP-10) in the serum of patients with autoimmune liver diseases and increase of its mRNA expression in hepatocytes. *Clin Exp Immunol* 2001; **123:** 271-279
25 **Apolinario A**, Majano PL, Alvarez-Perez E, Saez A, Lozano C, Vargas J, Garcia-Monzon C. Increased expression of T cell chemokines and their receptors in chronic hepatitis C: relation-

ship with the histological activity of liver disease. *Am J Gastroenterol* 2002; **97:** 2861-2870

26 **Shields PL**, Morland CM, Salmon M, Qin S, Hubscher SG, Adams DH. Chemokine and chemokine receptor interactions provide a mechanism for selective T cell recruitment to specific liver compartments within hepatitis C-infected liver. *J Immunol* 1999; **163:** 6236-6243

27 **Haydon G**, Lalor PF, Hubscher SG, Adams DH. Lymphocyte recruitment to the liver in alcoholic liver disease. *Alcohol* 2002; **27:** 29-36

28 **Qin S**, Rottman JB, Myers P, Kassam N, Weinblatt M, Loetscher M, Koch AE, Moser B, Mackay CR. The chemokine receptors CXCR3 and CCR5 mark subsets of T cells associated with certain inflammatory reactions. *J Clin Invest* 1998; **101:** 746-754

29 **Kunkel EJ**, Boisvert J, Murphy K, Vierra MA, Genovese MC, Wardlaw AJ, Greenberg HB, Hodge MR, Wu L, Butcher EC, Campbell JJ. Expression of the chemokine receptors CCR4, CCR5, and CXCR3 by human tissue-infiltrating lymphocytes. *Am J Pathol* 2002; **160:** 347-355

30 **Tilton B**, Ho L, Oberlin E, Loetscher P, Baleux F, Clark-Lewis I, Thelen M. Signal transduction by CXC chemokine receptor 4. Stromal cell-derived factor 1 stimulates prolonged protein kinase B and extracellular signal-regulated kinase 2 activation in T lymphocytes. *J Exp Med* 2000; **192:** 313-324

31 **Stupack DG**, Cho SY, Klemke RL. Molecular signaling mechanisms of cell migration and invasion. *Immunol Res* 2000; **21:** 83-88

32 **Marshall CJ**. Specificity of receptor tyrosine kinase signaling: transient versus sustained extracellular signal-regulated kinase activation. *Cell* 1995; **80:** 179-185

33 **Sauty A**, Colvin RA, Wagner L, Rochat S, Spertini F, Luster AD. CXCR3 internalization following T cell-endothelial cell contact: preferential role of IFN-inducible T cell alpha chemoattractant (CXCL11). *J Immunol* 2001; **167:** 7084-7093

34 **Morris AJ**, Malbon CC. Physiological regulation of G protein-linked signaling. *Physiol Rev* 1999; **79:** 1373-1430

35 **Kurt RA**, Baher A, Wisner KP, Tackitt S, Urba WJ. Chemokine receptor desensitization in tumor-bearing mice. *Cell Immunol* 2001; **207:** 81-88

36 **Kakumu S**, Ito S, Ishikawa T, Mita Y, Tagaya T, Fukuzawa Y, Yoshioka K. Decreased function of peripheral blood dendritic cells in patients with hepatocellular carcinoma with hepatitis B and C virus infection. *J Gastroenterol Hepatol* 2000; **15:** 431-436

37 **Liu Y**, Poon RT, Feng X, Yu WC, Luk JM, Fan ST. Reduced expression of chemokine receptors on peripheral blood lymphocytes in patients with hepatocellular carcinoma. *Am J Gastroenterol* 2004; **99**: 1111-1121

38 **Jones RL**, Young LS, Adams DH. Immunotherapy in hepatocellular carcinoma. *Lancet* 2000; **356:** 784-785

39 **Kershaw MH**, Wang G, Westwood JA, Pachynski RK, Tiffany HL, Marincola FM, Wang E, Young HA, Murphy PM, Hwu P. Redirecting migration of T cells to chemokine secreted from tumors by genetic modification with CXCR2. *Hum Gene Ther* 2002; **13:** 1971-1980

40 **Uekusa Y**, Yu WG, Mukai T, Gao P, Yamaguchi N, Murai M, Matsushima K, Obika S, Imanishi T, Higashibata Y, Nomura S, Kitamura Y, Fujiwara H, Hamaoka T. A pivotal role for CC chemokine receptor 5 in T-cell migration to tumor sites induced by interleukin 12 treatment in tumor-bearing mice. *Cancer Res* 2002; **62:** 3751-3758

Edited by Wang XL **Proofread by** Zhu LH

PO Box 2345, Beijing 100023, China
Fax: +86-10-85381893
E-mail: wjg@wjgnet.com www.wjgnet.com

ELSEVIER

World J Gastroenterol 2005;11(2):171-175
World Journal of Gastroenterology ISSN 1007-9327

• LIVER CANCER •

Do the expressions of gap junction gene connexin messenger RNA in noncancerous liver remnants of patients with hepatocellular carcinoma correlate with postoperative recurrences?

I-Shyan Sheen, Kuo-Shyang Jeng, Shou-Chuan Shih, Chin-Roa Kao, Po-Chuan Wang, Chih-Zen Chen, Wen-Hsing Chang, Horng-Yuan Wang, Li-Rung Shyung

I-Shyan Sheen, Division of Hepatogastroenterology, Chang Gung Memorial Hospital, Taipei, Taiwan, China
Kuo-Shyang Jeng, Departments of Surgery, Mackay Memorial Hospital, Taipei, Taiwan, China
Shou-Chuan Shih, Chin-Roa Kao, Po-Chuan Wang, Chih-Zen Chen, Wen-Hsing Chang, Horng-Yuan Wang, Li-Rung Shyung, Departments of Internal Medicine, Mackay Memorial Hospital, Taipei, Taiwan, China
Kuo-Shyang Jeng, Mackay Medicine, Nursing and Management College, Taipei, Taiwan, China
Supported by the Grants From Department of Health, National Science Council, Executive Yuan, Taiwan (NSC-89-2314-B-195-027), China
Correspondence to: Kuo-Shyang Jeng, M.D., F.A.C.S, Department of Surgery, Mackay Memorial Hospital, No. 92, Sec 2, Chung-San North Road, Taipei, Taiwan, China. issheen.jks@msa.hinet.net
Telephone: +886-2-25433535 **Fax:** +886-2-27065704
Received: 2004-05-31 **Accepted:** 2004-07-05

Abstract

AIM: To investigate whether the changes of gap junction gene connexin messenger RNA in the noncancerous liver tissue of patients with hepatocellular carcinoma (HCC) could play a significant role in its postresection recurrence.

METHODS: Seventy-nine consecutive patients having undergone curative resection for HCC entered this study. Using a reverse-transcription polymerase chain reaction (RT-PCR)-based assay, connexin (Cx) 26, connexin (Cx) 32 and connexin (Cx) 43 mRNAs were determined prospectively in noncancerous liver tissues from these 79 patients and in the liver tissues from 15 controls. The correlations between connexin mRNA expression and the clinicopathological variables and outcomes (tumor recurrence and recurrence related mortality) were studied.

RESULTS: Compared with liver tissues of control patients, the expression of Cx 32 mRNA in noncancerous liver tissues was significantly lower (mean: 0.715 *vs* control 1.225, $P<0.01$), whereas the decreased Cx 26 mRNA (mean: 0.700 *vs* of control 1.205, $P>0.05$) and increased Cx 43 mRNA (mean: 0.241 *vs* control 0.100, $P>0.05$) had no statistical significance. We defined the value of Cx 32 mRNA or Cx 26 mRNA below 0.800 as a lower value. By multivariate analysis for noncancerous livers, a lower value of Cx 32 mRNA correlated significantly with a risk of HCC recurrence and recurrence-related mortality. The lower value of Cx 26 mRNA did not correlate with recurrence and mortality. The increased value of Cx43 mRNA also did not correlate with postoperative recurrence and recurrence-related mortality. By multivariate analysis, other significant predictors of HCC recurrence included vascular permeation, cellular dedifferentiation, and less encaps-ulation. The other significant parameter of recurrence related mortality was vascular permeation.

CONCLUSION: The decreased expression of Cx 32 mRNA in noncancerous liver tissues plays a significant role in the prediction of postoperative recurrence of HCC.

Key words: Hepatocellular carcinoma; Gap junctions; Connexins; Local neoplasm recurrences

Sheen IS, Jeng KS, Shih SC, Kao CR, Wang PC, Chen CZ, Chang WH, Wang HY, Shyung LR. Do the expressions of gap junction gene connexin messenger RNA in noncancerous liver remnants of patients with hepatocellular carcinoma correlate with postoperative recurrences? *World J Gastroenterol* 2005; 11(2): 171-175
http://www.wjgnet.com/1007-9327/11/171.asp

INTRODUCTION

Hepatocellular carcinoma (HCC) is one of the most common malignant tumors that carries a poor prognosis. Surgery remains the best potentially curative treatment for patients with HCC. The high recurrence rate after resection is one of the main factors that limits the long-term outcome of HCC. However, despite the recent advances in surgery, postoperative recurrence is still common[1-7]. How to predict the prognosis remains a challenging problem to surgeons.

Noncancerous liver tissues from some HCC patients may be at a preneoplastic stage, which may develop postresection recurrence. The association between the shift of γ-glutamyl transpeptidase and the recurrence of HCC has been reported[5].

Gap junctional intercellular communication (GJIC) is performed by intercellular hemichannels, which are formed by six basic protein subunits named connexin (Cx) expressed in neighboring cells[8,9]. GJIC mediated via gap junctions plays important roles in embryonic development, metabolic cooperation, growth control, cell proliferation, cell differentiation, tissue homeostasis, as well as carcinogenesis[10-23]. Uncontrolled tumor cell growth because of the loss of GJIC due to the down-regulated expression of Cx genes appears to be an important event in cell transformation. Transformed cells *in vitro* and *in vivo* having a decreased GJIC capacity among themselves or with surrounding normal cells have been reported[10-13,17].

Connexin 32 (Cx32) and connexin 26 (Cx26) are the major gap junction forming proteins in hepatocytes. Moreover, another gap junction protein, connexin 43 (Cx43) (or α1) is prominent in the liver capsule, and between other liver cell types, including Ito (fat-storing) cells, cholangiocytes, and endothelial cells lining the venules. Some authors reported that Cx32 and Cx26 mRNA and their proteins were significantly decreased in HCC tissues and cell lines whereas expression of Cx43 protein was increased in hepatoma cell line SMMC-7721[8,19,20,24].

To the best of our knowledge, little is known about the prognostic correlation between the changes of connexin mRNA

expression in noncancerous liver tissues and postresection recurrence of HCC. We chose measuring connexin mRNA instead of measuring connexin protein because RT-PCR is thought to provide a more objective quantitification method than immunohistochemistry. We conducted this prospective study to investigate the correlation between connexin mRNA (Cx32, 26, 43 mRNA) expression in noncancerous liver tissues from HCC patients and the development of postoperative recurrence.

MATERIALS AND METHODS

Study population

Seventy-nine patients with HCC who underwent curative hepatectomy at the Department of Surgery, Mackay Memorial Hospital, between January 1997 and December 1998, whose tissue specimens were histopathologically found to have no degeneration or necrosis, were enrolled in this study. The mean age of patients was 56.4±12.6 years (range 16-82 years) with a male to female ratio of 52:27. Clinical details were available from medical records on all patients (Table 1). Surgeries included 73 major resections (38 partial lobectomies,28 lobectomies and 7 extended lobectmies) and 6 minor resections (4 segmentectomies and 2 subsegmentectomy).

Table 1 Characteristics of 79 patients with HCC undergoing curative resection

Variables	No. of patients (%)
Age (mean, yr)	56.4±12.6
Male	52 (65.8)
Cirrhosis	57 (72.2)
Child-Pugh's class A	55 (70.0)
Serum AFP <20 ng/mL	30 (38.0)
20-10^3 ng/mL	29 (36.7)
>10^3 ng/mL	20 (25.3)
HBsAg (+)	60 (57.8)
Anti-HCV (+)	41 (51.9)
Size of HCC <3 cm	24 (30.4)
3-10 cm	25 (31.6)
>10 cm	30 (38.0)
Edmondson-Steiner's grade I	4 (5.1)
grade II	30 (38.0)
grade III	42 (53.2)
grade IV	3 (3.8)
Complete capsule	61 (77.3)
Vascular permeation	56 (70.9)
Daughter nodules	44 (55.7)
Tumor necrosis	55 (70.0)
Tumor hemorrhage	24 (30.4)

AFP: serum alpha fetoprotein; HBsAg (+): positive hepatitis B surface antigen; Anti-HCV (+): positive hepatitis C virus antibody; Edmondson Steiner grade: differentiation grade.

Both cancerous and noncancerous liver tissues were studied for connexin. A control group including 5 healthy volunteers, 5 individuals with chronic active hepatitis without HCC and 5 individuals with liver cirrhosis without HCC also received liver biopsies for connexin mRNA study during exploratory laparotomy for other reasons. The surgically removed fresh liver samples were immediately transferred to the pathology laboratory, dissected, frozen in liquid nitrogen, and stored at -80 ℃ until RNA extraction. The dissected tumor and surrounding tissues were also studied by pathological examination. No obvious ischemic changes were observed in surrounding liver tissues, suggesting that duration between removal and freezing of samples did not cause problematic artifacts.

Clinicopathological parameters analyzed included sex (male *vs* female), age, presence of liver cirrhosis, hepatitis B virus (HBV) infection (hepatitis B surface antigen), hepatitis C virus (HCV) infection (anti-hepatitis C virus antibody), serum AFP level (<20 ng/mL *vs* 20 to 1 000 ng/mL *vs* >1 000 ng/ mL), cirrhosis, Child-Pugh class of liver functional reserve (A *vs* B), tumor size (<3 cm *vs* 3 to 10 cm *vs* >10 cm), tumor encapsulation (complete *vs* incomplete or absent), presence of daughter nodules, vascular permeation (including vascular invasion and/or tumor thrombi in either the portal or hepatic vein), and cell differentiation grade (Edmondson and Steiner grades I to IV).

After discharge, the patients were assessed regularly to detect HCC recurrence with abdominal ultrasonography (every 2-3 mo during the first 5 years, then every 4-6 mo thereafter), serum alpha fetoprotein (AFP) and liver biochemistry (every 2 mo during the first 2 years, then every 4 mo during the following 3 years, and every 6 mo thereafter), abdominal computed tomography (CT) (every 6 mo during the first 5 years, then annually), and chest X-ray and bone scans (every 6 mo). Hepatic arteriography was obtained if other studies suggested possible cancer recurrence. Detection of tumors on any imaging study was defined as recurrence.

Extraction of RNA

We homogenized resected tissues completely in 1 mL of RNA-bee™ (Tel-Test, Protech Technology Enterprises Co., Ltd, Friendswood, TX, USA), added 0.2 mL chloroform, and shook vigorously for 15 to 30 s. We stored the samples on ice for 5 min and then centrifuged them at 12 000 *g* for 15 min. We transferred the supernatant to a new 1.5 mL Eppendorf tube and precipitated the solution with 0.5 mL of isopropanol for 5 min at 4 ℃.We centrifuged the tube at 12 000 *g* for 5 min at 4 ℃ before removing the supernatant and washing the RNA pellet with 1 mL of isopropanol, shaking to dislodge the pellet from the side of the tube. We centrifuged the pellet again at 12 000 *g* for 5 min at 4 ℃, removed the supernatant, and washed the RNA pellet once with 75% ethanol, shaking to dislodge the pellet from the side of the tube. We suspended the pellet in at least 1 mL of 75% ethanol and centrifuged it at 7 500 *g* for 5 min at 4 ℃ before carefully removing the ethanol. The RNA was allowed to air dry and then dissolved in DEPC-H_2O (50 to 100 uL) and stored at -80 ℃.

Reverse transcription

We heated the RNA sample at 55 ℃ for 10 min, chilled it on ice, and then added the following reagents: 4 μL 5× RT buffer containing Tris-HCl (pH 8.3), 75 mmol/L KCl, 3 mmol/L $MgCl_2$, and 10 mmol/L DTT (dithiothreitol); 3 μL 10 mmol/L dNTP (deoxyribonucleoside triphosphate); 1.6 μL Oligo-d $(T)_{18}$ and 0.4 μL random hexamers (N) 6 (1 ug/uL); 0.5 μL RNase inhibitor (40 units/μL); 3 μL 25 mmol/L $MnCl_2$; 6 μL RNA in DEPC-H_2O; and 0.5 μL DEPC-H_2O. We incubated the mixture at 70 ℃ for 2 min and then chilled it to 23 ℃ to anneal the primer to the RNA. We added 1 μL of Moloney murine leukemia virus reverse transcriptase (M-MLV RTase), 200 units/μL, (Promega) and incubated it for 10 min at 23 ℃ followed by 60 min at 40 ℃. We then heated it at 94 ℃ for 5 min, chilled it on ice, and stored the cDNA at -20 ℃.

Amplification of connexins26, 32, 43, and GAPDH cDNA by PCR

First-strand cDNA synthesis was carried out using 2 μg of total RNA purified from 50-mg tissue. Reverse transcription was performed in a 20-μL final volume containing 2 μg of random hexamer (Gene Teks Bioscience Inc., Taipei), and 1.5 mmol/L each of dATP, dCTP, dGTP, and dTTP. Each reaction mixture was incubated for 8 min at 23 ℃ with 20 U of rRNasin (RNase

inhibitor; Promega, Madison, WI) followed by incubation with 200 U of Moloney murine leukemia virus reverse transcriptase (Gibco-BRL, Paisley, UK) for 60 min at 40 ℃ followed by 5 min at 94 ℃. PCR was performed in a final volume of 50 μL, by using 2 μL of cDNA solution in a mixture containing 0.4 mmol/L deoxynucleotide triphosphates, 40 pmoL of both sense and antisense oligonucleotide primers according to Cx 32, Cx 26 and Cx 43 to be detected, 2.5 mmol/L $MgCl_2$, 2.5 U of Taq DNA polymerase (Promega) and 5 μL of 10X Taq DNA polymerase reaction buffer (500 mmol/L KCl, 100 mmol/L Tris-HCl [pH9.0], 1% Triton-X-100). PCR primer sequences of the sense and antisense oligonucleotides for Cx 32, Cx 26 and Cx 43 as well as the direction, size and reaction conditions are shown in Table 2. For example, Cx 32 sense oligonucleotide (5'-CTGCTCTACCCG GGCTATGC-3') and its anti-sense sequence (5'-CAGGCTGAG CATCGGTCGCTCTT-3') were synthesized (by Sigma-Genosys Ltd, Woodlands, TX, USA). GAPDH was used as a control, with the quantities of the other mRNA products reported as a fraction of their intensity compared to GAPDH mRNA. To eliminate any possibility of genomic DNA contamination, PCR amplification reaction was carried out on each sample of the RNA extraction. As another internal contamination control, PCR amplification was also carried out on a sample of reaction mixture in the absence of cDNA.

Table 2 Nucleotide sequences of the primer sets and specific oligonucleotide probes to each type of connexin 5'-noncoding mRNA

Type of connexin mRNA	Primers Probes	Nucleotide sequences
Cx32	Sense	5 CTGCTCTACCCGGGCTATGC
	Antisense	5 CAGGCTGAGCATCGGTCGCTCTT
Cx26	Sense	5 CCGAAGTTCATGAAGGGAGAGAT
	Antisense	5 GGTCTTTTGGACTTCCCTGAGCA
Cx43	Sense	5 TACCATGCGACCAGTGGTGCGCT
	Antisense	5 GAATTCTGGTTATCATCGTCGGGGAA

The intensity of bands was measured using Fujifilm Science Lab 98 (Image Gauge V3.12). The sensitivity of our assay was assessed using human hepatocytes. A HepG2 (hepatoblastoma) cell line served as a positive control for connexin mRNA expression. For negative controls, we used EDTA-treated water (filtered and vaporized).

Statistical analysis

A statistical software (SPSS for Windows, version 8.0, Chicago, IL) was employed, Student's *t*-test was used to analyze continuous variables and a chi-square test or Fisher's exact test for categorical variables. A Cox proportional hazard model was used for multivariate stepwise analysis to identify significant factors for predicting recurrence and mortality. *P* value <0.05 was considered statistically significant.

RESULTS

RT-PCR analysis of connexin transcript in liver and HCC tissues

Compared with the mean values of mRNAs of Cx 32, 26 and 43 in livers obtained from 15 controls (1.225, 1.205, 0.100, respectively), the values of Cx 32 mRNA of noncancerous liver tissues from HCC patients (mean: 0.715) were significantly lower ($P<0.01$), whereas lower Cx 26 mRNA (mean: 0.700) and higher Cx 43 mRNA (mean: 0.241) were not found ($P>0.05$).

Correlation between clinical and histopathological features and different connexin mRNA expressions in liver remnants

We defined the value of Cx 32 mRNA or Cx 26 mRNA below 0.800 as a lower value. According to the value of Cx 32 mRNA, we categorized the 79 study patients into group A (lower than 0.800) and group B (higher than 0.800). When the clinicopathological characteristics of primary HCC were compared between the two groups, the difference was statistically significant in poor cellular differentiation ($P = 0.0203$), less encapsulation ($P = 0.0088$), and vascular permeation ($P = 0.0107$) respectively by univariate analysis. The presence of daughter nodules achieved a borderline significance ($P = 0.0527$, Table 3).

Whereas, no significant difference was noted between the two groups in age, gender, tumor size, coexisting cirrhosis, Child-Pugh's class, chronic HBV or HCV carriage, serum AFP level, tumor necrosis, or tumor hemorrhage ($P>0.05$, Table 3).

Table 3 Comparison of characteristics of primary HCC between different levels of connexin 32 mRNA in noncancerous liver tissues

Characteristics	Group A (n = 64,%)	Group B (n = 15,%)	*P*
Age (mean, yr)	52.3	48.8	NS
Male	65.6	66.7	NS
Liver cirrhosis	68.8	73.3	NS
Child- Pugh's class A	76.6	53.3	NS
Tumor size <3 cm	35.9	40.0	
>10 cm	34.4	13.3	NS
HBsAg (+)	53.1	46.6	NS
Anti-HCV (+)	78.1	66.7	NS
Serum AFP <20 ng/mL	21.9	40.0	
>1 000 ng/mL	37.5	40.0	NS
Tumor necrosis	76.6	53.3	NS
Tumor hemorrhage	35.9	40.0	NS
Edmondson-Steiner grade I[a]	1.6	20	0.0203
Capsule incomplete or absent[b]	78.1	40	0.0088
Daughter nodules	60.9	33.3	0.0527
Vascular permeation[c]	76.6	40	0.0107

Low Cx 32 mRNA: <0.800 (group A), high Cx 32 mRNA: ⩾0.800 (group B). *P*: The *P* value of univariate analysis. a, b, and c: the significant variables in multivariate analysis with *P* values of 0.0120, 0.0420 and 0.019 respectively. AFP: alpha-fetoprotein, NS: no statistical significance.

Correlation of connexin mRNA expression and tumor recurrence and recurrence related death

Fifty-five patients (69.6%) had clinically detectable recurrence during the follow-up period (median 58 mo; range 38 to 72 mo), of whom 26 died. A lower Cx 32 mRNA in liver remnant correlated significantly with tumor recurrence both univariately ($P = 0.0107$) (Table 4) and multivariately ($P = 0.0203$) (Table 5). The lower level of Cx 32 mRNA in noncancerous liver tissues significantly correlated with death from recurrence both univariately ($P = 0.0002$) (Table 4) and multivariately ($P = 0.0333$) (Table 5). However, the differences of the recurrence-free interval and the duration of survival between group A and group B did achieve borderline significance ($P = 0.0595$, $P = 0.0620$), respectively (Table 4). The lower Cx 26 mRNA and the increased Cx 43 mRNA had no significant correlation either with recurrence ($P = 0.0880$, $P = 0.0710$, respectively) or mortality ($P = 0.1240$, $P = 0.0866$, respectively) (Table 5).

Table 4 Comparison of recurrence, death, recurrence, free interval and survival between different levels of Cx 32 mRNA in noncancerous liver tissues

Outcome	Group A (n = 64)	Group B (n = 15)	P
Recurrence (number) (%)	49 (76.6)	6 (40.0)	0.0107
Death[1] (number) (%)[2]	25 (39.0)	1 (6.7)	0.0002
Recurrence free interval (median, mo)	8.5	43.0	0.0595
Duration of survival (median, mo)	11.5	41.5	0.0620

Note: Low Cx 32 mRNA: <0.800 (group A), high Cx 32 mRNA: ≥0.800 (group B), Death[1] : patients died of HCC recurrence. 2: percent of recurrence patients.

By multivariate analysis, other significant predictors of recurrence included vascular permeation (P = 0.0002), poor cellular differentiation (P = 0.0203), and less encapsulation (P = 0.0160) (Table 5). Whereas, by multivariate analysis, only vascular permeation significantly correlated with mortality (P<0.0001) (Table 5).

Table 5 Factors influencing tumor recurrence and death of patients in multivariate analysis

Variables	P	OR
Recurrence		
Vascular permeation	0.0002	5.36
Cellular dedifferentiation	0.0203	4.18
Incomplete or absent capsule	0.0160	3.10
Lower Cx 32 mRNA in liver remnant	0.0203	4.18
Lower Cx 26 mRNA in liver remnant	0.0880	2.29
Higher Cx 43 mRNA in liver remnant	0.0710	2.38
Death		
Vascular permeation	<0.0001	8.35
Lower Cx 32 mRNA in liver remnant	0.0333	3.80
Lower Cx 26 mRNA in liver remnant	0.1240	2.10
Higher Cx 43 mRNA in liver remnant	0.0866	2.40

OR: odds ratio; Lower Cx 32 mRNA: value <0.800.

DISCUSSION

Our study showed that compared with control group liver tissues, a lower value of Cx 32 mRNA in the noncancerous liver remnant tissues was significantly associated with an increased risk of postoperative recurrence and disease mortality. The lower value of Cx 26 mRNA and the increased value of Cx 43 mRNA were not significantly predictive of outcomes. The reasons remain unknown.

To explain this discrepancy, we propose the following five possible reasons.

The first is that among the three connexins, Cx 32 gene may be more predominant in tumor suppression. Some studies suggested that Cx32 and Cx26 genes, the specific genes expressing in normal liver tissues, be the potential unmutated tumor suppressor genes though some authors have suggested Cx32 and Cx43 genes[24-26]. When the liver remnants in some patients develop a preneoplastic transformation, a reduction between either homologous or heterologous GJIC, which has been demonstrated in many tumors, may contribute to neoplastic progression by allowing tumor cells to escape from intercellular signals involving regulations of proliferation, differentiation and apoptosis[10-26]. Ma *et al*[12] found that HCC cells often expressed less connexin, but the mechanisms are unknown. Eghbali *et al*[25] found that transfection of tumor cells with connexin 32 cDNA could retard tumor growth *in vivo*. Oyamada *et al*[19] suggested that the molecular mechanism might be different from those in rat hepatocarcinogenesis. However, in rat multistage hepatocarcinogenesis studies, several authors found that a significant decrease in connexin 32 expression at the mRNA or protein level occurred in preneoplastic nodules and HCCs induced by chemicals[24,27].

The second is that though both Cx 32 and Cx 26 are the main connexins in hepatocytes, they have differences. According to Plante *et al*[28] Cx 32 is about 10 times more abundant than Cx 26 in the liver, the importance of both connexins in promoter-induced tumors may therefore be different. Animal experiments found that Cx32 was involved in tumor promotion by chemicals[29].

The third is that the detailed mechanisms of the discrepancy of their decrease in HCC recurrence is unknown. We attribute it to that the pathways for Cx 32 and Cx 26 in liver may be different. There was a dramatic increase in the presence of Golgi in the case of Cx 32[30]. Sixty percent of Cx 26 present in the gap junction plaques support the possible existence of an alternative trafficking pathway for Cx 26 in liver. The alternative pathway proposed may not contain conventional signal peptide sequences and does not require endoplasmic reticulum (ER)/Golgi postranstational modification. Connexins lack a signal peptide sequence and Cx 26 is not phosphorylated.

The fourth is that Cx 32 may be more important in the shift of host-cancer cell coupling, which may be important in developing recurrence. Krutovskikh V highlighted that the direct intercellular host-tumor interactions may play a role in natural host resistance against neoplastic growth, and emphasized on the underlying connexin function impairment[31]. Among the 3 connexins, the change of Cx 32 may be earlier and more evident.

The fifth is that some authors have previously found that after partial hepatectomy, there was a reciprocal correlation between the expression of connexin and the mitotic activity of hepatocytes during liver regeneration[32]. The significant reduction of Cx32 expression in S-phase cells may play an important role in the control of proliferation in liver. More Cx 32 in the liver[28] may contribute to this significant reduction. Timmen *et al*[20] found that the partial loss of gap junctions provided a selective advantage for the preneoplastic liver cells to rapidly proliferate into carcinoma cells.

In our study, the decreased connexin 32 mRNA in liver remnants significantly correlated with some tumor invasiveness variables[33,34], including the grade of cellular differentiation, less encapsulation, and vascular permeation, which correlate with recurrence. The more invasive the HCC is, the earlier the recurrence in the remnant liver may develop.

Three characteristics during cellular differentiation have been emphasized, namely the rate of cell division, the adhesive properties of cell membranes that influence cells to migrate or metastasize, and specific patterns of cellular metabolism[35]. Among them, connexin may be important in the adhesive properties. An altered pattern of adhesion molecules on the surface of tumorigenic hepatocyte may influence the distribution of gap junctions in preneoplastic tissues.

Among patients with recurrence, 10.9% (6 among 55) patients had no decrease in Cx 32 mRNA. Not all patients revealed connexin mutations, suggesting that there may be both connexin-dependent and connexin-independent pathways leading to liver cancer. The identification of contributing genetic alterations related to connexin changes remains a considerable challenge in the field of liver cancer research.

In conclusion, decreased expression of Cx 32 mRNA in noncancerous liver tissues plays a significant role in the prediction of postoperative recurrence of HCC. Such patients may be the candidates for neoadjuvant therapy after surgery.

REFERENCES

1 **Yamamoto J,** Kosuge T, Takayama T, Shimada K, Yamasaki S, Ozaki H, Yamaguchi N, Makuuchi M. Recurrence of hepatocellular carcinoma after surgery. *Br J Surg* 1996; **83**: 1219-1222
2 **Lee PH,** Lin WJ, Tsang YM, Hu RH, Sheu JC, Lai MY, Hsu HC, May W, Lee CS. Clinical management of recurrent hepatocellular carcinoma. *Ann Surg* 1995; **222**: 670-676
3 **Poon RT,** Fan ST, Lo CM, Liu CL, Wong J. Intrahepatic recurrence after curative resection of hepatocellular carcinoma: long-term results of treatment and prognostic factors. *Ann Surg* 1999; **229**: 216-222
4 **Jeng KS,** Sheen IS, Chen BF, Wu JY. Is the p53 gene mutation of prognostic value in hepatocellular carcinoma after resection? *Arch Surg* 2000; **135**: 1329-1333
5 **Jeng KS,** Sheen IS, Tsai YC. Gamma glutamyl transpeptidase messenger RNA may serve as a diagnostic aid in hepatocellular carcinoma. *Br J Surg* 2001; **88**: 986-987
6 **Jeng KS,** Chen BF, Lin HJ. En bloc resection for extensive hepatocellular carcinoma: is it advisable? *World J Surg* 1994; **18**: 834-839
7 **Jeng KS,** Yang FS, Chiang HJ, Ohta I. Repeat operation for nodular recurrent hepatocellular carcinoma within the cirrhotic liver remnant: a comparison with transcatheter arterial chemoembolization. *World J Surg* 1992;16:1188-1191; discussion 1192
8 **Krutovskikh V,** Mazzoleni G, Mironov N, Omori Y, Aguelon AM, Mesnil M, Berger F, Partensky C, Yamasaki H. Altered homologous and heterologous gap-junctional intercellular communication in primary human liver tumors associated with aberrant protein localization but not gene mutation of connexin 32. *Int J Cancer* 1994; **56**: 87-94
9 **Bennett MV,** Barrio LC, Bargiello TA, Spray DC, Hertzberg E, Saez JC. Gap junctions: new tools, new answers, new questions. *Neuron* 1991; **6**: 305-320
10 **Rose B,** Mehta PP, Loewenstein WR. Gap-junction protein gene suppresses tumorigenicity. *Carcinogenesis* 1993; **14**: 1073-1075
11 **Iwai M,** Harada Y, Muramatsu A, Tanaka S, Mori T, Okanoue T, Katoh F, Ohkusa T, Kashima K. Development of gap junctional channels and intercellular communication in rat liver during ontogenesis. *J Hepatol* 2000; **32**: 11-18
12 **Ma XD,** Ma X, Sui YF, Wang WL. Expression of gap junction genes connexin32 and connexin43 mRNAs and proteins, and their role in hepatocarcinogenesis. *World J Gastroenterol* 2002; **8**: 64-68
13 **Niessen H,** Willecke K. Strongly decreased gap junctional permeability to inositol 1, 4, 5-trisphosphate in connexin32 deficient hepatocytes. *FEBS Lett* 2000; **466**: 112-114
14 **Robenek H,** Rassat J, Themann H. A quantitative freeze-fracture analysis of gap and tight junctions in the normal and cholestatic human liver. *Virchows Arch B Cell Pathol Incl Mol Pathol* 1981; **38**: 39-56
15 **Wilson MR,** Close TW, Trosko JE. Cell population dynamics (apoptosis, mitosis, and cell-cell communication) during disruption of homeostasis. *Exp Cell Res* 2000; **254**: 257-268
16 **Yamaoka K,** Nouchi T, Kohashi T, Marumo F, Sato C. Expression of gap junction protein connexin 32 in chronic liver diseases. *Liver* 2000; **20**: 104-107
17 **Loewenstein WR,** Kanno Y. Intercellular communication and the control of tissue growth: lack of communication between cancer cells. *Nature* 1966; **209**: 1248-1249
18 **Shimoyama Y,** Hirohashi S. Cadherin intercellular adhesion molecule in hepatocellular carcinomas: loss of E-cadherin expression in an undifferentiated carcinoma. *Cancer Lett* 1991; **57**: 131-135
19 **Oyamada M,** Krutovskikh VA, Mesnil M, Partensky C, Berger F, Yamasaki H. Aberrant expression of gap junction gene in primary human hepatocellular carcinomas: increased expression of cardiac-type gap junction gene connexin 43. *Mol Carcinog* 1990; **3**: 273-278
20 **Janssen-Timmen U,** Traub O, Dermietzel R, Rabes HM, Willecke K. Reduced number of gap junctions in rat hepatocarcinomas detected by monoclonal antibody. *Carcinogenesis* 1986; **7**: 1475-1482
21 **Hirschi KK,** Xu CE, Tsukamoto T, Sager R. Gap junction genes Cx26 and Cx43 individually suppress the cancer phenotype of human mammary carcinoma cells and restore differentiation potential. *Cell Growth Differ* 1996; **7**: 861-870
22 **Lee SW,** Tomasetto C, Paul D, Keyomarsi K, Sager R. Transcriptional downregulation of gap-junction proteins blocks junctional communication in human mammary tumor cell lines. *J Cell Biol* 1992; **118**: 1213-1221
23 **Yamaoka K,** Nouchi T, Tazawa J, Hiranuma S, Marumo F, Sato C. Expression of gap junction protein connexin 32 and E-cadherin in human hepatocellular carcinoma. *J Hepatol* 1995; **22**: 536-539
24 **Omori Y,** Krutovskikh V, Mironov N, Tsuda H, Yamasaki H. Cx32 gene mutation in a chemically induced rat liver tumour. *Carcinogenesis* 1996; **17**: 2077-2080
25 **Eghbali B,** Kessler JA, Reid LM, Roy C, Spray DC. Involvement of gap junctions in tumorigenesis: transfection of tumor cells with connexin 32 cDNA retards growth *in vivo*. *Proc Natl Acad Sci U S A* 1991; **88**: 10701-10705
26 **Zhang JT,** Nicholson BJ. Sequence and tissue distribution of a second protein of hepatic gap junctions, Cx26, as deduced from its cDNA. *J Cell Biol* 1989; **109**: 3391-3401
27 **Krutovskikh VA,** Mesnil M, Mazzoleni G, Yamasaki H. Inhibition of rat liver gap junction intercellular communication by tumor-promoting agents *in vivo*. Association with aberrant localization of connexin proteins. *Lab Invest* 1995; **72**: 571-577
28 **Plante I,** Charbonneau M, Cyr DG. Decreased gap junctional intercellular communication in hexachlorobenzene-induced gender-specific hepatic tumor formation in the rat. *Carcinogenesis* 2002; **23**: 1243-1249
29 **Schwarz M,** Wanke I, Wulbrand U, Moennikes O, Buchmann A. Role of connexin 32 and beta-catenin in tumor promotion in mouse liver. *Toxicol Pathol* 2003; **31**: 99-102
30 **Florkiewicz RZ,** Majack RA, Buechler RD, Florkiewicz E. Quantitative export of FGF-2 occurs through an alternative, energy-dependent, non-ER/Golgi pathway. *J Cell Physiol* 1995; **162**: 388-399
31 **Krutovskikh V.** Implication of direct host-tumor intercellular interactions in non-immune host resistance to neoplastic growth. *Semin Cancer Biol* 2002; **12**: 267-276
32 **Traub O,** Druge PM, Willecke K. Degradation and resynthesis of gap junction protein in plasma membranes of regenerating liver after partial hepatectomy or cholestasis. *Proc Natl Acad Sci USA* 1983; **80**: 755-759
33 **Ng IO,** Lai EC, Fan ST, Ng MM, So MK. Prognostic significance of pathologic features of hepatocellular carcinoma. A multivariate analysis of 278 patients. *Cancer* 1995; **76**: 2443-2448
34 **Nakashima O.** Pathological diagnosis of hepatocellular carcinoma. *Nihon Rinsho* 2001;**59** Suppl 6: 333-341
35 **Markert CL.** Neoplasia: a disease of cell differentiation. *Cancer Res* 1968; **28**: 1908-1914

Edited by Wang XL

PO Box 2345, Beijing 100023, China
Fax: +86-10-85381893
E-mail: wjg@wjgnet.com www.wjgnet.com

ELSEVIER

World J Gastroenterol 2005;11(2):176-181
World Journal of Gastroenterology ISSN 1007-9327

• LIVER CANCER •

Clinicopathological and prognostic implications of endoglin (CD105) expression in hepatocellular carcinoma and its adjacent non-tumorous liver

Joanna W. Ho, Ronnie T. Poon, Chris K. Sun, Wei-Cheng Xue, Sheung-Tat Fan

Joanna W. Ho, Ronnie T. Poon, Chris K. Sun, Wei-Cheng Xue, Sheung-Tat Fan, Centre for the Study of Liver Disease, and Departments of Surgery and Pathology, The University of Hong Kong, Pokfulam, Hong Kong, China
Supported by the Sun C.Y. Research Foundation for Hepatobiliary and Pancreatic Surgery of The University of Hong Kong
Correspondence to: Dr. Ronnie T. Poon, University of Hong Kong, Department of Surgery, Queen Mary Hospital, 102 Pokfulam Road, Hong Kong, China. poontp@hkucc.hku.hk
Telephone: +852-28553641 **Fax:** +852-28175475
Received: 2004-05-25 **Accepted:** 2004-07-27

Abstract

AIM: The expression pattern of endoglin (CD105) in hepatocellular carcinoma (HCC) has not been reported so far. We hypothesized that CD105 could differentially highlight a subset of microvessels in HCC, and intratumoral microvessel density (IMVD) by CD105 immunostaining (IMVD-CD105) could provide better prognostic information than IMVD by CD34 immunostaining (IMVD-CD34).

METHODS: Paraffin blocks of tumor and adjacent non-tumorous liver tissues from 86 patients who underwent curative resection of HCC were used for this study. Serial sections were stained for CD105 and CD34, respectively, to highlight the microvessels. IMVD was counted according to a standard protocol.

RESULTS: In the HCC tissues, CD105 was either negatively or positively stained only in a subset of microvessels. In contrast, CD34 showed positive and more extensive microvessel staining in all cases examined. However, in the adjacent non-tumorous liver sections, CD105 showed a diffuse pattern of microvessel staining in 20 of 86 cases, while CD34 showed negative or only focal staining of the sinusoids around portal area. Correlation with clinicopathological data demonstrated that lower scores of IMVD-CD105 were found in larger sized tumors [mean 41.4/0.74 mm^2 (>5 cm tumor) *vs* 65.9/0.74 mm^2 ($\leqslant$5 cm tumor), $P = 0.043$] and more aggressive tumors, as indicated by venous infiltration [36.8/0.74 mm^2 (present) *vs* 64.2/0.74 mm^2 (absent), $P = 0.020$], microsatellite nodules [35.1/0.74 mm^2 (present) *vs* 65.9/0.74 mm^2 (absent), $P = 0.012$], and advanced TNM tumor stage [38.8/0.74 mm^2 (stage 3 or 4) *vs* 68.3/0.74 mm^2 (stage 1 or 2), $P = 0.014$]. No prognostic significance was observed when median values were used as cut-off points using either IMVD-CD105 or IMVD-CD34. However, the presence of the diffuse pattern of CD105 expression in the adjacent non-tumorous liver tissues predicted a poorer disease-free survival (median 8.6 *vs* 21.5 mo, $P = 0.026$).

CONCLUSION: Our data demonstrate that a lower IMVD-CD105 is associated with larger and more aggressive tumors. In this study, IMVD-CD105 did not provide significant prognostic information. However, active angiogenesis as highlighted by diffuse CD105 staining of the microvessels in the adjacent non-tumorous liver tissues is predictive of early recurrence.

Key words: Hepatocellular carcinoma; Endoglin; Intratumoral microvessel density

Ho JW, Poon RT, Sun CK, Xue WC, Fan ST. Clinicopathological and prognostic implications of endoglin (CD105) expression in hepatocellular carcinoma and its adjacent non-tumorous liver. *World J Gastroenterol* 2005; 11(2): 176-181
http://www.wjgnet.com/1007-9327/11/176.asp

INTRODUCTION

Angiogenesis, the formation of new capillaries from a pre-existing vasculature, is implicated in tumor development, growth, progression, and metastasis[1-3]. Different from that in the normal physiological condition, the fine balance of modulation between proangiogenic and antiangiogenic factors is disturbed in tumor microenvironment, thus leading to abnormal vessel growth. It is known that tumor-associated endothelial cells in the neovasculature proliferate 20 to 2000 times more rapidly than those found in the normal vasculature[4,5]. The characteristics of microvessels in tumors are different from that developed under normal physiological conditions[6]. In fact, intratumoral microvessel density (IMVD) has been extensively investigated and was found to be a useful prognostic marker in many types of cancers[7].

Hepatocellular carcinoma (HCC) is a highly vascularized tumor on angiography. Its neovascularization is featured by sinusoidal capillarization[8]. However, not much is known about the exact mechanism and contribution of angiogenesis in different stages of HCC development. Several studies have shown that certain endothelial markers, in particular CD34, are expressed diffusely in the microvessels of HCC, and that their levels of expression correlate with prognosis of the patients[9-11]. A previous study by our group showed that IMVD assessed by CD34 immunostaining (IMVD-CD34) was a good prognostic marker of recurrence after hepatectomy in patients whose tumors were less than or equal to 5 cm in diameter[11]. However, CD34 is a pan-endothelial cell marker that reacts not only with proliferating vessels but also with established vessels in the tumor. Therefore, CD34 might not be an ideal marker of tumor neovascularization in HCC.

Endoglin (CD105) is a homodimeric membrane glycoprotein expressed on endothelial cells that can bind to transforming growth factor-β1 and transforming growth factor-β3[12]. CD105 is only weakly expressed in normal tissues, but it is strongly expressed in tumor endothelia[13-18]. Recent studies have

suggested that CD105 is a proliferation-associated marker of endothelial cells[13], and that its expression correlates strongly with cell proliferation markers in tumor endothelia[12]. Moreover, CD105 has been demonstrated to be a good tumor angiogenesis marker in breast cancer[19], brain tumor[20], malignant melanoma[21] and colorectal carcinoma[22]. Detection of CD105 in endothelial cells by immunohistochemical staining has been reported to provide a superior angiogenesis marker compared with the conventional CD34 staining in non-small cell lung cancer[18] and multiple myeloma[23]. Evaluation of tumor tissue expression of CD105 in correlation with clinicopathological parameters has revealed its diagnostic and prognostic significance in cancers such as breast cancer[24,25], squamous cell carcinoma of the oral cavity[26], prostate cancer[27], and renal cell carcinoma[28].

To date, not much is known about the exact mechanism of tumor angiogenesis in HCC, and the expression pattern of CD105 in HCC has not been reported before. Supported by the evidence shown in other tumors, we hypothesized that CD105 might be able to differentially highlight a subset of newly sprouted and immature microvessels in HCC, and tumor IMVD by CD105 immunostaining (IMVD-CD105) might provide a more informative angiogenesis score than IMVD-CD34, especially in terms of correlation with clinicopathological parameters.

MATERIALS AND METHODS

Patients and tissue samples

Eighty-six patients (67 men, 19 women) who underwent curative resection of HCC, defined as macroscopically complete removal of the tumor, in the Department of Surgery of the University of Hong Kong at Queen Mary Hospital were studied. None of the patients had received any preoperative treatment such as transarterial chemoembolization, and no postoperative adjuvant therapy was given. The study was approved by the Institutional Review Board of our institution.

The mean±SD maximum diameter of the tumors was 8.0 +/- 5.0 cm (range 1.5 cm to 22.0 cm). Thirty-three patients (38%) had tumor ≤5 cm in diameter. Tissue specimens were taken from the tumors and from adjacent non-tumorous livers. Fresh tissue specimens were fixed in 10% buffered formalin and embedded in paraffin, and 4-μm-thick sections were prepared for immunohistochemical study.

Immunohistochemical staining for CD34 and CD105

Tumorous and non-tumorous sections were immunostained with human CD34 monoclonal antibody (1:100; QBEND-10, Dako, Carpenteria, CA, USA) and CD105 monoclonal antibody (1:1 000; SN6H, Dako, Carpenteria, CA, USA). Consecutive paraffin sections were used for the staining of CD34 and CD105. Vascularization was demonstrated by an immunohistochemical analysis for CD105 using a catalyzed signal amplification system (Dako), based on the peroxidase-catalyzed deposition of a biotinylated phenol compound tyramide, while LSAB kit from Dako was used for CD34 staining. The negative controls were obtained by substituting the primary antibodies with mouse immunoglobulin G. IMVD was evaluated according to Gasparini's criteria[29] by two independent observers as described in a previous report[11]. The mean microvessel count of the five most vascular areas was taken as the MVD, which was expressed as the absolute number of microvessels per 0.74 mm^2 (×200 field).

Clinicopathological and follow-up data

All clinicopathological data were collected prospectively in a computerized database, and all patients were followed and monitored regularly for tumor recurrence by serum alpha fetoprotein (AFP) level monthly and chest X-ray together with computed tomography (CT) scan every 3 mo. The median follow-up time of all patients was 36 mo (range 20 to 50 mo). A diagnosis of recurrence was based on typical imaging appearance in CT scan and an elevated AFP level, and if necessary, fine needle aspiration cytology.

Statistical analysis

Student *t*-test was used for comparison of continuous variables between groups. The correlation between continuous variables was performed using the Spearman rank correlation test. Cumulative disease-free survival was computed using the Kaplan-Meier method and comparison between groups was done by the log-rank test.

Clinicopathological variables that were correlated with IMVD included gender, age (≤ or >60 years), hepatitis B surface antigen (HBsAg) status, presence or absence of cirrhosis in the non-tumorous livers, tumor size (≤ or >5 cm), tumor differentiation by Edmonson grade (1-2 or 3-4), any tumor encapsulation, venous invasion, microsatellite nodules, and pTNM stage (I/II or III/IVA). All statistical analyses were performed using the SPSS statistical software (SPSS/PC+, SPSS Inc., Chicago, IL, USA). $P < 0.05$ was considered statistically significant.

RESULTS

CD105 and CD34 staining in tumor and adjacent non-tumorous liver

Figure 1 shows the typical staining patterns of CD105 immunostaining in the tumor and the adjacent non-tumorous sections of the liver. The mean score of IMVD-CD105 was 50.8±54.8/0.74 mm^2 (range 0-240.0), whereas the mean score of IMVD-CD34 was 125.6±53.2/0.74 mm^2 (range 28.2-283.4) ($P<0.001$). There were no significant differences between IMVD values obtained by the two independent scorers.

Results from this study of 86 HCC cases revealed some similarities but also some differences between CD34 and CD105 staining. Similar to the CD34 staining observed in the present study, and that from others reported in HCC[9-11,30], highlighted microvessels by CD105 also showed three patterns of expression on the tumor tissue sections: sinusoid-like, branching, and small without apparent lumina (endothelial sprouts). Distinctively, the expression pattern of CD105 in HCC differed from that of CD34 in the following aspects. First, when consecutive slides of tumor tissue sections were compared, the number of vessels highlighted by CD105 was considerably lower than that by CD34, although a statistically significant positive correlation was observed between the MVD scores by the two markers (Figure 2). Second, in all tumor sections examined, CD105 was completely negative in 28/86 cases, while CD34 was positive in all of the cases examined. Third, in non-tumorous tissues, CD105 showed variable patterns of staining, including a diffuse pattern of staining in some cases, whereas CD34 was uniformly negative in non-tumorous liver except for sparse sinusoid staining distributed focally around the portal tract.

Correlation between IMVD and clinicopathological parameters

Table 1 summarizes the analysis of IMVD-CD105 and IMVD-CD34 in relation to various clinicopathological parameters. No significant differences were found between either IMVD-CD105 or IMVD-CD34 and gender, age or hepatitis B infection status of the patients. However, IMVD-CD105 and IMVD-CD34 were significantly related to several pathological variables. Both IMVD-CD105 and IMVD-CD34 were significantly lower in tumors > 5 cm compared to tumors ≤5 cm in diameter ($P = 0.043$ and 0.002, respectively). Furthermore, both showed a significant

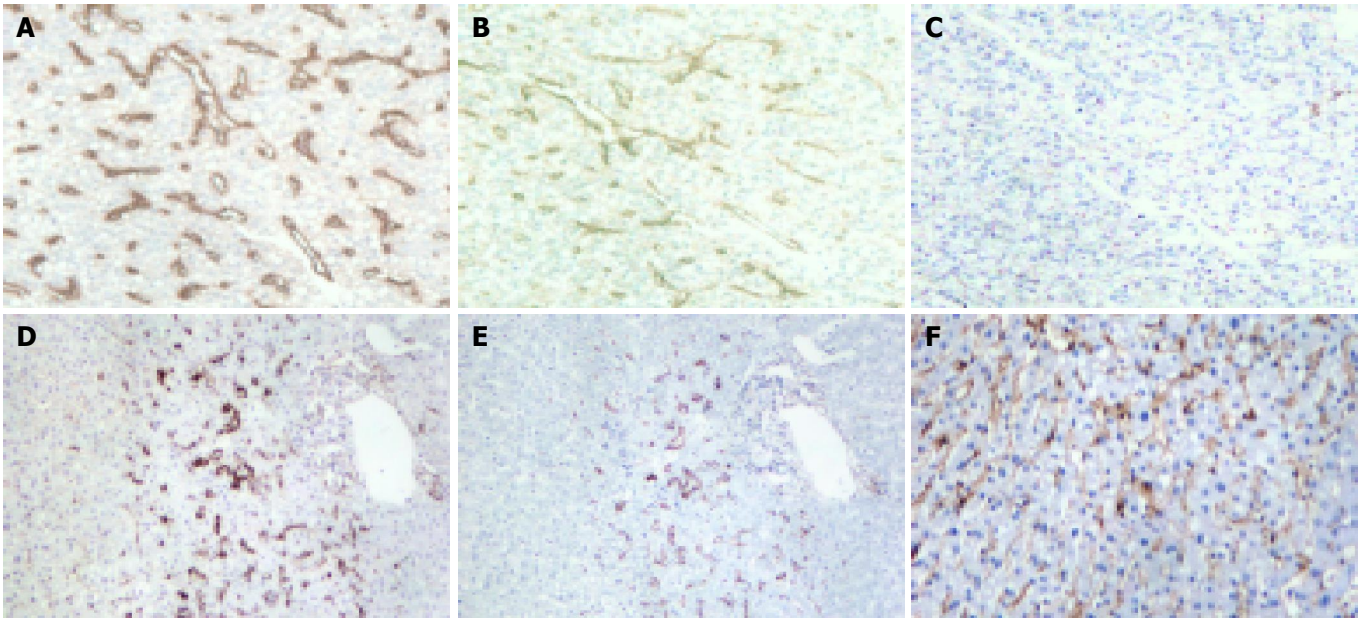

Figure 1 Expression of CD105 and CD34 as shown by the brown staining of the vasculature in tumor and adjacent non-tumorous liver (×100). A-C are serial sections of tumor tissue, where A shows the CD34 expression, B shows the CD105 expression, and C shows the negative control. D and E are serial sections of adjacent non-tumorous liver, where D shows the CD34 expression, and E shows the CD105 expression. Both D and E illustrate typical focal staining of vessels around the portal vein. F shows a case of diffuse CD105 staining in the non-tumorous liver, whereas such pattern of staining was not seen in the non-tumorous liver by CD34 staining.

Table 1 Correlation of IMVD-CD105 and IMVD-CD34 with clinicopathological parameters

Clinical parameters	IMVD-CD105 (/0.74 mm^2)				IMVD-CD34 (/0.74 mm^2)			
	n	mean	SD	*P*	*n*	mean	SD	*P*
Gender								
Male	67	49.29	55.17	0.631	67	124.94	53.51	0.823
Female	19	56.19	54.40		19	128.07	53.54	
Age (yr)								
≤60 years	58	43.96	48.21	0.095	58	121.09	58.19	0.257
>60 years	28	65.01	64.99		28	135.04	40.39	
HBsAg								
Positive	69	46.35	49.36	0.121	69	121.52	53.02	0.227
Negative	17	70.08	73.87		17	139.37	52.48	
Histopathological parameters								
Tumor size								
≤ 5 cm	33	65.90	58.98	0.043	33	147.76	53.41	0.002
>5 cm	53	41.42	50.26		53	111.85	48.68	
Tumor encapsulation								
Absent	53	48.31	48.00	0.497	53	120.29	54.19	0.193
Present	33	56.72	65.04		33	135.94	52.01	
Venous invasion								
Absent	44	64.17	60.96	0.020	44	133.59	50.14	0.157
Present	42	36.83	43.91		42	117.29	55.64	
Microsatellite lesions								
Absent	48	65.88	62.15	0.012	48	129.63	52.55	0.401
Present	38	35.06	41.02		38	119.65	52.53	
Adjacent non-tumorous liver								
Normal (0)	6	59.26	52.46	0.602 (0&1)	6	102.95	40.09	0.602 (0&1)
Chronic hepatitis (1)	38	43.14	57.47	0.817 (0&2)	38	118.37	47.69	0.118 (1&2)
Cirrhosis (2)	42	53.84	53.49	0.537 (1&2)	42	135.44	58.31	0.158 (0&2)
Edmonson grade								
1 & 2	21	83.73	65.87	0.079	21	162.94	41.95	0.013
≥3	65	48.47	54.21		65	117.28	51.12	
TNM stage								
I & II	35	68.26	63.67	0.014	35	144.89	55.42	0.005
III & IVA	51	38.84	44.52		51	112.41	47.84	

HBsAg, hepatitis B surface antigen; TNM, tumor-node-metastasis.

correlation with pTNM staging, and a lower IMVD observed in tumors with more advanced staging (P = 0.014 and 0.005, respectively). However, only lower scores of IMVD-CD105 showed a statistically significant association with venous invasion [36.8/0.74 mm^2 (present) *vs* 64.2/0.74 mm^2 (absent), P = 0.02], and microsatellite nodules [35.1/0.74 mm^2 (present) *vs* 65.9/0.74 mm^2 (absent), P = 0.012].

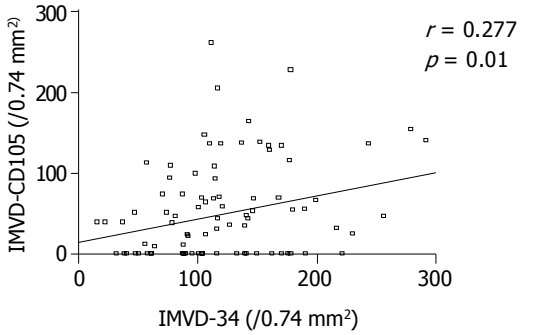

Figure 2 Graph of scatter plots showing correlation between scores of IMVD-CD105 *vs* IMVD-CD34.

Disease-free survival analysis

Disease-free survival analysis was performed in 81 patients after 5 patients with hospital mortality or palliative resection (i.e., positive resection margin) were excluded. No prognostic significance was observed when median values were used as cut-off points using either IMVD-CD105 or IMVD-CD34. However, as shown in Figure 3, when the patients were segregated by the presence and absence of diffuse CD105 staining patterns in the adjacent non-tumorous liver tissues, the patients with diffuse CD105 staining in the adjacent non-tumorous livers had a much poorer prognosis than those patients without such a pattern of CD105 staining (median disease-free survival 8.6 *vs* 21.5 mo, P = 0.026).

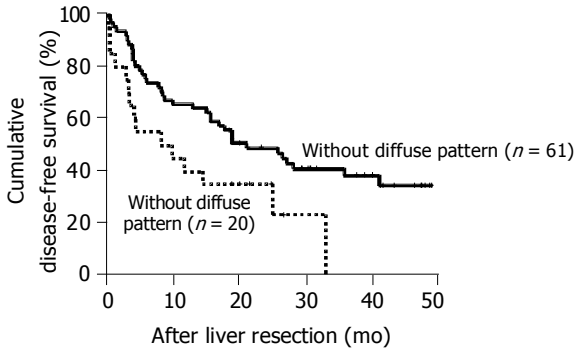

Figure 3 Disease-free survival analysis shows the differences in disease-free survival in patients with or without diffuse pattern of CD105 staining in non-tumorous livers. Five patients were excluded from the analysis because of hospital mortality or palliative resection with positive resection margins.

DISCUSSION

Previous reports have demonstrated that IMVD-CD34 is a better prognostic marker for HCC than IMVD assessed by many other endothelial markers, such as von Willebrand marker (vWF), CD31, and UEA-1[10,11,31]. However, CD34 is a pan-endothelial cell marker, therefore, it may not be able to reflect the exact angiogenesis activity in a tumor. According to some previous reports, CD105 is an endothelial marker that appears to react only with the endothelial cells in the newly formed vessels, and in particular, the immature tumor blood vessels[13-18]. Moreover, studies in other cancers have suggested that scores of IMVD-CD105 might be superior to those of IMVD-CD34 in terms of prognostic information[18,23]. To our knowledge, this is the first study that evaluated the clinicopathological significance of IMVD-CD105 in HCC, which is of particular interest because HCC is one of the most vascular solid tumors. Overall, in agreement with those reported for other cancers in the literature, our immunostaining confirmed that CD105 could stain a subset of microvessels and the staining patterns of CD105 in both tumors and non-tumorous liver differed from those stained by CD34 in certain aspects.

Correlation with clinicopathological parameters in this study demonstrated significantly lower IMVD scores in larger and more advanced stage tumors with both CD105 and CD34 as the endothelial markers. Moreover, lower scores of IMVD-CD105 were associated with more aggressive tumors as indicated by microscopic venous invasion and microsatellite nodules (Table 1). The latter correlations were probably indirect ones related to the higher frequencies of microscopic venous invasion and microsatellite nodules in larger tumors. The findings of a clinicopathological correlation with IMVD-CD105 were apparently contrary to those reported in other solid tumor types such as breast cancer and non-small cell lung cancer[18,24,25], in which higher rather than lower IMVD scores were associated with more aggressive tumors. However, as reviewed by Gasparini *et al*[32], most retrospective studies in breast cancer were on early-stage tumors, and hence angiogenesis appears to be a good prognostic marker only in early-stage group of breast cancer. Similarly, our previous study also illustrated that IMVD-CD34 was a good prognostic marker in small tumors $\leqslant$5 cm only[11]. The HCC cases studied by Tanigawa *et al*[10], who demonstrated a worse prognosis with a higher IMVD-CD34, were also mainly small tumors $\leqslant$5 cm in diameter. In this study, the majority of tumors were >5 cm in diameter, and both IMVD-CD105 and IMVD-CD34 decreased with increase in tumor size. In support of our data, the IMVD-CD34 analysis of 71 HCC cases by El-Assal *et al*[9] also found that the larger (>5 cm) tumors showed a trend to decrease IMVD. Neither IMVD-CD105 nor IMVD-CD34 showed a prognostic influence in this study of predominantly large HCCs.

Blood vessels could provide support for oxygen and nutrients, as well as many paracrine factors to its surrounding tumor cells[1,33,34]. Although it has been well accepted that tumor growth is dependent on angiogenesis[1], whether IMVD could truly reflect the angiogenic activity of tumors remains controversial. As pointed out by a recent review on IMVD from Folkman's group[7], IMVD reflects intercapillary distance, and therefore it may reflect the metabolic need of its surrounding tumor cells. While our finding of a lower IMVD in larger tumors should not be interpreted as suggesting that a bigger size tumor is less angiogenesis dependent, it may, however, indicate that tumor cells in a bigger sized tumor adapt to survive with less metabolic demand. It has been reported that oxygen consumption was much less in tumor tissues as compared with normal counterparts[1,35]. Another plausible explanation is that the turnover of tumor cells is much shorter than that of endothelial cells, resulting in an increased intercapillary distance as the tumor size increases[36,37]. This is particularly interesting in the case of HCC, which could grow very much larger in size compared to other types of tumors, as indicated by a mean diameter of 8.0 cm in our group of patients. Our results seem to support the notion that as the tumor cells expand in HCC, they can become more and more accustomed to a lower metabolic demand with an increase in

tumor size[35].

The adjacent non-tumorous livers were also included in this study. Interestingly, when we segregated the patients by CD105 stained vessel patterns in the adjacent non-tumorous livers according to the presence or absence of a well-diffuse pattern, the disease-free survival in those patients with a diffuse pattern of CD105 staining in the adjacent non-tumorous livers was statistically worse than that of patients without a diffuse pattern of CD105 expression in the adjacent non-tumorous livers. The finding that the diffuse pattern of CD105 staining in the adjacent non-tumorous liver can predict early recurrence is interesting but not surprising, because unlike other cancer types, the adjacent non-tumorous tissues in HCC patients were not normal in most cases. The liver of HCC patients is usually infected with chronic hepatitis B or C viruses, which lead to chronic hepatitis or even cirrhosis. Angiogenesis might have an important role in these disease processes too. Angiogenesis in the non-tumorous liver may enhance the growth of intrahepatic metastasis or development of multicentric tumors, both of which contribute to postoperative recurrence. Although the exact mechanism is unknown, our data suggest that the detection of the diffuse pattern of CD105 in the adjacent non-tumorous liver represents an unfavorable factor to those patients recovering from HCC resection. The relationship between angiogenesis in the non-tumorous liver and postoperative recurrence of HCC warrants further investigation.

In conclusion, contrary to those reported on other types of cancers where CD105 was found to be a good prognostic marker or even better than CD34, our data showed that IMVD-CD105 in HCC did not correlate with the prognosis of patients. However, our data illustrated that CD105 could stain a subset of microvessels differently from that stained by CD34 in HCC tissues. Our clinicopathological analysis demonstrated that lower scores of IMVD-CD105 were found in larger sized and more aggressive tumors. Furthermore, different from CD34, CD105 could also stain microvessels in the adjacent non-tumorous liver. The presence of well-diffuse patterns of CD105 expression in the adjacent non-tumorous liver could predict early disease recurrence. Further studies are merited to clarify the mechanisms involved in these associations.

REFERENCES

1 **Folkman J**. What is the evidence that tumors are angiogenesis dependent? *J Natl Cancer Inst* 1990; **82**: 4-6
2 **Folkman J**. Tumor angiogenesis. *Adv Cancer Res* 1985; **43**: 175-203
3 **Liotta LA**, Steeg PS, Stetler-Stevenson WG. Cancer metastasis and angiogenesis: an imbalance of positive and negative regulation. *Cell* 1991; **64**: 327-336
4 **Hobson B**, Denekamp J. Endothelial proliferation in tumours and normal tissues: continuous labelling studies. *Br J Cancer* 1984; **49**: 405-413
5 **Herlyn M**. Endothelial cells as targets for tumor therapy. *J Immunother* 1999; **22**: 185
6 **Nagy JA**, Brown LF, Senger DR, Lanir N, Van de Water L, Dvorak AM, Dvorak HF. Pathogenesis of tumor stroma generation: a critical role for leaky blood vessels and fibrin deposition. *Biochim Biophys Acta* 1989; **948**: 305-326
7 **Hlatky L**, Hahnfeldt P, Folkman J. Clinical application of antiangiogenic therapy: microvessel density, what it does and doesn't tell us. *J Natl Cancer Inst* 2002; **94**: 883-893
8 **Kin M**, Torimura T, Ueno T, Inuzuka S, Tanikawa K. Sinusoidal capillarization in small hepatocellular carcinoma. *Pathol Int* 1994; **44**: 771-778
9 **El-Assal ON**, Yamanoi A, Soda Y, Yamaguchi M, Igarashi M, Yamamoto A, Nabika T, Nagasue N. Clinical significance of microvessel density and vascular endothelial growth factor expression in hepatocellular carcinoma and surrounding liver: possible involvement of vascular endothelial growth factor in the angiogenesis of cirrhotic liver. *Hepatology* 1998; **27**: 1554-1562
10 **Tanigawa N**, Lu C, Mitsui T, Miura S. Quantitation of sinusoid-like vessels in hepatocellular carcinoma: its clinical and prognostic significance. *Hepatology* 1997; **26**: 1216-1223
11 **Poon RT**, Ng IO, Lau C, Yu WC, Yang ZF, Fan ST, Wong J. Tumor microvessel density as a predictor of recurrence after resection of hepatocellular carcinoma: a prospective study. *J Clin Oncol* 2002; **20**: 1775-1785
12 **Vermeulen PB**, Gasparini G, Fox SB, Toi M, Martin L, McCulloch P, Pezzella F, Viale G, Weidner N, Harris AL, Dirix LY. Quantification of angiogenesis in solid human tumours: an international consensus on the methodology and criteria of evaluation. *Eur J Cancer* 1996; **32A**: 2474-2484
13 **Burrows FJ**, Derbyshire EJ, Tazzari PL, Amlot P, Gazdar AF, King SW, Letarte M, Vitetta ES, Thorpe PE. Up-regulation of endoglin on vascular endothelial cells in human solid tumors: implications for diagnosis and therapy. *Clin Cancer Res* 1995; **1**: 1623-1634
14 **Seon BK**, Matsuno F, Haruta Y, Kondo M, Barcos M. Long-lasting complete inhibition of human solid tumors in SCID mice by targeting endothelial cells of tumor vasculature with antihuman endoglin immunotoxin. *Clin Cancer Res* 1997; **3**: 1031-1044
15 **Wang JM**, Kumar S, Pye D, van Agthoven AJ, Krupinski J, Hunter RD. A monoclonal antibody detects heterogeneity in vascular endothelium of tumours and normal tissues. *Int J Cancer* 1993; **54**: 363-370
16 **Westphal JR**, Willems HW, Schalkwijk CJ, Ruiter DJ, de Waal RM. A new 180-kDa dermal endothelial cell activation antigen: *in vitro* and *in situ* characteristics. *J Invest Dermatol* 1993; **100**: 27-34
17 **Matsuno F**, Haruta Y, Kondo M, Tsai H, Barcos M, Seon BK. Induction of lasting complete regression of preformed distinct solid tumors by targeting the tumor vasculature using two new anti-endoglin monoclonal antibodies. *Clin Cancer Res* 1999; **5**: 371-382
18 **Tanaka F**, Otake Y, Yanagihara K, Kawano Y, Miyahara R, Li M, Yamada T, Hanaoka N, Inui K, Wada H. Evaluation of angiogenesis in non-small cell lung cancer: comparison between anti-CD34 antibody and anti-CD105 antibody. *Clin Cancer Res* 2001; **7**: 3410-3415
19 **Bodey B**, Bodey B, Siegel SE, Kaiser HE. Over-expression of endoglin (CD105): a marker of breast carcinoma-induced neovascularization. *Anticancer Res* 1998; **18**: 3621-3628
20 **Bodey B**, Bodey B, Siegel SE, Kaiser HE. Upregulation of endoglin (CD105) expression during childhood brain tumor-related angiogenesis. Anti-angiogenic therapy. *Anticancer Res* 1998; **18**: 1485-1500
21 **Bodey B**, Bodey B, Siegel SE, Kaiser HE. Immunocytochemical detection of endoglin is indicative of angiogenesis in malignant melanoma. *Anticancer Res* 1998; **18**: 2701-2710
22 **Akagi K**, Ikeda Y, Sumiyoshi Y, Kimura Y, Kinoshita J, Miyazaki M, Abe T. Estimation of angiogenesis with anti-CD105 immunostaining in the process of colorectal cancer development. *Surgery* 2002; **131**: S109-S113
23 **Pruneri G**, Ponzoni M, Ferreri AJ, Decarli N, Tresoldi M, Raggi F, Baldessari C, Freschi M, Baldini L, Goldaniga M, Neri A, Carboni N, Bertolini F, Viale G. Microvessel density, a surrogate marker of angiogenesis, is significantly related to survival in multiple myeloma patients. *Br J Haematol* 2002; **118**: 817-820
24 **Kumar S**, Ghellal A, Li C, Byrne G, Haboubi N, Wang JM, Bundred N. Breast carcinoma: vascular density determined using CD105 antibody correlates with tumor prognosis. *Cancer Res* 1999; **59**: 856-861
25 **Dales JP**, Garcia S, Bonnier P, Duffaud F, Andrac-Meyer L, Ramuz O, Lavaut MN, Allasia C, Charpin C. CD105 expression is a marker of high metastatic risk and poor outcome in breast carcinomas. Correlations between immunohistochemical analysis and long-term follow-up in a series of 929 patients. *Am J Clin Pathol* 2003; **119**: 374-380

26 **Schimming R**, Marme D. Endoglin (CD105) expression in squamous cell carcinoma of the oral cavity. *Head Neck* 2002; **24**: 151-156
27 **Wikstrom P**, Lissbrant IF, Stattin P, Egevad L, Bergh A. Endoglin (CD105) is expressed on immature blood vessels and is a marker for survival in prostate cancer. *Prostate* 2002; **51**: 268-275
28 **Yagasaki H**, Kawata N, Takimoto Y, Nemoto N. Histopathological analysis of angiogenic factors in renal cell carcinoma. *Int J Urol* 2003; **10**: 220-227
29 **Gasparini G**, Harris AL. Clinical importance of the determination of tumor angiogenesis in breast carcinoma: much more than a new prognostic tool. *J Clin Oncol* 1995; **13**: 765-782
30 **Cui S**, Hano H, Sakata A, Harada T, Liu T, Takai S, Ushigome S. Enhanced CD34 expression of sinusoid-like vascular endothelial cells in hepatocellular carcinoma. *Pathol Int* 1996; **46**: 751-756
31 **Anthony PP**, Ramani P. Endothelial markers in malignant vascular tumours of the liver: superiority of QB-END/10 over von Willebrand factor and Ulex europaeus agglutinin 1. *J Clin Pathol* 1991; **44**: 29-32
32 **Gasparini G**. Clinical significance of determination of surrogate markers of angiogenesis in breast cancer. *Crit Rev Oncol Hematol* 2001; **37**: 97-114
33 **Rak J**, Filmus J, Kerbel RS. Reciprocal paracrine interactions between tumour cells and endothelial cells: the 'angiogenesis progression' hypothesis. *Eur J Cancer* 1996; **32A**: 2438-2450
34 **Weidner N**. Tumour vascularity and proliferation: clear evidence of a close relationship. *J Pathol* 1999; **189**: 297-299
35 **Steinberg F**, Rohrborn HJ, Otto T, Scheufler KM, Streffer C. NIR reflection measurements of hemoglobin and cytochrome aa3 in healthy tissue and tumors. Correlations to oxygen consumption: preclinical and clinical data. *Adv Exp Med Biol* 1997; **428**: 69-77
36 **Vaupel P**. Hypoxia in neoplastic tissue. *Microvasc Res* 1977; **13**: 399-408
37 **Tannock IF**, Steel GG. Quantitative techniques for study of the anatomy and function of small blood vessels in tumors. *J Natl Cancer Inst* 1969; **42**: 771-782

Assistant Editor Guo SY **Edited by** Wang XL

PO Box 2345, Beijing 100023, China
Fax: +86-10-85381893
E-mail: wjg@wjgnet.com www.wjgnet.com

ELSEVIER

World J Gastroenterol 2005;11(2):182-186
World Journal of Gastroenterology ISSN 1007-9327

• LIVER CANCER •

Construction of recombinant eukaryotic expression plasmid containing murine CD40 ligand gene and its expression in H22 cells

Yong-Fang Jiang, Yan He, Guo-Zhong Gong, Jun Chen, Chun-Yan Yang, Yun Xu

Yong-Fang Jiang, Yan He, Guo-Zhong Gong, Jun Chen, Chun-Yan Yang, Yun Xu, Center for Liver Diseases, Second Xiangya Hospital, Central South University, Changsha 410011, Hunan Province, China
Supported by the Public Health Department Foundation of Hunan province, China, No. Y02-42
Correspondence to: Dr Yong-Fang Jiang, Center for Liver Diseases, Second Xiangya Hospital, Central South University, No 139 Renmin Zhong Street, Changsha 410011, Hunan Province, China. jiangyongfang@hotmail.com
Telephone: +86-731-5524222-2263 **Fax:** +86-731-4896920
Received: 2004-03-30 **Accepted:** 2004-05-13

Abstract

AIM: To construct a recombinant murine CD40 ligand (mCD40L) eukaryotic expression vector for gene therapy and target therapy of hepatocellular carcinoma (HCC).

METHODS: mCD40L cDNA was synthesized by RT-PCR with the specific primers and directly cloned into T vector to generate middle recombinant. After digestion with restriction endonuclease, the target fragment was subcloned into the multi-clone sites of the eukaryotic vector. The constructed vector was verified by enzyme digestion and sequencing, and the product expressed was detected by RT-PCR and immunofluorescence methods.

RESULTS: The full-length mCD40L-cDNA was successfully cloned into the eukaryotic vector through electrophoresis, and mCD40L gene was integrated into the genome of infected H22 cells by RT-PCR. Murine CD40L antigen molecule was observed in the plasma of mCD40L-H22 by indirect immuno-fluorescence staining.

CONCLUSION: The recombined mCD40L eukaryotic expression vector can be expressed in H22 cell line. It provides experimental data for gene therapy and target therapy of hepatocellular carcinoma.

Key words: Hepatocellular carcinoma; Murine CD40 ligand; Plasmids; Genetic vectors

Jiang YF, He Y, Gong GZ, Chen J, Yang CY, Xu Y. Construction of recombinant eukaryotic expression plasmid containing murine CD40 ligand gene and its expression in H22 cells. *World J Gastroenterol* 2005; 11(2): 182-186
http://www.wjgnet.com/1007-9327/11/182.asp

INTRODUCTION

In China, the incidence of HCC is very high[1], and surgical operation, chemotherapy, and interventional therapy are the common therapies. But only a few patients of early stage without extrahepatic malignancy are indicated for operation, and for the advanced cases, chemotherapy and interventional therapy usually can not achieve a satisfactory effect. Therefore, it is urgent to find a novel strategy to prevent the proliferation of malignant cells. It is a hot spot at present to study immunogene therapy.

CD40 ligand (CD40L) is a 39 kD glycoprotein which is expressed on lymphocytes and non-lymphocytic leukocytes[2]. It is a member of the tumor necrosis factor family, and binds to CD40 on the membrane of antigen-presenting cells (APC)[3,4]. CD40-CD40L interaction plays a crucial role in the activation of APC and the initiation of both humoral and cellular immune responses[5-7].

Thus, gene transfer of CD40L has been proposed as an efficient means to treat malignancies[8]. CD40L may be used as a target molecule for immunotherapy or prophylaxis against HCC. For this purpose, we constructed the recombinant mCD40L eukaryotic expression vector, and expected that it would provide experimental data for the treatment of HCC.

MATERIALS AND METHODS

Cell lines and culture condition

Mouse splenocytes were obtained from female BALB/c mice. Cells were maintained in RPMI 1640 medium, supplemented with 10 mL/L FCS and 1 mmol/L glutamine, activated with Con A for 5 h. H22 cell line was provided by the Department of Biochemistry, Fourth Military Medical University, Xi'an, China. Cells were maintained in RPMI 1640 medium, supplemented with 10 mL/L FCS, 1 mmol/L glutamine, and 100 kU/L penicillin.

Plasmids and strain

The eukaryotic expression vector pcDNA3.1$^+$ was presented by Dr. Chun Deng, Michigan College, USA. The T vector pUCm-T was provided by the Bioasia, Shanghai. *E.coli* strain JM109 was purchased from Invitrogen Life Technologies (Burlington, ON, Canada).

Construction of recombinant mCD40L eukaryotic expression vector

A cDNA fragment coding for the full open reading frame of mouse CD40L gene was cloned by reverse transcription polymerase chain reaction (RT-PCR) from Con A stimulated mouse spleen cells using Taq polymerase. Two primers specific for the mouse CD40L gene were used, namely, the sense primer (5'-GAC GCT AGC ATG ATA GAA ACA TAC AGC CAA CCT-3') and the antisense primer (5'-GCC GAA TTC TCA GAG TTT GAG TAA GCC AAA AGA-3'). PCR conditions included 1 cycle at 94 ℃ for 5 min for pre-denaturation; 35 amplification cycles each consisting of denaturation at 94 ℃ for 60 s, annealing at 60 ℃ for 50 s, and extension at 72 ℃ for 90 s; followed by a further extension at 72 ℃ for 10 min. The cloned cDNA fragment was ligated into the pUCm-T vector to form pUCm-T-CD40L. The cDNA fragment of mCD40L from pUCm-T-mCD40L vector was further subcloned into the pcDNA3.1$^+$ to form eukaryotic expression vector pcDNA3.1$^+$-mCD40L. The recombinant expression vector pcDNA3.1$^+$-mCD40L was amplified in *E.coli* JM109 and then extracted by Wizard® Plus SV Minipreps

DNA Purification System (Promega, USA) according to the manufacturer's instructions.

Identification of recombinant mCD40L eukaryotic expression vector

The full-length mCD40L-cDNA was retrieved from the gel. pcDNA3.1$^+$-mCD40L was digested by *Nhe* I and *EcoR* I according to the afore-mentioned methods. The digested products were evaluated with 1.0% agarose gel electrophoresis. The full-length mCD40L-cDNA was successfully inserted into pcDNA3.1$^+$.

Nucleotide sequence analysis

The correct plasmids of recombinant mCD40L eukaryotic expression vector identified by the restriction analysis were sequenced using fluorescent dideoxynucleotides (Bioasia, Shanghai, China) on an automated DNA sequencer (ABI Prism 377). The sequences were compared with the published cDNA sequence[4].

Transfection of H22 cells

H22 cells were transfected with pcDNA3.1$^+$-mCD40L by liposome, LipofectamineTM 2000 (Gibco, USA). All the procedures were performed according to the guidance of the reagent. After 24-h exposure, cells were washed three times with medium and cultured in normal medium. Twenty-four hours after medium exchange, cells were selected in medium containing 800 μg/mL G418 (Gibco, USA). After 18 d of selection, G418-resistant clones were selected randomly from the surviving colonies. H22 cells were also transfected with pcDNA3.1$^+$ as control group, and H22 cells that were not transfected also served as control.

Detection of mCD40L expression by RT-PCR

To demonstrate the expression of mCD40L mediated by pcDNA3.1$^+$-mCD40L vector, total cellular RNA was extracted from the H22 cells. Synthesis and amplification of mCD40L cDNA were performed using RT-PCR. The cDNA was amplified with primers specific for mCD40L and the synthesis conditions according to the afore-mentioned methods.

Detection of mCD40L expression by immunofluorescence

The transfected cells were stabilized with 10 g/L formaldehydum polymerisatum for 30 min at 4 ℃, and blocked with 100 g/L bovine serum albumin (BSA) for 1 h at room temperature, then coated with rabbit anti-mouse CD40L antibody (Dako, Japan) for 45 min at 37 ℃, followed by goat anti-rabbit IgG-FITC (Boster, Wuhan) for 30 min at 37 ℃. The antibody-coated cells were observed under a fluorescence microscope (Optiphot XIF, Nicon, Japan) within 24 h.

RESULTS

Evaluation of pcDNA3.1$^+$-mCD40L

To demonstrate whether the full-length mouse CD40L-cDNA was inserted into the multi-clone sites of pcDNA3.1$^+$ correctly, pcDNA3.1$^+$-mCD40L was digested by *Nhe* I and *EcoR* I and evaluated with electrophoresis. Figure 1 shows that mCD40L-cDNA was successfully inserted into pcDNA3.1$^+$.

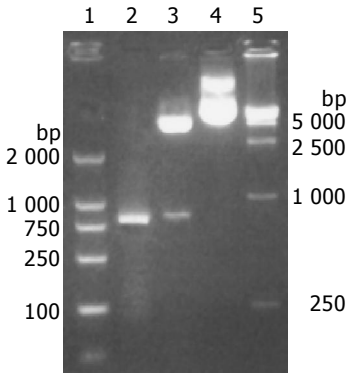

Figure 1 Electrophoresis of recombinant plasmid pcDNA3.1$^+$-mCD40L. Lanes 1 and 5: DNA molecular weight marker; lane 2: The RT-PCR product of mCD40L; lane 3: pcDNA3.1$^+$-mCD40L digested with *Nhe*I and *Eco*RI, pcDNA3.1$^+$ in the upper, full-length mCD40L-cDNA in the lower; and lane 4: pcDNA3.1$^+$-mCD40L not digested with *Nhe*I and *Eco*RI.

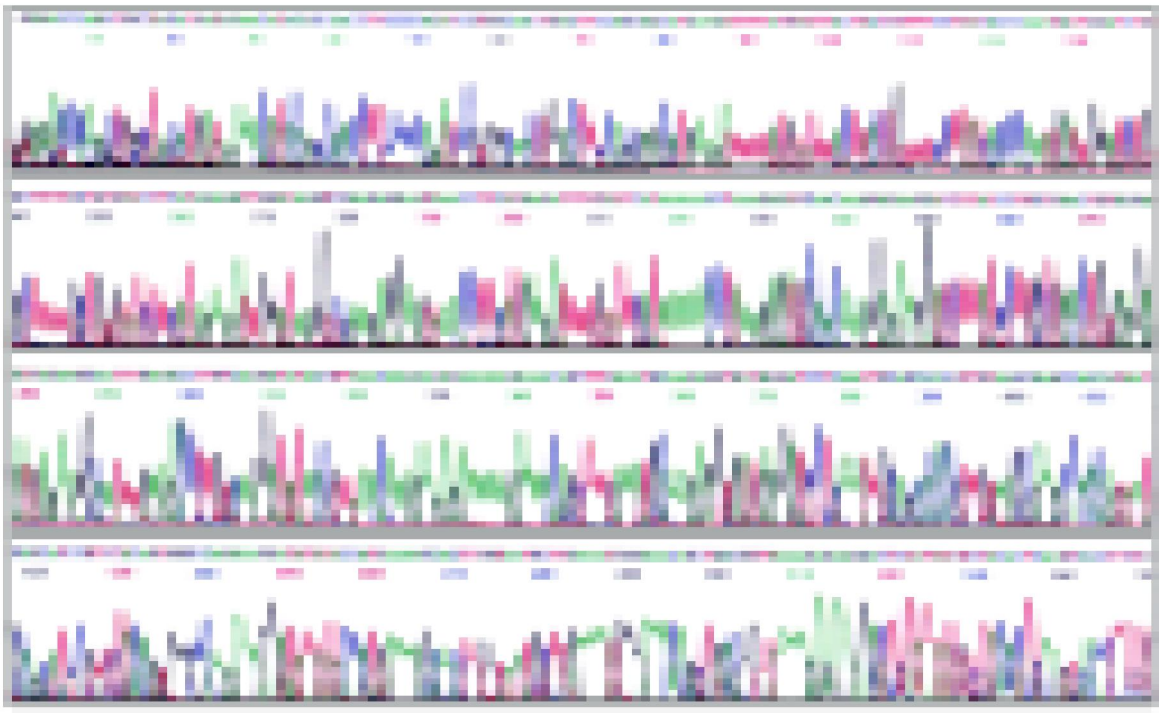

Figure 2 The sequencing map of pcDNA3.1$^+$-mCD40L with M13F primer.

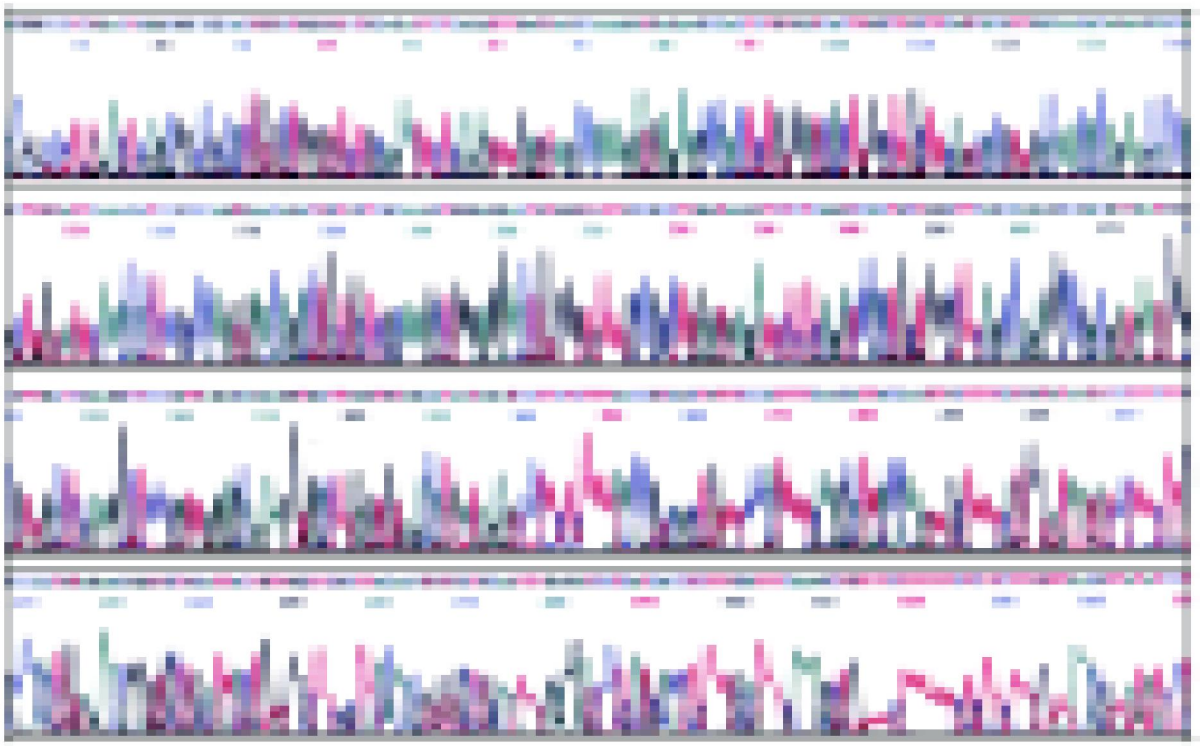

Figure 3 Sequencing map of pcDNA3.1$^+$-mCD40L with M13R primer.

GGAGACCCAAGCTG*GCTAGC*ATGATAGAAACATACAGCCAACCTTCCCCCAGATCCG

TGGCAACTGGACTTCCAGCGAGCATGAAGATTTTTATGTATTTACTTACTGTTTTCCTT

ATCACCCAAATGATTGGATCTGTGCTTTTTGCTGTGTATCTTCATAGAAGATTGGATA

AGGTCGAAGAGGAAGTAAACCTTCATGAAGATTTTGTATTCATAAAAAACCTAAAGAG

ATGCAACAAAGGAGAAGGATCTTTATCCTTGCTGAACTGTGAGGAGATGAGAAGGCA

ATTTGAAGACCTTGTCAAGGATATAACGTTAAACAAAGAAGAGAAAAAAGAAAACAG

CTTTGAAATGCAAAGAGGTGATGAGGATCCTCAAATTGCAGCACACGTTGTAAGCGA

AGCCAACAGTAATGCAGCATCCGTTCTACAGTGGGCCAAGAAAGGATATTATACCAT

GAAAAGCAACTTGGTAATGCTTGAAAATGGGAAACAGCTGACGGTTAAAAGAGAAG

GACTCTATTATGTCTACACTCAAGTCACCTTCTGCTCTAATCGGGAGCCTTCGAGTCA

ACGCCCATTCATCGTCGGCCTCTGGCTGAAGCCCAGCAGTGGATCTGAGAGAATCTT

ACTCAAGGCGGCAAATACCCACAGTTCCTCCCAGCTTTGCGAGCAGCAGTCTGTTCA

CTTGGGCGGAGTGTTTGAATTACAAGCTGGTGCTTCTGTGTTTGTCAACGTGACTGA

AGCAAGCCAAGTGATCCACAGAGTTGGCTTCTCATCTTTTGGCTTACTCAAACTCTG

A*GAATTC*TGCAGATATCCAGCACAGTGGCGGCCGCTCGAGTCTAGAGGGCCCGT

Figure 4 Nucleotide splicing sequence result of pcDNA3.1$^+$-mCD40L with DNAstar software analysis.

Recombinant plasmid pcDNA3.1$^+$-mCD40L sequence analysis

Plasmid DNA was extracted. The correct plasmids identified by restriction analysis were sequenced. The result of sequencing is shown in Figures 2-4. It demonstrated that integral mCD40L cDNA containing start codon, stop codon and endonuclease sites was cloned into eukaryotic expression vector pcDNA3.1$^+$.

RT-PCR

RT-PCR analysis showed that 0.8 kb fragments corresponding to the mCD40L cDNA were amplified with the total cellular RNA only from pcDNA3.1$^+$-mCD40L-transduced H22 cells, but not from the cells transduced with pcDNA3.1$^+$ (Figure 5).

Immunofluorescence staining of transfected cells

The transfected cells were coated with mCD40L antibody and fluorescent antibody. Under fluorescence microscopes, it was observed that the fluorescence staining was positive in the cytoplasm of H22 cells transfected with pcDNA3.1$^+$-mCD40L and negative in the controls (Figure 6).

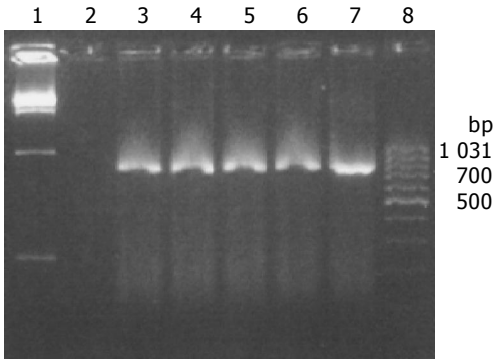

Figure 5 mCD40L gene expression in H22 cells by RT-PCR. Lanes 1 and 8: marker; Lane 2: negative control; Lanes 3-6: RT-PCR products from transfected H22 cells; Lane 7: RT-PCR product from BALB/C mouse splenocytes.

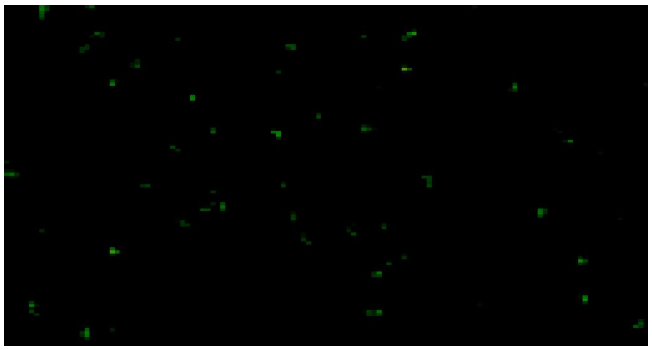

Figure 6 H22 cells transfected with pcDNA3.1$^+$-mCD40L. The fluorescence staining in the cytoplasm was positive. ×400.

DISCUSSION

Hepatocellular carcinoma (HCC) is a very common malignancy in China, and has a very poor prognosis[1]. Despite recent increases in therapeutic options, such as total vascular exclusion (TVE) technique used in hepatectomies of advanced and complicated hepatocellular carcinomas, combined multimodal interventional therapies which have revealed their advantages as compared with any single therapeutic regimen and play more important roles in treating unresectable HCC[9], and hepatic arterial infusion chemotherapy which may be a useful alternative for the treatment of patients with advanced HCC[10], percutaneous cryoablation which offers a safe and possibly curative treatment option for patients with HCC that can not be surgically removed[11], HCC remains one of the leading causes of death. The malignancies are often resistant to chemotherapy and metastasize to distant organs in the early stage of the disease. Even after the primary tumor is removed surgically, relapse at the primary or distant sites frequently occurs. Surgical resection itself may not accelerate cancer dissemination and increase postoperative recurrence significantly[12]. Preoperative level of circulating VEGF mRNA, especially isoform VEGF165, plays a significant role in the prediction of postoperative recurrence of HCC. Gene therapy provides new possibilities for the treatment of incurable diseases, including hepatocellular carcinoma[13].

However, the host immunity frequently fails to eliminate malignant tumors caused either by the lack of recognizable tumor antigens or by the inability of tumor antigens to stimulate an effective immune response[14,15], thus most malignant tumors evade host immune surveillance. The use of gene therapy with immunostimulatory molecules aiming at enhancing antitumoral immunity has emerged as a promising new approach to treat cancer[16,17].

CD40L-CD40 interactions on menbranes of APC, including dendritic cells (DCs), can activate APC, promote effective antigen presentation, express costimulatory and adhesion molecules, and up-regulate cytokine and chemokine production. For instance, CD40L-CD40 interactions strongly promote Th1 differentiation and provide a strong signal for interleukin (IL)-12 production, even in the presence of Th2 cytokines[18]. The endogenous production of IL-12 resulting from CD40L-CD40 interaction may play a role in the persistence of antitumor effects[19]. CD40 activation through CD40L-CD40 interaction may be used as a potential treatment tool of malignant neoplasms[20]. The rational for transducing tumor cells with CD40L is to convert these cells into stimulators of APC, an effect leading to enhanced presentation of tumor antigens to T cells and activation of antitumor immune responses. In fact, CD40L-CD40 interactions have been demonstrated to overcome tumor-specific CD4+ and CD8+ tolerance and induce antitumor immunity[21,22]. It remains possible that combining CD40L gene with another immunotherapeutic modality (*e.g.*, IL-12, CD80) or with a tumor associated antigen (*e.g.*, alpha fetoprotein, AFP) gene therapy would be still better. Using mCD40L gene or combining with IL-12 gene transduced leukemia cell therapy for chronic lymphocytic leukemia (CLL)[23], primary B-CLL[24,25] and acute leukemia[26] has provided encouraging results. Treatment not only appears capable of inducing a cellular anti-leukemia immunity, but also may have a direct effect on leukemia cells by inducing latent sensitivity to Fas (CD95)-dependent leukemia cell apoptosis[26]. Recently, many investigators have reported that *ex vivo* transduction of tumor cells with the mCD40L gene or *in vivo* transfer of the mCD40L gene is able to induce antitumor immunity against different tumor cell lines in subcutaneous tumor models, such as lung cancer[27,28], colon cancer[29,30], urologic malignancies[31-33], melanoma[34] and malignant mesothelioma[35]. In HCC, Schmitz *et al*[8] used adenovirus-mediated CD40 ligand gene therapy for orthotopic hepatocellular carcinoma, and demonstrated that it abrogated HCC cell tumorigenicity when expressing mCD40L gene, and led to complete tumor eradication and long-term survival in most of the treated animals. Yanagi *et al*[36] showed that Flt3L and CD40L significantly induced antitumor immunity against MH134 cells presumably through both innate and adaptive immunity. These data reveal that administration of mCD40L gene might provide an efficient and safe treatment for HCC.

In summary, mCD40L gene has shown its profound effect on HCC treatment in animal models. In our experiment, we could successfully construct the recombined mCD40L eukaryotic expression vector, and the mCD40L expressed in H22 cells effectively. This, we believe, provides experimental data for gene therapy and immunotherapy of HCC.

REFERENCES

1 **Tang ZY**. Hepatocellular carcinoma-cause, treatment and metastasis. *World J Gastroenterol* 2001; **7**: 445-454
2 **Mach F**, Schonbeck U, Sukhova GK, Bourcier T, Bonnefoy JY, Pober JS, Libby P. Functional CD40 ligand is expressed on human vascular endothelial cells, smooth muscle cells, and macrophages: implications for CD40-CD40 ligand signaling in atherosclerosis. *Proc Natl Acad Sci USA* 1997; **94**: 1931-1936
3 **Grewal IS,** Flavell RA. CD40 and CD154 in cell-mediated immunity. *Annu Rev Immunol* 1998; **16**: 111-135
4 **Roy M,** Waldschmidt T, Aruffo A, Ledbetter JA, Noelle RJ. The regulation of the expression of gp39, the CD40 ligand, on normal and cloned CD4+ T cells. *J Immunol* 1993; **151**: 2497-2510
5 **Ridge JP**, Di Rosa F, Matzinger P. A conditioned dendritic cell can be a temporal bridge between a CD4+ T-helper and a T-

killer cell. *Nature* 1998; **393**: 474-478
6 **Bennett SR**, Carbone FR, Karamalis F, Flavell RA, Miller JF, Heath WR. Help for cytotoxic-T-cell responses is mediated by CD40 signalling. *Nature* 1998; **393**: 478-480
7 **Schoenberger SP**, Toes RE, van der Voort EI, Offringa R, Melief CJ. T-cell help for cytotoxic T lymphocytes is mediated by CD40-CD40L interactions. *Nature* 1998; **393**: 480-483
8 **Schmitz V**, Barajas M, Wang L, Peng D, Duarte M, Prieto J, Qian C. Adenovirus-mediated CD40 ligand gene therapy in a rat model of orthotopic hepatocellular carcinoma. *Hepatology* 2001; **34**: 72-81
9 **Miyazaki M**, Ito H, Nakagawa K, Shimizu H, Yoshidome H, Shimizu Y, Ohtsuka M, Togawa A, Kimura F. An approach to intrapericardial inferior vena cava through the abdominal cavity, without median sternotomy, for total hepatic vascular exclusion. *Hepatogastroenterology* 2001; **48**: 1443-1446
10 **Mazzanti R,** Giallombardo AL, Mini E, Nobili S, Neri B, Arena U, Pantaleo P, Fabbroni V, Ghilardi M, Gattai R, Bandettini L. Treatment of locally advanced hepatocellular carcinoma by hepatic intra-artery chemotherapy: a pilot study. *Dig Liver Dis* 2004; **36**: 278-285
11 **Qian GJ,** Chen H, Wu MC. Percutaneous cryoablation after chemoembolization of liver carcinoma: report of 34 cases. *Hepatobiliary Pancreat Dis Int* 2003; **2**: 520-524
12 **Chen WT**, Chau GY, Lui WY, Tsay SH, King KL, Loong CC, Wu CW. Recurrent hepatocellular carcinoma after hepatic resection: prognostic factors and long-term outcome. *Eur J Surg Oncol* 2004; **30**: 414-420
13 **Ruiz J**, Mazzolini G, Sangro B, Qian C, Prieto J. Gene therapy of hepatocellular carcinoma. *Dig Dis* 2001; **19**: 324-332
14 **Chouaib S**, Asselin-Paturel C, Mami-Chouaib F, Caignard A, Blay JY. The host-tumor immune conflict: from immunosuppression to resistance and destruction. *Immunol Today* 1997; **18**: 493-497
15 **Gabrilovich DI**, Chen HL, Girgis KR, Cunningham HT, Meny GM, Nadaf S, Kavanaugh D, Carbone DP. Production of vascular endothelial growth factor by human tumors inhibits the functional maturation of dendritic cells. *Nat Med* 1996; **2**: 1096-1103
16 **Ruiz J**, Qian C, Drozdzik M, Prieto J. Gene therapy of viral hepatitis and hepatocellular carcinoma. *J Viral Hepat* 1999; **6**: 17-34
17 **Melero I**, Mazzolini G, Narvaiza I, Qian C, Chen L, Prieto J. IL-12 gene therapy for cancer: in synergy with other immunotherapies. *Trends Immunol* 2001; **22**: 113-115
18 **Bullens DM**, Kasran A, Thielemans K, Bakkus M, Ceuppens JL. CD40L-induced IL-12 production is further enhanced by the Th2 cytokines IL-4 and IL-13. *Scand J Immunol* 2001; **53**: 455-463
19 **Harada M**, Tamada K, Abe K, Yasumoto K, Kimura G, Nomoto K. Role of the endogenous production of interleukin 12 in immunotherapy. *Cancer Res* 1998; **58**: 3073-3077
20 **Ottaiano A**, Pisano C, De Chiara A, Ascierto PA, Botti G, Barletta E, Apice G, Gridelli C, Iaffaioli VR. CD40 activation as potential tool in malignant neoplasms. *Tumori* 2002; **88**: 361-366
21 **Sotomayor EM**, Borrello I, Tubb E, Rattis FM, Bien H, Lu Z, Fein S, Schoenberger S, Levitsky HI. Conversion of tumor-specific CD4+ T-cell tolerance to T-cell priming through *in vivo* ligation of CD40. *Nat Med* 1999; **5**: 780-787
22 **Diehl L**, den Boer AT, Schoenberger SP, van der Voort EI, Schumacher TN, Melief CJ, Offringa R, Toes RE. CD40 activation *in vivo* overcomes peptide-induced peripheral cytotoxic T-lymphocyte tolerance and augments anti-tumor vaccine efficacy. *Nat Med* 1999; **5**: 774-779
23 **Wierda WG**, Cantwell MJ, Woods SJ, Rassenti LZ, Prussak CE, Kipps TJ. CD40-ligand (CD154) gene therapy for chronic lymphocytic leukemia. *Blood* 2000; **96**: 2917-2924
24 **Wendtner CM**, Kofler DM, Theiss HD, Kurzeder C, Buhmann R, Schweighofer C, Perabo L, Danhauser-Riedl S, Baumert J, Hiddemann W, Hallek M, Buning H. Efficient gene transfer of CD40 ligand into primary B-CLL cells using recombinant adeno-associated virus (rAAV) vectors. *Blood* 2002; **100**: 1655-1661
25 **von Bergwelt-Baildon M,** Maecker B, Schultze J, Gribben JG. CD40 activation: potential for specific immunotherapy in B-CLL. *Ann Oncol* 2004; **15**: 853-857
26 **Saudemont A**, Buffenoir G, Denys A, Desreumaux P, Jouy N, Hetuin D, Bauters F, Fenaux P, Quesnel B. Gene transfer of CD154 and IL12 cDNA induces an anti-leukemic immunity in a murine model of acute leukemia. *Leukemia* 2002; **16**: 1637-1644
27 **Noguchi M,** Imaizumi K, Kawabe T, Wakayama H, Horio Y, Sekido Y, Hara T, Hashimoto N, Takahashi M, Shimokata K, Hasegawa Y. Induction of antitumor immunity by transduction of CD40 ligand gene and interferon-gamma gene into lung cancer. *Cancer Gene Ther* 2001; **8**: 421-429
28 **Tada Y**, O-Wang J, Yu L, Shimozato O, Wang YQ, Takiguchi Y, Tatsumi K, Kuriyama T, Takenaga K, Sakiyama S, Tagawa M. T-cell-dependent antitumor effects produced by CD40 ligand expressed on mouse lung carcinoma cells are linked with the maturation of dendritic cells and secretion of a variety of cytokines. *Cancer Gene Ther* 2003; **10**: 451-456
29 **Sun Y**, Peng D, Lecanda J, Schmitz V, Barajas M, Qian C, Prieto J. *In vivo* gene transfer of CD40 ligand into colon cancer cells induces local production of cytokines and chemokines, tumor eradication and protective antitumor immunity. *Gene Ther* 2000; **7**: 1467-1476
30 **Buning C**, Kruger K, Sieber T, Schoeler D, Schriever F. Increased expression of CD40 ligand on activated T cells of patients with colon cancer. *Clin Cancer Res* 2002; **8**: 1147-1151
31 **Loskog A**, Totterman TH, Bohle A, Brandau S. *In vitro* activation of cancer patient-derived dendritic cells by tumor cells genetically modified to express CD154. *Cancer Gene Ther* 2002; **9**: 846-853
32 **Loskog A**, Bjorkland A, Brown MP, Korsgren O, Malmstrom PU, Totterman TH. Potent antitumor effects of CD154 transduced tumor cells in experimental bladder cancer. *J Urol* 2001; **166**: 1093-1097
33 **Hussain SA**, Ganesan R, Hiller L, Murray PG, el-Magraby MM, Young L, James ND. Proapoptotic genes BAX and CD40L are predictors of survival in transitional cell carcinoma of the bladder. *Br J Cancer* 2003; **88**: 586-592
34 **Peter I**, Naweath M, Kamarashev J, Odermatt B, Mezzacasa A, Hemmi S. Immunotherapy for murine K1735 melanoma: combinatorial use of recombinant adenovirus expressing CD40L and other immunomodulators. *Cancer Gene Ther* 2002; **9**: 597-605
35 **Friedlander PL**, Delaune CL, Abadie JM, Toups M, LaCour J, Marrero L, Zhong Q, Kolls JK. Efficacy of CD40 ligand gene therapy in malignant mesothelioma. *Am J Respir Cell Mol Biol* 2003; **29**: 321-330
36 **Yanagi K**, Nagayama Y, Nakao K, Saeki A, Matsumoto K, Ichikawa T, Ishikawa H, Hamasaki K, Ishii N, Eguchi K. Immuno-gene therapy with adenoviruses expressing fms-like tyrosine kinase 3 ligand and CD40 ligand for mouse hepatoma cells *in vivo*. *Int J Oncol* 2003; **22**: 345-351

Edited by Kumar M and Zhu LH

PO Box 2345, Beijing 100023, China
Fax: +86-10-85381893
E-mail: wjg@wjgnet.com www.wjgnet.com

ELSEVIER

World J Gastroenterol 2005;11(2):187-192
World Journal of Gastroenterology ISSN 1007-9327

• LIVER CANCER •

Clinical significance of the expression of isoform 165 vascular endothelial growth factor mRNA in noncancerous liver remnants of patients with hepatocellular carcinoma

I-Shyan Sheen, Kuo-Shyang Jeng, Shou-Chuan Shih, Chih-Roa Kao, Wen-Hsing Chang, Horng-Yuan Wang, Po-Chuan Wang, Tsang-En Wang, Li-Rung Shyung, Chih-Zen Chen

I-Shyan Sheen, Liver Research Unit, Division of Hepatogastroenterology, Chang Gung Memorial Hospital, Taipei, Taiwan, China
Kuo-Shyang Jeng, Department of Surgery, Mackay Memorial Hospital, Taipei, Taiwan, China
Shou-Chuan Shih, Chih-Roa Kao, Wen-Hsing Chang, Horng-Yuan Wang, Po-Chuan Wang, Tsang-En Wang, Li-Rung Shyung, Chih-Zen Chen, Medical Department, Mackay Memorial Hospital, Taipei, Taiwan, China
Kuo-Shyang Jeng, Mackay Junior School of Nursing, Taipei, Taiwan, China
Supported by the Grants from the Department of Medical Research, Mackay Memorial Hospital, Taiwan, China (MMH9237)
Correspondence to: Kuo-Shyang Jeng, M.D., F.A.C.S., Department of Surgery, Mackay Memorial Hospital, No. 92, Sec 2, Chung-San North Road, Taipei, Taiwan, 10449, China. issheen.jks@msa.hinet.net
Telephone: +886-2-5433535 **Fax:** +886-2-27065704
Received: 2004-05-07 **Accepted:** 2004-07-05

Abstract

AIM: To investigate the prognostic role of isoform 165 vascular endothelial growth factor messenger RNA ($VEGF_{165}$ mRNA) in noncancerous liver tissues from patients with primary hepatocellular carcinoma (HCC).

METHODS: Using a reverse-transcription polymerase chain reaction (RT-PCR)-based assay, VEGF mRNA was determined prospectively in noncancerous liver tissues from 60 consecutive patients with HCC undergoing curative resection. We categorized the patients with $VEGF_{165}$ mRNA over 0.500 in noncancerous liver tissues as group A, and those below 0.500 as group B.

RESULTS: Among the isoforms of VEGF mRNA by multivariate analysis, a higher level of $VEGF_{165}$ mRNA in noncancerous liver tissue correlated significantly with a higher risk of HCC recurrence ($P = 0.039$) and recurrence-related mortality ($P = 0.048$), but $VEGF_{121}$ did not. The other significant predictors of recurrence consisted of vascular permeation ($P = 0.022$), daughter nodules ($P = 0.033$), cellular dedifferentiation ($P = 0.033$), an absent or incomplete capsule ($P = 0.037$). A significant variable of recurrence-related mortality was vascular permeation ($P = 0.012$). As to the clinical manifestations of 16 patients who developed recurrence, the recurrent tumor number over 2, recurrent extent over two-liver segments, and the median survival after recurrence, all significantly correlated with group A patients ($P = 0.043$, 0.043, and 0.048, respectively). However, the presence of extrahepatic metastasis was not ($P>0.05$). The difference in recurrence after treatment between the two groups had no statistical significance ($P>0.05$).

CONCLUSION: The higher expression of isoform $VEGF_{165}$ mRNA in noncancerous liver remnant of patients with HCC may be a significant biological indicator of the invasiveness of postoperative recurrence.

Key words: Hepatocellular carcinoma; VEGF protein; Messenger RNA

Sheen IS, Jeng KS, Shih SC, Kao CR, Chang WH, Wang HY, Wang PC, Wang TE, Shyung LR, Chen CZ. Clinical significance of the expression of isoform 165 vascular endothelial growth factor mRNA in noncancerous liver remnants of patients with hepatocellular carcinoma. *World J Gastroenterol* 2005; 11 (2): 187-192
http://www.wjgnet.com/1007-9327/11/187.asp

INTRODUCTION

Hepatocellular carcinoma (HCC) is one of the most common malignant tumors with a poor prognosis. During the last 10 years, efforts have been made worldwide toward earlier detection and safer surgical resection of HCC. However, despite these recent diagnostic and therapeutic advances, postoperative recurrence is still common[1-3]. How to early predict the prognosis after resection is a challenging problem for surgeons.

It is well known that the development of a tumor requires oxygen and nutrients, which are supplied through neovascularization. Angiogenic potential is a prerequisite for tumor growth[4-9]. Thus, enhanced gene expression of angiogenic factors in a developing tumor is strongly expected. The release of angiogenic factors from malignant tumors, in turn, would lead to the production of vascular endothelial cells via a paracrine mechanism. Among the potential angiogenic factors, vascular endothelial growth factor (VEGF) is the most potently direct acting and specific one. The variation in size due to alternative exon splicing may produce four different isoforms of 121, 165, 189 and 206 amino acids (monomeric size)[10,11]. According to Ferrara's analysis, $VEGF_{165}$ is the predominantly expressed form in human cDNA libraries as in most normal cells and tissues[12]. Different cancers may have different expressions of the isoforms. The majority of HCCs expresses an abundance of $VEGF_{121}$ and $VEGF_{165}$[10-12].

Angiogenesis in tumors has been proven to be an independent factor of prognosis and metastasis in many carcinomas[13-15]. Mise *et al*[16] found that VEGF mRNA was also expressed in nontumorous portions of the livers. It remains unknown whether the degree of angiogenesis in nontumorous liver tissues contributes to the grade of HCC malignancy and the potential of postresection recurrence[16].

This study was to elucidate the correlation between VEGF mRNA expression in noncancerous liver tissues and the clinicopathological manifestations of postoperative recurrence, so to provide a useful prognostic parameter for predicting the recurrence.

MATERIALS AND METHODS

Study population

Sixty consecutive patients (35 men and 25 women, with a mean age of 54.5±13.5 years) with HCC undergoing curative hepatectomy from November 2000 to November 2003, were enrolled in this prospective study. Patients who had a previous history of hepatectomy or preoperative neoadjuvant ethanol injection or hepatic arterial chemoembolization (TACE) were all excluded. Surgical procedures performed included 44 major resections (8 extended right lobectomies, 14 right lobectomies, 9 left lobectomies, and 13 two-segmentectomies) and 16 minor resections (14 one-segmentectomies, 1 subsegmentectomy, and 1 wedge resection). Noncancerous liver tissues were obtained from the contralateral lobe remnant of all 60 patients during hepatectomy. The liver tissue was taken at least 3 cm far from the resection margin of HCC. We changed instruments in this procedure to avoid seeding or contaminating the liver biopsy tissues by HCC cells. A control group including 10 healthy volunteers without liver disease (5 men, 5 women, mean age 50 years) and 20 patients with chronic liver disease (10 with liver cirrhosis, 5 with hepatitis B carrier but no cirrhosis, 5 with hepatitis C carrier but no cirrhosis) but without any evidence of HCC also received liver biopsies during laparotomy for other reasons. All liver tissues were examined for VEGF mRNA. All of the patients agreed to participate in this study preoperatively.

Demographic data analysis

Clinicopathological variables analyzed included age, sex (male *vs* female), presence of liver cirrhosis, Child-Pugh class of liver functional reserve (A *vs* B), hepatitis B virus (HBV) infection (hepatitis B surface antigen, HBsAg), hepatitis C virus (HCV) infection (anti-hepatitis C virus antibody, Anti-HCV), serum alfafetoprotein (AFP) level (< 20 ng/mL *vs* 20 to 1 000 ng/mL *vs* ⩾ 1 000 ng/mL), tumor size (<3 cm *vs* 3 to 10 cm *vs* ⩾ 10 cm), tumor encapsulation (complete *vs* incomplete or absent), presence of daughter nodules, vascular permeation (including vascular invasion and/or tumor thrombi in either the portal or hepatic vein), and cell differentiation grade (Edmondson and Steiner grades I to IV) (Table 1).

Table 1 Characteristics of 60 patients with HCC undergoing curative resection

Variables	No. of patients (%)
Age (mean, yr) (±SD)	50.4±12.6
Male	44 (73)
Cirrhosis	47 (78)
Child- Pugh's class A	43 (72)
Serum AFP < 20 ng/mL	19 (32)
20-10^3 ng/mL	29 (48)
>10^3 ng/mL	12 (20)
HBsAg (+)	47 (78)
Anti-HCV (+)	32 (53)
Size of HCC <3 cm	17 (28)
3-10 cm	22 (37)
>10 cm	2 (35)
Edmondson-Steiner's grade I	13 (22)
Grade II	11 (18)
Grade III	18 (30)
Grade IV	18 (30)
Absent or incomplete capsule	39 (65)
Vascular permeation	33 (55)
Daughter nodules	31 (52)

AFP: serum alpha fetoprotein; HBsAg (+): positive hepatitis B surface antigen; Anti-HCV (+): positive hepatitis C virus antibody; Edmondson Steiner grade: differentiation grade.

Detection of VEGF mRNA

It included extraction of RNA and reverse transcription, and amplification of cDNA of VEGF and GAPDH by PCR.

Extraction of RNA and reverse transcription We homogenized each resected tissue (including noncancerous liver tissues and control liver tissues) completely in 1 mL of RNA-bee™, and added 0.2 mL chloroform and shook it vigorously for 15-30 s. We stored the sample on ice for 5 min and centrifuged at 12 000 *g* for 15 min. We transferred the supernatant to a new 1.5 mL Eppendorf tube and precipitated it with 0.5 mL of isopropanol. The precipitation was as short as 5 min at 4 ℃. We centrifuged it at 12 000 *g* for 5 min at 4 ℃. Then we removed the supernatant and washed the RNA pellet with 1 mL of 75% ethanol, shaking to dislodge the pellet from the side of the tube. We centrifuged it at 7 500 *g* for 5 min at 4 ℃ and carefully removed ethanol, the supernatant and dissolved RNA in DEPC-H_2O (usually between 50-100 uL), and stored it at -80 ℃.

We heated the RNA sample at 55 ℃ for 10 min and chilled it on ice. We added into it the following components: (1) 4 μL 5×RT butter containing a composition of 50 mmol/L Tris-HCl (pH 8.3), 75 mmol/L KCl, 3 mmol/L $MgCl_2$ and 10 mmol/L DTT (dithiothreitol), (2) 3 μL 10 mmol/L dNTP, (3) 1.6 μL Oligo-d$(T)_{18}$ and 0.4 μL random hexamers (N)6 (1 μg/μL), (4) 0.5 μL RNase inhibitor (40 units/ μL), (5) 3 μL 25 mmol/L $MnCl_2$, (6) 6 μL RNA in DEPC-H_2O, (7) 0.5 μL DEPC-H_2O. We incubated at 70 ℃ for 2 min, chilled it to 23 ℃ to anneal primer to RNA. We added 1 μL of M-MLV RTase to (Moloney murine leukemia virus revers transcriptase, 200 units/μL, Promega product). We incubated it for 8 min at 23 ℃, then for 60 min at 40 ℃. We heated the reaction at 94 ℃ for 5 min and chilled it on ice and stored cDNA at -20 ℃.

Amplification of cDNA of VEGF and GAPDH by PCR The sequences of the sense primers were 5'-AGTGTGTGCCC ACTGAGGA-3' (VEGF) and 5'-AGTCAACGGATTTGGTC GTA-3'(GAPDH) and those of the antisense primers were 5'-AGTCAACGGATTTGGTCGTA-3'(VEGF) and 5'-GGAACA TGTAAACCATGTAG-3' (GAPDH). The first polymerase chain reaction (RT-PCR) solution contained 5 μL of the synthesized cDNA solution, 10 μL of 10× polymerase reaction buffer, 500 μmol/L each of dCTP, dATP, dGTP and dTTP, 15 pmoL of each external primer (EX-sense and EX-antisense), 4 units of Thermus Brockiamus Prozyme DNA polymerase (PROtech Technology Ent. Co., Ltd., Taipei, Taiwan) and water. The PCR cycles were denatured at 94 ℃ for 1 min, annealed at 52 ℃ for 1 min, and primer extension at 72 ℃ for 1 min. The cycles were repeated 40 times. The PCR products were reamplified with internal primers for nested PCR to obtain a higher sensitivity. The first and second PCR components were the same, but for the primer pairs (IN-sense and IN-antisense), the final products were electrophoresed on 2% agarose gel and stained with ethidium bromide. Four different isoforms of human VEGF were identified, arising from alternative splicing of the primary transcript of a single gene. The majority were $VEGF_{121}$ (165 bp) and $VEGF_{165}$ (297 bp). The percentage intensity of the VEGF PCR fragment for each liver was relative to a GAPDH PCR fragment (122 bp). The intensity of bands was measured using Fujifilm Science Lab 98 (Image Gauge V3.12). The sensitivity of our assay was assessed using human hepatocytes.

For a positive control for VEGF mRNA expression , we used a hepatoblastoma cell line (HepG2). EDTA-treated water (filtered and vaporized) served as negative controls.

Follow-up study after recurrence

From the value of $VEGF_{165}$ mRNA of noncancerous liver remnant, we divided the HCC patients into two groups, i.e., those with a higher level of $VEGF_{165}$ mRNA (over 0.500) as group A, and

those with a lower level of $VEGF_{165}$ mRNA (below 0.500) as group B.

After discharge, all the patients were assessed regularly to detect tumor recurrence with abdominal ultrasonography (every 2-3 mo during the first 5 years, then every 4-6 mo thereafter), serum AFP and liver biochemistry (every 2 mo during the first 2 years, then every 4 mo during the following 3 years, and every 6 mo thereafter), abdominal computed tomography (CT) (every 6 mo during the first 5 years, then annually), and chest x-ray and bone scans (every 6 mo). Hepatic arteriography was obtained if other studies suggested possible cancer recurrence. Detection of tumors on any imaging study was defined as clinical recurrence.

After the detection of recurrence, the following prognostic factors were analyzed and compared between group A and group B: extrahepatic metastasis (presence or absence), the number of recurrent tumor lesions (solitary or multiple), and the extent of recurrent tumors (affecting more than or less than two segments), treatments for recurrent tumors (surgical or non surgical treatment), and survival time after recurrence. The number and extent of recurrent tumors were evaluated and counted from abdominal CT scan and hepatic arteriography.

Statistical analysis

A statistical software (SPSS for Windows, version 8.0, Chicago, Illinois) was employed, Student's *t*-test was used to analyze continuous variables and chi-square test or Fisher's exact test was used for categorical variables. Parameters relating to the presence of VEGF mRNA in liver tissue were analyzed by stepwise logistic regression. A Cox proportional hazard model was used for multivariate stepwise analysis to identify significant variables for outcome of recurrence and mortality. $P<0.05$ was considered statistically significant.

RESULTS

RT-PCR analysis of VEGF transcript in liver tissues

VEGF mRNA was detected in the liver tissues of 10 ($VEGF_{165}$ in 10 and $VEGF_{121}$ in 6) of 30 control patients but the values were very low (all below 0.005). In the HCC group, isoform $VEGF_{165}$ was expressed in noncancerous liver tissues of all 60 patients (100%) (with a value ranging from 0.176 to 0.784) and isoform $VEGF_{121}$ in 36 patients (60.0%) (with a value ranging from 0.285 to 1.030). As to $VEGF_{165}$ mRNA values, 49 (81.7%) patients belonged to group A and 11 patients (18.3%) belonged to group B.

We did not detect isoforms $VEGF_{189}$ and/or $VEGF_{206}$ in any noncancerous liver tissues or control liver tissues.

Correlation between VEGF mRNA expression in noncancerous liver tissues and clinical histopathologic characteristics

Amongall the patients' characteristics, age, gender, liver cirrhosis, Child-Pugh class A or B, size of HCC, positivity of HBsAg or anti-HCV, and level of serum AFP showed no statistically significant difference between groups A and B (Table 2). From both univariate and multivariate analyses, the correlation between higher $VEGF_{165}$ mRNA expression in liver remnant tissues and grade of cellular differentiation (Edmondson Steiner grade), incomplete or absent capsule, presence of daughter nodules, and vascular permeation was significant respectively (Table 2).

Table 3 shows that group A patients had more tumor recurrence (28.6% *vs* 18.2%, $P = 0.039$), and more recurrence-related death (26.5% *vs* 9.1%, $P = 0.048$). After analysis with Cox proportional hazard model, a higher expression of $VEGF_{165}$ mRNA in the liver remnant had a significant correlation with both a shorter recurrence-free interval and a shorter survival time ($P = 0.037$ and 0.040, respectively) (Table 3). Factors influencing HCC recurrence and time lapse to recurrence were vascular permeation ($P = 0.022$, OR = 5.36), daughter nodules ($P = 0.033$, OR = 4.18), cellular dedifferentiation ($P = 0.033$, OR = 4.18), incomplete or absent capsule ($P = 0.037$, OR = 3.10), and higher $VEGF_{165}$ mRNA expression in the liver remnant ($P = 0.039$, OR = 2.29) (Table 4). The significant variables affecting death resulting from recurrence included vascular permeation ($P = 0.012$, OR = 8.35) and higher $VEGF_{165}$ mRNA expression in the liver remnant ($P = 0.048$, OR = 2.38) (Table 4).

During the follow-up period (range 1 to 3 years, median 2 years), 16 patients (26.7%) had clinically detected recurrence. In 16 patients with recurrent HCCs, there was no statistically significant correlation between the status of a higher $VEGF_{165}$ mRNA expression in the liver remnant and the treatment for recurrent tumors, and the existence of extrahepatic metastasis ($P>0.05$, respectively) (Table 5). However, compared with the extent of intrahepatic recurrence and the outcome, group A patients had a greater number of HCC nodules ($P = 0.043$), and a greater involvement of over two-liver segments ($P = 0.043$). The median survival after recurrence was significantly shorter (4.4 mo *vs* 11.0 mo) in group A ($P = 0.048$) (Table 5).

Table 2 Comparison of characteristics of primary HCC between different levels of $VEGF_{165}$ mRNA in noncancerous liver tussues

Characteristics	Group A (%) (n = 49)	Group B (%) (n = 11)	P
Age (yr, mean)	52	48	NS
Male	73.5	72.7	NS
Liver cirrhosis	79.6	72.7	NS
Child-Pugh class A	71.4	72.7	NS
Tumor size <3 cm	28.6	27.2	NS
>10 cm	34.7	36.4	NS
HBsAg (+)	79.6	72.7	NS
Anti-HCV (+)	53.1	54.5	NS
AFP <20 ng/mL	32.7	27.2	NS
>1 000 ng/mL	20.4	18.2	NS
Edmondson-Steiner grade I[1]	10.2	72.7	0.009
Capsule incomplete or absent[2]	75.5	18.2	0.007
Daughter nodules[3]	61.2	9.1	0.001
Vascular permeation[4]	65.3	9.1	0.001

Notes: high $VEGF_{165}$ mRNA: ⩾0.500 (group A); low $VEGF_{165}$ mRNA: <0.500 (group B). *P*: by univariate analysis. 1, 2, 3 and 4: the significant variables in multivariate analysis with *P* values of 0.036, 0.048, 0.024, and 0.019 respectively. HBsAg: hepatitis B surface antigen; Anti-HCV: antibody to hepatitis C virus; AFP: alpha-fetoprotein; NS: no statistical significance.

Table 3 Correlation between $VEGF_{165}$ mRNA expression in liver remnant and the outcome of patients with HCC

Outcome	Group A (n = 49)	Group B (n = 11)	P
Recurrence (number; %)	14 (28.6)	2 (18.2)	0.039
Death[1] (number; %)	13 (26.5)	1 (9.1)	0.048
Recurrence-free interval (median, mo)	8.5	43.0	0.037
Duration of survival (median, mo)	11.5	41.5	0.040

Notes: high $VEGF_{165}$ mRNA: ⩾0.500 (group A), low $VEGF_{165}$ mRNA: <0.500 (group B), death[1]: patients died of HCC recurrence.

Table 4 Factors influencing tumor recurrence and death of patients in multivariate analysis

Variables	*P*	OR
Recurrence		
Vascular permeation	0.022	5.36
Daughter nodules	0.033	4.18
Cellular dedifferentiation	0.033	4.18
Incomplete or absent capsule	0.037	3.10
Higher $VEGF_{165}$ mRNA in liver remnant	0.039	2.29
Death		
Vascular permeation	0.012	8.35
Higher $VEGF_{165}$ mRNA in liver remnant	0.048	2.38

OR: odds ratio; higher $VEGF_{165}$ mRNA: value $\geqslant$0.500.

Table 5 Correlation between the clinical features of recurrent hepatocellular carcinoma and the expression of $VEGF_{165}$ mRNA in primary lesions

Clinical features	$VEGF_{165}$ mRNA		*P*
	high (n = 14)	low (n = 2)	
Extent of recurrent tumors:			
Extrahepatic metastasis (number, %)	8 (57.1)	1 (50.0)	NS
Multiple recurrent tumors (number, %)	10 (71.4)	1 (50.0)	0.043
Involvement over two-segments (number, %)	10 (71.4)	1 (50.0)	0.043
Survival after recurrence (median mo)	4.4	11.0	0.048
Treatment for recurrent tumors			
Surgery (number)	0	0	NS
Non-surgical treatment[1] (number, %)	8 (57.1)	1 (50.0)	NS
No treatment (number, %)	6 (42.9)	1 (50.0)	NS

Notes: NS: no statistical significance; non-surgical treatments[1]: treatment with transcatheter arterial chemoembolization or/and percutaneous ethanol injection. High $VEGF_{165}$ mRNA: $\geqslant$0.500; low $VEGF_{165}$ mRNA: <0.500.

DISCUSSION

Our study revealed that a higher value of VEGF mRNA isoform $_{165}$ in noncancerous liver remnant tissues of HCC patients was significantly associated with an increased risk of postoperative recurrence and disease mortality. Even after recurrence, those with a higher $VEGF_{165}$ mRNA expression had a larger extent of recurrence and a worse outcome. The value of VEGF mRNA isoform $_{121}$ in liver remnant tissues was not significantly predictive of the outcome.

Studies reporting the correlation between VEGF of noncancerous liver tissues and the potential recurrence were rare. Mise *et al*[16] found that vascular endothelial cells in tumorous tissues showed a dense VEGF immunostaining, whereas those in nontumorous tissues did not show any appreciable staining. In contrast, Feng *et al*[17] found VEGF protein was heterogeneously expressed both in almost all the noncarcinoma portions of the liver and in HCC portions of the liver with HCC. According to Feng *et al*, the nearer the non-cancerous liver cells were to cancerous cells, the stronger the VEGF expression they showed. In HCC cases, VEGF expression in non-cancerous liver cells was a little stronger than that in HCC cells, although there was no significant difference.

To be more accurate, we measured mRNA expression of VEGF in liver tissues rather than the protein itself. According to the study of El-Assal *et al*[18], the level of VEGF mRNA did not always correlate with the protein concentration. Immunohistochemistry could not distinguish small amounts of protein, which may partly explain the discrepancy in protein and mRNA levels. From the study of Mise *et al*, the level of VEGF mRNA in tumorous tissues was higher than that in corresponding nontumorous ones in 12 of 20 patients by more than 1.2-fold. In contrast, in only 2 cases VEGF mRNA levels were lower in tumorous tissues than that in nontumorous tissues (ratio<0.8)[16]. From our study, the level of VEGF mRNA in tumorous tissues was higher than that in corresponding nontumorous ones in 48 (80%) of 60 patients. In 9 patients, the two values were similar and their difference was less than 0.0005. In other 3 patients, VEGF mRNA levels were lower in tumorous tissues than that in nontumorous tissues. We attributed this discrepancy with the result of Mise *et al* to the different methods of mRNA examination and different backgrounds of study patients. The method we used was the nested RT-PCR which was more accurate than conventional RT-PCR.

The value of $VEGF_{165}$ mRNA in remnant livers was a ratio of its expression value to the expression value of GAPDH. We defined it as high if it was over 0.5000. There were 81.7% of our study patients belonging to the high-value group. The detailed mechanisms underlying the increase of VEGF mRNA in the remnant liver remain unclear.

In the literature, the tumor invasiveness variables included high-serum AFP, hepatitis, vascular permeation, grade of cellular differentiation, infiltration or absence of capsule, tumor size, coexisting cirrhosis, presence of daughter nodules, multiple lesions, p53 gene mutation, and gamma glutamyl transpeptidase expression[19-30]. Based on the study of Yamaguchi *et al*[31], VEGF expression in HCC tissues was thought to be related to the histological grade. Suzuki *et al*[32] found that VEGF mRNA expression in HCC was associated with fibrous capsule formation and septal formation. Whereas, as to the higher level of $VEGF_{165}$ mRNA in noncancerous liver tissues but not HCC itself from Table 2, we could find it corresponded significantly with some invasiveness variables (cellular differentiation, capsule status, daughter nodules, and vascular permeation) of primary HCC. We propose the following three possible pathogenetic mechanisms.

The first is that if HCC cells have a more invasive behavior, then they may secrete a higher level of VEGF. VEGF may enter the circulation and increase angiogenesis of the remnant liver via its paracrine growth factor function. Some authors reported that VEGF might be synthesized both in HCC cells and in liver cells, and accumulated in their target endothelial cells[32-39]. Yamaguchi *et al*[31] found VEGF was expressed in surrounding HCC tissues. The noncarcinoma liver cells themselves stimulated by VEGF might also secrete VEGF protein. This effect thus results in a longer and higher VEGF level in remnant liver.

The second is that the noncancerous liver remnant itself has a precancerous change. It is developing into an angiogenetic environment which may secrete a higher VEGF. The mechanism of the precancerous change may be complex, not only influenced by the original HCC itself. Coexisting cirrhosis might contribute to VEGF level[18]. Sasaki *et al*[24] emphasized that cirrhosis had a higher carcinogenic potential. The association of liver cirrhosis with HCC in our patients was as high as 78% (Table 1). Angiogenesis, the sprouting of new capillaries from a pre-existing vascular bed, could provide a route favoring for the malignantly degenerated hepatocytes to develop and to progress[40]. Regeneration in the cirrhotic liver would pose a potential of malignant degeneration[34]. Akiyoshi *et al*[34] suggested that serum VEGF level might be associated with hepatocyte regeneration grade. Suzuki *et al*[32] also supported that VEGF might play an important role in the development of HCC. This could also result in a high level of VEGF in liver remnants.

The third is that the microscopic metastasis from primary HCC to the remnant liver takes place very early. The metastatic lesions may be too small to be detected by the conventional imaging studies including ultrasound, CT scan or arteriography. However, these metastatic HCC cells may also produce a high level of VEGF, resulting in a high expression of $VEGF_{165}$ mRNA in the remnant liver. Miura *et al*[33] observed VEGF expression both in HCC and in non-HCC liver tissues, and supported the hypothesis that VEGF may be involved in the development and/or progression of HCC. Yoshiji *et al*[41] suggested that VEGF played a critical role in the development of HCC in cooperation with endothelial cells, because they found that VEGF-transduced cells showed a marked increase in their invasion activity. Torimura *et al* considered that HCC seemed to originate as a well-differentiated tumor, becoming progressively less differentiated with enlargement. They concluded that VEGF production could increase with tumor progression[40].

The prognosis after recurrence in relation to $VEGF_{165}$ mRNA in the noncancerous liver remnant was rarely reported. VEGF, may also increase the permeability of microvessels to 50 000-fold over that of histamine, thus causing a significant vascular leakiness. An increase in tumor vessel permeability could increase the change of the entry of tumor cells into the circulation, and newly formed vessels or capillaries may have leaky and weak basement membranes through which tumor cells could penetrate more easily than those of mature vessels, thus accelerating the hematogenous metastasis[5-10]. In addition, VEGF could induce both urokinase-type and tissue-type plasmins in endothelial cells which are the key proteases involved in the degradation of the extracellular matrix. These could result in the progression of recurrent HCC in remnant livers. Our findings suggest that remnant livers with a higher $VEGF_{165}$ mRNA have a higher malignant potential manifested as a greater number of recurrent tumors, and a larger extent of involved hepatic segments, a higher recurrence rate and mortality, a shorter recurrence-free interval and a shorter survival. All these factors correlated with an aggressive hematogenous metastasis as the majority of our patients had diffuse multiple recurrent nodules over the remnant liver. Repeat surgery was not undertaken on any patient.

Examination of VEGF mRNA expression in liver remnants during hepatectomy may give us information on the risk of postoperative recurrence. Neoadjuvant antiangiogenic therapy after surgery may be considered for such patients. From this prospective study, we suggest that VEGF mRNA expression in noncancerous liver tissues, especially isoform $VEGF_{165}$, not only plays a significant role in the prediction of postresection recurrence of HCC, but also correlates with a vigorous invasive behavior after recurrence.

REFERENCES

1 **Poon RT**, Fan ST, Lo CM, Liu CL, Wong J. Intrahepatic recurrence after curative resection of hepatocellular carcinoma: long-term results of treatment and prognostic factors. *Ann Surg* 1999; **229**: 216-222

2 **Jeng KS**, Chen BF, Lin HJ. En bloc resection for extensive hepatocellular carcinoma: is it advisable? *World J Surg* 1994; **18**: 834-839

3 **Lai EC**, Ng IO, Ng MM, Lok AS, Tam PC, Fan ST, Choi TK, Wong J. Long–term results of resection for large hepatocellular carcinoma: a multivariate analysis of clinicopathological features. *Hepatology* 1990; **11**: 815-818

4 **Folkman J**. What is the evidence that tumors are angiogenesis dependent? *J Natl Cancer Inst* 1990; **82**: 4-6

5 **Folkman J**. Endothelial cells and angiogenic growth factors in cancer growth and metastasis. Introduction. *Cancer Metastasis Rev* 1990; **9**:171-174

6 **Zhou J**, Tang ZY, Fan J, Wu ZQ, Li XM, Liu YK, Liu F, Sun HC, Ye SL. Expression of platelet-derived endothelial cell growth factor and vascular endothelial growth factor in hepatocellular carcinoma and portal vein tumor thrombus. *J Cancer Res Clin Oncol* 2000; **126**: 57-61

7 **Fox SB**, Gatter KC, Harris AL. Tumour angiogenesis. *J Pathol* 1996; **179**: 232-237

8 **Marme D**. Tumor angiogenesis: the pivotal role of vascular endothelial growth factor. *World J Urol* 1996; **14**: 166-174

9 **Folkman J**. Angiogenesis in cancer, vascular, rheumatoid and other disease. *Nat Med* 1995; **1**: 27-31

10 **Dvorak HF**, Brown LF, Detmar M, Dvorak AM. Vascular permeability factor/vascular endothelial growth factor, microvascular hyperpermeability, and angiogenesis. *Am J Pathol* 1995; **146**: 1029-1039

11 **Houck KA**, Ferrara N, Winer J, Cachianes G, Li B, Leung DW. The vascular endothelial growth factor family: identification of a fourth molecular species and characterization of alternative splicing of RNA. *Mol Endocrinol* 1991; **5**: 1806-1814

12 **Ferrara N**, Houck K, Jakeman L, Leung DW. Molecular and biological properties of the vascular endothelial growth factor family of proteins. *Endocr Rev* 1992; **13**: 18-32

13 **Anan K**, Morisaki T, Katano M, Ikubo A, Kitsuki H, Uchiyama A, Kuroki S, Tanaka M, Torisu M. Vascular endothelial growth factor and platelet-derived growth factor are potential angiogenic and metastatic factors in human breast cancer. *Surgery* 1996; **119**: 333-339

14 **Sun HC**, Tang ZY, Li XM, Zhou YN, Sun BR, Ma ZC. Microvessel density of hepatocellular carcinoma: its relationship with prognosis. *J Cancer Res Clin Oncol* 1999; **125**: 419-426

15 **Inoue K**, Ozeki Y, Suganuma T, Sugiura Y, Tanaka S. Vascular endothelial growth factor expression in primary esophageal squamous cell carcinoma. Association with angiogenesis and tumor progression. *Cancer* 1997; **79**: 206-213

16 **Mise M**, Arii S, Higashituji H, Furutani M, Niwano M, Harada T, Ishigami S, Toda Y, Nakayama H, Fukumoto M, Fujita J, Imamura M. Clinical significance of vascular endothelial growth factor and basic fibroblast growth factor gene expression in liver tumor. *Hepatology* 1996; **23**: 455-464

17 **An FQ**, Matsuda M, Fujii H, Matsumoto Y. Expression of vascular endothelial growth factor in surgical specimens of hepatocellular carcinoma. *J Cancer Res Clin Oncol* 2000; **126**: 153-160

18 **El-Assal ON**, Yamanoi A, Soda Y, Yamaguchi M, Igarashi M, Yamamoto A, Nabika T, Nagasue N. Clinical significance of microvessel density and vascular endothelial growth factor expression in hepatocellular carcinoma and surrounding liver: possible involvement of vascular endothelial growth factor in the angiogenesis of cirrhotic liver. *Hepatology* 1998; **27**: 1554-1562

19 **Ng IO**, Lai EC, Fan ST, Ng MM, So MK. Prognostic significance of pathologic features of hepatocellular carcinoma. A multivariate analysis of 278 patients. *Cancer* 1995; **76**: 2443-2448

20 **Arii S**, Tanaka J, Yamazoe Y, Minematsu S, Morino T, Fujita K, Maetani S, Tobe T. Predictive factors for intrahepatic recurrence of hepatocellular carcinoma after partial hepatectomy. *Cancer* 1992; **69**: 913-919

21 **Shirabe K**, Kanematsu T, Matsumata T, Adachi E, Akazawa K, Sugimachi K. Factors linked to early recurrence of small hepatocellular carcinoma after hepatectomy: univariate and multivariate analyses. *Hepatology* 1991; **14**: 802-805

22 **Jwo SC**, Chiu JH, Chau GY, Loong CC, Lui WY. Risk factors linked to tumor recurrence of human hepatocellular carcinoma after hepatic resection. *Hepatology* 1992; **16**: 1367-1371

23 **Nagao T**, Inoue S, Goto S, Mizuta T, Omori Y, Kawano N, Morioka Y. Hepatic resection for hepatocellular carcinoma. Clinical features and long-term prognosis. *Ann Surg* 1987; **205**: 33-40

24 **Sasaki Y**, Imaoka S, Masutani S, Ohashi I, Ishikawa O, Koyama H, Iwanaga T. Influence of coexisting cirrhosis on long-term prognosis after surgery in patients with hepatocellular carcinoma. *Surgery* 1992; **112**: 515-521

25 **Hsu HC**, Wu TT, Wu MZ, Sheu JC, Lee CS, Chen DS. Tumor invasiveness and prognosis in resected hepatocellular carcinoma.

Cancer 1988; **61**: 2095-2099
26 **Hsu HC**, Sheu JC, Lin YH, Chen DS, Lee CS, Hwang LY, Beasley RP. Prognostic histologic features of resected small hepatocellular carcinoma (HCC) in Taiwan. A comparison with resected large HCC. *Cancer* 1985; **56**: 672-680
27 **el-Assal ON**, Yamanoi A, Soda Y, Yamaguchi M, Yu L, Nagasue N. Proposal of invasiveness score to predict recurrence and survival after curative hepatic resection for hepatocellular carcinoma. *Surgery* 1997; **122**: 571-577
28 **Yamamoto J**, Kosuge T, Takayama T, Shimada K, Yamasaki S, Ozaki H, Yamaguchi N, Makuuchi M. Recurrence of hepatocellular carcinoma after surgery. *Br J Surg* 1996; **83**: 1219-1222
29 **Jeng KS**, Sheen IS, Chen BF, Wu JY. Is the p53 gene mutation of prognostic value in hepatocellular carcinoma after resection? *Arch Surg* 2000; **135**: 1329-1333
30 **Jeng KS**, Sheen IS, Tsai YC. Gamma glutamyl transpeptidase messenger RNA may serve as a diagnostic aid in hepatocellular carcinoma. *Br J Surg* 2001; **88**: 986-987
31 **Yamaguchi R**, Yano H, Iemura A, Ogasawara S, Haramaki M, Kojiro M. Expression of vascular endothelial growth factor in human hepatocellular carcinoma. *Hepatology* 1998; **28**: 68-77
32 **Suzuki K**, Hayashi N, Miyamoto Y, Yamamoto M, Ohkawa K, Ito Y, Sasaki Y, Yamaguchi Y, Nakase H, Noda K, Enomoto N, Arai K, Yamada Y, Yoshihara H, Tujimura T, Kawano K, Yoshikawa K, Kamada T. Expression of vascular permeability factor/vascular endothelial growth factor in human hepatocellular carcinoma. *Cancer Res* 1996; **56**: 3004-3009
33 **Miura H**, Miyazaki T, Kuroda M, Oka T, Machinami R, Kodama T, Shibuya M, Makuuchi M, Yazaki Y, Ohnishi S. Increased expression of vascular endothelial growth factor in human hepatocellular carcinoma. *J Hepatol* 1997; **27**: 854-861
34 **Akiyoshi F**, Sata M, Suzuki H, Uchimura Y, Mitsuyama K, Matsuo K, Tanikawa K. Serum vascular endothelial growth factor levels in various liver diseases. *Dig Dis Sci* 1998; **43**: 41-45
35 **Chow NH**, Hsu PI, Lin XZ, Yang HB, Chan SH, Cheng KS, Huang SM, Su IJ. Expression of vascular endothelial growth factor in normal liver and hepatocellular carcinoma: an immunohistochemical study. *Hum Pathol* 1997; **28**: 698-703
36 **Li XM**, Tang ZY, Zhou G, Lui YK, Ye SL. Significance of vascular endothelial growth factor mRNA expression in invasion and metastasis of hepatocellular carcinoma. *J Exp Clin Cancer Res* 1998; **17**: 13-17
37 **Qin LX**, Tang ZY. The prognostic molecular markers in hepatocellular carcinoma. *World J Gastroenterol* 2002; **8**: 385–392
38 **Chao Y**, Li CP, Chau GY, Chen CP, King KL, Lui WY, Yen SH, Chang FY, Chan WK, Lee SD. Prognostic significance of vascular endothelial growth factor, basic fibroblast growth factor, and angiogenin in patients with resectable hepatocellular carcinoma after surgery. *Ann Surg Oncol* 2003; **10**: 355-362
39 **Motoo Y**, Sawabu N, Nakanuma Y. Expression of epidermal growth factor and fibroblast growth factor in human hepatocellular carcinoma: an immunohistochemical study. *Liver* 1991; **11**: 272-277
40 **Torimura T**, Sata M, Ueno T, Kin M, Tsuji R, Suzaku K, Hashimoto O, Sugawara H, Tanikawa K. Increased expression of vascular endothelial growth factor is associated with tumor progression in hepatocellular carcinoma. *Hum Pathol* 1998; **29**: 986-991
41 **Yoshiji H**, Kuriyama S, Yoshii J, Yamazaki M, Kikukawa M, Tsujinoue H, Nakatani T, Fukui H. Vascular endothelial growth factor tightly regulates in vivo development of murine hepatocellular carcinoma cells. *Hepatology* 1998; **28**: 1489-1496

Edited by Wang XL **Proofread by** Zhu LH

PO Box 2345, Beijing 100023, China
Fax: +86-10-85381893
E-mail: wjg@wjgnet.com www.wjgnet.com

ELSEVIER

World J Gastroenterol 2005;11(2):193-199
World Journal of Gastroenterology ISSN 1007-9327

• LIVER CANCER •

Survivin antisense compound inhibits proliferation and promotes apoptosis in liver cancer cells

De-Jian Dai, Cai-De Lu, Ri-Yong Lai, Jun-Ming Guo, Hua Meng, Wei-Sheng Chen, Jun Gu

De-Jian Dai, Hua Meng, Department of Surgery, Second Affiliated Hospital of Zhejiang University Medical School, Hangzhou 310009, Zhejiang Province, China
Cai-De Lu, Department of Surgery, Lihuili Hospital of Ningbo Medical Center, Ningbo University Medical School, Ningbo 315040, Zhejiang Province, China
Ri-Yong Lai, Department of Biochemistry and Molecular Biology, Gannan Medical College, Ganzhou 341000, Jiangxi Province, China
Jun-Ming Guo, Medical School, Ningbo University, Ningbo 315211, Zhejiang Province, China
Wei-Sheng Chen, Jun Gu, Ningbo Institute of Microcirculation and Henbane, Ningbo 315040, Zhejiang Province, China
Supported by the National Natural Science Foundation of China, No. 30171059
Correspondence to: Cai-De Lu, M.D., Department of Surgery, Lihuili Hospital of Ningbo Medical Center, Ningbo University Medical School, Ningbo 315040, Zhejiang Province, China. lucd71@hotmail.com
Telephone: +86-574-87392290-7707 **Fax:** +86-574-87392232
Received: 2004-04-07 **Accepted:** 2004-05-24

Abstract

AIM: To evaluate the effects of survivin on cell proliferation and apoptosis in liver cancer.

METHODS: MTT assay was used to generate and optimize phosphorothioate antisense oligonucleotides (ODNs)-Lipofectamine™2000 (LiP) compound by varying ODNs (μg): LiP (μL) ratios from 1:0.5 to 1:5. Then, liver cancer cells (HepG2) were transfected with the compound. By using RT-PCR and Western blot, the expression levels of survivin mRNA and proteins were detected in HepG2 cells treated with antisense compounds (ODNs:LiP = 1:4), and compared with those treated with sense compounds (1:4) as control. MTT assay was applied to the determination of cell proliferation in HepG2 cells. Active caspase-3 was evaluated by flow cytometric analysis. The morphological changes were assessed by electron microscopy. Laser scanning confocal microscopy was performed to detect the subcellular localization of survivin proteins in treated and untreated cells.

RESULTS: Antisense compounds (1:4) down-regulated survivin expression (mRNA and protein) in a dose-dependent manner with an IC_{50} of 250 nmol/L. Its maximum effect was achieved at a concentration of 500 nmol/L, at which mRNA and protein levels were down-regulated by 80%. The similar results were found in MTT assay. Antisense compound (1:4)-treated cells revealed increased caspase-3-like protease activity compared with untreated cells. Untreated cells as control were primarily negative for the presence of active-caspase-3. As shown by transmission electron microscopy, treated cells with antisense compounds (1:4) resulted in morphological changes such as blebbing and loss of microvilli, vacuolization in the cytoplasm, condensation of the cytoplasm and nuclei, and fragmented chromatin. Immunofluorescence analysis confirmed the presence of survivin protein pool inside the cytoplasm in untreated cells. Labeled-FITC immunofluorescence staining of survivin clearly showed that survivin was distributed mainly in a spotted form inside the cytoplasm. Whereas cells treated with antisense compounds were rare and weak inside the cytoplasm.

CONCLUSION: Down-regulation of survivin expression induced by the antisense compounds reduces tumor growth potential, promotes apoptosis and affects the localization of survivin proteins in HepG2 cells. Furthermore, survivin protein is a key molecule associated with proliferation and apoptosis, and antisense oligonucleotides targeting survivin have a bright prospect in the therapy of liver cancer.

Key words: Liver cancer; Survivin; Cell proliferation; Apoptosis

Dai DJ, Lu CD, Lai RY, Guo JM, Meng H, Chen WS, Gu J. Survivin antisense compound inhibits proliferation and promotes apoptosis in liver cancer cells. *World J Gastroenterol* 2005; 11(2): 193-199
http://www.wjgnet.com/1007-9327/11/193.asp

INTRODUCTION

Diminished apoptosis plays a critical role in tumor initiation, progression, as well as in cancer therapy[1]. Several proteins that inhibit apoptosis have been identified, including bcl-2 family members bcl-2, bcl-xl and IAP[2]. Certain members of the latter family directly inhibit terminal effector caspases engaged in the execution of cell death[3]. Among molecules of the IAP family, survivin is unique in having a single baculovirus IAP repeat (BIR) and extended C-terminal x-helix[4] and dimeric architecture that is essential for the inhibition of apoptosis[5,6]. Although survivin protein lacks the ability to directly inhibit caspase-3[7], it binds quantitatively to a new IAP-inhibiting protein, Smac/Diablo[8,9], raising the possibility that it might suppress caspases indirectly by freeing other IAP family members from the constraints of protein. Taken together, these studies support the notion that survivin exerts an anti-apoptotic effect. Survivin is expressed during embryonal development but lacks expression in terminally differentiated adult tissues[2,4]. Interestingly, it becomes reexpressed in transformed cell lines and in a variety of human tumors[3,4]. Survivin is expressed in the G_2/M phase of the cell cycle and associates with microtubules of the mitotic spindle in a specific and saturable reaction that is regulated by microtubule dynamics[10]. This implies that overexpression of survivin has oncogenic potential because it may overcome the G_2/M phase checkpoint to enforce progression of cells through mitosis, thus promoting proliferation. Recent studies suggest an alternative distribution of survivin localized to kinetochores of metaphase chromosomes, and to microtubules of the central spindle midzone at anaphase[11-13]. Approximately 80% of the total cellular survivin content in mitotic cells is bound to centrosomes and microtubules of the metaphase and anaphase spindles[10]. These studies reveal that survivin could connect the cell cycle with apoptosis, thus

providing a death switch for the termination of defective mitosis. These lines of evidence make survivin an attractive therapeutic target in cancer treatment.

Liver cancer is a leading cause of cancer death, and its incidence continues to rise. The main reasons for the unfavorable prognosis of these tumors are their propensity to metastasizing early and developing resistance to a wide range of functionally anticancer agents. Recent studies show that expression of survivin is not only detected in stomach cancer[14,15], non-small cell lung cancer[16], breast cancer[17], esophageal cancer[18], colon cancer, ovarian carcinoma[19], but also in HepG2, Huh7, sk-Hep1 cell lines and hepatocellular carcinoma tissues, and it has a close correlation with apoptosis and proliferation of liver cancer[4,20]. In addition, skin cancer HaCat cells transfected with antisense oligonucleotide down regulate expression of survivin, promote apoptosis and diminish proliferation[21]. Consequently, targeting expression of survivin has a potential value in cancer therapy. Although antisense oligonucleotide has been widely recognized as an efficient tool for the inhibition of gene expression in a sequence specific way, during practical application of antisense approach, many key problems need to be solved, such as to find an effective targeting site of survivin mRNA that is likely to be accessible to antisense oligonucleotides, to select an adaptable vector combined with antisense oligonucleotides in the formation of a potent compound to facilitate apoptosis of tumor, to optimize transfection conditions in a cell line with high expression of survivin.

In the present study, we generated a series of antisense compounds, with the strongest efficient antisense oligonucleotides designed by Olie *et al*[22] and highly efficient vector Lipofectamine 2000. Using MTT assay and the survivin-overexpressing liver cancer cell line HepG2, one antisense compound was identified that could most efficiently down-regulate survivin expression levels (mRNA and protein) and directly induce apoptosis. Furthermore, in a double immunofluorescence staining experiment with FITC-labelled antibody against survivin and Allexa-labelled concanavalin A, evidence is provided that antisense mediated down-regulation of survivin has the potential to affect subcellular localization of survivin proteins in HepG2 cells.

MATERIALS AND METHODS

Antisense oligonucleotides

According to the method of Olie *et al*[22], antisense and sense oligonucleotides for survivin were designed. The antisense oligonucleotides targeting nucleotides 232-251 revealed the strongest effect and were used in the following experiments. Their sequences are shown in Table 1. Phosphorothioate oligonucleotides ODNs were purchased from Sangon (Shanghai, China), and delivered in the form of complex with Lipofectamine 2000 (Lip) (Invitrogen, USA).

Table 1 Sequences of oligonucleotides for survivin

Antisense	5'-CCCAGCCTTCCAGCTCCTTG-3'
Sense	5'-CAAGGAGCTGGAAGGCTGGG-3'

Cell line

Liver cancer cell line HepG2, which was reported to express high levels of survivin[19], was obtained from Shanghai Institute of Cell Biology. Cells were grown in DMEM (Gibco, USA) supplemented with 10% heat-inactivated fetal bovine serum (Sijiqing, Hangzhou, China). Cells were maintained in monolayer cultures at 37 ℃ in a humidified atmosphere consisting of 5 mL/L CO_2 and 95% air.

Generation and optimization of phosphorthioate antisense oligonucleotides (ODNs)-Lipofectamine 2000 (LiP) compound

To obtain the highest transfection efficiency and low non-specific effects, transfection conditions were optimized by varying ODNs, LiP concentrations and cell density. Cells should be greater than 80% confluence and ODNs (μg):LiP (μL) ratios were varied from 1:0.5 to 1:5. ODNs were diluted in the appropriate amount of DMEM without serum, at the final concentration of 0.2 μg/25 μL, and they were mixed gently. LiP was gently mixed before use, then diluted in an appropriate amount of DMEM without serum at the final concentrations of 0.1 μg/25 μL, 0.2 μg/25 μL, 0.4 μg/25 μL, 0.6 μg/25 μL, 0.8 μg/25 μL, 1 μg/25 μL. These ODNs solutions were gently mixed and incubated for 5 min at room temperature. After incubated for 5 min, the diluted ODNs were mixed with the six different concentrations of diluted LiP (1:0.5-1:5), and incubated for 20 min at room temperature to form the ODNs-LiP compounds. Fifty microliters of ODNs-LiP compounds was added to each well (96-well plates) containing cells and media, gently mixed again by rocking the plate back and forth, the cells were incubated at 37 ℃ in a CO_2 incubator for 48 h. Then, MTT assay was performed.

Treatment of HepG2 cells with survivin oligonucleotides

One day before transfection, HepG2 cells were plated in 96-, 24-, or 6-well tissue culture plates. Oligonucleotides were delivered in the form of compound LiP as described above. After a 24-h transfection, the transfection medium was replaced by medium without transfection reagents. HepG2 cells were harvested 24, 48 or 72 h after the start of transfection.

Measurement of cell growth

Growth inhibition in HepG2 cell line was determined by a colorimetric MTT assay. HepG2 cells were cultured in 96-well plates with an initial concentration of 1×10^4 cells/well in DMEM supplemented with 10% fetal bovine serum. ODNs were delivered in the form of compound LiP, as described above. Briefly, after transfection for 48 h at 37 ℃, 20 μL of MTT reagent (Sangon, Shanghai, China) was added and allowed to react for 4 h at 37 ℃. Subsequently, the MTT was discarded, 150 μL of DMSO reagent (Sangon, Shanghai, China) was added and allowed to react for 15 min at 37 ℃. Substrate cleavage was monitored at 570 nm by a microplate reader (Tosoh, Yamaguchi, Japan) and the rate of inhibition was calculated. Experiments were repeated three times.

RNA extraction

Total cellular RNA was extracted using RNeasy Plant Mini kit reagent according to the manufacturer's recommendations (QIAGEN, Germany). The quantity and quality of RNA were assessed spectrophotometrically at 260 nm and 280 nm (the A_{260} to A_{280} ratio of pure RNA was approximately 2).

RT-PCR

RT-PCR amplification product was synthesized with 0.1 μg of total RNA using OneStep RT-PCR kit (QIAGEN, Germany) according to the manufacturer's instructions. Primers used for amplification were human survivin sense primer corresponding to nucleotides 47-66 (5'-GGCATGGGTGCCCCGACGTT-3'), and antisense primer complementary to nucleotides 466-485 (5'-AGAGGCCTCAATCCATGGCA-3'). Amplification of human β-actin served as an internal control, β-actin sense primer was corresponding to nucleotides 578-609 (5'-ATCTGGCACC ACACCTTCTACAATGAGCTGCG-3'), and antisense primer was complementary to nucleotides 1 415-1 384 (5'- CGTCATA

CTCCTGCTTCCTGATCCACATCTGC-3'). Optimization conditions were as follows: reverse transcription for 30 min at 50 ℃, initial PCR activation step for 15 min at 95 ℃. Three-step cycling was denaturation for 1 min at 94 ℃, annealing for 1 min at 62 ℃, extension for 1 min at 72 ℃, and a final extension for 10 min at 72 ℃ using the Eppendorf PCR System (Eppendorf, Germany). PCR products were analysed on a 2% agarose gel by electrophoresis and the bands were visualized by ethidium bromide staining.

Western blot

Cells were collected on ice and centrifuged at 1 500 rm for 5 min at 4 ℃. The cells were resuspended and washed with ice-cold PBS and centrifuged again at 1 500 rm for 5 min at 4 ℃. Supernatants were discarded and cell pellets were lysed in 2× cell lysis buffer [2% Triton X-100, 300 mmol/L NaCl, 20 mmol/L Tris-Cl pH 7.2, 10% glycerol and 4% SDS] and heated to 95 ℃ for 10 min. The lysates were centrifuged at 14 000 rm for 30 min at 4 ℃ and the protein supernatants were collected and stored at -20 ℃. The protein concentrations were determined by BCA assay according to the manufacturer's instructions (Pierce Co). Equal quantities of proteins (20 μg/well) were separated on 7.5-12% sodium dodecyl sulfate polyacrylamide gel electrophoretic gels for the detection of survivin. Following electrophoretic transfer of protein onto nitrocellulose membranes, immunoblots were sequentially incubated in 5% skimmed milk blocking solution at room temperature for 2 h. The membranes were incubated in a solution containing antihuman survivin antibody (1:800; Oncogene, USA) overnight at 4 ℃. After washed three times with 1% PBS-Tween solution at room temperature for 1 h, the membranes were incubated with horseradish peroxidase-conjugated secondary antibodies (1:2 000; Oncogene, USA) at room temperature for 2 h. Finally, after the membranes were washed for 1 h, protein bands were detected by using the ECL system according to the manufacturer's instructions (Amersham Life Sciences). β-actin was used as a protein loading control.

Measurement of caspase activation

Caspase-3-like protease activity in cells was analyzed by flow cytometry (FACS Calibur, Bection Dikinson, USA) using a PE-conjugated polyclonal rabbit anti-active caspase-3 antibody kit (Becton Dickinson, USA). Zero, 24, 48, 72 h after antisense compound induction respectively, cells were harvested and washed twice with PBS, fixed in ice-cold 70% ethanol and stored at 4 ℃. Prior to analysis, cells were again washed with PBS. Cytometric analyses were performed using a flow cytometer and Cell Quest software. Approximately 20 000 cells were calculated for each determination.

Electron microscopic examination

Cells were seeded into 30-mm dishes, treated as described above, collected on ice with media by gently scraping, and washed three times in ice-cold PBS. The cell pellets were fixed with a solution of 2% formaldehyde and 3% glutaraldehyde in 0.1 mol/L sodium cacodylate buffer (pH 7.4) for 1 h at 48 ℃. The fixed cells were washed three times in cacodylate buffer (pH 7.2) containing 0.2 mol/L sucrose, postfixed with 1% osmic acid in 0.3 mol/L cacodylate buffer, dehydrated in a graded series of acetone, and embedded in epoxy resin. Ultrathin sections were cut, stained with uranyl acetate and lead citrate, and assessed by using a TECNA10 electron microscope (Philips, Holand).

Immunofluorescence and confocal laser scanning microscopy

Cells were cultured on microscope slides, then treated or untreated with antisense compounds (1:4) for 48 h. Cells were washed three times with PBS for 15 min and fixed in ice-cold paraformaldehyde for 30 min. Cells were fixed in ice-cold CAM (chloroform:acetone:methanol = 1:1:2) at -20 ℃ for 30 min, and washed three times with PBS for 15 min. Cells were incubated overnight at 4 ℃ with polyclonal anti-survivin (1:400 diluted; rabbit polyclonal IgG; Oncogene, USA), washed three times with PBS for 30 min, incubated for 2 h at room temperature with fluorescein (FITC)-conjugated anti-rabbit-IgG (1:1 000; Oncogene, USA). After a further washing step, cell membranes were stained for 2 min with a 5×10^{-3}% (w/v) solution of Alexa-labelled concanavalin A (MoBiTec, Gottingen, Germany) in BPS. Finally, the cells were embedded in a gel containing 22.73% (w/w) glycerine, 9.1% (w/w) Mowiol4-88 (present from Ningbo Institute of Microcirculation and Henbane), 22.73% (w/w) double-distilled water, 45.45% (w/w) 0.2 mol/L Tris buffer, pH 8.5, and 2.5% (w/w) DABCO (present from Ningbo Institute of Microcirculation and Henbane) as an antifading agent. After 12 h, confocal microscopy was performed with a microscope (TCS-SP2, Leica, Germany) equipped with an argon/krypton laser. Two-channer image recording at 488 nm and 633 nm laser excitation was used. Optical filters were chosen for the FITC and TRLTC range. All optical sections were recorded with the same laser and detector settings using software (Leica Confocal, Germany). Further image processing was performed with software (Leica Confocal, Germany) on a computer system. Confocal stacks of green and red fluorescence were visualized in section view mode.

Statistical methods

All statistical analyses were performed by the SPSS11.0 software package for Windows (SPSS Inc., Chicago, IL). The *t* test was used to compare the distribution of individual variables. A two-tailed *P* value less than 0.05 was considered statistically significant.

RESULTS

Generation and optimization of antisense compound

With the aim of obtaining the highest transfection efficiency and low non-specific effects, the compounds were generated using the antisense phosphorothioate oligonucleotides (ODNs) and highly effective Lipofectamine 2 000 (LiP) by varying ODNs (μg):LiP (μL) ratios from 1:0.5 to 1:5. The ODNs designed by Olie *et al*[22], which targeted nucleotides (232-251) revealed the strongest effect. MTT was performed to test the effect of those compounds in surviving-HepG2 high-expression cells. As shown in Figure 1, the antisense compounds (1:4, 1:5) were identified as the most potent compounds. There was no significant difference in the effect between the compounds (1:4) and (1:5). Because the antisense compounds (1:0.5-1:3) could not achieve the best effect, and LiP had slight cytotoxicity, we only used the antisense compounds (1:4) in the following experiments.

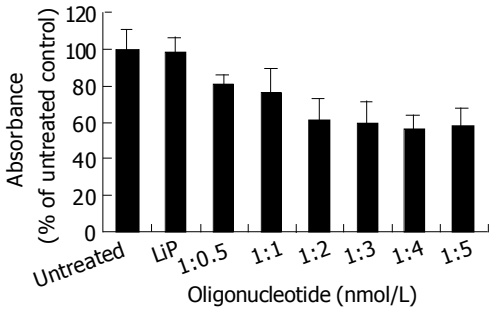

Figure 1 Generation and optimization of antisense compound. Each value represents the mean±SD of three independent experiments.

Down-regulatory effects of antisense oligonucleotides on survivin expression levels

To further characterize the potency of antisense compounds (1:4) and their dose dependent effect on survivin expression levels (mRNA and protein) in HepG2 cells, the cells highly expressing survivin were transfected with different concentrations of antisense compounds (100-600 nmol/L), whereas the cells transfected with sense compound (600 nmol/L), LiP (600 nmol/L) and untreated cells were used as controls. Forty-eight hours after the start of transfection, the cells were examined by RT-PCR and Western blot. As shown in Figure 2, antisense compounds (1:4) down-regulated the survivin expression level in a dose-dependent manner with an IC_{50} of about 250 nmol/L. At a concentration of 500 nmol/L, a maximum down-regulation to 20% of the initial mRNA level was achieved. A further increase in oligonucleotide concentration did not result in increased antisense efficacy. The sense compound (600 nmol/L), LiP (600 nmol/L) and antisense compound controls without LiP (600 nmol/L) did not down-regulate the survivin expression level.

Inhibition of cell growth by antisense compound (1:4)

To analyze the biological effect associated with the down-regulation of survivin expression, the growth of HepG2 cells treated with antisense compounds was investigated by MTT assay. As shown in Figure 3 A, 48 h after the start of transfection, antisense compounds reduced the growth of HepG2 cells dose-dependently, with an IC_{50} of 300 nmol/L. The unspecific growth-inhibitory effect of the sense compound (600 nmol/L) control was comparatively low, LiP (600 nmol/L) control had no growth-inhibitory effect. Antisense compounds induced death in HepG2 cells, as revealed by detachment from the culture surface (Figure 3: B, C, D, E).

Anti-active caspase-3 antibodies for measuring apoptosis by flow cytometric analysis

Having demonstrated that down-regulation of survivin expression reduced the viability of HepG2 cells, we analyzed whether cell death was due to the induction of apoptosis. As shown in Figure 4, HepG2 cells were treated with antisense compounds 24, 48, 72 h after the start of transfection. Then, the cells were analyzed by flow cytometry using PE-conjugated polyclonal rabbit anti-active caspase-3 antibody. Antisense compound-treated cells revealed increased caspase-3-like protease activity compared with untreated cells. Cells treated for 24 h had detectable active caspase-3 corresponding to a measurable value 23, whereas about 16% of the cells were induced to undergo apoptosis. Cells treated for 48 h had detectable active caspase-3 corresponding to a measurable value 33 corresponding to a 60% apoptosis ratio, while cells treated for 72 h had a measurable value 42 corresponding to a 70% apoptotic ratio. Untreated cells as control were primarily negative for the presence of active-caspase-3, a measurable value 16 corresponding to 5% apoptotic cells.

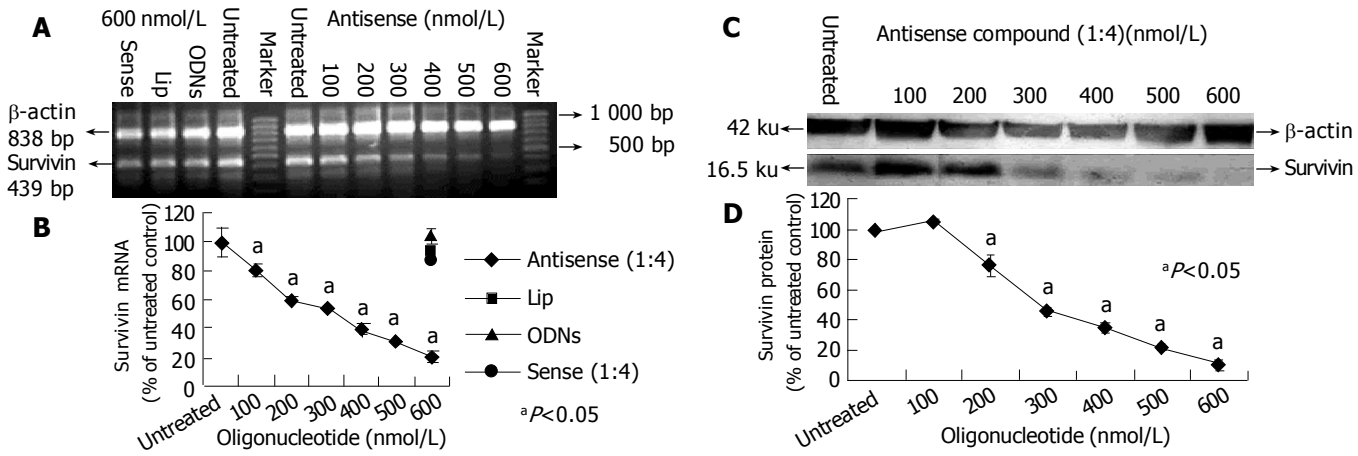

Figure 2 Survivin expression level (mRNA and protein) in HepG2 cells treated with antisense compound (1:4). A: Sensitivity of survivin mRNA in RT-PCR assay; B: Level of survivin mRNA expression in HePG2; C and D: Western blot analysis of survivin protein expression in HePG2 cells.

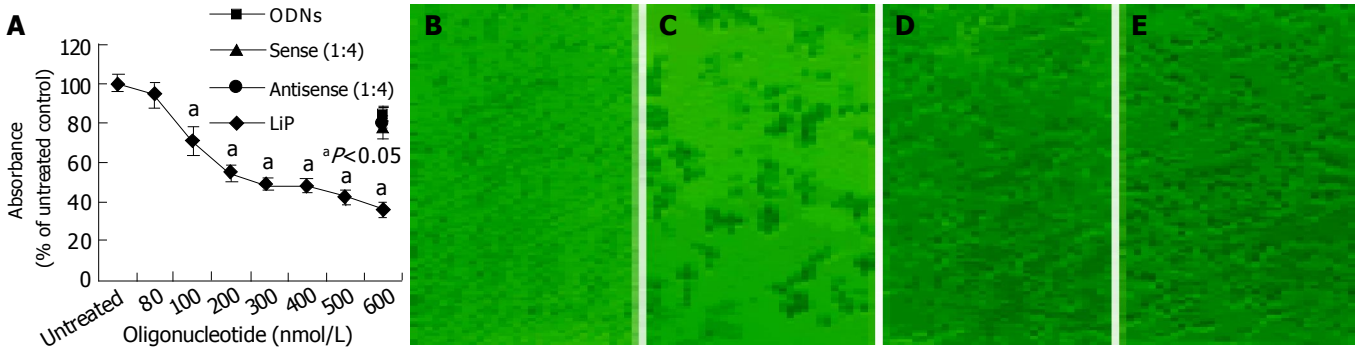

Figure 3 Effect of antisense compound (1:4) on the growth and viability of HepG2 cells. A: Cells incubated with an increasing concentration of antisense compound (1:4), 600 nmol/L sense compound (1:4), 600 nmol/L LiP, or 600 nmol/L (ODNs) for 48-h after the start of transfection; B: untreated cells; C-E: photomicrographs of HepG2 cells after a 48-h transfection with (C) 600 nmol/L antisense comound (1:4), (D) 600 nmol/L sense compound (1:4) or (E) 600 nmol/L LiP.

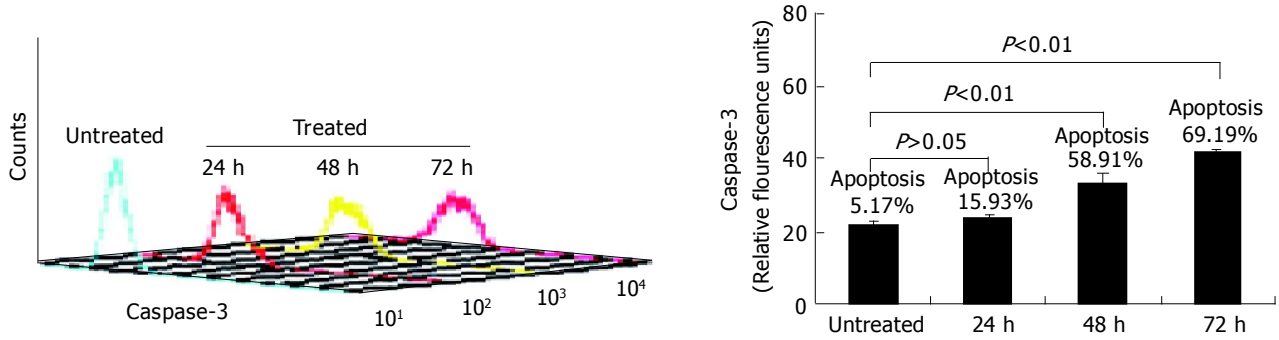

Figure 4 Anti-active caspase-3 antibodies for measuring apoptosis by flow cytometric analysis.

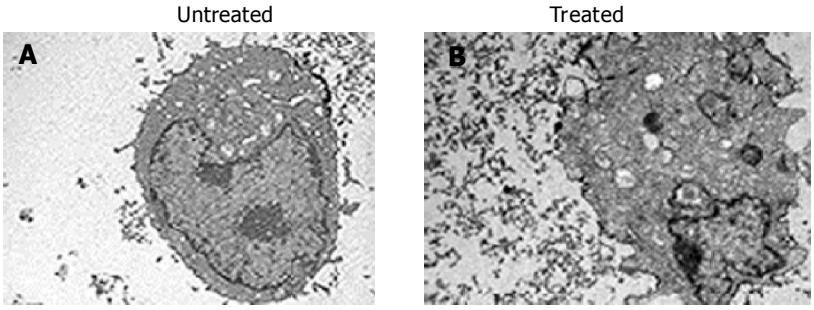

Figure 5 Morphological evaluation of HepG2 cells(original magnification, ×4 000). A: Normal structure in the nuclei and cytoplasm of untreated cell; B: Morphological changes of apoptosis in treated cells.

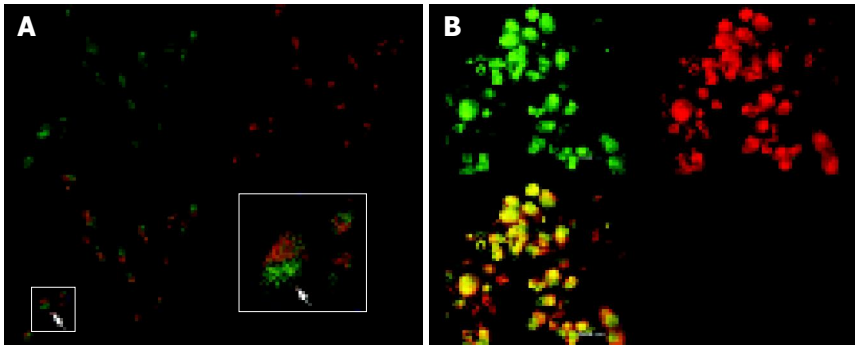

Figure 6 Laser scanning confocal microscopy of localization of survivin protein in HepG2 cells. A: Expression and localization of endogenous survivin proteins with immunofluorescence analysis of untreated cells by using the polyclonal anti-survivin antibody and FITC-labeled anti-rabbit-IgG as secondary antibody; B: Rare and weakly stained cells treated with antisense compound inside the cytoplasm and morphological changes corresponding to apoptosis.

Morphological changes of apoptosis induced by antisense compound

In order to confirm the cell apoptosis induced by treatment with antisense compounds, the morphological signs of apoptosis were evaluated by transmission electron microscopy. As shown in Figure 5, untreated HepG2 cells showed normal morphology in the nuclei and cytoplasm (Figure 5A). Treatment of HepG2 cells with antisense compounds resulted in changes such as blebbing and loss of microvilli, vacuolation in cytoplasm, condensation of cytoplasm and nuclei, and fragmented chromatin, providing further evidence for the induction of apoptosis as a consequence of survivin antisense treatment (Figure 5B).

Localization of survivin protein in HepG2 cells

We carried out double immunofluorescence staining using FITC-labelled antibody against survivin and Alexa-labelled concanavalin A, with which cells of the membranes were counterstained. The stained cells were investigated by confocal laser scanning microscopy. As shown in Figures 6 A,B in cells untreated with antisense compounds, green-immunofluorescence staining of survivin clearly showed that survivin was expressed mainly in the form of a spotted distribution inside the cytoplasm, which was named as survivin pool (Figure 6A). In cells treated with antisense compounds, however, there was rare and weak green fluorescence inside the cells, of which the membranes were counterstained with Alexa -labeled concanavalin A (Figure 6B).

DISCUSSION

Survivin, a member of the inhibitors of apoptosis protein family, deserves growing attention as "an ideal target" for cancer therapy[23,24] due to its differential expression in tumors *vs* normal tissues, distribution of subcellular localization, and the evidence for a dual role in both cell apoptosis and proliferation. It is expressed during embryonal development, lacks expression in terminally differentiated adult tissues, and becomes reexpressed

in transformed cell lines and a variety of human tumors, with highest levels in liver cancer[4,20]. The expression of survivin in tumors is correlated with a shorter survival of patients with liver cancer, non-small cell lung cancer, colorectal cancer. Despite survivin represents an attractive target for therapy[25,26], the promise of survivin antisense ODNs to facilitate apoptosis of HepG2 cells, localization of survivin, and how the localization of survivin proteins is affected by transfection of antisense oligonucleotides in HepG2 cells remain to be determined. In the present study, we generated and optimized sequence-specific antisense compounds to down-regulate survivin expression (mRNA and protein) in HepG2 cell lines to demonstrate its ability to induce apoptosis, and how to localize survivin protein affected by antisense compounds.

Antisense approaches are efficient tools for the inhibition of gene expression in a sequence specific way[27]. Most antisense approaches rely on empirical targeting of oligonucleotides against the translation initiation site of mRNA, where the ATG start codon lies. The rationale for choosing this site is that it likely presents in single-stranded conformation, thus being accessible to antisense oligonucleotides. In a study by Olie *et al*[22], survivin antisense oligonucleotides, which target nucleotides 232-251, were identified, and most efficiently down-regulated the survivin mRNA level and directly induced apoptosis. In our study, we successfully transfected HepG2 cells with the above antisense oligonucleotides incorporating a vector of LiP, and generated and optimized the compounds by varying ODNs:LiP ratios from 1:0.5 to 1:5. Moreover, we identified that the compounds (1:4) were the most potent. As measured by RT-PCR and Western blot, the antisense compounds (1:4) also most efficiently down-regulated the survivin expression level in HepG2 cells, achieving its maximum effect at a concentration of 500 nmol/L, at which the expression level of survivin was down-regulated by 80%. By transfection of these compounds, we were also able to witness increased caspase-3-like protease activity by flow cytometric analysis, and morphological changes of apoptosis induced by antisense compounds such as vacuolation in cytoplasm, condensation of cytoplasm and nuclei and fragmented chromatin, with a parallel inhibition seen in cell proliferative activity by MTT assay.

A previous study reported that survivin could prevent apoptosis by targeting the terminal effectors caspase-3 and caspase-7, which act downstream in two major apoptotic pathways [3]. Survivin is believed to be expressed in the G_2/M phase of the cell cycle in a cell cycle-regulated manner and is associated with microtubule formation of the mitotic spindle[10]. Antisense compounds (1:4) induce a strong growth-inhibitory effect and apoptosis in HepG2 cells in the absence of any further cytotoxic stimulus. These data suggest that targeting survivin with transfection of antisense ablates expression of endogenous survivin. However, loss of survivin expression is sufficient to trigger caspase-dependent apoptosis in HepG2 cells. Moreover, it has been suggested that the survivin antisense approach may be able to facilitate apoptosis through the two major apoptotic pathways. This observation is in agreement with the findings of others describing the necessity of interaction between survivin and microtubules of the mitotic spindle apparatus to prevent a default induction of apoptosis at the G_2/M phase of cell cycle[10].

One of the most significant features of survivin is expressed in the G_2/M phase of cell cycle in a cell-regulated manner. At the beginning of mitosis, survivin is associated with microtubules of the mitotic spindle in a specific and saturable reaction that is regulated by microtubule dynamics[10]. Recent studies have suggested an alternative distribution of survivin localized to kinetochores, centrosomes (microtubule-organizing centers), spindle microtubules, central spindle midzone and midbodies. Approximately 80% of the total cellular survivin content in mitotic cells is bound to centrosomes and microtubules of the metaphase and anaphase spindles. Survivin's localizations in the mitotic spindle apparatus might be essential for anti-apoptotic function[28].

In the present study, double immunofluorescence analysis has confirmed the presence of survivin protein pool in cytoplasm. In untreated HepG2 cells, labeled-FITC-immunofluorescence staining of survivin clearly showed that survivin was expressed mainly in the form of a spotted distribution inside the cytoplasm. Whereas, in treated cells, survivin was rare and weak in immunoreactivity. As demonstrated by Western blot, in cells treated with antisense compounds, survivin expression level was in a dose-dependent manner. It is suggested that the survivin antisense approach may be able to affect the localization of survivin. Recent experiments demonstrate that survivin exists in an immunochemically distinct pool of survivin[10]. A more recent study suggests that overexpression of survivinDsRed fusion proteins is diffusely distributed in cytoplasm with distinct spots[29]. We also found that survivin was expressed in cytoplasm in the form of pools or spots, suggesting that survivin plays an important role in linking cell death and proliferation. In the context, antisense disruption of survivin-microtubule interactions can result in two effects during mitosis: increased caspase-3 activity-a mechanism involved in cell death and loss of anti-apoptosis function of survivin.

In summary, down-regulation of survivin expression by antisense compounds facilitates apoptosis, and localization of survivin proteins is affected by antisense compounds in HepG2 cells. Survivin protein is a key molecule connecting cell proliferation with apoptosis. Antisense targeting survivin has a bright prospect in liver cancer therapy.

REFERENCES

1 **Makin G,** Hickman JA. Apoptosis and cancer chemotherapy. *Cell Tissue Res* 2000; **301**: 143-152

2 **Adida C,** Crotty PL, McGrath J, Berrebi D, Diebold J, Altieri DC. Developmentally regulated expression of the novel cancer anti-apoptosis gene survivin in human and mouse differentiation. *Am J Pathol* 1998; **152**: 43-49

3 **Tamm I,** Wang Y, Sausville E, Scudiero DA, Vigna N, Oltersdorf T, Reed JC. IAP-family protein survivin inhibits caspase activity and apoptosis induced by Fas (CD95), Bax, caspases, and anticancer drugs. *Cancer Res* 1998; **58**: 5315-5320

4 **Ambrosini G,** Adida C, Altieri DC. A novel anti-apoptosis gene, survivin, expressed in cancer and lymphoma. *Nat Med* 1997; **3**: 917-921

5 **Deveraux QL,** Reed JC. IAP family proteins-suppressors of apoptosis. *Genes Dev* 1999; **13**: 239-252

6 **LaCasse EC,** Baird S, Korneluk RG, MacKenzie AE. The inhibitors of apoptosis (IAPs) and their emerging role in cancer. *Oncogene* 1998; **17**: 3247-3259

7 **Verdecia MA,** Huang H, Dutil E, Kaiser DA, Hunter T, Noel JP. Structure of the human anti-apoptotic protein survivin reveals a dimeric arrangement. *Nat Struct Biol* 2000; **7**: 602-608

8 **Du C,** Fang M, Li Y, Li L, Wang X. Smac, a mitochondrial protein that promotes cytochrome c-dependent caspase activation by eliminating IAP inhibition. *Cell* 2000; **102**: 33-42

9 **Verhagen AM,** Ekert PG, Pakusch M, Silke J, Connolly LM, Reid GE, Moritz RL, Simpson RJ, Vaux DL. Identification of DIABLO, a mammalian protein that promotes apoptosis by binding to and antagonizing IAP proteins. *Cell* 2000; **102**: 43-53

10 **Li F,** Ambrosini G, Chu EY, Plescia J, Tognin S, Marchisio PC, Altieri DC. Control of apoptosis and mitotic spindle checkpoint by survivin. *Nature* 1998; **396**: 580-584

11 **Skoufias DA,** Mollinari C, Lacroix FB, Margolis RL. Human survivin is a kinetochore-associated passenger protein. *J Cell Biol* 2000; **151**: 1575-1582

12 **Uren AG,** Wong L, Pakusch M, Fowler KJ, Burrows FJ, Vaux

DL, Choo KH. Survivin and the inner centromere protein INCENP show similar cell-cycle localization and gene knockout phenotype. *Curr Biol* 2000; **10**: 1319-1328

13 **Wheatley SP,** Carvalho A, Vagnarelli P, Earnshaw WC. INCENP is required for proper targeting of Survivin to the centromeres and the anaphase spindle during mitosis. *Curr Biol* 2001; **11**: 886-890

14 **Lu CD,** Altieri DC, Tanigawa N. Expression of a novel antiapoptosis gene, survivin, correlated with tumor cell apoptosis and p53 accumulation in gastric carcinomas. *Cancer Res* 1998; **58**: 1808-1812

15 **Zhu XD,** Lin GJ, Qian LP, Chen ZQ. Expression of survivin in human gastric carcinoma and gastric carcinoma model of rats. *World J Gastroenterol* 2003; **9**: 1435-1438

16 **Monzo M,** Rosell R, Felip E, Astudillo J, Sanchez JJ, Maestre J, Martin C, Font A, Barnadas A, Abad A. A novel anti-apoptosis gene: Re-expression of survivin messenger RNA as a prognosis marker in non-small-cell lung cancers. *J Clin Oncol* 1999; **17**: 2100-2104

17 **Tanaka K,** Iwamoto S, Gon G, Nohara T, Iwamoto M, Tanigawa N. Expression of survivin and its relationship to loss of apoptosis in breast carcinomas. *Clin Cancer Res* 2000; **6**: 127-134

18 **Kato J,** Kuwabara Y, Mitani M, Shinoda N, Sato A, Toyama T, Mitsui A, Nishiwaki T, Moriyama S, Kudo J, Fujii Y. Expression of survivin in esophageal cancer: correlation with the prognosis and response to chemotherapy. *Int J Cancer* 2001; **95**: 92-95

19 **Yoshida H,** Ishiko O, Sumi T, Matsumoto Y, Ogita S. Survivin, bcl-2 and matrix metalloproteinase-2 enhance progression of clear cell- and serous-type ovarian carcinomas. *Int J Oncol* 2001; **19**: 537–542

20 **Ito T,** Shiraki K, Sugimoto K, Yamanaka T, Fujikawa K, Ito M, Takase K, Moriyama M, Kawano H, Hayashida M, Nakano T, Suzuki A. Survivin promotes cell proliferation in human hepatocellular carcinoma. *Hepatology* 2000; **31**: 1080-1085

21 **Grossman D,** McNiff JM, Li F, Altieri DC. Expression of the apoptosis inhibitor, survivin, in nonmelanoma skin cancer and gene targeting in a keratinocyte cell line. *Lab Invest* 1999; **79**: 1121-1126

22 **Olie RA,** Simoes-Wust AP, Baumann B, Leech SH, Fabbro D, Stahel RA, Zangemeister-Wittke U. A novel antisense oligonucleotide targeting survivin expression induces apoptosis and sensitizes lung cancer cells to chemotherapy. *Cancer Res* 2000; **60**: 2805-2809

23 **Jaattela M.** Escaping cell death: survival proteins in cancer. *Exp Cell Res* 1999; **248**: 30-43

24 **Kawasaki H,** Altieri DC, Lu CD, Toyoda M, Tenjo T, Tanigawa N. Inhibition of apoptosis by survivin predicts shorter survival rates in colorectal cancer. *Cancer Res* 1998; **58**: 5071-5074

25 **Nakagawara A.** Molecular basis of spontaneous regression of neuroblastoma: role of neurotrophic signals and genetic abnormalities. *Hum Cell* 1998; **11**: 115-124

26 **Saitoh Y,** Yaginuma Y, Ishikawa M. Analysis of Bcl-2, Bax and Survivin genes in uterine cancer. *Int J Oncol* 1999; **15**: 137-141

27 **Urban E,** Noe CR. Structural modifications of antisense oligonucleotides. *Farmaco* 2003; **58**: 243-258

28 **Shin S,** Sung BJ, Cho YS, Kim HJ, Ha NC, Hwang JI, Chung CW, Jung YK, Oh BH. An anti-apoptotic protein human survivin is a direct inhibitor of caspase-3 and -7. *Biochemistry* 2001; **40**: 1117-1123

29 **Temme A,** Rieger M, Reber F, Lindemann D, Weigle B, Diestelkoetter-Bachert P, Ehninger G, Tatsuka M, Terada Y, Rieber EP. Localization, dynamics, and function of survivin revealed by expression of functional survivinDsRed fusion proteins in the living cell. *Mol Biol Cell* 2003; **14**: 78-92

Edited by Wang XL and Zhu LH

PO Box 2345, Beijing 100023, China
Fax: +86-10-85381893
E-mail: wjg@wjgnet.com www.wjgnet.com

ELSEVIER

World J Gastroenterol 2005;11(2):200-203
World Journal of Gastroenterology ISSN 1007-9327

Detection of hypervascular hepatocellular carcinoma: Comparison of multi-detector CT with digital subtraction angiography and Lipiodol CT

Xiao-Hua Zheng, Yong-Song Guan, Xiang-Ping Zhou, Juan Huang, Long Sun, Xiao Li, Yuan Liu

Xiao-Hua Zheng, Yong-Song Guan, Xiang-Ping Zhou, Juan Huang, Long Sun, Xiao Li, Yuan Liu, Department of Radiology, Huaxi Hospital, Sichuan University, Chengdu 610041, Sichuan Province, China
Supported by the Medical Science Research Fund of Sichuan Province, No. 200054
Correspondence to: Dr. Yong-Song Guan, Department of Radiology, Huaxi Hospital, Sichuan University, 37 Guoxuexiang, Chengdu 610041, Sichuan Province, China. yongsongguan@yahoo.com
Telephone: +86-28-85421008 **Fax:** +86-28-85421008
Received: 2004-04-19 **Accepted:** 2004-05-9

Abstract

AIM: The purpose of this study was to compare the diagnostic accuracy of biphasic multi-detector row helical computed tomography (MDCT), digital subtraction angiography (DSA) and Lipiodol computed tomography (CT) in detection of hypervascular hepatocellular carcinoma (HCC).

METHODS: Twenty-eight patients with nodular HCC underwent biphasic MDCT examination: hepatic arterial phase (HAP) 25 s and portal venous phase (PVP) 70 s after injection of the contrast medium (1.5 mL/kg). They also underwent hepatic angiography and intra-arterial infusion of iodized oil. Lipiodol CT was performed 3-4 wk after infusion. MDCT images were compared with DSA and Lipiodol CT images for detection of hepatic nodules.

RESULTS: The three imaging techniques had the same sensitivity in detecting nodules >20 mm in diameter. There was no significant difference in the sensitivity among HAP-MDCT, Lipiodol CT and DSA for nodules of 10-20 mm in diameter. For the nodules <10 mm in diameter, HAP-MDCT identified 47, Lipiodol CT detected 27 ($\chi^2 = 11.3$, $P = 0.005 < 0.01$, HAP-MDCT *vs* Lipiodol CT) and DSA detected 16 ($\chi^2 = 9.09$, $P = 0.005 < 0.01$ *vs* Lipiodol CT and $\chi^2 = 29.03$, $P = 0.005 < 0.01$ *vs* HAP-MDCT). However, six nodules <10 mm in diameter were detected only by Lipiodol CT.

CONCLUSION: MDCT and Lipiodol CT are two complementary modalities. At present, MDCT does not obviate the need for DSA and subsequent Lipiodol CT as a preoperative examination for HCC.

Key words: Hypervascular hepatocellular carcinoma; Multi-detector CT; Digital subtraction angiography; Lipiodol CT

Zheng XH, Guan YS, Zhou XP, Huang J, Sun L, Li X, Liu Y. Detection of hypervascular hepatocellular carcinoma: Comparison of multi-detector CT with digital subtraction angiography and Lipiodol CT. *World J Gastroenterol* 2005; 11(2): 200-203
http://www.wjgnet.com/1007-9327/11/200.asp

INTRODUCTION

Hepatocellular carcinoma (HCC) is one of the most common malignancies in the world, causing an estimated one million deaths annually. In China, HCC has ranked second in cancer mortality since 1 990s[1]. It has a poor prognosis due to its rapid infiltrating growth and complicating liver cirrhosis. Surgical resection, liver transplantation and cryosurgery are considered the best curative options, achieving a high rate of complete response, especially in patients with small HCC and good residual liver function. Moreover, nonsurgical, regional interventional therapies have led to a major breakthrough in the management of unresectable HCC, which include transarterial chemoembolization (TACE), percutaneous ethanol injection (PEI), radiofrequency ablation (RFA), microwave coagulation therapy (MCT), laser-induced thermotherapy (LITT) and other biotherapies.

Liver resection remains a good treatment for HCC in patients with cirrhosis. Satisfactory results have been obtained in patients with small, non-invasive tumors[2]. However, only a small number of patients are suitable for curative resection due to many factors such as multicentric tumors, intrahepatic metastases, early vascular invasion, coexisting advanced liver cirrhosis and comorbidities[3]. Liver transplantation seems to be the choice for monofocal HCC less than 5 cm in diameter and in selected cases of plurifocal HCC[4]. Therefore, accurate evaluation of intrahepatic metastases, or daughter nodules, is important to determine appropriate treatment for the disease. Because the prognosis after surgical treatment depends on the initial staging, performance of the most accurate preoperative evaluation is crucial. The main difficulty for diagnosis and staging of HCC resides in the detection of small nodular lesions (including intrahepatic metastases and multicentric tumors). Underestimation of these lesions may lead to inappropriate surgical resection. Therefore, accurate preoperative imaging evaluation of HCC nodules is essential for selecting appropriate patients for surgical intervention and for determining the extent of hepatoectomy.

It has been recognized that the majority of HCCs are hypervascular. During the hepatic arterial phase (HAP), hypervascular lesions are greatly enhanced, and become iso- or hypodense in the portal venous phase (PVP), which is a sensitive and specific feature for diagnosing HCC. A biphasic hepatic acquisition helical CT scanning technique has become a standard method for clinical diagnosis of HCC[5-10]. Meanwhile, hepatic angiography is widely used as an imaging technique for HCC. Moreover, Lipiodol CT, which involves CT after intrahepatic arterial injection of iodized oil, has been reported to be the most sensitive preoperative imaging modality for HCC, especially in detecting intrahepatic metastastic nodules[11-13].

Recently, a new generation of multi-detector row helical CT (MDCT) has been used in clinical practice. It is a technologic advance that allows the simultaneous acquisition of multiple images during a single rotation of the X-ray tube. The scanning time can be shortened to 0.5 s. If the 16-detector array CT scanner is used, the entire hepatic acquisition can be accomplished in a very short period of time (4-8 s). Reformations provide a unique perspective to view the liver, and may improve diagnostic

capacity[14]. However, consensus has not been reached as to whether biphasic MDCT obviates the need for other invasive imaging modalities such as digital subtraction angiography (DSA) and Lipiodol CT.

The purpose of this study was to compare the diagnostic accuracy of biphasic MDCT, DSA and Lipiodol CT in detection of hypervascular HCC.

MATERIALS AND METHODS

Patients

From January 2003 to February 2004, 28 patients (24 men, 4 women, mean age 49 years) with nodular HCC were enrolled in this study. The diagnosis was based on the results of percutaneous needle biopsy (n = 12) and operation (n = 2) or test of the serum alpha-fetoprotein levels in combination with imaging appearance and follow-up images (n = 14) according to the diagnostic criteria for HCC formulated by Chinese National Association of Anticancer Committee (1999).

MDCT

MDCT scans of liver were performed with Sensation16 CT scanner (Siemens Medical System, Germany) using the following parameters: 0.5 s scanning time, 5-μm-thick section, 24 mm/s table speed, 120 KVP and 140 mA .

Before examination, 800-1 000 mL water was taken as an oral contrast. The patients underwent unenhanced and biphasic helical CT scanning as follows. First, patients were imaged with a helical MDCT scanner in a cranial-caudal direction beginning at top of the liver. Then, nonionic contrast medium (Ultravist 300, Schering Pharmaceutical Lt., Guangzhou, China) was administered at a dose of 1.5 mL/kg and an injection rate of 3 mL/s via the antecubital vein. Biphase acquisition was performed with a scanning delay set for HAP and PVP at 25 s and 70 s, respectively. Each of the whole liver scanning by cephalad-caudal orientation was completed in 4-8 s with breath held.

DSA and Lipiodol CT

The DSA procedure was obtained with a digital angiographic system (AXIOM Artis FA, Siemens Medical System, Germany). Under local anesthesia, the focal segmental or sub-segmental artery was detected carefully by celiac arteriography, and variants were excluded by superior mesenteric arteriography and phrenic arteriography. When the tip of the catheter arrived at the appropriate focal artery, 30-40 mL of the contrast medium (Ultravist 300, Schering Pharmaceutical Lt., Guangzhou, China) was injected at about 6-8 mL/s. After angiography was performed, 8-15 mL iodized oil (Huaihai Pharmaceutical Factory, Shanghai, China) was dripped through the 5-Fr catheter under fluoroscopic monitoring. CT examination of the liver was performed within 3 to 4 wk after intra-arterial injection of iodized oil to evaluate areas of Lipiodol retention.

Imaging analysis

The images for each radiological method were interpreted in conference by at least two attending radiologists who were unaware of the results of previously performed imaging studies. The HAP and PVP of MDCT images were evaluated in separate sessions, thus keeping the readers unaware of the results of the other phase. Images of each phase were compared at the same hepatic window settings throughout the liver. Images were evaluated to determine lesion size, number, and detectability. Because detectability represents a subjective determination of the ease of visualization of a nodule, detectability depends on the attenuation of the tumor and the liver and the presence of a tumor capsule. Biphasic MDCT scans were compared with DSA and Lipiodol CT scans.

Statistical analysis

To compare the various techniques, Chi-square test was performed, and P values less than 0.05 were considered statistically significant.

RESULTS

The results are summarized in Table 1 and Figure 1. A total of 98 nodules were detected in 28 patients by at least one modality. Two patients had one nodule, four had two nodules, 10 had three nodules, and 12 had four or more nodules. The mean number of HCC nodules per patient was 3.5.

Table 1 Nodule detectability according to size by each imaging technique

Tumor Size (mm)	MDCT		Lipiodol CT	DSA
	HAP	PVP		
<10 mm	47	11	27	16
10-20 mm	19	14	13	11
>20 mm	26	24	26	26
Total	92	49	66	53

MDCT: multi-detector row helical computed tomography; HAP: hepatic arterial phase; PVP: portal venous phase; DSA: digital subtraction angiography.

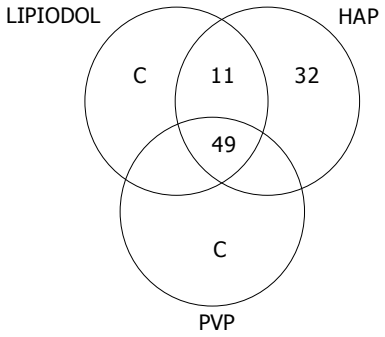

Figure 1 Diagram of nodule detectability by each imaging technique.

Lipiodol CT detected one or more hepatic nodules in 26 of 28 patients for a total 66 nodules. In the remaining 2 patients with negative Lipiodol CT, HAP-MDCT detected 2 nodules. MDCT identified 92 hepatic nodules, HAP-MDCT detected all while PVP-MDCT detected only 49 of these nodules (Table 1). None of the 53 nodules detected by DSA was missed using either Lipiodol CT or HAP-MDCT. When data obtained with Lipiodol CT were compared with those of MDCT, 60 nodules were detected by both techniques, 6 were detected only by Lipiodol CT, and 32 were detected only by HAP-MDCT (Figure 1).

The three imaging techniques used in this study (MDCT, DSA, Lipiodol CT) had the same sensitivity in detecting nodules >20 mm in diameter since the 26 nodules >20 mm in diameter were detected by DSA as well as HAP-MDCT and Lipiodol CT. MDCT and Lipiodol CT were also comparable in detection of nodules with diameters of 10-20 mm in diameter. In fact, 19 of these nodules were seen by HAP-MDCT (14 by PVP-MDCT), and 13 by Lipiodol CT. For nodules < 10 mm in diameter, HAP-MDCT identified 47 nodules, Lipiodol CT showed 27 including the six nodules not detected by MDCT (HAP-MDCT *vs* Lipiodol CT: $\chi^2 = 11.3$, $P = 0.005 < 0.01$), DSA showed 16 ($\chi^2 = 9.09$, $P = 0.005 < 0.01$, *vs* Lipiodol CT and $\chi^2 = 29.03$, $P = 0.005 < 0.01$, *vs* HAP-MDCT) and PVP showed 11 (Figures 2, 3).

Figure 2 A hepatocellular carcinoma nodule identified by Lipiodol CT but not by biphasic MDCT in a 53-year-old man. A: MDCT scan during the arterial phase shows a 3-cm hypervascular tumor in S5 (arrowhead); B: DSA confirms the MDCT findings (arrowhead); C: Lipiodol CT identifies another tumor in S6 (arrowhead) in addition to S5.

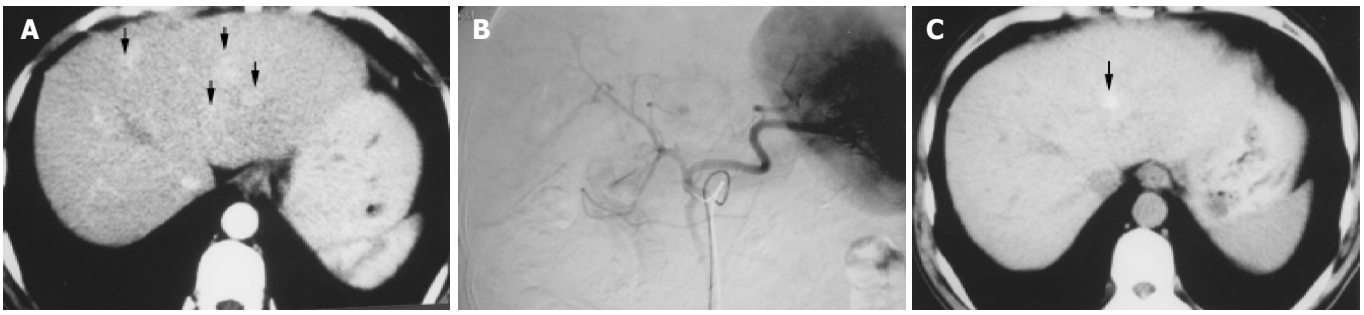

Figure 3 Hepatocellular carcinoma nodules identified by MDCT, but not by Lipiodol CT in a 46-year-old man. A: Four nodules measuring 1-cm in diameter (arrowhead) were depicted as hyperattenuating lesions during the arterial phase by MDCT; B: These lesions were not detected by DSA; C: Only one lesion was deposited by Lipiodol CT (arrowhead).

DISCUSSION

In preoperative evaluation of hepatic tumors, the imaging studies used must be highly sensitive and specific for the detection of malignant neoplasms to enable the selection of appropriate surgical candidates and avoid unnecessary surgery. Several authors have evaluated the accuracy of Lipiodol CT imaging in detecting HCC nodules. They used histologic assessment of liver biopsy specimens, liver parenchyma taken by partial liver resection, or explanted liver at the time of liver transplantation as references and have reported a wide variety of sensitivities (40% to >90%)[12,15-21]. Still, the question of whether Lipiodol CT provides information beyond that obtained with other noninvasive modalities, as preoperative evaluation in the era of MDCT, remains to be addressed. In recent years, a few studies[14,22-25] have evaluated the role of multiphasic scanning by MDCT in detecting small hypervascular HCC. They have drawn a conclusion that the utility of faster speed and thinner slice (6 mm) MDCT can improve the detectability of hypervascular small HCC, and additional early arterial phase imaging does not improve the detection of HCC compared with biphasic CT images. With these in mind, we reviewed the experience with DSA, Lipiodol CT and biphasic MDCT performed at our institution.

It has been known that the imaging techniques for detection and staging of HCC take advantages of two basic events: 1) the disappearance of portal vessels, which are substituted with arterial vessels; and 2) a progressive disappearance of the reticuloendothelial system (RES)[26]. The latter has been exploited by Lipiodol CT: the iodized oil that reaches the hepatic parenchyma via the hepatic artery is eliminated within 3-4 wk by Kuppfer cells, but not by neoplastic nodules, which can be easily detected by performing a second CT scan 3-4 wk later. Unfortunately, this technique gives both false positive and false negative results. False positive results are due to the persistence of Lipiodol in non-neoplastic areas of the liver due to an altered RES, within angiomas, or at the site of a previous liver biopsy[27]. False negative results are due to the presence of neoplastic foci not reached by Lipiodol and/or tracer eliminated from the foci. In the current investigation, false negative results were more frequent in the case of small neoplastic nodules (<2 cm)[15,17]. The phenomenon may attribute to a greater degree of differentiation of these small HCC nodules, with persistence of some reticuloendothelial cells, less developed arterial vascularization, or both.

MDCT focuses on the other main characteristic of HCC, which is the development of new arterial vascularization, probably an earlier phenomenon than the disappearance of RES. The results of this study clearly indicate that MDCT has a remarkably greater sensitivity than DSA and Lipiodol CT in detecting small neoplastic nodules (<20 mm). The advantage of MDCT scan is mainly due to the possibility of imaging the liver in the arterial phase, as demonstrated by the comparison between HAP and PVP.

In this study, all 28 patients had at least one overt HCC. We defined the largest lesions as the main lesions, while called the other lesions as small nodular lesions (including intrahepatic metastases and multicentric tumors). It is not possible to discriminate completely between daughters (i.e., intrahepatic metastatic) and multicentric tumors based solely on imaging or pathologic findings. However, it is generally accepted that a tumor becomes less differentiated (i.e., well to moderately or poorly) as its size increases, whereas daughter nodules are small but their grade of differentiation is moderate to poor[12]. In light of these considerations, the present results strongly suggest that MDCT is superior to Lipiodol CT in delineating early HCC nodules, but the latter method is superior for detecting intrahepatic metastatic lesions.

This study has limitations. Firstly, histologic confirmation of each nodule was not obtained, not allowing a precise CT-histopathologic correlation of each nodule, although we

performed biopsy on the main lesion in some patients. Specificity was not confirmed, but a combination of the clinical course, laboratory values, and imaging appearance is believed to be sufficient for a presumptive diagnosis of hypervascular HCC nodules. On the other hand, ultrasound or CT-guided needle biopsy is less sensitive than imaging in the detection of this kind of malignancy (75% of needle biopsy *vs* 97% of imaging), as needle sampling involves only a small part of the lesion, and this may not include the area of neoplastic degeneration. Secondly, some lesions might be missed by all three imaging techniques used in this study since there is a possibility that the three techniques do not have 100% sensitivity for the detection of nodular HCC. Consequently, we could not obtain the true sensitivity, specificity, and accuracy of the three techniques. However, Torzilli *et al* reported that the respective accuracy, sensitivity, specificity, and positive and negative predictive values were 99.6%, 100%, 98.9%, 99.3%, and 100% for diagnosis of HCC using a combination of ultrasonography, spiral CT, angiography, magnetic resonance imaging (MRI), and Lipiodol CT. Thirdly, hypovascular HCC cases were excluded because of the difficult verification of these tumors by the methods we used. Although this type of HCC is not common, the overall detectability of nodular HCC cannot be estimated.

Further studies based on accurate follow-up of patients with HCC or a pathologic correlation with livers studied at surgery or autopsy are needed to clarify the nature of hepatic nodules detected with the three techniques.

From the present study, we conclude that biphasic MDCT and Lipiodol CT appear to be complementary, although the overall ability of biphasic MDCT scan to detect hypervascular HCC nodules is superior to that of Lipiodol CT. At present, MDCT does not obviate the need for DSA and subsequent Lipiodol CT as a preoperative examination for HCC. In addition, intra-arterial infusion of iodized oil can be also used for therapy.

REFERENCES

1 **Tang ZY.** Hepatocellular carcinoma-cause, treatment and metastasis. *World J Gastroenterol* 2001; **7**: 445-454
2 **Franco D,** Usatoff V. Resection of hepatocellular carcinoma. *Hepatogastroenterology* 2001; **48**: 33-36
3 **Alsowmely AM,** Hodgson HJ. Non-surgical treatment of hepatocellular carcinoma. *Aliment Pharmacol Ther* 2002; **16**: 1-15
4 **Colella G,** Bottelli R, De Carlis L, Sansalone CV, Rondinara GF, Alberti A, Belli LS, Gelosa F, Iamoni GM, Rampoldi A, De Gasperi A, Corti A, Mazza E, Aseni P, Meroni A, Slim AO, Finzi M, Di Benedetto F, Manochehri F, Follini ML, Ideo G, Forti D. Hepatocellular carcinoma: comparison between liver transplantation, resective surgery, ethanol injection, and chemoembolization. *Transpl Int* 1998; **11** Suppl 1: S193-S196
5 **Baron RL,** Oliver JH, Dodd GD, Nalesnik M, Holbert BL,Carr B. Hepatocellular carcinoma: evaluation with biphasic, contrast-enhanced, helical CT. *Radiology* 1996; **199**: 505-511
6 **Oliver JH,** Baron RL, Federle MP, Rockette HE. Detecting hepatocellular carcinoma: value of unenhanced or arterial phase CT imaging or both used in conjunction with conventional portal venous phase contrast-enhanced CT imaging. *AJR Am J Roentgenol* 1996; **167**: 71-77
7 **Oliver JH,** Baron RL. Helical biphasic contrast-enhanced CT of the liver: technique, indications, interpretation, and pitfalls. *Radiology* 1996; **201**: 1-14
8 **Oliver JH,** Baron RL, Federle MP, Jones BC, Sheng R. Hypervascular liver metastases: do unenhanced and hepatic arterial phase CT images affect tumor detection? *Radiology* 1997; **205**: 709-715
9 **Paulson EK,** McDermott VG, Keogan MT, DeLong DM, Frederick MG, Nelson RC. Carcinoid metastases to the liver: role of triple-phase helical CT. *Radiology* 1998; **206**: 143-150
10 **Mitsuzaki K,** Yamashita Y, Ogata I, Nishiharu T, Urata J, Takahashi M. Multiple-phase helical CT of the liver for detecting small hepatomas in patients with liver cirrhosis: contrast-injection protocol and optimal timing. *AJR Am J Roentgenol* 1996; **167**: 753-757
11 **Bartolozzi C,** Lencioni R, Caramella D, Palla A, Bassi AM, Di Candio G. Small hepatocellular carcinoma. Detection with US, CT, MR imaging, DSA, and Lipiodol-CT. *Acta Radiol* 1996; **37**: 69-74
12 **Lencioni R,** Pinto F, Armillotta N, Di Giulio M, Gaeta P, Di Candio G, Marchi S, Bartolozzi C. Intrahepatic metastatic nodules of hepatocellular carcinoma detected at lipiodol-CT: imaging-pathologic correlation. *Abdom Imaging* 1997; **22**: 253-258
13 **Itai Y.** Lipiodol-CT for hepatocellular carcinoma. *Abdom Imaging* 1997; **22**: 259-260
14 **Wong K,** Paulson EK, Nelson RC. Breath-hold three-dimensional CT of the liver with multi-detector row helical CT. *Radiology* 2001; **219**: 75-79
15 **Veltri A,** Robba T, Anselmetti GC, Martina MC, Regge D, Grosso M, Fava C. Computerized tomography with lipiodol in hepatocarcinoma. Assessment of its diagnostic accuracy with anatomo-pathological control. *Radiol Med* 1998; **96**: 81-86
16 **Bizollon T,** Rode A, Bancel B, Gueripel V, Ducerf C, Baulieux J, Trepo C. Diagnostic value and tolerance of Lipiodol-computed tomography for the detection of small hepatocellular carcinoma: correlation with pathologic examination of explanted livers. *J Hepatol* 1998; **28**: 491-496
17 **Spreafico C,** Marchiano A, Mazzaferro V, Frigerio LF, Regalia E, Lanocita R, Patelli G, Andreola S, Garbagnati F, Damascelli B. Hepatocellular carcinoma in patients who undergo liver transplantation: sensitivity of CT with iodized oil. *Radiology* 1997; **203**: 457-460
18 **Valls C,** Figueras J, Jaurrieta E, Sancho C, Dominguez J, Benasco C, Moreno P, Rafecas A, Virgili J, Castellsague X. Hepatocellular carcinoma: iodized-oil CT TNM classification. *AJR Am J Roentgenol* 1996; **167**: 477-481
19 **Taourel PG,** Pageaux GP, Coste V, Fabre JM, Pradel JA, Ramos J, Larrey D, Domergue J, Michel H, Bruel JM. Small hepatocellular carcinoma in patients undergoing liver transplantation: detection with CT after injection of iodized oil. *Radiology* 1995; **197**: 377-380
20 **Bhattacharya S,** Dhillon AP, Rees J, Savage K, Saada J, Burroughs A, Rolles K, Davidson B. Small hepatocellular carcinomas in cirrhotic explant livers: identification by macroscopic examination and lipiodol localization. *Hepatology* 1997; **25**: 613-618
21 **Saada J,** Bhattacharya S, Dhillon AP, Dick R, Burroughs AK, Rolles K, Davidson BR. Detection of small hepatocellular carcinomas in cirrhotic livers using iodised oil computed tomography. *Gut* 1997; **41**: 404-407
22 **Laghi A,** Iannaccone R, Rossi P, Carbone I, Ferrari R, Mangiapane F, Nofroni I, Passariello R. Hepatocellular carcinoma: detection with triple-phase multi-detector row helical CT in patients with chronic hepatitis. *Radiology* 2003; **226**: 543-549
23 **Ichikawa T,** Kitamura T, Nakajima H, Sou H, Tsukamoto T, Ikenaga S, Araki T. Hypervascular hepatocellular carcinoma: can double arterial phase imaging with multidetector CT improve tumor depiction in the cirrhotic liver? *AJR Am J Roentgenol* 2002;**179**: 751-758
24 **Kawata S,** Murakami T, Kim T, Hori M, Federle MP, Kumano S, Sugihara E, Makino S, Nakamura H, Kudo M. Multidetector CT: diagnostic impact of slice thickness on detection of hypervascular hepatocellular carcinoma. *AJR Am J Roentgenol* 2002; **179**: 61-66
25 **Kim SK,** Lim JH, Lee WJ, Kim SH, Choi D, Lee SJ, Lim HK, Kim H. Detection of hepatocellular carcinoma: comparison of dynamic three-phasecomputed tomography images and four-phase computed tomography images using multidetector row helical computed tomography. *J Comput Assist Tomogr* 2002; **26**: 691-698
26 **Choi BI,** Takayasu K, Han MC. Small hepatocellular carcinomas and associated nodular lesions of the liver: pathology, pathogenesis, and imaging findings. *AJR Am J Roentgenol* 1993; **160**: 1177-1187
27 **Veltri A,** Robba T, Anselmetti GC, Martina MC, Regge D, Grosso M, Fava C. Computerized tomography with lipiodol in hepatocarcinoma. Assessment of its diagnostic accuracy with anatomo-pathological control. *Radiol Med* 1998; **96**: 81-86

Edited by Xia HHX and Wang XL **Proofread by** Ma JY

PO Box 2345, Beijing 100023, China
Fax: +86-10-85381893
E-mail: wjg@wjgnet.com www.wjgnet.com

ELSEVIER

World J Gastroenterol 2005;11(2):204-207
World Journal of Gastroenterology ISSN 1007-9327

Specific COX-2 inhibitor NS398 induces apoptosis in human liver cancer cell line HepG2 through BCL-2

Dong-Sheng Huang, Ke-Zhen Shen, Jian-Feng Wei, Ting-Bo Liang, Shu-Sen Zheng, Hai-Yang Xie

Dong-Sheng Huang, Ke-Zhen Shen, Jian-Feng Wei, Ting-Bo Liang, Shu-Sen Zheng, Hai-Yang Xie, Department of Hepatobiliary Pancreatic Surgery, The First Affiliated Hospital, Zhejiang University, College of Medicine, Hangzhou 310003, Zhejiang Province, China
Correspondence to: Dr. Hai-Yang Xie, Department of Hepatobiliary Pancreatic Surgery, The First Affiliated Hospital, College of Medicine, Zhejiang University, Hangzhou 310003, Zhejiang Province, China. xiehaiyang@zju.edu.cn
Telephone: +86-571-87236570 **Fax:** +86-571-87236570
Received: 2003-06-21 **Accepted:** 2003-09-25

Abstract

AIM: To evaluate the effects of NS-398, a cyclooxygenase-2 (COX-2) inhibitor, on the proliferation and apoptosis of HepG2 cells.

METHODS: The effects of NS-398 on the proliferation of HepG2 cells were evaluated by MTT. DNA fragmentation gel analysis was used to analyze the apoptotic cells. DNA ploidy and apoptotic cell percentage were calculated by flow cytometry. The expression of COX-2 and Bcl-2 mRNA was identified by competitive RT-PCR. Furthermore, expression level of Bcl-2 was detected using Western blot in HepG2 after treated with NS-398.

RESULTS: NS-398 inhibited cell proliferation and induced apoptosis of HepG2 cells in a concentration-dependent manner. DNA ploidy analysis showed that S phase cells were significantly decreased with increase of NS-398 concentration. The quiescent G0/G1 phase was accumulated with decrease of Bcl-2 mRNA. Whereas NS-398 had no effect on the expression of COX-2 mRNA, and no correlations were found between COX-2 mRNA and HepG2 cell proliferation and apoptosis induced by NS-398 (r = 0.056 and r = 0.119, respectively). Bcl-2 protein level was inhibited after treated with NS-398.

CONCLUSION: NS-398 significantly inhibits the proliferation and induces apoptosis of HepG2 cells. Mechanisms involved may be accumulation of quiescent G0/G1 phase and decrease of Bcl-2 expression.

Key words: Liver cancer; NS-398; Bcl-2 protein; COX-2

Huang DS, Shen KZ, Wei JF, Liang TB, Zheng SS, Xie HY. Specific COX-2 inhibitor NS398 induces apoptosis in human liver cancer cell line HepG2 through BCL-2. *World J Gastroenterol* 2005; 11(2): 204-207
http://www.wjgnet.com/1007-9327/11/204.asp

INTRODUCTION

Two forms of cyclooxygenase, Cox-1 and Cox-2, which can convert arachidonic acid to prostaglandins, have been identified. Cox-1 is constitutively expressed and synthesizes cytoprotective prostaglandins mainly in the gastrointestinal tract while Cox-2 is highly inducible by the oncogenes *ras* and *scr* and other cytokines at the sites of inflammation and cancer[1]. Preview studies have shown that most cancer cells are found to exhibit over-expression of Cox-2, which can stimulate cellular division and angiogenesis and inhibit apoptosis[2].

In hepatocellular carcinoma (HCC), the expression pattern of Cox-2 protein is well correlated with the differentiation grade, suggesting that abnormal Cox-2 expression plays an important role in hepatocarcinogenesis while inhibition of Cox-2 can induce growth suppression of hepatoma cell lines via induction of apoptosis[3].

Nonsteriodal anti-inflammatory drugs (NSAIDs) have been shown to exert anti-proliferative and pro-apoptotic effects on a variety of cell lines by inhibiting the expression of Cox[4]. Epidemiological studies also show a lower risk of cancers of the colon, breast, esophagus, and stomach following ingestion of NSAIDs[5]. On the other hand, classic NSAIDs inhibit both Cox-2, and Cox-1, resulting in the common side-effect of gastric mucosal damage. To reduce the gastrointestinal side-effects of NSAIDs, selective Cox-2 inhibitors have been developed[6], and the effect of these selective inhibitors on the proliferation and apoptosis of liver cancer cells has been the subject of investigation in recent years[7-9]. However, the underlying mechanism how Cox-2 inhibitor executes anti-proliferation and proapoptotic effect on liver cancer cells is still unclear. To address this issue, we investigated the mechanism of Cox-2 specific inhibitor, NS-398 on the proliferation and apoptosis of HepG2 cells.

MATERIALS AND METHODS

Materials

HepG2 human hepatocellular carcinoma cells (ATCC CCL2) were maintained in DMEM supplemented with 10% FBS, 100 units/mL penicillin and 100 μg/mL streptomycin.

TRIzol reagent, RNase A and MuLV transcriptase were purchased from Invitrogen (Gibco, BRL). NS-398 and all other reagents were purchased from Sigma. The Bcl-2 antibody was purchased from Santa Cruz (USA).

Methods

MTT test MTT test was used to monitor cell proliferation and apoptosis according to Hansen's protocol[10]. Briefly, HepG2 cells were first cultured in 96-well microplates (1×10^4 cells/well) in 100 μL of complete DMEM for 12 h. Cells were then treated with indicated concentrations of NS-398 in FBS-free MEM for 72 h. At the end of incubation, 25 μL of MTT (5 mg/mL) was added to each well and incubation was allowed to continue for further 4 h. Finally, 100 μL of DMSO was added to each well. The plate was read using a microplate reader (BIO-RAD, USA) at a wavelength of 590 nm.

Flow cytometry assay DNA content assay was carried out to detect cell cycle change of HepG2 cells under NS-398. HepG2 cells were seeded in a 6-well plate and treated with NS-398 for 72 h. The cells were trypsinized and fixed with 70% (vol/vol, -20 ℃) ethanol in PBS. After centrifugation, the pellet was

resuspended with staining solution (0.1% Triton X-100, 0.2 mg/mL RNase A and propidium iodide in PBS). The samples were analysed in a flow cytometer (Couter, USA) after incubated for 30 min at room temperature in dark.

DNA ladder Cell apoptosis induced by NS-398 was analyzed by agarose gel-electrophoresis. Briefly, cells (1×10^6) were lysed with 0.5 mL lysis buffer and suspended, followed by the addition of RNase A to a final concentration of 200 μg/mL, and incubated for 1 h at 37 ℃. Cells were then treated with 300 μg/mL of proteinase K for 1 h at 37 ℃. After addition of 4 μL loading buffer, 20 μL samples in each lane was subjected to electrophoresis on an 1.5% agarose at 50 V for 3 h. DNA was stained with ethidium bromide and laddering was visualized under UV light.

Reverse transcription polymerase chain reaction To study cytokine gene expression patterns, we used competitive template reverse transcription-polymerase chain reaction (RT-PCR). Total RNA was extracted from HepG2 cells using TRIzol reagent according to the manufacturer's recommendations. For cDNA synthesis, 4 μg total RNA was reverse transcribed with MuLV reverase transcriptase. Sequences of the primers used for RT-PCR analysis are described in Table 1. Thirty-two cycles of amplifications were performed under the following conditions: at 95 ℃ for 2 min, at 94 ℃ for 45 s, at 56 ℃ for 45 s, at 72 ℃ for 45 s. The final extension step was performed by one cycle at 72 ℃ for 10 min. twenty-five reaction system was used, including 2 μL cDNA template, 1 μL sense primer, 1 μL anti-sense primer, 2 μL 25 mmol $MgCl_2$, 1 μL dNTP and 1.5 u Taq DNA polymerase. Reaction products were run by electrophoresis on an 1.5% agarose gel for 30-40 min at 100 V in 0.5×TBE buffer, and visualized with ethidium bromide staining under UV light. Relative expression level of BCL-2 and COX-2 was defined as optical density ratio (Target gene/GAPDH) analyzed by Kodak digital science scanning system.

Table 1 Sequences of primers for amplifed cDNA of *Cox-2*, *Bcl-2* and *GAPDH*

Gene	Primer	Sequence	Length of product
Cox-2	Sense	5′-TGAAACCCACTCCAAACACACAG-3′	232 bp
	Anti-sense	5′-TCATCAGGCACAGGAGGAAG-3′	
Bcl-2	Sense	5′-GACTTCGCCGAGATGTCCAG-3′	225 bp
	Anti-sense	5′-CAGGTGCCGGTTCAGGTACT-3′	
GAPDH	Sense	5′-ATGGCACCGTCAAGGCTGAG-3′	379 bp
	Anti-sense	5′-GCAGTGATGGCATGGACTGT-3′	

Antibodies and Western blot Total proteins were extracted using Western blot lysis buffer containing 5 mmol/L EDTA, 150 mmol/L NaCl, 50 mmol/L TrisHCl, 1% TritonX-100 and 0.1% SDS. The protease inhibitor cocktail prepared from protease inhibitor cocktail tablets (Roche) was added and used for no more than 2 wk. Protein extracts (20 μg) were run on 10% SDS-PAGE gels and transfered to PVDF membrane (Amersham Biosciences, USA). Following this, the membrane was blocked with 5% non-fat dry milk in TBS-T buffer for 1h and incubated with appropriate dilution ratio of first antibody overnight at 4 ℃. The membranes were incubated with secondary antibody for 1 h at room temperature and detected with ECL reagent (Santa Cruz, USA).

Statistical analysis

All data were expressed as mean±SD and analyzed by one-way of variance (ANOVA) using SPSS software (version 11.0 for Windows). Pearson correlation analysis was used between parameters. $P<0.05$ was considered statistically significant.

RESULTS

Inhibition of HepG2 cell proliferation by NS-398

To determine the effect of the selective Cox-2 inhibitor NS-398 on HepG2 cell apoptosis, we measured the cell viability with the MTT assay for 72 h at different concentrations. As shown in Figure 1, the cell proliferation was inhibited significantly in a dose-dependent manner at the final concentrations of 50 μmol/L, 100 μmol/L and 200 μmol/L ($P<0.05$ *vs* control).

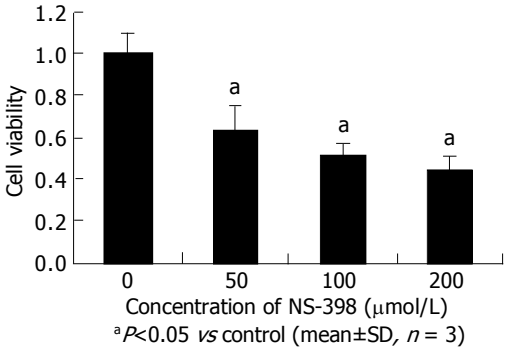

Figure 1 Inhibition of HepG2 cell proliferation by NS-398.

G0/G1 arrest and apoptosis of HepG2 cells induced by NS-398

To assess the effect of NS-398 on inducing HepG2 cell apoptosis, we used DNA content test by flow cytometry. HepG2 cells were treated with NS-398 at indicated concentrations and harvested after 72 h. Then the cells were stained with propidium iodide (PI) and analyzed by flow cytometry. Figure 2A shows that NS-398, at concentrations of 100 μmol/L and 200 μmol/L, significantly increased the number of cells in G0/G1 by 67.5% and 73.1% respectively in comparison to control cells in which 61.2% of cells were in G0/G1. A reciprocal reduction in the number of cells in S phase was also observed. We detected the further effect of NS-398 on induction of HepG2 cell apoptosis. The nucleosome-sized DNA fragments, typical signs of programmed cell death, are shown in Figure 2B. The results showed that HepG2 liver cancer cell apoptosis was induced in a dose-dependent manner after treated with NS-398.

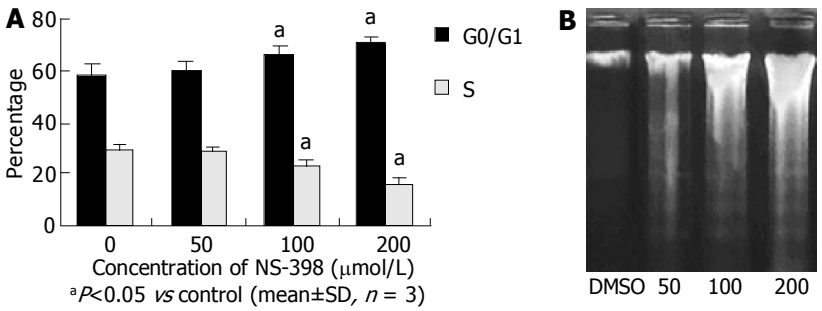

Figure 2 G0/G1 arrest and apoptosis of HepG2 cells induced by NS-398. A: G0/G1 arrest in HepG2 cells after treated with NS-398 for 72 h; B: Typical signs of programmed cell death after treated with NS-398.

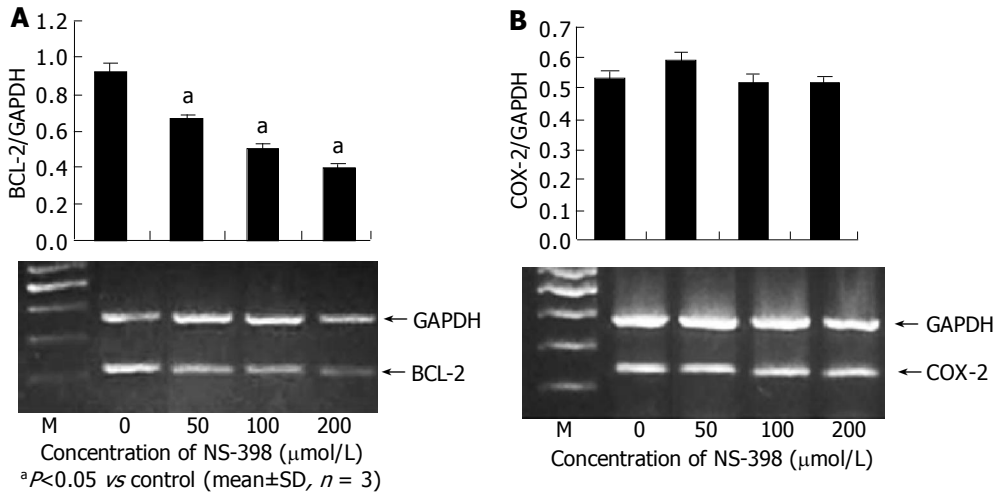

[a] $P<0.05$ *vs* control (mean±SD, $n = 3$)

Figure 3 Inhibition of Bcl-2 mRNA (A) and Bcl-2 protein expression by NS-398 (B).

Inhibition of Bcl-2 expression

Cox-2 and Bcl-2 mRNA expressions by NS-398 were confirmed by semi-quantitive RT-PCR analysis. The cDNA was prepared from HepG2 cells after treated with NS-398 at different concentrations for 72 h. Bcl-2 mRNA levels were decreased in a dose-dependent manner after treated with NS-398 while no significant change was found in Cox-2 mRNA (Figure 3A). Equal loading was confirmed by the housekeeping gene GAPDH.

Specific antibodies were used to detect Bcl-2 protein by Western blot. As shown in Figure 3B, the Bcl-2 protein levels decreased after treated with NS-398 in a dose-dependent manner.

DISCUSSION

Recently, accumulated evidence suggests that many cancers are associated with abnormal expression of Cox-2[11-13]. Several reports have shown that over-expression of Cox-2 is found in a variety of carcinomas including liver cancer[3,14], colon cancer[15,16], breast cancer[17,18], pancreatic cancer[19], lung cancer[20] and uterine carcinoma[21], *etc*. Cox-2 can be induced by a variety of proteins, including cytokines, growth factors, and tumor promoters[22]. It is thought that over-expression of Cox-2 can increase cell survival by inhibition of apoptosis and stimulation of angiogenesis, and enhancement of cellular adhesion to matrix proteins[23]. Although NSAIDs have been used in clinical cancer prevention and can induce tumor cells to undergo apoptosis[24], long-term use is limited in clinic because of its no-specific and high frequency of side-effects[25]. Therefore, selective Cox-2 inhibitors have become a focus of attention as potential chemopreventive and chemotherapeutic agents.

NS-398, one of the selective Cox-2 inhibitors, has been shown to inhibit proliferation and induce apoptosis in carcinomas including colon[26], breast, lung[27] and liver cancers[28]. But the detail mechanism is unclear. In this study, we used the HepG2 cell line to explore the mechanism of liver cancer apoptosis after treatment with NS-398.

Our data show that selective Cox-2 inhibitor NS-398 can inhibit proliferation and induce apoptosis of HepG2 liver cancer cells in a dose-dependent manner. We also found that the dose to induce apoptosis was much higher than that to inhibit expression of Cox-2, indicating that COX-2-independent actions of NS398 may exist[29]. Although most previous studies have shown that induction of apoptosis by NS398 is associated with Cox-2 expression, Cox-2 independent effects of NS398 may exist[30]. Several other studies, however, have shown that there is no correlation between COX-2 expression and apoptosis induced by NSAIDs, including NS398[31]. We compared the Cox-2 expression between the cells treated and untreated with NS-398. The results showed that expression Cox-2 was not associated with apoptosis HepG2 cells.

The Bcl-2 gene has been implicated as a major player in apoptosis pathway[32]. Aspirin-induced apoptosis is associated with the down-regulation of Bcl-2 expression in HEC cells[33]. We also compared the level of anti-apoptotic gene Bcl-*2* after treated with NS-398 and found that NS-398 could down-regulate the expression of Bcl-2, suggesting that down-regulation of Bcl-2 may be required for HepG2 cell apoptosis induced by NS-398, thus increasing mitochondrial permeability and cytochrome C release, which will initiate the progress of apoptosis[34].

In conclusion, selective Cox-2 inhibitor, NS-398, can suppress the growth of HepG2 cells by reducing proliferation and induction of apoptosis. Cox-2-specific inhibitor offers a potential candidate as an effective chemotherapeutic and chemopreventive strategy against human cancer.

REFERENCES

1 **Turini ME,** DuBois RN. Cyclooxygenase-2: a therapeutic target. *Annu Rev Med* 2002; **53**: 35-57
2 **Dempke W,** Rie C, Grothey A, Schmoll HJ. Cyclooxygenase-2: a novel target for cancer chemotherapy? *J Cancer Res Clin Oncol* 2001; **127**: 411-417
3 **Bae SH,** Jung ES, Park YM, Kim BS, Kim BK, Kim DG, Ryu WS. Expression of cyclooxygenase-2 (COX-2) in hepatocellular carcinoma and growth inhibition of hepatoma cell lines by a COX-2 inhibitor, NS-398. *Clin Cancer Res* 2001; **7**: 1410-1418
4 **Subbaramaiah K,** Dannenberg AJ. Cyclooxygenase 2: a molecular target for cancer prevention and treatment. *Trends Pharmacol Sci* 2003; **24**: 96-102
5 **Moran EM.** Epidemiological and clinical aspects of nonsteroidal anti-inflammatory drugs and cancer risks. *J Environ Pathol Toxicol Oncol* 2002; **21**: 193-201
6 **Stratton MS,** Alberts DS. Current application of selective COX-2 inhibitors in cancer prevention and treatment. *Oncology (Williston Park)* 2002; **16**: 37-51
7 **Qiu DK,** Ma X, Peng YS, Chen XY. Significance of cyclooxygenase-2 expression in human primary hepatocellular carcinoma. *World J Gastroenterol* 2002; **8**: 815-817
8 **Kern MA,** Schubert D, Sahi D, Schoneweiss MM, Moll I, Haugg AM, Dienes HP, Breuhahn K, Schirmacher P. Proapoptotic and antiproliferative potential of selective cyclooxygenase-2 inhibitors in human liver tumor cells. *Hepatology* 2002; **36**: 885-894
9 **Cheng J,** Imanishi H, Amuro Y, Hada T. NS-398, a selective cyclooxygenase 2 inhibitor, inhibited cell growth and induced cell cycle arrest in human hepatocellular carcinoma cell lines.

Int J Cancer 2002; **99**: 755-761
10 **Hansen MB,** Nielsen SE, Berg K. Re-examination and further development of a precise and rapid dye method for measuring cell growth/cell kill. *J Immunol Methods* 1989; **119**: 203-210
11 **Mohan S,** Epstein JB. Carcinogenesis and cyclooxygenase: the potential role of COX-2 inhibition in upper aerodigestive tract cancer. *Oral Oncol* 2003; **39**: 537-546
12 **Iniguez MA,** Rodriguez A, Volpert OV, Fresno M, Redondo JM. Cyclooxygenase-2: a therapeutic target in angiogenesis. *Trends Mol Med* 2003; **9**: 73-78
13 **Dang CT,** Shapiro CL, Hudis CA. Potential role of selective COX-2 inhibitors in cancer management. *Oncology (Williston Park)* 2002; **16**: 30-36
14 **Shiota G,** Okubo M, Noumi T, Noguchi N, Oyama K, Takano Y, Yashima K, Kishimoto Y, Kawasaki H. Cyclooxygenase-2 expression in hepatocellular carcinoma. *Hepatogastroenterology* 1999; **46**: 407-412
15 **Fournier DB,** Gordon GB. COX-2 and colon cancer: potential targets for chemoprevention. *J Cell Biochem Suppl* 2000; **34**: 97-102
16 **Taketo MM.** COX-2 and colon cancer. *Inflamm Res* 1998; **47** Suppl 2: S112-116
17 **Costa C,** Soares R, Reis-Filho JS, Leitao D, Amendoeira I, Schmitt FC. Cyclo-oxygenase 2 expression is associated with angiogenesis and lymph node metastasis in human breast cancer. *J Clin Pathol* 2002; **55**: 429-434
18 **Singh-Ranger G,** Mokbel K. The role of cyclooxygenase-2 (COX-2) in breast cancer, and implications of COX-2 inhibition. *Eur J Surg Oncol* 2002; **28**: 729-737
19 **Ding XZ,** Tong WG, Adrian TE. Blockade of cyclooxygenase-2 inhibits proliferation and induces apoptosis in human pancreatic cancer cells. *Anticancer Res* 2000; **20**: 2625-2631
20 **Takahashi T,** Kozaki K, Yatabe Y, Achiwa H, Hida T. Increased expression of COX-2 in the development of human lung cancers. *J Environ Pathol Toxicol Oncol* 2002; **21**: 177-181
21 **Kim YB,** Kim GE, Cho NH, Pyo HR, Shim SJ, Chang SK, Park HC, Suh CO, Park TK, Kim BS. Overexpression of cyclooxygenase-2 is associated with a poor prognosis in patients with squamous cell carcinoma of the uterine cervix treated with radiation and concurrent chemotherapy. *Cancer* 2002; **95**: 531-539
22 **Subongkot S,** Frame D, Leslie W, Drajer D. Selective cyclooxygenase-2 inhibition: a target in cancer prevention and treatment. *Pharmacotherapy* 2003; **23**: 9-28
23 **Richter M,** Weiss M, Weinberger I, Furstenberger G, Marian B. Growth inhibition and induction of apoptosis in colorectal tumor cells by cyclooxygenase inhibitors. *Carcinogenesis* 2001; **22**: 17-25
24 **Husain SS,** Szabo IL, Tamawski AS. NSAID inhibition of GI cancer growth: clinical implications and molecular mechanisms of action. *Am J Gastroenterol* 2002; **97**: 542-553
25 **Kune GA.** Colorectal cancer chemoprevention: aspirin, other NSAID and COX-2 inhibitors. *Aust N Z J Surg* 2000; **70**: 452-455
26 **Hara A,** Yoshimi N, Niwa M, Ino N, Mori H. Apoptosis induced by NS-398, a selective cyclooxygenase-2 inhibitor, in human colorectal cancer cell lines. *Jpn J Cancer Res* 1997; **88**: 600-604
27 **Rioux N,** Castonguay A. Prevention of NNK-induced lung tumorigenesis in A/J mice by acetylsalicylic acid and NS-398. *Cancer Res* 1998; **58**: 5354-5360
28 **Leng J,** Han C, Demetris AJ, Michalopoulos GK, Wu T. Cyclooxygenase-2 promotes hepatocellular carcinoma cell growth through Akt activation: evidence for Akt inhibition in celecoxib-induced apoptosis. *Hepatology* 2003; **38**: 756-768
29 **Souza RF,** Shewmake K, Beer DG, Cryer B, Spechler SJ. Selective inhibition of cyclooxygenase-2 suppresses growth and induces apoptosis in human esophageal adenocarcinoma cells. *Cancer Res* 2000; **60**: 5767–5772
30 **Li M,** Wu X, Xu XC. Induction of apoptosis by cyclo-oxygenase-2 inhibitor NS398 through a cytochrome C-dependent pathway in esophageal cancer cells. *Int J Cancer* 2001; **93**: 218-223
31 **Elder DJ,** Halton DE, Hague A, Paraskeva C. Induction of apoptotic cell death in human colorectal carcinoma cell lines by a cyclooxygenase-2 (COX-2)-selective nonsteroidal anti-inflammatory drug: independence from COX-2 protein expression. *Clin Cancer Res* 1997; **3**: 1679–1683
32 **Kroemer G,** Reed JC. Mitochondrial control of cell death. *Nat Med* 2000; **6**: 513–519
33 **Li M,** Lotan R, Levin B, Tahara E, Lippman SM, Xu XC. Aspirin induction of apoptosis in esophageal cancer: a potential for chemoprevention. *Cancer Epidemiol Biomarkers Prev* 2000; **9**: 545–549
34 **Hirpara JL,** Seyed MA, Loh KW, Dong H, Kini RM, Pervaiz S. Induction of mitochondrial permeability transition and cytochrome C release in the absence of caspase activation is insufficient for effective apoptosis in human leukemia cells. *Blood* 2000; **95**: 1773-1780

Edited by Zhang JZ and Wang XL

PO Box 2345, Beijing 100023, China
Fax: +86-10-85381893
E-mail: wjg@wjgnet.com www.wjgnet.com

ELSEVIER

World J Gastroenterol 2005;11(2):208-211
World Journal of Gastroenterology ISSN 1007-9327

Prediction of HLA-A2-restricted CTL epitope specific to HCC by SYFPEITHI combined with polynomial method

Hai-Long Dong, Yan-Fang Sui

Hai-Long Dong, Yan-Fang Sui, Department of pathology, Fourth Military Medical University, Xi'an 710032, Shaanxi Province, China
Supported by Natural Scientific Foundation of China, No. 39830420
Correspondence to: Professor Yan-Fang Sui, Department of Pathology, Fourth Military Medical University, Xi'an 710032, Shaanxi Province, China. suiyanf@fmmu.edu.cn
Telephone: +86-29-3374541-211 **Fax:** +86-29-3374597
Received: 2003-11-04 **Accepted:** 2003-12-16

Abstract

AIM: To predict the HLA-A2-restricted CTL epitopes of tumor antigens associated with hepatocellular carcinoma (HCC).

METHODS: MAGE-1, MAGE-3, MAGE-8, P53 and AFP were selected as objective antigens in this study for the close association with HCC. The HLA-A*0201 restricted CTL epitopes of objective tumor antigens were predicted by SYFPEITHI prediction method combined with the polynomial quantitative motifs method. The threshold of polynomial scores was set to -24.

RESULTS: The SYFPEITHI prediction values of all possible nonamers of a given protein sequence were added together and the ten high-scoring peptides of each protein were chosen for further analysis in primary prediction. Thirty-five candidates of CTL epitopes (nonamers) derived from the primary prediction results were selected by analyzing with the polynomial method and compared with reported CTL epitopes.

CONCLUSION: The combination of SYFPEITHI prediction method and polynomial method can improve the prediction efficiency and accuracy. These nonamers may be useful in the design of therapeutic peptide vaccine for HCC and as immunotherapeutic strategies against HCC after identified by immunology experiment.

Key words: Hepatocellular carcinoma; HLA-A*0201; Cytotoxic T Lymphocyte; Epitope

Dong HL, Sui YF. Prediction of HLA-A2-restricted CTL epitope specific to HCC by SYFPEITHI combined with polynomial method. *World J Gastroenterol* 2005; 11(2): 208-211
http://www.wjgnet.com/1007-9327/11/208.asp

INTRODUCTION

Cancer immunotherapy has become one of the most important therapeutic procedures in the past two decades. Induction of potent anti-tumor cytotoxicity T lymphocytes (CTL) responses can result in regression and prevention of metastasis, as demonstrated in experimental model systems. Thus, efforts towards the development of cancer immunotherapy have recently focused on the generation of tumor-specific T cell responses. Over the last few years, several human genes that code for tumor antigens recognized by autologous CTL have been isolated[1-3] and the epitopes derived from these tumor antigens have been further identified to serve as targets for CTL in the context of HLA class I molecules[4].

Hepatocellular carcinoma (HCC) is one of the commonest malignant diseases in China and some other parts of Asia. Although encouraging advances have been made in the past few decades, there are still many difficulties in treating advanced-stage patients and in preventing recurrence and metastasis[5]. Immunotherapy is considered promising despite the fact that it is still a supplementary method in clinical practice[6,7]. The frequency of HLA-A2 allele in HCC patients is 53.5% in Chinese population[8]. It is very valuable to identify the tumor antigen epitopes which are presented by HLA-A2 and able to induce epitope-specific CTL against HCC cells.

In this study, we report a simple and efficient prediction method to identify candidate HLA-A2 restricted CTL epitopes from the tumor antigen that is closely associated with HCC.

MATERIALS AND METHODS

Materials

MAGE-1(309aa), MAGE-3(314aa), MAGE-8(234aa), P53(393aa) and AFP (609aa) were selected as objective antigens in this study for the close association with HCC. The amino acid sequences of these tumor antigens were quoted from EMBL database.

Methods

SYFPEITHI prediction Database retrieval can be performed on any HTML-browser supporting JavaScript. The main page of the database (http://www.uni-tuebingen.de/uni/kxi/) offers three sections: "Find Your Motif", "Epitope prediction" and "Information". After a preselection of one or multiple MHC-types, the "Epitope prediction" section allows the user to predict candidate epitope from protein sequence of a tumor antigen. The sequences of the protein or its gene, the restriction element are available.

The frequent of HLA-A2 types in HCC patients is 53.5% in the Chinese population and HLA-A*0201 is the major subtype of HLA-A2 allele, the HLA-A*0201 type was chosen from the frame of "Select MHC type". In this study, the nonamers (9aa) were chosen from the frame of "Choose a nonamer" due to the typical length of a class I ligand comprised 9 amino acids (nonamers). Following the amino acid sequences of each tumor antigen were inputted, the epitope prediction program was processed immediately. The values of all possible nonamers of a given sequence were added together and the ten high-scoring peptides of each antigen were selected as optimal T-cell epitope for further study.

Polynomial method analysis

The basic premise of this method is independent binding of individual side-chains (IBS). When residue *R* occurs at position *i* in the peptide, it is assumed to contribute a constant amount *Ri* to the free energy of binding of the peptide irrespective of the sequence of the rest of the peptide. Parameters *Ri* are estimated

Table 1 Coefficients for the polynomial method

Res	Position								
	1	2	3	4	5	6	7	8	9
A	-2.38	-3.22	-2.8	-2.66	-2.89	-2.7	-2.35	-3.07	-2.49
C	-2.94	-15.0	-2.58	-1.96	-3.29	-2.22	-2.97	-2.37	-15.0
D	-3.69	-15.0	-3.46	-2.71	-2.26	-2.63	-3.61	-3.03	-15.0
E	-3.64	-15.0	-3.51	-2.65	-3.39	-3.41	-3.21	-2.63	-15.0
F	-1.89	-15.0	-2.35	-2.5	-1.34	-2.43	-2.18	-1.71	-15.0
G	-2.32	-15.0	-3.04	-2.63	-2.56	-2.3	-3.13	-2.96	-15.0
H	-2.67	-15.0	-2.58	-2.58	-2.05	-3.32	-3.13	-2.16	-15.0
I	-1.65	-2.55	-2.8	-3.44	-2.74	-2.79	-2.2	-2.69	-2.1
K	-2.51	-15.0	-3.65	-2.93	-3.34	-3.77	-2.97	-3.27	-15.0
L	-2.32	-1.7	-2.09	-2.49	-2.71	-2.63	-2.62	-2.01	-2.74
M	-0.39	-1.39	-1.79	-3.01	-3.43	-1.38	-1.33	-0.97	-2.96
N	-3.12	-15.0	-3.31	-2.22	-2.36	-2.3	-3.14	-3.31	-15.0
P	-3.61	-15.0	-2.97	-2.64	-2.42	-2.31	-1.83	-2.42	-15.0
Q	-2.76	-15.0	-2.81	-2.63	-3.06	-2.84	-2.12	-3.05	-15.0
R	-1.92	-15.0	-3.41	-2.61	-3.05	-3.76	-3.43	-3.02	-15.0
S	-2.39	-15.0	-2.04	-2.12	-2.83	-3.04	-2.73	-2.02	-15.0
T	-2.89	-3.58	-2.6	-2.48	-2.17	-2.58	-2.67	-3.14	-3.7
V	-2.44	-2.64	-2.68	-3.29	-2.49	-2.25	-2.68	-2.8	-1.7
W	-0.14	-15.0	-1.01	-2.94	-1.77	-2.77	-2.85	-2.13	-15.0
Y	-1.46	-15.0	-1.67	-2.7	-1.92	-2.39	-1.35	-3.37	-15.0

Coefficients of the polynomial method. For each of the 20 amino acid residues, the amount they contribute to the polynomial score is shown (for all nine positions in which they may occur).

from a training set of 161 peptides by a method analogous to that used by epidemiologists to calculate risk factors for developing a disease. All peptides in the training set contain the canonical motif for HLA-A2.1, so that they all contain the "correct" residue at the anchor positions (2 and 9). For *i* other than 2 and 9 (for the non-anchor positions), the average negative $\log_{10}$ of IC_{50} of all the peptides carrying *R* at position *i* is calculated and used as the estimate of *Ri*. This is a slightly modified version of the method reported by Ruppert *et al*[9]. The values of the *Ri* terms of HLA-A2 specificity are shown in Table 1.

To calculate the polynomial method score of peptides in this study, the *Ri* values corresponding to the sequence of the given peptide were added together. If this sum exceeded a chosen threshold, the peptide was predicted to bind. The threshold was chosen as the number that gave a relatively clean separation between binders and non-binders in the training set. In the present study the threshold was -24.

Prediction result analysis

The previously reported CTL epitope of the antigens investigated in this study were obtained from the "Find Your Motif" section of SYFPEITHI database. These epitopes were screened out from the primary predicted epitopes.

RESULTS

SYFPEITHI prediction

The SYFPEITHI prediction values of all possible nonamers of a given protein sequence were added together and the ten high-scoring peptides of each protein were selected for further analysis. Scores for all predicted epitopes specifically for HLA-A*0201 are given in Table 2. The predicted epitopes were accorded with the simple motif (SM) of HLA-A2.1 (the presence of L, M or I at position 2 and L, V or I at position 9). The SYFPEITHI predicted scores of these epitopes were usually higher than 20.

Polynomial method analysis

The primary predicted epitopes were compared with epitopes that were demonstrated in previous research. Six reported HLA-A2 restricted CTL epitopes (MAGE-$1_{278-286}$KVLEYVIKV[10], MAGE-$3_{112-120}$KVAELVHFL[11], MAGE-$3_{271-279}$FLWGPRALV[12], $P53_{187-197}$GLAPPQHLIRV[13], $P53_{322-330}$ PLDGEYFTL[14], $AFP_{158-166}$ FMNKFIYEI[15]) were eliminated from the SYFPEITHI prediction results. The polynomial scores of predicted epitopes are shown in Table 2. The epitopes which polynomial scores less than -24 (MAGE-$1_{101-109, 301-309, 15-23}$, MAGE-$8_{20-28}$, $P53_{129-137, 193-201, 256-264, 113-121}$, $AFP_{410-418}$) were eliminated from the prediction results. At last, thirty-five epitopes were selected from the predicted results for further study.

Table 2 HLA-A2 restricted epitope prediction results

Antigens	AApos	Sequence	SYFPEITHI score	Polynomial score
MAGE-1 (MAG1)	194	FLIIVLVMI	27	-17.07
	38	LVLGTLEEV	26	-20.77
	278	**KVLEYVIKV**	**26**	**-21.23**
	101	VITKKVADL	25	-24.23
	301	ALREEEEGV	25	-24.81
	187	QIMPKTGFL	24	-23.24
	93	ILESLFRAV	23	-22.32
	105	KVADLVGFL	23	-23.12
	15	ALEAQQEAL	22	-25.17
	89	STSCILESL	22	-23.31
MAGE-3 (MAG3)	108	ALSRKVAEL	31	-22.04
	201	LLIIVLAII	28	-22.52
	200	GLLIIVLAI	27	-22.33
	271	**FLWGPRALV**	**27**	**-19.47**
	220	KIWEELSVL	26	-23.01
	112	**KVAELVHFL**	**25**	**-23.14**
	237	SILGDPKKL	25	-22.73

	176	Y I F A T C L G L	23	-21.73
	238	I L G D P K K L L	23	-23.01
	174	H L Y I F A T C L	22	-21.30
MAGE-8 (MAG8)	111	A L D E K V A E L	33	-23.5
	45	L I M G T L E E V	29	-21.63
	204	L L I I V L G M I	26	-21.58
	115	K V A E L V R F L	24	-23.44
	179	Y I L V T C L G L	24	-22.10
	71	S L T V T D S T L	23	-23.39
	203	G L L I I V L G M	23	-23.08
	205	L I I V L G M I L	23	-22.73
	20	G E A P G L M D V	21	-34.01
	25	L M D V Q I P T A	21	-23.75
P53 (P53)	24	K L L P E N N V L	26	-23.31
	187	**G L A P P Q H L I**	**25**	**-21.96**
	264	L L G R N S F E V	24	-21.58
	129	A L N K M F C Q L	23	-24.94
	132	K M F C Q L A K T	22	-23.22
	193	H L I R V E G N L	22	-24.86
	65	R M P E A A P P V	21	-20.47
	322	**P L D G E Y F T L**	**21**	**-25.24**
	256	T L E D S S G N L	20	-25.86
	113	F L H S G T A K S	19	-34.05
AFP (FETA)	90	Q L P A F L E E L	27	-22.64
	257	K L V L D V A H V	27	-20.10
	158	**F M N K F I Y E I**	**26**	**-20.37**
	172	F L Y A P T I L L	25	-19.87
	410	A L A K R S C G L	25	-24.57
	218	L L N Q H A C A V	24	-22.45
	242	K L S Q K F T K V	24	-22.29
	571	V I A D F S G L L	23	-22.76
	599	L I S K T R A A L	23	-23.93
	8	F L I F L L N F T	22	-22.78

A: the epitopes were reported; A: the prediction epitopes whose polynomial scores were less than -24.

DISCUSSION

The induction of antigen-specific cytotoxic T lymphocytes (CTL) has been suggested to be efficacious in the prevention and treatment of various types of tumor. Determination of peptides that elicit a T-cell response *in vivo* is important for identifying autoimmune and CTL epitopes and for peptide vaccine design. About 120 CTL epitopes presented by HLA-A, B, C molecules have been reported in recent study[4] and some epitopes have been used as peptide vaccine in animal and clinical experiments[16,17].

While sufficient conditions for a peptide to be a T-cell epitope are not well known, one well established necessary condition is that they bind to MHC molecules. Hence considerable effort has been made to measure the binding affinities of peptides to MHC molecules. A reliable theoretical method that rapidly predict whether a peptide bind is of great practical utility. The methods of epitope prediction were constructed by immunologists in recent decades. These predictions are based on comparisons of precursor peptide sequences known to contain T cell epitopes. It is the discovery of allele-specific motifs shared by eluted natural MHC ligands that finally allow the exact prediction of peptides from a given protein sequence presented on MHC class I molecules. Currently, several algorithms are publicly available for predicting the HLA-binding affinities of peptides, such as the SYFPEITHI database (http://uni-tuebingen.de/uni/kxi/)[18]. SYFPEITHI uses motif matrices deduced from refined motifs based on the pool sequence and single peptide analysis exclusively of natural ligands. Potential binders for various MHC class I molecules are ranked according in the presence of primary and secondary anchor amino acids as well as favored and disfavored amino acids.

However, motifs are the simplest independent binding site models: they specify positions with required residues and certain other positions with prohibited residues. One way to include more detail than motifs in an independent binding model is the polynomial method. Polynomial method is based on statistical parameter estimation assuming independent binding of the side-chains of residues[9]. Its sensitivity and positive predictive value are better than the simple motif (such as syfpeithi database)[19]. This and other[20-22] independent binding site methods that assign a score to a peptide have been called quantitative motifs[23]. Threshold is an integral part of the polynomial method. In the above analysis the threshold was set to -24. In this study, 35 candidate epitopes were selected for further immunology experiments by the SYFPEITHI prediction combined with polynomial methods.

Hepatocellular carcinoma (HCC) is one of the most common neoplasms worldwide. It is the major cause of death in China and some regions of Asia. The pathogenic mechanisms responsible for HCC are not well defined, and therapeutic means, especially in unresectable HCCs, are still unsatisfactory. In Chinese HCC patients, the proportion of HLA-A2 is higher than other alleles[8]. Therefore, identification of HLA-A2 restricted CTL epitopes of tumor antigen closely associated with HCC is very valuable for HCC immunotherapy in China. In this study, the antigens of MAGE gene family(MAGE-1, MAGE-3 and MAGE-8), P53 mutation gene and AFP were selected as objective proteins because these antigens have been demonstrated to be closely associated with HCC[24-26,15]. The candidate HLA-A2 restricted CTL epitopes of these antigens were predicted using the syfpeithi prediction combined with polynomial methods.

The epitope prediction has been carried in tumor antigen specificity for CTL epitope identification in most studies recently. Schirle *et al*[14] reported that two new CTL epitopes of gastrointestinal tumor were identified by epitope prediction combined with acid eluted methods. Epitope prediction also has been combined with epitope reconstruction and immunology assay by Pascolo *et al*[10] and a new CTL epitope of MAGE-1 was identified.

If immunological activity of the candidate epitopes has been identified by further immunology assay, most of the patients with HCC could be potentially candidates for specific immunotherapy against these epitopes, including vaccination using APC pulsed with HLA-A2-restricted CTL epitopes or the adoptive transfer of specific CTL generated from PBMC by stimulation with the epitopes. The results of this study will benefit to most patients with HCC in the future.

REFERENCES

1 **Dong HL**, Sui YF, Li ZS, Qu P, Wu W, Ye J, Zhang XM, Lu SY. Efficient induction of cytotoxic T lymphocytes specific to hepatocellular carcinoma using HLA-A2-restricted MAGE-n peptide *in vitro*. *Cancer Lett* 2004; **211**: 219-225

2 **van der Bruggen P,** Traversari C, Chomez P, Lurquin C, De Plaen E, Van den Eynde B, Knuth A, Boon T. A gene encoding an antigen recognized by cytolytic T lymphocytes on a human melanoma. *Science* 1991; **254**: 1643-1647

3 **Katsura F,** Eura M, Chikamatsu K, Oiso M, Yumoto E, Ishikawa T. Analysis of individual specific cytotoxic T lymphocytes for two MAGE-3-derived epitopes presented by HLA-A24. *Jpn J Clin Oncol* 2000; **30**: 117-121

4 **Renkvist N,** Castelli C, Robbins PF, Parmiani G. A listing of

human tumor antigens recognized by T cells. *Cancer Immunol Immunother* 2001; **50**: 3-15

5 **Gebo KA**, Chander G, Jenckes MW, Ghanem KG, Herlong HF, Torbenson MS, El-Kamary SS, Bass EB. Screening tests for hepatocellular carcinoma in patients with chronic hepatitis C: a systematic review. *Hepatology* 2002; **36**: S84-S92

6 **Butterfield LH,** Ribas A. Immunotherapy of hepatocellular carcinoma. *Expert Opin Biol Ther* 2002; **2**: 123-133

7 **Ladhams A,** Schmidt C, Sing G, Butterworth L, Fielding G, Tesar P, Strong R, Leggett B, Powell L, Maddern G, Ellem K, Cooksley G. Treatment of non-resectable hepatocellular carcinoma with autologous tumor-pulsed dendritic cells. *J Gastroenterol Hepatol* 2002; **17**: 889-896

8 **Ming LH,** Zhu YR, Harris CC, Wang XH, Wu ZY, Sun ZT. Association of HLA-A02 genotype with hepatocellular carcinoma in a prevalent area of China. *Chin J Immunol* 1999; **15**: 305-310

9 **Ruppert J,** Sidney J, Celis E, Kubo RT, Grey HM, Sette A. Prominent role of secondary anchor residues in peptide binding to HLA-A2.1 molecules. *Cell* 1993; **74**: 929-937

10 **Pascolo S,** Schirle M, Guckel B, Dumrese T, Stumm S, Kayser S, Moris A, Wallwiener D, Rammensee HG, Stevanovic S. A MAGE-A1 HLA-A*0201 epitope identified by mass spectrometry. *Cancer Res* 2001; **61**: 4072-4077

11 **Kawashima I,** Hudson SJ, Tsai V, Southwood S, Takesako K, Appella E, Sette A, Celis E. The multi-epitope approach for immunotherapy for cancer: identification of several CTL epitopes from various tumor-associated antigens expressed on solid epithelial tumors. *Hum Immunol* 1998; **59**: 1-14

12 **van der Bruggen P,** Bastin J, Gajewski T, Coulie PG, Boel P, De Smet C, Traversari C, Townsend A, Boon T. A peptide encoded by human gene MAGE-3 and presented by HLA-A2 induces cytolytic T lymphocytes that recognize tumor cells expressing MAGE-3. *Eur J Immunol* 1994; **24**: 3038-3043

13 **Theobald M,** Biggs J, Hernandez J, Lustgarten J, Labadie C, Sherman LA. Tolerance to p53 by A2.1-restricted cytotoxic T lymphocytes. *J Exp Med* 1997; **185**: 833-841

14 **Schirle M,** Keilholz W, Weber B, Gouttefangeas C, Dumrese T, Becker HD, Stevanovic S, Rammensee HG. Identification of tumor-associated MHC class I ligands by a novel T cell-independent approach. *Eur J Immunol* 2000; **30**: 2216-2225

15 **Butterfield LH,** Meng WS, Koh A, Vollmer CM, Ribas A, Dissette VB, Faull K, Glaspy JA, McBride WH, Economou JS. T cell responses to HLA-A*0201-restricted peptides derived from human alpha fetoprotein. *J Immunol* 2001; **166**: 5300-5308

16 **Thurner B,** Haendle I, Röder C, Dieckmann D, Keikavoussi P, Jonuleit H, Bender A, Maczek C, Schreiner D, von den Driesch P, Bröcker EB, Steinman RM, Enk A, Kämpgen E, Schuler G. Vaccination with mage-3A1 peptide-pulsed mature, monocyte-derived dendritic cells expands specific cytotoxic T cells and induces regression of some metastases in advanced stage IV melanoma. *J Exp Med* 1999; **190**: 1669-1678

17 **Dagher R,** Long LM, Read EJ, Leitman SF, Carter CS, Tsokos M, Goletz TJ, Avila N, Berzofsky JA, Helman LJ, Mackall CL. Pilot trial of tumor-specific peptide vaccination and continuous infusion interleukin-2 in patients with recurrent Ewing sarcoma and alveolar rhabdomyosarcoma: an inter-institute NIH study. *Med Pediatr Oncol* 2002; **38**: 158-164

18 **Rammensee H,** Bachmann J, Emmerich NP, Bachor OA, Stevanović S. SYFPEITHI: database for MHC ligands and peptide motifs. *Immunogenetics* 1999; **50**: 213–219

19 **Gulukota K,** Sidney J, Sette A, DeLisi C. Two complementary methods for predicting peptides binding major histocompatibility complex molecules. *J Mol Biol* 1997; **267**: 1258-1267

20 **Marshall KW,** Wilson KJ, Liang J, Woods A, Zaller D, Rothbard JB. Prediction of peptide affinity to HLA DRB1*0401. *J Immunol* 1995; **154**: 5927-5933

21 **Parker KC,** Bednarek MA, Coligan JE. Scheme for ranking potential HLA-A2 binding peptides based on independent binding of individual peptide side-chains. *J Immunol* 1994; **152**: 163-175

22 **Hammer J,** Bono E, Gallazzi F, Belunis C, Nagy Z, Sinigaglia F. Precise prediction of major histocompatibility complex class II-peptide interaction based on peptide side chain scanning. *J Exp Med* 1994; **180**: 2353-2358

23 **Hammer J.** New methods to predict MHC-binding sequences within protein antigens. *Curr Opin Immunol* 1995; **7**: 263-269

24 **Tahara K,** Mori M, Sadanaga N, Sakamoto Y, Kitano S, Makuuchi M. Expression of the MAGE gene family in human hepatocellular carcinoma. *Cancer* 1999; **85**: 1234-1240

25 **Kobayashi Y,** Higashi T, Nouso K, Nakatsukasa H, Ishizaki M, Kaneyoshi T, Toshikuni N, Kariyama K, Nakayama E, Tsuji T. Expression of MAGE, GAGE and BAGE genes in human liver diseases: utility as molecular markers for hepatocellular carcinoma. *J Hepatol* 2000; **32**: 612-617

26 **Charuruks N,** Tangkijvanich P, Voravud N, Chatsantikul R, Theamboonlers A, Poovorawan Y. Clinical significance of p53 antigen and anti-p53 antibodies in the sera of hepatocellular carcinoma patients. *J Gastroenterol* 2001; **36**: 830-836

Edited by Wang XL and Xu FM

PO Box 2345, Beijing 100023, China
Fax: +86-10-85381893
E-mail: wjg@wjgnet.com www.wjgnet.com

ELSEVIER

World J Gastroenterol 2005;11(2):212-215
World Journal of Gastroenterology ISSN 1007-9327

• LIVER CANCER •

Adhesion of different cell cycle human hepatoma cells to endothelial cells and roles of integrin β_1

Guan-Bin Song, Jian Qin, Qing Luo, Xiao-Dong Shen, Run-Bin Yan, Shao-Xi Cai

Guan-Bin Song, Jian Qin, Qing Luo, Xiao-Dong Shen, Run-Bin Yan, Shao-Xi Cai, Key Laboratory for Biomechanics and Tissue Engineering of the State Ministry of Education, College of Bioengineering, Chongqing University, Chongqing 400044, China
Supported by the National Natural Science Foundation of China, No. 19972077 and No.10372121
Correspondence to: Dr. Guan-Bin Song, Key Laboratory for Biomechanics and Tissue Engineering of the State Ministry of Education, College of Bioengineering, Chongqing University, Chongqing 400044, China. song9973@tom.com
Telephone: +86-23-65102507 **Fax:** +86-23-65111633
Received: 2004-02-02 **Accepted:** 2004-04-05

Abstract

AIM: To investigate the adhesive mechanical properties of different cell cycle human hepatoma cells (SMMC-7721) to human umbilical vein endothelial cells (ECV-304), expression of adhesive molecule integrinβ_1 in SMMC-7721 cells and its contribution to this adhesive course.

METHODS: Adhesive force of SMMC-7721 cells to endothelial cells was measured using micropipette aspiration technique. Synchronous G_1 and S phase SMMC-7721 cells were achieved by thymine-2-deoxyriboside and colchicines sequential blockage method and double thymine-2-deoxyriboside blockage method, respectively. Synchronous rates of SMMC-7721 cells and expression of integrinβ_1 in SMMC-7721 cells were detected by flow cytometer.

RESULTS: The percentage of cell cycle phases of general SMMC-7721 cells was 11.01% in G_2/M phases, 53.51% in G_0/G_1 phase, and 35.48% in S phase. The synchronous rates of G_1 and S phase SMMC-7721 cells amounted to 74.09% and 98.29%, respectively. The adhesive force of SMMC-7721 cells to endothelial cells changed with the variations of adhesive time and presented behavior characteristics of adhesion and de-adhesion. S phase SMMC-7721 cells had higher adhesive forces than G_1 phase cells [$(307.65\pm92.10)\times10^{-10}$N *vs* $(195.42\pm60.72)\times10^{-10}$N, $P<0.01$]. The expressive fluorescent intensity of integrinβ_1 in G_1 phase SMMC-7721 cells was depressed more significantly than the values of S phase and general SMMC-7721cells. The contribution of adhesive integrinβ_1 was about 53% in this adhesive course.

CONCLUSION: SMMC-7721 cells can be synchronized preferably in G_1 and S phases with thymine-2-deoxyriboside and colchicines. The adhesive molecule integrinβ_1 expresses a high level in SMMC-7721 cells and shows differences in various cell cycles, suggesting integrin β_1 plays an important role in adhesion to endothelial cells. The change of adhesive forces in different cell cycle SMMC-7721 cells indicates that S phase cells play predominant roles possibly while they interact with endothelial cells.

Key words: Hepatoma; Cell cycle; Integrin β_1; Endothelial cells; Cell adhesion

Song GB, Qin J, Luo Q, Shen XD, Yan RB, Cai SX. Adhesion of different cell cycle human hepatoma cells to endothelial cells and roles of integrin β_1. *World J Gastroenterol* 2005; 11(2): 212-215
http://www.wjgnet.com/1007-9327/11/212.asp

INTRODUCTION

Tumor is a malignant disease caused by disorganized cell cycle and the uncontrollable growth of cells, which is very harmful to human's health. Invasion and metastasis are the representations of malignancy and also the direct causes of terminal deterioration and death of tumor patients[1,2]. The metastasis of tumor cells through blood circulation is a complicated continuous process with many steps, of which the adhesion of tumor cells to extra cellular matrix (ECM) and endothelial cells is one of the definitive steps in tumor metastasis, and the expression of adhesive molecules is the important factor in determining the adhesion of cells. Integrinβ_1 is the main mediating adhesive molecule in locking phase of the adhesion between tumor cells and vascular endothelial cells[3].

Primary hepatocellular carcinoma is one of the ten important frequent cancers in the world, but its biomechanical mechanism in the course of invasion and metastasis has not been elucidated completely up to now, the adhesive mechanical properties of different cell cycle hepatoma cells to endothelial cells and the expressions and roles of correlative adhesive molecules in the adhesive course have not been fully understood. In this paper, we put emphasis on studying the adhesive mechanical properties of different cell cycle hepatoma cells to endothelial cells using micropipette aspiration technique from the view of cell cycle. Furthermore, the expression and contribution of adhesive molecule integrinβ_1 were investigated quantitatively. The experimental results may provide the quantitative biomechanical basis in understanding the metastasis mechanism of hepatoma cells.

MATERIALS AND METHODS

Cells and cell culture

Human hepatoma SMMC-7721 cells, purchased from the Second Military Medical University in Shanghai, were cultivated in RPMI-1640 medium (Gibco product) supplemented with 10% calf serum in a standard incubator at 37 ℃.

Human umbilical vein endothelial ECV-304 cells, purchased from Shanghai Institute of Cell Biology, Chinese Academy of Sciences, were cultivated in M199 medium (Gibco product) supplemented with 15% fetal bovine serum (FBS, Hyclone product). ECV-304 cells were identified as endothelial cells by the presence of factor VIII-related antigen and typical endothelial morphology. Experiments were performed by using ECV-304 cells from passages 3-5.

Synchronization of SMMC-7721 cells

G_1 phase SMMC-7721 cells were achieved by thymine-2-

deoxyriboside (Sigma-Aldrich product) and colchicine (Serva product) sequential blockage method. S phase SMMC-7721 cells were achieved by double thymine-2-deoxyriboside blockage method[4,5]. The synchronized SMMC-7721 cells were washed twice in 0.01 mol/L pH7.4 phosphate buffered solution (PBS), and fixed with 75% cooled ethanol, dyed for 30 min by propidium iodide (PI), then the synchronizing rate was measured by flow cytometer (BD FACS Caliber, BD Bioscience, USA).

Flow cytometer to detect the expression of integrin β_1 in SMMC-7721 cells

About 1.5 mL cell suspension (1×10^6 cells/mL) was put into a 2.0-mL test tube and centrifuged at 1 500 rpm for 5 min. The cells were washed twice in 0.01 mol/L pH7.4 PBS, the supernatant was swilled out and about 200 μL solution was left, the solution was mixed gently and put into two 1.5-mL test tubes averagely. Then, 2.5 μL monoclonal mouse anti-human IgG1k/FITC (Ancell product, USA) was added into one test tube (as control) and 2.5 μL monoclonal mouse anti-human integrin β_1/FITC (Ancell product, USA) was added into the other tube, they were let to react at 4 ℃ for 30 min. The cells were washed three times as before and the expression of integrin β_1 was detected by a flow cytometer (BD FACS Caliber, BD Bioscience, USA).

Measurement of adhesive forces of SMMC-7721 cells to ECV-304 cells

Micropipette aspiration technique[6-9] was adopted to measure the adhesive force of SMMC-7721 cells to ECV-304 cells. Briefly, monolayer ECV-304 cells were cultivated in a special chamber, about 0.5 mL SMMC-7721 single cell suspension (1×10^5 cells/mL) was added into the chamber, adhesive experiments were started about 30 min later. The pressure was adjusted to zero (zero-pressure state) using the pressure controlling and recording system. SMMC-7721 cells were chosen under a microscope and the tip of the micropipettes was positioned close to the surface of SMMC-7721 cells by a micromanipulator, a small portion of the cells was aspirated into the micropipettes with a step-rise negative pressure produced by the pressure control system. Then the micropipettes were pulled using the micromanipulator flatly and slowly, SMMC-7721 cells were detached gradually from the surface of adhered ECV-304 cells, and the negative pressure was adjusted simultaneously until the SMMC-7721 cells were drawn out from the surface of adhered ECV-304 cells. The whole experimental process was recorded using a video tape recorder continuously, the experimental data were measured through the image processing system. All micropipette manipulations were carried out at room temperature (about 25 ℃) and completed within 2 h.

Calculation of adhesive forces and data processing

The formula for calculating the adhesive force (F) was defined as[10,11], $F=\pi\times R_p^2\times \Delta P\times\cos\theta$, where Rp is the inner radius of the micropipettes (2.5-3.0 μm inner radius was used in this experiment), ΔP is the critical negative pressure, and θ is the angle between the micropipettes and the plane of ECV-304. In our experiments, θ angle was regulated to about 10°, therefore $\cos\theta\approx\cos10^\circ=0.985\approx1$ and the formula could be simplified as $F=\pi\times R_p^2\times\Delta P$.

The adhesive force values were described as mean±SD and Student's t test was used for statistical analysis.

RESULTS

Synchronization of SMMC-7721 cells

Cell cycle phases were analyzed with a flow cytometer. The percentage of cell cycle phase of general SMMC-7721 cells (non-synchronized) was 53.51% in G_0/G_1 phase, 11.01% in G_2/M phases, 35.48% in S phase, as shown in Figure 1A. On the other hand, we synchronized SMMC-7721 cells by the methods of thymine-2-deoxyriboside and colchicines sequential blockage and double thymine-2-deoxyriboside blockage, the average synchronizing rates of G_1 and S phase cells amounted to 74.09% and 98.29%, respectively (Figure 1B, 1C). It was suggested that SMMC-7721 cells could be synchronized preferably in G_1 and S phases using this method.

Time dependency of adhesive forces of SMMC-7721 cells to ECV-304 cells

Using the micropipette aspiration technique, we investigated the time dependency of adhesive forces of SMMC-7721 cells to ECV-304, the results are shown in Table 1.

Table 1 Time dependence of adhesive forces of SMMC-7721 cells to ECV-304 (mean±SD)

Period of time (min)	Adhesion forces ($F\times10^{-10}$N)	n
0-30	39.98±25.77	16
30-60	297.32±82.35	20
60-90	336.49±73.51	18
90-120	301.09±62.04	21

n: number of cells measured.

Cell cycle dependency of adhesive forces of SMMC-7721 cells to ECV-304 cells

The adhesive forces of different cell cycle SMMC-7721 cells to ECV-304 cells were investigated, and the results are shown in

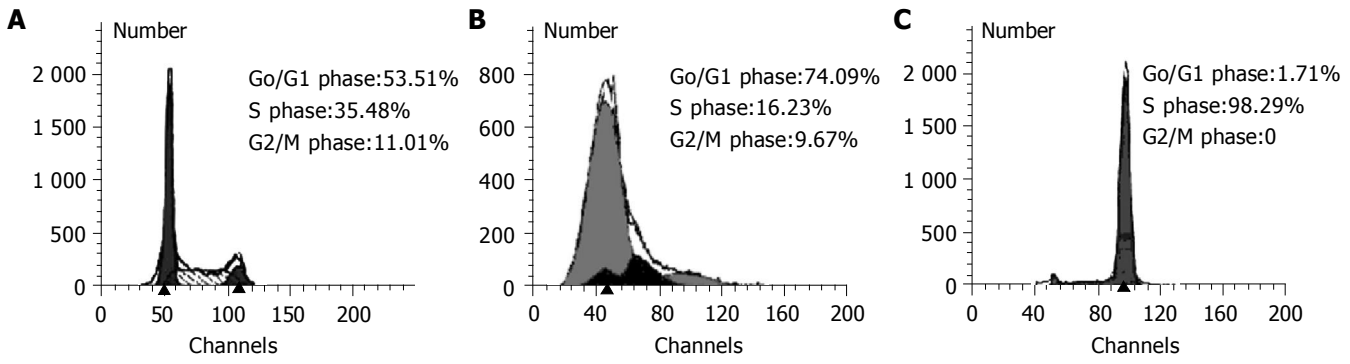

Figure 1 Flow cytometer diagram of general SMMC-7721 cells, G_1 phase and S phase SMMC-7721 cells. A: Flow cytometer diagram of general SMMC-7721 cells; B: Flow cytometer diagram of G_1 phase SMMC-7721 cells; C: Flow cytometer diagram of S phase SMMC-7721 cells.

Table 2. The adhesive forces of G_1 phase SMMC-7721 cells to ECV-304 cells were much lower than the corresponding value of S phase ($P<0.01$) and general SMMC-7721 cells ($P<0.01$). However, there was no obvious difference in the adhesive forces between S phase and general SMMC-7721 cells.

Table 2 Adhesion forces of different cell cycle SMMC-7721 cells to ECV-304 cells (mean±SD)

Treatment	Adhesion forces ($F\times10^{-10}N$)	*n*
General SMMC-7721	281.26±70.15	38
G_1 phase SMMC-7721	195.42±60.72[b,d]	31
S phase SMMC-7721	307.65±92.10	35

[b]$P<0.01$ *vs* compared with general SMMC-7721 cells; [d]$P<0.01$, compared with S phase SMMC-7721 cells; *n*: number of cells measured.

Expression of integrin β_1 in SMMC-7721 cells

The expressed fluorescent intensity of integrin β_1 in different cell cycle SMMC-7721 cells is shown in Table 3, which indicates that the average fluorescent intensity of integrin β_1 in general, G_1 phase and S phase SMMC-7721 cells was 95.7±1.2, 76.9±1.9, and 94.1±1.6, respectively. It could also be known from the table that the expression of integrin β_1 in G_1 phase was decreased obviously when compared with the corresponding value of S phase and general SMMC-7721 cells. These results suggested that there were cell cycle differences of expressions of integrin β_1 in SMMC-7721 cells.

Table 3 Expression of integrin β_1 in different cell cycle SMMC-7721 cells (mean±SD)

Treatments	Expressed fluorescent intensity of integrin β_1	*n*
General SMMC-7721	95.7±1.2	3
G_1 phase SMMC-7721	76.9±1.9[b,d]	3
S phase SMMC-7721	94.1±1.6	3

[b]$P<0.01$ *vs* compared with general SMMC-7721 cells; [d]$P<0.01$, compared with S phase SMMC-7721 cells; *n*: number of samples measured.

Blockage roles of integrin β_1 antibody in adhesion of SMMC-7721 cells to ECV-304 cells

To study the contributions of integrin β_1 to the adhesion of hepatoma cells to endothelial cells, we measured the adhesive forces quantitatively of general SMMC-7721 cells to ECV-304 cells with micropipette aspiration technique, using monoclonal mouse anti-human IgG1k/FITC (nonspecific antibody) and monoclonal mouse anti-human integrin β_1/FITC (specific antibody) to block these adhesive courses, respectively. The results are shown in Figure 2. The adhesive behavior of SMMC-7721 cells to ECV-304 cells was obviously blocked by monoclonal antibody of integrin β_1, the block rate was 53.01% and the adhesive force was distinctly lower than that of general SMMC-7721($P<0.01$). However, the block rate of nonspecific antibody was only 1.52% and the adhesive force had no difference when compared with control experiment.

DISCUSSION

Adhesion of tumor cells to vascular endothelial cells is one of the key steps in metastasis. It has been proved that there is much commonness in the course of interactions between tumor cells and different vascular endothelial cells despite of organic metastasis[12]. Now adhesive behaviors of tumor cells to human umbilical vein endothelial cells have been used as a "gold model" for studying interactions of tumor cells and endothelial cells[13], and this model has been accepted by academic communities[14]. In this paper, we explored the adhesive mechanical properties of human hepatoma cells and human umbilical vein endothelial cells from the view of cell cycle and found that the adhesive forces of SMMC-7721 cells to ECV-304 cells changed with adhesive time, and increased rapidly within 30-60 min and then kept steady after 60 min. This suggests that the expression of adhesive molecules is time-dependent in SMMC-7721 cells and ECV-304 cells, thas showing behavior characteristics of adhesion and de-adhesion.

With a series of ordinary biochemical events in space-time, cells could control their growth, proliferation, differentiation to ensure the natural process of cell cycle[15]. The abnormity of cell cycle regulating function is one of the mechanisms that result in the abnormal proliferation of tumor cells. Therefore it is very important to understand the proliferation, differentiation and the biophysical characteristics of cells from the view of cell cycle, while the cellular synchronization is the important way to investigate cell modalities, structures, functions and other characteristics in each cycle phase. The synchronous results have shown that thymine-2-deoxyriboside and colchicine sequential blockage and double thymine-2-deoxyriboside blockage methods could synchronize SMMC-7721 cells preferably in G_1 phase and S phase, respectively. Comparing the synchronous results, we found that the synchronizing rate of G_1 phase SMMC-7721 cells was lower than that of S phase, which might be caused by different synchronizing ways.

To some extent, the occurrence, evolution and metastasis of malignant tumors are related to the abnormal expression or structural change of integrin[16]. There is a decrease or lack of the integrin expression in some tumor cells while a distinct increase in other tumors[17]. This indicates that the relation between integrin and tumors might be twofold. In the early period of tumor occurrence, the decrease of expression of integrin might result in the weakening of adhesion between tumor cells and basement membranes or extra cellular matrix, which is proportional to the local growth of tumor cells. After tumor cells enter blood circulation, increased expression of integrin would be proportional for tumor cells to adhere to vascular endothelial cells and its metastasis. Integrin β_1 is the main mediating adhesive molecule in locking phase of adhesions between tumor cells and vascular endothelial cells. In this experiment, we found that strong fluorescence of expressed integrin β_1 occurred in SMMC-7721 cells, but the expression of integrin β_1 in G_1 phase SMMC-7721 cells was

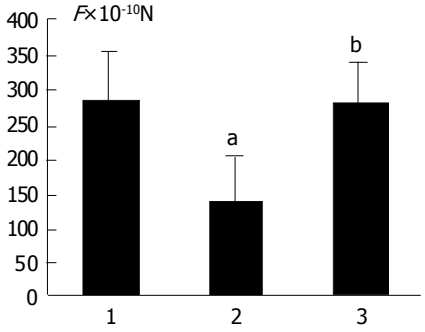

Figure 2 Adhesion forces of general SMMC-7721 cells to ECV-304 cells blocked by integrinβ_1 antibody. 1. General SMMC-7721+ECV-304 (n = 38), 2. General SMMC-7721+specific antibody+ECV-304 (n = 29), 3.General SMMC-7721+nonspecific antibody+ECV-304 (n = 36). [b]$P<0.01$, compared with 1 and 3; [a]$P>0.05$, compared with 1; *n*: number of measured cells.

decreased obviously when compared with the corresponding values of S phase and general SMMC-7721 cells, there were cell cycle differences in expression of integrin β_1 in SMMC-7721 cells.

In our study, we found that the adhesive force was obviously decreased after the blockage using the specific monoclonal antibody of mouse integrin β_1 ($P<0.01$), the block rate was 53%. Meanwhile blocked by nonspecific monoclonal antibody under the same condition, the adhesive force was almost equal to that of the control experiment and the block rate was only 2%. These results indicate that the expression of integrin β_1 plays very important roles in the adhesion of SMMC-7721 cells to ECV-304 cells, and the contribution of this adhesive molecule is about 50% in these adhesive processes.

We also discovered that the adhesive force of G_1 phase SMMC-7721 cells was distinctly lower than the corresponding value of S phase cells ($P<0.01$), but there was no obvious difference when S phase was compared with general SMMC-7721 cells. This result suggests that S phase SMMC-7721 cells probably play a very important role in the adhesive course between SMMC-7721 cells and ECV-304 cells. Compared to the results we achieved in the investigation of the adhesive force of different cell cycle SMMC-7721 cells to surfaces coated with collagen IV[18], we conclude that G_1 phase SMMC-7721 cells might be very important in promoting the interaction with basement membranes in the course of metastasis through blood circulation. However, S phase SMMC-7721 cells might play predominant roles in the adhesion of SMMC-7721 cells to ECV-304 cells.

Invasion and metastasis of hepatoma cells are a complicated process, the adhesive behaviors of hepatoma cells are mediated by the cooperation of many adhesive molecules. The functions, contributions and rules of other adhesive molecules in these adhesive courses should be further studied.

ACKNOWLEDGEMENTS

We would thank Professor Long Mian (Institute of Mechanics, The Chinese Academy of Sciences) for his advise in this experiment.

REFERENCES

1 **Thiery JP**. Cell adhesion in cancer. *Comptes Rendus Physigue* 2003; **4**: 289-304
2 **Jiang XN**, Zhou RL. The Relatiosnhip Between Adhesion,Migration of Cancer Cellsand Mestastasis. *Shengwu Huaxue Yu Shengwu Wuli Jinzhan* 1998; **25**: 404-407
3 **Karmakar S**, Mukherjee R. Integrin receptors and ECM proteins involved in preferential adhesion of colon carcinoma cells to lung cells. *Cancer Lett* 2003; **196**: 217-227
4 **Uzbekov R**, Chartrain I, Philippe M, Arlot-Bonnemains Y. Cell cycle analysis and synchronization of the *Xenopus* cell line XL2. *Exp Cell Res* 1998; **242**: 60-68
5 **Song GB**, Yu WQ, Liu BA, Long M, Wu ZZ, Wang BC, Cai SX. Investigation on the viscoelasticity of synchronous human hepatocellular carcinoma cells. *Colloids and Surfaces B*: *Biointerfaces* 2002; **24**: 327-332
6 **Geiger S,** Jager-Lezer N, Tokgoz S, Seiller M, Grossiord JL. Characterization of the mechanical properties of a water/oil/water multiple emulsion oily membrane by a micropipette aspiration technique. *Colloids and surfaces A*: *Physicochemical and Engineering Aspects* 1999; **157**: 325-332
7 **You J**, Mastro AM, Dong C. Application of the dual-micropipet technique to the measurement of tumor cell locomotion. *Exp Cell Res* 1999; **248**: 160-171
8 **Zhao H**, Dong X, Wang X, Li X, Zhuang F, Stoltz JF, Lou J. Studies on single-cell adhesion probability between lymphocytes and endothelial cells with micropipette technique. *Microvasc Res* 2002; **63**: 218-226
9 **Wu ZZ**, Wang BC, Shao KF, Akio S. Adhesion of normal and carcinoma hepatic cells on the membrane containing collagen IV using a micropipette technique. *Colloids and Surfaces B: Biointerfaces* 1998; **11**: 273-279
10 **Wu ZZ**, Shao KF, Song GB, Wang HB, Wang YJ, Cai SX. Adhesion of hepatocellular carcinoma cells to collagen IV coated surfaces. *Natl Med J China* 1999; **79**: 369-372
11 **Song GB**, Liu BA, Qin J, Long M, Cai SX. Studies on the adhesive mechanical properties between hepatocellular carcinoma cells and endothelial cells. *Shengwu Wuli Xuebao* 2003; **19**: 84-87
12 **Weber GF**, Ashkar S. Molecular mechanisms of tumor dissemination in primary and metastatic brain cancers. *Brain Res Bull* 2000; **53**: 421-424
13 **Simiantonaki N**, Jayasinghe C, Kirkpatrick CJ. Effect of pro-inflammatory stimuli on tumor cell-mediated induction of endothelial cell adhesion molecules *in vitro*. *Exp Mol Pathol* 2002; **73**: 46-53
14 **Andrews EJ**, Wang JH, Winter DC, Laug WE, Redmond HP. Tumor cell adhesion to endothelial cells is increased by endotoxin via an upregulation of beta-1 integrin expression. *J Surg Res* 2001; **97**: 14-19
15 **Crowe DL**, Brown TN, Kim R, Smith SM, Lee MK. A c-fos/Estrogen receptor fusion protein promotes cell cycle progression and proliferation of human cancer cell lines. *Mol Cell Biol Res Commun* 2000; **3**: 243-248
16 **Han JY**, Kim HS, Lee SH, Park WS, Lee JY, Yoo NJ. Immunohistochemical expression of integrins and extracellular matrix proteins in non-small cell lung cancer: correlation with lymph node metastasis. *Lung Cancer* 2003; **41**: 65-70
17 **Armulik A**, Svineng G, Wennerberg K, Fassler R, Johansson S. Expression of integrin subunit beta1 B in integrin beta1-deficient GD25 cells does not interfere with alphaVbeta3 functions. *Exp Cell Res* 2000; **254**: 55-63
18 **Yu W**, Song G, Long M. Investigation on the adhesive properties of different cycle hepatoma cells. *Zhonghua Ganzangbing Zazhi* 1999; **7**: 153-155

Assistant Editor Guo SY **Edited by** Wang XL and Ma JY

PO Box 2345, Beijing 100023, China
Fax: +86-10-85381893
E-mail: wjg@wjgnet.com www.wjgnet.com

ELSEVIER

World J Gastroenterol 2005;11(2):216-220
World Journal of Gastroenterology ISSN 1007-9327

Effects of thalidomide on angiogenesis and tumor growth and metastasis of human hepatocellular carcinoma in nude mice

Zhong-Lin Zhang, Zhi-Su Liu, Quan Sun

Zhong-Lin Zhang, Zhi-Su Liu, Quan Sun, Department of General Surgery, Zhongnan Hospital, Wuhan University, Wuhan 430071, Hubei Province, China
Correspondence to: Professor Zhi-Su Liu, Department of General Surgery, Zhongnan Hospital, Wuhan University, Wuhan 430071, Hubei Province, China. zhangzhonglin221@sina.com
Telephone: +86-27-67813007 **Fax:** +86-27-87330795
Received: 2004-01-15 **Accepted:** 2004-02-24

Abstract

AIM: To investigate the effects of thalidomide on angiogenesis, tumor growth and metastasis of hepatocellular carcinoma in nude mice.

METHODS: Twenty-four nude mice were randomly divided into therapy group and control group, 12 mice in each group. Thalidomide dissolved in 0.5% sodium carboxyl methyl cellulose (CMC) suspension was administered intraperitoneally once a day at the dose of 200 mg/kg in therapy group, and an equivalent volume of 0.5% CMC in control group. Mice were sacrificed on the 30th d, tumor size and weight and metastases in liver and lungs were measured. CD34 and VEGF mRNA in tumor tissue were detected by immunohistochemistry and semi-quantitative RT-PCR respectively and microvessel density (MVD) was counted. Serum concentrations of TNF-α and ALT and AFP were also tested.

RESULTS: MVD and VEGF mRNA in therapy group were less than those in control group (31.08±16.23 vessels/HP *vs* 80.00±26.27 vessels/HP, 0.0538±0.0165 *vs* 0.7373±0.1297, respectively, $P<0.05$). No statistical difference was observed in tumor size and weight and metastases in liver and lungs. TNF-α was significantly lower in therapy group than in control group (28.64±4.64 ng/L *vs* 42.69±6.99 ng/L, $P<0.05$). No statistical difference in ALT and AFP was observed between groups.

CONCLUSION: Thalidomide can significantly inhibit angiogenesis and metastasis of hepatocellular carcinoma. It also has inhibitory effects on circulating TNF-α.

Key words: Hepatocellular carcinoma; Thalidomide; Angiogenesis; Neoplasm metastasis

Zhang ZL, Liu ZS, Sun Q. Effects of thalidomide on angiogenesis and tumor growth and metastasis of human hepatocellular carcinoma in nude mice. *World J Gastroenterol* 2005; 11(2): 216-220
http://www.wjgnet.com/1007-9327/11/216.asp

INTRODUCTION

Malignant tumor's growth, invasion and metastasis depend on the process of angiogenesis[1,2], obliteration of the feeding vessels to a tumor could cause its shrinkage or death[3]. As a result, antiangiogenic therapy has become a hotspot in the field of tumor treatment. Hepatocellular carcinoma (HCC) is the fourth most common cause of cancer death, and accounts for 53% of all liver cancer deaths in China[4]. Poor prognosis of hepatocellular carcinomas is mainly due to its high recurrence and metastasis. HCC also a kind of typical hypervascular malignant tumor, for which antiangiogenic therapy is particularly promising.

It has been found in a recent research that thalidomide, having been removed from medical markets for its severe side effects of teratogenesis, has antiangiogenic effects[5]. Thalidomide first entered medical care markets as a non-barbital sedative with remarkable anti-emetic effects on nausea of first-trimester morning sickness in pregnant women. Unprecedented epidemic of babies' birth defects in late 1950s and early 1960s was due to its serious potential side effects of teratogenicity, and then the drug has been prohibited and removed from markets since 1963. But research on this agent has never stopped and in 1994 D'A mato *et al*[5] firstly reported it could remarkably reduce neovascularization in rabbit corneas after stimulation by basic fibroblast growth factor (bFGF), and following studies[6-8] confirmed its antiangiogenic effects. As a result, thalidomide has been employed in the studies of solid tumor as an antiangiogenic agent in recent years. Some preclinical and clinical trials for the treatment of several types of solid tumor using thalidomide have been reported[9-11]. However, the effectiveness and mechanism of this antiangiogenic agent for the treatment of hepatocellular carcinoma have not been fully investigated. In the current study we established nude mice models bearing xenografts of human hepatocellular carcinoma with a high metastatic potential, by which we examined the effect of thalidomide on angiogenesis and tumor growth and metastasis of human hepatocellular carcinoma. Its influence on tumor necrosis factor α (TNF-α) and liver function was also investigated.

MATERIALS AND METHODS

Animals

Male athymic BALB/c nu/nu mice, 4-6 wk old, were obtained from Shanghai Institute of Materia Medica, Chinese Academy of Sciences and maintained under specific pathogen-free (SPF) conditions. The study protocol on mice was approved by Shanghai Medical Experimental Animal Care Commission.

Metastatic model of human HCC in nude mice

Human hepatocellular carcinoma cell line HCCLM3 was established by Liver Cancer Institute of Fudan University[12], in which a metastatic model of human hepatocellular carcinoma in nude mice was constructed via orthotopic implantation of histologically intact metastatic tumor tissue. Briefly, HCCLM3 derived 5×10^6 (0.2 mL) cells were injected subcutaneously into the nude mice. When the subcutaneous tumor reached about 1.5 cm in diameter, mice were sacrificed and small pieces of tumor tissue (approximately 1 mm^3) were implanted into the

liver of new recipient mice, which were kept in standard facilities. This animal model represents 100% spreading in liver and metastasis to lungs. Besides, alpha-fetoprotein (AFP) was excreted and hepatitis B virus was integrated into host cellular genome as previously reported[12].

Grouping and drug administration

Twenty-four nude mice were randomly divided into therapy group and control group, 12 mice in each group. Thalidomide was dissolved in 0.5% sodium carboxyl methyl cellulose (CMC) as an even suspension due to its poor solubility in water. Thalidomide (200 mg/kg·d) was intraperitoneally administered once a day in the therapy group and an equivalent volume of 0.5% CMC suspension simply in the control group. The injection started from the second day of inoculation and continued in the following consecutive 30 d. Body weight of mice was recorded once a week.

Parameters observed

On the 30th d all mice were sacrificed and 1 mL of blood sample was collected. After separated, tumors were weighed and the longest (a) and the smallest (b) diameters were measured by slide gauge under operating microscope. Tumor volume was calculated with the following formulation: $V = a \cdot b^2/2$. Liver tissues were carefully anatomized and visible metastases were counted. Paraffin blocks of 10% buffered formalin-fixed samples of lungs were prepared. Each lung sample was consecutively cut into 10 slices. Serial sections were cut at 5-μm and stained with hematoxylin and eosin to determine the presence of lung metastases. After blood samples were coagulated, centrifugation at 2 000×g for 10 min was performed and serum was obtained for the test of AFP and alanine aminotransferase (ALT) and TNF-α by radioimmunoassay and immunosorbent assay respectively. Part of each tumor tissue was embedded in paraffin block for advanced immunohistochemistry analysis of CD34 and the rest was stored at -70 ℃ for following RT-PCR study.

Immunohistochemical assessment of vascular density

Paraffin-embedded tumor tissues were sectioned (4 μm) and the slides were deparaffinized as usual and washed with tris buffered saline (TBS), and then incubated with 10% normal goat serum (Zhongshan Bio. CA). Sections were then incubated with appropriately diluted (1:10) rat-anti-mouse CD34 monoclonal antibody (Santa Cruz Biotechnology, Inc., Santa Cruz, CA) for 24 h at 4 ℃. Primary antibody was removed and washed with TBS, goat-anti-rat IgG peroxidase (Zhongshan Bio. CA) was then added. Finally the slices were stained as usual with haematoxylin and washed with distilled water. Quantification of blood vessels was carried out as previously described[13]. Any brown-stained endothelial cell cluster distinct from adjacent microvessels, tumor cells, or other stromal cells was considered as a single countable microvessel. The most vascularized areas of tumors were identified in a low-power field (×100), and vessels were counted in five high-power fields (×200). The data were presented as mean±SD of five high-power fields.

Semi-quantitative reverse transcription-PCR

Total RNA was extracted with Trizol reagent (Promega, USA) following the manufacturer's instructions and quantitated by absorbance analysis at 260 nm. For the reverse transcription polymerase chain reaction, RNA PCR kit (AMV) (TakaRa Bio, JP) was used. Total volume of reverse transcription reaction was 10 μL. Reaction temperature was 30 ℃ for 10 min, 42 ℃ for 20 min and 45 ℃ for 30 min. For PCR reaction the total reacting volume was 50 μL. PCR reaction was performed in GeneAmp PCR system 2400 (Perkin Elmer, USA). Primers were designed according to previous publications[14,15]. Primer sequences and PCR reaction conditions are shown in Table 1. Glyceraldehyde 3-phosphate dehydrogenase (G3PDH) was used as the internal standard. Of the PCR products 5 μL was visualized by electrophoresis on 1.5% agarose gel stained with ethidium bromide and quantitated by densitometry using the Image Master VDS system and associated software (Pharmacia, Sweden).

Enzyme-linked immunosorbent assay for TNF-α

Serum TNF-α was tested by enzyme-linked immunosorbent assay (ELISA) using TNF-α ELISA kit (Basic Medical Institute of Shanghai, Chinese Academy of Military Medical Sciences). Procedure was designed according to manufacturer's instructions, concentrations of unknown samples were determined by comparing the optical density of samples to the standard curve.

Statistical analysis

Data were analyzed for significance with unpaired *t* test and chi-square test. Statistical software SPSS 11.5 was used in the analysis. *P* value less than 5% was considered statistically significant.

RESULTS

Effects of thalidomide on growth of HCC

Lumps in stomach and skin invasion could be observed at the 5th wk when mice were sacrificed. The separated tumors are shown in Figure 1. The changes of body weight (g) and tumor weight (g) and tumor volume (cm^3) in treatment group were all smaller than those in control group (4.3000±1.9980 *vs* 5.1833±0.9827, 1.0333±0.2842 *vs* 1.1483±0.3633 and 0.9950±0.3987 *vs* 1.2806±0.3188, respectively) There was no statistical significance ($P>0.05$).

Effects of thalidomide on metastasis of HCC

Visible metastases ranging from 1 to 10 mm in diameter were observed when seven lobes of liver were carefully anatomized and the number of visible metastases was recorded. Gross pathological examination of the lungs found scattered hemorrhagic spots, which were confirmed by histopathology to be metastases (Figure 2). The metastatic rate in liver and lungs in treatment group and control group was both 100%, but the number of metastases in both liver and lungs in therapy group was significantly less than that in control group ($P<0.05$, Figure 3).

Table 1 Primer sequences and PCR reaction conditions

Gene	Primers	Products size	Annealing Temp/Time	Cycles
VEGF (all isoforms)	Upper: CCTGGTGGACATCTTCCAGGAGTACC Lower: GAAGCTCATCTCTCCTATGTGCTGGC	196 bp	58 ℃/30 s	30
G3PDH	Upper: ACCACAGTCCATGCCATCAC Lower: TCCACCACCCTGTTGCTGTA	450 bp	58 ℃/30 s	30

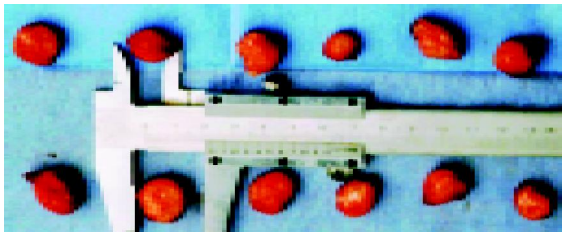

Figure 1 Tumors in nude mice on the 30th d. Upper line of tumors was HCC in the control group, the lower in therapy group.

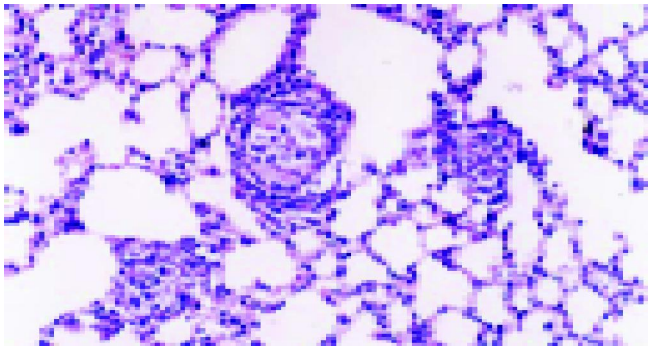

Figure 2 Metastases of hepatocellular carcinoma in lungs. Magnification: ×200.

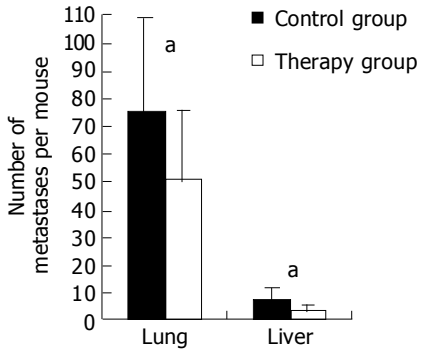

Figure 3 Metastases of hepatocellular carcinoma in lungs and liver. [a]$P<0.05$. Liver metastases were recorded in a gross manner by examining each lobe of liver and counting macroscopic tumors on the surface. Lung metastases were counted under microscope by observing consecutive paraffin slices of lung.

CD34 expression and microvessel counting

Expression of CD34 in therapy group was weak or even negative, whereas it was strong in control group. The newborn endothelial cells were stained brown or yellow and sinusoidly distributed in capillary walls of portal area and fiber interval of liver tissue (Figure 4). Microvessel counting revealed that MVD in control group was 80.00±26.27 per high-power field (×200), whereas it was 31.08±16.23 in therapy group ($P<0.05$).

Semi-quantitative RT-PCR

As shown in Figure 5, the PCR products of VEGF and G3PDH were visualized at the expected locations on agarose gels and in direct cDNA sequencing. All the obtained PCR products had the same cDNA sequences as the gene bank sequences (data not shown). The degree of VEGF mRNA by semi-quantitative RT-PCR was 0.0538±0.0165 in the therapy group, and 0.7373±0.1297 in the control group ($P<0.05$).

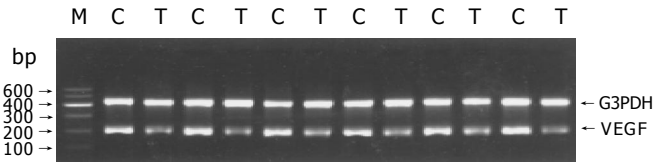

Figure 5 RT-PCR of VEGF mRNA in HCC tissue. M: Marker, 100 bp DNA ladder, ranging from 100 bp to 600 bp; C: Control group; T: Therapy group. The band of VEGF (all isoforms, 196 bp) and G3PDH (450 bp) are shown at expected location in the gel. G3PDH used as an internal standard. VEGF mRNA was expressed strongly in control group, whereas weakly in therapy group.

Effects on serum TNF-α and liver function indexes

Concentrations of serum ALT, AFP and TNF-α are shown in Table 2. The level of TNF-α in therapy group was lower than that in control group ($P<0.05$). No significant difference was observed in the in serum concentrations of ALT and AFP.

Table 2 Comparison of serum concentrations of ALT and AFP and TNF-α between groups (mean±SD)

Groups	ALT (IU/L)	AFP (μg/L)	TNF-α (ng/L)
Control (n = 12)	102.35±39.29	25.68±14.38	42.69±6.99
Therapy (n = 12)	87.88±35.38	19.40±13.58	28.64±4.64[a]

[a]$P<0.05$ *vs* control group.

DISCUSSION

Angiogenesis is a neovascularization process during which endothelial cells of the pre-existing capillaries proliferate and migrate to form new vascular tips or so called "vascular sprouts" or "endothelial buds". It is critical for the growth, invasion and

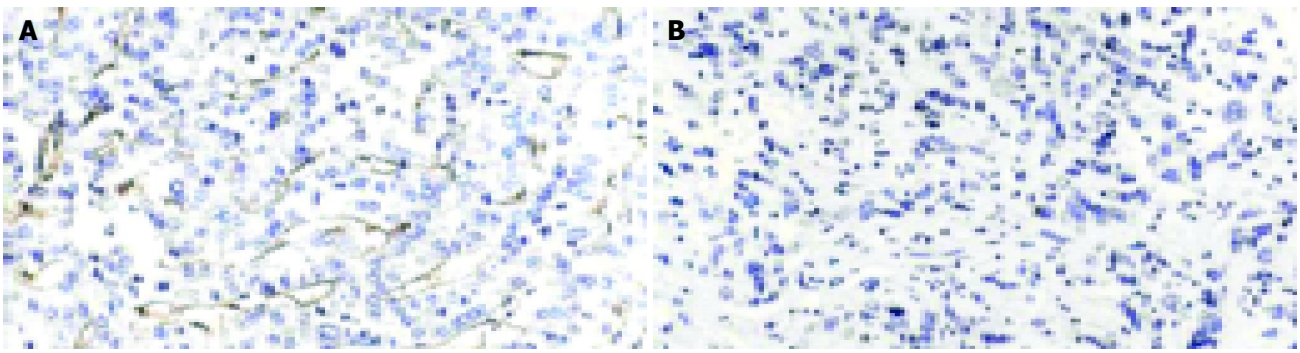

Figure 4 Immunohistochemical expression of CD34. A: control group; B: thalidomide treated group. Magnification: ×200.

metastasis of cancer[1,2,16]. Solid tumors would not grow beyond the volume of 2-3 mm^3 when sprouting new capillary blood vessels are tack, and the small cancer blocks, so-called micrometastases, would be kept in a hibernating state for a long term. Antiangiogenic therapy for malignant tumors has opened a brand new way to the treatment of carcinomas, and is regarded as one of the most promising and hopeful strategies. Different inhibitory effects of thalidomide on angiogenesis and tumor growth have been reported[17-19]. The current study was to examine the effect of thalidomide on angiogenesis and tumor growth and metastasis of human hepatocellular carcinoma.

In our study intraperitoneal administration was employed as previously described[14,15] at the dose of 200 mg/kg body weight every day. Kotoh *et al*[15] reported the antitumor and antiangiogenic effect of thalidomide on human esophageal cancer ES63 in nude mice by intraperitoneal administration. Whereas same effects were not observed when mice were treated by gavage administration. However, experiments *in vitro* have failed to demonstrate that thalidomide or any of its metabolites has any direct effect on cell proliferation or cytotoxic effect[20]. The mechanisms underlying the strong effect of antiangiogenesis by intraperitoneal route but poor efficiency by oral route remain unclear, the reason might be the bioavailability of the active form of thalidomide at tumor site. Results in this study reveal that changes of body weight and tumor weight and tumor volume in treatment group were smaller than those in control group, but statistical analysis showed no significant difference ($P>0.05$). Metastases in both liver and lung were observed. The metastatic rate in liver and lungs in treatment group and control group was 100%, but metastasis counting showed that the number of metastases in liver and lungs in treatment group was both statistically lower than those in control group ($P<0.05$). Minchinton *et al*[6] reported that thalidomide did not alter primary tumor growth of Lewis lung tumor xenoplanted in mice, and additionally reduced the radiosensitivity of the tumor, but did increase its sensitivity of combined treatment with radiation and cytotoxin tirapazamine. In another report[17], thalidomide alone inhibited tumor growth by 55% in the rabbit oral carcinoma model. However, Gutman *et al*[19] failed to find any antiangiogenic effect and tumor inhibition effect of thalidomide in syngeneic mice. Results reported are very different, it might be partly due to thalidomide's species specificity and tissue specificity[21]. Stephens *et al*[22] believe that various species and tissues depend on different angiogenesis or vascular pathways, the extent of dependence on integrin $\alpha_v\beta_3$ determines their sensitivity to thalidomide.

Angiogenesis is a highly complex and closely regulated process, which is influenced by the balance between stimulatory and inhibitory factors released by tumor and surrounding host cells. VEGF, bFGF and patelet-derived endothelial cell growth factor (PD-ECGF) are the main stimulatory factors, of which VEGF is the most important; it could promote the growth of malignant cells by increasing vascular permeability[23]. Researches have revealed that expression of VEGF in hepatocellular carcinoma is much higher than that in non-tumor tissues[24]. Concentration of VEGF in serum is also closely related to tumor's pathologic progress and patients' prognosis after operation[25]. In the current study we examined VEGF mRNA in cancer by semi-quantitative RT-PCR. It showed that the level of VEGF mRNA in thalidomide-treated group was significantly lower than that in control group. Also we immunohistochemically examined the expression of CD34 which was considered as an endothelial-specific marker, using monoclonal antimouse CD34 antibody. Results suggested that the expression of CD34 in therapy group was very weak, whereas in control group it was strongly expressed. Accordingly, MVD in the former was much less than that in the later ($P<0.05$). VEGF and MVD are the most common parameters reflecting neovascularisation. The effects of down-regulation in this study suggest thalidomide has inhibitory effects on angiogenesis. Its inhibitory effects on metastases in liver and lung might mainly attribute to its inhibition on VEGF[14], and its inhibition on integrin $\alpha_v\beta_3$ may also involve the process. Whether its obvious inhibition on metastasis but poor effects on tumor growth are due to its modulation on integrin $\alpha_v\beta_3$ is yet to be investigated.

The pharmaceutical role of thalidomide is very extensive, the most significant is to decrease the level of TNF-α in circulation so as to modulate immune system[26]. TNF-α, an important inflammatory factor, is also a critical factor to induce inflammatory reaction in hepatitis[27]. Raufman *et al*[28] reported a case of hepatitis C who's ALT in circulation was induced to normal by thalidomide. Serum TNF-α and liver function indexes such as ALT and AFP were tested in the study so as to try to find thalidomide's influence on liver function. Results suggest thalidomide could dramatically down-regulate serum TNF-α as previously reported[26], but no statistical variance was observed in serum concentration of ALT and AFP. Whether inhibition of TNF-α synthesis plays a different role in the inhibition of angiogenesis compared with immunomodulation has yet to be investigated. The remarkably inhibitory effect of thalidomide on TNF-α might be valuable for clinical treatment of liver cancer, because in China about 90% of hepatocellular carcinomas are accompanied with hepatitis B and abnormal liver function, the continuous inflammatory states of liver and liver failure after operation at least could partly contribute to the prognosis and poor life quality of patients. Although in this animal model hepatitis B virus genome was carried and AFP was expressed, its biological state of hepatitis might be very different from that of human beings. Further studies about the drug's effect on liver function are needed.

The molecular mechanisms and specific antitumor effects of thalidomide are yet to be elucidated, although some clinical trials have been performed[29]. Current clinical trials on thalidomide are mainly performed on unoperable malignant cases of middle or final phase, and in most cases tumor's volume change and disappearance are taken as standards to evaluate the drug's efficiency. Studies should be focused on elucidating the antitumor and antiangiogenic effects of thalidomide on specific cancers. Then in clinical trials this drug should be used as an adjunct treatment modality, its accumulating effects in long term and influence on the life quality of patients may be the most valuable, because thalidomide, as an antiangiogenic agent, does not have a remarkable dose-effect relationship as cytotoxic drugs. The results of this study suggest that thalidomide can be used as an adjunct treatment modality in the treatment of hepatocellular carcinoma.

REFERENCES

1 **Folkman J**. The role of angiogenesis in tumor growth. *Semin Cancer Biol* 1992; **3**: 65-71
2 **Folkman J**. Role of angiogenesis in tumor growth and metastasis. *Semin Oncol* 2002; **29**: 15-18
3 **Kuiper RA**, Schellens JH, Blijham GH, Beijnen JH, Voest EE. Clinical research on antiangiogenic therapy. *Pharmacol Res* 1998; **37**: 1-16
4 **Pisani P**, Parkin DM, Bray F, Ferlay J. Estimates of the world-wide mortality from 25 cancers in 1990. *Int J Cancer* 1999; **83**: 18-29
5 **D'Amato RJ**, Loughnan MS, Flynn E, Folkman J. Thalidomide is an inhibitor of angiogenesis. *Proc Natl Acad Sci USA* 1994; **91**: 4082-4085
6 **Minchinton AI**, Fryer KH, Wendt KR, Clow KA, Hayes MM. The effect of thalidomide on experimental tumors and metastases. *Anticancer Drugs* 1996; **7**: 339-343

7 **Kenyon BM**, Browne F, D'Amato RJ. Effects of thalidomide and related metabolites in a mouse corneal model of neovascularization. *Exp Eye Res* 1997; **64**: 971-978
8 **Kruse FE**, Joussen AM, Rohrschneider K, Becker MD, Volcker HE. Thalidomide inhibits corneal angiogenesis induced by vascular endothelial growth factor. *Graefes Arch Clin Exp Ophthalmol* 1998; **236**: 461-466
9 **Tseng JE**, Glisson BS, Khuri FR, Shin DM, Myers JN, El-Naggar AK, Roach JS, Ginsberg LE, Thall PF, Wang X, Teddy S, Lawhorn KN, Zentgraf RE, Steinhaus GD, Pluda JM, Abbruzzese JL, Hong WK, Herbst RS. Phase II study of the antiangiogenesis agent thalidomide in recurrent or metastatic squamous cell carcinoma of the head and neck. *Cancer* 2001; **92**: 2364-2473
10 **Govindarajan R**. Irinotecan and thalidomide in metastatic colorectal cancer. *Oncology (Williston Park)* 2000; **14**: 29-32
11 **Baidas SM**, Winer EP, Fleming GF, Harris L, Pluda JM, Crawford JG, Yamauchi H, Isaacs C, Hanfelt J, Tefft M, Flockhart D, Johnson MD, Hawkins MJ, Lippman ME, Hayes DF. Phase II evaluation of thalidomide in patients with metastatic breast cancer. *J Clin Oncol* 2000; **18**: 2710-2717
12 **Li Y**, Tang Y, Ye L, Liu B, Liu K, Chen J, Xue Q. Establishment of a hepatocellular carcinoma cell line with unique metastatic characteristics through *in vivo* selection and screening for metastasis-related genes through cDNA microarray. *J Cancer Res Clin Oncol* 2003; **129**: 43-51
13 **Weidner N**, Semple JP, Welch WR, Folkman J. Tumor angiogenesis and metastasis-correlation in invasive breast carcinoma. *N Engl J Med* 1991; **324:** 1-8
14 **Myoung H**, Hong SD, Kim YY, Hong SP, Kim MJ. Evaluation of the anti-tumor and anti-angiogenic effect of paclitaxel and thalidomide on the xenotransplanted oral squamous cell carcinoma. *Cancer Lett* 2001; **163:** 191-200
15 **Kotoh T**, Dhar DK, Masunaga R, Tabara H, Tachibana M, Kubota H, Kohno H, Nagasue N. Antiangiogenic therapy of human esophageal cancers with thalidomide in nude mice. *Surgery* 1999; **125**: 536-544
16 **Folkman J**. Fundamental concepts of the angiogenic process. *Curr Mol Med* 2003; **3**: 643-651
17 **Verheul HM**, Panigrahy D, Yuan J, D'Amato RJ. Combination oral antiangiogenic therapy with thalidomide and sulindac inhibits tumour growth in rabbits. *Br J Cancer* 1999; **79**: 114-118
18 **Eisen T**, Boshoff C, Mak I, Sapunar F, Vaughan MM, Pyle L, Johnston SR, Ahern R, Smith IE, Gore ME. Continuous low dose Thalidomide: a phase II study in advanced melanoma, renal cell, ovarian and breast cancer. *Br J Cancer* 2000; **82:** 812-817
19 **Gutman M**, Szold A, Ravid A, Lazauskas T, Merimsky O, Klausner JM. Failure of thalidomide to inhibit tumor growth and angiogenesis *in vivo*. *Anticancer Res* 1996; **16**: 3673-3677
20 **Santos-Mendoza T**, Favila-Castillo L, Oltra A, Tamariz J, Labarrios F, Estrada-Parra S, Estrada-Garcia L. Thalidomide and its metabolites have no effect on human lymphocyte proliferation. *Int Arch Allergy Immunol* 1996; **111**: 13-17
21 **Belo AV**, Ferreira MA, Bosco AA, Machado RD, Andrade SP. Differential effects of thalidomide on angiogenesis and tumor growth in mice. *Inflammation* 2001; **25**: 91-96
22 **Stephens TD**, Bunde CJ, Fillmore BJ. Mechanism of action in thalidomide teratogenesis. *Biochem Pharmacol* 2000; **59**: 1489-1499
23 **Yamaguchi R**, Yano H, Nakashima Y, Ogasawara S, Higaki K, Akiba J, Hicklin DJ, Kojiro M. Expression and localization of vascular endothelial growth factor receptors in human hepatocellular carcinoma and non-HCC tissues. *Oncol Rep* 2000; **7**: 725-729
24 **Shimamura T**, Saito S, Morita K, Kitamura T, Morimoto M, Kiba T, Numata K, Tanaka K, Sekihara H. Detection of vascular endothelial growth factor and its receptor expression in human hepatocellular carcinoma biopsy specimens. *J Gastroenterol Hepatol* 2000; **15**: 640-646
25 **Poon RT**, Ng IO, Lau C, Yu WC, Fan ST, Wong J. Correlation of serum basic fibroblast growth factor levels with clinicopathologic features and postoperative recurrence in hepatocellular carcinoma. *Am J Surg* 2001; **182:** 298-304
26 **Meierhofer C**, Dunzendorfer S, Wiedermann CJ. Theoretical basis for the activity of thalidomide. *BioDrugs* 2001; **15**: 681-703
27 **Powell EE**, Edwards-Smith CJ, Hay JL, Clouston AD, Crawford DH, Shorthouse C, Purdie DM, Jonsson JR. Host genetic factors influence disease progression in chronic hepatitis C. *Hepatology* 2000; **31**: 828-833
28 **Raufman JP**, Lamps LW. Thalidomide-induced normalization of serum ALT levels in a patient with hepatitis C. *Am J Gastroenterol* 2001; **96:** 3209-3211
29 **Patt YZ**, Hassan MM, Lozano RD, Ellis LM, Peterson JA, Waugh KA. Durable clinical response of refractory hepatocellular carcinoma to orally administered thalidomide. *Am J Clin Oncol* 2000; **23**: 319-321

Edited by Wang XL and Zhu LH

PO Box 2345, Beijing 100023, China
Fax: +86-10-85381893
E-mail: wjg@wjgnet.com www.wjgnet.com

ELSEVIER

World J Gastroenterol 2005;11(2):221-227
World Journal of Gastroenterology ISSN 1007-9327

• LIVER CANCER •

TIP30 regulates apoptosis-related genes in its apoptotic signal transduction pathway

Mei Shi, Xia Zhang, Ping Wang, Hong-Wei Zhang, Bai-He Zhang, Meng-Chao Wu

Mei Shi, Hong-Wei Zhang, Shandong University, Jinan 250014, Shandong Province, China
Mei Shi, Ping Wang, Bai-He Zhang, Meng-Chao Wu, Department of Clinical Surgery, Eastern Hepatobiliary Surgery Hospital, The Second Military Medical University, 225 Changhai Road, Shanghai 200438, China
Xia Zhang, Department of Oncology, Fuzhou General Hospital of Nanjing Military Command, Fuzhou 350025, Fujian Province, China
Correspondence to: Meng-Chao Wu, Department of Clinical Surgery, Eastern Hepatobiliary Surgery Hospital, The Second Military Medical University, 225 Changhai Road, Shanghai 200438, China. tupa@vip.sina.com
Telephone: +86-21-25075388
Received: 2004-01-02 **Accepted:** 2004-02-09

Abstract

AIM: To investigate the role of TIP30 in apoptotic signal pathway in hepatoblastoma cells and to provide a basis for TIP30 as a gene therapy candidate in the regression of hepatoblastoma cells.

METHODS: Apoptosis of human hepatoblastoma cell lines HepG2 (p53 wild), Hep3B (p53 null) and PLC/RPF/5 (p53 mutant) infected with Ad-TIP30 (bearing a wild type human Tip30 gene) were analyzed and p53, Bax and Bcl-xl expression levels were compared among these cells. MTT assay, DNA fragmentation, *in situ* 3′ end labeling of DNA, annexin-V FITC staining were used to detect cell death and apoptosis in cells at various time intervals subsequent to infection, and to determine whether TIP30 had an effect on the expression levels of some apoptosis-related gene products such as Bax, p53 and Bcl-xl. A similar time course experiment was performed by Western blotting.

RESULTS: In MTT assay, the viability of HepG2 cells decreased significantly from 99.7% to 10% and displayed more massive cell death within 5-8 d than Hep3B and PLC/RPF/5 cells, with their viability decreased from 97.8% to 44.3% and 98.1% to 50.4%, respectively. In annexin-V FITC assay, the percentage of apoptosis cells in HepG2 cells was two to three-fold higher than that in control cells (infected with Ad-GFP), two-fold higher than that in Hep3B cells and 1.4-fold higher than that in PLC/RPF/5 cells 36 h after infection, respectively. Moreover, in HepG2 cells, the p53 began to increase 6-8 h after infection, reaching a maximum level between 8 and 12 h after infection and then dropped. Bax showed a similar increase in the cells as p53 reached the maximum at 8-12 h and subsequently decreased. Interestingly, Bcl-xl protein levels were down regulated during 24 to 36 h after Ad-TIP30 infection. In contrast, ectopic expression of TIP30 in Hep3B and PLC/RPF/5 cells had no effect on the regulation of Bax expression, but had an effect on Bcl-xl levels. In comparison with HepG2 cells, these data suggested that up-regulation of p53 levels by TIP30 might be a pre-requisite for Bax and Bax/Bcl-xl ratio increase. We hypothesized that TIP30 might regulate Bax gene partly through p53, which sensitizes cells to apoptosis by involving a p53 apoptosis signal transduction pathway.

CONCLUSION: TIP30 plays an important role in predisposing hepatoblastoma cells to apoptosis through regulating expression levels of these genes. Ad-TIP30 carrying exogenous TIP30-anti-tumor genes may be regarded as a potential candidate for the treatment of hepatocellular carcinoma.

Key words: Hepatoblastoma; TIP30; Apoptosis; Signal transduction

Shi M, Zhang X, Wang P, Zhang HW, Zhang BH, Wu MC. TIP30 regulates apoptosis-related genes in its apoptotic signal transduction pathway. *World J Gastroenterol* 2005; 11(2): 221-227
http://www.wjgnet.com/1007-9327/11/221.asp

INTRODUCTION

TIP30 is an evolutionarily conserved gene that is expressed ubiquitously in human tissues and some tumor tissues with properties of serine/threonine kinase, coding a polypeptide of 242 amino acids. It is identified as a cofactor to specially enhance human immunodeficiency virus-1 (HIV-1) Tat-activated transcription by phosphorylating heptapeptide repeats of C-terminal domain (CTD) of the largest RNA polymerase II subunit in a Tat-dependent manner[1,2]. Furthermore, Baker *et al*[2] have shown that TIP30 is an important metastasis suppression factor that accounts for a significant suppression growth retardation in small cell lung carcinoma (SCLC), which could be largely mediated by the ability of TIP30 to promote the apoptosis pathway. Moreover, ectopic expression of TIP30 in SCLC cells induces activation of apoptosis-related genes: Bad and Siva. Nevertheless, the molecular mechanism by which the TIP30 gene mediates apoptosis remains largely unknown.

We employed *in vitro* analysis to gain an insight into the molecular candidates other than Tat with which TIP30 interacted. In this respect, many pro-apoptotic proteins were investigated to reveal a TIP30 triggering apoptosis pathway. Among them, p53 is considered as one of the best target genes because of its pivotal role in regulating cell cycle progression as well as apoptotic cell death[3,4]. The biochemical activity of p53 closely associated with apoptosis is its function as a sequence-specific DNA-binding protein and a transcriptional factor that controls the expression of a large panel of genes implicated in engagement of apoptosis[5]. Moreover, p53 protein levels have been shown to dramatically rise in response to diverse stresses including ionizing radiation, UV radiation, growth factor deprivation or virus infection[6]. Bax gene is a pro-apoptosis member of Bcl-2 whose promoter is highly p53-responsive. Furthermore, Bcl-xl is another member of Bcl-2 family

that has been found to express high levels in more than half of all human tumors[7-9]. Consistent with its anti-apoptotic role by antagonizing the Bax-dependent apoptosis pathway, it prevents all mitochondrial changes including release of cytochrome *C* and loss of mitochondrial membrane potential as well as caspase activation by sequestering Apaf-1[10,11]. It seems that in some cells, p53 protein-involving apoptosis modification can result in a general up-regulation of protein expression of pro-apoptotic members and down-regulation of anti-apoptotic proteins in Bcl-2 family, shifting the balance in favor of apoptosis[12]. In hepatocellular carcinoma, Bax and Bcl-xl proteins are especially involved in the regulation[13]. Although the central role of p53 as a pro-apoptotic-focus protein has been established, the complicated mechanism by which p53 exerts its interaction with some components and how many regulating factors are involved in p53-dependent pathway are far unknown.

Our study was designed to evaluate the expression of TIP30 and its target gene after infection with Ad-TIP30 to enhance our understanding of molecular basis of human hepatoma and to raise the realistic possibility of targeting the p53 pathway in cancer therapy. With the advantages of both maximum effect and minimum cytotoxicity to the target cells in genetic therapeutic approaches, adenovirus vectors are being wildly developed for gene therapy[14].

MATERIALS AND METHODS

Cells, chemicals and antibodies

Human heptoblastoma carcinoma cell lines HepG2, Hep3B and PLC/RPF/5 were grown in DMEM supplemented with 10% FBS (Hyclone). Anti-p53 antibody (Ab-2) was purchased from Sigma (Stlouis, MO, USA). Anti-Bax and anti-Bcl-xl antibodies were obtained from Oncogene Research Products (San Diego, CA).

Recombinant adenovirus infection

Cells were grown in 96-well and 6-well dishes at a density of 5×10^3 or 5×10^6 per well. Then the cells were infected with either Ad-TIP30 or Ad-GFP (no TIP30) at MOI of 20-50 MOI by co-culturing with viruses at 37 ℃ for 1 hour in 200-500 μL of serum free medium. An additional 100-1 000 μL of complete medium was then added and cells were cultured in the presence of viruses for the indicated length of time.

Cell viability assays

XTT colorimetric assay (Oncogene Research Products, San Diego, CA) was used to determine cell proliferation and death. Briefly, cells were plated in a 96-well-plate at a concentration of 8 000-10 000 cells/well and infected with adenoviruses. After cells were incubated for 24 h per day, XTT reaction mixture was added, which contained XTT labeling reagent and the electron-coupling reagent in a 20:1 ratio. Cell/solution mixture was then read using a colormetric plate reader at a wavelength of 500 nm. Each sample was assayed in triplicate. Data were then analyzed with Microsoft Excel software. Cells were continually cultured for 8 d after-infection.

Apoptosis assay

Flow cytometry Cells were infected with Ad-TIP30 and Ad-GFP with mock (no virus) as control. Afterwards, infected and control cells were disassociated with 0.25% trypsin and collected by centrifugation at 8 000 g with cells floating in the culture, washed twice with PBS and stained with annexin-V-FITC and propidium iodide. Fluorescence was measured with a minimum of 10 000 events for each sample in a FACSCAN according to the method suggested by the manufacturers. Data analysis was performed.

DNA fragmentation analysis (DNA ladder) Infected and control cells were lysed at 0, 12, 24 or 36 h after infection. The lysate buffer contained 10 mmol/L Tris-HCl (pH7.5), 10 mmol/L EDTA, 0.3% Triton X-100, 100 μg/mL RNase and 200 μg/mL proteinase K. After incubated at 50 ℃ for 4 h or overnight, lysate was extracted twice with phenol/chloroform, then precipitated at -20 ℃ for 10 min by adding sodium acetate/ethanol. DNA concentration was determined, and an equal amount of DNA (10 μg) was electrophoresed on 2% agarose gel containing 0.1 μg/mL ethidium bromide. DNA bands were examined using UVPC system.

***In situ* 3' end labeling of DNA in apoptotic cells** 3' end labeling of DNA *in situ* was performed using the Apoptag Plus Kit (Oncogene Research Products, San Diego, CA). Cells grown *in vitro* were spun onto a plastic slide and fixed with buffered 4% formaldehyde at 0, 12, 24 h after infection. The percentage of positive cells was also determined by flow cytometry.

Western blotting

Cells were harvested and lysed in ice-cold lysis buffer containing 10 mmol/L Tris-HCl (pH7.5), 20% SDS, and 1mmol/L PMSF. After 30 min incubation on ice, lysate was stored at -80 ℃ before use. Protein concentration was determined by the Bradford method[35]. Equal amounts of protein (50 μg) were loaded onto SDS-polyacrylamide gels and the protein was electrophoretically transferred to a PVDF film (Millipore, Bedford, MA). Immunoblots were analyzed using specific primary antibodies (antibodies to Bcl-2, Bcl-xl, Bax, p53, β-actin), and protein was visualized using a chemiluminescence detection kit (Amersham, Ayesbury, UK). β-actin was used as an internal control to confirm whether the amount of protein was equal.

Statistical analysis

The data in this paper were the mean of three replications. Unless otherwise stated. Test of significant differences in significance was performed with Student's *t-test*. $P<0.05$ was considered statistically significant and $P<0.01$ very statistically significant.

RESULTS

Cooperation of TIP30 and p53 predisposed cells to death

The effect of TIP30 and p53 gene products on the *in vitro* growth characteristics of HepG2, Hep3B and PLC/RPF/5 cells was examined by colorimetric XTT assay. The three kinds of cells infected with Ad-TIP30 and Ad-GFP and mock (no virus) were incubated in DMEM medium and monitored by viability staining for 8 d. As shown in Figure 1, the viability of HepG2 cells decreased significantly from 99.7%, 68.3% to 10% and further displayed more massive cell deaths within 5-8 d than Hep3B and PLC/RPF/5 cells, with the latter decreased from 97.8%, 62.1% to 44.3% and 98.1%, 68.6% to 50.4%, respectively. All the three kinds of cells infected with Ad-GFP were found to have relatively lower cell deaths until 5-8 d. On the contrary, control cells (no virus) displayed a relatively high growth rate and maintained a high percentage of live cells even until 8-10 d after plating. These results demonstrated that expression of exogenous TIP30 in HepG2 cells could cooperate with p53 to reduce cell proliferation and then led them to massive deaths.

TIP30 induced cell death was due to apoptosis

To verify whether the cell death induced by TIP30 was ascribed to the activation of apoptosis in cells, *in situ* 3' end labeling of DNA assay was performed to examine 3'-OH groups at the end of DNA fragments in apoptotic cells (Figure 2), which was a hallmark of apoptosis. Percentage of apoptotic was calculated by FACS assay. This quantitative analysis indicated that the proportion of apoptosis cells progressively increased in cells

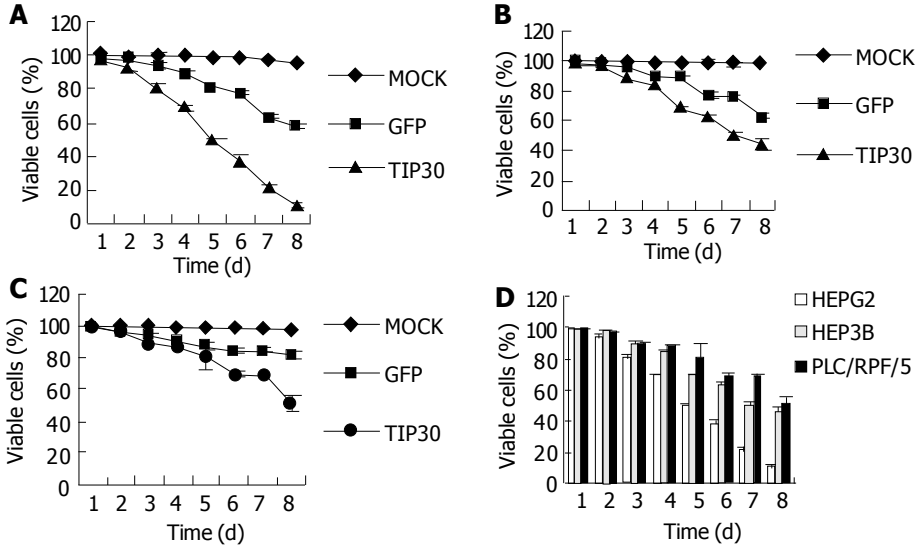

Figure 1 Cell viability of hepatoblastoma cell lines: HepG2, Hep3B and PLC/RPF/5 on indicated days as measured by XTT assay following infection with Ad-TIP30 and GFP at MOI of 20 or treatment of PBS (mock) (A, B, C). Three cell lines were infected with TIP30 at MOI of 20 in 8 continuous days (D). Values in the figures are mean±SD.

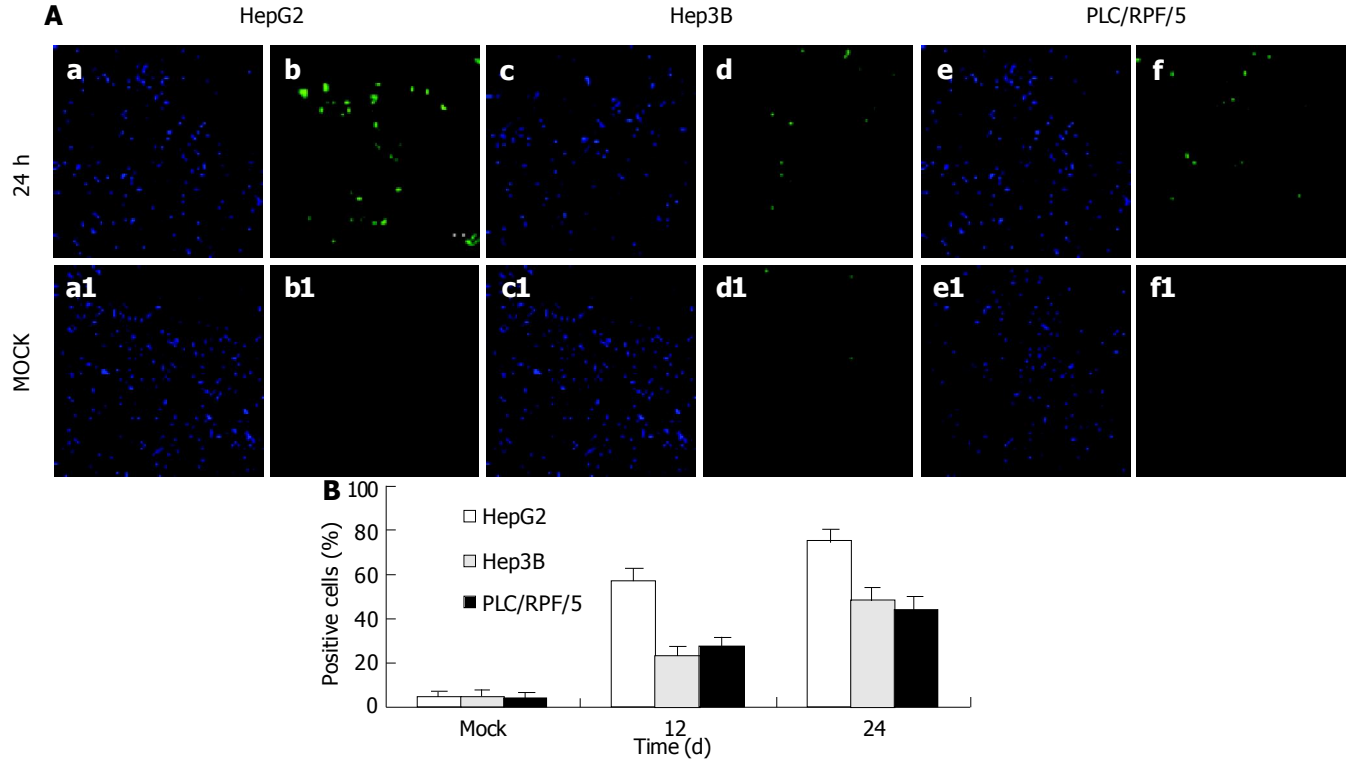

Figure 2 TUNEL (*in situ*) assay for TIP30 infection induced apoptosis at 24 h after infection and description of cell population with DAPI (a, c, d) and fluorescent (b, d, f) microscopy with mock as control. A: The mean of percentages of positive cells was calculated from the analysis; B: Data in the figure are mean±SD (P<0.01).

bearing Ad-TIP30. The maximum cell apoptosis was obtained at 24 h in HepG2, Hep3B, and PLC/RPF/5 cells, respectively. Quantitative analysis of apoptosis revealed that the percentage of apoptotic cells in HepG2 cells at 24 h was 1.5-to 2-fold (P<0.01) higher than those in Hep3B (48.1%) and PLC/RPF/5 (46.3%) cells. However, there was almost no apoptotic cell in mock (no virus).

Similar results were attained by flow cytometry assay with cells treated as previously. Cells were labeled with annexin-V-FITC followed by propidium staining in order to differentiate the necrosis-cells or apoptotic cells. The apoptotic cell proportions in HepG2 cells were 32.36%, 61.04%, and 81.67% at 12, 24 and 36 h after infection respectively. Meanwhile, in Hep3B and PLC/RPF/5 cells, the apoptotic cell proportions were only 12.38%, 34.08%, 50.71% and 11.26%, 23.17%, 53.52% at the same time after infection respectively, while mock cells did not display significant apoptosis (Figure 3).

To further confirm the kinetics of this programmed cell death, DNA fragmentation assay was performed with the same treatment in cells as previously. As indicated in Figure 4, DNA fragmentation became detectable at 24 h in HepG2 cells infected with Ad-TIP30, whereas it was detectable at 36 h in Hep3B and PLC/RPF/5 cells. Nevertheless, DNA ladder never emerged during the whole incubation process (72 h and more) of control cells (infected with Ad-GFP and mock, data not shown).

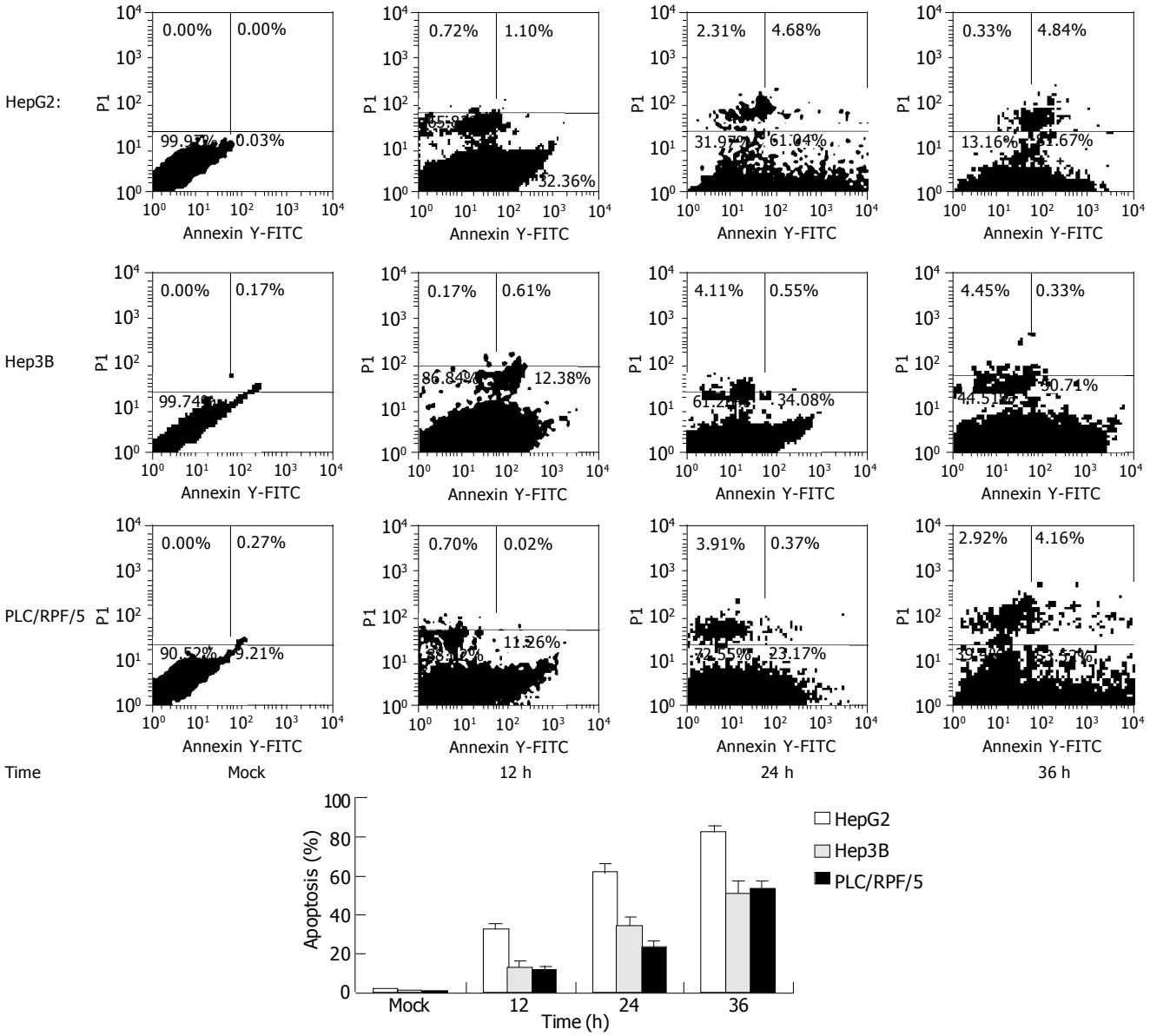

Figure 3 FACS analyses of annexin-V-FITC and PI double-stained cells. Cells were infected with Ad-TIP30 and mock as control (no virus). After treatment for 12, 24, 36 h, cells were double-stained at various indicated time points with annexin-V-FITC and PI and analyzed by flow cytometry. Cells appearing in the lower right quadrant showed positive annexin-V-FITC staining, which indicated phosphatidylserine translocation to the cell surface and no DNA staining by PI. Data in the figures are mean±SD. The percentage of apoptosis cells of three cell lines treated as previously (P<0.01).

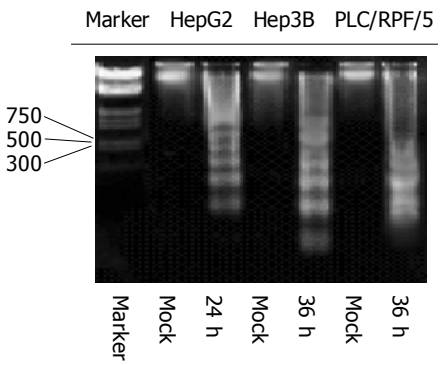

Figure 4 Kinetics of apoptosis in HepG2 and Hep3B and PLC/RPF/5 cells infected with Ad-TIP30. Twelve, twenty-four or thirty-six hours after infection, analysis of DNA laddering was performed by gel electrophoresis. An overexposed photograph was provided to show the beginning of DNA laddering at 24 h in HepG2 cells and at 36 h in Hep3B and PLC/RPF/5 cells.

Infection with Ad-TIP30 induced profound elevation of p53 protein

In response to DNA damage, the tumor suppressor protein, p53, was stabilized, accumulated inside the cells and was detectable by Western blotting. It was found to be a reliable initiator of apoptosis. We used HepG2 to study the expression level of p53 after infection with Ad-TIP30. Levels of p53 protein in HepG2 cells were examined at 6, 8, 12, 24 and 36 h after infection with 50 MOI of Ad-TIP30. In Figure 5, at 6-8 h after infection, p53 protein levels were significantly higher than those at other time points and drastically reduced at 12-24 h (Figure 5). Although the level of p53 after infection with Ad-GFP was a little higher than that of mock cells, no changes were observed at different time points (data not shown). According to the data quantified by densitometry, levels of p53 protein in Ad-TIP30 infected HepG2 cells were elevated by a range of 2-to 3- fold compared with cells infected with Ad-GFP. A comparable reduction in p53 protein was observed at 36 h, when a large percentage of apoptotic HepG2 cells was found. Expression of exogenously

introduced wild type TIP30 gene was confirmed in Ad-TIP30 infected cells by Western blotting (data not shown).

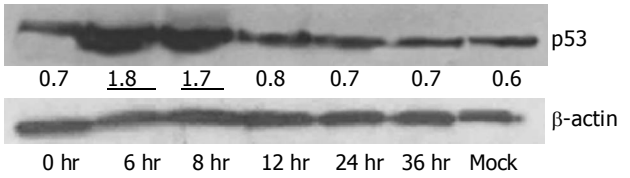

Figure 5 Western blotting analysis of p53 protein in HepG2 cells infected with Ad-TIP30. HepG2 cells were infected with Ad-TIP30. Harvested protein (50 ug/lane) was applied to 12% SDS-polyacrylamide electrophoresis. Proteins were transferred to PVDF film and probed with anti-serum specific for p53. p53 levels were quantified by densitometric analysis and normalized to β-actin. The data shown here were representative of three independent experiments with a similar result.

Expression of Bcl-2 family members after Ad-TIP30 infection

Expression of Bcl-2 family members was examined in three cell lines. Levels of Bax at 8-10 h after infection with Ad-TIP30 were 2-fold higher than those of Ad-GFP infected cells and mock in HepG2 cells, while there was no change in Hep3B and PLC/RPF/5 cells (Figure 6).

We examined Bcl-xl level in the three cell lines treated as previously. Its levels in HepG2, Hep3B and PLC/RPF/5 cells infected with AD-TIP30 were 2-fold to 1.5-fold lower than those infected with Ad-GFP (data not shown). Furthermore, in HepG2 cells, at 24-36 h after infection, Bax/Bcl-xl ratio reached the maximum of 2-fold higher than at other time points, with a requisite increase in p53 levels (Figure 7). In the mean time, a little decrease was found in Hep3B and PLC/RPF/5 cells at 36 h after infection.

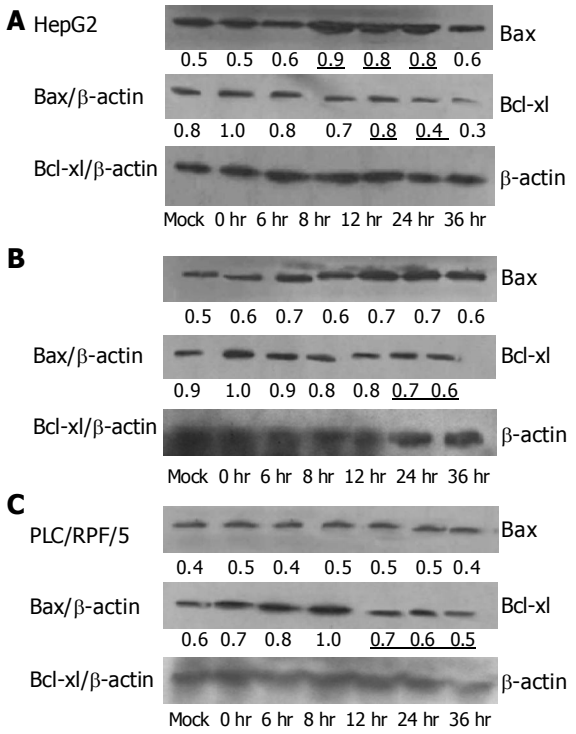

Figure 6 Expression of Bax and Bcl-xl after infection with Ad-TIP30 and mock as control in the three cell lines. Lysates were collected at 0, 6, 8, 12, 24, 36 h after infection. Ad-TIP30 infection resulted in increased Bax protein expression which was at its peak at 12-24 h after infection in HepG2 cells (Figure 6A), and decreased Bcl-xl protein levels in three cell lines (Figures 6A-C).

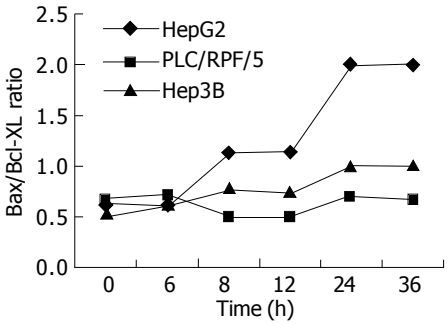

Figure 7 Infection of Ad-TIP30 with immunoblot analysis: densitometric analysis of the bands. The cells were infected with Ad-TIP30 and mock (no virus) as control in HepG2, Hep3B and PLC/RF/5 cells. The variation of Bax/Bcl-xl ratio in the three cell lines with time course was shown.

DISCUSSION

TIP30 is a novel Tat-cooperation protein that enhances human immunodeficiency virus-1 (HIV-1) by phosphorylating RNA polymerase II subunit. Recently, Xiao *et al*[1] and Baller *et al*[2] have shown that the 242- amino-acid-long- protein TIP30 plays an important role in suppression of metastasis of small cell lung carcinoma (SCLC) leading it to apoptosis.

We are in favor of connecting TIP30 with some genes as a preferential representative in apoptosis pathway. p53 gene and its related genes have been regarded as a model for the following reasons. P53 is a key factor in regulating apoptosis and shares one common down-regulator with TIP30: pig12[15]. The manner of p53 activation appears to be primarily controlled through phosphorylating its N-terminal for its stability. Sherr *et al*[16] and several other studies suggest that the major manner of evaluating its levels is at post-transcription. Xiao *et al*[17] demonstrated that TIP30 had a characteristic of phosphorylase kinase activity to trigger apoptosis.

Additionally, the pro-apoptotic activity of TIP30 by stresses such as chemical oxidants, growth factor deprivation, leads to the expression of a number of genes such as Bad and Siva, which are responsible for apoptosis[2]. Despite the fact that TIP30 is defined unambiguously as a tumor suppressor and a pro-apoptotic factor, the molecular mechanism by which TIP30 gene mediates apoptosis and which component is involved in TIP30 pathway remain largely unknown. Therefore, we employed *in vitro* analysis to reveal the apoptosis pathway in which TIP30 takes part.

p53 protein is a transcription factor that can inhibit cell cycle progression or induce apoptosis in response to stress or DNA damage, with a short life and a low expression level in normal cells[5]. Normally, the half-life of p53 is attributable to degradation mediated by Mdm2, which targets p53 for ubiquitin-dependent proteolysis[18]. Several stress-responsive kinases have been shown to phosphorylate p53 in a manner that could potentially inhibit Mdm2-mediated degradation. Avantaggiati *et al*[19] showed that DNA damage triggered accumulation and functional activation of p53 by converting the protein from a latent to an active form. Two proteins have been recently identified as potential regulators of p53 stability: one is kinase CHK2, which could inhibit Mdm2-mediated ubiquitination and proteolysis of p53[18]. Hemmatip *et al*[20] have shown that introduction of Ad-P14^{ARF} into U-20s osteosarcoma cells could efficiently induce apoptosis in p53 pathway, in turn upregulation of P14^{ARF} could mediate accumulation of p53 via sequestration of the p53-antagonist Mdm2 through the ubiquitin /proteasome pathway. Thus, P14^{ARF} relieves the Mdm2-mediated degradation of p53, thereby prolonging the

half-life of p53 protein[21]. In human breast cancer cells-MCF-7, Ad-P14^{ARF} has cytotoxicity to MCF-7 cells (p53 wild type), resulting in a considerable increase of p53. Jiang *et al*[13] demonstrated that staurosprine, quinacrine and ultraviolet irradiation were all capable of triggering apoptosis of HepG2 cells by affecting the expression levels of p53. A cytotoxic agent of rodent liver, 7H-dibenzocc carbazole (DBC) could increase p53 protein levels followed by apoptotic cell death[22]. In our studies, when HepG2 cells were infected with Ad-TIP30, to our expectation, levels of wide p53 were increased in a time-dependent manner with an asynchronous apoptosis, indicating that apoptosis induced by TIP30 is attributable to the accumulation of p53, which supports the hypothesis that TIP30 is involved in apoptosis pathway partly by cooperating with p53 protein.

It is well known that one mechanism by which p53 is stabilized within infected cells is that p53 is substantially modified post-translationally via serine targeted phosphorlation at both the N-terminus and C-terminus as well as acetylation at lysine residues in C-terminus[23], implicating that p53 appears to be optimal in post-translation level under a stress response. In addition, the primary consequence of this induction is cell cycle arrest or apoptotic cell death. Xiao *et al*[17] found that TIP30 had an intrinsic kinase activity in phosphorylating the heptapeptide repeats of the C-terminal domain (CTD) of the largest subunit of RNA polymerase II in concurrence with the ability to trigger SCLC cells to apoptosis. We also speculate that TIP30 might phosphorylate the p53 C- or N- terminus in advance to enhance the p53-dependent pathway. Nevertheless, verification of the hypothesis requires further experiment. Interestingly, in Hep3B and PLC/RPF/5 cells where p53 protein is absent or mutational, introduction of TIP30 also predispose cells to apoptosis at a less extent than in HepG2 cells, implicating that TIP30 might trigger apoptosis through other pathways that occur independently of the p53/Bax pathway. Further investigation might be essential and helpful.

In p53/mitochondrial pathway, members of Bcl-2 family are critical regulators of the apoptotic pathway[24]. Bcl-xl, an anti-apoptotic member of Bcl-2 family, inhibits the release of cytochrome *C* from mitochondria whereas Bax, a pro-apoptotic member of Bcl-2 family, has been shown to stimulate release of cytochrome *C* from mitochondria thereby enhancing apoptotic response[25].

In the present study, we evaluated the role of Bax and Bcl-xl in Ad-TIP30 mediated apoptosis. Early studies have shown that Bax gene plays an important role in the course of carcinogenesis in stomach, colorectum and endometrium in humans[26]. Furthermore, the Bax gene promoter is highly p53-responsive and its expression is upregulated by p53[27].

Pearson and Francis[28] have shown that adenovirus-mediated over-expression of p53 in lung cancer cell lines H1299, H358 and HK322 simultaneously upregulates Bax protein levels 18 to 36 h after introduction. In Tu-138 and Tu-167 cells, after infection with Ad5CMV-p53[29], Bax levels were elevated 2-to 6-fold higher than controls, demonstrating that influence upon Bax is caused by asynchronous activation of p53. Mohiuddin *et al*[30] reported that in hepablastoma cells multiple stimuli such as ultraviolet and carcumin could not change Bax levels. On the contrary, in this case, exogenous TIP30 and endogenous p53 expression in HepG2 cells led to elevation of Bax level at 18-24 h after infection whereas no change was found in Hep3B cells with absence of p53, indicating that it is alternatively possible that the Bax levels are not influenced directly by TIP30, but rather through p53 involvement when apoptotic cell death is initiated. In support of this model, more observations have shown that in many other cancer cell lines, a high level of Bax follows the activation and stabilization of p53[31].

Previous reports have shown that alternation in the ratio of proapoptotic to anti-apoptotic members of the Bcl-2 family, rather than the absolute expression level of any single Bcl-2 family member, determines apoptotic sensitivity[32]. As to hepatoblastoma cells[33], the ratio of Bax to Bcl-xl protein plays a major role in sensitivity to apoptotic stimuli, because the expression of Bcl-2 is uncommon in hepatoblastoma cells according to several researches. Ectopic expression of transcriptionally active p53 alone is not sufficient for the activation of apoptosis in p53-null Hep3B cells, except when endogenous Bcl-xl is simultaneously inhibited by anti-sense oligonucleotide in these cells[34-36]. In our studies, immunoblot analysis revealed decreased Bcl-xl levels and increased Bax levels in HepG2 cells after Ad-TIP30 infection. In addition, in Hep3B and PLC/RPF/5 cells, Bcl-xl decrease was observed at a less extent than in HepG2 cells, while there was no significant change in Bax levels, indicating that TIP30 might regulate the Bax and Bcl-xl ratio in a p53 dependent and independent manner. Therefore, our studies clearly suggest that shift in the ratio of proapoptotic factor (Bax) to anti-apoptotic factor (Bcl-xl) in favor of proapoptotic factor (Bax) is an important factor for determining the response toward Ad-TIP30 triggering apoptosis.

What are the mechanisms by which TIP30 causes apoptosis in hepotablastoma cells? We suggest that wild type p53 upregulates Bax expression with concomitant down-regualtion of Bcl-xl is the consequence of p53 accumulation due to exogenous TI*P*30 expression. Thus, TIP30 gene may serve as a good sample for heptoblastoma gene therapy, not only because it may kill cancer cells directly, but also because it may be regarded as a useful mediator in elevating apoptosis-related gene expression in its apoptotic pathway.

ACKNOWLEDGEMENTS

We thank Dr. Hua Xiao for generously providing a cDNA encoding full-length human TIP30.

REFERENCES

1 **Xiao H**, Tao Y, Greenblatt J, Roeder RG. A cofactor, TIP30, specifically enhances HIV-1 Tat-activated transcription. *Proc Natl Acad Sci USA* 1998; **95:** 2146-2151
2 **Baker ME**, Yan L, Pear MR. Three-dimensional model of human TIP30, a coactivator for HIV-1 Tat-activated transcription, and CC3, a protein associated with metastasis suppression. *Cell Mol Life Sci* 2000; **57:** 851-858
3 **Chene P**. Inhibition of the p53-MDM2 interaction: targeting a protein-protein interface. *Mol Cancer Res* 2004; **2:** 20-28
4 **Batinac T,** Gruber F, Lipozencic J, Zamolo-Koncar G, Stasic A, Brajac I. Protein p53-structure, function, and possible therapeutic implications. *Acta Dermatovenerol Croat* 2003; **11:** 225-230
5 **Mirza A**, Wu Q, Wang L, McClanahan T, Bishop WR, Gheyas F, Ding W, Hutchins B, Hockenberry T, Kirschmeier P, Greene JR, Liu S. Global transcriptional program of p53 target genes during the process of apoptosis and cell cycle progression. *Oncogene* 2003; **22:** 3645-3654
6 **Courageot MP**, Catteau A, Despres P. Mechanisms of dengue virus-induced cell death. *Adv Virus Res* 2003; **60:** 157-186
7 **Hayward RL**, Macpherson JS, Cummings J, Monia BP, Smyth JF, Jodrell DI. Enhanced oxaliplatin-induced apoptosis following antisense Bcl-xl down-regulation is p53 and Bax dependent: Genetic evidence for specificity of the antisense effect. *Mol Cancer Ther* 2004; **3:** 169-178
8 **Chipuk JE**, Kuwana T, Bouchier-Hayes L, Droin NM, Newmeyer DD, Schuler M, Green DR. Direct activation of Bax by p53 mediates mitochondrial membrane permeabilization and apoptosis. *Science* 2004; **303:** 1010-1014
9 **Groeger AM**, Esposito V, De Luca A, Cassandro R, Tonini G, Ambrogi V, Baldi F, Goldfarb R, Mineo TC, Baldi A, Wolner E.

Prognostic value of immunohistochemical expression of p53, bax, Bcl-2 and Bcl-xL in resected non-small-cell lung cancers. *Histopathology* 2004; **44:** 54-63

10 **Feng WY**, Liu FT, Patwari Y, Agrawal SG, Newland AC, Jia L. BH3-domain mimetic compound BH3I-2' induces rapid damage to the inner mitochondrial membrane prior to the cytochrome c release from mitochondria. *Br J Haematol* 2003; **121:** 332-340

11 **Moreau C**, Cartron PF, Hunt A, Meflah K, Green DR, Evan G, Vallette FM, Juin P. Minimal BH3 peptides promote cell death by antagonizing anti-apoptotic proteins. *J Biol Chem* 2003; **278:** 19426-19435

12 **Dimitrakakis C**, Konstadoulakis M, Messaris E, Kymionis G, Karayannis M, Panoussopoulos D, Michalas S, Androulakis G. Molecular markers in breast cancer: can we use c-erbB-2, p53, bcl-2 and bax gene expression as prognostic factors? *Breast* 2002; **11:** 279-285

13 **Jiang MC**, Yen HF. Differential regulation of p53, c-myc,Bcl-2 and Bax protein expression during apoptosis induced by wildly divergent stimuli in human hepatoblastoma cells. *Oncogene* 1996; **22:** 609

14 **Shi M**, Wang FS, Wu ZZ. Synergetic anticancer effect of combined quercetin and recombinant adenoviral vector expressing human wild-type p53, GM-CSF and B7-1 genes on hepatocellular carcinoma cells *in vitro*. *World J Gastroenterol* 2003; **9**: 73-78

15 **Lee SH**, DeJong J. Microsomal GST-I: genomic organization, expression, and alternative splicing of the human gene. *Biochim Biophys Acta* 1999; **1446:** 389-396

16 **Sherr CJ**. Tumor surveillance via the ARF-p53 pathway. *Genes Dev* 1998; **12:** 2984-2991

17 **Xiao H**, Palhan V, Yang Y, Roeder RG. TIP30 has an intrinsic kinase activity required for up-regulation of a subset of apoptotic genes. *EMBO J* 2000; **19:** 956-963

18 **Mocanu MM**, Yellon DM. p53 down-regulation: a new molecular mechanism involved in ischaemic preconditioning. *FEBS Lett* 2003; **555:** 302-306

19 **Avantaggiati ML**, Ogryzko V, Gardner K, Giordano A, Levine AS, Kelly K. Recruitment of p300/CBP in p53-dependent signal pathways. *Cell* 1997; **89:** 1175-1184

20 **Hemmati PG**, Gillissen B**,** von Haefen C, Wendt J, Starck L, Guner D, Dorken B, Daniel PT. Adenovirus-mediated overexpression of p14(ARF) induces p53 and Bax-independent apoptosis. *Oncogene* 2002; **21:** 3149-3161

21 **Sturzenhofecker B**, Schlott T, Quentin T, Kube D, Jung W, Trumper L. Abundant expression of spliced HDM2 in Hodgkin lymphoma cells does not interfere with p14(ARF) and p53 binding. *Leuk Lymphoma* 2003; **44:** 1587-1596

22 **Chen YN**, Chen JC, Yin SC, Wang GS, Tsauer W, Hsu SF, Hsu SL. Effector mechanisms of norcantharidin-induced mitotic arrest and apoptosis in human hepatoma cells. *Int J Cancer* 2002; **100:** 158-165

23 **Deng X**, Kim M, Vandier D, Jung YJ, Rikiyama T, Sgagias MK, Goldsmith M, Cowan KH. Recombinant adenovirus-mediated p14(ARF) overexpression sensitizes human breast cancer cells to cisplatin. *Biochem Biophys Res Commun* 2002; **296:** 792-798

24 **Kasai H**, Yamamoto K, Koseki T, Yokota M, Nishihara T. Involvement of caspase activation through release of cytochrome c from mitochondria in apoptotic cell death of macrophages infected with Actinobacillus actinomycetemcomitans. *FEMS Microbiol Lett* 2004; **233:** 29-35

25 **Tsujimoto Y**. Cell death regulation by the Bcl-2 protein family in the mitochondria. *J Cell Physiol* 2003; **195:** 158-167

26 **Scorrano L**, Korsmeyer SJ. Mechanisms of cytochrome c release by proapoptotic BCL-2 family members. *Biochem Biophys Res Commun* 2003; **304:** 437-444

27 **Ohtsuka T**, Ryu H, Minamishima YA, Macip S, Sagara J, Nakayama KI, Aaronson SA, Lee SW. ASC is a Bax adaptor and regulates the p53-Bax mitochondrial apoptosis pathway. *Nat Cell Biol* 2004; **6:** 121-128

28 **Pearson AS**, Spitz FR, Swisher SG, Kataoka M, Sarkiss MG, Meyn RE, McDonnell TJ, Cristiano RJ, Roth JA. Upregulation of the proapoptotic mediators Bax and Bak after adenovirus-mediated p53 gene transfer in lung cancer cells. *Clin Cancer Res* 2000; **6:** 887-890

29 **Frederick MJ,** Holton PR, Hudson M, Wang M, Clayman GL. Expression of apoptosis-related genes in human head and neck squamous cell carcinomas undergoing p53-mediated programmed cell death. *Clin Cancer Res* 1999; **5:** 361-369

30 **Mohiuddin I**, Cao X, Fang B, Nishizaki M, Smythe WR. Significant augmentation of pro-apoptotic gene therapy by pharmacologic bcl-xl down-regulation in mesothelioma. *Cancer Gene Ther* 2001; **8:** 547-554

31 **Thornborrow EC**, Manfredi JJ. The tumor suppressor protein p53 requires a cofactor to activate transcriptionally the human BAX promoter. *J Biol Chem* 2001; **276:** 15598-15608

32 **Srivastava M**, Ahmad N, Gupta S, Mukhtar H. Involvement of Bcl-2 and Bax in photodynamic therapy-mediated apoptosis. Antisense Bcl-2 oligonucleotide sensitizes RIF 1 cells to photodynamic therapy apoptosis. *J Biol Chem* 2001; **276:** 15481-15488

33 **Ahn SG**, Kim HS, Jeong SW, Kim BE, Rhim H, Shim JY, Kim JW, Lee JH, Kim IK. Sox-4 is a positive regulator of Hep3B and HepG2 cells' apoptosis induced by prostaglandin (PG) A(2) and delta (12)-PGJ(2). *Exp Mol Med* 2002; **34:** 243-249

34 **Takehara T,** Liu X, Fujimoto J, Friedman SL, Takahashi H. Expression and role of Bcl-xL in human hepatocellular carcinomas. *Hepatology* 2001; **34:** 55-61

35 **Bradford MM**. A rapid and sensitive method for the quantitation of microgram quantities of protein utilizing the principle of protein-dye binding. *Anal Biochem* 1976; **72:** 248-254

36 **Chun E**, Lee KY. Bcl-2 and Bcl-xL are important for the induction of paclitaxel resistance in human hepatocellular carcinoma cells. *Biochem Biophys Res Commun* 2004; **315:** 771-779

Assistant Editor Guo SY **Edited by** Zhang JZ and Wang XL

PO Box 2345, Beijing 100023, China
Fax: +86-10-85381893
E-mail: wjg@wjgnet.com www.wjgnet.com

ELSEVIER

World J Gastroenterol 2005;11(2):228-231
World Journal of Gastroenterology ISSN 1007-9327

• LIVER CANCER •

Expression of fragile histidine triad in primary hepatocellular carcinoma and its relation with cell proliferation and apoptosis

Ke-Jun Nan, Zhi-Ping Ruan, Zhao Jing, Hai-Xia Qin, Hong-Yan Wang, Hui Guo, Rui Xu

Ke-Jun Nan, Zhi-Ping Ruan, Zhao Jing, Hai-Xia Qin, Hui Guo, Rui Xu, Department of Oncology, First Hospital of Xi'an Jiaotong University, Xi'an 710061, Shaanxi Province, China
Hong-Yan Wang, Department of Pathology, First Hospital of Xi'an Jiaotong University, Xi'an 710061, Shaanxi Province, China
Correspondence to: Dr. Ke-Jun Nan, Department of Oncology, First Hospital of Xi'an Jiaotong University, 1 Jiankang Xilu, Xi'an 710061, Shaanxi Province, China. zoporun@hotmail.com
Telephone: +86-29-85324086 **Fax:** +86-29-85324086
Received: 2004-02-02 **Accepted:** 2004-04-07

Abstract

AIM: To evaluate the expression of fragile histidine triad (FHIT) gene protein, product of a candidate tumor suppressor, and to investigate the relationship between FHIT, cell apoptosis and proliferation, and pathological features of primary hepatocellular carcinoma (HCC).

METHODS: Forty-seven HCC and ten normal liver specimens were collected during surgical operation between 2001 and 2003. FHIT and proliferating cell nuclear antigen (PCNA) expression were detected by immunohistochemistry, and apoptotic level was evaluated by terminal deoxynucleotidyl transferase-mediated dUTP nick end labeling (TUNEL) assay on the tissue sections.

RESULTS: All normal liver tissues showed a strong expression of FHIT, whereas 28 of 47 (59.6%) carcinomas showed a significant loss or absence of FHIT expression ($P = 0.001$). The proportion of reduced FHIT expression in those carcinomas at stages III-IV (70.6%) and in those with extrahepatic metastasis (86.7%) showed an increasing trend compared with those at stages I-II (30.8%, $P = 0.013$) and those without metastasis (46.9%, $P = 0.010$) respectively. Apoptotic incidence in advanced TNM stage carcinoma and those with positive FHIT expression was higher than that in early stage carcinoma ($P = 0.030$) and in those with negative FHIT expression ($P = 0.044$) respectively. The proliferating potential of hepatocellular carcinoma was associated with FHIT expression ($P = 0.016$) and the aggressive feature ($P = 0.019$). Kaplan-Meier analysis demonstrated that the survival time of these 47 patients correlated with TNM stage, FHIT expression and metastasis.

CONCLUSION: There is marked loss or absence of FHIT expression, as well as abnormal apoptosis-proliferation balance in HCC. FHIT may play an important role in carcinogenesis and development of HCC.

Key words: Hepatocellular carcinoma; Fragile histidine triad protein; Cell proliferation; Apoptosis

Nan KJ, Ruan ZP, Jing Z, Qin HX, Wang HY, Guo H, Xu R. Expression of fragile histidine triad in primary hepatocellular carcinoma and its relation with cell proliferation and apoptosis. *World J Gastroenterol* 2005; 11(2): 228-231
http://www.wjgnet.com/1007-9327/11/228.asp

INTRODUCTION

Fragile histidine triad gene has been cloned and is located on 3p14.2[1], which encompasses the most common human fragile site, FRA3B. Alterations of FHIT and loss of its product have been found frequently in several human tumors and tumor-derived cell lines associated with environmental carcinogens. Disturbance of cell number regulation is one of the characteristics of malignant tumors, which could lead to tumor cell proliferation out of control. We have known that a variety of oncogenes, tumor suppressor genes and some modifiers are involved in the regulation mechanism[2]. Human hepatocellular carcinoma is a familiar lethal cancer which is closely related to some carcinogens such as hepatitis B virus infection, dietary aflatoxin and alcohol consumption. It is imperative to speculate on whether FHIT, as a putative tumor suppressor gene, plays a role in the development of hepatocellular carcinoma by participating in the process of apoptosis or cell cycle. From this study, the indices of apoptosis and cell proliferation showed a certain association with the aberrant FHIT expression in hepatocellular carcinoma, which may elucidate one aspect of carcinogenesis of malignant tumors.

MATERIALS AND METHODS

Materials

Forty-seven liver cancer specimens and ten normal liver specimens as controls were obtained from surgical resections in the First Hospital of Xi'an Jiaotong University during 2001 to 2003. The patients included 38 men and 9 women with a mean age of 48.62±10.99 years (range 29-77 years). The pathological types of all specimens were confirmed tobe hepatocellular carcinoma by pathologists in Pathology Department of the First Hospital of Xi'an Jiaotong University. Of these patients, 39 were at grades I and II, 8 at grade III according to Edmondson grading and local invasion or extrahepatic metastasis was observed in 15; and 13 were at stages I-II, 34 at stages III-IV according to the pTNM criteria of UICC. The follow-up for all cases was terminated in April of 2004.

Methods

All surgical specimens were fixed in 10% formaldehyde, embedded in paraffin and cut into 4-μm thick sections. One section of each specimen was stained with H&E and used for histological identification, and the rest were used for immunostaining.

Immunohistochemical analysis for FHIT and PCNA

Slides were deparaffinized in xylene twice for 10 min, rehydrated through graded ethanol to distilled water, incubated for 15 min with 3% hydrogen peroxidase to inhibit endogenous peroxidase activity, and then heated in 0.01 mol/L citrate buffer (pH 6.0) in a microwave oven for 5 min at 100 ℃ for antigen retrieval. After cooled down at room temperature for 30 min, the sections were incubated for 15 min in a blocking solution containing 10%

normal goat serum in PBS [0.01 mol/L phosphate (pH 7.4)] and then incubated for 1 h at 37 ℃ in a humidified chamber with rabbit polyclonal antibody to human FHIT (Zymed Laboratories Inc., South San Francisco, CA) at a dilution of 1:50, followed by incubation for 30 min with goat anti-rabbit IgG conjugated to horseradish peroxidase (Santa Cruz Biotechnology). 3,3'-diaminobenzidine was used as the chromogen. Slides were counterstained for 3 min with hematoxylin solution, then dehydrated and coverslipped. Normal liver tissue was used as a positive control, whereas the primary antibody was replaced by PBS for a negative control. PCNA was detected by mouse monoclonal antibody to human PCNA (1:50, Santa Cruz Biotechnology).

Apoptosis detection in situ with TUNEL

Paraffin-embedded sections on polylysine-coated slides were deparaffinized and rehydrated as described in immunohistochemistry method and then incubated for 15 min with 40 mg/L trypsin at 37 ℃, rinsed in PBS and incubated for 1 h at 37 ℃ with TUNEL reaction mixture (buffer solution mixed with terminal deoxynucleotidyl transferase and nucleotide labeled solution; Roche, Germany), rinsed again in PBS and incubated for 30 min at 37 ℃ with converter-AP. 5-bromo-4-chloro-3-indalylphosphate/nitro blue tetrazolium (BCIP/NBT) was used as the chromogen. Slides were counterstained for 5 min with nuclear fast red solution, then dehydrated and coverslipped.

Evaluation of scores

Cells filled with yellow or brown granules in cytoplasm were considered as positive immunostained cells. Both the extent and intensity of immunostaining were considered when FHIT protein expression of a section was scored according to Hao *et al*[3]. The extent of positivity was scored as follows: 0, <5%; 1, 5-25%; 2, 25-50%; 3, 50-75%; and 4, >75% of hepatocytes in respective lesions. The intensity was scored as follows: 0, negative; 1, weak; 2, moderate; and 3, as strong as in normal hepatocytes. The final score was obtained by multiplying the extent of positivity and intensity scores in the range of 0-12. Scores 8-12 were defined as strong staining, scores 0-6 as markedly reduced or lost expression.

PCNA positively immunostained cells were filled with brown granules in nuclei. The apoptotic cells were stained blue in nuclei, whereas the normal nuclei were stained pink. Regardless of the extent or intensity of the PCNA and apoptosis staining, the positive cells were observed and calculated under a light microscope in 5 high power fields (×400). Proliferation index (PI) and apoptosis index (AI), expressed as the ratio of positively stained cells to total cells of the fields, were used to evaluate the proliferation and apoptosis features respectively.

Statistical analysis

Pearson chi-square test and Fisher's exact test (two sided) for trends in proportions were used to assess the association between FHIT expression and pathological indices. Student's *t*-test was adopted to determine the difference between two sample means. Survival time was analyzed by Kaplan-Meier method (SPSS 11.0 for windows). $P<0.05$ was considered statistically significant.

RESULTS

FHIT expression in normal tissues and HCC

All the 10 normal liver tissues and para-neoplastic tissues showed a strong FHIT expression in the cytoplasm of hepatocytes (Figure 1A). Some lymphocytes and fibroblasts were positively stained, also. FHIT was expressed in 19 carcinomas as strongly as or more strongly than in normal, whereas it was expressed negatively in 28 of 47 (59.6%) carcinomas (Figure 1B). The absence of FHIT expression in carcinoma was significant ($\chi^2=11.709$, $P=0.001$).

Relationship between FHIT expression and clinicopathological indices

The proportion of reduced FHIT expression in carcinomas at stages III-IV was significantly higher (24/34) than that at stages I-II (4/13) ($P=0.013$). This proportion in carcinomas with extrahepatic metastasis (13/15) was higher than that in those without metastasis (15/32). No evidence indicated the relation between FHIT expression and other clinicopathological features such as age, sex, histological grade and tumor size (Table 1).

Table 1 Relationship between FHIT expression and clinicopathological indices of HCC

	n	FHIT score		*P*
		-	+	
Age (yr)				
≤45	18	10	8	0.658
>45	29	18	11	
Sex				
Male	38	21	18	0.278
Female	9	7	2	
Histological grade				
I-II	39	21	18	0.119
III	8	7	1	
TNM stage				
I-II	13	4	9	0.013
III-IV	34	24	10	
Tumor size (diameter)				
<50 mm	19	12	7	0.680
≥50 mm	28	16	12	
Extrahepatic metastasis				
Positive	15	13	2	0.010
Negative	32	15	17	

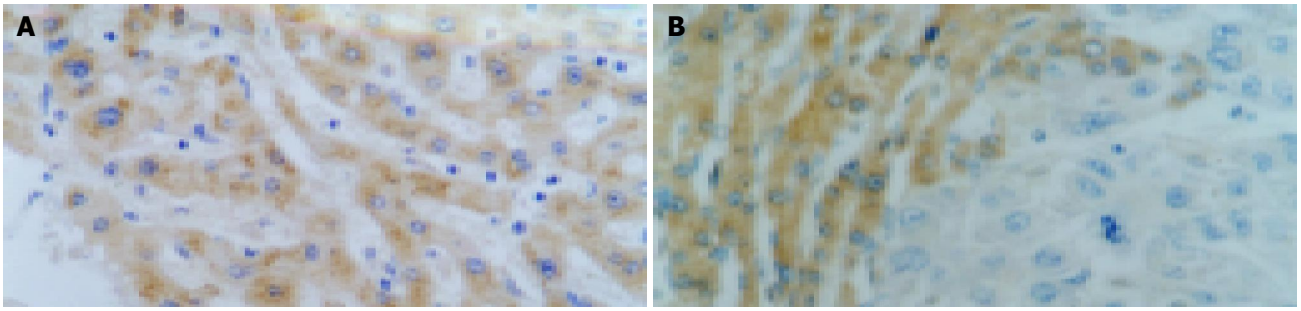

Figure 1 FHIT expression in normal tissues and HCC. A: Yellow granules in normal liver tissues, and para-neoplastic tissues; B: non-stained cytoplasm of tumor cells.

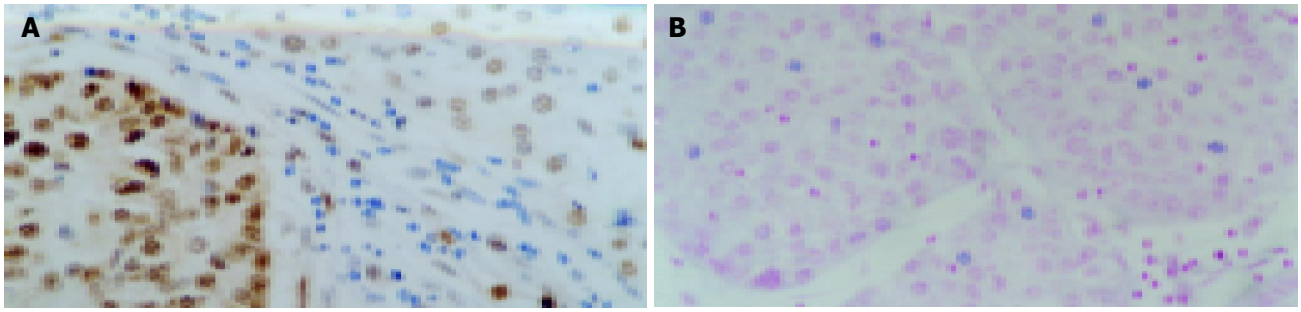

Figure 2 Expression of PCNA in normal and cancer tissues. A: Positive PCNA expression manifested brown granules in nuclei. B: nuclei of apoptic cells were stained blue but normal nuclei were stained pink.

Table 2 Relationship between PI, AI and clinicopathological indices (mean±SD)

	N	AI (%)	*P* value	PI (%)	*P* value
FHIT expression					
Positive	19	9.42±2.85	0.044	28.47±4.22	0.016
Negative	28	8.07±1.63		31.61±4.24	
Histological grade					
I-II	39	8.87±2.38	0.091	30.46±4.46	0.686
III	8	7.38±1.19		29.75±4.74	
TNM stage					
I-II	13	7.46±2.30	0.030	28.85±3.85	0.158
III-IV	34	9.06±2.15		30.91±4.60	
Tumor size (diameter)					
<50 mm	19	8.11±2.03	0.208	29.79±4.85	0.492
⩾50 mm	28	8.96±2.41		30.71±4.23	
Extrahepatic metastasis					
Positive	15	9.00±1.89	0.436	32.53±3.93	0.019
Negative	32	8.44±2.45		29.31±4.38	

Proliferation and apoptosis features in HCC

PCNA was localized in nuclei. Positive PCNA expression manifested brown granules in nuclei (Figure 2A). Nuclei of apoptotic cells were stained blue but normal nuclei were stained pink (Figure 2B).

Table 2 summarizes the relationship between AI, PI and clinicopathological indices. AI showed a similar association with TNM stage and FHIT expression, i.e., those HCCs at stages III-IV and those with positive FHIT expression showed a higher AI compared with those at stages I-II and those with negative FHIT expression ($P<0.05$) respectively. PI showed a relationship with FHIT expression and metastasis ($P<0.05$).

Survival analysis

The survival time of the forty-seven patients undergoing surgical resection varied from 1 to 34 mo. Patients with positive FHIT expression, or those at stages I-II, or those without metastasis had a longer survival time as shown by Kaplan-Meier analysis (data not shown).

DISCUSSION

Unregulation of cell proliferation homeostasis results in unlimited proliferation of malignant cells, which would enlarge the tumor size and cause cancer. However, its opposite antagonistic way, apoptosis, determines the cell death. Apoptosis is an efficacious approach to protect human beings from adverse carcinogens which may induce mutation or canceration. PCNA is an auxiliary protein for DNA polymerase delta, which could perform an essential function in DNA replication and repair process[4]. The amount of PCNA mRNA varies with DNA synthesis cycle[5], and reflects the proliferating activity of cancer cells. Thus, it has been regarded as a proliferation marker for cancer cells[6,7]. The PCNA labeling index is one useful marker for evaluating the malignant feature of tumors, and for predicting recurrence and the prognosis of patients[8].

Apoptosis with necrosis, plays an important role in the cell life including cell growth, differentiation and proliferation[9]. It is a regulation mechanism to maintain the homeostasis of tissues. Malignant tumor tissues lose this regulation and obtain infinite proliferating potential. There is a controversy concerning the relationship between proliferation and apoptosis in cancers[10-12]. Our study showed a significant association between PI, AI and some clinicopathological indices of HCC, such as TNM stage and extrahepatic metastasis.

FHIT gene spans the most active common fragile site in the human genome, FRA3B, which is susceptible to inactivation by environmental carcinogenic factors[13], such as hepatitis B virus infection, dietary aflatoxin and alcohol consumption[14]. Aberrant FHIT expression has been detected in other tumors, including lung[15], esophageal[16], stomach[17], colorectal[18], cervical[19], and prostate[20] carcinomas. Our research demonstrated a high proportion (59.6%) of reduced FHIT expression in HCC, compared with positive expression in all 10 normal liver tissues, as reported previously[14]. Moreover, the aberrant FHIT expression was correlated with TNM stage and extrahepatic metastasis of HCC. The patients with positive FHIT expression showed a longer survival time than those with negative expression. Some findings indicate that loss of FHIT expression might be an early event in the development of human carcinoma[16,21]. Therefore, detection of FHIT expression in malignant tissues by immunohistochemistry may provide some important diagnostic and prognostic information[22].

FHIT gene consists of 10 exons and encodes FHIT protein (M_r 16 800), which consists of 147 amino acids. FHIT protein is a member of histidine triad superfamily and a diadenosine 5', 5'-P1, P3-triphosphate (Ap3A) asymmetrical hydrolase which cleaves Ap3A into adenosine 5'-diphosphate and AMP[23]. Siprashvili *et al*[24] designed a structure similar to FHIT, in which

the middle histidine in histidine triad was replaced by asparagine. This artificial product significantly lost its enzymatic activity but still maintained tumor suppressor function. It has been found that hydrolysis for Ap3A is not required for tumor suppression of FHIT. Researches on the tumor suppression mechanism of FHIT indicate the active suppressor of FHIT might function in the form of FHIT-substrate complex[25,26]. Our study showed a higher AI but a lower PI in carcinomas with positive FHIT expression, suggesting that FHIT might play a role in the regulation of cell proliferation and apoptosis. The conceivable mechanism is that the FHIT-substrate binding complex participates in signal transduction and induces accumulation of cells at S to G2-M phase, and then these arrested cells are cleaned out in manner of apoptosis. This hypothesis is supported by some molecular experiments[27,28]. Furthermore, some more detailed researches have revealed that FHIT-induced apoptosis is practiced in a p53-independent apoptotic pathway[29,30]. This may provide a new method and opportunity in gene therapy for malignant tumors.

Carcinogenesis of HCC is a multi-sequential process involving various oncogenes and tumor suppression genes. Inactivation of FHIT may play a role in the development and progression of HCC. FHIT as a valuable target in gene therapy has a bright future.

REFERENCES

1 **Ohta M,** Inoue H, Cotticelli MG, Kastury K, Baffa R, Palazzo J, Siprashvili Z, Mori M, McCue P, Druck T, Croce CM, Huebner K. The FHIT gene, spanning the chromosome 3p14.2 fragile site and renal carcinoma-associated t(3;8) breakpoint, is abnormal in digestive tract cancers. *Cell* 1996; **84**: 587-597

2 **Qin LX,** Tang ZY. The prognostic molecular markers in hepatocellular carcinoma. *World J Gastroenterol* 2002; **8**: 385-392

3 **Hao XP,** Willis JE, Pretlow TG, Rao JS, MacLennan GT, Talbot IC, Pretlow TP. Loss of fragile histidine triad expression in colorectal carcinomas and premalignant lesions. *Cancer Res* 2000; **60**: 18-21

4 **Morris GF,** Bischoff JR, Mathews MB. Transcriptional activation of the human proliferating-cell nuclear antigen promoter by p53. *Proc Natl Acad Sci USA* 1996; **93**: 895-899

5 **Morris GF,** Mathews MB. Regulation of proliferating cell nuclear antigen during the cell cycle. *J Biol Chem* 1989; **264**: 13856-13864

6 **Hall PA,** Levison DA, Woods AL, Yu CC, Kellock DB, Watkins JA, Barnes DM, Gillett CE, Camplejohn R, Dover R. Proliferating cell nuclear antigen (PCNA) immunolocalization in paraffin sections: an index of cell proliferation with evidence of deregulated expression in some neoplasms. *J Pathol* 1990; **162**: 285-294

7 **Weber JC,** Nakano H, Bachellier P, Oussoultzoglou E, Inoue K, Shimura H, Wolf P, Chenard-Neu MP, Jaeck D. Is a proliferation index of cancer cells a reliable prognostic factor after hepatectomy in patients with colorectal liver metastases? *Am J Surg* 2001; **182**: 81-88

8 **al-Sheneber IF,** Shibata HR, Sampalis J, Jothy S. Prognostic significance of proliferating cell nuclear antigen expression in colorectal cancer. *Cancer* 1993; **71**: 1954-1959

9 **Kerr JF.** History of the events leading to the formulation of the apoptosis concept. *Toxicology* 2002; **181-182**: 471-474

10 **Park YN,** Chae KJ, Kim YB, Park C, Theise N. Apoptosis and proliferation in hepatocarcinogenesis related to cirrhosis. *Cancer* 2001; **92**: 2733-2738

11 **Hino N,** Higashi T, Nouso K, Nakatsukasa H, Tsuji T. Apoptosis and proliferation of human hepatocellular carcinoma. *Liver* 1996; **16**: 123-129

12 **Paiva C,** Oshima CT, Lanzoni VP, Forones NM. Apoptosis, PCNA and p53 in hepatocellular carcinoma. *Hepatogastroenterology* 2002; **49**: 1058-1061

13 **Nelson HH,** Wiencke JK, Gunn L, Wain JC, Christiani DC, Kelsey KT. Chromosome 3p14 alterations in lung cancer: evidence that FHIT exon deletion is a target of tobacco carcinogens and asbestos. *Cancer Res* 1998; **58**: 1804-1807

14 **Yuan BZ,** Keck-Waggoner C, Zimonjic DB, Thorgeirsson SS, Popescu NC. Alterations of the FHIT gene in human hepatocellular carcinoma. *Cancer Res* 2000; **60**: 1049-1053

15 **Mascaux C,** Martin B, Verdebout JM, Meert AP, Ninane V, Sculier JP. Fragile histidine triad protein expression in nonsmall cell lung cancer and correlation with Ki-67 and with p53. *Eur Respir J* 2003; **21**: 753-758

16 **Mori M,** Mimori K, Shiraishi T, Alder H, Inoue H, Tanaka Y, Sugimachi K, Huebner K, Croce CM. Altered expression of Fhit in carcinoma and precarcinomatous lesions of the esophagus. *Cancer Res* 2000; **60**: 1177-1182

17 **Rocco A,** Schandl L, Chen J, Wang H, Tulassay Z, McNamara D, Malfertheiner P, Ebert MP. Loss of FHIT protein expression correlates with disease progression and poor differentiation in gastric cancer. *J Cancer Res Clin Oncol* 2003; **129**: 84-88

18 **Andachi H,** Yashima K, Koda M, Kawaguchi K, Kitamura A, Hosoda A, Kishimoto Y, Shiota G, Ito H, Makino M, Kaibara N, Kawasaki H, Murawaki Y. Reduced Fhit expression is associated with mismatch repair deficiency in human advanced colorectal carcinoma. *Br J Cancer* 2002; **87**: 441-445

19 **Takizawa S,** Nakagawa S, Nakagawa K, Yasugi T, Fujii T, Kugu K, Yano T, Yoshikawa H, Taketani Y. Abnormal Fhit expression is an independent poor prognostic factor for cervical cancer. *Br J Cancer* 2003; **88**: 1213-1216

20 **Fouts RL,** Sandusky GE, Zhang S, Eckert GJ, Koch MO, Ulbright TM, Eble JN, Cheng L. Down-regulation of fragile histidine triad expression in prostate carcinoma. *Cancer* 2003; **97**: 1447-1452

21 **Skopelitou AS,** Mitselou A, Katsanos KH, Alexopoulou V, Tsianos EV. Immunohistochemical expression of Fhit protein in *Helicobacter pylori* related chronic gastritis, gastric precancerous lesions and gastric carcinoma: correlation with conventional clinicopathologic parameters. *Eur J Gastroenterol Hepatol* 2003; **15**: 515-523

22 **Croce CM,** Sozzi G, Huebner K. Role of FHIT in human cancer. *J Clin Oncol* 1999; **17**: 1618-1624

23 **Barnes LD,** Garrison PN, Siprashvili Z, Guranowski A, Robinson AK, Ingram SW, Croce CM, Ohta M, Huebner K. Fhit, a putative tumor suppressor in humans, is a dinucleoside 5′, 5‴-P1, P3-triphosphate hydrolase. *Biochemistry* 1996; **35**: 11529- 11535

24 **Siprashvili Z,** Sozzi G, Barnes LD, McCue P, Robinson AK, Eryomin V, Sard L, Tagliabue E, Greco A, Fusetti L, Schwartz G, Pierotti MA, Croce CM, Huebner K. Replacement of Fhit in cancer cells suppresses tumorigenicity. *Proc Natl Acad Sci USA* 1997; **94**: 13771-13776

25 **Pace HC,** Garrison PN, Robinson AK, Barnes LD, Draganescu A, Rosler A, Blackburn GM, Siprashvili Z, Croce CM, Huebner K, Brenner C. Genetic, biochemical, and crystallographic characterization of Fhit-substrate complexes as the active signaling form of Fhit. *Proc Natl Acad Sci USA* 1998; **95**: 5484-5489

26 **Trapasso F,** Krakowiak A, Cesari R, Arkles J, Yendamuri S, Ishii H, Vecchione A, Kuroki T, Bieganowski P, Pace HC, Huebner K, Croce CM, Brenner C. Designed FHIT alleles establish that Fhit-induced apoptosis in cancer cells is limited by substrate binding. *Proc Natl Acad Sci USA* 2003; **100**: 1592-1597

27 **Dumon KR,** Ishii H, Vecchione A, Trapasso F, Baldassarre G, Chakrani F, Druck T, Rosato EF, Williams NN, Baffa R, During MJ, Huebner K, Croce CM. Fragile histidine triad expression delays tumor development and induces apoptosis in human pancreatic cancer. *Cancer Res* 2001; **61**: 4827-4836

28 **Ji L,** Fang B, Yen N, Fong K, Minna JD, Roth JA. Induction of apoptosis and inhibition of tumorigenicity and tumor growth by adenovirus vector-mediated fragile histidine triad (FHIT) gene overexpression. *Cancer Res* 1999; **59**: 3333-3339

29 **Sard L,** Accornero P, Tornielli S, Delia D, Bunone G, Campiglio M, Colombo MP, Gramegna M, Croce CM, Pierotti MA, Sozzi G. The tumor-suppressor gene FHIT is involved in the regulation of apoptosis and in cell cycle control. *Proc Natl Acad Sci USA* 1999; **96**: 8489-8492

30 **Gopalakrishnan VK,** Banerjee AG, Vishwanatha JK. Effect of FHIT gene replacement on growth, cell cycle and apoptosis in pancreatic cancer cells. *Pancreatology* 2003; **3**: 293-302

Edited by Wang XL and Zhu LH

PO Box 2345, Beijing 100023, China
Fax: +86-10-85381893
E-mail: wjg@wjgnet.com www.wjgnet.com

ELSEVIER

World J Gastroenterol 2005;11(2):232-236
World Journal of Gastroenterology ISSN 1007-9327

• BASIC RESEARCH •

Prostacyclin inhibition by indomethacin aggravates hepatic damage and encephalopathy in rats with thioacetamide-induced fulminant hepatic failure

Chi-Jen Chu, Ching-Chin Hsiao, Teh-Fang Wang, Cho-Yu Chan, Fa-Yauh Lee, Full-Young Chang, Yi-Chou Chen, Hui-Chun Huang, Sun-Sang Wang, Shou-Dong Lee

Chi-Jen Chu, Ching-Chin Hsiao, Fa-Yauh Lee, Full-Young Chang, Yi-Chou Chen, Hui-Chun Huang, Shou-Dong Lee, Division of Gastroenterology, Department of Medicine, Taipei Veterans General Hospital, Taipei, Taiwan, China
Teh-Fang Wang, Armed Forces Sungshan Hospital, Taipei, Taiwan, China
Cho-Yu Chan, Department of Medical Research and Education, Taipei Veterans General Hospital, Taipei, Taiwan, China
Fa-Yauh Lee, Division of General Medicine, Department of Medicine, Taipei Veterans General Hospital, Taipei, Taiwan, China
Sun-Sang Wang, Taipei Municipal Gan-Dau Hospital, Taipei, Taiwan, China
Chi-Jen Chu, Ching-Chin Hsiao, Cho-Yu Chan, Fa-Yauh Lee, Full-Young Chang, Hui-Chun Huang, Sun-Sang Wang, Shou-Dong Lee, National Yang-Ming University School of Medicine, Taipei, Taiwan, China
Supported by the National Science Council of Taiwan (grant no. NSC 92-2314-B-075-036) and Taipei Veterans General Hospital (VGH-93-212)
Correspondence to: Dr. Fa-Yauh Lee, Division of Gastroenterology, Department of Medicine, Taipei Veterans General Hospital, Taipei, Taiwan, China. fylee@vghtpe.gov.tw
Telephone: +886-2-28757308 **Fax:** +886-2-28739318
Received: 2004-03-09 **Accepted:** 2004-04-09

Abstract

AIM: Vasodilatation and increased capillary permeability have been proposed to be involved in the pathogenesis of acute and chronic form of hepatic encephalopathy. Prostacyclin (PGI_2) and nitric oxide (NO) are important contributors to hyperdynamic circulation in portal hypertensive states. Our previous study showed that chronic inhibition of NO had detrimental effects on the severity of encephalopathy in thioacetamide (TAA)-treated rats due to aggravation of liver damage. To date, there are no detailed data concerning the effects of PGI_2 inhibition on the severity of hepatic encephalopathy during fulminant hepatic failure.

METHODS: Male Sprague-Dawley rats weighing 300-350 g were used. Fulminant hepatic failure was induced by intraperitoneal injection of TAA (350 mg/(kg·d) for 3 d. Rats were divided into two groups to receive intraperitoneal injection of indomethacin (5 mg/(kg·d), n = 20) or normal saline (N/S, n = 20) for 5 d, starting 2 d before TAA administration. Severity of encephalopathy was assessed by the counts of motor activity measured with Opto-Varimex animal activity meter. Plasma tumor necrosis factor-α (TNF-α, an index of liver injury) and 6-keto-$PGF_{1\alpha}$ (a metabolite of PGI_2) levels were measured by enzyme-linked immunosorbent assay.

RESULTS: As compared with N/S-treated rats, the mortality rate was significantly higher in rats receiving indomethacin (20% *vs* 5%, P<0.01). Inhibition of PGI_2 created detrimental effects on total movement counts (indomethacin *vs* N/S: 438±102 *vs* 841±145 counts/30 min, P<0.05). Rats treated with indomethacin had significant higher plasma levels of TNF-α (indomethacin *vs* N/S: 22±5 *vs* 10±1 pg/mL, P<0.05) and lower plasma levels of 6-keto-$PGF_{1\alpha}$ (P<0.001), but not total bilirubin or creatinine (P>0.05), as compared with rats treated with N/S.

CONCLUSION: Chronic indomethacin administration has detrimental effects on the severity of encephalopathy in TAA-treated rats and this phenomenon may be attributed to the aggravation of liver injury. This study suggests that PGI_2 may provide a protective role in the development of fulminant hepatic failure.

Key words: Hepatic Encephalopathy; Fulminant hepatic failure; Prostacyclin; Indomethacin

Chu CJ, Hsiao CC, Wang TF, Chan CY, Lee FY, Chang FY, Chen YC, Huang HC, Wang SS, Lee SD. Prostacyclin inhibition by indomethacin aggravates hepatic damage and encephalopathy in rats with thioacetamide-induced fulminant hepatic failure. *World J Gastroenterol* 2005; 11(2): 232-236
http://www.wjgnet.com/1007-9327/11/232.asp

INTRODUCTION

Hepatic encephalopathy is a neuropsychiatric syndrome associated with acute liver failure, chronic parenchymal liver disease, or portal-systemic anastomosis[1-3]. The spectrum of symptoms may vary from subtle mental changes or a disrupted circadian rhythm to hepatic coma. The pathogenesis of hepatic encephalopathy has not been fully established and a delineation of pathogenetic factors for hepatic encephalopathy, as well as developing therapeutic modalities, are highly warranted today.

Hyperdynamic circulation observed in portal hypertension is characterized by pronounced vasodilatation, increased systemic and regional blood flows, and augmented cardiac index[4]. Vasodilatation and increased capillary permeability have been proposed to be involved in the pathogenesis of acute and chronic form of hepatic encephalopathy[5-8]. Recent studies demonstrated that excessive formation of nitric oxide (NO) and prostacyclin (PGI_2), the endogenous vasodilators synthesized by the vascular endothelium[9], are important contributors to the hyperdynamic circulation[10-13]. Our recent study[14] demonstrated that chronic inhibition of NO had detrimental effects on the severity of encephalopathy in thioacetamide (TAA)-treated rats due to aggravation of liver damage, suggesting a protective role for NO in the development of hepatic encephalopathy. Concerning the relationship between prostaglandins and the liver, some studies suggested that prostaglandins could protect the liver against the damage by a wide variety of toxins (carbon

tetrachloride, acetaminophen, galactosamine, alcohol), hypoxia, ischemia, and immune injury[15-23] although the mechanisms remain unclear. To date, there are no detailed data concerning the effects of PGI_2 inhibition on the severity of hepatic encephalopathy during the condition of fulminant hepatic failure.

The aim of this study was to investigate the effects of indomethacin, a PGI_2 inhibitor[24], on the severity of encephalopathy in rats with TAA-induced fulminant hepatic failure[25-27]. For more accurate quantification of the degree of hepatic encephalopathy, motor activities of rats were measured in automated open field boxes equipped with infrared cells[28-30]. Plasma levels of tumor necrosis factor-α (TNF-α, an index of liver injury), 6-keto-prostaglandin $F_{1\alpha}$ (6-keto-$PGF_{1\alpha}$ a metabolite of PGI_2), aminotransferase (ALT), total bilirubin, and creatinine were also determined.

MATERIALS AND METHODS

Animal model

Sprague-Dawley rats weighing 300-350 g were used. Fulminant hepatic failure was induced by intraperitoneal injection of TAA (350 mg/(kg.d) in normal saline, Sigma Chemical Co, St. Louis, MO, USA) for 3 consecutive days. Rats were divided into two groups to receive intraperitoneal injection of indomethacin (5 mg/(kg·d), $n = 20$)[24] or placebo (normal saline, N/S, $n = 20$) from two days prior to the starting of TAA administration and lasted for 5 d. To avoid hypoglycemia and electrolyte imbalance, subcutaneous injections of a solution containing 10% glucose water mixed with lactate ringer (25 mL/kg) was performed every 12 h after the first injection of TAA[31]. Motor activity measurements and blood sample collection were performed 3 d after the first administration of TAA. All rats were caged at 24 ℃ with a 12-h light-dark cycle and allowed free access to water and food. The experiments reported here were conducted according to the American Physiological Society guiding principles for the care and use of laboratory animals.

Measurement of motor activities

Motor activities in an open field were determined by using the Opto-Varimex animal activity meter (Columbus Instruments Inc., Columbus, OH, USA)[28-30]. The Opto-Varimex activity sensors utilize high-intensity, modulated infrared light beams to detect animal motion. Animals were housed in transparent cages (17 inches ×17 inches ×8 inches) through which 30 infrared beams pass in the horizontal plane, 15 on each axis. This device differentiates non-ambulatory movements (scratching, gnawing) from ambulation on the basis of consecutive interruption of the infrared monitoring beams. An additional row of infrared beams in the horizontal plane (15 on each axis) about 10 cm above the floor was used to count the vertical movements. During the activity measurements, animals had no access to food or chow. All studies were performed under strictly standardized conditions in the dark room for 30 min. The number of total movements, ambulatory movements, and vertical movements was separately recorded to reflect the motor activities of rats with fulminant hepatic failure.

Determination of plasma TNF-α, 6-keto-$PGF_{1\alpha}$, ALT, total bilirubin, and creatinine

After the abdominal skin was cleaned twice with iodine tincture and 70% alcohol, the abdomen was opened using a sterile technique. A 3 mL of blood sample was collected from the inferior vena cava into a pyrogen-free syringe containing 75 units of heparin sodium, then placed in an ice bath and transported immediately to the laboratory. Plasma was centrifuged at 4 ℃ and 2 935 *g* for 10 min, then stored at -70 ℃ in pyrogen-free polyethylene tubes for subsequent analysis within 6 wk.

We measured plasma TNF-α levels[32] with a commercially available solid phase sandwich enzyme-linked immunosorbent assay (rat TNF-α kits; R&D systems, Minneapolis, MN, USA) according to the protocol supplied by the manufacturer. The standards and samples were incubated with a TNF-α antibody coating a 96-well microtiter plate. The wells were washed with buffer and then incubated with anti-TNF-α antibody conjugated to horseradish peroxidase for 2 h. This was washed away and a yellow-brownish color was developed in the presence of tetramethyl benzidine chromogen substrate. The intensity of the color was measured in a Bio-kinetics reader (Bio-Tek Instruments Inc., Winooski, VT, USA) by reading the absorbance at 450 nm with a correction wavelength of 570 nm. We compared the samples against the standard curve to determine the amount of TNF-α present. All samples were run in duplicate. The lower limit of sensitivity for TNF-α by this assay was 5 pg/mL. The intra-assay and inter-assay coefficients of variation were 5.1% and 9.7%, respectively.

The measurement of 6-keto-$PGF_{1\alpha}$ was based on a competitive binding technique in which 6-keto-$PGF_{1\alpha}$ present in a sample competes with a fixed amount of alkaline phosphatase-labeled 6-keto-$PGF_{1\alpha}$ for sites on a sheep polyclonal antibody (6-keto-$PGF_{1\alpha}$ Kits; R&D systems, Minneapolis, MN, USA). During the incubation, the polyclonal antibody became bound to the donkey anti-sheep antibody coated onto the microplate. Following a wash to remove excess conjugates and unbound samples, a substrate solution was added to the wells to determine the bound enzyme activity. The color development was stopped and the absorbance was read at 405 mm in a Bio-kinetics reader (Bio-Tek Instruments Inc., Winooski, VT, USA). The intensity of the color was inversely proportional to the concentration of 6-keto-$PGF_{1\alpha}$ in the sample. All samples were run in duplicate. The lower limit of the sensitivity for 6-keto-$PGF_{1\alpha}$ by this assay was 1.4 pg/mL.

We determined plasma levels of ALT, total bilirubin and creatinine by colorimetric assay with a Clinical Systems 700 analyzer (Beckman Instruments, Fullerton, CA, USA).

Statistical analysis

Results were expressed as mean±SE. Statistical analyses for categorical variables were performed by Chi-square and Fisher exact tests. Student's *t*-test was used for continuous variables. Results were considered statistically significant at $P<0.05$.

RESULTS

Effects of chronic indomethacin administration on mortality rate in rats with fulminant hepatic failure

Four rats in the indomethacin group and one rat in the N/S group died during chronic administration of TAA before the measurement of motor activities. As compared with N/S-treated rats, the mortality rate was significantly higher in rats receiving chronic indomethacin administration (20% *vs* 5%, $P<0.01$).

Effects of chronic indomethacin administration on degree of hepatic encephalopathy in rats with fulminant hepatic failure (Figure 1)

In rats receiving indomethacin, the total movements were significantly decreased (indomethacin *vs* N/S: 438±102 *vs* 841±145 counts/30 min, $P<0.05$). The counts of ambulatory movements (256±62 *vs* 385±95 counts/30 min, $P = 0.29$) and vertical movements (28±12 *vs* 68±27 counts/30 min, $P = 0.20$) in the rats treated with indomethacin tended to be lower; however, the differences did not reach a significant level.

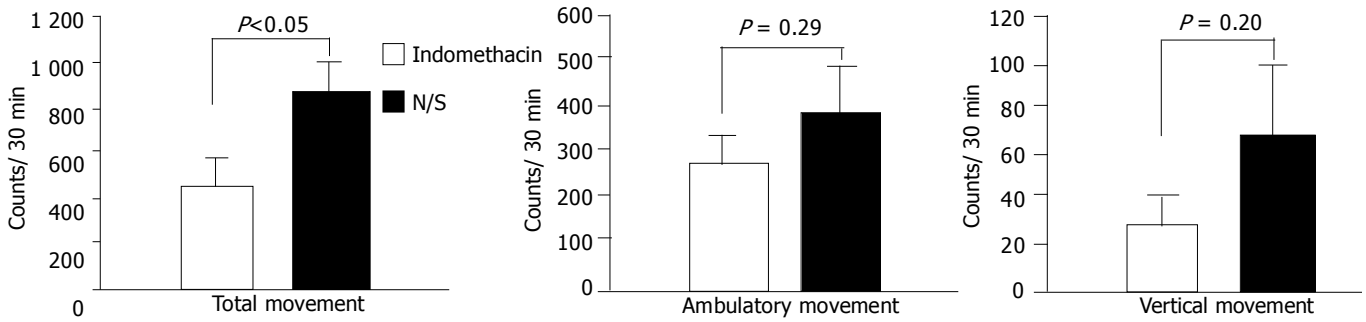

Figure 1 Comparison of the degree of hepatic encephalopathy by total, ambulatory and vertical movement counts between rats with fulminant hepatic failure treated with indomethacin (n = 19) or N/S (n = 16).

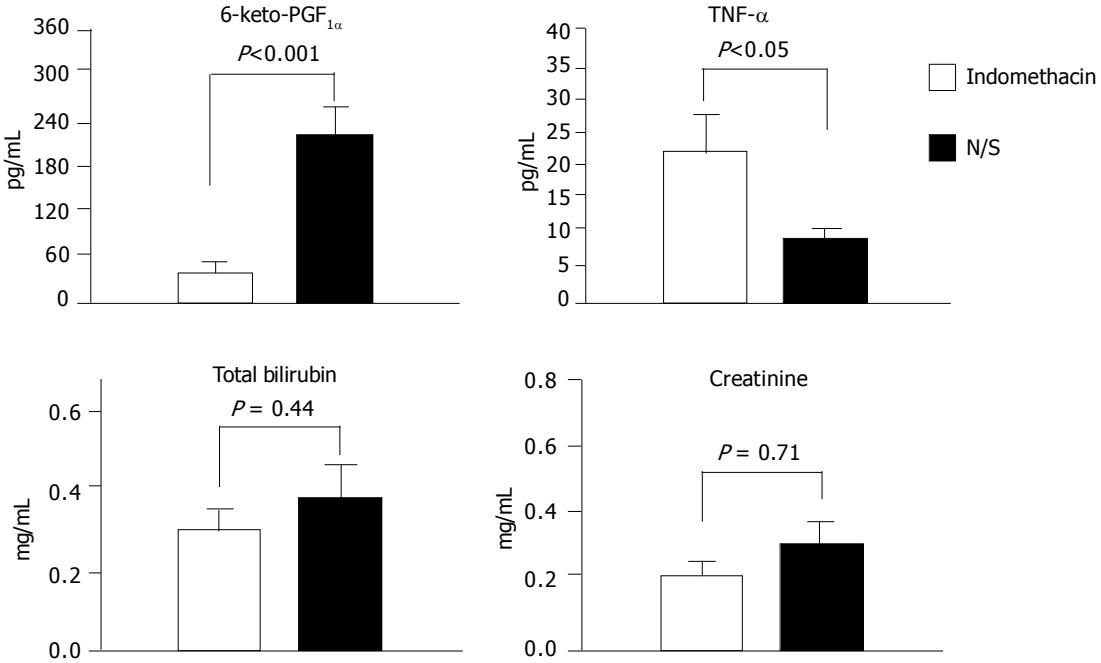

Figure 2 Comparison of the plasma levels of 6-keto-$PGF_{1\alpha}$, TNF-α, total bilirubin, and creatinine between rats with fulminant hepatic failure treated with indomethacin (n = 19) or N/S (n = 16).

Effects of chronic indomethacin administration on plasma levels of 6-keto-$PGF_{1\alpha}$, TNF-α, ALT, total bilirubin, and creatinine in rats with fulminant hepatic failure (Figure 2)

Rats treated with indomethacin had significantly lower plasma levels of 6-keto-$PGF_{1\alpha}$ (indomethacin *vs* N/S: 32±11 *vs* 213±47 pg/mL, P<0.001) and higher plasma levels of TNF-α (indomethacin *vs* N/S: 22±5 *vs* 10±1 pg/mL, P<0.05) as compared to N/S-treated rats. The indomethacin group of rats had a higher serum ALT (indomethacin *vs* N/S: 172±35 *vs* 141±31 IU/L, P>0.05); however, it did not reach a significant level. Serum levels of total bilirubin (indomethacin *vs* N/S: 0.3±0.1 *vs* 0.4±0.1 mg/dL, P>0.05) and creatinine (indomethacin *vs* N/S: 0.2±0.1 *vs* 0.3±0.1 mg/dL, P>0.05) were comparable between these two groups.

DISCUSSION

Regarding the relationships between the liver and arachidonic acid derivatives, in the last decade much has been learned between the interactions of liver and prostaglandins (PGs) under normal and pathological conditions. However, the puzzle is far from complete. Physiologically, the liver synthesizes all the major metabolites of the arachidonate cascade, including PGs. It has been found that PGs are involved in various physiological processes in the liver, including vasoregulation, platelet aggregation and mediation of inflammation[33]. As we stated previously, some studies suggested that PGs could protect the liver against damage by a wide variety of toxins (carbon tetrachloride, acetaminophen, galactosamine, alcohol), hypoxia, ischemia, and immune injury[15-23]. Although the precise mechanism underlying the cytoprotective effects of PGs in acute liver injury remains to be precisely defined, it may be related to the alleviation of vasoconstriction with tissue hypoxia, lipid peroxidation, and release of inflammatory cytokines or cytotoxic factors[34-36]. In agreement with previous studies[15-23], our current study showed that inhibition of PGI_2 by indomethacin during acute liver injury could aggravate hepatic damage. In addition, this is the first study which demonstrated that indomethacin administration could result in detrimental effects on encephalopathy in rats with TAA-induced fulminant hepatic failure. This finding was similar to NO inhibition in our previous research[14] suggesting that maintaining tissue oxygenation by vasodilators is important in fulminant hepatic failure. Besides, evidence from animal studies suggested indomethacin administration might affect neurotransmission and concentrations of neuropeptides in the brain[37-39]. Since our current study did not have data on the above issues, it is hard

to tell whether the deleterious effects of indomethacin injection on encephalopathy may be partially attributed to this and further studies are warranted.

Physiologically, TNF-α has been found to be a peptide mediator released by mononuclear cells on activation by endotoxin, tissue injury and tumor cells[40]. The metabolism of TNF-α was located within the liver after it was bound to a specific receptor[41]. Therefore, plasma levels of TNF-α, together with serum bilirubin, could be regarded as an index for evaluating the degree of hepatocellular damage and tissue necrosis.

Grading of hepatic encephalopathy is crucial in the research field for causally related pathogenetic factors. Various tests such as equilibrium test, corneal, auditory startle, and righting reflexes have been used but the interpretation of these tests may be subjective and cannot be quantified. Thus, a mechanical scoring system was applied in the present study. These tests are of great benefit in monitoring the minor changes in motivated behavior. On the basis of consecutive interruption of the infrared monitoring beams, we could differentiate non-ambulatory (scratching, gnawing) from ambulatory movements. The additional row of infrared cells above the plane could provide us more information concerning the movements toward the vertical direction. In the current study, the time interval from the first dose of TAA administration to the measurement of motor counts was fixed (72 h). The advantage of this model is that it can provide a therapeutic window for treatment modalities.

Indomethacin acts by inhibiting cyclooxygenase (COX), the rate-limiting enzyme in metabolic conversion of arachidonic acids into PGs. Two isoforms of COX have been identified[42] and both can be inhibited by indomethacin. COX-1 is expressed constitutively in most tissues and plays an important function in the protection of gastric mucosa and maintaining physiological homeostasis. COX-2 is thought to be the enzyme induced in inflammatory states and tumorigenesis. Recently, the intervention of selective COX-2 inhibitors was shown to preserve the anti-inflammatory efficacy of non-steroid antiinflammatory drugs (NSAIDs) and to achieve greater safety than traditional NSAIDs[43-45]. It is unknown whether using selective COX-2 inhibitors may have different effects on hepatic encephalopathy other than detrimental effect and this issue deserves further evaluations.

Results of preliminary clinical trials using PGs as therapeutic agents in patients with severe acute liver injury have been encouraging[46]. However, most of these trials were lack of control groups. To accept that PGs as a standardized treatment in some forms of liver injury, there is still much to learn about the intimate mechanisms responsible for the hepatoprotective effect. We acknowledge that this study may not be 100% extrapolated to patients with acute or chronic forms of hepatic encephalopathy in conditions of liver insufficiency. However, we want to point out that using NSAIDs in patients who potentially suffer from hepatic encephalopathy should be closely monitored.

In summary, chronic indomethacin administration had detrimental effects on the severity of encephalopathy in TAA-treated rats and this phenomenon may be partly attributed to the aggravation of liver injury. It is possible that prostacyclin inhibition may affect neurotransmission, brain microcirculation, or changes of blood-brain-barrier permeability. However, the detailed responsible mechanisms remained to be elucidated. Our current study suggests that PGI_2 may provide a protective role in the development of fulminant hepatic failure.

ACKNOWLEDGEMENTS

The authors gratefully acknowledge Chun-Ching Tai, Yu-Yao Kau and Yun-Ni Hsieh for their excellent technical assistance.

REFERENCES

1 **Gammal SH**, Jones EA. Hepatic encephalopathy. *Med Clin North Am* 1989; **73**: 793-813
2 **Sherlock S**. Fulminant hepatic failure. *Adv Intern Med* 1993; **38**: 245-267
3 **Mousseau DD**, Butterworth RF. Current theories on the pathogenesis of hepatic encephalopathy. *Proc Soc Exp Biol Med* 1994; **206**: 329-344
4 **Palmer RM**, Ashton DS, Moncada S. Vascular endothelial cells synthesize nitric oxide from L-arginine. *Nature* 1988; **333**: 664-666
5 **Groszmann RJ**. Hyperdynamic circulation of liver disease 40 years later: pathophysiology and clinical consequences. *Hepatology* 1994; **20**: 1359-1363
6 **Lockwood AH**, Yap EW, Wong WH. Cerebral ammonia metabolism in patients with severe liver disease and minimal hepatic encephalopathy. *J Cereb Blood Flow Metab* 1991; **11**: 337-341
7 **Janigro D**, West GA, Nguyen TS, Winn HR. Regulation of blood-brain barrier endothelial cells by nitric oxide. *Circ Res* 1994; **75**: 528-538
8 **Jaworowicz DJ**, Korytko PJ, Singh Lakhman S, Boje KM. Nitric oxide and prostaglandin E_2 formation parallels blood-brain barrier disruption in an experimental rat model of bacterial meningitis. *Brain Res Bull* 1998; **46**: 541-546
9 **Smith WL**. Prostaglandin biosynthesis and its compartmentation in vascular smooth muscle and endothelial cells. *Annu Rev Physiol* 1986; **48**: 251-262
10 **Pizcueta P**, Piqué JM, Fernandéz M, Bosch J, Rodés J, Whittle BJ, Moncada S. Modulation of the hyperdynamic circulation of cirrhotic rats by nitric oxide inhibition. *Gastroenterology* 1992; **103**: 1909-1915
11 **Lee FY**, Colombato LA, Albillos A, Groszmann RJ. N omega-nitro-L-arginine administration corrects peripheral vasodilation and systemic capillary hypotension and ameliorates plasma volume expansion and sodium retention in portal hypertensive rats. *Hepatology* 1993; **17**: 84-90
12 **Sitzmann JV**, Bulkley GB, Mitchell MC, Campbell K. Role of prostacyclin in the splanchnic hyperemia contributing to portal hypertension. *Ann Surg* 1989; **209**: 322-327
13 **Bruix J**, Bosch J, Kravetz D, Mastai R, Rodéz J. Effects of prostaglandin inhibition on systemic and hepatic hemodynamics in patients with cirrhosis of the liver. *Gastroenterology* 1985; **88**: 430-435
14 **Chu CJ**, Wang SS, Lee FY, Chang FY, Lin HC, Hou MC, Chan CC, Wu SL, Chen CT, Huang HC, Lee SD. Detrimental effects of nitric oxide inhibition on hepatic encephalopathy in rats with thioacetamide-induced fulminant hepatic failure. *Eur J Clin Invest* 2001; **31**: 156-163
15 **Rush B**, Merritt MV, Kaluzny M, Van Schoick T, Brunden MN, Ruwart M. Studies on the mechanism of the protective action of 16,16-dimethylPGE2 in carbon tetrachloride induced acute hepatic injury in the rat. *Prostaglandins* 1986; **32**: 439-455
16 **Araki H**, Lefer AM. Cytoprotective actions of prostacyclin during hypoxia in the isolated perfused cat liver. *Am J Physiol* 1980; **238**: H176-H181
17 **Davis DC**, Potter WZ, Jollow DJ, Mitchell JR. Species differences in hepatic glutathione depletion, covalent binding and hepatic necrosis after acetaminophen. *Life Sci* 1974; **14**: 2099-2109
18 **Mizoguchi Y**, Tsutsui H, Miyajima K, Sakagami Y, Seki S, Kobayashi K, Yamamoto S, Morisawa S. The protective effects of prostaglandin E_1 in an experimental massive hepatic cell necrosis model. *Hepatology* 1987; **7**: 1184-1188
19 **Noda Y**, Hughes RD, Williams R. Effect of prostacyclin (PGI_2) and a prostaglandin analogue BW245C on galactosamine-induced hepatic necrosis. *J Hepatol* 1986; **2**: 53-64
20 **Ogawa M**, Mori T, Mori Y, Ueda S, Yoshida H, Kato I, Iesato K, Wakashin Y, Wakashin M, Okuda K. Inhibitory effects of prostaglandin E1 on T-cell mediated cytotoxicity against iso-

lated mouse liver cells. *Gastroenterology* 1988; **94**: 1024-1030
21 **Alp MH**, Hickman R. The effect of prostaglandins, branched-chain amino acids and other drugs on the outcome of experimental acute porcine hepatic failure. *J Hepatol* 1987; **4**: 99-107
22 **Guarner F**, Boughton-Smith NK, Blackwell GJ, Moncada S. Reduction by prostacyclin of acetaminophen-induced liver toxicity in the mouse. *Hepatology* 1988; **8**: 248-253
23 **Masaki N**, Ohta Y, Shirataki H, Ogata I, Hayashi S, Yamada S, Hirata K, Nagoshi S, Mochida S, Tomiya T. Hepatocyte membrane stabilization by prostaglandins E_1 and E_2: favorable effects on rat liver injury. *Gastroenterology* 1992; **102**: 572-576
24 **Hou MC**, Cahill PA, Zhang S, Wang YN, Hendrickson RJ, Redmond EM, Sitzmann JV. Enhanced cyclooxygenase-1 expression within the superior mesenteric artery of portal hypertensive rats: role in the hyperdynamic circulation. *Hepatology* 1998; **27**: 20-27
25 **Albrecht J**, Hilgier W, Rafalowska U. Activation of arginine metabolism to glutamate in rat brain synaptosomes in thioacetamide-induced hepatic encephalopathy: an adaptive response? *J Neurosci Res* 1990; **25**: 125-130
26 **Osada J**, Aylagas H, Miro-Obradors MJ, Arce C, Palacios-Alaiz E, Cascales M. Effect of acute thioacetamide administration on rat brain phospholipid metabolism. *Neurochem Res* 1990; **15**: 927-931
27 **Steindl P**, Püspök A, Druml W, Ferenci P. Beneficial effect of pharmacological modulation of the $GABA_A$-benzodiazepine receptor on hepatic encephalopathy in the rat: comparison with uremic encephalopathy. *Hepatology* 1991; **14**: 963-968
28 **Bengtsson F**, Gage FH, Jeppsson B, Nobin A, Rosengren E. Brain monoamine metabolism and behavior in portacaval shunted rats. *Exp Neurol* 1985; **90**: 21-35
29 **Ribeiro J**, Nordlinger B, Ballet F, Cynober L, Coudray-Lucas C, Baudrimont M, Legendre C, Delelo R, Panis Y. Intrasplenic hepatocellular transplantation corrects hepatic encephalopathy in portacaval–shunted rats. *Hepatology* 1992; **15**: 12-18
30 **Chu CJ**, Lee FY, Wang SS, Chang FY, Lin HC, Wu SL, Chan CC, Tsai YT, Lee SD. Establishment of an animal model of hepatic encephalopathy. *J Chin Med Assoc* 2000; **63**: 263-269
31 **Gammal SH**, Basile AS, Geller D, Skolnick P, Jones EA. Reversal of the behavioral and electrophysiological abnormalities of an animal model of hepatic encephalopathy by benzodiazepine receptor ligands. *Hepatology* 1990; **11**: 371-378
32 **Chu CJ**, Lee FY, Wang SS, Lu RH, Tsai YT, Lin HC, Hou MC, Chan CC, Lee SD. Hyperdynamic circulation of cirrhotic rats with ascites: role of endotoxin, tumour necrosis factor-a and nitric oxide. *Clin Sci* 1997; **93**: 219-225
33 **Needleman P**, Turk J, Jakschik BA, Morrison AR, Lefkowith JB. Arachidonic acid metabolism. *Annu Rev Biochem* 1986; **55**: 69-102
34 **Iwai M**, Jungermann K. Leukotrienes increase glucose and lactate output decrease flow in perfused rat liver. *Biochem Biophys Res Commun* 1988; **151**: 283-290
35 **Busam KJ**, Bauer TM, Bauer J, Gerok W, Decker K. Interleukin-6 release by rat liver macrophages. *J Hepatol* 1990; **11**: 367-373
36 **Nagai H**, Aoki M, Shimazawa T, Yakuo I, Koda A, Kasahara M. Effect of OKY-046 and ONO-3708 on liver injury in mice. *Jpn J Pharmacol* 1989; **51**: 191-197
37 **Matsukawa R**, Takiguchi H. Effect of indomethacin on Ca2+-stimulated adenosine triphosphatase in the synaptic vesicles of rat brain *in vitro*. *Int J Biochem* 1982; **14**: 713-717
38 **Hemker DP**, Aiken JW. Actions of indomethacin and prostaglandins E2 and D2 on nerve transmission in the nictitating membrane of the cat. *Prostaglandins* 1981; **22**: 599-611
39 **Theodorsson E**, Mathe AA, Stenfors C. Brain neuropeptides: tachykinins, neuropeptide Y, neurotensin and vasoactive intestinal polypeptide in the rat brain: modifications by ECT and indomethacin. *Prog Neuropsychopharmacol Biol Psychiatry* 1990; **14**: 387-407
40 **Old LJ**. Tumor necrosis factor (TNF). *Science* 1985; **230**: 630-632
41 **Andus T**, Bauer J, Gerok W. Effects of cytokines on the liver. *Hepatology* 1991; **13**: 364-375
42 **FitzGerald GA**, Patrono C. The coxibs, selective inhibitors of cyclooxygenase-2. *N Engl J Med* 2001; **345**: 433-442
43 **Cannon GW**, Caldwell JR, Holt P, McLean B, Seidenberg B, Bolognese J, Ehrich E, Mukhopadhyay S, Daniels B. Rofecoxib, a specific inhibitor of cyclooxygenase-2, with clinical efficacy comparable with that of diclofenac sodium: results of a one-year, randomized, clinical trial in patients with osteoarthritis of the knee and hip. Rofecoxib Phase III Protocol 035 Study Group. *Arthritis Rheum* 2000; **43**: 978-987
44 **Clemett D**, Goa KL. Celecoxib: a review of its use in osteoarthritis, rheumatoid arthritis and acute pain. *Drugs* 2000; **59**: 957-980
45 **Day R**, Morrison B, Luza A, Castaneda O, Strusberg A, Nahir M, Helgetveit KB, Kress B, Daniels B, Bolognese J, Krupa D, Seidenberg B, Ehrich E. A randomized trial of the efficacy and tolerability of the COX-2 inhibitor rofecoxib *vs* ibuprofen in patients with osteoarthritis. Rofecoxib/Ibuprofen Comparator Study Group. *Arch Intern Med* 2000; **160**: 1781-1787
46 **Sinclair SB**, Greig PD, Blendis LM, Abecassis M, Roberts EA, Phillips MJ, Cameron R, Levy GA. Biochemical and clinical response of fulminant viral hepatitis to administration of prostaglandin E. A preliminary report. *J Clin Invest* 1989; **84**; 1063-1069

Edited by Wang XL **Proofread by** Chen WW

PO Box 2345, Beijing 100023, China
Fax: +86-10-85381893
E-mail: wjg@wjgnet.com www.wjgnet.com

ELSEVIER

World J Gastroenterol 2005;11(2):237-241
World Journal of Gastroenterology ISSN 1007-9327

• BASIC RESEARCH •

Increase in neurokinin-1 receptor-mediated colonic motor response in a rat model of irritable bowel syndrome

Jun-Ho La, Tae-Wan Kim, Tae-Sik Sung, Hyn-Ju Kim, Jeom-Yong Kim, Il-Suk Yang

Jun-Ho La, Tae-Sik Sung, Hyn-Ju Kim, Il-Suk Yang, Department of Physiology, College of Veterinary Medicine, Seoul National University, Republic of Korea
Tae-Wan Kim, Department of Physiology, College of Veterinary Medicine, Kyungpuk National University, Republic of Korea
Jeom-Yong Kim, Institute of Bioscience and Biotechnology, Daewoong Pharm Co. Ltd. Republic of Korea
Correspondence to: Il-Suk Yang, D.V.M. Ph.D., Department of Physiology, College of Veterinary Medicine, Seoul National University, San 56-1 Sillim-Dong, Kwanak-Gu, Seoul, 151-742, Republic of Korea. isyang@snu.ac.kr
Telephone: +82-2-880-1261 **Fax:** +82-2-885-2732
Received: 2004-05-10 **Accepted:** 2004-06-18

Abstract

AIM: Irritable bowel syndrome (IBS) is a functional bowel disorder. Its major symptom is bowel dysmotility, yet the mechanism of the symptom is poorly understood. Since the neurokinin-1 receptor (NK_1R)-mediated signaling in the gut is important in the control of normal bowel motor function, we aimed to investigate whether the NK_1R-mediated bowel motor function was altered in IBS, using a rat IBS model that was previously reported to show colonic dysmotility in response to restraint stress.

METHODS: IBS symptoms were produced in male Sprague-Dawley rats by inducing colitis with acetic acid. Rats were left to recover from colitis for 6 d, and used for experiments 7 d post-induction of colitis. Motor activities of distal colon were recorded *in vitro*.

RESULTS: The contractile sensitivity of isolated colon to a NK_1R agonist [Sar^9,$Met(O_2)^{11}$]-substance P (1-30 nmol/L) was higher in IBS rats than that in normal rats. After the enteric neurotransmission was blocked by tetrodotoxin (TTX, 1 μmol/L), the contractile sensitivity to the NK_1R agonist was increased in normal colon but not in IBS rat colon. The NK_1R agonist-induced contraction was not different between the two groups when the agonist was challenged to the TTX-treated colon or the isolated colonic myocytes. A nitric oxide synthase inhibitor N^{ω}-nitro-L-arginine methyl ester (L-NAME, 100 μmol/L) augmented the NK_1R agonist-induced contraction only in normal rat colon.

CONCLUSION: These results suggest that the NK_1R-meidated colonic motor response is increased in IBS rats, due to the decrease in the nitrergic inhibitory neural component.

Key words: Irritable bowel syndrome; Neurokinin-1 receptor

La JH, Kim TW, Sung TS, Kim HJ, Kim JY, Yang IS. Increase in neurokinin-1 receptor-mediated colonic motor response in a rat model of irritable bowel syndrome. *World J Gastroenterol* 2005; 11(2): 237-241
http://www.wjgnet.com/1007-9327/11/237.asp

INTRODUCTION

IBS is a functional bowel disorder, and its major clinical symptom is disordered defecation associated with abdominal pain/discomfort[1,2]. The disordered defecation can be diarrhea or constipation, or an alternating bowel habit from one to the other over time[3]. Based on the disordered defecation patterns, patients diagnosed with IBS have been divided into different subtypes such as diarrhea-predominant IBS or constipation-predominant IBS[4]. It has been suggested that the disordered defecation in IBS patients results from abnormal motor function of the colon[5-8]. However, the mechanisms underlying the disordered defecation in IBS are still poorly understood.

Researchers have consistently reported that substance P (SP) is an important enteric transmitter in the control of bowel motility[9]. Interacting mainly with the neurokinin-1 receptor (NK_1R), SP can both stimulate and inhibit bowel motility by direct activation of the muscle cells and stimulation of enteric neural circuits[10]. Thus, it is highly conceivable that alterations in the NK_1R-mediated signaling can cause bowel dysmotility. Indeed, pathophysiological involvement of NK_1R has been shown in inflammation or stress-induced colonic dysmotility[11-14].

Considering the importance of the NK_1R-mediated signaling in normal bowel motility, one can hypothesize that the disordered defecation in IBS might be related to a disturbance in the NK_1R-mediated control of colonic motility. We aimed to test this hypothesis using an animal model of IBS. Previously we reported that rats developed IBS symptoms after subsidence of acetic acid-induced colitis[15]. This animal model showed a visceral hypersensitivity and an altered defecation pattern in the absence of histological and biochemical signs of intestinal inflammation. In the colon of this rat model of IBS, we investigated whether the NK_1R-mediated motor response was altered.

MATERIALS AND METHODS

Experimental animals and induction of IBS

Male Sprague-Dawley rats, weighing 270-310 g, were housed in stainless steel hanging cages in a colony room maintained under a 12 h light/dark cycle with a room temperature of 22±1 ℃ and a humidity of 65-70%. Water and food were available *ad libitum*. IBS symptoms were produced as described previously[15]. Briefly, colitis was induced by intracolonic instillation of 1 mL 4% acetic acid. Control animals received saline instead of acetic acid. Rats were left to recover from colitis for 6 d, and used for experiments 7 d post-induction of colitis.

Recording of colonic motor activities

Motor activity of isolated colonic segment On the day of experiments, rats were killed by cervical dislocation, and a 2 cm distal colonic segment was removed. The segment was suspended in a 20 mL organ bath containing oxygenated (95% O_2 and 50 mL/L CO_2) Krebs solution maintained at 37 ℃. The distal end of the segment was tied around the mouth of J-tube that was connected via a 3-way connector to a syringe and to a pressure transducer (RP-1500, Narco Bio-systems Inc., USA). The proximal end of the segment was ligated with a thread that was connected to an isometric force displacement transducer

(FT-03, Grass-Telefactor, USA). The signals from both transducers were acquired by PowerLab/400 (AD Instruments, Castle Hill, Australia) and recorded on an IBM-compatible computer.

Initial 1-g tension was loaded on the colonic segment and the lumen of the segment was filled with a 0.2 mL Krebs solution per 1 cm length of the segment. The mechanical activities of the colonic segment were detected as changes in intraluminal pressure. This parameter was reported to reflect the motor activity of intestinal circular muscles[16]. After a 60-min equilibration period, drugs were cumulatively administered into the bath with a 5-min exposure time at each concentration. The effect of a drug on the colonic motor activity was quantified by measuring the mean intraluminal pressure at a given concentration. The mean intraluminal pressure was digitally calculated by dividing an integral value of pressure (area under the pressure trace) by the number of data points (tracing time). At the end of each experiment, the tonic contraction by KCl (60 mmol/L) was measured to normalize the motor activity of the isolated colon at each concentration of drugs (% of the maximal amplitude of the KCl-induced tonic contraction, % KCl).

Contractility of isolated colonic smooth muscle cells

Smooth muscle layers from the colon were isolated, cut into small pieces and placed in nominal Ca^{2+}-free physiological salt solution (Ca^{2+}-free PSS). These segments were incubated in a medium modified from Kraft-Brühe (KB) medium[17] for 30-60 min at room temperature. They were then incubated for 20-30 min at 37 ℃ in digestion medium (Ca^{2+}-free PSS) containing 1.5 mg/mL collagenase type 2, 2.0 mg/mL trypsin inhibitor, 2.0 mg/mL bovine serum albumin and 0.5 mg/mL dithioerythritol. After digestion, the supernatant was discarded, the softened muscle segments were transferred again into modified KB medium, and single cells were dispersed by gentle agitation with a wide-bore glass pipette. Isolated colonic myocytes were kept in modified KB medium at 4 ℃ until use. All experiments were carried out at room temperature within 12 h of harvesting cells.

Isolated colonic myocytes were transferred to a stage on an inverted microscope (Olympus CK2, Japan) and allowed to stick lightly to the glass coverslip bottom of a small chamber for 10 min. The cells were then perfused with physiological salt solution (PSS) to remove cellular debris. Single smooth muscle cells were identified and cell image was digitally captured using CCD camera (TMC-7, PULNiX Inc., USA) at 0.05 frame per second (fps) rate. Cell length was measured using software for image analysis. Cell contraction was expressed as a percent decrease in cell length by a drug from control length (the length of cells before the application of drugs).

Solutions and chemicals

The Krebs solution contained (in mmol/L) 118 NaCl, 4.7 KCl, 2.5 $CaCl_2$, 1.2 $MgSO_4$, 1.2 KH_2PO_4, 25 $NaHCO_3$, and 11 glucose. The Ca^{2+}-free PSS contained (in mmol/L) 135 NaCl, 5 KCl, 1.2 $MgCl_2$, 10 glucose, and 10 HEPES (adjusted to pH 7.4 with Tris). PSS contained (in mmol/L) 135 NaCl, 5 KCl, 2 $CaCl_2$, 10 glucose, and 10 HEPES. [Sar^9, $Met(O_2)^{11}$]-substance P (SP) was purchased from Tocris Cookson (Avonmouth, UK). Collagenase type 2 was purchased from Worthington (Lakewood, NJ, USA). All the following chemicals were purchased from Sigma (St. Louis, MO, USA): tetrodotoxin (TTX), N^{ω}-nitro-L-arginine methyl ester (L-NAME), dithioerythritol, trypsin inhibitor.

Statistical analysis

Data were expressed as mean±SE with *n*, the number of animals. Unpaired Student's *t*-test was used for statistical comparison (at $P<0.05$ significance level). In case of analyzing the effect of a NK_1R agonist on normal and IBS colon before and after TTX-treatment, the significance level was adjusted using Bonferroni procedure.

RESULTS

Spontaneous motor activities of isolated colon

The isolated colonic segments showed spontaneous motor activities in rest, and tonically contracted under a high KCl (60 mmol/L) solution (Figure 1). There was no difference in the KCl-induced contraction (normalized by dividing by wet weight of the colonic segment) between normal and IBS rat colons (329±31 mmHg/g *vs* 326±37 mmHg/g, $P>0.95$, $n = 10$). The frequency of the spontaneous phasic contraction was 0.79±0.08 beat per minute (BPM) ($n = 10$) in normal and 0.77±0.07 BPM ($n = 10$) in IBS rat colon. The amplitude of the spontaneous contraction was 13.1±1.6% KCl and 13.3±1.2% KCl in normal rat colon and IBS rat colon, respectively ($P>0.9$).

Effect of NK_1R agonist on the motor activities of isolated colon

As shown in Figure 2A, a selective NK_1R agonist, [Sar^9,$Met(O_2)^{11}$]-substance P (SP), contracted the circular muscle of an isolated distal colonic segment. The contractile effect of [Sar^9, $Met(O_2)^{11}$]-SP was more prominent in IBS rat colon than that in normal rat colon at 10 and 30 nmol/L ($P<0.05$).

Blocking the enteric neurotransmission with TTX (1 μmol/L) increased the resting mean intraluminal pressure by 9.7±1.1% KCl ($n = 8$) in normal rat colon and by 8.0±1.7% KCl ($n = 7$) in IBS rat colon ($P = 0.4$). The contractile effect of [Sar^9,$Met(O_2)^{11}$]-SP was not different between the two groups under the presence of TTX (Figure 2B). In the TTX-pretreated normal rat colon ($n = 8$), the contractile effect of [Sar^9,$Met(O_2)^{11}$]-SP was increased to 19.0±2.2% KCl ($P<0.01$ *vs* 11.2±0.9% KCl) and to 33.5±3.8% KCl ($P<0.01$ *vs* 16.3±0.9% KCl) at 10 and 30 nmol/L, respectively (Figure 2C), which implied that an inhibitory neural component was involved in the NK_1R agonist-induced contraction in

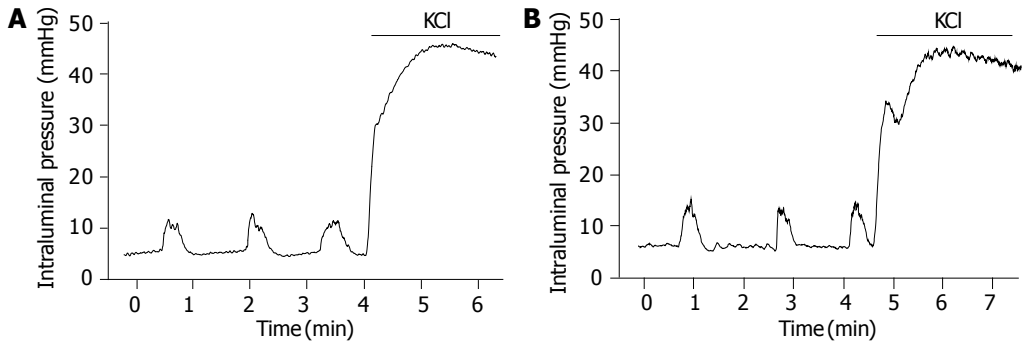

Figure 1 Motor activities of circular muscle in isolated colonic segments. Motor activities of circular muscle were measured as changes in intraluminal pressure in (A) normal rat colon and (B) IBS rat colon. No difference was observed between groups in the spontaneous rhythmic phasic contraction and in the KCl (60 mmol/L)-induced tonic contraction.

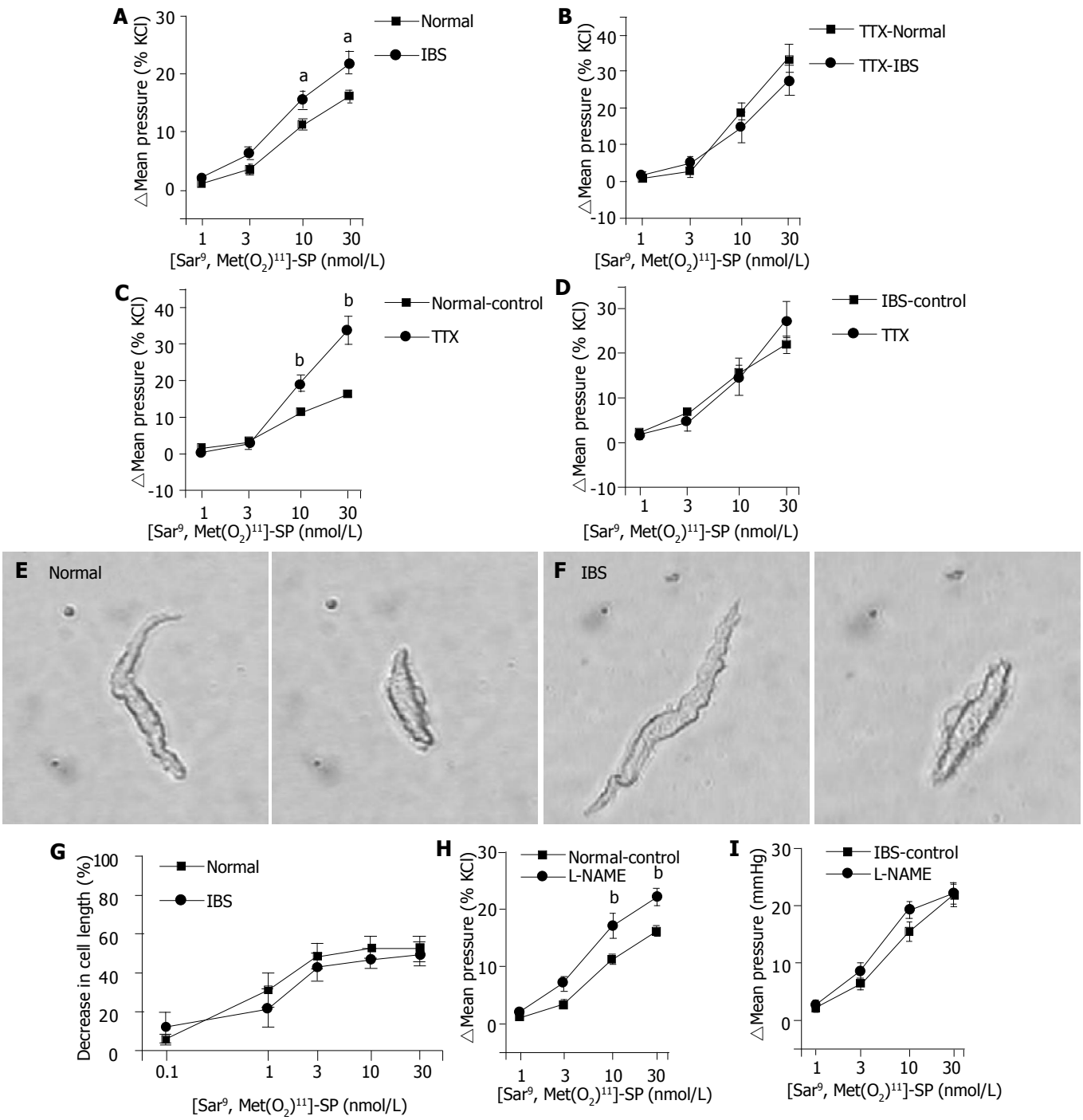

Figure 2 Contractile effect of NK_1R agonist on isolated distal colonic segments, isolated colonic myocytes, and NOS inhibitor-pretreated isolated colonic segments. A: The contractile sensitivity of IBS rat colon to [Sar^9,Met$(O_2)^{11}$]-SP was higher than that of normal rat colon. $^aP<0.05$ *vs* normal by Student's *t*-test with Bonferroni correction; B: Under the presence of TTX (1 μmol/L), no statistical difference was detected between groups in the [Sar^9,Met$(O_2)^{11}$]-SP-induced contraction; C and D: TTX increased the [Sar^9,Met$(O_2)^{11}$]-SP-induced contraction in normal rat colon but not in IBS rat colon. $^bP<0.01$ *vs* control by Student's *t*-test with Bonferroni correction (n = 12 in normal control, 9 in IBS control, 8 in TTX-normal, 7 in TTX-IBS); E and F: Photographs of myocytes in normal and IBS groups under control condition (left), and under the presence of 30 nmol/L [Sar^9,Met$(O_2)^{11}$]-SP (right). Bar = 30 μm. G: Dose-response plot showing the contractile effect of [Sar^9,Met$(O_2)^{11}$]-SP on the isolated colonic myocytes. The [Sar^9,Met$(O_2)^{11}$]-SP-induced contraction was measured as a percent decrease in cell length (n = 7 in normal, 8 in IBS); H and I: Normal and IBS rat colonic segments were incubated with a NOS inhibitor L-NAME (0.1 mmol/L) for 10 min before the cumulative administration of [Sar^9,Met$(O_2)^{11}$]-SP. $^bP<0.01$ *vs* control by Student's *t*-test (H: n = 12 in control, 7 in L-NAME. I: n = 9 in control, 6 in L-NAME).

normal rat colon. In IBS rat colon (n = 7), the contraction at each concentration of [Sar^9,Met$(O_2)^{11}$]-SP was not significantly changed by TTX pretreatment (Figure 2D).

Effect of NK_1R agonist on the motor activities of isolated colonic myocytes

The initial length of isolated colonic myocytes was 77.8±3.2 μm (n = 7) and 70.5±2.7 μm (n = 8) in normal and IBS groups, respectively ($P>0.09$). [Sar^9,Met$(O_2)^{11}$]-SP concentration-dependently decreased the length of isolated muscle cells. At the highest concentration (30 nmol/L), the cell length was decreased by 52.3±6.4% in normal group and 50.1±6.0% in IBS group. The response of muscle cells to [Sar^9,Met$(O_2)^{11}$]-SP was not different between the two groups (Figures 2E-G).

Effect of NK_1R agonist on the motor activities of isolated colon under the presence of NOS inhibitor

Pretreatment of a NOS inhibitor L-NAME (0.1 mmol/L) increased the resting mean intraluminal pressure by 10.7±1.5% KCl (n = 7) in normal rat colon and by 12.9±3.4% KCl (n = 6) in IBS rat colon (P = 0.55). In normal rat colon (n = 7), the contractile effect of [Sar^9,$Met(O_2)^{11}$]-SP was increased by the pretreatment of L-NAME to 17.2±2.2% KCl (P<0.01 *vs* 11.2±0.9% KCl), and to 22.1±1.5% KCl (P<0.01 *vs* 16.3±0.9% KCl) at 10 and 30 nmol/L, respectively. On the other hand, L-NAME was ineffective to augment the contractile effect of [Sar^9,$Met(O_2)^{11}$]-SP in IBS rat colon (Figure 2H, 2I).

DISCUSSION

In the present study, we found that the NK_1R-mediated colonic motor response was altered in a rat model of IBS. A selective NK_1R agonist [Sar^9,$Met(O_2)^{11}$]-SP contracted IBS rat colon more potently than normal rat colon. Because SP could stimulate both intestinal smooth muscle cells and enteric inhibitory nerves[10], we hypothesized that the higher contractile sensitivity of IBS rat colon to the NK_1R agonist resulted from increased contractile response of muscle cells, and/or decreased response of enteric inhibitory nerves to the NK_1R agonist. Our results support the second hypothesis. In normal rat colon, the contractile effect of [Sar^9,$Met(O_2)^{11}$]-SP was enhanced by a neurotransmission blocker TTX, whereas that in IBS rat colon was not significantly changed by TTX. Furthermore, the [Sar^9,$Met(O_2)^{11}$]-SP-induced contraction was not different between the two groups when the agonist was challenged to the TTX-treated isolated colon or directly to the isolated myocytes. These data indicate that the higher contractile sensitivity of IBS rat colon to [Sar^9,$Met(O_2)^{11}$]-SP results from the decreased enteric inhibitory neural components rather than the increased contractile response of muscle cells.

Recently, enteric nitrergic inhibitory nerves were reported to participate in the NK_1R-mediated control of peristalsis in isolated guinea-pig ileum[18] and in isolated rabbit distal colon[19]. Therefore, we supposed that nitrergic inhibitory nerves were the inhibitory neural components activated by [Sar^9,$Met(O_2)^{11}$]-SP. Expectedly, we found that the [Sar^9,$Met(O_2)^{11}$]-SP-induced contraction was augmented by the suppression of nitrergic inhibitory transmission with L-NAME in normal rat colon but not in IBS rat colon. Putting these lines of evidence together, it can be concluded that the increased NK_1R-mediated contraction in IBS rat colon results from the decreased NK_1R-mediated activation of enteric nitrergic inhibitory nerves.

Considering that the IBS rats used in this study developed IBS symptoms after subsidence of colitis, it is worthy to mention that intestinal inflammation could induce profound changes in enteric nerves, which might persist long after the inflammation subsided[20,21]. In addition, there have been studies reporting the dysfunction of enteric nitrergic nerves in animals with gut inflammation. Researchers have shown the decreased nNOS-immunoreactivities in TNBS-induced colitic rats[22], the reduced activity and synthesis of nNOS in DSS-induced colitic rats[23], and the diminished NO-mediated relaxation in nematode-infected mice[24]. Thus, it seems likely that alterations of enteric nitrergic neural function by colitis can persist in the colon of IBS rats, causing a higher contractile sensitivity of IBS colon to the NK_1R agonist.

Since nitrergic nerves are tonically active in rat colon[25,26], one would expect that dysfunction of enteric nitrergic nerves results in alterations of the resting colonic motility. However, we observed that the resting motility of the isolated colon was not different between normal group and IBS group (Figure 1). Moreover, the extent of the increase in the resting colonic motor activities by a NOS inhibitor was similar in the two groups, suggesting that the tonic nitrergic inhibition of resting motility is maintained in IBS rat colon. This seems incompatible with our aforementioned conclusion that the decreased enteric nitrergic inhibitory neural components in IBS rat colon causes the increased NK_1R-mediated colonic motor response. One of the possible explanations for this discrepancy is that the NK_1R-mediated signaling pathways do not modulate the tonic inhibitory action of nitrergic nerves and hence have no influence on the resting colonic motility. Supporting this notion, Mule *et al*[27] reported that the resting spontaneous motility of rat colon was not affected by a NK_1R antagonist but inhibited by several NK_2R antagonists, indicating that the NK_1R-mediated signaling pathways do not contribute to the control of the resting motility in rat colon.

In conclusion, the present results indicate that the NK_1R-mediated contraction is exaggerated in the colon of rat IBS model. The higher contractile sensitivity of IBS rat colon to the NK_1R agonist appears to result from the decreased enteric nitrergic inhibitory neural components rather than the increased contractile response of muscle cells. These results suggest that disordered defecation in IBS patients, especially who develop IBS after intestinal inflammation, might be related to the alterations in the NK_1R-mediated control of bowel motility.

REFERENCES

1 **Camilleri M,** Heading RC, Thompson WG. Clinical perspectives, mechanisms, diagnosis and management of irritable bowel syndrome. *Aliment Pharmacol Ther* 2002; **16**: 1407-1430
2 **Drossman DA.** Review article: an integrated approach to the irritable bowel syndrome. *Aliment Pharmacol Ther* 1999; **13**: 3-14
3 **Wood JD.** Neuropathophysiology of irritable bowel syndrome. *J Clin Gastroenterol* 2002; **35**: S11-S22
4 **Clemens CH,** Samsom M, Van Berge Henegouwen GP, Smout AJ. Abnormalities of left colonic motility in ambulant nonconstipated patients with irritable bowel syndrome. *Dig Dis Sci* 2003; **48**: 74-82
5 **Chaudhary NA,** Truelove SC. Human colonic motility. A comparative study of normal subjects, patients with ulcerative colitis, and patients with the irritable colon syndrome. *Gastroenterology* 1968; **54**: 777-uppl:778
6 **Chey WY,** Jin HO, Lee MH, Sun SW, Lee KY. Colonic motility abnormality in patients with irritable bowel syndrome exhibiting abdominal pain and diarrhea. *Am J Gastroenterol* 2001; **96**: 1499-1506
7 **Connell AM.** Intestinal motility and the irritable bowel. *Postgrad Med J* 1984; **60**: 791-796
8 **Vassallo MJ,** Camilleri M, Phillips SF, Steadman CJ, Talley NJ, Hanson RB, Haddad AC. Colonic tone and motility in patients with irritable bowel syndrome. *Mayo Clin Proc* 1992; **67**: 725-731
9 **Holzer P,** Holzer-Petsche U. Tachykinins in the gut. Part I. Expression, release and motor function. *Pharmacol Ther* 1997; **73**: 173-217
10 **Scheurer U,** Drack E, Halter F. Substance P activates rat colonic motility via excitatory and inhibitory neural pathways and direct action on muscles. *J Pharmacol Exp Ther* 1994; **271**: 7-13
11 **Castagliuolo I,** Lamont JT, Qiu B, Fleming SM, Bhaskar KR, Nikulasson ST, Kornetsky C, Pothoulakis C. Acute stress causes mucin release from rat colon: role of corticotropin releasing factor and mast cells. *Am J Physiol* 1996; **271**: G884-G892
12 **Di Sebastiano P,** Grossi L, Di Mola FF, Angelucci D, Friess H, Marzio L, Innocenti P, Buchler MW. SR140333, a substance P receptor antagonist, influences morphological and motor changes in rat experimental colitis. *Dig Dis Sci* 1999; **44**: 439-444
13 **Ikeda K,** Miyata K, Orita A, Kubota H, Yamada T, Tomioka

K. RP67580, a neurokinin1 receptor antagonist, decreased restraint stress-induced defecation in rat. *Neurosci Lett* 1995; **198**: 103-106

14 **Okano S,** Nagaya H, Ikeura Y, Natsugari H, Inatomi N. Effects of TAK-637, a novel neurokinin-1 receptor antagonist, on colonic function *in vivo*. *J Pharmacol Exp Ther* 2001; **298**: 559-564

15 **La JH,** Kim TW, Sung TS, Kang JW, Kim HJ, Yang IS. Visceral hypersensitivity and altered colonic motility after subsidence of inflammation in a rat model of colitis. *World J Gastroenterol* 2003; **9**: 2791-2795

16 **Coupar IM,** Liu L. A simple method for measuring the effects of drugs on intestinal longitudinal and circular muscle. *J Pharmacol Toxicol Methods* 1996; **36**: 147-154

17 **Isenberg G,** Klockner U. Calcium tolerant ventricular myocytes prepared by preincubation in a "KB medium". *Pflugers Arch* 1982; **395**: 6-18

18 **Holzer P.** Involvement of nitric oxide in the substance P-induced inhibition of intestinal peristalsis. *Neuroreport* 1997; **8**: 2857-2860

19 **Onori L,** Aggio A, Taddei G, Loreto MF, Ciccocioppo R, Vicini R, Tonini M. Peristalsis regulation by tachykinin NK1 receptors in the rabbit isolated distal colon. *Am J Physiol Gastrointest Liver Physiol* 2003; **285**: G325-G331

20 **Sanovic S,** Lamb DP, Blennerhassett MG. Damage to the enteric nervous system in experimental colitis. *Am J Pathol* 1999; **155**: 1051-1057

21 **Tornblom H,** Lindberg G, Nyberg B, Veress B. Full-thickness biopsy of the jejunum reveals inflammation and enteric neuropathy in irritable bowel syndrome. *Gastroenterology* 2002; **123**: 1972-1979

22 **Miampamba M,** Sharkey KA. Temporal distribution of neuronal and inducible nitric oxide synthase and nitrotyrosine during colitis in rats. *Neurogastroenterol Motil* 1999; **11**: 193-206

23 **Mizuta Y,** Isomoto H, Takahashi T. Impaired nitrergic innervation in rat colitis induced by dextran sulfate sodium. *Gastroenterology* 2000; **118**: 714-723

24 **Barbara G,** Vallance BA, Collins SM. Persistent intestinal neuromuscular dysfunction after acute nematode infection in mice. *Gastroenterology* 1997; **113**: 1224-1232

25 **Middleton SJ,** Cuthbert AW, Shorthouse M, Hunter JO. Nitric oxide affects mammalian distal colonic smooth muscle by tonic neural inhibition. *Br J Pharmacol* 1993; **108**: 974-979

26 **Mule F,** D'Angelo S, Amato A, Contino I, Serio R. Modulation by nitric oxide of spontaneous mechanical activity in rat proximal colon. *J Auton Pharmacol* 1999; **19**: 1-6

27 **Mule F,** D'Angelo S, Tabacchi G, Serio R. Involvement of tachykinin NK2 receptors in the modulation of spontaneous motility in rat proximal colon. *Neurogastroenterol Motil* 2000; **12**: 459-466

Edited by Wang XL

PO Box 2345, Beijing 100023, China
Fax: +86-10-85381893
E-mail: wjg@wjgnet.com www.wjgnet.com

ELSEVIER

World J Gastroenterol 2005;11(2):242-248
World Journal of Gastroenterology ISSN 1007-9327

• BASIC RESEARCH •

Screening of stimulatory effects of dietary risk factors on mouse intestinal cell kinetics

Pooja Shivshankar, Shyamala C. S. Devi

Pooja Shivshankar, Shyamala C. S. Devi, Department of Biochemistry and Molecular Biology, University of Madras, Guindy Campus, Chennai- 600 025, India
Supported by Senior Research fellowship from Council of Scientific and Industrial Research (CSIR), New Delhi, India, SRF No. [9/115 (462) / 98 EMR-1- BKR]
Correspondence to: Dr. Pooja Shivshankar, Ph D, Geriatric Research Education and Clinical Center (GRECC), 182, VA Medical Center, 7400 Merton Minter Blvd., San Antonio, Texas-78229, USA. poojashivshankar@yahoo.co.in
Telephone: +1-210-692-9298 **Fax:** +1-210-617-5312
Received: 2004-02-03 **Accepted:** 2004-03-02

Abstract

AIM: Although epidemiological and experimental studies validate influence of genetic, environmental and dietary factors in the causation of various types of cancers including colon, results from all these sources are inconclusive. Hypothesizing that high fat diet and obesity are among the major predisposing factors in the incidence of colon cancer, we evaluated the role of diet constituted with food material derived from a tropical plant, *Tamarindus indica* Linn (TI).

METHODS: A two part randomized double-blind study was conducted employing inbred Swiss albino mice from a single generation for the whole investigation. One day-old neonates (n = 12) were subcutaneously administered with monosodium glutamate (MSG) to induce obesity (OB). At weaning these animals were maintained on modified AIN-76 diet supplemented with 10% TI and 10% fat bolus (w/w, TIFB) for 8 wk. Subsequently, in the second part of study, four groups of animals belonging to the same generation, age and gender (n = 12 per group), were maintained on: AIN-76 control diet (CD); AIN-76 mixed with 10% TI extract (TI); and, mixed with 10% TI and 10% FB (TIFB) for 8 wk, to determine intestinal crypt cell proliferation, functionally-specific enzyme activities, fermentation profile, and energy preferences.

RESULTS: We observed a significant increase in the crypt cell production rate in distal colonic segment of experimental animals when compared with the controls. This segment also contained significantly low butyrate levels compared to control and TIFB groups. All the experimental groups showed a gross decrease in the enzyme activities viz., succinate dehydrogenase, acid-galactosidase and dipeptidyl amino peptidase IV demonstrating pathological stress caused by the test regimens, and an altered metabolic flux in the cellular environment.

CONCLUSION: We have demonstrated a cumulative response to the three dietary factors, one of which (TI) is reported, herein, for the first time to modulate kinetics of large intestinal mucosa, contributing to total risk posed by these test agents.

Key words: Large intestinal mucosa; Kinetics; Tamarindus indica Linn; Diet

Shivshankar P, Devi SCS. Screening of stimulatory effects of dietary risk factors on mouse intestinal cell kinetics. *World J Gastroenterol* 2005; 11(2): 242-248
http://www.wjgnet.com/1007-9327/11/242.asp

INTRODUCTION

Dietary factors have been estimated to be responsible for up to 40% of cancers including those of the gastrointestinal tract (GIT)[1-4]. Numerous life style factors have also been included such as, high fat diet consumption, inadequate physical activity and obesity[5-7]. High fat/low fiber diet has been found to have greater influence on the development of colon cancer[8]. Several studies have been conducted worldwide to relate obesity with cancer risk especially of the large intestine[9-13].

Tamarind forms an important ingredient of Indian cookery. Tamarind pulp powder (hereafter referred as TI) as used in the present study is prepared by concentrating, drying and milling the pulp into a powdered form. It is one of the convenient food products produced commercially by several manufacturers in India. Manjunath *et al*[14] reported that on average the total solid content of tamarind pulp powder varied between 18.6 and 25%, and acidity between 8.7 and 11.1% with an average value of 9.9% (as tartaric acid). The moisture content ranges between 3.5 and 8. 8%. Digestible starch is the major ingredient in tamarind pulp powder (20-41%). In some recent reports, the presence of nicotinic acid (about 5%), and primary amines (148.8 ppm) were discussed with emphasis on precursor carcinogens that added up to the list of environmental hazards to human beings[15-17]. The average composition of the dried pulp powder of TI is given in Table 1.

Table 1 Proximate composition of dried pulp of tamarind fruit

Constituents	Proximate composition of the dried pulp powder (%)[1]
Moisture	3.5-8.8
Protein	1.7-2.4
Total sugars	15.8-25.0
Ash	2.1-3.2
Free tartaric acid	8.7-11.1
Starch	20-41.3

[1]Source: Reference[14].

In view of the above literature, we wondered if the type of starch and high content of sugar present in the dried pulp of T. indica (hereafter referred as TI) might exert its effect on the colonic cell kinetics, either positively or negatively, when fed to the experimental animals chronically as a mix with AIN-76 control diet *ad libitum*. Influence of dietary sugars/starch and microbial contents on colonic cell proliferation has been studied extensively[18]. It is likely that non-digestible starch increases

apoptotic cell death and inhibits cellular growth in colonic mucosa. DNA damage is considered to play a crucial role in the induction of almost every type of cancer including that of colon. Studies have been carried out until recently on the DNA damage events by the exposure to various forms of starch using animal models[19,20].

In addition, we attempted to evaluate the influence of TI-derived components with fat bolus in experimental animals post-challenged with neonatal obesity. It is neither evident from the previous literature that TI might trigger genesis of any type of cancer in humans epidemiologically, nor is it experimentally demonstrated to cause any inductive/promotive response towards carcinogenesis. However, Block[21] and Patterson[22] reported that plant-derived components had significant impact on the mucosal properties in the entire gastrointestinal tract.

Hence, a protocol was designed to evaluate whether TI could act independently on the colonic mucosal architecture of the host system, and/or facilitate the fatty diet and/or obesity - mediated cellular damage and upregulate the proliferation rate, a basic prerequisite of neoplastic transformation. For the present communication, crypt cell proliferation rate (CCPR) and tritiated thymidine incorporation assays, biochemical enzyme profile, short chain fatty acids profile (SCFAs) and energy preferences such as lactate, were chosen to address possible effects of TI, *per se* as well as in combination with the well-established predisposing factors, on colonic mucosa of Swiss albino mice.

MATERIALS AND METHODS

Chemicals and isotopes

All the chemicals and solvents used in this study were of analytical grade. The isotope [^{3}H] - thymidine was purchased from Board of Radiation and Isotope Technology, Bombay, India. Monosodium glutamate (marketed as "aginomoto salt") and the dried pulp of tamarind (marketed as "dry tam- without mess") were purchased from the local market.

Preparation of T. indica fruit pulp extract

The dried fruit pulp of T. indica weighing 100 g was taken in conical flask and about 500 mL of boiled water was added and allowed to soak for 1 h. The cooled, aqueous extract[16] was filtered through a sieve (100 mesh) and used as an ingredient in the synthetic diet. The particular preparation method logically simulated the conditions applied by the Indian cookery system.

Experimental design

Swiss albino mice were purchased from Tamil Nadu Veterinary and Animal Science University (TNVASU), Chennai, India, and bred in the department's animal house. Inbred animals belonging to a single generation were selected for all the experimental conditions. In the first part of investigation, 75 animals from the third day of their birth were subcutaneously administered with 100 µL of 20 mg/mL MSG at two spots, regularly for eleven days[23]. A mortality rate of about 60% was observed during the induction of obesity and remaining 40% live animals developed obesity successfully, eighteen animals of which were chosen for the present study plan (OB), and therefore, caged separately. They were fed the AIN-76 modified diet[24], constituted with 10% (w/w) TI, 10% (w/w) fat bolus and 2% cholesterol, as designated for the TIFB-treated group.

For the second set of study, animals were divided into four groups (twenty four animals in each group). Control animals received controlled AIN-76 synthetic diet (CD). Animals belonging to TI - treated group (TI) were maintained on the synthetic diet mixed with 10% TI. Further, for TIFB - treated group (TIFB) of animals, the diet was mixed with 10% TI, 2% cholesterol, and 10% fat bolus.

Table 2 describes the diet composition of control and experimental groups of animals. Adjustment on caloric value of the diet was done with respect to the chemical composition of TI fruit extract, saturated animal fat and cholesterol. Choline and corn oil were excluded from the dietary regimens so as to analyze the effects of pure animal fat and cholesterol on the cellular membrane integrity without the interference of choline and other lipids. Treatment of animals with the present study setup was within the permissible criteria proposed by Government of India's Ministry of Social Justice and Empowerment, and Committee for the Purpose of Control and Supervision of Experiments on Animals (CPCSEA), (as published recently in Volume 19, Issue 23, November 9-22, 2002 Frontline). The rules and laws were followed from Poynter Center for the Study of Ethics and American Institutions, Indiana University, 410 N. Park Ave., Bloomington, IN, USA.

Table 2 Composition of the diet administered to control and experimental animals

Constituents	Control diet	Experimental diet
Caesin (%)	23.8	23.8
DL- methionine (%)	0.5	0.5
Corn starch (%)	30.0	22.7
Sucrose (%)	30.0	27.5
Cellulose (%)	6.5	6.5
Corn oil (%)	5.0	5.0
Salt mix (%)	3.0	3.0
Vitamin mix (%)	1.0	1.0
Choline bitartrate (%)	0.2	0.2
TI (10%)[1]- mixed		
Sucrose (%)	-	2.5
Tartaric/Malic/Citric acid (%)	-	3.3
Starch (%)	-	4.0
Animal fat (%)[2] - mixed	-	10.0
Cholesterol (%)	-	2.0

[1]TI was mixed (10%) in the total diet and compensated with corn starch and sucrose of the control diet for the nutrients composition for preparing experimental diet [2]Choline bitartrate and corn oil were excluded from the dietary regimens of groups3 and 4.

Crypt cell proliferation rate assay

At intervals of 2, 4 and 8 wk, 6 animals from the experimental and control groups were given 1 mg/kg of colchicine intraperitoneally. The tissue samples were excised from different parts of the large intestine. The number of arrested metaphases increased with time after injection. To prevent variation in the kinetic results due to diurnal changes[25], in each group, the first animal was killed 30 min after injection with colchicine and thereafter one animal was killed every 15 min up to 90 min. Three segments were taken viz., cecum, ascending colon, and descending colon. Fixing of the segments was carried out with glacial acetic acid for 24 h and stored in 750 mL/L ethanol. For measurement of the crypt cell proliferation rate, the tissue specimens were rehydrated on an alcohol gradient and hydrolyzed in 1 N HCl for 10 min and stained using periodic acid Schiff's reagent. The focal areas of crypts exhibiting abnormal characteristics were microscopically dissected and squashed under cover slips. The number of arrested metaphases was counted in ten crypts per sample. The mean metaphase count per crypt was plotted against the time that the samples were taken (five points, 30 to 90 min). A linear regression curve was drawn for each site in each group, and from the slope of the graph mean CCPR/crypt/h was calculated and plotted.

^{3}H-Thymidine incorporation assay

Control and experimental animals (six in each) after 2, 4 and 8 wk of experimental period were taken for this assay. For the determination of [^{3}H]-dThd into DNA, 100 µci/kg body weight of [^{3}H]-dThd (3H-(methyl) thymidine; specific activity

18 μci/mmole) was injected intraperitoneally to the animals of experimental and control groups. Animals were sacrificed by cervical dislocation after 3 h of injection of [^{3}H]-dThd. The three colonic segments were excised and placed in saline at 4 ℃. During the analysis, the mucosa was scraped and DNA content was extracted and counted as described previously[26-28]. The results are represented as counts per minute (cpm) per μg DNA.

Measurement of SCFAs and lactate

Colonic contents were collected at respective intervals from 6 animals in each group. The contents were acidified with 500 mL/L sulphuric acid solution. The solution was then extracted with 2 mL ether and 1 μL of the extract was injected into a capillary column containing a column stationary phase of 10% fatty acids, of 30 m long (inner diameter: 0.32 mm, thickness: 0.5 μm, split, 1:80). A Hewlett Packard gas chromatograph (Model 6890) equipped with a flame ionization detector was used. A column temperature of 70 ℃ and a detector temperature of 230 ℃ were used. Peaks of SCFAs were confirmed by running known standards under similar conditions. Integration of the peaks was carried out using the HP 3389A software; values are represented as percentage distribution of each SCFA in the profile. Lactate levels in the control and experimental samples were measured by UV- enzymatic method as described in the commercial kit (Boehringer, Mannheim, Germany) and calculated as μmol/g wet content by establishing the standard curve.

Enzymatic analysis

In this study, activities of mitochondrial succinate dehydrogenase (SDH), brush border dipeptidyl amino peptidase IV (DAP IV) and lysosomal acid β-galactosidase (acid β-gal) were measured by histochemical quantitation (Table 3). Colon tissues were removed and cut opened longitudinally and washed thoroughly with physiological saline. Serial 10 μm cryostat sections of the colon tissues were mounted on the cover slips. Histochemical quantitation of the enzymes was carried out using specific substrate solutions and stains according to the established procedures[29-31].

Statistical analysis

In the calculation of CCPR, linear regression analysis was carried out to determine the correlation coefficient. The standard deviations of the slopes were also calculated but, as is normal practice in this analysis, they were not quoted[32]. Cell kinetics data between each experimental group and the control group for each segment were compared for statistical significance using two tailed Student's *t*-test. Chi-square test was applied to determine the significance of counts of tritiated thymidine incorporation into DNA. ANOVA was employed for calculating the statistical significance of the means of SCFA and lactate levels obtained for the experimental and control groups. Histochemical analysis was performed on rank data as low (1), moderate (2), and high (3) levels of staining. ANOVA was used to get the statistical significance with respect to the colonic segments and treatment groups. Statistical analyses were also aided by MicroCal Origin software (version 2.9, USA).

RESULTS

CCPR assay

Linear regression curve (Figure 1) was drawn by taking the mean number of cells produced at five different time intervals, 30 min after the administration of colchicine. It might be noted that each CCPR/crypt/h measurement at different sites at their specific exposure levels was carried out in a similar manner. Figures 2A, B, C show the crypt cell production rate in cecum, ascending colon and descending colon tissues isolated from the experimental and normal animals at wk 2, 4, and 8. It was observed that the rate of cell proliferation in the TI-supplemented group was approximately equal to its normal counterpart, up to 4 wk in all the three segments of GIT. Combination of TI and saturated fat (TIFB) did not influence the production of cells significantly at wk 2 in all the tissue sections. However, at four weeks of study, this group had a significantly greater rate of cell production compared to the controls. While for the OB treated animals, influence of obese condition on the production rate of crypt cells in the presence of TIFB-supplemented diet was evidently significant in all the three segments four weeks onwards.

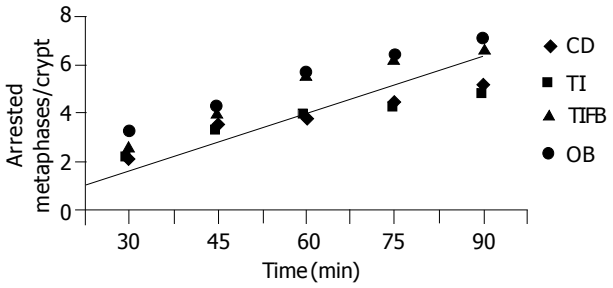

Figure 1 Linear relationship of metaphase arrest to time used to calculate CCPR.

[^{3}H]-dThd incorporation assay

Figures 3A, B, C demonstrate the amount of [^{3}H] - dThd incorporation into the colonocyte DNA of cecum, ascending and descending colon tissues at three different exposure levels. At wk 8, the OB animals exhibited a significantly increased incorporation in the mucosa obtained from all three segments followed by TIFB-treated group in comparison to their normal counterparts. However, on a par with the analysis of CCPR, TI-fed animals presented reduced levels of incorporation in all three tissue sections up to 4 wk. Nevertheless this group was indicated to incorporate significant numbers of radiolabeled precursor in the colonocyte DNA of ascending and descending segments at eight weeks as compared to controls.

Table 3 Activities of succinate dehydrogenase, acid-B- galactosidase and dipeptidyl amino peptidase IV (values are expressed as absorbance units, mean±SE; n = 6)

Enzymes	Crypt segments	CD	TI	TIFB	OB
SDH	Luminal epithelium	0.596±0.053	0.533±0.038	0.512±0.053[a]	0.524±0.067[a]
DAP IV	Luminal epithelium	0.178±0.027	0.163±0.008	0.156±0.019	0.125±0.014[a]
	Basal crypt epithelium	0.196±0.012	0.179±0.003	0.162±0.005	0.151±0.030
Acid-β-Gal	Luminal epithelium	0.526±0.046	0.443±0.035	0.381±0.028[a]	0.314±0.029[a]
	Basal crypt epithelium	0.592±0.061	0.527±0.036	0.493±0.058	0.397±0.011[b]
	Apical crypt epithelium	0.863±0.067	0.639±0.057[c]	0.587±0.009[c]	0.452±0.065[c]

[a]P<0.05 *vs* CD in the crypt segment of luminal epithelium; [b]P<0.01 *vs* CD in the crypt segment of basal crypt epithelium; [c]P<0.05 *vs* CD in the crypt segment of apical crypt epithelium.

Fermentation profile

TI - *per se* fed animals showed a significant decrease in the levels of butyrate and lactate at 8 wk, in the ascending and descending colon segments, while there was no significant change at 2 and 4 wk of exposure (Figure 4). Acetate and propionate were as equal as that of control samples. However, insignificant changes were observed in the cecum tissue of TI -fed animals compared to control group with regard to all of these SCAFs. The TIFB-and OB-induced groups produced significantly increased amount of lactate in the two colon segments, whereas, the cecum tissues of these groups producd more propionate and butyrate. Acetate concentrations in all the three segments from these two treated groups were not altered. The changes in these two groups were significant at 4 wk and increases continued thereafter.

In the cecum, lactate concentrations in the animals of control and experimental groups showed a positive correlation with other SCFAs, indicating the fate of microbial content of the mucosa at different dietary exposures (Figure 5). TI fed group showed an insignificant change in its lactate content compared to that of controls at 2 wk. While this group showed a significant elevation in the levels of lactate at wk 4 and 8 ($P<0.004$ and $P<0.016$, respectively). Ascending and descending colon tissues showed elevated lactate concentrations at 2 wk ($P<0.047$, and $P<0.002$, respectively). However, decreased lactate production was evident in these two segments later on (P = NS). The results were attributed to the amount of starch that escaped digestion producing high lactate at about 2 wk. The animals were seemed to get acclimatized to the dietary conditions thereafter. Upon analysis of the same samples isolated from the other two groups, viz., TIFB and OB, there seemed to be a significant production of lactate from 4 wk onwards in all the three segments indicating a close association with the high acetate levels (about 73%) and propionate levels (around 45% in the cecum specifically) found in these experimental animals.

Enzyme activities

The selection of the three enzymes was dependent upon the occurrence of these enzymes in colonic crypts. The distribution of these enzymes in the crypt follows a function-specific pattern. The activity of succinate dehydrogenase is pronounced in the luminal epithelium of the colonic crypt, whereas the basal epithelium contains DAP IV activity and the activity of acid β-gal occupies the apical crypt at a high level. Distribution of reactive DAP IV is also seen in the luminal crypt. Similarly, a moderate level distribution of acid β-gal is seen in the luminal and basal portions of the colonic crypt[33]. Histochemical analysis of the enzymes indicated a gross decrease in the activities of all the three enzymes along the entire large intestine suggesting impaired metabolic activities of the colonic mucosa, due in part to the dietary exposures. The effect was more prominent when observed critically in the OB - group, as there was an additive influence of TIFB in association with obese condition. Distribution patterns of enzyme activities in the tissue sections of cecum region of TI *per se* - treated group did not reveal much variation in their activities at all the three time points. However, in combination with other two factors, viz., FB and OB, it was shown to have an impact as a positive stimulator. There was of course, a reduction of enzyme activities observed in the other two segments after 4 wk of treatment with TI.

DISCUSSION

Our investigation has shown that dietary factors had a significant impact on large intestine of experimental animals. It was critically noted that all the parameters included in this study were dependent on each other. Generally, epithelial restitution is a basic physiologic response elicited against any kind of mucosal damage causing an insult to the epithelial layer. Rate of cell proliferation was increased in such instances and normal differentiated cells migrated towards and replaced the damaged epithelia. Crypt fission occurred under these conditions leading to increased numbers of crypts thereby stabilizing mode of spread of mutated clones in the mucosa[34]. Our findings go in parallel with the literature cited with respect to colonic epithelial cell proliferation. Crypt cell proliferation rate was increased in

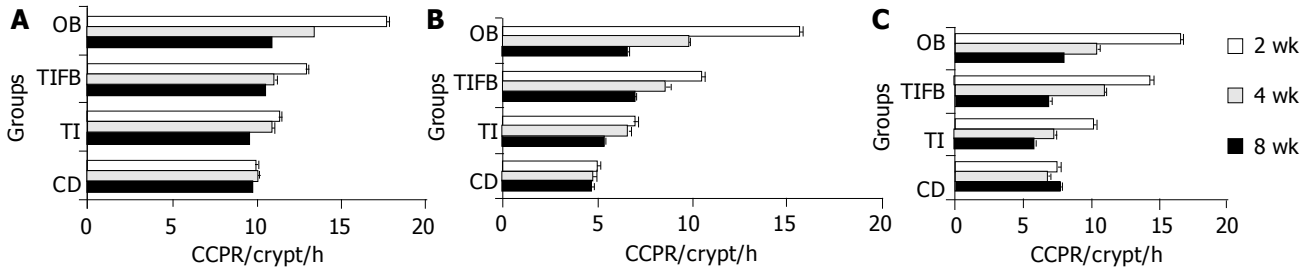

Figure 2 Crypt cell production rate/Crypt/h in caecum at (A), ascending colon (B) and descending colon (C) tissues isolated from experimental and control groups of animals (mean±SE) at 2, 4 and 8 wk treatment. Significance was seen between CD and the experimental groups TI, TIFB and OB.

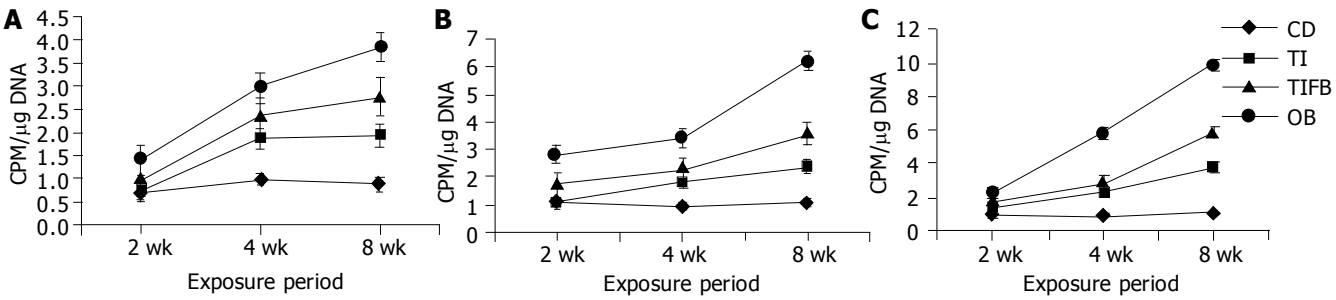

Figure 3 Incorporation of [^{3}H] – dThd into the DNA of cecum (A), ascending colon (B) and descending colon (C) tissues at different exposure periods in experimental and control groups (mean±SE). Significance was seen between CD and the experimental groups TI, TIFB and OB.

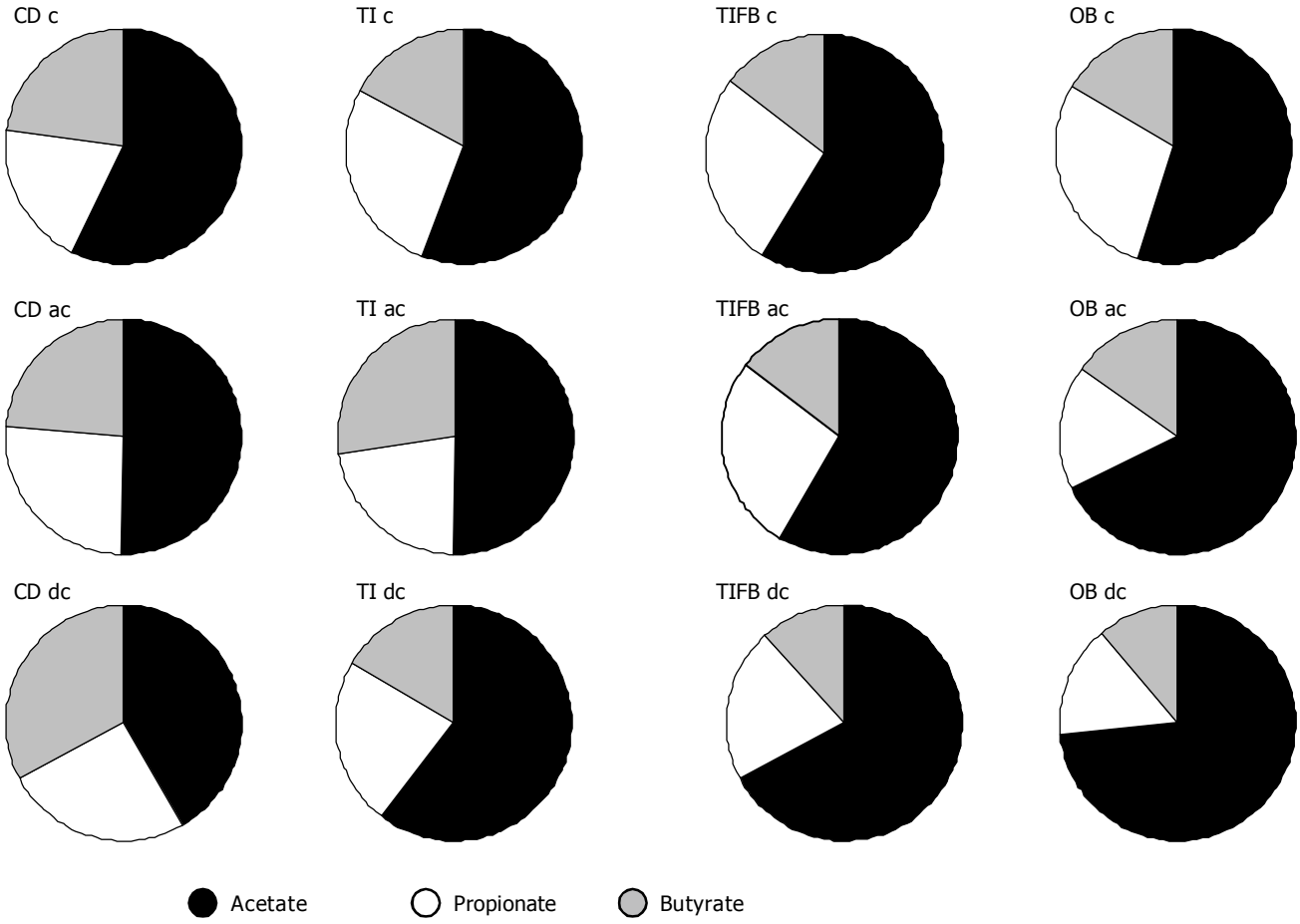

Figure 4 Mean (%) of acetic, propionic and butyric acids in the mucosal contents of cecum (c), ascending colon (ac) and descending colon (dc) tissue segments isolated from mice of CD, TI, TIFB and OB groups. Results were drawn from the total mean(%) distribution of SCFAs throughout the experimental period (n = 6).

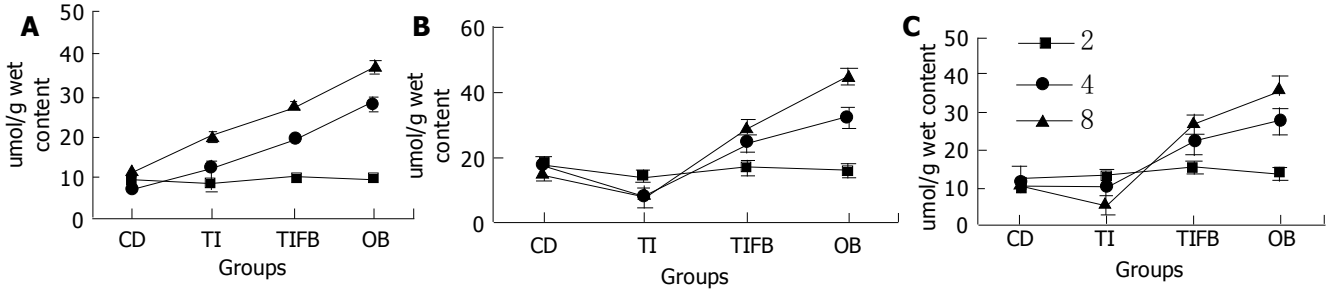

Figure 5 Levels of lactate in mice fed with various dietary factors in CD, TI, TIFB and OB groups for 2, 4 and 8 wk of test periods in the isolated cecum (A), ascending colon (B) and descending colon (C). Values are represented as μmol/g wet mucosal content, mean±SE.

all the three segments of OB- and TIFB- treated animals with a positive correlation with decreased levels of butyrate and enzyme activities. It was reported that butyrate acted as an inducer of apoptosis under *in vivo* conditions and in contrast it was implied as an inducer of cellular differentiation under *in vitro* conditions[35-37]. A biopsy obtained from human cecum showed a response to SCFA supplementation with an increase in cell proliferation when cultured *in vitro*[38]. In our study butyrate levels went down in the groups of TIFB and OB at an early stage compared to the TI- *per se* treated group and controls, leading to uncontrolled proliferation of mucosal epithelium. Earlier reports also suggested similar hypotheses[6,12]. It was also noted that distribution of mitotic cells (in OB and TIFB-treated groups) was seen in the upper 40% of the crypt, which was considered to be a sensitive biomarker of cancer risk[39].

Interestingly, in the present study, alterations in the colonic mucosa were evident due in part to the high digestible starch and acidic content of TI which might have affected the microfloral content of the colon as shown by altered short chain fatty acids profile and impaired enzyme profile, thereby aggravating the adverse effects of fatty diet and obese condition. Large bowel microfloral contents were found to be very low when the cecum and distal colon tissues were weighed in comparison to that of control tissues, as it is evident[40,41] that microbial digestion of the partially digested food that escape from the small intestine are ultimately digested by the microflora of the cecum (wherein the digested material stays for a maximum time period, approximately 4 h in the case of mouse). In addition, our suggested hypothesis is in agreement with the findings of McIntyre *et al*[42], who suggested the beneficial effects of

increased butyrate production in the large bowel due to consumption of fiber-enriched diet which helps protect the rat from developing colon cancer. In our study, lactate production showed an indifferent pattern of results with a close similarity to other SCFAs profiles. The profile indicated that the amount of lactate produced in the TIFB and OB - groups was a reflection to some extent of high bacterial glycolysis in combination with a high proliferative index of mucosal cells as noted with an increased CCP rate and radioactive labeling. Other reports of Fleming *et al*[43] and Caderni *et al*[44] also suggested these two phenomena in the mucosa under carcinogenic/pathological conditions induced by high fat diet.

Further, the rate of proliferation of the crypt epithelium and radiolabeled precursor incorporated DNA content in the cells of colon tissues isolated from OB and TIFB - fed groups, were increased in a linear fashion from 4 to 8 wk . It is speculated that both physiological and biochemical parameters seem to be affected significantly after 4 wk attributing to the fact that acclimatization of animals to their respective diets *ad libitum* might take nearly 2 wk. Previous reports also supported our findings that *ad libitum* feeding of high-fat diet enhanced formation of aberrant crypt/ foci in experimental animals after four weeks[45-47]. Patients with familial polyposis coli, clinically manifested in association with obesity, have been indicated to have increased thymidine - labeled cells in the upper third of the morphologically normal crypt[45]. It was demonstrated by another scientific group that specified pathogen-free gut conditions might have a positive impact on the development of polyps[48]. Association of fatty diet consumption and obesity has been studied extensively[5]. Ogus *et al*[49] have described that high fat diet - induced obesity in normal and transgenic mice results in an increase in body weight and decrease in energy expenditure thus establishing a leptin - resistant state. High fat intake rich in saturated fatty acids promotes colon cancer risk in azoxy methane (AOM) - induced rats.

On the other hand, TI - treated group showed an insignificant correlation between CCPR and thymidine labeling at four weeks, supporting the hypothesis that DNA synthesizing cells remain microscopically unaltered[50,51]. A further continuation of DNA synthesis in those cells in which it normally ceased was the earliest and most reliable pathological sign of the commencement of neoplastic alterations[52], as we have observed in the OB and TIFB - treated groups, suggesting that obesity and fatty diet influenced the intensity of response to TI. It was likely that the colonocytes of TI- *per se* treated group stayed in phase I, according to Lipkin[53] wherein, cells remained microscopically normal and moved towards medial two thirds of the crypt, and in TIFB- and OB- treated groups, the cells stayed in phase II stage, wherein proliferating cells were not shed into the lumen and, due to inadequate suppression of the DNA synthesis, accumulated in the mucosa, leading to neoplastic transformation.

Observations of a highly significant reduction of SDH levels in OB and TIFB - treated animals could be attributed to the fact that the exposures to TI and FB of normal and obese animals might have caused damage to the mitochondrial membrane and impaired the aerobic metabolism and electron transport chain in the mitochondria[54]. Further, attenuation and dispersal of cell organelles were affected due to fusion of cells during proliferation. This may also lead to decreased enzyme activities[55].

Dipeptidyl amino peptidase IV is a brush border enzyme. It plays an important role perhaps, together with other amino peptidases, in the final digestion of nutritional constituents[56]. Dipeptidyl aminopeptidase liberates dipeptides from the amino terminal end of the polypeptides, derived from other digestive enzymes such as trypsin, chymotrypsin and pepsin. Transport of these amino acids as well as dipeptides is done by the brush border hydrolases, therefore known as carriers[57,58]. A decrease in such an enzyme activity as observed in this study might lead to an increase in the intracellular amino acids pool. In addition, obesity induction has been found to be associated with alterations in the cholesterol and membrane bound- lipid components[59]. We, therefore, suggested that altered membrane fluidity due in part to the effects of TI and FB, might have affected the glycoprotein constituents of the cell membrane resulting in decreased peptidase activity. A similar pattern of reduction in the activity of acid β-galactosidase has been observed in the entire crypt segment, the reduction of this enzyme was found to be more pronounced in the apical crypt epithelium, with respect to TIFB treatment and OB induction. Literature evidenced[60] that cellular membrane damage caused release of lysosomal enzymes into the blood stream, leading to an insult to the cellular integrity.

Finally, our design involved a multifactorial exposure to dietary components of either sex of animals. It excluded typical chemical inducers to cause genetic susceptibility. In addition, we employed a method of inducing obesity with MSG, so as to relate with the realistic regular human diets constituted with this typical flavoring agent, classified as a non-nutritional factor by World Health Organization[61]. Apart from the probable mechanisms so far discussed, there might be some other parameters, such as intestinal enzyme activities and gross metabolic alterations, detailed studies on these aspects have been carried out and results are yet to be communicated.

ACKNOWLEDGEMENTS

Thanks are due to Professor S. Govindasamy, our former Head, Department of Biochemistry and Molecular Biology, University of Madras, Guindy Campus, Chennai - 600025 India.

REFERENCES

1 **Deng DJ.** Progress of gastric cancer etiology: *N*-nitrosamides 1999s. *World J Gastroenterol* 2000; **6**: 613-618
2 **O'Brien H,** Mathew JA, Gee JM, Watson M, Rhodes M, Speakman CT, Stebbings WS, Kennedy HJ, Johnson IT. K-ras mutations, rectal crypt cells proliferation and meat consumption in patients with left-sided colorectal carcinoma. *Eur J Cancer Prev* 2000; **9**: 41-47
3 **Giovannucci E.** Obesity, gender, and colon cancer. *Gut* 2002; **51**: 147
4 **Kaaks R,** Lukanova A. Effects of weight control and physical activity in cancer prevention: role of endogenous hormone metabolism. *Ann N Y Acad Sci* 2002; **963**: 268-281
5 **Woods SC,** Seeley RJ, Rushing PA, D'Alessio D, Tso P. A controlled high-fat diet induces an obese syndrome in rats. *J Nutr* 2003; **133**: 1081-1087
6 **Saglam K,** Aydur E, Yilmaz M, Goktas S. Leptin influences cellular differentiation and progression in prostate cancer. *J Urol* 2003; **169**: 1308 -1311
7 **Rock CL,** Demark-Wahnefried W. Can lifestyle modification increase survival in women diagnosed with breast cancer? *J Nutr* 2002; **132**: 3504S-3507S
8 **Reddy BS,** Hedges AR, Laakso K, Wynder EL. Metabolic epidemiology of large bowel cancer: fecal bulk and constituents of high-risk North American and low-risk Finnish population. *Cancer* 1978; **42**: 2832–2838
9 **Terry PD,** Miller AB, Rohan TE. Obesity and colorectal cancer risk in women. *Gut* 2002; **51**: 191–194
10 **Nelson DE,** Bland S, Powell-Griner E, Klein R, Wells HE, Hogelin G, MarkS JS. State trends in health risk factors and receipt of clinical preventive services among US adults during the 1990 s. *JAMA* 2002; **287**: 2659-2667
11 **Deslypere JP.** Obesity and cancer. *Metabolism* 1995; **44**: 24–27
12 **Weber RV,** Stein DE, Scholes J, Kral JG. Obesity potentiates AOM- induced colon cancer. *Dig Dis Sci* 2000; **45**: 890–895
13 **Alfieri M,** Pomerleau J, Grace DM. A comparison of fat intake of normal weight, moderately obese and severely obese subjects.

Obes Surg 1997; **7**: 9 -15
14 **Manjunath MN,** Sattigeri VD, Rama Rao SN, Udah Rani M, Nagaraja KV. Physico-chemical composition of commercial tamarind powder. *Indian Food Packer* 1991; **45**: 39-42
15 **Shankaracharya NB.** Tamarind–chemistry, technology and uses–A critical appraisal. *J Food Sci Tech Mysore* 1988; **35**: 193-203
16 **Mustapha A,** Yakasai IA, Aguye IA. Effect of Tamarindus indica L. on the bioavailability of aspirin in healthy human volunteers. *Eur J Drug Metab Pharmacokinet* 1996; **21**: 223-226
17 **Kobayashi A,** Adenan MI, Kajiyama S, Kanzaki H, Kawazu K. A cytotoxic principle of Tamarindus indica, di-n-butyl malate and the structure-activity relationship of its analogues. *Z Naturforsch C* 1996; **51**: 233–242
18 **Poulsen M,** Molck AM, Thorup I, Breinholt V, Meyer O. The influence of simple sugars and starch given during pre- or post-initiation on aberrant crypt foci in rat colon. *Cancer Lett* 2001; **167**: 135–143
19 **Le Leu RK,** Brown IL, Hu Y, Young GP. Effect of resistant starch on genotoxin-induced apoptosis, colonic epithelium, and lumenal contents in rats. *Carcinogenesis* 2003; **24**: 1347-1352
20 **Le Leu RK,** Hu Y, Young GP. Effects of resistant starch and nonstarch polysaccharides on colonic luminal environment and genotoxin-induced apoptosis in the rat. *Carcinogenesis* 2002; **23**: 713–719
21 **Block G,** Patterson B, Subar A. Fruit, vegetables, and cancer prevention: a review of the epidemiological evidence. *Nutr Cancer* 1992; **18**: 1-29
22 **Patterson BH**, Block G. Food choices and the cancer guidelines. *Am J Public Health* 1988; **78**: 282-286
23 **Bunyan J,** Murrell EA, Shah PP. The induction of obesity in rodents by means of monosodium glutamate. *Br J Nutr* 1976; **35**: 25-39
24 **Report of the American Institute of Nurtition ad hoc Committee on Standards for Nutritional Studies**. *J Nutr* 1977; **107**: 1340–1348
25 **Deschner EE,** Lipkin M. In: Gastrointestinal tract cancer. Ed: Lipkin M, Good RA. *Sloane kettering Institute, Cancer Series, New York* 1978: 14
26 **DeRubertis FR,** Craven PA, Saito R. Role of prostaglandins in bile salt-induced changes in rat colonic structure and function. *J Clin Invest* 1984; **74**: 1614-1624
27 **Burton K.** A study of the conditions and mechanism of the diphenylamine reaction for the colorimetric estimation of deoxyribonucleic acid. *Biochem J* 1956; **62**: 315-323
28 **Kornblum HI**, Loughlin SE, Leslie FM. Effects of morphine on DNA synthesis in neonatal rat brain. *Brain Res* 1987;**428**:45-52
29 **Pearse AGE.** Histochemistry, Theoritical and applied. Third edition. *Churchill Livingstone London* 1972; **2**: 1342-1343
30 **Gossrau R.** Splitting of naphthol AS-BI beta-galactopyranoside by acid beta-galactosidase. *Histochemie* 1973; **37**: 89–91
31 **McDonald JK,** Schwabe C. In: Proteinases in mammalian cells and tissues, *North Holland, Amsterdam* 1977: 311
32 **Goeting N,** Trotter GA, Cooke T, Kirkham N, Taylor I. Effect of warfarin on cell kinetics, epithelial morphology and tumour incidence in induced colorectal cancer in the rat. *Gut* 1985; **26**: 807-815
33 **Sandforth F,** Heimpel S, Balzer T, Gutschmidt S, Riecken EO. Characterization of stereomicroscopically identified preneoplastic lesions during dimethylhydrazine-induced colonic carcinogenesis. *Eur J Clin Invest* 1988; **18**: 655-662
34 **Wright NA.** Epithelial stem cell repertoire in the gut: clues to the origin of cell lineages, proliferative units and cancer. *Int J Exp Pathol* 2000; **81**: 117-143
35 **Sakata T.** Stimulatory effect of short-chain fatty acids on epithelial cell proliferation in the rat intestine: a possible explanation for trophic effects of fermentable fibre, gut microbes and luminal trophic factors. *Br J Nutr* 1987; **58**: 95–103
36 **Whitehead RH,** Young GP, Bhathal PS. Effects of short chain fatty acids on a new human colon carcinoma cell line (LIM1215). *Gut* 1986; **27**: 1457-1463
37 **Cummings JH.** Colonic absorption: the importance of SCFAs in man. *Scand J Gastroenterol Suppl* 1984; **93**: 117-131
38 **Samelson SL,** Nelson RL, Nyhus LM. Protective role of faecal pH in experimental colon carcinogenesis. *J R Soc Med* 1985; **78**: 230-233
39 **Barthold SW.** Relationship of colonic mucosal background to neoplastic proliferative activity in dimethylhydrazine-treated mice. *Cancer Res* 1981; **41**: 2616-2620
40 **Goodlad RA,** Ratcliffe B, Fordham JP, Wright NA. Does dietary fibre stimulate intestinal epithelial cell proliferation in germ-free rats? *Gut* 1989; **30**: 820-825
41 **Folino M,** McIntyre A, Young GP. Dietary fibers differ in their effects on large bowel epithelial proliferation and fecal fermentation-dependent events in rats. *J Nutr* 1995; **125**: 1521-1528
42 **McIntyre A,** Gibson PR, Young GP. Butyrate production from dietary fibre and protection against large bowel cancer in a rat model. *Gut* 1993; **34**: 386-391
43 **Fleming SE,** Fitch MD, De Vries S. The influence of dietary fiber on proliferation of intestinal mucosal cells in miniature swine may not be mediated primarily by fermentation. *J Nutr* 1992; **122**: 906-916
44 **Caderni G,** Stuart EW, Bruce WR. Dietary factors affecting the proliferation of epithelial cells in the mouse colon. *Nutr Cancer* 1988; **11**: 147-153
45 **Lupton JR,** Coder DM, Jacobs LR. Influence of luminal pH on rat large bowel epithelial cell cycle. *Am J Physiol* 1985; **249**: G382-G388
46 **Freeman HJ,** San RH. Use of unscheduled DNA synthesis in freshly isolated human intestinal mucosal cells for carcinogen detection. *Cancer Res* 1980; **40**: 3155-3157
47 **Reddy BS,** Wang CX, Maruyama H. Effects of restricted caloric intake on azoxymethane-induced colon tumor incidence in wale f344 rats. *Cancer Res* 1987; **74**: 1226-1228
48 **Rasmussen RE,** Boyd CH, Dansie DR, Kouri RE, Henry CJ. DNA replication and unscheduled DNA synthesis in lungs of mice exposed to cigarette smoke. *Cancer Res* 1981; **41**: 2583-2588
49 **Ogus S,** Ke Y, Qiu J, Wang B, Chehab FF. Hyperleptinemia precipitates diet-induced obesity in transgenic mice overexpressing leptin. *Endocrinology* 2003; **144**: 2865-2869
50 **Deschner EE,** Lipkin M. Study of human rectal epithelial cells *in vitro*. III. RNA, protein, and DNA synthesis in polyps and adjacent mucosa. *J Natl Cancer Inst* 1970; **44**: 175-185
51 **Lieb LM,** Lisco H. *In vitro* uptake of tritiated thymidine by carcinoma of the human colon. *Cancer Res* 1966; **26**: 733-740
52 **Zhuang XQ,** Yuan SZ, Wang XH, Lai RQ, Luo ZQ. Oncoprotein expression and inhibition of apoptosis during colorectal tumorigenesis. *China Nati J New Gastroenterol* 1996; **2**: 3-5
53 **Lipkin M.** Proliferative changes in the colon. *Cancer Suppl* 1974; **34**: 878-888
54 **Borthwick GM,** Johnson MA, Ince PG, Shaw PJ, Turnbull DM. Mitochondrial enzyme activity in amyotrophic lateral sclerosis: implications for the role of mitochondria in neuronal cell death. *Ann Neurol* 1999; **46**: 787-790
55 **Maskens AP,** Dujardin-Loits RM. Experimental adenomas and carcinomas of the large intestine behave as distinct entities: most carcinomas arise de novo in flat mucosa. *Cancer* 1981; **47**: 81-89
56 **Gutschmidt S,** Gossrau R. A quantitative histochemical study of dipeptidylpeptidase IV (DPP IV). *Histochemistry* 1981; **73**: 285-304
57 **Ward PE,** Sheridan MA, Hammon KJ, Erdos EG. Angiotensin I converting enzyme (kininase II) of the brush border of human and swine intestine. *Biochem Pharmacol* 1980; **29**: 1525-1529
58 **Matthews DM,** Adibi SA. Peptide Absorption. *Gastroenterology* 1976; **71**: 151-161
59 **Reynier M,** Sari H, d'Anglebermes M, Kye EA, Pasero L. Differences in lipid characteristics of undifferentiated and enterocytic-differentiated HT29 human colonic cells. *Cancer Res* 1991; **51**: 1270-1277
60 **Kyriacou K,** Garrett JR. Histochemistry of hydrolytic enzymes in resting submandibular glands of rabbits. *Histochem J* 1985; **17**: 683-698
61 **Robert HR.** In: Food Safety. Ed: Roberts Hr, *New York Wiley* 1999: 239

Edited by Wang XL and Zhu LH

PO Box 2345, Beijing 100023, China
Fax: +86-10-85381893
E-mail: wjg@wjgnet.com www.wjgnet.com

ELSEVIER

World J Gastroenterol 2005;11(2):249-254
World Journal of Gastroenterology ISSN 1007-9327

• BASIC RESEARCH •

Expression of sialyl Lewis^a relates to poor prognosis in cholangiocarcinoma

Apa Juntavee, Banchob Sripa, Ake Pugkhem, Narong Khuntikeo, Sopit Wongkham

Apa Juntavee, Sopit Wongkham, Department of Biochemistry, Faculty of Medicine and Liver Fluke and Cholangiocarcinoma Research Center, Khon Kaen University, Khon Kaen, 40002, Thailand
Banchob Sripa, Department of Pathology, Faculty of Medicine and Liver Fluke and Cholangiocarcinoma Research Center, Khon Kaen University, Khon Kaen, 40002, Thailand
Ake Pugkhem, Narong Khuntikeo, Department of Surgery, Faculty of Medicine and Liver Fluke and Cholangiocarcinoma Research Center, Khon Kaen University, Khon Kaen, 40002, Thailand
Supported by research grants of Faculty of Medicine (#I46007), and Graduate School (#4432201), Khon Kaen University, Thailand
Co-first-authors: Apa Juntavee and Sopit Wongkham
Co-correspondents: Banchob Sripa
Correspondence to: Dr. Sopit Wongkham, Department of Biochemistry, Faculty of Medicine, Khon Kaen University, Khon Kaen, 40002, Thailand. sopit@kku.ac.th
Telphone: +66-43-348386 **Fax:** +66-43-348375
Received: 2004-06-24 **Accepted:** 2004-07-17

Abstract

AIM: High levels of serum sialyl Lewis^a (sLe^a) are frequently found in cholangiocarcinoma (CCA) patients and have been suggested to be a serum marker for CCA. However, the significance of this antigen in CCA is unknown. In this study, the clinical significance of sLe^a expression in CCA tissues and the possible role of sLe^a in vascular invasion *in vitro* were elucidated.

METHODS: Expression of sLe^a in tumor tissues of 77 patients with mass-forming CCA and 33 with periductal infiltrating CCA was determined using immunohistochemistry. The *in vitro* assays on adhesion and transmigration of CCA cells to human umbilical vein endothelial cells were compared between CCA cell lines with and without sLe^a expression.

RESULTS: sLe^a was aberrantly expressed in 60% of CCA tumor tissues. A significant relationship was found between the frequency of sLe^a expression and the mass-forming type CCA (P = 0.041), well differentiated histological grading (P = 0.029), and vascular invasion (P = 0.030). Patients with positive sLe^a expression had a significantly poorer prognosis (21.28 wk, 95% CI = 16.75-25.81 wk) than those negative for sLe^a (37.30 wk, 95% CI = 27.03-47.57 wk) (P<0.001). Multivariate analysis with adjustment for all covariates showed that patients positive for sLe^a possessed a 2.3-fold higher risk of death than patients negative for sLe^a (P<0.001). The role of sLe^a in vascular invasion was demonstrated using *in vitro* adhesion and transmigration assays. KKU-M213, a human CCA cell-line with a high expression of sLe^a, adhered and transmigrated to IL-1β-activated endothelial cells of the human umbilical vein more than KKU-100, the line without sLe^a expression (P<0.001). These processes were significantly diminished when the antibodies specific to either sLe^a or E-selectin were added to the assays (P<0.001).

CONCLUSION: This study demonstrates the clinical significance of sLe^a expression in vascular invasion, and an unfavorable outcome in CCA. The role of sLe^a in vascular invasion which may lead to poor prognosis is supported by the *in vitro* adhesion and transmigration studies.

Key words: Cholangiocarcinoma; Sialyl Lewis^a; Poor prognosis

Juntavee A, Sripa B, Pugkhem A, Khuntikeo N, Wongkham S. Expression of sialyl Lewis^a relates to poor prognosis in cholangiocarcinoma. *World J Gastroenterol* 2005; 11(2): 249-254
http://www.wjgnet.com/1007-9327/11/249.asp

INTRODUCTION

Metastasis spreads malignant cells from a primary tumor throughout the body resulting in growth of secondary tumors in other tissues or organs. The ability of disseminated cancer cells to re-establish themselves is regulated by a combination of factors, including access to microvasculature and host-tumor cell interaction[1]. Attachment to vascular endothelia is the start of the metastatic cascade and evidence suggests that attachment precedes, and is required for, tumor cell extravasation and subsequent invasion into the target organ parenchyma[2]. Organ-specific receptors have been identified on the luminal surface of microvascular endothelia, specifically recognized by tumor cell ligands, thereby facilitating tumor cell arrest and transmigration into the extravascular space.

Sialyl Lewis^a (sLe^a) antigen, discovered by Koprowski *et al*[3] with the use of monoclonal antibody CA19-9, is a tetrasaccharide epitope (sialylated lacto-N-fucopentaose II) on the tumor cell membrane which may have a role in cancer dissemination[4,5]. There is evidence that sLe^a expressed on tumor cells plays an important role in the adhesion of tumor cells to E-selectin on endothelial cells in the extravasation process[6,7]. Detection of sLe^a, in either tissue or pre- and post-operative serum is a prediction of increased cancer mortality[8]. The association of high levels of serum sLe^a with tumor invasion is common in cancer patients[5,9-11].

Cholangiocarcinoma (CCA), a bile duct cancer, is highly prevalent in Northeast Thailand[12]. Early stage CCA often goes undetected, most patients are diagnosed at an advanced or disseminated stage with a poor prognosis. High levels of serum sLe^a are frequently found in CCA patients and have been suggested to be a serum marker for CCA[13-17]. However, the role of sLe^a in CCA is unclear. We therefore evaluated the association of sLe^a expression in tumor tissues with the clinicopathology and survival of CCA patients. The role of sLe^a antigen in the adhesion and transmigration of human CCA cells to human umbilical vein endothelial cells (HUVEC) *in vitro* was demonstrated.

MATERIALS AND METHODS

Patients

Surgical specimens of 110 CCAs were obtained from the files of the Liver Fluke and Cholangiocarcinoma Research Center, Khon Kaen University, Thailand. The specimens were classified into 2 types: 77 cases of mass forming CCA and 33 cases of periductal infiltrating CCA. The mean age of patients was 55 years (range, 32 to 75 years). Seventy-two were males, and 31 were females. Informed consent was obtained from each subject and the Human Research Ethics Committee, Khon Kaen University, approved our research protocol. Cancer diagnosis was verified by histology with UICC TNM classification. Clinical follow-up was available for 104 (94.5%) of the patients. Survival of each CCA patient was recorded after surgery until May 15, 2001. Ninety-one patients (82.7%) died by the end of the follow-up period.

Human cholangiocarcinoma cell-lines and HUVECs

The two human cholangiocarcinoma cell-lines used (KKU-M213 and KKU-100) were from the Liver Fluke and Cholangiocarcinoma Research Center, Faculty of Medicine, Khon Kaen University, Thailand. The human umbilical vein endothelial cells (HUVECs) were from the American Type Culture Collection (Manassas, VA).

CCA cells were cultured in a HAM-F12 medium (Life Technologies, Rockville, MD) supplemented with 10% fetal calf serum, 100 U/mL penicillin, 100 μg/mL streptomycin and 2.5 μg/mL fungizone. sLe^a expression in CCA cell-lines was determined by immunocytochemistry using anti-CA19-9 antibody (Novocastra, Newcastle upon Tyne, UK). sLe^a was highly expressed in KKU-M213, more than 95% of cells had strong, positive staining. In contrast, KKU-100 cells showed no reaction (data not shown).

Immunohistochemical detection of sLe^a

All specimens were fixed in 10% neutral buffered formalin, embedded in paraffin, and cut into 4-μm-thick serial sections for immunohistochemical staining using avidin-biotin complex technique. Briefly, the paraffin sections were deparaffinized, hydrated and endogenous peroxidase-blocked with hydrogenperoxide. After non-specific staining was blocked with normal horse serum, the sections were incubated with 1:100 anti-sLe^a (anti CA19-9) overnight, followed by biotinylated anti-mouse IgG (Vector Laboratories, Burlingame, CA) and streptavidin-peroxidase (Vector). After washed, the sections were developed in 0.05% 3,3'-diaminobenzidine tetrahydrochloride (DAB; Sigma Chemical Co., St Louis, MO), counterstained with hematoxylin, dehydrated, cleared and mounted. When PBS was applied instead of the primary antibody, there was no positive staining.

The intensity of sLe^a expression was semi-quantitatively classified into 4 groups on the basis of the percentage of positive tumor cells: 0%, negative; 1-25%, +1; 26-50%, +2 and >50%, +3.

Adhesion assay

The adhesion assay procedure[18] was as follows. In briefly: HUVECs (2 to 5 passages) were grown in Kaighn's F12K medium, supplemented with endothelial cell growth supplement (Life Technologies, Rockville, MD) and seeded at 4×10^4 cells/well in a 96-well plate, pre-coated with 0.1% gelatin. The plate was then incubated at 37 ℃ in an atmosphere containing 50 mL/L CO_2 for 24 h. After activation of the rIL-1β (100 U/mL) (Life Technologies, Rockville, MD) for 4 h, the medium was removed and the cells were blocked with 1% bovine serum albumin complete media for 1 h.

Cell suspensions of KKU-M213 or KKU-100 (2×10^4 cells), in phosphate-buffered saline (PBS) with 1 mmol/L $CaCl_2$, were added to the HUVEC in each well and incubated for further 45 min. Unbound cells were removed by washing the wells with PBS. Adhered cells were fixed for 15 min with 2.5% glutaraldehyde, then stained with an antibody of 1:400 of pan-cytokeratin (Novocastra Lab, Newcastle upon Tyne, UK) and 1:100 horseradish peroxidase-conjugated goat anti-mouse IgG (Zymed Laboratories, South San Francisco, CA).

The cells that adhered to the HUVECs were counted by microscopy in nine low power fields (×100 magnification). Non-stimulated HUVECs were used as the controls. Triplicate assays were performed and at least two separate experiments were done.

Transmigration assays

A modified transmigration *in vitro* assay was performed as per Yoshida[19]. Approximately 8×10^4 HUVECs were plated on a 0.3-mg pre-coated-Matrigel-culture insert (Becton-Dickinson, San Jose, CA). The monolayer was activated with 100 U/mL IL-1β for 4 h. After blocked with 1% bovine serum albumin complete media for 1 h, 4×10^4 cells of KKU-M213 cells in PBS with 1 mmol/L $CaCl_2$ were added to each insert and incubated for 30 min. Cells on the upper face of the membrane were scraped using a cotton swab and cells on the lower face were fixed with 25% methanol for 15 min and stained with 0.5% crystal violet in 25% methanol. The number of migrated cells on the lower face of the filter was counted under microscopy in nine fields (×100 magnification). KKU-M213 cells incubated in the pre-coated-Matrigel insert without HUVECs were used as control. Assays were done in triplicate and repeated at least twice.

Inhibition of adhesion and transmigration by antibodies to sLe^a and anti-E-selectin

KKU-M213 cells were incubated with 50 μg/mL of anti-sLe^a monoclonal antibody (Chemicon International, Temecula, CA) for 30 min prior to the adhesion or transmigration assays. For HUVEC, a monolayer of activated HUVEC was pre-incubated with 10 μg/mL anti-human E-selectin (Santa Cruz Biotechnology, Santa Cruz, CA) at 37 ℃ for 15 min[7]. The excess anti-E-selectin was washed out with PBS before incubated with tumor cells in the adhesion or transmigration assays. The viability of treated cells determined using trypan blue exclusion dye was 96.86%, which was not significantly different from that of the non-treated sample.

Statistical analysis

Data were presented as mean±SD. The Student *t* test was used for comparisons and $P<0.05$ was considered statistically significant. The association of two categorical variables was analyzed by the χ^2-test or Fisher's exact probability test.

Survival of the patients was compared between the group with positive sLe^a antigen expression and the group with negative sLe^a antigen expression according the Kaplan-Meier method. The significance of the difference in survival between the 2 groups was tested by the log-rank test. Several clinicopathologic factors were subjected to univariate and multivariate analysis using the Cox proportional-hazard regression model. The relative risk of death was compared using the assessment of hazard ratio. Differences were considered statistically significant at $P<0.05$.

RESULTS

Expression of sLe^a and association with clinicopathologic features

By immunohistochemistry, sLe^a was constitutively expressed in normal biliary epithelial cells. It was localized at the apical surface, cytoplasm and/or stroma of CCA tissues (Figure 1).

The expression of sLe[a] was detected in 60% (66/110) of CCA patients. There were 79% (26/33) of periductal infiltrating CCA patients and 52% (40/77) of mass-forming CCA patients who expressed sLe[a] ($P = 0.015$) (Table 1).

The association of sLe[a] expression in CCA patients with clinico-pathologic features was determined. Three variables, mass-forming CCA, well differentiated adenocarcinoma histological grading and vascular invasion were statistically significant and were associated with the expression of tumor sLe[a] (Table 2).

Table 1 Expression of sLe[a] in tumor tissues of CCA patients

Expression of sLe[a]	Tumor type		Total
	Mass-forming	Periductal infiltrating	
0	37	7	44
1+	7	7	14
2+	8	6	14
3+	25	13	38
Total	77	33	110

Table 2 Correlation between expression of tissue sLe[a] and clinicopathologic features

		Expression of sLe[a]				*P*
		0	1+	2+	3+	
CCA type						
Mass-forming		37	7	8	25	0.041
Periductal-infiltrating		7	7	6	13	
Histology type						
Papillary		2	3	1	8	0.029
Well differentiated		8	5	6	14	
Moderately differentiated		8	3	4	5	
Poorly differentiated		19	2	0	9	
Squamous/adenosquamous		7	1	3	2	
Vascular invasion	- No	13	8	9	11	0.030
	- Yes	31	6	5	21	
Neural invasion	- No	27	8	4	14	0.054
	- Yes	17	6	10	24	
Lymphatic invasion	- No	9	5	2	9	0.560
	- Yes	35	9	12	29	

Correlation between sLe[a] expression and cumulative survival rate

Median overall survival in CCA patients with positive and negative sLe[a] expressions was 21.28 wk (95% CI = 16.75-25.81) and 37.30 wk (95% CI = 27.03-47.57), respectively. The survival rate of the patients with positive sLe[a] expression was significantly poorer than that of the patients with negative sLe[a] expression ($P = 0.021$, log-rank test, Figure 2). Well differentiated type CCA ($P = 0.027$) and the expression of sLe[a] ($P = 0.001$) were independently poor prognostic indicators contributing to disease-free survival of CCA (Table 3).

Table 3 Significant prognostic factors contributing to disease-free survival by multivariate Cox's proportion-hazard regression model

Variable	Coefficient	SE	Hazard ratio	*P*
Age (55 *vs* >55 yr)	-0.013	0.011	0.987	0.257
Sex (male *vs* female)	0.294	0.250	1.342	0.239
CCA type (mass-forming *vs* periductal-infiltrating)	0.440	0.322	1.552	0.173
Histology				
Papillary	-0.830	0.471	0.436	0.078
Well differentiated	-0.891	0.402	0.410	0.027
Moderately differentiated	-0.736	0.462	0.479	0.111
Poorly differentiated	-0.356	0.405	0.701	0.379
Squamous/adenosquamous	0.264	0.756	1.302	0.727
Vascular invasion (present *vs* absent)	-0.234	0.272	0.791	0.390
Neural invasion (present *vs* absent)	-0.362	0.247	0.696	0.143
Lymphatic invasion (present *vs* absent)	0.053	0.313	1.055	0.865
Tissue sLe[a] (present *vs* absent)	0.834	0.260	2.302	0.001

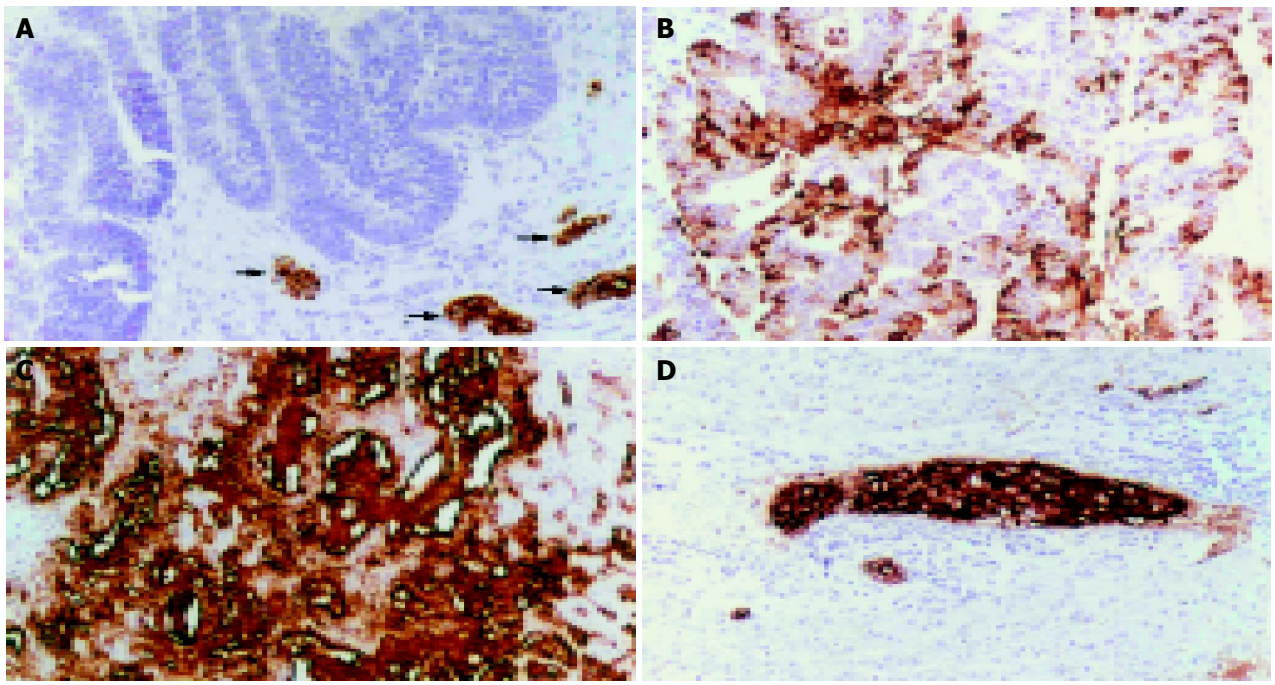

Figure 1 Immunohistochemical detection of sLe[a] in CCA. A: A CCA case with no sLe[a] expression in tumor but with positive staining in the normal bile ducts (arrows); B: and C: CCA cases with positive sLe[a], showing apical and stromal staining, respectively; D: Vascular metastasis of sLe[a] positive CCA cells. (Immunoperoxidase staining, original magnification ×100).

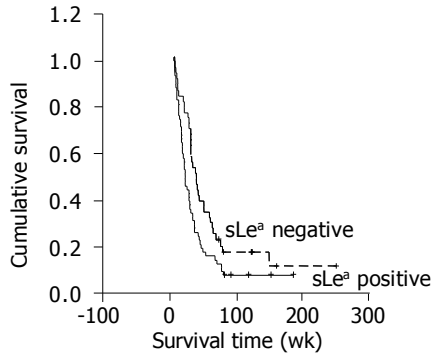

Figure 2 Correlation between expression and cumulative survival rate (Kaplan-Meier method). Patients who were positive for tumor sLe^a had a less favorable prognosis compared to those who were negative (P<0.001).

Role of sLe^a in adhesion and transmigration of CCA cell lines

The adhesion of CCA cells with high positive sLe^a expression (KKU-M213) was compared to that of CCA cells with negative sLe^a expression (KKU-100). The basal adhesion level of these two cell-lines to non-activated endothelial cells was not significantly different. However, in the cytokine-activated HUVECs, the adhesion of KKU-M213 cells was significantly greater than that of KKU-100 cells (P<0.001) (Figure 3). This finding was confirmed by the inhibition assay in which tumor cells were pre-treated with monoclonal antibodies for sLe^a before added to the HUVEC. The number of cancer cells that adhered to the rIL-1β activated HUVECs decreased to base levels, and was significantly less than that without anti-sLe^a (P<0.001) (Figure 3).

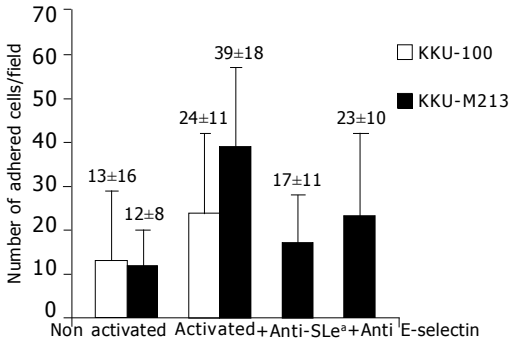

Figure 3 Adhesion of CCA cells to epithelial cells of the human umbilical vein endothelial cells (HUVEC). KKU-M213 or KKU-100 cells were incubated with non-activated or IL-1β activated HUVECs for 45 min at 37 ℃. The basal adhesion levels of KKU-100 and KKU-M213 to non-activated HUVECs were not statistically different, whereas the adhesion levels to activated HUVECs were significantly different (P<0.001). A significant difference occurred between the levels of KKU-100 and KKU-M213 adhesion to non-activated and IL-1β-activated HUVECs (P<0.001). The adhesion level of KKU-M213 significantly declined (P<0.001), when anti-sLe^a or anti E-selectin was added to KKU-M213 or IL-1β-activated HUVECs before the adhesion assay. The results were expressed as mean±SD of triplicate samples of a representative experiment.

To evaluate the contribution of E-selectin to the adhesion of CCA cells, adhesion assays of KKU-M213 to HUVECs were performed with and without rIL-1β-activation. rIL-1β had a clear stimulatory effect on the adhesion of cancer cells to HUVECs (Figure 3). The adhesion of KKU213 to rIL-1β-activated HUVECs was about 4-fold greater than that without activation (P<0.001). The significant contribution of E-selectin was confirmed by showing that incubation of the activated HUVECs with monoclonal antibody to E-selectin, before addition of cancer cells, clearly inhibited cell adhesion (Figure 3) (P<0.001). However, the number of adhered cells was still greater than the basal level (P<0.001).

The contributions of sLe^a and E-selectin to transmigration of KKU-M213 via the HUVECs were evident. The number of cancer cells that transmigrated through HUVEC was significantly reduced, when prior to the transmigration assay. The KKU-M213 cells were treated with anti-sLe^a (P<0.001) or the activated HUVECs were pre-treated with anti-E-selectin (P<0.001) (Figure 4). This observation was contributed mainly via transmigration of KKU-213 through the HUVECs since no KKU-213 cells or HUVECs migrated through the control insert within 30 min of incubation.

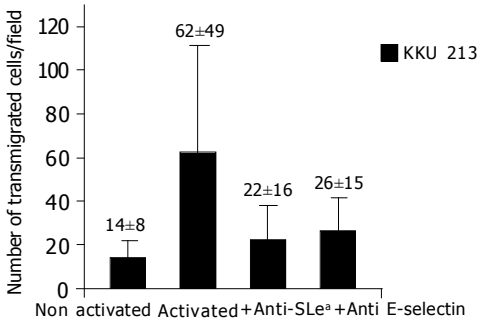

Figure 4 Contributions of sLe^a and E-selectin to transmigration of KKU-M213 to activated HUVECs. Transmigration of KKU-M213 was significantly reduced (P<0.001) when either sLe^a or E-selectin was blocked with specific corresponding antibodies before the transmigration assay. Experiments were carried out in triplicate. The mean±SD of a representative experiment and similar patterns was obtained in the two repeated experiments.

DISCUSSION

The present study demonstrated that 60% of CCA tumor tissues were aberrantly expressed sLe^a. The univariate analysis revealed mass-forming type CCA, well-differentiated histological type and presence of vascular invasion tumor associated with the expression of tumor sLe^a. Tsuji *et al*[15] and Minato *et al*[20] supported our immunohistology results that sLe^a was expressed in 60% of intrahepatic CCAs and the expression of sLe^a antigen was more frequent in well-differentiated adenocarcinoma cells. In addition, the high level of serum sLe^a (CA19-9) in CCA patients was recently demonstrated to be related to venous invasion, perineural invasion and lymph node metastases[14].

The multivariate analysis indicated the expression of tumor sLe^a as an independent prognostic factor affecting disease-free survival and overall survival. From our literature search, this appears to be the first report on the association of sLe^a expression with poor prognosis in CCA. Patients with positive sLe^a in tumor tissues had significantly shorter survival than those with negative sLe^a. Therefore, the presence of tumor sLe^a can be used as a prognostic risk factor related to survival of CCA patients and may help select patients with poor prognoses that can then be offered adjuvant therapy.

A key event in cancer metastasis is the transendothelial migration of tumor cells. This process involves multiple adhesive interactions between tumor cells and the endothelium. After adhering to the surface of endothelial cells, tumor cells must penetrate the endothelial junction. The contribution of sLe^a to the adhesion of tumor cells to endothelial cells via E-selectin has been observed in various cancer cell-lines[21-23]. In the present

study, the contribution of sLe[a] to vascular invasion was demonstrated not only by a statistical association analysis but also in the *in vitro* adhesion and transmigration assays of CCA cells to E-selectin-mediated human endothelial cells.

The role of sLe[a] in endothelial cell adhesion was assessed by comparing the adhesion levels of two CCA cell lines: one with a high expression of sLe[a] (KKUM213) and one with undetectable sLe[a] (KKU-100). These two cell lines had comparable basal adhesion to non-activated HUVECs. However, upon rIL-1β-activation, the number of cells adhering to the activated-HUVECs of KKU-M213 was significantly greater than that of KKU-100.

Our *in vitro* studies with KKU-M213 and KKU-100 had a low, but measurable basal adhesion to non-activated endothelial cells. Blocking-activated HUVECs with antibody to E-selectin did not completely keep adhesion at a basal level, suggesting the involvement of other, as yet unknown, carbohydrate ligands on CCA cells, and/or receptors on activated HUVECs, in the adhesion of these cell-lines.

The importance of sLe[a] to allow or enable attachment of CCA cells to endothelial cells has therefore been confirmed by the selective blocking of sLe[a] (marked reduction of adhesion of KKU-M213) by specific antibodies. Moreover, the treatment inhibited the binding of KKU-M213 to activated HUVECs close to the basal level obtained from KKU-M213, with non-activated HUVECs. The observation indicates that the KKU-M213 cells adhering to the activated HUVECs was mainly via sLe[a]. The same conclusion is drawn from the transmigration study.

Blocking either sLe[a] or E-selectin, with a specific neutralizing antibody, can inhibit adhesion and transmigration of CCA cells to endothelial cells, confirming the involvement of sLe[a] and E-selectin in these processes.

The sLe[a] antigen is expressed at trace levels in normal biliary cells but is expressed in a high level in tumor cells and can be detected as a tumor marker in serum. The increased serum level of sLe[a] in CCA has been reported ranging from 57 to 100%[13-16]. The discrepancies between various investigators might be due to the differences in etiology and incidence[24-29].

Several lines of evidence and our results point to the cancer-associated carbohydrate antigen, sLe[a], in the vascular invasion via the adhesion and transmigration of cancer cells to vascular endothelial cells. It may also contribute to the hematogenous metastasis of cancer and unfavorable outcome. SLe[a] is immunogenic and potentially a target for passive-and active-specific immunotherapy for human cancers in which the sLe[a] antigen could be expressed as a tumor-differentiation antigen[30]. CCA is a highly metastatic cancer with a poor prognosis. The association of sLe[a] expression with a poor prognosis in CCA and the contribution of sLe[a] to CCA-cell adhesion and transmigration via E-selectin-mediated HUVECs demonstrated in this study suggest the possible use of this ligand as a target for specific immunotherapy of CCA in the prevention of metastases, especially in patients with aberrant expression of sLe[a].

ACKNOWLEDGEMENTS

The authors thank Professor James Will, University of Wisconsin-Madison, for assistance with the English-language presentation of the manuscript.

REFERENCES

1 **Radinsky R**, Fidler IJ. Regulation of tumor cell growth at organ-specific metastases. *In Vivo* 1992; **6**: 325-331
2 **Brodt P.** Adhesion recrptors and proteolytic mechanisms in cancer invasion and metastasis. In: *Cell adhesion and invasion in cancer metastasis*, edited by Brodt P. Berlin: *Springer-Verlag* 1996: 167-242
3 **Koprowski H**, Steplewski Z, Mitchell K, Herlyn M, Herlyn D, Fuhrer P. Colorectal carcinoma antigens detected by hybridoma antibodies. *Somatic Cell Genet* 1979; **5**: 957-971
4 **Zenita K**, Kirihata Y, Kitahara A, Shigeta K, Higuchi K, Hirashima K, Murachi T, Miyake M, Takeda T, Kannagi R. Fucosylated type-2 chain polylactosamine antigens in human lung cancer. *Int J Cancer* 1988; **41**: 344-349
5 **Kannagi R**, Kitahara A, Itai S, Zenita K, Shigeta K, Tachikawa T, Noda A, Hirano H, Abe M, Shin S. Quantitative and qualitative characterization of human cancer-associated serum glycoprotein antigens expressing epitopes consisting of sialyl or sialyl-fucosyl type 1 chain. *Cancer Res* 1988; **48**: 3856-3863
6 **Phillips ML**, Nudelman E, Gaeta FC, Perez M, Singhal AK, Hakomori S, Paulson JC. ELAM-1 mediates cell adhesion by recognition of a carbohydrate ligand, sialyl-Lex. *Science* 1990; **250**: 1130-1132
7 **Takada A**, Ohmori K, Yoneda T, Tsuyuoka K, Hasegawa A, Kiso M, Kannagi R. Contribution of carbohydrate antigens sialyl Lewis A and sialyl Lewis X to adhesion of human cancer cells to vascular endothelium. *Cancer Res* 1993; **53**: 354-361
8 **Weston BW**, Hiller KM, Mayben JP, Manousos G, Nelson CM, Klein MB, Goodman JL. A cloned CD15s-negative variant of HL60 cells is deficient in expression of FUT7 and does not adhere to cytokine-stimulated endothelial cells. *Eur J Haematol* 1999; **63**: 42-49
9 **Del Villano BC**, Brennan S, Brock P, Bucher C, Liu V, McClure M, Rake B, Space S, Westrick B, Schoemaker H, Zurawski VR. Radioimmunometric assay for a monoclonal antibody-defined tumor marker, CA 19-9. *Clin Chem* 1983; **29**: 549-552
10 **Magnani JL**, Steplewski Z, Koprowski H, Ginsburg V. Identification of the gastrointestinal and pancreatic cancer-associated antigen detected by monoclonal antibody 19-9 in the sera of patients as a mucin. *Cancer Res* 1983; **43**: 5489-5492
11 **Lowe JB,** Stoolman LM, Nair RP, Larsen RD, Berhend TL, Marks RM. ELAM-1-dependent cell adhesion to vascular endothelium determined by a transfected human fucosyltransferase cDNA. *Cell* 1990; **63**: 475-484
12 **Vatanasapt V**, Tangvoraphonkchai V, Titapant V, Pipitgool V, Viriyapap D, Sriamporn S. A high incidence of liver cancer in Khon Kaen Province, Thailand. *Southeast Asian J Trop Med Public Health* 1990; **21**: 489-494
13 **Torzilli G**, Makuuchi M, Ferrero A, Takayama T, Hui AM, Abe H, Inoue K, Nakahara K. Accuracy of the preoperative determination of tumor markers in the differentiation of liver mass lesions in surgical patients. *Hepatogastroenterology* 2002; **49**: 740-745
14 **Siqueira E**, Schoen RE, Silverman W, Martin J, Rabinovitz M, Weissfeld JL, Abu Elmaagd K, Madariaga JR, Slivka A. Detecting cholangiocarcinoma in patients with primary sclerosing cholangitis. *Gastrointest Endosc* 2002; **56**: 40-47
15 **Tsuji M**, Kashihara T, Terada N, Mori H. An immunohistochemical study of hepatic atypical adenomatous hyperplasia, hepatocellular carcinoma, and cholangiocarcinoma with alpha-fetoprotein, carcinoembryonic antigen, CA19-9, epithelial membrane antigen, and cytokeratins 18 and 19. *Pathol Int* 1999; **49**: 310-317
16 **Qin XL**, Wang ZR, Shi JS, Lu M, Wang L, He QR. Utility of serum CA19-9 in diagnosis of cholangiocarcinoma: in comparison with CEA. *World J Gastroenterol* 2004; **10**: 427-432
17 **Patel AH**, Harnois DM, Klee GG, LaRusso NF, Gores GJ. The utility of CA 19-9 in the diagnoses of cholangiocarcinoma in patients without primary sclerosing cholangitis. *Am J Gastroenterol* 2000; **95**: 204-207
18 **Aubert M**, Panicot L, Crotte C, Gibier P, Lombardo D, Sadoulet MO, Mas E. Restoration of alpha(1,2) fucosyltransferase activity decreases adhesive and metastatic properties of human pancreatic cancer cells. *Cancer Res* 2000; **60**: 1449-1456
19 **Yoshida M**, Chien LJ, Yasukochi Y, Numano F. Differentiation-induced transmigration of HL60 cells across activated HUVEC monolayer involves E-selectin-dependent mechanism. *Ann N Y Acad Sci* 2000; **902**: 307-310
20 **Minato H**, Nakanuma Y, Terada T. Expression of blood group-

related antigens in cholangiocarcinoma in relation to non-neoplastic bile ducts. *Histopathology* 1996**; 28**: 411-419

21 **Takada A**, Ohmori K, Takahashi N, Tsuyuoka K, Yago A, Zenita K, Hasegawa A, Kannagi R. Adhesion of human cancer cells to vascular endothelium mediated by a carbohydrate antigen, sialyl Lewis A. *Biochem Biophys Res Commun* 1991; **179**: 713-719

22 **Tyrrell D**, James P, Rao N, Foxall C, Abbas S, Dasgupta F, Nashed M, Hasegawa A, Kiso M, Asa D. Structural requirements for the carbohydrate ligand of E-selectin. *Proc Natl Acad Sci USA* 1991**; 88**: 10372-10376

23 **Yoon WH**, Park HD, Lim K, Hwang BD. Effect of O-glycosylated mucin on invasion and metastasis of HM7 human colon cancer cells. *Biochem Biophys Res Commun* 1996; **222**: 694-699

24 **Lindberg B**, Arnelo U, Bergquist A, Thorne A, Hjerpe A, Granqvist S, Hansson LO, Tribukait B, Persson B, Broome U. Diagnosis of biliary strictures in conjunction with endoscopic retrograde cholangiopancreaticography, with special reference to patients with primary sclerosing cholangitis. *Endoscopy* 2002; **34**: 909-916

25 **Ozkan H**, Kaya M, Cengiz A. Comparison of tumor marker CA 242 with CA 19-9 and carcinoembryonic antigen (CEA) in pancreatic cancer. *Hepatogastroenterology* 2003; **50**: 1669-1674

26 **Torok N,** Gores GJ. Cholangiocarcinoma. *Semin Gastrointest Dis* 2001; **12**: 125-132

27 **Chalasani N**, Baluyut A, Ismail A, Zaman A, Sood G, Ghalib R, McCashland TM, Reddy KR, Zervos X, Anbari MA, Hoen H. Cholangiocarcinoma in patients with primary sclerosing cholangitis: a multicenter case-control study. *Hepatology* 2000; **31**: 7-11

28 **Ahrendt SA,** Pitt HA, Nakeeb A, Klein AS, Lillemoe KD, Kalloo AN, Cameron JL. Diagnosis and management of cholangiocarcinoma in primary sclerosing cholangitis. *J Gastrointest Surg* 1999; **3**: 357-367; discussion 367-368

29 **Hultcrantz R**, Olsson R, Danielsson A, Jarnerot G, Loof L, Ryden BO, Wahren B, Broome U. A 3-year prospective study on serum tumor markers used for detecting cholangiocarcinoma in patients with primary sclerosing cholangitis. *J Hepatol* 1999; **30**: 669-673

30 **Ravindranath MH**, Amiri AA, Bauer PM, Kelley MC, Essner R, Morton DL. Endothelial-selectin ligands sialyl Lewis(x) and sialyl Lewis(a) are differentiation antigens immunogenic in human melanoma. *Cancer* 1997; **79**: 1686-1697

Edited by Wang XL

PO Box 2345, Beijing 100023, China
Fax: +86-10-85381893
E-mail: wjg@wjgnet.com www.wjgnet.com

ELSEVIER

World J Gastroenterol 2005;11(2):255-259
World Journal of Gastroenterology ISSN 1007-9327

• CLINICAL RESEARCH •

Clinical usefulness of biochemical markers of liver fibrosis in patients with nonalcoholic fatty liver disease

Hiroshi Sakugawa, Tomofumi Nakayoshi, Kasen Kobashigawa, Tsuyoshi Yamashiro, Tatsuji Maeshiro, Satoru Miyagi, Joji Shiroma, Akiyo Toyama, Tomokuni Nakayoshi, Fukunori Kinjo, Atsushi Saito

Hiroshi Sakugawa, Tomofumi Nakayoshi, Kasen Kobashigawa, Tsuyoshi Yamashiro, Tatsuji Maeshiro, Satoru Miyagi, Joji Shiroma, Akiyo Toyama, Tomokuni Nakayoshi, Fukunori Kinjo, Atsushi Saito, First Department of Internal Medicine, Faculty of Medicine, School of Medicine, University of the Ryukyus, Okinawa, Japan
Correspondence to: Hiroshi Sakugawa, M.D., First Department of Internal Medicine, University Hospital, Faculty of Medicine, University of the Ryukyus, 207 Uehara, Nishihara, Okinawa, 903-0215 Japan. b987607@med.u-ryukyu.ac.jp
Telephone: +98-895-1144 **Fax:** +98-895-1414
Received: 2004-04-22 **Accepted:** 2004-06-18

Abstract

AIM: Nonalcoholic steatohepatitis (NASH) is a severe form of nonalcoholic fatty liver disease (NAFLD), and progresses to the end stage of liver disease. Biochemical markers of liver fibrosis are strongly associated with the degree of histological liver fibrosis in patients with chronic liver disease. However, data are few on the usefulness of markers in NAFLD patients. The aim of this study was to identify better noninvasive predictors of hepatic fibrosis, with special focus on markers of liver fibrosis, type VI collagen 7S domain and hyaluronic acid.

METHODS: One hundred and twelve patients with histologically proven NAFLD were studied.

RESULTS: The histological stage of NAFLD correlated with several clinical and biochemical variables, the extent of hepatic fibrosis and the markers of liver fibrosis were relatively strong associated. The best cutoff values to detect NASH were assessed by using receiver operating characteristic analysis: type VI collagen 7S domain $\geqslant$5.0 ng/mL, hyaluronic acid $\geqslant$43 ng/mL. Both markers had a high positive predictive value: type VI collagen 7S domain, 86% and hyaluronic acid, 92%. Diagnostic accuracies of these markers were evaluated to detect severe fibrosis. Both markers showed high negative predictive values: type VI collagen 7S domain ($\geqslant$5.0 ng/mL), 84% and hyaluronic acid ($\geqslant$50 ng/mL), 78%, and were significantly and independently associated with the presence of NASH or severe fibrosis by logistic regression analysis.

CONCLUSION: Both markers of liver fibrosis are useful in discriminating NASH from fatty liver alone or patients with severe fibrosis from patients with non-severe fibrosis.

Key words: Liver fibrosis; Nonalcoholic fatty liver disease; Collagen type IV; Hyaluronic acid

Sakugawa H, Nakayoshi T, Kobashigawa K, Yamashiro T, Maeshiro T, Miyagi S, Shiroma J, Toyama A, Nakayoshi T, Kinjo F, Saito A. Clinical usefulness of biochemical markers of liver fibrosis in patients with nonalcoholic fatty liver disease. *World J Gastroenterol* 2005; 11(2): 255-259
http://www.wjgnet.com/1007-9327/11/255.asp

INTRODUCTION

The prevalence of overweight persons is increasing in developed and developing countries[1,2]. Fatty metamorphosis in the liver is common in these obese subjects and nonalcoholic fatty liver disease (NAFLD) has become widespread with the increasing prevalence of obesity[3-6]. In Japan, the prevalence of NAFLD has been recently increasing[7], which may be attributable to lifestyle change including physical inactivity and an increase in daily fat consumption.

Most patients with NAFLD have a benign clinical course, but some patients progress to advanced liver disease, liver cirrhosis or even hepatocellular carcinoma[3,8-10]. Nonalcoholic steatohepatitis (NASH) is a severe form of NAFLD, and is strongly associated with female gender, older age, obesity and type 2 diabetes mellitus[3,4,11-15]. The definitive diagnosis of NASH requires liver biopsy, but it is an invasive procedure that may cause undesirable complications. Clinical indications for liver biopsy should be limited in patients with NAFLD who are likely to have NASH or significant fibrosis. Liver fibrotic change is an important pathological finding to stage NAFLD or to determine the prognosis of NAFLD[16,17]. NAFLD patients with severe fibrosis have a poor prognosis[18].

Many clinical variables have been proposed as predictors of severe fibrosis in patients with NAFLD: old age, type 2 diabetes mellitus, obesity, serum transaminase levels, peripheral platelet counts, *etc*.[19-22]. Biochemical markers of liver fibrosis are strongly associated with the degree of histological fibrosis in patients with chronic viral hepatitis[23-25]. However, data are few on the usefulness of markers of liver fibrosis to evaluate the degree of liver fibrosis among patients with NAFLD or for distinguishing NASH from benign NAFLD[22].

The aim of the present study was to identify better noninvasive predictors of liver fibrosis, with special focus on the markers of liver fibrosis.

MATERIALS AND METHODS

Patients

From January 1993 to August 2003, NAFLD was diagnosed in 112 patients who visited our hospital or affiliated hospitals. The patients included 36 men and 76 women aged between 19 and 78 years, 87% were 40 years of age or older. All denied regular alcohol use and definitions of nonalcoholic use were 30 g/d or less for men and 20 g/d or less for women. No patient had conditions related to secondary NAFLD: regular use of drugs known to produce steatosis (corticosteroids, tamoxifen, amiodarone), previous gastrointestinal surgery, total parenteral nutrition, *etc*.[3]. Other liver diseases were appropriately excluded:

chronic viral hepatitis, autoimmune hepatitis, drug-induced liver disease, primary biliary cirrhosis, metabolic liver diseases. For all patients, the body mass index (BMI; kg/m^2) was calculated.

Methods

NAFLD was diagnosed histologically. All liver biopsy samples were examined by two of us (HS, KK) who were unaware of the clinical and biochemical conditions of each patient. Specimens were fixed in 10% neutral buffered formalin and stained with hematoxylin and eosin and Azan-Mallory. Fatty change was defined as 10% or more fatty metamorphosis in the hepatocytes. Histological criteria of NASH were based on steatosis ($\geqslant$10% of hepatocytes affected) and two of the following three: lobular inflammation, ballooning degeneration, and pericellular fibrosis. Different histological parameters were evaluated including steatosis, pericellular fibrosis, portal/septal fibrosis, portal inflammation, periportal necrosis, lobular inflammation, ballooning, Mallory body. Pericellular fibrosis was graded on a scale of absent, mild, moderate, severe fibrosis. Portal/septal fibrosis was graded according to the histological criteria for chronic viral hepatitis: 0, none; 1, portal expanding or periportal fibrosis; 2, partial bridging fibrosis; 3, diffuse bridging fibrosis with lobular remodeling, 4, cirrhosis. Histological staging was done according to Brunt *et al*[16,17] with slight modifications: stage 0, no fibrosis (fatty liver alone or fatty liver plus lobular inflammation); stage 1, perisuinasoidal fibrosis without portal fibrosis; stage 2, perisuinasoidal fibrosis plus portal fibrosis; stage 3, presence of bridging fibrosis; stage 4, cirrhosis. Written informed consent was obtained from all patients, and the study was conducted in conformance with the Helsinki Declaration.

Laboratory tests included peripheral blood cell counts, and measurements of albumin, aspartate aminotransferase (AST), alanine aminotransferase (ALT), γ-glutamyl transpeptidase (GGT), alkaline phosphatase (ALP), fasting glucose, fasting insulin, total cholesterol and triglyceride levels, glycosylated hemoglobin A1c (HbA1c), free fatty acid (FFA), ferritin, immunoglobulin G (IgG), IgA, IgM, type VI collagen 7S domain, hyaluronic acid , hepatitis B surface antigen, antibody to hepatitis C virus. Insulin resistance was calculated by homeostasis model assessment (HOMA-R: fasting glucose (mg/dL) ×fasting insulin (μU/mL) ÷405). Standard liver tests were performed on a multichannel autoanalyzer. Hepatitis B surface antigen was measured by a commercially available enzyme immunoassay (Enzygnost, Berling, Germany). Antibody to hepatitis C virus was tested by a second generation enzyme immunoassay (Ortho Diagnostics, Raritan, NJ).

Type VI collagen 7S domain was measured with a type VI collagen 7S domain RIA kit (Nippon CPC Co., Tokyo, Japan) and serum hyaluronic acid was tested by sandwich binding protein assay by using a commercially available kit (Chugai Co., Tokyo, Japan).

Statistical analysis

The continuous variables were compared using the 2-tailed Student's *t* test. The correlation between these variables was analyzed by Pearson's correlation coefficient or Spearman's correlation coefficient. Categorical variables were compared with Fisher's exact test. The diagnostic values of the clinical variables were assessed by calculating the areas under the receiver operating characteristic (ROC) curves, which were used to assess the best cutoff points to identify the presence of NASH or severe fibrosis. The diagnostic accuracy was calculated by sensitivity, specificity, and positive and negative predictive values (PPV and NPV). Multivariate analysis was tested using logistic regression analysis. The SPSS statistical software (Ver. 11.0) was used for statistical analysis. A P value less than 0.05 was considered statistically significant.

RESULTS

Of the 112 patients with NAFLD, 35 (31.3%) were classified as stage 0, 12 (10.7%) as stage 1, 17 (15.2%) as stage 2, 39 (34.8%) as stage 3 and 9 (8.0%) as stage 4. Seventy patients were diagnosed as NASH, and all of them had liver fibrotic change at stage 1 or at a more severe stage. The remaining 42 patients were diagnosed as having nonalcoholic fatty liver. When the 112 patients were divided into two groups by the severity of fibrosis (mild: stage 0-2 and severe: stage 3 and 4), women were more frequently seen in the severe group ($P = 0.04$), (Table 1).

Correlations were examined between the degree of fibrosis or the stage of NAFLD and the following clinical variables: age, BMI, blood pressure, peripheral platelet counts, serum levels of albumin, total bilirubin, fasting blood glucose, AST, ALT, GGT, ALP, total cholesterol, triglyceride, FFA, IgG, IgA, IgM, type VI collagen 7S domain, hyaluronic acid, ferritin, HbA1c, HOMA-R.

The degree of all three histological criteria of fibrosis and the following quantitative variables were significantly correlated:

Table 1 Correlation between degree of liver fibrosis and clinical and laboratory data (n = 112)

Clinical/laboratory data	Degree of liver fibrosis		
	Portal/Septal	Pericellular	Fibrosis stage
Age (yr)	0.265 (P = 0.005)	0.172 (P = 0.07)	0.302 (P = 0.001)
BMI	0.220 (P = 0.020)	0.236 (P = 0.012)	0.238 (P = 0.011)
Platelet	-0.331 (P<0.001)	-0.133 (P = 0.2)	-0.298 (P = 0.001)
Albumin	-0.295 (P = 0.002)	-0.078 (P = 0.4)	-0.291 (P = 0.002)
AST	0.306 (P = 0.001)	0.384 (P P<0.001)	0.340 (P<0.001)
AST/ALT	0.458 (P<0.001)	0.420 (P P<0.001)	0.438 (P<0.001)
IgG (n=100)	0.261 (P =0.009)	0.141 (P = 0.1)	0.208 (P = 0.038)
IgA (n=94)	0.281 (P<0.006)	0.285 (P = 0.005)	0.291 (P = 0.004)
IgM (n=100)	0.256 (P =0.010)	0.188 (P = 0.06)	0.266 (P = 0.008)
Type IV Ccollagen 7S	0.580 (P<0.001)	0.516 (P<0.001)	0.607 (P<0.001)
Hyaluronic acid	0.543 (P<0.001)	0.387 (P<0.001)	0.553 (P<0.001)
Ferritin (n = 98)	0.205 (P = 0.043)	0.120 (P = 0.2)	0.252 (P = 0.012)
HbA1c (n = 96)	0.309 (P = 0.002)	0.211 (P = 0.039)	0.315 (P = 0.002)
FFA (n = 80)	0.238 (P = 0.033)	0.271 (P = 0.015)	0.276 (P = 0.013)
HOMA-R (n = 82)	0.224 (P = 0.043)	0.164 (P = 0.1)	0.222 (P = 0.045)

age, BMI, platelet counts, albumin, AST, AST/ALT ratio, IgA, type VI collagen 7S domain, hyaluronic acid, HbA1c, FFA. Serum IgG and IgM concentrations, ferritin and HOMA-R were significantly correlated with either the degree of portal/septal fibrosis or fibrosis stage, but were not significantly correlated with the degree of pericellular fibrosis. Among these variables, the markers of liver fibrosis, type VI collagen 7S domain and hyaluronic acid, showed relatively high correlation coefficients. ALT, GGT, ALP, total serum cholesterol, triglyceride, peripheral hemoglobin concentration, systolic blood pressure, diastolic blood pressure, and fasting blood glucose level were not significantly correlated with any degree of the three histological criteria (Table 1).

When the patients having fatty liver alone were compared with the patients having NASH, the BMI, ALT, GGT, IgG, IgA, fasting glucose, ferritin, and HOMA-R were not significantly different, but several clinical variables were significantly different between the two groups, particularly the differences in AST level, AST/ALT ratio, and the markers of liver fibrosis were highly significant (Table 2).

Table 2 Comparison between patients with fatty liver and with NASH (mean±SD)

	Fatty liver alone	NASH	*P* value
Number	42	70	
Age (yr)	45.2±13.6	53.8±14.4	0.002
Gender (female)	22 (52.4%)	54 (77.1%)	0.012
BMI	28.2±4.9	29.6±5.2	NS
Diabetes mellitus (%)	8 (19.0%)	26 (37.1%)	0.044
Platelet count (×10⁴/μL)	23.8±4.8	21.1±6.8	0.036
Prothrombin time (%)	98.5±11.1	91.6±13.6	0.009
Albumin (g/dL)	4.4±0.3	4.3±0.4	0.017
AST (IU/L)	56.7±30.8	87.5±48.1	<0.001
ALT (IU/L)	110.1±68.2	117.1±65.1	NS
AST/ALT ratio	0.56±0.2	0.82±0.4	<0.001
GGT (IU/L)	124.9±96.6	106.2±129.3	NS
IgG (mg/dL)	1 377.1±366.7	1 526.9±423.3	NS
IgA (mg/dL)	313.1±191.3	356.9±134.1	NS
IgM (mg/dL)	124.2±47.9	162.8±82.4	0.004
Type IV collagen 7S (ng/mL)	4.1±0.9	6.0±2.0	<0.001
Hyaluronic acid (ng/mL)	29.0±20.0	103.4±116.8	<0.001
Fasting glucose (mg/dL)	107.8±34.4	120.2±51.8	NS
HbA1c (%)	5.4±1.0	6.2±1.7	0.005
Ferritin (ng/mL)	151.7±107.0	351.5±455.7	0.001
FFA (mEq/L)	0.6±0.2	0.7±0.3	0.022
HOMA-R	5.1±6.3	6.0±6.6	NS

When the patients having stage 0-2 fibrosis were compared with the patients having stage 3 and 4 fibrosis, the BMI, ALT level, any subclass of immunoglobulins, fasting glucose and HOMA-R were not significantly different. The frequency of diabetes mellitus was not significantly different between these groups, but the difference was significant between patients having fatty liver alone and patients having NASH (Table 3).

Table 3 Comparison between NAFLD patients with stage 0-2 fibrosis and those with stage 3 and 4 fibrosis (mean±SD)

	Stages 0-2 fibrosis	Stages 3,4 fibrosis	*P* value
Number	64	48	
Age (yr)	47.8±14.5	54.3±14.0	0.02
Gender (female)	38 (59.4%)	38 (79.2%)	0.04
BMI	28.3±4.8	30.1±5.4	NS
Diabetes mellitus (%)	15 (23.4%)	19 (39.6%)	NS
Platelet count (×10⁴/μL)	23.8±5.1	20.3±7.1	0.004
Prothrombin time (%)	96.9±11.1	90.1±14.7	0.018
Albumin (g/dL)	4.4±0.3	4.3±0.4	0.03
AST (IU/L)	67.0±37.5	87.9±51.2	0.02
ALT (IU/L)	113.1±65.2	116.3±67.9	NS
AST/ALT ratio	0.66±0.4	0.82±0.3	0.015
GGT (IU/L)	133.5±141.6	85.7±66.6	0.019
IgG (mg/dL)	1 408.1±367.0	1 555.5±446.4	NS
IgA (mg/dL)	316.3±172.3	371.0±133.5	NS
IgM (mg/dL)	137.2±79.1	163.8±64.9	NS
Type IV collagen 7S (ng/mL)	4.6±1.5	6.3±2.0	<0.001
Hyaluronic acid (ng/mL)	50.4±74.3	108.8±118.7	0.004
Fasting glucose (mg/dL)	115.1±49.4	116.6±43.1	NS
HbA1c (%)	5.6±1.2	6.4±1.9	0.01
Ferritin (ng/mL)	253.8±52.6	320.1±373.0	NS
FFA (mEq/L)	0.6±0.3	0.8±0.3	0.007
HOMA-R	5.7±5.8	5.8±4.6	NS

Relatively high correlation coefficients were seen between the degree of hepatic fibrosis and the markers of fibrosis. We therefore examined the diagnostic accuracy of the markers of fibrosis for NASH and severe fibrosis. To detect NASH, the area under the curves for type VI collagen 7S domain and hyaluronic acid were 0.828 and 0.797, respectively, by ROC analysis (Table 4). The best cutoff values to detect NASH were also assessed using the ROC analysis, and sensitivity, specificity, PPV, and NPV were calculated. Both markers had high PPV: type VI collagen 7S domain, 86.0% and hyaluronic acid, 92.0%. A combination of these markers was also useful to discriminate NASH from fatty liver alone. If both markers combined were positive, the PPV was high (97.1%) (Table 4). To detect severe

Table 4 Diagnostic accuracy of the markers of liver fibrosis for NASH

	ROC analysis		Cutoff value	Accuracy			
	AUC (95% CI)	*P* value		Se (%)	Sp (%)	PPV (%)	NPV (%)
(a) Type IV collagen 7S	0.828 (0.754-0.902)	0.000	≥5.0 ng/mL	70.0	81.0	86.0	61.8
(b) Hyaluronic acid	0.797 (0.716-0.879)	0.000	≥43 ng/mL	65.7	90.5	92.0	61.3
Combination of Markers			a≥5.0 ng/mL or b≥43 ng/mL	87.1	73.8	84.7	77.5
			a≥5.0 ng/mL and b≥43 ng/mL	48.6	97.6	97.1	53.2

Abbreviations: ROC, receiver operating characteristic; AUC, area under the ROC curve; CI, confidence interval; Se, sensitivity; Sp, specificity; PPV, positive predictive value; NPV, negative predictive value.

Table 5 Diagnostic accuracy of the markers of liver fibrosis for severe fibrosis

	ROC analysis		Cutoff value	Accuracy			
	AUC (95% CI)	*P* value		Se (%)	Sp (%)	PPV (%)	NPV (%)
(a) Type IV collagen 7S	0.817 (0.736-0.897)	0.000	≥5.0 ng/mL	81.3	71.4	68.4	83.6
(b) Hyaluronic acid	0.797 (0.652-0.845)	0.000	≥50 ng/mL	68.8	82.8	75.0	77.9
Combination of Markers			a≥5.0 ng/mL or b≥50 ng/mL	95.8	62.5	65.7	95.2
			a≥5.0 ng/mL and b≥50 ng/mL	54.2	92.2	83.9	72.8

Abbreviations: ROC, receiver operating characteristic; AUC, area under the ROC curve; CI, confidence interval; Se, sensitivity; Sp, specificity; PPV, positive predictive value; NPV, negative predictive value.

fibrosis, the type VI collagen 7S domain cutoff value for the best compromise sensitivity-specificity was 5.0 ng/mL. This value was the same as in detecting NASH. Type VI collagen 7S domain and hyaluronic acid showed relatively high NPVs in detecting severe fibrosis. If both markers were concomitantly negative, severe fibrosis was unlikely to be present, the NPV of either type VI collagen 7S domain ≥5.0 ng/mL or hyaluronic acid ≥50 ng/mL in detecting severe fibrosis was high (95.2%) (Table 5).

Although several clinical variables were associated with the presence of NASH or severe fibrosis by univariate analysis (Tables 2, 3), these factors were too many to be evaluated in logistic regression analysis. We therefore selected eight variables (age, gender, BMI, peripheral platelet counts, AST/ALT ratio, type VI collagen 7S domain, hyaluronic acid, presence of diabetes) for logistic regression analysis. The cutoff values for continuous variables (age, peripheral platelet counts, AST/ALT ratio, type VI collagen 7S domain, hyaluronic acid) were determined based on ROC analysis. The cutoff value for BMI was adopted as ≥30 kg/m^2. The logistic regression analysis indicated that three (AST/ALT ratio ≥0.55, type VI collagen 7S domain ≥5.0 ng/mL, hyaluronic acid ≥43 ng/mL) out of the eight variables were significantly and independently associated with NASH. Odds ratios for the three independent predictors of NASH were AST/ALT ratio 10.1, 95% confidence interval (CI) 2.0-52.3, $P=0.006$; type VI collagen 7S domain 6.9, 95% CI 2.1-23, $P=0.002$; hyaluronic acid 12.7, 95% CI 3.0-54, $P=0.001$. The logistic regression analysis also indicated that two (type VI collagen 7S domain ≥50 ng/mL, hyaluronic acid ≥50 ng/mL) of the eight variables were significantly and independently associated with severe fibrosis. Odds ratios of the two markers of liver fibrosis were type VI collagen 7S domain 10.4, 95% CI 3.2-34, $P=0.000$; hyaluronic acid 5.6, 95% CI 1.7-19, $P=0.005$.

DISCUSSION

In this study, the markers of liver fibrosis (type VI collagen 7S domain and hyaluronic acid) correlated well with the degree of liver fibrosis among patients with NAFLD compared with several clinical variables (age, serum AST level, AST/ALT ratio, BMI, presence of diabetes mellitus, peripheral platelet count, *etc*.) previously reported to be useful to diagnose NASH and severe fibrosis. The performances of these markers in predicting NASH and severe fibrosis were examined by either univariate analysis, ROC analysis, or multiple logistic regression analysis. The likelihood of having NASH could be 97% if patients showed a positive level of serum type VI collagen 7S domain and hyaluronic acid. Also, 96% of the NASH patients had a positive level of either type VI collagen 7S domain or hyaluronic acid.

Most NASH patients were asymptomatic, and had abnormally increased ALT levels[4]. The diagnosis of NASH should be suspected in people who have an asymptomatic increase in liver enzymes, and increased liver echogenicity by ultrasound examination. In Japan, health check-ups usually include ultrasound examination. Persons with ultrasonographic evidence of fatty liver and an increased ALT level unrelated to chronic hepatitis virus infection are frequently found among health check-up participants, and then are referred to hepatologists. Some of them may have NASH and may include cases of severe fibrosis, and others may have fatty liver alone or fat plus inflammation despite of increased ALT levels. The discrimination between NASH and fatty liver alone is difficult without liver biopsy. However, liver biopsy is not always justified in those cases. Clinicians need a sensible reason to obtain agreement for liver biopsy from reluctant patients.

The degree of liver fibrosis is important to evaluate the prognosis in patients with NAFLD. Inter- and intra-observer discrepancies in assessing the extent of liver fibrosis were small compared with assessing the extent of inflammation[26]. Prediction of liver fibrosis is challenging, and many investigations have been made of patients with chronic hepatitis C[23-25,27-29]. However, such investigations have been limited to patients with NAFLD[19-22]. Angulo *et al*[19] reported that age, presence of diabetes, AST/ALT ratio were the predictors of severe fibrosis in patients with NASH. However, these clinical predictors were not useful to discriminate NASH from fatty liver alone or patients with severe fibrosis from those with non-severe fibrosis in this study.

The usefulness of markers of liver fibrosis (type VI collagen 7S domain or hyaluronic acid) has been assessed for patients with chronic viral hepatitis[23-25]. However, studies are few on the clinical usefulness of markers of liver fibrosis to predict severe fibrosis in patients with NAFLD[22]. The serum level of type VI collagen 7S domain type, but not hyaluronic acid, was reported to be significantly different between NASH patients with severe fibrosis and those with mild to moderate fibrosis. Platelet count and AST/ALT ratio might be more useful predictors of the presence of severe fibrosis compared with markers of liver fibrosis[22]. However, the fibrotic markers were more useful predictors of NASH or severe fibrosis in this study.

Our study showed discrepancies with other previous studies[19-22] in the assessment of useful predictors of NASH or severe fibrosis in patients with NAFLD. The discrepancies may be attributed to a difference in percentage of patients with severe fibrosis. The percentage of patients with liver cirrhosis in this study was 8% (9/112), but in previous studies the percentages of patients with liver cirrhosis among NASH patients were 17[19] and 21%[22]. Only 10% of patients in this study showed AST/ALT ratio>1, which was a useful predictor in previous studies[19]. We experienced patients with cryptogenic liver cirrhosis who were suspected of having sequelae of NASH, but they were excluded from this study because of inadequate fatty change (<10%).

In conclusion, the biochemical markers of liver fibrosis, type 4 collagen 7S domain and hyaluronic acid, are useful predictors to evaluate the degree of hepatic fibrosis in patients with NAFLD. These markers are also useful to discriminate NASH from fatty liver alone or patients with severe fibrosis from patients with non-severe fibrosis.

REFERENCES

1 **Kuczmarski RJ**, Carroll MD, Flegal KM, Troiano RP. Varying body mass index cutoff points to describe overweight prevalence among U.S. adults: NHANES III (1988 to 1994). *Obes Res* 1997; **5**: 542-548
2 **Kopelman PG**. Obesity as a medical problem. *Nature* 2000; **404**: 635-643
3 **Falck-Ytter Y**, Younossi ZM, Marchesini G, McCullough AJ. Clinical features and natural history of nonalcoholic steatosis syndromes. *Semin Liver Dis* 2001; **21**: 17-26
4 **Day CP**. Non-alcoholic steatohepatitis (NASH): where are we now and where are we going? *Gut* 2002; **50**: 585-588
5 **Shen L**, Fan JG, Shao Y, Zeng MD, Wang JR, Luo GH, Li JQ, Chen SY. Prevalence of nonalcoholic fatty liver among administrative officers in Shanghai: an epidemiological survey. *World J Gastroenterol* 2003; **9**: 1106-1110
6 **Chitturi S**, Farrell GC, George J. Non-alcoholic steatohepatitis in the Asia-Pacific region: future shock? *J Gastroenterol Hepatol* 2004; **19**: 368-374
7 **Kojima S**, Watanabe N, Numata M, Ogawa T, Matsuzaki S. Increase in the prevalence of fatty liver in Japan over the past 12 years: analysis of clinical background. *J Gastroenterol* 2003; **38**: 954-961
8 **Bugianesi E**, Leone N, Vanni E, Marchesini G, Brunello F, Carucci P, Musso A, De Paolis P, Capussotti L, Salizzoni M, Rizzetto M. Expanding the natural history of nonalcoholic steatohepatitis: from cryptogenic cirrhosis to hepatocellular carcinoma. *Gastroenterology* 2002; **123**: 134-140
9 **Hui JM**, Kench JG, Chitturi S, Sud A, Farrell GC, Byth K, Hall P, Khan M, George J. Long-term outcomes of cirrhosis in nonalcoholic steatohepatitis compared with hepatitis C. *Hepatology* 2003; **38**: 420-427
10 **Sakugawa H**, Nakasone H, Nakayoshi T, Kawakami Y, Yamashiro T, Maeshiro T, Kobashigawa K, Kinjo F, Saito A. Clinical characteristics of patients with cryptogenic liver cirrhosis in Okinawa, Japan. *Hepatogastroenterology* 2003; **50**: 2005-2008
11 **Ludwig J**, Viggiano TR, McGill DB, Oh BJ. Nonalcoholic steatohepatitis: Mayo Clinic experiences with a hitherto unnamed disease. *Mayo Clin Proc* 1980; **55**: 434-438
12 **Sheth SG**, Gordon FD, Chopra S. Nonalcoholic steatohepatitis. *Ann Intern Med* 1997;**126**: 137-145
13 **James OF**, Day CP. Non-alcoholic steatohepatitis (NASH): a disease of emerging identity and importance. *J Hepatol* 1998; **29**: 495-501
14 **Bacon BR**, Farahvash MJ, Janney CG, Neuschwander-Tetri BA. Nonalcoholic steatohepatitis: an expanded clinical entity. *Gastroenterology* 1994; **107**: 1103-1109
15 **Harrison SA**, Kadakia S, Lang KA, Schenker S. Nonalcoholic steatohepatitis: what we know in the new millennium. *Am J Gastroenterol* 2002; **97**: 2714-2724
16 **Brunt EM**, Janney CG, Di Bisceglie AM, Neuschwander-Tetri BA, Bacon BR. Nonalcoholic steatohepatitis: a proposal for grading and staging the histological lesions. *Am J Gastroenterol* 1999; **94**: 2467-2474
17 **Neuschwander-Tetri BA**, Caldwell SH. Nonalcoholic steatohepatitis: summary of an AASLD Single Topic Conference. *Hepatology* 2003; **37**: 1202-1219
18 **Matteoni CA**, Younossi ZM, Gramlich T, Boparai N, Liu YC, McCullough AJ. Nonalcoholic fatty liver disease: a spectrum of clinical and pathological severity. *Gastroenterology* 1999; **116**: 1413-1419
19 **Angulo P**, Keach JC, Batts KP, Lindor KD. Independent predictors of liver fibrosis in patients with nonalcoholic steatohepatitis. *Hepatology* 1999; **30**: 1356-1362
20 **Ratziu V**, Giral P, Charlotte F, Bruckert E, Thibault V, Theodorou I, Khalil L, Turpin G, Opolon P, Poynard T. Liver fibrosis in overweight patients. *Gastroenterology* 2000; **118**: 1117-1123
21 **Dixon JB**, Bhathal PS, O'Brien PE. Nonalcoholic fatty liver disease: predictors of nonalcoholic steatohepatitis and liver fibrosis in the severely obese. *Gastroenterology* 2001; **121**: 91-100
22 **Shimada M**, Hashimoto E, Kaneda H, Noguchi S, Hayashi N. Nonalcoholic steatohepatitis: risk factors for liver fibrosis. *Hepatol Res* 2002; **24**: 429-438
23 **Guechot J**, Poupon RE, Giral P, Balkau B, Giboudeau J, Poupon R. Relationship between procollagen III aminoterminal propeptide and hyaluronan serum levels and histological fibrosis in primary biliary cirrhosis and chronic viral hepatitis C. *J Hepatol* 1994; **20**: 388-393
24 **Murawaki Y**, Ikuta Y, Koda M, Kawasaki H. Serum type III procollagen peptide, type IV collagen 7S domain, central triple-helix of type IV collagen and tissue inhibitor of metalloproteinases in patients with chronic viral liver disease: relationship to liver histology. *Hepatology* 1994; **20**: 780-787
25 **Takamatsu S,** Nakabayashi H, Okamoto Y, Nakano H. Noninvasive determination of liver collagen content in chronic hepatitis. Multivariate regression modeling with blood chemical parameters as variables. *J Gastroenterol* 1997; **32**: 355-360
26 **Younossi ZM**, Gramlich T, Liu YC, Matteoni C, Petrelli M, Goldblum J, Rybicki L, McCullough AJ. Nonalcoholic fatty liver disease: assessment of variability in pathologic interpretations. *Mod Pathol* 1998; **11**: 560-565
27 **Imbert-Bismut F**, Ratziu V, Pieroni L, Charlotte F, Benhamou Y, Poynard T. Biochemical markers of liver fibrosis in patients with hepatitis C virus infection: a prospective study. *Lancet* 2001; **357**: 1069-1075
28 **Forns X**, Ampurdaners S, Llovet JM, Aponte J, Quinto L, Martinez-Bauer E, Bruguera M, Shanchez-Tapias JM, Rodes J. Identification of chronic hepatitis C without hepatic fibrosis by a simple predictive model. *Hepatology* 2002; **36**: 986-992
29 **Wai CT**, Greenson JK, Fontana RJ, Kalbleisch JD, Marrero JA, Conjeevaram HS, Lok AS. A simple noninvasive index can predict both significant fibrosis and cirrhosis in patients with chronic hepatitis C. *Hepatology* 2003; **38**: 518-526

Edited by Wang XL

PO Box 2345, Beijing 100023, China
Fax: +86-10-85381893
E-mail: wjg@wjgnet.com www.wjgnet.com

ELSEVIER

World J Gastroenterol 2005;11(2):260-263
World Journal of Gastroenterology ISSN 1007-9327

• CLINICAL RESEARCH •

Giant malignant gastrointestinal stromal tumors: Recurrence and effects of treatment with STI-571

Teng-Wei Chen, Hsiao-Dung Liu, Rong-Yaun Shyu, Jyh-Cherng Yu, Ming-Lang Shih, Tzu-Ming Chang, Chung-Bao Hsieh

Teng-Wei Chen, Hsiao-Dung Liu, Jyh-Cherng Yu, Ming-Lang Shih, Chung-Bao Hsieh, Division of General Surgery, Department of Surgery, Tri-Service General Hospital, National Defense Medical Center, Taipei, Taiwan, China
Rong-Yaun Shyu, Division of Gastrointestinal Medicine, Department of Internal Medicine, Tri-Service General Hospital, National Defense Medical Center, Taipei, Taiwan, China
Tzu-Ming Chang, Department of Surgery, Tungs' Taichung Metroharbor Hospital, Taichung, Taiwan, China
Correspondence to: Dr. Chung-Bao Hsieh, 325, Sec 2, Cheng-Kung Rd, Taipei, Taiwan, China. albert0920@yahoo.com.tw
Telephone: +886-2-87927191 **Fax:** +886-2-87927372
Received: 2004-04-10 **Accepted:** 2004-06-07

Abstract

AIM: Malignant gastrointestinal stromal tumors (GISTs) are rare. Tumors larger than 10 cm tend to recur earlier: the larger the volume of the tumor, the worse the prognosis. We hypothesized that treatment with imatinib mesylate (Gleevec; STI-571), a *c-kit* tyrosine kinase inhibitor, as palliative therapy would prolong the survival of patients with recurrent giant malignant GISTs after resection.

METHODS: We performed a retrospective analysis of the effects of resection on patients with giant GISTs (>10 cm in diameter) to determine the overall survival and recurrence rates. Twenty-three patients diagnosed with giant GISTs were included from June 1996 to December 2003. STI-571 was not available until January 2000. After that time, 9 patients received this drug. The factors of age, sex, tumor location, histological surgical margin, and STI-571, tumor size changes and drug side effects were reviewed. We compared the survival rate to determine the prognostic factors and the effects of STI-571 on patients with recurrent malignant gastrointestinal stromal tumor.

RESULTS: The positive surgical margin group had a significantly higher recurrence rate than the negative margin group ($P = 0.012$). A negative surgical margin and palliative treatment with STI-571 were significant prognostic variables (Log-rank test, $P<0.05$). Age, sex and tumor location were not significant prognostic variables. The 5-year survival rate of the surgical margin free patients was 80% and the 2-year survival rate of the surgical margin positive patients was 28%. The 5-year survival rate was 80% for the patients given STI-571 and 30% for the patients not given STI-571. The use of STI-571 gave a significant tumor shrinkage (6/9) rate in patients with giant GIST recurrence after resection.

CONCLUSION: A negative surgical margin and the use of STI-571 after surgical resection were good prognostic indicators. Achieving a tumor-free surgical margin is still the best primary treatment for patients with such tumors. If STI-571 is used immediately when the surgical margin is positive and the tumor recurs after resection, then the prognosis of patients with giant GISTs can be improved.

Key words: Giant malignant gastrointestinal stromal tumors; STI-571

Chen TW, Liu HD, Shyu RY, Yu JC, Shih ML, Chang TM, Hsieh CB. Giant malignant gastrointestinal stromal tumors: Recurrence and effects of treatment with STI-571. *World J Gastroenterol* 2005; 11(2): 260-263
http://www.wjgnet.com/1007-9327/11/260.asp

INTRODUCTION

Gastrointestinal stromal tumors (GISTs) are specific mesenchymal tumors that can occur through the entire gastrointestinal tract, and in the omentum and mesentery. They range from small, benign, incidentally detected nodules to large malignant tumors. GISTs have been proposed to originate from the interstitial cells of Cajal, which are intestinal pacemakers[1]. They are derived from the myeloid stem cells, being positive for the CD34 antigen in 52-72% of cases[2], and are frequently marked by the presence of the *c-kit* proto-oncogene (85-94%)[3]. Cajal cells have the characteristics of both smooth muscle and neural cells, and neoplastic Cajal cells might preferentially express one, both, or neither of these features, thus explaining the variant forms of GISTs.

Surgical removal remains the only curative treatment for patients with GISTs[4]. Tumor size[5,6], mitotic index[6], anatomic location[7], tumor rupture and disease-free interval[8] are the classic characteristics used to predict the clinical course of patients who undergo complete gross resection. DeMatteo analyzed 200 patients with malignant GISTs and found that patients with tumors larger than 10 cm had shorter disease-free intervals (tumor recurrence)[5]. Tumor size was a predictor of tumor recurrence, age, sex, and surgical margins were not[5]. However, the results of Pierie *et al*[9] and Clary *et al*[10] showed that surgical margin was a predictor of tumor recurrence, this needs confirmation.

Immunohistochemical studies have shown that up to 94% of patients with GISTs could express CD117 (the *c-kit* gene product). The c-Kit protein, a typical type-III tyrosine-kinase receptor, is encoded by the proto-oncogene *c-kit*[11-13], and is essential for the development of the interstitial cells of Cajal[14]. The occurrence of activating mutations involving exon II of *c-kit* in sporadic GISTs indicates the importance of this protein in GIST tumorigenesis. There is the same mutation gene in intestinal gastric carcinoma[15]. The first case in which imatinib mesylate (Gleevec; STI-571), an inhibitor of *c-kit* tyrosine kinase activity, was used successfully to treat a patient with a GIST was reported in Finland by Joensuu in 2001[16].

We retrospectively analyzed the clinical outcomes of GIST patients who did and did not receive STI-571 to determine which factors in GIST patients might predict early recurrence and to show the benefit from immediate treatment with STI-571. We hypothesized that treatment with STI-571 would be successful in treating patients with recurrent giant malignant GISTs after

resection. The aim of this study was to evaluate the factors determining early recurrence, prognostic factors for giant GISTs, and the effect of imatinib on recurrent GISTs after resection.

MATERIALS AND METHODS

Patient selection

The medical records of all patients from June 1996 through December 2003 referred to the Tri-Service General Hospital were reviewed. Inclusion criteria were that the tumor originated from the gastrointestinal tract, GISTs were diagnosed by immunochemical staining for *c-kit*, and the tumor size was larger than 10 cm, pathologists confirmed the latter two items. Patients with a primary tumor less than 10 cm in size (n = 47) were excluded.

Twenty-three patients (11 men, 12 women) were included in this retrospective analysis. All data for the included patients were recorded, such as basic characteristics, tumor size and location, surgical margin, recurrence, palliative treatment pattern, and survival results. The timing of applying STI-571 was at tumor recurrence after surgical resection, proved by imaging studies. A dose of 400 mg twice a day was used.

Definitions

The pathologists at Tri-Service General Hospital determined the tumor grade, tumor size and the presence of a tumor-free surgical margin. A negative surgical margin was defined as removal of all gross tumor tissues at operation (n = 12) and a histological examination that confirmed the margin to be free of tumor invasion. A positive surgical margin implied that total removal of gross tumor tissues was not confirmed by histological examination. This condition was usually combined with multiple organ involvement, tumor rupture during operation, or perforation (n = 11). Local recurrence was defined as a tumor recurring within the abdominal cavity, exclusive of the liver. Metastasis was defined as tumor recurrence occurring in the liver or in extra-abdominal sites. The tumor shrinkage effect of STI-571 was defined using computed tomography scans of tumor size before and after 6 mo of treatment. Complete response was tumor disappearance, partial response was tumor shrinkage by 25-75%, stable disease was tumor unchanged in size, and disease progress was tumor enlargement by more than 150%.

Statistical analysis

When the interval to tumor recurrence was calculated, the initial event was taken as the time of curative surgery and the terminal event was defined as the time of detection of the recurrent tumor at a specific site (peritoneum, liver, or extra-abdominal). For survival analysis after the onset of recurrence, the terminal event was taken as death resulting from the malignant neoplasm, or the last follow-up date for surviving patients. The survival analysis was tested by the Kaplan-Meier method, and statistical differences were tested using the Log-rank test. The numeric data were tested by Student's t test and the category data were tested by the Fisher's exact test. $P<0.05$ was considered statistically significant for all comparisons.

RESULTS

The mean age of the patients was 56.2±16.9 years and the mean follow-up time of patients who were alive was 29.1±25.8 mo (range 4.6-87.9 mo). The mean tumor size was 15.9±8.4 cm.

The clinical characteristics of GIST patients are shown in Table 1. Nine patients received STI-571 and 13 did not. These two groups were not different in any of the clinical characteristics. Among the patients who received STI-571 in the palliative treatment, three received repeated resection, two received trans-arterial chemo-embolization, and two received chemotherapy. Among the patients who did not receive STI-571, only two received chemotherapy.

Table 1 Clinical characteristics of giant GISTs patients

	Total (n = 23)	STI-571 (n = 9)	No STI-571 (n = 14)	P
Age (yr)	56.2±16.9			
≤50 yr		40.2±11.9(5)	39.0±10.8(4)	0.8
>50 yr		67.3±5.8(4)	66.7±11.0(10)	0.9
Sex				
Male	11	2	9	0.08
Female	12	7	5	
Tumor size (cm)	15.9±8.4	20.7±9.9	12.8±5.4	0.06
Location				
Gastroduodenal	14	6	8	0.9
Intestinal	9	3	6	
Surgical margin				
Negative	12	4	8	0.68
Positive	11	5	6	
Recurrence	14	7	7	
Local	11	5	6	0.59
Distal metastasis	6	4	2	
Treatment of recurrence	14	7	7	
Repeat resection	3	3	0	
TACE	2	2	0	
Chemotherapy	3	2	2	
Mean recurrence time (mo)		15.2±11.8	6.9±5.7	0.15

TACE = Trans-arterial chemo-embolization.

Seven patients who had tumor recurrence and did not receive STI-571, all died within 21 mo (Figure 1). Of the seven patients who had tumor recurrence but received STI-571, one died after 17.3 mo. The general characteristics of these two groups were not different.

The effects and side effects of STI-571 are shown in Table 2. The tumor shrinkage rate was 66% (6/9). Complete response occurred in two patients, partial response in four, disease progress in one, and disease re-progression after stopping STI-571 occurred in one. The side effects were skin rash, edema, gastrointestinal upset, disease progress, and abnormal liver function.

Table 2 Effects and side effects of STI-571

	Number (n = 9)
Tumor shrinkage	6
Complete response	2
Tumor shrinkage ≥75%	0
50% <Tumor shrinkage <75%	3
25% <Tumor shrinkage <50%	1
Tumor shrinkage ≤25%	2
Tumor enlargement (150%)	1
Tumor re-enlargement (150%)	1
Side effect	8
Skin rash	4
Edema	5
Gastrointestinal upset	1
Disease progress	1
Abnormal liver function	1

In our series, the effect of STI-571 on tumor shrinkage was obvious, the mean shrinkage of tumor size was 5.3±2.4 cm (range, 2 cm to 8 cm). Seven of nine patients who received STI-571 had tumor shrinkage, tumors completely disappeared in two patients (2/7), and partially disappeared in four (4/7). Only one patient had his tumor enlarged from 10 cm to 15 cm (1/7). The tumor in one special patient showed shrinkage after STI-571 was used for the first time, but proved resistant to re-treatment with imatinib for tumor enlargement. Two patients received STI-571 immediately after surgical resection due to their very large GISTs (25 and 30 cm). These two patients had no tumor recurrence within 14 and 4 mo of follow-up.

Table 3 shows the prognostic variables for survival analysis in GIST patients. Surgical margin and use of STI-571 were significant prognostic variables (log-rank test, $P<0.05$), while age, sex, and tumor location were not significant prognostic variables.

Table 3 Prognostic variables for survival analysis

Variable	Mortality (n = 8)	Log-rank test
Age (yr)		0.085
≤50 yr	1/9	
>50 yr	7/14	
Sex		
Male	4/11	0.95
Female	4/12	
Location		0.872
Gastroduodenal	5/14	
Intestinal	3/9	
Surgical margin		0.047
Negative	2/12	
Positive	6/11	
STI-571		0.045
Yes	1/9	
No	7/14	

Figure 2 shows that there was a statistical relationship between surgical margin and disease-free rate. When the surgical margin was negative, the 5-year disease-free rate was nearly 40%. Conversely, when the surgical margin was positive, the two-year disease-free rate was 0%. The relation between surgical margin and survival rate is shown in Figure 3. The 5-year survival rate of patients with a negative surgical margin was 80% and the 2-year survival rate of patients with a positive surgical margin was 28%. The effect of STI-571 is shown in Figure 1. The 5-year survival rate of patients who received STI-571 was 80%, and that of patients who did not receive STI-571 was 30%. The effect of STI-571 in prolonging life span was significant.

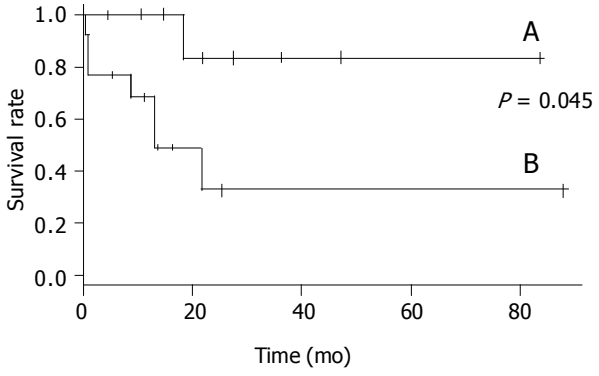

Figure 1 Kaplan-Meier survival curves of GIST patients who (A) received STI-571 and (B) did not receive STI-571.

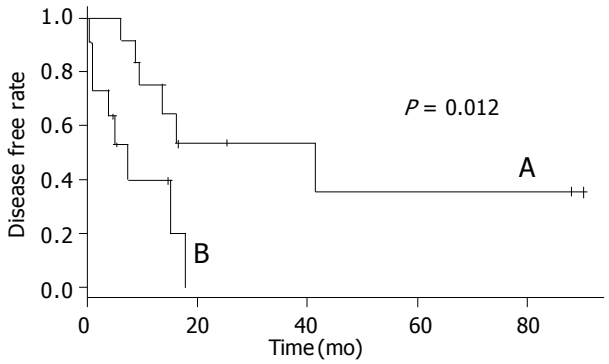

Figure 2 Kaplan-Meier plots of the disease-free rate of GIST patients with (A) negative and (B) positive surgical margins.

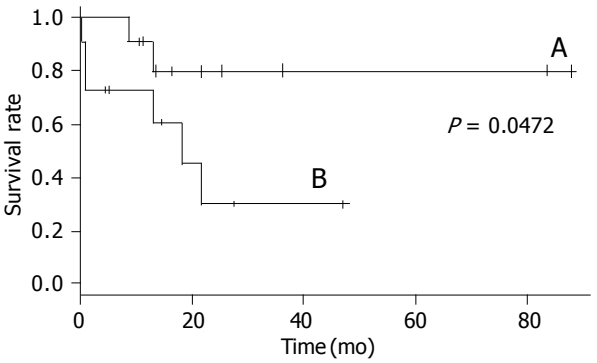

Figure 3 Kaplan-Meier survival curves of GIST patients with (A) negative and (B) positive surgical margins.

DISCUSSION

In this series, we retrospectively analyzed 23 patients with giant GISTs (tumor size >10 cm) and found that surgical margin was an independent factor for tumor recurrence (Figure 2). A negative surgical margin meant total tumor removal by surgical resection. This is similar to previous studies[9,10]. This result indicated that the factors that could cause a positive surgical margin were the risk factors for tumor recurrence, such as tumor rupture, multiple organ involvement, and margin involvement on histological examination.

The 5-year survival rate was significantly better in patients with a negative surgical margin (Figure 3). Tumor rupture before or during resection is another predictor of poor outcome[6]. Lewis also showed that gross margin-free tumor resection gave a good prognosis[17].

In our series, good results were obtained for patients who received STI-571, and the survival rate of patients who received STI-571 was significantly higher than that of the patients who did not receive STI-571. A European Organization for Research and Treatment of Cancer (EORTC) in a soft tissue and bone sarcoma group phase II study[18] showed that STI-571 was well tolerated at a dose of 400 mg twice a day. Response rate in the EORTC study for GISTs was 7% complete response, 25% partial response, 24% stable disease and 14% disease progression, respectively. Tumor resistance could have been primary or acquired after several months of drug administration, but the mechanism is unknown[19]. The most common side effects were anemia (92%), periorbital edema (84%), skin rashes (69%), and fatigue (76%)[18]. This was consistent with our results.

A tumor size greater than 10 cm is the worst prognostic factor for malignant GISTs[20,21]. In a study of 100 patients with GISTs, multivariate analysis showed that tumor size was an independent prognostic factor for survival. Patients with giant

GISTs (>10 cm) had a disease-specific 5-year survival of only 20% after resection[5]. Although our study was retrospective, treatment in the STI-571 and non-STI-571 eras was also different. The average size of the STI-571 group (20.7 cm) was larger than that of the non-STI-571 group (12.8 cm), although the difference was not significant. All included patients had a tumor diameter greater than 10 cm. In patients not given STI-571, the 5-year survival rate was 30%, similar to the previous study. The 5-year survival rate of patients given STI-571 was nearly 80%, and STI-571 treatment could prolong the survival time even with tumor recurrence after surgical resection.

In our series, two patients had tumor recurrences within 15 and 9 mo after resection and received only systemic chemotherapy. These two patients died within six months of chemotherapy. In contrast, the patients with giant GISTs who received STI-571 obtained good results. We conclude that patients who need palliative therapy should be treated in combination with STI-571 to give a better prognosis.

Surgical treatment is still essential, even for the largest GISTs[4], and complete surgical resection remains the only curative treatment for malignant GISTs[22]. However, significant risks of recurrence remain particularly in those tumors that demonstrate necrosis, high mitotic activity, and large size[22]. The diagnostic accuracy of *c-kit* staining, careful surgical planning to achieve a complete resection, and the availability of imatinib to treat metastatic diseases contribute to the high five-year overall survival rate (76%)[22]. We believe that aggressive complete resection, avoidance of tumor rupture and spillage, and en-bloc resection of other involved organs remain a good policy for treating malignant giant GISTs[21,23,24].

In conclusion, surgery is still the best primary treatment for patients with GIST tumors[21]. We suggest that immediate use of STI-571 when the surgical margin is positive would improve the prognosis of patients with giant GISTs.

REFERENCES

1 **Kindblom LG,** Remotti HE, Aldenborg F, Meis-Kindblom JM. Gastrointestinal pacemaker cell tumor (GIPACT): gastrointestinal stromal tumors show phenotypic characteristics of the interstitial cells of Cajal. *Am J Pathol* 1998; **152**: 1259-1269

2 **Miettinen M,** Virolainen M. Gastrointestinal stromal tumors-value of CD_{34} antigen in their identification and separation from true leiomyomas and schwannomas. *Am J Surg Pathol* 1995; **19**: 207-216

3 **Hirota S,** Isozaki K, Moriyama Y, Hashimoto K, Nishida T, Ishiguro S, Kawano K, Hanada M, Kurata A, Takeda M, Muhammad Tunio G, Matsuzawa Y, Kanakura Y, Shinomura Y, Kitamura Y. Gain-of-function mutations of *c-kit* in human gastrointestinal stromal tumors. *Science* 1998; **279**: 577-580

4 **Miettinen M,** El-Rifai W, H L Sobin L, Lasota J. Evaluation of malignancy and prognosis of gastrointestinal stromal tumors: a review. *Hum Pathol* 2002; **33**: 478-483

5 **DeMatteo RP,** Lewis JJ, Leung D, Mudan SS, Woodruff JM, Brennan MF. Two hundred gastrointestinal stromal tumors: recurrence patterns and prognostic factors for survival. *Ann Surg* 2000; **231**: 51-58

6 **Ng EH,** Pollock RE, Munsell MF, Atkinson EN, Romsdahl MM. Prognostic factors influencing survival in gastrointestinal leiomyosarcomas. Implications for surgical management and staging. *Ann Surg* 1992; **215**: 68-77

7 **Emory TS,** Sobin LH, Lukes L, Lee DH, O'Leary TJ. Prognosis of gastrointestinal smooth-muscle (stromal) tumors: dependence on anatomic site. *Am J Surg Pathol* 1999; **23**: 82-87

8 **Ng EH,** Pollock RE, Romsdahl MM. Prognostic implications of patterns of failure for gastrointestinal leiomyosarcomas. *Cancer* 1992; **69**: 1334-1341

9 **Pierie JP,** Choudry U, Muzikansky A, Yeap BY, Souba WW, Ott MJ. The effect of surgery and grade on outcome of gastrointestinal stromal tumors. *Arch Surg* 2001; **136**: 383-389

10 **Clary BM,** DeMatteo RP, Lewis JJ, Leung D, Brennan MF. Gastrointestinal stromal tumors and leiomyosarcoma of the abdomen and retroperitoneum: a clinical comparison. *Ann Surg Oncol* 2001; **8**: 290-299

11 **Yarden Y,** Kuang WJ, Yang-Feng T, Coussens L, Munemitsu S, Dull TJ, Chen E, Schlessinger J, Francke U, Ullrich A. Human proto-oncogene *c-kit*: a new cell surface receptor tyrosine kinase for an unidentified ligand. *EMBO J* 1987; **6**: 3341-3351

12 **Chabot B**, Stephenson DA, Chapman VM, Besmer P, Bernstein A. The proto-oncogene *c-kit* encoding a transmembrane tyrosine kinase receptor maps to the mouse W locus. *Nature* 1988; **335**: 88-89

13 **Geissler EN,** Ryan MA, Housman DE. The dominant-white spotting (W) locus of the mouse encodes the *c-kit* proto-oncogene. *Cell* 1988; **55**: 185-192

14 **Maeda H,** Yamagata A, Nishikawa S, Yoshinaga K, Kobayashi S, Nishi K, Nishikawa S. Requirement of *c-kit* for development of intestinal pacemaker system. *Development* 1992; **116**: 369-375

15 **Liu YQ,** Zhao H, Ning T, Ke Y, Li JY. Expression of 1A6 gene and its correlation with intestinal gastric carcinoma. *World J Gastroenterol* 2003; **9**: 238-241

16 **Joensuu H,** Roberts PJ, Sarlomo-Rikala M, Andersson LC, Tervahartiala P, Tuveson D, Silberman S, Capdeville R, Dimitrijevic S, Druker B, Demetri GD. Effect of the tyrosine kinase inhibitor STI571 in a patient with a metastatic gastrointestinal stromal tumor. *N Engl J Med* 2001; **344**: 1052-1056

17 **Lewis JJ,** Leung D, Woodruff JM, Brennan MF. Retroperitoneal soft-tissue sarcoma: analysis of 500 patients treated and followed at a single institution. *Ann Surg* 1998; **228**: 355-365

18 **Verweij J,** van Oosterom A, Blay JY, Judson I, Rodenhuis S, van der Graaf W, Radford J, Le Cesne A, Hogendoorn PC, di Paola ED, Brown M, Nielsen OS. Imatinib mesylate (STI-571 Glivec®, Gleevec™) is an active agent for gastrointestinal stromal tumours, but does not yield responses in other soft-tissue sarcomas that are unselected for a molecular target. Results from an EORTC Soft Tissue and Bone Sarcoma Group phase II study. *Eur J Cancer* 2003; **39**: 2006-2011

19 **Dematteo RP,** Heinrich MC, El-Rifai WM, Demetri G. Clinical management of gastrointestinal stromal tumors: before and after STI-571. *Hum Pathol* 2002; **33**: 466-477

20 **Bilimoria MM,** Holtz DJ, Mirza NQ, Feig BW, Pisters PW, Patel S, Pollock RE, Benjamin RS, Papadopoulos NE, Plager C, Murphy A, Griffin JR, Burgess MA, Hunt KK. Tumor volume as a prognostic factor for sarcomatosis. *Cancer* 2002; **94**: 2441-2446

21 **Mudan SS,** Conlon KC, Woodruff JM, Lewis JJ, Brennan MF. Salvage surgery for patients with recurrent gastrointestinal sarcoma: prognostic factors to guide patient selection. *Cancer* 2000; **88**: 66-74

22 **Wu PC,** Langerman A, Ryan CW, Hart J, Swiger S, Posner MC. Surgical treatment of gastrointestinal stromal tumors in the imatinib (STI-571) era. *Surgery* 2003; **134**: 656-665; discussion 665-666

23 **Crosby JA,** Catton CN, Davis A, Couture J, O'Sullivan B, Kandel R, Swallow CJ. Malignant gastrointestinal stromal tumors of the small intestine: a review of 50 cases from a prospective database. *Ann Surg Oncol* 2001; **8**: 50-59

24 **Pidhorecky I,** Cheney RT, Kraybill WG, Gibbs JF. Gastrointestinal stromal tumors: current diagnosis, biologic behavior, and management. *Ann Surg Oncol* 2000; **7**: 705-712

Assistant Editor Guo SY **Edited by** Wang XL and Ma JY

PO Box 2345, Beijing 100023, China
Fax: +86-10-85381893
E-mail: wjg@wjgnet.com www.wjgnet.com

ELSEVIER

World J Gastroenterol 2005;11(2):264-267
World Journal of Gastroenterology ISSN 1007-9327

• BRIEF REPORTS •

Mitochondrial DNA sequence analysis of two mouse hepatocarcinoma cell lines

Ji-Gang Dai, Xia Lei, Jia-Xin Min, Guo-Qiang Zhang, Hong Wei

Ji-Gang Dai, Xia Lei, Jia-Xin Min, Guo-Qiang Zhang, Hong Wei, Department of Thoracic Surgery, Xinqiao Hospital, Third Military Medical University, Chongqing 400037, China
Supported by the National Natural Science Foundation of China, No. 39900173
Correspondence to: Jia-Xin Min, Department of Thoracic Surgery, Xinqiao Hospital, Third Military Medical University, Chongqing 400037, China. daijigang@vip.sina.com
Telephone: +86-23-68755616 **Fax:** +86-23-68755616
Received: 2003-12-28 **Accepted:** 2004-01-15

Abstract

AIM: To study genetic difference of mitochondrial DNA (mtDNA) between two hepatocarcinoma cell lines (Hca-F and Hca-P) with diverse metastatic characteristics and the relationship between mtDNA changes in cancer cells and their oncogenic phenotype.

METHODS: Mitochondrial DNA D-loop, $tRNA^{Met+Glu+Ile}$ and ND3 gene fragments from the hepatocarcinoma cell lines with 1 100, 1 126 and 534 bp in length respectively were analysed by PCR amplification and restriction fragment length polymorphism techniques. The D-loop 3' end sequence of the hepatocarcinoma cell lines was determined by sequencing.

RESULTS: No amplification fragment length polymorphism and restriction fragment length polymorphism were observed in $tRNA^{Met+Glu+Ile}$, ND3 and D-loop of mitochondrial DNA of the hepatocarcinoma cells. Sequence differences between Hca-F and Hca-P were found in mtDNA D-loop.

CONCLUSION: Deletion mutations of mitochondrial DNA restriction fragment may not play a significant role in carcinogenesis. Genetic difference of mtDNA D-loop between Hca-F and Hca-P, which may reflect the environmental and genetic influences during tumor progression, could be linked to their tumorigenic phenotypes.

Key words: Hepatocarcinoma; Mitochondrial DNA; Base Sequence

Dai JG, Lei X, Min JX, Zhang GQ, Wei H. Mitochondrial DNA sequence analysis of two mouse hepatocarcinoma cell lines. *World J Gastroenterol* 2005; 11(2): 264-267
http://www.wjgnet.com/1007-9327/11/264.asp

INTRODUCTION

Mammalian mitochondrial DNA (mtDNA) is a 15-16 kb circular double-stranded DNA. The genome contains genes coding for 13 polypeptides involved in respiration and oxidative phosphorylation, 2 rRNAs and a set of 22 tRNAs that are essential for protein synthesis of mitochondria. In contrast to the nuclear DNA, mtDNA is a naked DNA molecule without introns and is replicated at a much higher rate without an effective DNA repair mechanism. Therefore, mtDNA is more vulnerable to reactive oxygen species and free radicals that are generated in electron leak pathway of the respiratory chain[1-3].

The possibility that the mitochondrial genome may be involved in carcinogenesis can be extrapolated back to Warburg, who demonstrated that increased anaerobic glycolysis was a common feature of tumor cells[4]. One scenario is that the somatic mtDNA mutations in tumor cells play an active role in shifting metabolism away from mitochondrial oxidative phosphorylation and towards enhanced glycolysis[5,6]. mtDNA mutation is a prominent feature of cancer cells and has been identified in various tumors and tumor cell lines[7]. However, the direct link between mtDNA mutations of cancer cells and their oncogenic phenotype has not been demonstrated.

Hca-F and Hca-P are two types of cell lines originating from an identical parent cell line, hepatocarcinoma H22, with high and low metastatic abilities, respectively. To inquire into the role of mtDNA mutations in tumorigenic phenotype, the genetic variations of mtDNA from Hca-F and Hca-P cell lines were analyzed by PCR and restriction fragment length polymorphism (RFLP) and DNA sequencing.

MATERIALS AND METHODS

Materials

The restriction endonucleases including *Hae* III, *Bam*H I, *Apa* I, *Nde* II, *Xho* I, *Xba* I, *Alu* I, *Rsa* I, *Stu* I, *Dra* I, *Ava* I, and *Hae* II were purchased from German Boehringer Mannheing and American Promega companies; PCR test kits were also obtained from German Boehringer Mannhening Company. Hca-F and Hca-P hepatocarcinoma cell lines were supplied by Professor Mao-Yin Lin of Dalian Medical University, China.

Amplification of PCR

The primers were synthesized by Shanghai Cell Biological Institute of China (Table 1). Mitochondrial DNA of the tumor cell lines was prepared by the method of nuclei/cytoplasm partition[8]. PCR amplification was carried out in a final volume of 100 μL containing 0.5 μg mtDNA, 0.5 mmol/L of each primer, 2.5 mmol/L $MgCl_2$, 200 mmol/L of each dNTP, and 2.5 U *Taq* DNA polymerase (TaKaRa Ex TaqTM). PCR (an initial incubation at 94 ℃ for 4 min, followed by 30 cycles at 94 ℃ for 30 s, at 55 ℃ for 1 min, and at 72 ℃ for 1 min; the final step at 72 ℃ was extended to 10 min) was performed in a Biometra Personal PCR system.

PCR-RFLP analysis of D-loop, $tRNA^{Met+Glu+Ile}$ and ND3 gene fragments

Two U restriction endonucleases and 1.2 μL 10×buffer were added to 5 μL of every PCR product separately and each dilution was mixed with sterilized water until the total volume was 12 μL; then incubated at 37 ℃ overnight. After digested by the restriction endonucleases, each sample was analyzed by 1% agarose gel electrophoresis (the buffer fluid was TBE buffer). Performed at 3 V/cm for 1-2 h, the electrophoresis was observed under ultraviolet and photographs were taken. The standard marker of Huamei Company was adopted as the molecular weight standard to determine the length of the fragments.

Table 1 Primer sequence and length of amplified fragments

Amplified fragment	Length (bp)	Location	Primer sequence
D-loop	1 100	L strand (15 294-15 320)	5′-TAAACATTACTCTGGTCTTGTAAACC-3′
		H strand (98-72)	5′-ATTAATAAGGCCAGGACCAAACCT-3′
$tRNA^{Met+Glu+Ile}$	1 126	L strand (3 401-3 419)	5′-CGGCCCATTCGCGTTATTC-3′
		H strand (4 527-4 508)	5′-AGGTTGAGTAGAGTGAGGGA-3′
ND3 fragment	534	L strand (9 364-9 385)	5′-ACGTCTCCATTTATTGATGAGG-3′
		H strand (9 897-9 876)	5′-GAGGTTGAAGAAGGTAGATGGC-3′
D-loop 3′ end fragment	437	L strand (15 950-15 968)	5′-AGGCATGAAAGGACAGCAC-3′
		H strand (91-73)	5′-ATAAGGCCAGGACCAAACC-3′

Table 2 Mitochondrial $tRNA^{Met+Glu+Ile}$, ND3 and D-loop restriction patterns

Enzyme	D-loop (1 100 bp)		$tRNA^{Met+Glu+Ile}$ (1 126 bp)		ND3 (534 bp)	
	Site	FL	Site	FL	Site	FL
Hae III	4	456 445 122, ...	4	470 290 136...	1	392 142
Apa I	1	655 445	1	658 469	0	534
Alu I	4	545 269 102, ...	3	665 318 135...	1	310 224
*Bam*H I	0	1 100	2	710 252 164	0	534
Dra I	0	1 100	1	634 493	1	45 183
Stu I	0	1 100	2	605 297 225	1	391 143
Nde II	2	84 511 837	0	1 126	0	534
Rsa I	6	720 178 125...	4	392 259 228...	2	35 310 378
Xba I	1	680 420	0	1 126	0	524

FL: fragment length.

DNA sequencing of PCR products

PCR products for the D-loop 3 end fragment of 437 bp in length were sent to United Gene Technology Company, Ltd, Shanghai, China for direct sequencing.

RESULTS

Mitochondrial DNA D-loop, $tRNA^{Met+Glu+Ile}$ and ND3 gene fragments from the hepatocarcinoma cell lines with 1 100, 1 126 and 534 bp in length respectively were analysed by PCR amplification. No amplification fragment length polymorphism and negative amplification were observed. Mitochondrial DNA D-loop, $tRNA^{Met+Glu+Ile}$ and ND3 fragments were cleaved respectively by 12 kinds of restriction endonucleases including *Hae* III, *Bam*H I, *Apa* I, *Nde* II, *Xho* I, *Xba* I, *Alu* I, *Rsa* I, *Stu* I, *Dra* I, *Ava* I and *Hae* II. But no difference was observed in all restriction maps of D-loop, $tRNA^{Met+Glu+Ile}$ and ND3 fragments of mtDNA from hepatocarcinoma cell lines and no variation was found in 41 restriction endonuclease sites (Figure 1, Table 2).

The D-loop 3' end fragment sequence of two hepatocarcinoma cell lines was determined by sequencing. Compared with published mouse mtDNA sequence, we had found 3 mutations: G:C→A:T transition was detected at nucleotide 16 007 in Hca-F and Hca-P cell lines and a T:A→C:G occurred at nucleotide 16 268 only in Hca-F cell line (Figure 2).

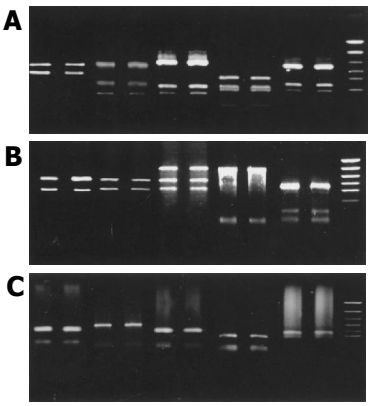

Figure 1 Restriction patterns of amplified fragments. F: Hca-F cells; P: Hca-P cells; M: PCR standard marker. A: Restriction patterns of tRNA Met+Glu+Ile digested by *Apa* I, *Alu* I, *Bam*H I, *Rsa* I and *Stu* I, respectively; B: Restriction patterns of D-loop digested by *Xba* I, *Apa* I, *Rsa* I, *Stu* I and *Alu* I, respectively; C: Restriction patterns of ND3 digested by *Hae* III, *Dra* I, *Stu* I, *Rsa* I and *Alu* I, respectively.

15 950	AGGCATGAAA	GGACAGCACA	CAGTCTAGAC	GCACCTACGG	TGAAGAATCA	TTAGTCCGCA A(2)
16 010	AAACCCAATC	ACCTAAGGCT	AATTATTCAT	GCTTGTTAGA	CATAAATGCT	ACTCAATACC
16 070	AAATTTTAAC	TCTCCAAACC	CCCCACCCCC	TCCTCTTAAT	GCCAAACCC	AAAAAACACT
16 130	AAGAACTTGA	AAGACATATA	ATATTAACTA	TCAAACCCTA	TGTCCTGATC	AATTCTAGTA
16 190	GTTCCCAAAA	TATGACTTAT	ATTTTAGTAC	TTGTAAAAAT	TTTACAAAAT	CAATGTTCCGT
16 250	GAACCAAAAC	TCTAATCATAC	CTCTATTACG	CAATAAACAT	TAACAA 1	GTTAATGTAG
11	CTTAATAACA	AAGCAAAGCA	CTGAAAATGC	TTAGATGGAT	AATTGTATCC	CATAAACACA
71	AAGGTTTGGT	CCTGGCCTTA	T			

Figure 2 Variations identified in the D-loop (bases 15 950-91) of mitochondrial DNA from two types of hepatocarcinoma cell lines. Sequence and base number were from the complete mouse mtDNA sequence reported by Bibb *et al*. (Cell 1981; 26: 167-180). The G at nucleotide 16 007 was mutated to A in two hepatocarcinoma cell lines and T at nucleotide 16 268 was mutated to C in Hca-F cell line.

DISCUSSION

Carcinogenesis is a multi-step process involving the accumulation of genetic changes that ends in malignant cell transformation. Much attention has been paid to the genetic events in the nDNA, such as activation of oncogene, inactivation of tumor suppressor gene, and defects of mismatch DNA repair gene. However, several aspects in the process of carcinogenesis are still unclear. Contribution of mtDNA mutations to carcinogenesis was postulated when wide spectra of the mtDNA alterations were reported in different types of cancer: colon, ovarian, lung, pancreatic, liver, thyroid, bladder, prostate, esophageal and gastric cancer[7,9-12]. Reported sequence changes include point mutations (mostly transitions), multiple deletions and microsatellite instability in coding and noncoding regions. However, of all these mutations and polymorphisms only a few can be linked to a known phenotypic effect. Alonso[13] suggested different mechanisms, such as clonal expansion, increased oxidative damage and mutator mutations, to explain this high frequency of homoplasmic mtDNA variation in cancer samples. Because most tumors are a clonal expansion of a single cell, it is possible that mtDNA homoplasmic mutations are just the results of clonal expansion of spontaneous somatic mutations, which occur at a very low frequency during previous replication of this precursor cell and later become predominant or homoplasmic by clonal expansion of its cell[14]. However, the selective advantage of mtDNA changes in the development of tumors cannot be excluded. In principle, these mutations could contribute to neoplastic transformation by changing cellular energy capacities, increasing mitochondrial oxidative stress, and/or modulating apoptosis.

In this study, large-scale deletion mutations of D-loop, $tRNA^{Met+Glu+Ile}$ and ND3 gene fragments in hot-spot regions of mtDNA were analysed by PCR amplification and RFLP techniques. There were no amplification fragment length polymorphism and negative amplification, and all restriction patterns of D-loop, $tRNA^{Met+Glu+Ile}$ and ND3 fragments from Hca-F and Hca-P hepatocarcinoma cell lines were also identical. In contrast to previous studies, we failed to find mtDNA large-scale deletions in tumor cell lines, which differ from the observation that multiple mtDNA deletions were detected in tumors and normal human tissue cells[15,16]. We propose possible mechanisms to explain the phenomenon. Firstly, the increased proliferation of tumor cell lines promotes the cytoplasmic segregation of deleted mtDNAs, and thus the mtDNA molecules with deletions are passively eliminated in tumor cells. Secondly, the mtDNA deletions accumulated in tumor cells may result in impaired mitochondrial respiration and decrease ATP synthesis. After cytoplasmic segregation of deleted mtDNAs, the cells harboring higher proportion of mtDNA deletions could not survive and lead to dropout from the population. So, we suggest that mtDNA fragment deletion mutations in tumors unlikely play a significant role in carcinogenesis, probably just as age-related increases in DNA damage due to cellular oxidative stress and environmental factors.

Mitochondrial DNA control region (non-coding region, D-loop), containing the origin of replication for H-strand synthesis, mitochondrial transcription promoters, mtTF1 binding site and conserved sequence block, *etc*, serves as the main site for mitochondrial genomic replication and transcription. Point mutations and genetic instabilities at the D-loop region are potentially involved in the maintenance of structure and function or even the expression of other mitochondrial genes, and probably also involved in the progressive stage of the disease[17,18]. In the present study, we have found sequence difference in mtDNA D-loop region between two types of hepatocarcinoma cell lines with diverse metastatic abilities. G:C→A:T transition was detected at nucleotide 16 007 in Hca-F and Hca-P cell lines and T:A→C:G occurred at nucleotide 16 268 only in Hca-F cell line. Little is known about the presence of genetic alterations, especially of point mutations, localized at crucial sites or adjacent place in the mtDNA control region, and their contribution to carcinogenesis. Although it is unlikely that mutations in the mtDNA control region are immediately deleterious or tumorigenic, the frequency of mtDNA mutations may reflect underlying genetic and environmental influences during tumor progression[19]. It is also possible that sequence variants in the mtDNA control region could influence disease-associated mutations in the coding regions[20,21]. There is considerable evidence that the mutation rate of both mitochondrial coding region and non-coding region loci is increased as a result of tumorigenicity[22-25]. It is likely, therefore, that the difference of mtDNA D-loop region observed in different hepatocarcinoma cell lines is a reflection of this increased mutation rate and can be linked to their tumorigenic phenotype. More extensive biochemical and molecular studies will be necessary for determining the pathological effect of these mtDNA genetic alterations.

REFERENCES

1 **Lee HC,** Lim ML, Lu CY, Liu VW, Fahn HJ, Zhang C, Nagley P, Wei YH. Concurrent increase of oxidative DNA damage and lipid peroxidation together with mitochondrial DNA mutation in human lung tissues during aging-smoking enhances oxidative stress on the aged tissues. *Arch Biochem Biophys* 1999; **362**: 309-316

2 **Taanman JW.** The mitochondrial genome: structure, transcription, translation and replication. *Biochim Biophys Acta* 1999; **1410**: 103-123

3 **Li JM,** Cai Q, Zhou H, Xiao GX. Effects of hydrogen peroxide on mitochondrial gene expression of intestinal epithelial cells. *World J Gastroenterol* 2002; **8**: 1117-1122

4 **Dang CV,** Semenza GL. Oncogenic alterations of metabolism. *Trends Biochem Sci* 1999; **24**: 68–72

5 **Polyak K,** Li Y, Zhu H, Lengauer C, Willson JK, Markowitz SD, Trush MA, Kinzler KW, Vogelstein B. Somatic mutations of the mitochondrial genome in human colorectal tumours. *Nat Genet* 1998; **20**: 291–293

6 **Yeh JJ,** Lunetta KL, van Orsouw NJ, Moore FD, Mutter GL, Vijg J, Dahia PL, Eng C. Somatic mitochondrial DNA (mtDNA) mutations in papillary thyroid carcinomas and differential mtDNA sequence variants in cases with thyroid tumours. *Oncogene* 2000; **19**: 2060–2066

7 **Carew JS,** Huang P. Mitochondrial defects in cancer. *Mol Cancer* 2002; **1**: 9

8 **Dai JG,** Wu YG, Wei H, Xiao YB. A simple and rapid method for the preparation the mtDNA. *Disan Junyi Daxue Xuebao* 2000; **15**: 391-392

9 **Fliss MS,** Usadel H, Caballero OL, Wu L, Buta MR, Eleff SM, Jen J, Sidransky D. Facile detection of mitochondrial DNA mutations in tumors and bodily fluids. *Science* 2000; **287**: 2017–2019

10 **Luciakova K,** Kuzela S. Increased steady-state levels of several mitochondrial and nuclear gene transcripts in rat hepatoma with a low content of mitochondria. *Eur J Biochem* 1992; **205**: 1187-1193

11 **Tamura G,** Nishizuka S, Maesawa C, Suzuki Y, Iwaya T, Sakata K, Endoh Y, Motoyama T. Mutations in mitochondrial control region DNA in gastric tumours of Japanese patients. *Eur J Cancer* 1999; **35**: 316-319

12 **Clayton DA,** Vinograd J. Circular dimer and catenate forms of mitochondrial DNA in human leukaemic leucocytes. *J Pers* 1967; **35**: 652-657

13 **Alonso A,** Martin P, Albarran C, Aquilera B, Garcia O, Guzman A, Oliva H, Sancho M. Detection of somatic mutations in the mitochondrial DNA control region of colorectal and gastric tumors by heteroduplex and single-strand conformation analysis. *Electrophoresis* 1997; **18**: 682-685

14 **Perucho M.** Microsatellite instability: the mutator that mutates the other mutator. *Nat Med* 1996; **2**: 630-631

15 **Lee HC,** Yin PH, Yu TN, Chang YD, Hsu WC, Kao SY, Chi CW, Liu TY, Wei YH. Accumulation of mitochondrial DNA deletions in human oral tissues-effects of betel quid chewing and oral cancer. *Mutat Res* 2001; **493**: 67-74
16 **Kotake K,** Nonami T, Kurokawa T, Nakao A, Murakami T, Shimomura Y. Human livers with cirrhosis and hepatocellular carcinoma have less mitochondrial DNA deletion than normal human livers. *Life Sci* 1999; **64**: 1785-1791
17 **Bianchi NO,** Bianchi MS, Richard SM. Mitochondrial genome instability in human cancers. *Mutat Res* 2001; **488**: 9-23
18 **Maximo V,** Soares P, Seruca R, Rocha AS, Castro P, Sobrinho-Simoes M. Microsatellite instability, mitochondrial DNA large deletions, and mitochondrial DNA mutations in gastric carcinoma. *Genes Chromosomes Cancer* 2001; **32**: 136-143
19 **Burgart LJ,** Zheng J, Shu Q, Strickler JG, Shibata D. Somatic mitochondrial mutation in gastric cancer. *Am J Pathol* 1995; **147**: 1105-1111
20 **Marchington DR,** Poulton J, Sellar A, Holt IJ. Do sequence variants in the major non-coding region of the mitochondrial genome influence mitochondrial mutations associated with disease? *Hum Mol Genet* 1996; **5**: 473-479
21 **Poulton J,** Macaulay V, Marchington DR. Mitochondrial genetics' 98 is the bottleneck cracked? *Am J Hum Genet* 1998; **62**: 752-757
22 **Loeb LA.** A mutator phenotype in cancer. *Cancer Res* 2001; **61**: 3230-3239
23 **Penta JS,** Johnson FM, Wachsman JT, Copeland WC. Mitochondrial DNA in human malignancy. *Mutat Res* 2001; **488**: 119-133
24 **Sanchez-Cespedes M,** Parrella P, Nomoto S, Cohen D, Xiao Y, Esteller M, Jeronimo C, Jordan RC, Nicol T, Koch WM, Schoenberg M, Mazzarelli P, Fazio VM, Sidransky D. Identification of a mononucleotide repeat as a major target for mitochondrial DNA alterations in human tumors. *Cancer Res* 2001; **61**: 7015-7019
25 **Richard SM,** Bailliet G, Paez GL, Bianchi MS, Peltomaki P, Bianchi NO. Nuclear and mitochondrial genome instability in human breast cancer. *Cancer Res* 2000; **60**: 4231-4237

Edited by Chen WW **Proofread by** Zhu LH

PO Box 2345, Beijing 100023, China
Fax: +86-10-85381893
E-mail: wjg@wjgnet.com www.wjgnet.com

ELSEVIER

World J Gastroenterol 2005;11(2):268-271
World Journal of Gastroenterology ISSN 1007-9327

• BRIEF REPORTS •

Effects of oxymatrine on experimental hepatic fibrosis and its mechanism *in vivo*

Guang-Feng Shi, Qian Li

Guang-Feng Shi, Qian Li, Department of Infectious Diseases, Hua Shan Hospital, Fu Dan University, Shanghai 200040, China
Supported by Foundation of "Bai Ren Ji Hua" of Shanghai Health Bureau, No. 98BR32
Correspondence to: Dr. Guang-Feng Shi, Department of Infectious Diseases, Hua Shan Hospital, Fu Dan University, 12 Wu Lu Mu Qi Zhong Road, Shanghai 200040, China. gfshi@shmu.edu.cn
Telephone: +86-21-62489999-6565 **Fax:** +86-21-62489015
Received: 2004-02-03 **Accepted:** 2004-03-18

Abstract

AIM: Hepatic fibrogenesis has close relation with hepatic stellate cells (HSC) and tissue inhibitors of metalloproteinase (TIMP). Oxymatrine (OM) is a kind of Chinese herb that is found to have some effects on liver fibrosis. We aimed to determine the effects of OM on hepatic fibrosis and explore the possible mechanism.

METHODS: Thirty-two rats were randomly divided into four groups; 16 were used to develop hepatic fibrosis by carbon tetrachloride (CCl_4) and treated with or without OM, and 16 were used as controls. The expression of tissue inhibitor of metalloproteinase-1 (TIMP-1) and α-smooth muscle actin (α-SMA) in the livers of rats was detected by immunohistochemical assay. Liver pathology was determined by H&E staining and reticulum staining.

RESULTS: In CCl_4-injured rats, the normal structure of lobules was destroyed, and pseudolobules were formed. Hyperplasia of fibers was observed surrounding the lobules. While the degree of fibrogenesis in liver tissues was significantly decreased in those rats with OM-treatment compared with those without OM treatment. The pseudolobules were surrounded by strong, multi-layer reticular fibers, which netted into pseudolobules in CCl_4-injured rats, however, there was a significant decrease in reticular fibers in OM-treated rats. The expression of TIMP-1 in hepatic cells was weak in control groups, but strong in CCl_4-injured groups, however, the expression of TIMP-1 was significantly inhibited by OM ($F = 52.93$, $P<0.05$). There was no significant change in the expression of α-SMA between CCl_4-injured rats with or without OM treatment ($F = 8.99$, $P>0.05$).

CONCLUSION: OM effectively inhibits CCl_4-induced fibrogenesis in rat liver tissues, probably by reducing the expression level of TIMP-1.

Key words: Experimental hepatic fibrosis; Oxymatrine; TIMP-1; α-SMA

Shi GF, Li Q. Effects of oxymatrine on experimental hepatic fibrosis and its mechanism *in vivo*. *World J Gastroenterol* 2005; 11(2): 268-271
http://www.wjgnet.com/1007-9327/11/268.asp

INTRODUCTION

Significant progress in the cellular and molecular mechanisms of hepatic fibrogenesis has been achieved over the last decades[1-5]. Hepatic fibrogenesis is known to be a gradual and dynamic process, which involves a series of complicated changes in cells, cytokines and extra cellular matrix (ECM). Especially, it has close relation with the hepatic stellate cells (HSC)[6] and tissue inhibitors of metalloproteinase (TIMP)[7].

Oxymatrine (OM) is a kind of Chinese herb which can inhibit hepatitis B and C viruses[8-12]. It was originally used for the treatment of chronic viral hepatitis. Later, it was found to have some effects on liver fibrosis[13]. However, there is little evidence of the underlying mechanism. In this study, we determined the effects of OM on experimental hepatic fibrosis, and explored the possible mechanism *in vivo*.

MATERIALS AND METHODS

Animal experiments

Thirty-two adult male Sprague Dawley rats, weighing 190-230 g (provided by Experimental Animal Center of Chinese Academy, Shanghai, China) were included in the experiments. A rat model of chronic hepatic injury was produced by carbon tetrachloride (CCl_4) IH (hypodermic injection) in 16 rats, and 16 rats were used as controls.

The rats were randomly divided into four groups. In group 1 (CCl_4 group, $n=8$), CCl_4 (0.3 mL/100 g weight, Shanghai Lingfeng Chemicals Reagent Company, Shanghai, China) was injected at the back hypodermically twice per wk for 10 wk to develop a model of hepatic fibrosis. In group 2 (CCl_4+OM group, $n = 8$), CCl_4 was given as in group 1 together with OM (60 mg/kg weight, Shanghai Chemicals Reagent Company, China Pharmaceutical Corporation, Shanghai, China), once daily for 10 wk. In group 3 (OM control group, $n = 8$), OM was given as in group 2 but without CCl_4. In group 4 (blank control group, $n = 8$), olive oil (0.3 mL/100 g weight, Ningxia Pharmaceutical Factory, Ningxia, China), instead of CCl_4, was injected at the back hypodermically. After 10-wk injection, all animals were sacrificed under narcosis, and their right liver lobes were immediately excised. The specimens were fixed in formaldehyde for the preparation of serial paraffin sections at 5-μm thickness.

Pathological observation and reticular collagen staining

Liver sections were stained with hematoxylin and eosin (H and E) for the assessment of liver cell degeneration and necrosis, infiltration of inflammatory cells, hyperplasia of the lattice fibers and formation of collagen bundles and pseudolobules. Other sections were stained with Von Gieson and Masson special staining for the assessment of fiber structure of the livers and analysis of hyperplasia of liver fiber tissues by computer image analysis system.

Expression of liver TIMP-1 and α-SMA

TIMP-1 expression was determined by the immunohistochemical ABC method. The serial paraffin sections of liver samples were deparaffinized and rehydrated after being immersed in 0.3% peroxide-ethanol solution at room temperature for 10 min, and

digested with 0.1% pancreatic protease at 37 ℃ for 60 min. Rabbit anti-TIMP-1 antibody (working concentration 1:100, Santa Cruz Biotechnology Company, LA, USA) was added at 37 ℃ for 60 min, then the samples were put at 4 ℃ overnight. Then biotinylated goat anti-rabbit antibody was added at 37 ℃ for 60 min, and ABC compound (working concentration 1:100, Huamei Company, Shanghai, China) was incubated at 37 ℃ for 45 min. Finally, diaminobenzidine tetrahydrochloride (DAB, Huamei Company) was added to develop color for microscopic examination and photography.

For immunohistochemical staining of α-SMA, the paraffin sections were deparaffinized and rehydrated after being immersed in 0.3% peroxide-ethanol solution at room temperature for 10 min and digested with microwave for 10 min. After incubation with the rat anti-human α-SMA monoclonal antibody (working concentration 1:100, Long-island Antibody Diagnosis Company, Shanghai, China) at 37 ℃ for 60 min and at 4 ℃ overnight, the sections were incubated with the rabbit anti-rat antibody (working concentration 1:100, Long-island Antibody Diagnosis Company) at 37 ℃ for 60 min, and finally with DAB to develop color for microscopic examination and photography.

Statistical analysis

χ^2-test was performed with SPSS 10.0.

RESULTS

Hepatic pathological findings

In the two control groups (OM control group and blank control group), the structure of liver lobules was normal, central vein was clear and the size and shape of hepatic cells were normal and distributed centrifugally (Figure 1A). In the CCl_4 group, the normal structure of lobules was destroyed, and pseudolobules were formed. Liver cells swelled, with lipid vacuoles in cytoplasm. Hyperplasia of fibers was observed surrounding the lobules. The hepatic lobules were encysted and separated by collagen bundles, and associated with bile duct "proliferation", infiltration of inflammatory cells, bordering of the portal areas. Abundant fiber tissues were present, extended outwards in stellar shape. Cholestasis was seen in some bile duct cells. Hyperplasia of ovum shape cells was observed in collagen bundles. Mitotic figures were seen in particular individual cells (Figure 1B). In CCl_4+OM group, the normal structure of lobules was also destroyed, with pseudolobule formation. Liver cells swelled and degenerated, with lipid vacuoles in cytoplasm. The hepatic lobules were encysted and separated by collagen bundles, with infiltration of inflammatory cells. However, these changes were significantly milder compared with CCl_4 group (Figure 1C).

Expression of liver reticular collagen

In the two control groups, there were only a few fiber tissues seen in portal areas. There was no significant difference between OM control group and blank control group (Figure 2A). However, in CCl_4 group, the pseudolobules were surrounded by strong, multi-layer reticular fibers, which netted into pseudolobules (Figure 2B). In CCl_4+OM group, the pseudolobules were surrounded by multi-layer reticular fibers,

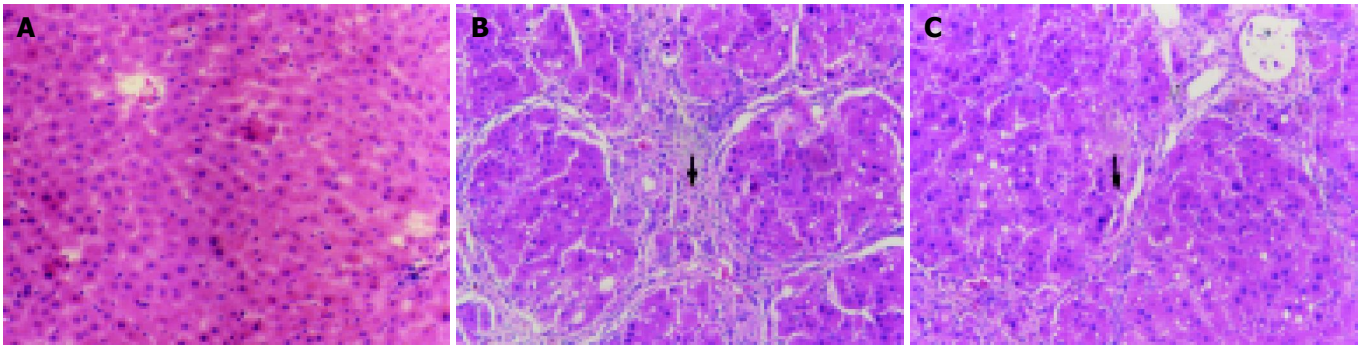

Figure 1 Pathological changes in rats' liver by H.E. staining. 10×10 A: (Control group): The structure of liver lobules was normal, the size and shape of hepatic cells were normal and distributed centrifugally; B: (CCl_4 group): The normal structure of lobules was destroyed, and pseudolobules were formed. Liver cells swelled and hepatic lobules were encysted and separated by collagen bundles, and associated with infiltration of inflammatory cells; C: (CCL_4+OM group): The normal structure of lobules was also destroyed, pseudolobules formed, and liver cells swelled at a milder extent. The hepatic lobules were encysted and separated by slimmer collagen bundles, with milder infiltration of inflammatory cells.

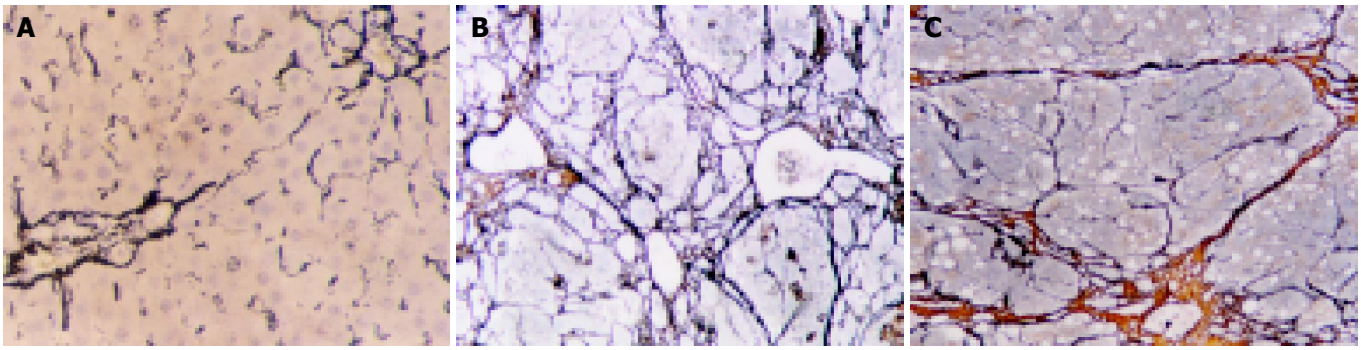

Figure 2 Observation on reticular collagen by reticular staining. 10×10. A: (Control group): A few fiber tissues were only seen in portal areas; B: (CCl_4 group): The pseudolobules were surrounded by strong, multi-layer reticular fibers, which netted into pseudolobules; C: (CCl_4+OM group): The pseudolobules were surrounded by slimmer, multi-layer reticular fibers; a significant decrease of reticular fibers was observed in this group, compared with CCl_4 group.

which netted into pseudolobules. However, there was a significant decrease in reticular fibers in this group, compared with CCl_4 group (Figure 2C).

Image pattern analysis showed that the expression of collagen in the experimental groups (CCl_4 group and CCl_4+OM group) was much stronger than that in the two control groups. Moreover, the expression of collagen in CCl_4 group was significantly stronger than that in CCl_4+OM group ($F = 31.89$, $P<0.05$) (Figure 3).

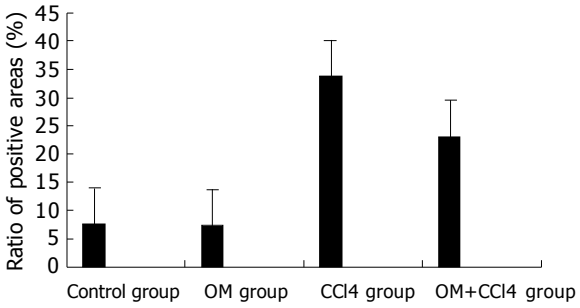

Figure 3 Contents of collagen in livers of rats in different groups.

Expression of TIMP-1 in the liver

Cytoplasmic expression of TIMP-1 antigen was detected in most hepatic cells in the experimental rats, but only in a few individual liver cells and hepatic stellate cells (HSCs) in the control rats (Figure 4A). The expression of TIMP-1 in hepatic cells was weak in control groups, but strong in experimental groups (Figure 4B). There was a significant decline in the expression of TIMP-1 in CCl_4+OM group, compared with that in CCL_4 group ($F = 52.93$, $P<0.05$) (Figure 4C, Table 1).

Table 1 Effects of oxymatrine on expression of tissue inhibitor of metalloproteinase-1 (TIMP-1) and α-smooth muscle actin (α-SMA) in the livers of rats with hepatic fibrosis (Ratio of positive areas)

Groups	*n*	TIMP-1	α-SMA
CCl_4 group	8	35.07±6.50	24.89±5.32
CCl_4+OM group	8	27.01±5.88[a]	21.64±2.36
OM group	8	2.16±1.16	4.46±1.47
Control group	8	2.48±1.40	12.52±17.6

[a]$P<0.05$ *vs* CCl_4 group.

Expression of α-SMA in the liver

α-SMA antigen in control rat liver was detected in myofibroblasts and vascular endothelial cells. The expression of α-SMA in experimental groups was significantly stronger than that in control groups (Figure 5A). There was no significant difference between CCl_4 group and CCL_4+OM group ($F = 8.99$, $P>0.05$) (Figure 5B, C, Table 1).

DISCUSSION

Studies on the pathogenesis of hepatic fibrosis have shown that HSCs within the space of Disse experience a transform, in the wake of liver injures by various causes. In normal liver, HSCs store vitamin A and show minimal proliferation and collagen synthesis. However, in an injured liver, HSCs lose vitamin A and transform into myofibroblasts (MFB), called

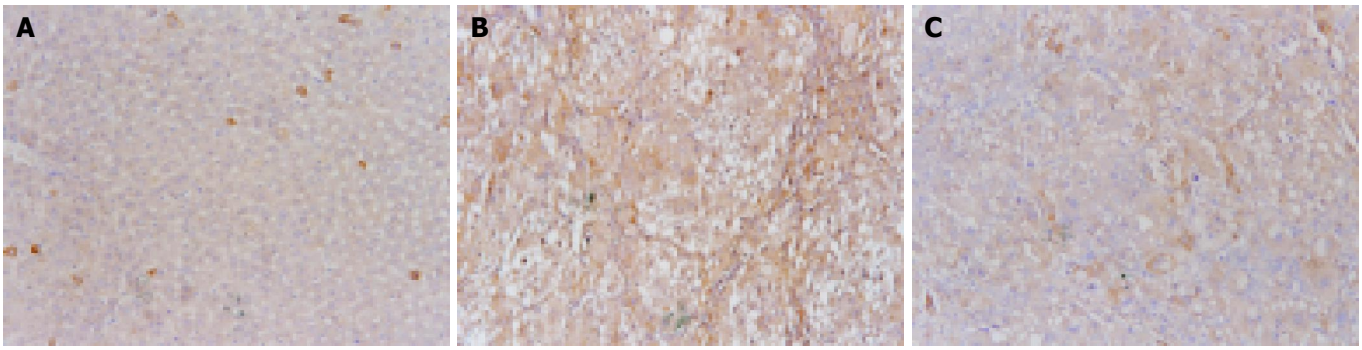

Figure 4 Expression of TIMP-1antigen by immunohistochemical staining. 10×10 A: (Control group): There was only a weak expression of TIMP-1 antigen in individual liver cells and hepatic stellate cells (HSCs); B: (CCl_4 group): The expression of TIMP-1 was detected in cytoplasm of most hepatic cells; C: (CCl_4+OM group): There was a significant decline of the expression of TIMP-1 in CCl_4+OM group, as compared with that in CCl_4 group.

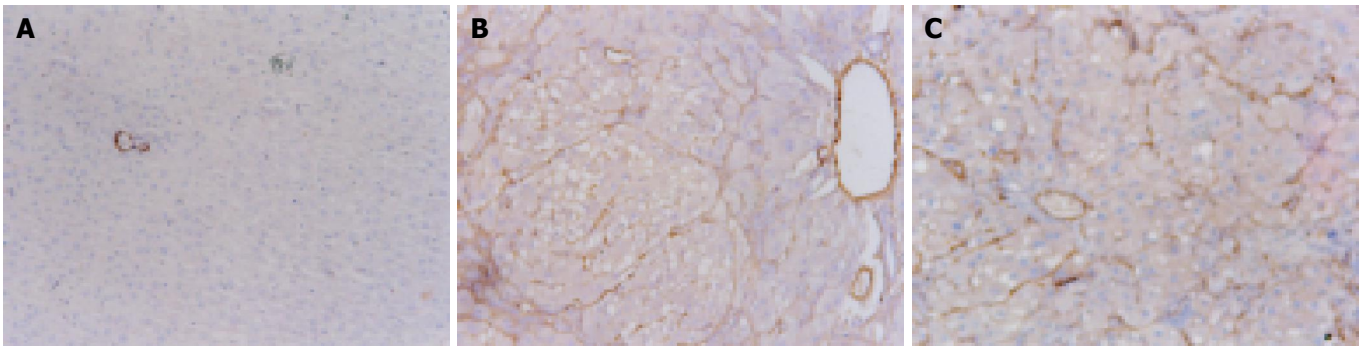

Figure 5 Expression of -SMA antigen by immunohistochemical staining. 10×10 A: (Control group): α-SMA antigen was detected in myofibroblasts and vascular endothelial cells; B: (CCl_4 group): The expression of α-SMA was significantly stronger than that in the control groups; C: (CCl_4+OM group): The expression of α-SMA was not significantly different from that in CCl_4 group.

activated HSCs, which express α-SMA and have the function of contractibility, proliferation and fibrogenesis[12]. HSCs synthesize a number of collagens, and enzymes that inhibit degeneration of extracellular matrix (ECM), and some cytokines that promote fibrosis. Thus, the balance between the deposition and degeneration of ECM is broken, leading to the startup and development of hepatic fibrosis. Some studies have shown that TIMP is a very important promoting factor of hepatic fibrosis, and it inhibits matrix metal protease (MMP) to deposit ECM[13]. Strong expression of TIMP-1 reflects the severity of hepatic fibrosis. On the other hand, OM is a kind of alkaloid, extracted from a Chinese herb, Guangdou Root. Some reports have shown that OM inhibits the secretion of IL-1, IL-6 and TNF-α from Kupffer cells, the proliferation of fibroblasts and expression of PIIIP mRNA[11]. To our knowledge, there are no reports on the effects of OM on activation of HSCs and expression of TIMP-1 in liver.

In our present study, the pathologic observation and reticular collagen staining demonstrated that the expression of collagen in CCl_4+OM group was significantly lower than that in CCl_4 group. Our results indicate that OM has a potent interference effect on hepatic fibrosis. In addition, the results of immunohistochemical staining showed that the expression of TIMP-1 in CCl_4+OM group was significantly lower than that in CCl_4 group. Combining the above quantitative data of reticular collagen, we noticed that the stronger the expression of TIMP-1 was the more reticular collagens were secreted, and *vice versa*. We suggest that TIMP-1 plays an important role in the process of hepatic fibrogenesis. One possible mechanism of OM's anti-fibrotic effect lies in its inhibition of expression of TIMP[14]. Several reports have shown that the expression levels of TIMP-1 reflect the severity of alcohol-induced hepatic fibrosis. Accordingly, there seems to be some correlation between the expression levels of TIMP-1 and the severity of hepatic fibrosis.

The present study showed that the expression of α-SMA in the liver in experimental groups was significantly stronger than that in control groups. However, there was no significant difference between CCl_4 group and CCl_4+OM group. It is presumed that OM does not have a direct effect on the activation of HSCs, whereas it influences the function of myofibroblasts[15]. Nevertheless, OM inhibits the secretion of collagen fibers and expression of TIMP-1, which in turn have interference effect on hepatic fibrosis.

In conclusion, OM has an interference effect on hepatic fibrosis, and one possible mechanism lies in its inhibitory effect on the expression of TIMP-1 in the liver.

ACKNOWLEDGEMENTS

The authors thank Mr. Gang Qin (Huashan Hospital) for the preparation of the manuscript.

REFERENCES

1 **Friedman SL.** Molecular regulation of hepatic fibrosis, an integrated cellular response to tissue injury. *J Biol Chem* 2000; **275**: 2247-2250
2 **Dodig M,** Mullen KD. New mechanism of selective killing of activated hepatic stellate cells. *Hepatology* 2003; **38**: 1051-1053
3 **Cai Y,** Shen XZ, Wang JY. Effects of glycyrrhizin on genes expression during the process of liver fibrosis. *Zhonghua Yixue Zazhi* 2003; **83**: 1122-1125
4 **Liu YK,** Shen W. Inhibitive effect of cordyceps sinensis on experimental hepatic fibrosis and its possible mechanism. *World J Gastroenterol* 2003; **9**: 529-533
5 **Nishio A,** Keeffe EB, Gershwin ME. Immunopathogenesis of primary biliary cirrhosis. *Semin Liver Dis* 2002; **22**: 291-302
6 **Eng FJ,** Friedman SL. Fibrogenesis I. New insights into hepatic stellate cell activation: the simple becomes complex. *Am J Physiol Gastrointest Liver Physiol* 2000; **279**: G7-G11
7 **Lee M,** Song SU, Ryu JK, Suh JK. Sp1-dependent regulation of the tissue inhibitor of metalloproteinases-1 promoter. *J Cell Biochem* 2004; **91**: 1260-1268
8 **Yu YY,** Wang QH, Zhu LM, Zhang QB, Xu DZ, Guo YB, Wang CQ, Guo SH, Zhou XQ, Zhang LX. A clinical research on oxymatrine for the treatment of chronic hepatitis B. *Zhonghua Ganzangbing Zazhi* 2002; **10**: 280-281
9 **Liu J,** Manheimer E, Tsutani K, Gluud C. Medicinal herbs for hepatitis C virus infection: a Cochrane hepatobiliary systematic review of randomized trials. *Am J Gastroenterol* 2003; **98**: 538-544
10 **Chen Y,** Li J, Zeng M, Lu L, Qu D, Mao Y, Fan Z, Hua J. The inhibitory effect of oxymatrine on hepatitis C virus *in vitro*. *Zhonghua Ganzangbing Zazhi* 2001; **9** Suppl: 12-14
11 **Song J,** Wang LL, Zhu L, Zhong HM, Yao P. Effects of oxymatrine on procollagen metabolism and its gene expression in experimental fibrotic rats. *Zhonghua Ganzangbing Zazhi* 2003; **11**: 697
12 **Hellemans K,** Rombouts K, Quartier E, Dittie AS, Knorr A, Michalik L, Rogiers V, Schuit F, Wahli W, Geerts A. PPARbeta regulates vitamin A metabolism-related gene expression in hepatic stellate cells undergoing activation. *J Lipid Res* 2003; **44**: 280-295
13 **Murphy F,** Waung J, Collins J, Arthur MJ, Nagase H, Mann D, Benyon RC, Iredale JP. N-Cadherin cleavage during activated hepatic stellate cell apoptosis is inhibited by tissue inhibitor of metalloproteinase-1. *Comp Hepatol* 2004; **3**(Suppl 1): S8
14 **Wang BE.** Treatment of chronic liver diseases with traditional Chinese medicine. *J Gastroenterol Hepatol* 2000; **15** Suppl: E67-E70
15 **Xiang X,** Wang G, Cai X, Li Y. Effect of oxymatrine on murine fulminant hepatitis and hepatocyte apoptosis. *Chin Med J (Engl)* 2002; **115**: 593-596

Edited by Xia HHX **Proofread by** Zhu LH

PO Box 2345, Beijing 100023, China
Fax: +86-10-85381893
E-mail: wjg@wjgnet.com www.wjgnet.com

ELSEVIER

World J Gastroenterol 2005;11(2):272-274
World Journal of Gastroenterology ISSN 1007-9327

• BRIEF REPORTS •

Polymorphism of glutathione *S*-transferase mu 1 and theta 1 genes and hepatocellular carcinoma in southern Guangxi, China

Zhuo-Lin Deng, Yi-Ping Wei, Yun Ma

Zhuo-Lin Deng, Yun Ma, Department of Pathology, Guangxi Medical University, Nanning 530021, Guangxi Zhuang Autonomous Region, China
Yi-Ping Wei, Nurse College, Guangxi Medical University, Nanning 530021, Guangxi Zhuang Autonomous Region, China
Supported by The Natural Scientific Foundation of China No. 39860032; by the Education Department of Guangxi Zhuang Autonomous Region No. 98-2-8
Correspondence to: Dr. Zhuo-Lin Deng, Department of Pathology, Guangxi Medical University, Nanning 530021, Guangxi Guangxi Zhuang Autonomous Region, China. zhuolindeng@hotmail.com
Telephone: +86-771-5358262
Received: 2004-03-06 **Accepted:** 2004-04-13

Abstract

AIM: Glutathione *S*-transferase mu 1 (GSTM1) and theta 1 (GSTT1) genes are involved in the metabolism of a wide range of carcinogens, but deletions of the genes are commonly found in the population. The present study was undertaken to evaluate the association between GSTM1 and GSTT1 gene polymorphisms and hepatocellular carcinoma (HCC) risk.

METHODS: The genetic polymorphisms were studied at an aflatoxin highly contaminated region in Guangxi, China. Polymerase chain reaction (PCR) technique was used to detect the presence or absence of the GSTM1 and GSTT1 genes in blood samples. The case group was composed of 181 patients of HCC identified by the pathologists and the control group was composed of 360 adults without any tumor.

RESULTS: The frequencies of GSTM1 and GSTT1 null genotypes in the control were 47.8% and 42.7%, while those in the HCC group were 64.6% and 59.7%, respectively. The differences between HCC group and control group were very significant ($P<0.01$). GSTM1 and GSTT1 combined null genotypes in HCC group and control group were 38.2% and 18.5% respectively, and the difference was significant ($P<0.05$).

CONCLUSION: The GSTM1 and GSTT1 null genotypes are associated with an increased risk of HCC in a special geographic environment. Combination of the two null genotypes in an individual is substantially increased twice the risk of HCC.

Key words: Hepatocellular carcinoma; Glutathione *S*-transferase mu 1; Glutathione *S*-transferase theta 1; Polymorphism

Deng ZL, Wei YP, Ma Y. Polymorphism of glutathione *S*-transferase mu 1 and theta 1 genes and hepatocellular carcinoma in southern Guangxi, China. *World J Gastroenterol* 2005; 11(2): 272-274
http://www.wjgnet.com/1007-9327/11/272.asp

INTRODUCTION

Glutathione *S*-transferases (GSTs) M1 and T1 are most important detoxified enzymes in the body that participate in the metabolism of a wide range of chemical carcinogens that are ubiquitous in the environment[1-3], but the enzyme deficiency is common in humans. Are there any cause and effect on the high prevalence of hepatocellular carcinoma (HCC) in a local region? Epidemiological investigations and animal experiments have identified that the major risk factors involved in the prevalence of HCC in southern Guangxi are hepatitis B virus (HBV) infection and aflatoxin B1 (AFB1) exposure[4,5], and etiological studies have given evidence to support the existence of a synergistic relationship between HBV and AFB1[6-8]. AFB1 is a mycotoxin that is produced by Aspergillus flavus. Since aflatoxin was discovered in food in early 1 960 s, the search for mycotoxins has led to the identification of over 100 toxigenic fungi and more than 300 mycotoxins. While AFB1 is the most vigorous carcinogen, its mutagenic metabolities binding to DNA are capable of inducing G to T transversions and the liver is a primary target organ[9,10]. It has been found that AFB1 could contaminate foods such as corn and peanut in the world, and it is known that the southwest of Guangxi is one of the areas with a rather high level of contamination and a high prevalence of HCC[10]. Therefore, study need to lay stress on detoxification of AFB1 by enzymes in an individual and susceptibility to HCC. AFB1 is not harmful prior to metabolic activation via oxidase of cytochrome P450 to form a DNA damaging agent, AFB1-8, 9-epoxide[11]. Several enzymes in the body can resist this toxin and are good for health. The present study emphasized the importance of polymorphisms of GSTM1 and GSTT1, especially their genetic deletion polymorphisms and susceptibility to HCC.

MATERIALS AND METHODS

Patients and controls

One hundred and eighty-one HCC patients and 360 controls participated in the present investigation. The HCC cases were recruited from the Affiliated Hospital of Guangxi Medical University from January 1998 to December 2002. All HCCs were confirmed by pathologic diagnosis. There were 145 male and 36 female patients aged from 28 to 70 years with an average age of 49 years. The control group came from the same hospital with their age and sex matched for the case group.

Blood samples

Three mL of blood was taken by venous puncture. The blood was used for lymphocyte isolation using buffy coat extraction kit. Genomic DNA was prepared by standard phenol-chloroform extraction.

Genotypes for the GSTM1 and GSTT1 deletions were determined by polymerase chain reaction (PCR) on the genomic DNA. Primers binding to the 5' region of exon 4 (5'-CTGCCCTA CTTGATTGATGGG-3') and the 3' region of exon 5 (5'-CTGGAT TGTAGCAGATCATGC-3') of GSTM1 were used to amplify a 273 base pair (bp) fragment. Primers for the 5' region of GSTT1 (5'-TTCCTTACTGGTCCTCACATCTC-3') and the 3' region (5'TCACCGGATGGCCAGCA-3') were used to amplify a 480 bp fragment. In both assays, the absence of PCR products was

indicative of the null genotypes[12,13]. In the cases of GSTM1 or GSTT1 null genotypes, the samples must have internal controls by a pair of β-globin or p53 gene primer co-amplification repeat analysis to monitor the quality control to exclude possible pseudo-negative reactions[13].

PCR reaction was carried out in a "BIO-RAD" amplified instrument. A commercial PCR kit was used with 5 μg of DNA, 2.5 mmol/L of dNTP, 5 umol/L of each primer, 25 mmol/L of $MgCl_2$ and 0.5 units of Taq polymerase in a total volume of 25 μL, then overlaid with a drop of mineral oil and proceeded to amplification.

PCR amplified conditions

The samples were denatured at 94 ℃ for 5 min, then treated in a different way for GSTM1 and GSTT1 gene amplification. As for the amplification of GSTM1 gene, the best condition was for 30 s at 93 ℃ and for 45 s at 50 ℃ and at 72 ℃ for 45 s, while for the GSTT1 gene, the best condition was for 45 s at 94 ℃ and 50 s at 61 ℃ and at 72 ℃ for 60 s, respectively. After 35 cycles, a final step of extension at 72 ℃ for 10 min was followed. The amplified products were subjected to electrophoresis on a 2% agarose gel and stained with ethidium bromide, observed under violet light.

Statistical analysis

The experimental results were analyzed by χ^2-test.

RESULTS

PCR products from amplification of GSTT1 (480 bp) and GSTM1 (273 bp) on agarose gels are shown in Figure 1.

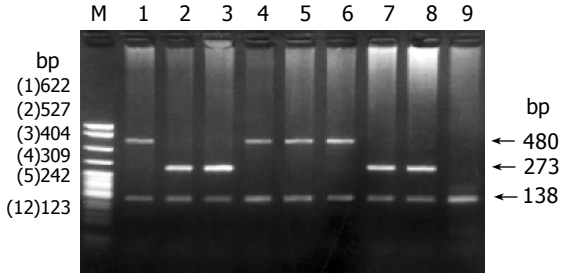

Figure 1 Amplification of GSTT1 (480 bp), GSTM1 (273 bp), and the control p53 (138 bp) gene products illustrated in agarose gel electrophoresis. M: pBR322 DNA/MspI. Lane 1: positive reaction of GSTT1 in a control case; Lane 2-3: positive reaction of GSTM1 in a control case; Lane 4-6: positive reaction of GSTT1 in HCC cases; Lane 7-8: positive reaction of GSTM1 in HCC cases; Lane 9: negative reaction of GSTM1 in a HCC case, p53 positive reaction in each case from lanes 1 to 9.

The frequencies of GSTT1 null genotype in HCC group and control group were 59.7% (108/181) and 42.7% (154/360) respectively. The frequencies of GSTM1 null genotype in HCC group and control group were 64.6% (117/181) and 47.8% (172/360) respectively. The differences were very significant (P<0.01, Table 1). In some of the cases, both GSTM1 and GSTT1 null genotypes that occurred in HCC group and control group were 38.2% and 18.5% respectively, and the difference was significant (P<0.05). GSTM1-positive but GSTT1-negative cases accounted for 21.8% and 20.7%, GSTM1-negative but GSTT1-positive cases were 25.5% and 28.9% respectively, and the two groups had no significant difference compared with the controls.

Table 1 Polymorphisms of GSTM1 and GSTT1 genes in HCC patients and controls

Group	*n*	GSTM1			GSTT1		
		Null	Present	Deletion rate (%)	Null	Present	Deletion rate (%)
HCC	181	117	64	64.6	108	73	59.7
Control	360	172	188	47.8[1]	154	206	42.7[2]

HCC group compared with control [1] χ^2 = 13.7643, P<0.01 [2]χ^2 = 13.7585, P<0.01.

DISCUSSION

GSTs are a super family, in which seven classes have been found, but only class μ (GSTM1) and class θ (GSTT1) have gene deficiency (null genotype)[14] and completely lack of respective enzyme activity. Carcinogen AFB1-8, 9-epoxide is a substrate of both GSTM1 and GSTT1[13,14]. GSTs are dimeric proteins that could catalyze conjugation reaction between glutathione and epoxides facilitate excretion and detoxification[17]. As a result, GSTs may play an important role in anti-carcinogenesis. The absence of these enzymes might susceptible to several cancers[18]. A previously report failed to detect a statistically significant relationship between GSTM1 genotype and HCC case/control status might be due to an inadequate sample size[11]. We investigated the GSTs genotypes in the area of high prevalence of HCC with enough cases and control participatants[16]. In our previous study[10] we found that HCC patients were significantly associated with tumor suppressor gene p53 mutation at codon 249 G to T transversion which may be involved in environmental mutagen AFB1[19]. Here, we are interested in the GSTM1 and GSTT1 genotypes associated with susceptibility to HCC in the natives of Guangxi and whether HCC patients possess more GSTM1 or GSTT1 null genotypes than other people.

Cheng[20] reported that smokers of deficiency in GSTM1 and GSTT1 genes were predisposed to head and neck squamous cell carcinoma. Dialyna[21] found that GSTM1 and GSTT1 null genotypes were correlated with lung cancer in heavy smokers. The present results suggest that natives in southwest Guangxi had a rather higher level of GSTM1 and GSTT1 null genotypes, their GSTM1 null genotype accounted for 47.8%, a high level in the world. While GSTT1 null genotype accounted for 42.7%, much higher than the average level reported[22-24]. It is known that people with high GSTs null genotypes who have never contacted with relevant chemical toxins such as AFB1 will never increase the risk of HCC. However, the people who live in an AFB1 contaminated area for a long time would fully reveal genetic defects and susceptibility to HCC. The present study showed that GSTM1 or GSTT1 null genotypes were higher in the HCC group than in control group, and the differences were very significant (P<0.01). There was not any relationship between their age and sex status (P>0.05). The frequency of combined GSTM1 and GSTT1 deletions in HCC group versus control group was 38.2% and 18.5%, respectively (P<0.05). Actually, there was twice more the risk of HCC in the GSTM1 and GSTT1 combined null genotypes in patients than in control.

In conclusion, the risk of HCC is associated with GSTM1 and GSTT1 null genotypes, especially in people contacted with AFB1. The natives in Guangxi have a high level of GSTM1 or/and GSTT1 null genotypes. AFB1 undergoes metabolism by GSTM1 and GSTT1 enzymes, an individual lacking of these enzymes should predispose to HCC. Genetic susceptibility due to GSTM1 and GSTT1 null genotypes in humans occurs in conjunction with exposure to environmental carcinogens such as AFB1 involved in the pathogenesis of HCC, especially in an area with hepatitis B prevalence.

REFERENCES

1 **Yeh FS,** Yu MC, Mo CC, Luo S, Tong MJ, Henderson BE. Hepatitis B virus, aflatoxins, and hepatocellular carcinoma in southern Guangxi, China. *Cancer Res* 1989; **49**: 2506-2509

2 **Stern MC,** Umbach DM, Yu MC, London SJ, Zhang ZQ, Taylor JA. Hepatitis B, aflatoxin B (1), and p53 codon 249 mutation in hepatocellular carcinomas from Guangxi, People's Republic of China, and a meta-analysis of existing studies. *Cancer Epidemiol Biomarkers Prev* 2001; **10**: 617-625

3 **Srivastava DS,** Kumar A, Mittal B, Mittal RD. Polymorphism of GSTM1 and GSTT1 genes in bladder cancer: a study from North India. *Arch Toxicol* 2004; **78**: 430-434

4 **Shupe T,** Sell S. Low hepatic glutathione S-transferase and increased hepatic DNA adduction contribute to increased tumorigenicity of aflatoxin B1 in newborn and partially hepatectomized mice. *Toxicol Lett* 2004; **148**: 1-9

5 **Sell S.** Mouse models to study the interaction of risk factors for human liver cancer. *Cancer Res* 2003; **63**: 7553-7562

6 **Kew MC.** Synergistic interaction between aflatoxin B1 and hepatitis B virus in hepatocarcinogenesis. *Liver Int* 2003; **23**: 405-409

7 **Su JJ,** Li Y, Ban KC, Qin LL, Wang HY, Yang C, Ou C, Duan XX, Lee Yl Yl, Yan RQ. Alteration of the p53 gene during tree shrews' hepatocarcinogenesis. *Hepatobiliary Pancreat Dis Int* 2003; **2**: 612-616

8 **Su JJ,** Li Y, Ban KC, Qin LL, Wang HY, Yang C, Ou C, Duan XX, Li YY, Yan RQ. Alteration of p53 gene during tree shrews' hepatocarcinogenesis. *Zhonghua Ganzangbing Zazhi* 2003; 11: 159-161

9 **Wang JS,** Groopman JD. DNA damage by mycotoxins. *Mutat Res* 1999; **424**: 167-181

10 **Deng ZL,** Ma Y. Aflatoxin sufferer and p53 gene mutation in hepatocellular carcinoma. *World J Gastroenterol* 1998; **4**: 28-29

11 **McGlynn KA,** Rosvold EA, Lustbader ED, Hu Y, Clapper ML, Zhou T, Wild CP, Xia XL, Baffoe-Bonnie A, Ofori-Adjei D. Susceptibility to hepatocellular carcinoma is associated with genetic variation in the enzymatic detoxification of aflatoxin B1. *Proc Natl Acad Sci USA* 1995; **92**: 2384-2387

12 **Shea TC,** Claflin G, Comstock KE, Sanderson BJ, Burstein NA, Keenan EJ, Mannervik B, Henner WD. Glutathione transferase activity and isoenzyme composition in primary human breast cancers. *Cancer Res* 1990; **50**: 6848-6853

13 **Garcia-Closas M,** Kelsey KT, Hankinson SE, Spiegelman D, Springer K, Willett WC, Speizer FE, Hunter DJ. Glutathione S-transferase mu and theta polymorphisms and breast cancer susceptibility. *J Natl Cancer Inst* 1999; **91**: 1960-1964

14 **Wiencke JK,** Kelsey KT, Lamela RA, Toscano WA. Human glutathione S-transferase deficiency as a marker of susceptibility to epoxide-induced cytogenetic damage. *Cancer Res* 1990; **50**: 1585-1590

15 **Tiemersma EW,** Omer RE, Bunschoten A, van't Veer P, Kok FJ, Idris MO, Kadaru AM, Fedail SS, Kampman E. Role of genetic polymorphism of glutathione-S-transferase T1 and microsomal epoxide hydrolase in aflatoxin-associated hepatocellular carcinoma. *Cancer Epidemiol Biomarkers Prev* 2001; **10**: 785-791

16 **Ma Y,** Deng ZL, Wei YP. Study of the deletion mutation of glutathione S-transferase M1 gene and its role in susceptibility to hepatocellular carcinoma. *Chinese J Can Res* 2001; **13**: 176-178

17 **Esaki H,** Kumagai S. Glutathione-S-transferase activity toward aflatoxin epoxide in livers of mastomys and other rodents. *Toxicon* 2002; **40**: 941-945

18 **Deng Z,** Wei Y, Ma Y. Glutathione-S-transferase M1 genotype in patients with hepatocellular carcinoma. *Zhonghua Zhongliu Zazhi* 2001; **23**: 477-479

19 **Olivier M,** Hussain SP, Caron de Fromentel C, Hainaut P, Harris CC. TP53 mutation spectra and load: a tool for generating hypotheses on the etiology of cancer. *IARC Sci Publ* 2004; **157**: 247-270

20 **Cheng L,** Sturgis EM, Eicher SA, Char D, Spitz MR, Wei Q. Glutathione-S-transferase polymorphisms and risk of squamous-cell carcinoma of the head and neck. *Int J Cancer* 1999; **84**: 220-224

21 **Dialyna IA,** Miyakis S, Georgatou N, Spandidos DA. Genetic polymorphisms of CYP1A1, GSTM1 and GSTT1 genes and lung cancer risk. *Oncol Rep* 2003; **10**: 1829-1835

22 **Kargas C,** Krupa R, Walter Z. Combined genotype analysis of GSTM1 and GSTT1 polymorphisms in a Polish population. *Hum Biol* 2003; **75**: 301-307

23 **Laso N,** Lafuente MJ, Mas S, Trias M, Ascaso C, Molina R, Ballesta A, Rodriguez F, Lafuente A. Glutathione S-transferase (GSTM1 and GSTT1)-dependent risk for colorectal cancer. *Anticancer Res* 2002; **22**: 3399-3403

24 **Dandara C,** Sayi J, Masimirembwa CM, Magimba A, Kaaya S, De Sommers K, Snyman JR, Hasler JA. Genetic polymorphism of cytochrome P450 1A1 (Cyp 1A1) and glutathione transferases (M1, T1, and P1) among Africans. *Clin Chem Lab Med* 2002; **40**: 952-957

Edited by Wang XL and Zhang JZ

PO Box 2345, Beijing 100023, China
Fax: +86-10-85381893
E-mail: wjg@wjgnet.com www.wjgnet.com

ELSEVIER

World J Gastroenterol 2005;11(2):275-279
World Journal of Gastroenterology ISSN 1007-9327

• BRIEF REPORTS •

Polymerase chain reaction-single strand conformational polymorphism analysis of rearranged during transfection proto-oncogene in Chinese familial hirschsprung's disease

Tao Guan, Ji-Cheng Li, Min-Ju Li, Jin-Fa Tou

Tao Guan, Ji-Cheng Li, Department of Lymphology, Institute of Cell Biology, Zhejiang University Medical College, Hangzhou 310031, Zhejiang Province, China
Min-Ju Li, Jin-Fa Tou, Children's Hospital, Zhejiang University Medical College, Hangzhou 310006, Zhejiang Province, China
Supported by the Fund for Excellent Young Talented Persons by Public Health Ministry of China, and Analysis and Testing Foundation of Zhejiang Province, No. 99075
Correspondence to: Professor. Ji-Cheng Li, Department of Lymphology, Institute of Cell Biology, Zhejiang University Medical College, Hangzhou 310031, Zhejiang Province, China. lijc@mail.hz.zj.cn
Telephone: +86-571-87217451 **Fax:** +86-571-87217145
Received: 2004-03-15 **Accepted:** 2004-05-13

Abstract

AIM: To investigate the relationship between mutations of rearranged during transfection (RET) proto-oncogene and Chinese patients with Hirschsprung's disease (HD), and to elucidate the genetic mechanism of familial HD patient at the molecular level.

METHODS: Genomic DNA was extracted from venous blood of probands and their relatives in two genealogies. Polymerase chain reaction (PCR) products, which were amplified using specific primers (RET, exons 11, 13, 15 and 17), were electrophoresed to analyze the single-strand conformational polymorphism (SSCP) patterns. The positive amplified products were sequenced. Forty-eight sporadic HD patients and 30 normal children were screened for mutations of RET proto-oncogene simultaneously.

RESULTS: Three cases with HD in one family were found to have a G heterozygous insertion at nucleotide 18 974 in exon 13 of RET cDNA (18 974insG), which resulted in a frameshift mutation. In another family, a heterozygosity for T to G transition at nucleotide 18 888 in the same exon which resulted in a synonymous mutation of Leu at codon 745 was detected in the proband and his father. Eight RET mutations were confirmed in 48 sporadic HD patients.

CONCLUSION: Mutations of RET proto-oncogene may play an important role in the pathogenesis of Chinese patients with HD. Detection of mutated RET proto-oncogene carriers may be used for genetic counseling of potential risk for HD in the affected families.

Key words: Hirschsprung's disease; Proto-oncogene proteins RET; Transfection; PCR-SSCP

Guan T, Li JC, Li MJ, Tou JF. Polymerase chain reaction-single strand conformational polymorphism analysis of rearranged during transfection proto-oncogene in Chinese familial hirschsprung's disease. *World J Gastroenterol* 2005; 11(2): 275-279
http://www.wjgnet.com/1007-9327/11/275.asp

INTRODUCTION

Hirschsprung's disease (HD) is a common congenital malformation affecting 1 in 5 000 live births. Absence of parasympathetic neuronal ganglia in the hindgut results in poor coordination of peristaltic movement and varying degrees of constipation[1-6]. Although the pathogenesis of HD has not been fully understood, the familial occurrence with an increased risk for siblings as well as an uneven gender distribution indicates a genetic cause of the disease. RET proto-oncogene, encoding a 1 114 residue receptor tyrosine kinase, is thought to be essential for neurogenesis of the enteric nervous system[7-11]. Through detailed examination more than 60 missense mutations or deletions have been found along the whole coding sequence of RET in HD[8,12-21]. It was reported that RET mutations were identified in approximately 50% of familial cases of HD and in 10-20% of sporadic cases abroad[7,22-24]. However, few studies on HD in Chinese population are reported.

In this study, we performed genetic analysis of exons 11, 13, 15 and 17 of RET proto-oncogene in two HD genealogies by using polymerase chain reaction-single strand conformation polymorphism (PCR-SSCP). In order to further investigate the pathogenic mechanism of HD, 48 sporadic HD patients and 30 normal children were also screened by SSCP.

MATERIALS AND METHODS

Case selection and extraction of DNA

Probands of two HD families were collected at Zhejiang Children's Hospital. The criteria[25] for HD were absence of enteric plexuses plus the aganglionlic tract and increased acetylcholinesterase staining of nerve fibers. Forty-eight Chinese patients with sporadic HD (35 males and 13 females) and 30 normal children were enrolled in this study. Genomic DNA was isolated from peripheral white blood cells according to standard procedures[26].

PCR amplification

Primers were designed to amplify the exons and flanking intronic sequences (Table 1). PCR amplification was performed in a reaction volume of 50 μL containing 200 ng of genomic DNA, 10 mmol/L Tris-HCl (pH 8.4), 50 mmol/L KCl, 1.5 mmol/L $MgCl_2$, 0.5 μmol/L each of two fragment-specific primers, 100 μmol/L each of dATP, dGTP, dTTP and dCTP, and 2 units of Taq DNA polymerase. The template-melting step of PCR amplification was at 94 ℃ for 5 min, followed by 30 cycles of serial incubation at 94 ℃ for 50, at 58 ℃ to 62 ℃ for 50 min, and at 72 ℃ for 10 min. PCR products were electrophoresed on 1% agarose gel and 100-bp ladder markers were used to compare the size of amplified fragments.

Table 1 Primers used in PCR amplification and DNA sequencing expriments

Exon	Sequence (5′→3′)	Annealing *t* (℃)	Product size (bp)
11	F: ACACCACCCCCACCCACAGAT	62	273
	R: AAGCTTGAAGGCATCCACGG		
13	F: GACCTGGTATGGTCATGGA	58	253
	R: AAGAGGGAGAACAGGGCTGTA		
15	F: GACTCGTGCTATTTTTCCTAC	60	234
	R: TATCTTTCCTAGGCTTCCC		
17	F: CCCCACTAGATGTATAAGGG	59	232
	R: TCACTGGTCCTTTCACTCTCT		

F: forward primer; R: reverse primer.

SSCP analysis

SSCP analysis of fragments was performed on a mini electrophoresis unit (Bio-Rad Company, USA). A total of 10 μL of the PCR product was diluted with 10 μL of sample buffer containing 900 mL/L formamide, 0.5 g/L bromphenol blue dye and 0.5 g/L xylene cyanol. The samples were heated at 100 ℃ for 8 min, transferred into an ice-cold water bath for 3 min, and analyzed by 80 g/L polyacryl amide gel electrophoresis (PAGE) in 45 mmol/L-Tris-borate (pH 8.0)/1 mmol/L-EDTA (TBE) buffer under 13 v/cm at 10 ℃.

DNA silver staining

Gels were fixed in 100 mL/L alcohol for 10 min and oxidized in 100 mL/L nitric acid. After 3 min, gels were washed for 1 min with double distilled water, then stained in 2 g/L silver nitric acid for 5 min, and again washed for 1 min with double distilled water. The gels showed appropriate color in 15 g/L anhydrous sodium carbonate and 4 mL/L formalin and ended reducing response by 7.5 mL/L glacial acetic acid. Subsequently, gels were washed with double distilled water. At last, the results of silver staining were analyzed and photographed.

Purification of PCR products and DNA sequencing

Abnormal PCR products screened by SSCP were cut from gel and purified according to Viogene kit manufacturer's instructions. Sequence analysis was carried out with a PE377 automated sequencer.

RESULTS

Analysis of PCR products

The increment of all DNA samples from HD patients was a single strand with the same length as normal controls, indicating that a large fragment insertion and deletion did not exist in the region in exons 11, 13, 15 and 17 of RET proto-oncogene among HD patients.

Mutations of RET proto-oncogene in family 1

HD was observed in 3 generations in patients III, II 1 and I 1 (Figure 1A). The female proband (III) carried a large aganglionic region in the colon that was removed by surgery at the age of 1 year. Her farther also developed the long aganglionic form of HD and underwent surgery at age of two years. The male I 1 in the first generation suffered from chronic obstipation. We analyzed the genomic DNA of the 5 familial members for mutations in exons 11, 13, 15 and 17 of RET proto-oncogene. All three HD patients demonstrated abnormal SSCP patterns in exon 13 (Figure 1A). DNA sequencing revealed a G heterozygous insertion at nucleotide 18 974 (18 974insG) in exon 13 of RET proto-oncogene encoding the intracellular part of RET receptors (Figure 2A), which resulted in a frameshift mutation. We failed to detect any additional mutation in RET proto-oncogene in DNA of the unaffected members in this family.

Mutation of RET proto-oncogene in family 2

In this family, one son (II) suffered from HD and was operated for the disease at the age of 3 mo. The aganglionosis in II was confined to the rectosigmoid colon. On SSCP screening of RET proto-oncogene, II and his father whose phenotype was normal showed distinct aberrant band patterns in exon 13 (Figure 1B). DNA sequencing showed a T to G transition in codon 745. This nucleotide was exchanged from CTT to CTG; however, it was mute and did not alter the tyrosine in this position. This synonymous mutation was found to be heterozygous (Figure 2B). In DNA of the unaffected mother, the nucleotide sequence at codon 745 was unaltered.

Mutation of RET proto-oncogene in 48 sporadic HD patients

Mutation changes were detected in 8 of 48 sporadic HD patients in RET proto-oncogene. But in 30 normal individuals no mutation change was observed. This mutation rate in the gene was estimated to be 16.7% (8/48). DNA sequence analysis showed that there were 5 patterns of nucleotide changes: A G to A substitution was observed at codon 667 (G667S) in exon 11 encoding the tyrosine kinase domain of the receptor in 3 samples (Figure 2D). Another a G to A substitution was identified at codon 916 (Q916Q) in exon 15 in one patient, but it was a synonymous mutation (Figure 2E). In exon 13, a A to G transition was found at colon 756 (K756E) in one patient (Figure 2C). A T to G mutation, although it seemed to be a silent mutation, was revealed in codon 745 (L745L) in another patient (Figure 2C). A G heterozygous insertion at nucleotide 18 974 (18 974insG) was found in 2 patients. Among the 8 patients with RET mutations, 5 were patients with sporadic long-segment (aganglionosis confined to the transverse colon) HD and 3 were patients with sporadic short-segment (aganglionosis confined to the rectosigmoid colon) HD. All these mutation changes were identified to be heterozygous, and are summarized in Table 2.

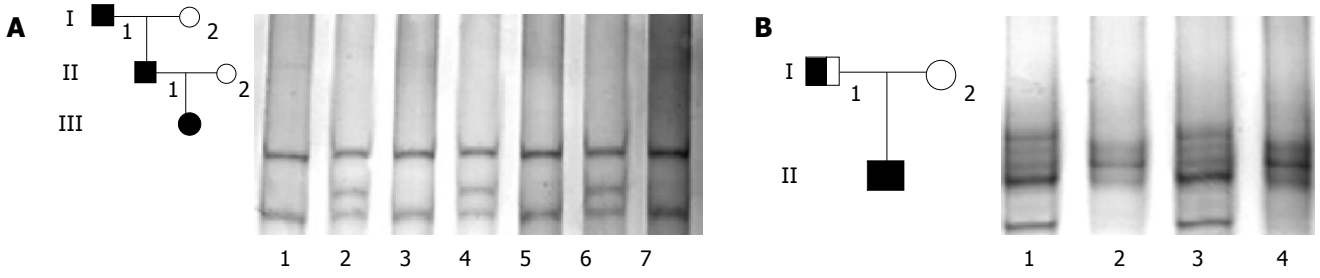

Figure 1 Pedigree of families one and two and SSCP analysis in exon 13 of RET proto-oncogene. A: Pedigree of family one and SSCP analysis in exon 13 of RET proto-oncogene Lane 1: healthy control; Lane 2: I 1; Lane 3: I 2; Lane 4: II 1; Lane 5: II 2; Lane 6: III (proband); Lane 7: healthy control; B: Pedigree of family two and SSCP analysis in exon 13 of RET proto-oncogene. Lane 1: II ; Lane 2: healthy control; Lane 3: I 1; Lane 4: I 2.

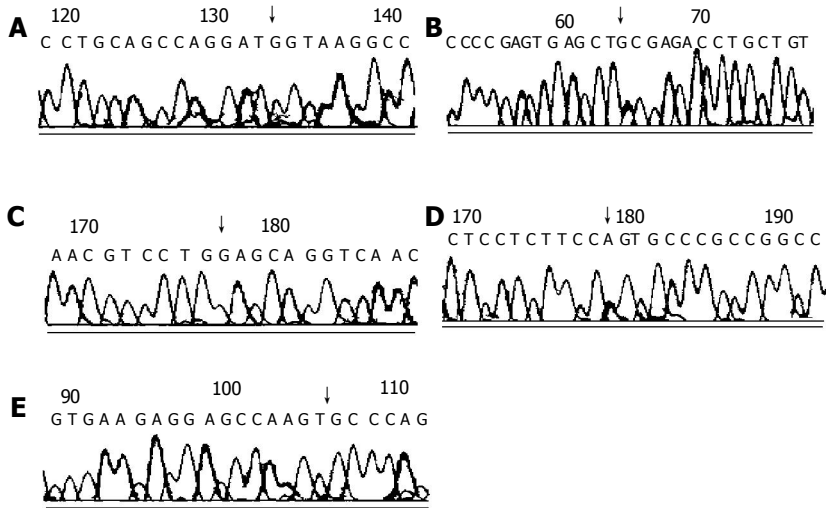

Figure 2 Sequence analysis of RET gene in patients with aberrant SSCP patterns. The arrows indicate the position of mutation. A: A G heterozygous insertion at nucleotide 18 974 in exon 13, resulted in a frameshift mutation; B: A T to G transition at codon 745 in exon 13 was exchanged from CTT to CTG, resulting in a silent mutation; C: An A to G transition at codon 756 in exon 13 resulted in a K→E missense mutation; D: A G to A substitution at codon 667 in exon 11 resulted in a G→S missense mutation; E: A G to A substitution at codon 916 in exon 15 resulted in a silent mutation.

Table 2 Mutated sites observed in RET proto-oncogenes in 48 sporadic HD patients

Case	Sex	Range of aganglionic segment	Exon	Nucleotide change	Amino acid change	Mutation types
1	M	Long-segment	11	G15165→A	G667S	Missense mutation
2	M	Short-segment	11	G15165→A	G667S	Missense mutation
3	F	Long-segment	11	G15165→A	G667S	Missense mutation
4	M	Long-segment	13	T18888→G	L745L	Silent mutation
5	M	Long-segment	13	A18919→G	K756E	Missense mutation
6	M	Long-segment	13	18974insG	- - - -	Frameshift mutation
7	M	Short-segment	13	18974insG	- - - -	Frameshift mutation
8	M	Short-segment	15	G20692→A	Q916Q	Silent mutation

M: male; F: female.

DISCUSSION

The human RET proto-oncogene has been mapped to chromosome band 10q11.2 and comprises 20 exons with a length of about 80 kb[27-30]. Receptor tyrosine kinase encoded by RET proto-oncogene consists of an intracellular tyrosine kinase domain, a transmembrane domain and an extracellular domain which includes a "cadherin-like" region. Receptor tyrosine kinases generally function as ligand-dependent dimmers, which phosphorylate "second messenger" proteins in the cytoplasm, and they are commonly associated with the regulation of cell growth and differentiation, development of normal nerves, and expressed in gangliogenic source cells, such as neurogenic ganglia and ganglia of peripheral nerve system, neuroendocrine cells, epidermic pigment cells, *etc*.[9]. RET proto-oncogene is controlled by a promoter harboring four randomly repeated 5'-CG-3' sequences that are part of a 5'-CG-3' dense region in proximity to the transcriptional start site[31]. Ninety-five unmethylated 5'-CG-3' dinucleotides are located in a region of about 900 bp in which the majority lie within the putative promoter segment. During embryogenesis, RET proto-oncogene expression is regulated in a temporally and spatially defined pattern. In adults, RET mRNA transcripts could be detected exclusively in substantia nigra, adrenal medulla, cerebellum and other parts of the brain[31-35]. RET proto-oncogene alterations as disease-causing mutations have been demonstrated in five different disease entities: HD, papillary thyroid carcinoma, and three types of inherited cancer syndromes, multiple endocrine neoplasia (MEN) 2A, MEN 2B and familial modullary thyroid carcinoma (FMTC)[21,36-42].

To date, only 15-20% of all HD cases were reported to be of familial origin, and 80% of these were reported to be caused by mutations in either RET proto-oncogene or other candidate genes[1,6]. Recently, Munnes *et al*[32] identified and analyzed six HD families living in Germany by PCR-DNA sequencing. They observed mutations at codon 609 (C609R) in one out of 6 cysteine residues encoded in exon 10 of RET proto-oncogene in one family with a joint occurrence of HD and FMTC. The other 2 patterns of RET mutations (R77C, Y204Y) were found in 2 different families. Up to now, mutation analysis of candidate genes has not been reported in Chinese HD pedigree[43]. In this study, we have found that three HD cases in one Chinese HD family carried a frame-shift mutation (18 974insG) in exon 13 of RET proto-oncogene. This novel mutation could alter the amino acid sequence in the tyrosine kinase domain of the RET receptor, and the signal conduction was obstructed, thereby finally causing HD. Therefore, in this family, RET mutation analysis enabled us to concentrate our clinical efforts on family members at high risk for HD. In mutated RET proto-oncogene carriers, theraputic planning could be made based on the natural history of this disease. Genetic information on RET genotye-phenotypic correlation might be used for genetic counseling of potential risk for HD. In another family, the sick child and his father had the same heterozygous silent mutation (L745L) in exon 13 of RET proto-oncogene. However, the father's phenotype was normal, and penetrance of HD was incomplete. It

is suggested that phenotypic expression of this disease might depend not only on the RET mutation pattern but also on other genetic or environmental determinants, although it has a genetic tendency.

In the 48 sporadic HD patients, we detected 6 disease-causing mutations and 2 silent mutations. These mutations were revealed to be heterozygous. Studies have reported that only a half quantity of RET proto-oncogene mutations is likely to cause HD in humans[44-46], which was also confirmed by our finding. We observed that 2 of the 6 disease-causing mutations were detected in HD patients with short-segment aganglionosis suggesting that mutations of RET proto-oncogene are associated not only with long-segment HD, but also with sporadically occurring short-segment HD in Chinese population with this disease.

Our results suggest that mutations of RET proto-oncogene may play an important role in the pathogenesis of Chinese patients with HD. Mutation analysis of the gene may provide an additive diagnostic value for this disease, especially familial cases. However, the low mutation rate and no spot of mutations in this gene indicate that other genes and microenvironmental factors can be involved in the development of HD. Further investigation is necessary to elucidate the pathogenesis of this disease.

REFERENCES

1 **Nogueira A,** Campos M, Soares-Oliveira M, Estevao-Costa J, Silva P, Carneiro F, Carvalho JL. Histochemical and immunohistochemical study of the intrinsic innervation in colonic dysganglionosis. *Pediatr Surg Int* 2001; **17**: 144-151

2 **Yoneda A,** Wang Y, O'Briain DS, Puri P. Cell-adhesion molecules and fibroblast growth factor signalling in Hirschsprung's disease. *Pediatr Surg Int* 2001; **17**: 299-303

3 **Li JC,** Mi KH, Zhou JL, Busch L, Kuhnel W. The development of colon innervation in trisomy 16 mice and Hirschsprung's disease. *World J Gastroenterol* 2001; **7**: 16-21

4 **Won KJ,** Torihashi S, Mitsui-Saito M, Hori M, Sato K, Suzuki T, Ozaki H, Karaki H. Increased smooth muscle contractility of intestine in the genetic null of the endothelin ETB receptor: a rat model for long segment Hirschsprung's disease. *Gut* 2002; **50**: 355-360

5 **Amiel J,** Lyonnet S. Hirschsprung disease, associated syndromes, and genetics: a review. *J Med Genet* 2001; **38**: 729-739

6 **Rice J,** Doggett B, Sweetser DA, Yanagisawa H, Yanagisawa M, Kapur RP. Transgenic rescue of aganglionosis and piebaldism in lethal spotted mice. *Dev Dyn* 2000; **217**: 120-132

7 **Iwashita T,** Kurokawa K, Qiao S, Murakami H, Asai N, Kawai K, Hashimoto M, Watanabe T, Ichihara M, Takahashi M. Functional analysis of RET with Hirschsprung mutations affecting its kinase domain. *Gastroenterology* 2001; **121**: 24-33

8 **Griseri P,** Pesce B, Patrone G, Osinga J, Puppo F, Sancandi M, Hofstra R, Romeo G, Ravazzolo R, Devoto M, Ceccherini I. A rare haplotype of the RET proto-oncogene is a risk-modifying allele in hirschsprung disease. *Am J Hum Genet* 2002; **71**: 969-974

9 **Manie S,** Santoro M, Fusco A, Billaud M. The RET receptor: function in development and dysfunction in congenital malformation. *Trends Genet* 2001; **17**: 580-589

10 **Japon MA,** Urbano AG, Saez C, Segura DI, Cerro AL, Dieguez C, Alvarez CV. Glial-derived neurotropic factor and RET gene expression in normal human anterior pituitary cell types and in pituitary tumors. *J Clin Endocrinol Metab* 2002; **87**: 1879-1884

11 **Gershon MD.** Lessons from genetically engineered animal models. II. Disorders of enteric neuronal development: insights from transgenic mice. *Am J Physiol* 1999; **277**: G262-267

12 **Onochie CI,** Korngut LM, Vanhorne JB, Myers SM, Michaud D, Mulligan LM. Characterisation of the human GFRalpha-3 locus and investigation of the gene in Hirschsprung disease. *J Med Genet* 2000; **37**: 674-679

13 **Inoue K,** Shimotake T, Iwai N. Mutational analysis of RET/GDNF/NTN genes in children with total colonic aganglionosis with small bowel involvement. *Am J Med Genet* 2000; **93**: 278-284

14 **Gath R,** Goessling A, Keller KM, Koletzko S, Coerdt W, Muntefering H, Wirth S, Hofstra RM, Mulligan L, Eng C, von-Deimling A. Analysis of the RET, GDNF, EDN3, and EDNRB genes in patients with intestinal neuronal dysplasia and Hirschsprung disease. *Gut* 2001; **48**: 671-675

15 **Julies MG,** Moore SW, Kotze MJ, du Plessis L. Novel RET mutations in Hirschsprung's disease patients from the diverse South African population. *Eur J Hum Genet* 2001; **9**: 419-423

16 **Inoue K,** Shimotake T, Tomiyama H, Iwai N. Mutational analysis of the RET and GDNF gene in children with hypoganglionosis. *Eur J Pediatr Surg* 2001; **11**: 120-123

17 **Shimotake T,** Go S, Inoue K, Tomiyama H, Iwai N. A homozygous missense mutation in the tyrosine E kinase domain of the RET proto-oncogene in an infant with total intestinal aganglionosis. *Am J Gastroenterol* 2001; **96**: 1286-1291

18 **Hofstra RM,** Wu Y, Stulp RP, Elfferich P, Osinga J, Maas SM, Siderius L, Brooks AS, vd Ende JJ, Heydendael VM, Severijnen RS, Bax KM, Meijers C, Buys CH. RET and GDNF gene scanning in Hirschsprung patients using two dual denaturing gel systems. *Hum Mutat* 2000; **15**: 418-429

19 **Sancandi M,** Ceccherini I, Costa M, Fava M, Chen B, Wu Y, Hofstra R, Laurie T, Griffths M, Burge D, Tam PK. Incidence of RET mutations in patients with Hirschsprung's disease. *J Pediatr Surg* 2000; **35**: 139-142; discussion 142-143

20 **Fitze G,** Cramer J, Ziegler A, Schierz M, Schreiber M, Kuhlisch E, Roesner D, Schackert HK. Association between c135G/A genotype and RET proto-oncogene germline mutations and phenotype of Hirschsprung's disease. *Lancet* 2002; **359**: 1200-1205

21 **Pigny P,** Bauters C, Wemeau JL, Houcke ML, Crepin M, Caron P, Giraud S, Calender A, Buisine MP, Kerckaert JP, Porchet N. A novel 9-base pair duplication in RET exon 8 in familial medullary thyroid carcinoma. *J Clin Endocrinol Metab* 1999; **84**: 1700-1704

22 **Borrego S,** Ruiz A, Saez ME, Gimm O, Gao X, Lopez-Alonso M, Hernandez A, Wright FA, Antinolo G, Eng C. RET genotypes comprising specific haplotypes of polymorphic variants predispose to isolated Hirschsprung disease. *J Med Genet* 2000; **37**: 572-578

23 **Martucciello G,** Ceccherini I, Lerone M, Jasonni V. Pathogenesis of Hirschsprung's disease. *J Pediatr Surg* 2000; **35**: 1017-1025

24 **Bolk S,** Pelet A, Hofstra RM, Angrist M, Salomon R, Croaker D, Buys CH, Lyonnet S, Chakravarti A. A human model for multigenic inheritance: phenotypic expression in Hirschsprung disease requires both the RET gene and a new 9q31 locus. *Proc Natl Acad Sci USA* 2000; **97**: 268-273

25 **Khan AR,** Vujanic GM, Huddart S. The constipated child: how likely is Hirschsprung's disease? *Pediatr Surg Int* 2003; **19**: 439-442

26 **Pepinski W,** Soltyszewski I, Janica J, Skawronska M, Koc-Zorawska E. Comparison of five commercial kits for DNA extraction from human blood, saliva and muscle samples. *Rocz Akad Med Bialymst* 2002; **47**: 270-275

27 **Lesueur F,** Corbex M, McKay JD, Lima J, Soares P, Griseri P, Burgess J, Ceccherini I, Landolfi S, Papotti M, Amorim A, Goldgar DE, Romeo G. Specific haplotypes of the RET proto-oncogene are over-represented in patients with sporadic papillary thyroid carcinoma. *J Med Genet* 2002; **39**: 260-265

28 **Melillo RM,** Santoro M, Ong SH, Billaud M, Fusco A, Hadari YR, Schlessinger J, Lax I. Docking protein FRS2 links the protein tyrosine kinase RET and its oncogenic forms with the mitogen-activated protein kinase signaling cascade. *Mol Cell Biol* 2001; **21**: 4177-4187

29 **Griseri P,** Sancandi M, Patrone G, Bocciardi R, Hofstra R, Ravazzolo R, Devoto M, Romeo G, Ceccherini I. A single-nucleotide polymorphic variant of the RET proto-oncogene is underrepresented in sporadic Hirschsprung disease. *Eur J Hum Genet* 2000; **8**: 721-724

30 **Hansford JR,** Mulligan LM. Multiple endocrine neoplasia type 2 and RET: from neoplasia to neurogenesis. *J Med Genet* 2000; **37**: 817-827

31 **Munnes M,** Patrone G, Schmitz B, Romeo G, Doerfler W. A 5'-CG-3'-rich region in the promoter of the transcriptionally frequently silenced RET protooncogene lacks methylated cytidine residues. *Oncogene* 1998; **17**: 2573-2583

32 **Munnes M,** Fanaei S, Schmitz B, Muiznieks I, Holschneider AM, Doerfler W. Familial form of hirschsprung disease: nucleotide sequence studies reveal point mutations in the RET proto-

oncogene in two of six families but not in other candidate genes. *Am J Med Genet* 2000; **94**: 19-27

33 **Parisi MA,** Kapur RP. Genetics of Hirschsprung disease. *Curr Opin Pediatr* 2000; **12**: 610-617

34 **Amiel J,** Salomon R, Attie-Bitach T, Touraine R, Steffann J, Pelet A, Nihoul-Fekete C, Vekemans M, Munnich A, Lyonnet S. Molecular genetics of Hirschsprung disease: a model of multigenic neurocristopathy. *J Soc Biol* 2000; **194**: 125-128

35 **Matera I,** De Miguel-Rodriguez M, Fernandez-Santos JM, Santamaria G, Puliti A, Ravazzolo R, Romeo G, Galera-Davidson H, Ceccherini I. cDNA sequence and genomic structure of the rat RET proto-oncogene. *DNA Seq* 2000; **11**: 405-417

36 **Sakai T,** Nirasawa Y, Itoh Y, Wakizaka A. Japanese patients with sporadic Hirschsprung: mutation analysis of the receptor tyrosine kinase proto-oncogene, endothelin-B receptor, endothelin-3, glial cell line-derived neurotrophic factor and neurturin genes: a comparison with similar studies. *Eur J Pediatr* 2000; **159**: 160-167

37 **De Vita G,** Melillo RM, Carlomagno F, Visconti R, Castellone MD, Bellacosa A, Billaud M, Fusco A, Tsichlis PN, Santoro M. Tyrosine 1062 of RET-MEN2A mediates activation of Akt (protein kinase B) and mitogen-activated protein kinase pathways leading to PC12 cell survival. *Cancer Res* 2000; **60**: 3727-3731

38 **Fugazzola L,** Cerutti N, Mannavola D, Ghilardi G, Alberti L, Romoli R, Beck-Peccoz P. Multigenerational familial medullary thyroid cancer (FMTC): evidence for FMTC phenocopies and association with papillary thyroid cancer. *Clin Endocrinol (Oxf)* 2002; **56**: 53-63

39 **Wohllk N,** Becker P, Youlton R, Cote GJ, Gagel RF. Germline mutations of the ret proto-oncogene in Chilean patients with hereditary and sporadic medullary thyroid carcinoma. *Rev Med Chil* 2001; **129**: 713-718

40 **Lore F,** Talidis F, Di Cairano G, Renieri A. Multiple endocrine neoplasia type 2 syndromes may be associated with renal malformations. *J Intern Med* 2001; **250**: 37-42

41 **Takano T,** Miyauchi A, Yoshida H, Hasegawa Y, Kuma K, Amino N. Large-scale analysis of mutations in RET exon 16 in sporadic medullary thyroid carcinomas in Japan. *Jpn J Cancer Res* 2001; **92**: 645-648

42 **Chiefari E,** Chiarella R, Crocetti U, Tardio B, Arturi F, Russo D, Trischitta V, Filetti S, Zingrillo M. A large family with hereditary MTC: role of RET genetic analysis in differential diagnosis between MEN 2A and FMTC. *Horm Metab Res* 2001; **33**: 52-56

43 **Garcia-Barcelo M,** Sham MH, Lee WS, Lui VC, Chen BL, Wong KK, Wong JS, Tam PK. Highly recurrent RET mutations and novel mutations in genes of the receptor tyrosine kinase and endothelin receptor B pathways in Chinese patients with sporadic Hirschsprung disease. *Clin Chem* 2004; **50**: 93-100

44 **Sakai T,** Wakizaka A, Nirasawa Y. Congenital central hypoventilation syndrome associated with Hirschsprung's disease: mutation analysis of the RET and endothelin-signaling pathways. *Eur J Pediatr Surg* 2001; **11**: 335-337

45 **Pasini B,** Rossi R, Ambrosio MR, Zatelli MC, Gullo M, Gobbo M, Collini P, Aiello A, Pansini G, Trasforini G, degli Uberti EC. RET mutation profile and variable clinical manifestations in a family with multiple endocrine neoplasia type 2A and Hirschsprung's disease. *Surgery* 2002; **131**: 373-381

46 **Mograbi B,** Bocciardi R, Bourget I, Juhel T, Farahi-Far D, Romeo G, Ceccherini I, Rossi B. The sensitivity of activated Cys Ret mutants to glial cell line-derived neurotrophic factor is mandatory to rescue neuroectodermic cells from apoptosis. *Mol Cell Biol* 2001; **21**: 6719-6730

Edited by Kumar M and Wang XL

PO Box 2345, Beijing 100023, China
Fax: +86-10-85381893
E-mail: wjg@wjgnet.com www.wjgnet.com

ELSEVIER

World J Gastroenterol 2005;11(2):280-284
World Journal of Gastroenterology ISSN 1007-9327

• BRIEF REPORTS •

Anticancer activity of resveratrol on implanted human primary gastric carcinoma cells in nude mice

Hai-Bo Zhou, Juan-Juan Chen, Wen-Xia Wang, Jian-Ting Cai, Qin Du

Hai-Bo Zhou, Juan-Juan Chen, Wen-Xia Wang, Jian-Ting Cai, Qin Du, Department of Gastroenterology, Second Hospital of Zhejiang University, Hangzhou 310009, Zhejiang Province, China
Correspondence to: Dr. Hai-Bo Zhou, Department of Gastroenterology, Second Affliated Hospital of Zhejiang University, Hangzhou 310009, Zhejiang Province, China. zhouhaibohz@163.com
Telephone: +86-571-87783564
Received: 2004-01-10 **Accepted:** 2004-03-12

Abstract

AIM: To investigate the apoptosis of implanted primary gastric cancer cells in nude mice induced by resveratrol and the relation between this apoptosis and expression of bcl-2 and bax.

METHODS: A transplanted tumor model was established by injecting human primary gastric cancer cells into subcutaneous tissue of nude mice. Resveratrol (500 mg/kg, 1 000 mg/kg and 1 500 mg/kg) was directly injected beside tumor body 6 times at an interval of 2 d. Then changes of tumor volume were measured continuously and tumor inhibition rate of each group was calculated. We observed the morphologic alterations by electron microscope, measured the apoptotic rate by TUNEL staining method, detected the expression of apoptosis-regulated genes *bcl-2* and *bax* by immunohistochemical staining and PT-PCR.

RESULTS: Resveratrol could significantly inhibit carcinoma growth when it was injected near the carcinoma. An inhibitory effect was observed in all therapeutic groups and the inhibition rate of resveratrol at the dose of 500 mg/kg, 1 000 mg/kg and 1 500 mg/kg was 10.58%, 29.68% and 39.14%, respectively. Resveratrol induced implanted tumor cells to undergo apoptosis with apoptotic characteristics, including morphological changes of chromatin condensation, chromatin crescent formation, nucleus fragmentation. The inhibition rate of 0.2 mL of normal saline solution, 1 500 mg/kg DMSO, 500 mg/kg resveratrol, 1 000 mg/kg resveratrol, and 1 500 mg/kg resveratrol was 13.68±0.37%, 13.8±0.43%, 48.7±1.07%, 56.44±1.39% and 67±0.96%, respectively. The positive rate of bcl-2 protein of each group was 29.48±0.51%, 27.56±1.40%, 11.86±0.97%, 5.7±0.84% and 3.92±0.85%, respectively by immunohistochemical staining. The positive rate of bax protein of each group was 19.34±0.35%, 20.88±0.91%, 40.02±1.20%, 45.72±0.88% and 52.3±1.54%, respectively by immunohistochemical staining. The density of bcl-2 mRNA in 0.2 mL normal saline solution, 1 500 mg/kg DMSO, 500 mg/kg resveratrol, 1 000 mg/kg resveratrol, and 1 500 mg/kg resveratrol decreased progressively and the density of bax mRNA in 0.2 mL normal saline solution, 1 500 mg/kg DMSO, 500 mg/kg resveratrol, 1 000 mg/kg resveratrol, and 1 500 mg/kg increased progressively with elongation of time by RT-PCR.

CONCLUSION: Resveratrol is able to induce apoptosis of transplanted tumor cells. This apoptosis may be mediated by down-regulating apoptosis-regulated gene *bcl-2* and up-regulating the expression of apoptosis-regulated gene bax.

Key words: Gastric carcinoma; Resveratrol; Neoplasm Transplantation; Apoptosis

Zhou HB, Chen JJ, Wang WX, Cai JT, Du Q. Anticancer activity of resveratrol on implanted human primary gastric carcinoma cells in nude mice. *World J Gastroenterol* 2005; 11(2): 280-284
http://www.wjgnet.com/1007-9327/11/280.asp

INTRODUCTION

Bcl-2 family plays a crucial role in the control of apoptosis. The family includes a number of proteins which have homologous amino acid sequences, including anti-apoptotic members such as bcl-2 and bcl-xl, as well as pro-apoptotic members including bax and bad. In *in vitro* experiments, overexpression of bcl-2 has been shown to inhibit apoptosis, but overexpression of bax has been shown to promote apoptosis.

Resveratrol, a phytoalexin found in grapes, fruits, and root extracts of the weed *Polygonum cuspidatum*, is an important constituent of Chinese folk medicine. Indirect evidence suggests that the presence of resveratrol in white and rose wine may be helpful to reduce risks of coronary heart disease which would be achieved by a moderate wine consumption. This effect has been attributed to the inhibition of platelet aggregation and coagulation, in addition to the anti-oxidant and anti-inflammatory activity of resveratrol. Moreover, a recent report showed that resveratrol was a potent cancer chemopreventive agent in three major stages of carcinogenesis. We found resveratrol was able to induce apoptosis in primary gastric cancer *in vitro*. This apoptosis may be mediated by down-regulating the expression of apoptosis-regulated gene *bcl-2* and up-regulating the expression of apoptosis-regulated gene *bax*.

This study was to investigate the apoptosis of implanted tumor of primary gastric cancer cells in nude mice induced by resveratrol and the relation between this apoptosis and expression of bcl-2 and bax *in vivo* and to provide the theoretical and methodological basis for its clinical application.

MATERIALS AND METHODS

Materials

Resveratrol was obtained from Sigma Chemical Co. Ltd and dissolved in DMSO. *In situ* cell detection kit, anti-bcl-2 and anti-bax monoclonal antibodies were purchased from Beijing Zhongshan Biotechnology Co. Ltd. Balb/C female nude mice (4 wk old, 16-18 g) were obtained from Chinese Academy of Medical Sciences.

Methods

Cell culture Fresh samples from a patient with low-differentiation gastric cancer were obtained at operating. A single-cell suspension of tumor cells with the concentration of 5×10^5/mL

was prepared for seeding. Primary gastric cancer cells were artificially purified after cultured with pancreatic proteinase.

Tumor implanted into nude mice A transplanted tumor model was established by injecting 1×10^9/L human primary gastric cancer cells into subcutaneous tissues of nude mice. After 10 d, 25 nude mice were divided into 5 groups at random and 0.2 mL normal saline solution, 1 500 mg/kg DMSO, 500 mg/kg resveratrol, 1 000 mg/kg resveratrol, and 1 500 mg/kg resveratrol were directly injected beside tumor body respectively 6 times at an interval of 2 d. Then changes of tumor volume ($V = (\pi/6) \times abc$) were measured 11 d after injecting drugs and tumor inhibition rate of each group was calculated according to the following formula.

$$\text{Inhibitory rate\{IR\} of tumor growth} = \frac{C(V_1-V_0) - T(V_1-V_0)}{C(V_1-V_0)}$$

Where C is control group, T is treated group, V_1 is the volume before treatment (mm^3), V_0 is the volume after treated (mm^3).

Transmission electron microscopy

Tumor samples were cut into 1 mm×1 mm×1 mm sections and fixed in 4% glutaral and immersed with Epon 821, imbedded for 72 h at 60 ℃. Cells were prepared into ultrathin section (60 nm) and stained with uranyl acetate and lead citrate. Cell morphology was observed by transmission electron microscopy.

TUNEL assay

Tumor samples were cryopreservated in liquid nitrogen and cut into 8-μm thick slices. Slices were fixed in ice-cold 80% ethanol for 24 h, treated with proteinase K and 0.3% H_2O_2, labeled with fluorescein dUTP in a humid box for 1 h at 37 ℃. Slices were then combined with POD-horseradish peroxidase, stained with DAB and counterstained with methyl green. Controls received the same management except the labeling of omission of fluorescein dUTP. Cells were visualized with light microscope. The apoptotic index (AI) was calculated as follows: AI = (number of apoptotic cells/total number) ×100%.

Immunohistochemical staining

Tumor samples were cryopreservated in liquid nitrogen, cut into 8-μm thick slices and fixed by acetone. After washed with PBS, slices were incubated in 0.3% H_2O_2 solution at room temperature for 5 min. Slices were then incubated with anti-bcl-2 or anti-bax monoclonal antibody at a 1:300 dilution at 4 ℃ overnight. After washed with PBS, the second antibody, biotinylated antirat IgG, was added and cells were incubated at room temperature for 1 h. After washed with PBS, ABC compound was added and incubated at room temperature for 10 min. DAB was used as the chromagen. After 10 min, the brown color signifying the presence of antigens bound to antibodies was detected by light microscopy. Controls were managed as the experimental group except the incubation of primary antibody. The positive rate (PR) was calculated as follows: PR = (number of positive cells/total number) ×100%.

RT-PCR

Tumor samples were cryopreservated in liquid nitrogen and total RNA was extracted. Concentration of RNA was determined by the absorption at 260 nm. The primers for bcl-2, bax and β-actin were as follows: β-actin (500 bp) 5' GTGGGGCGCCCCAGGCACCA3' (sense); 5' CTCCTTAATGTCACGCACGATTTC3' (anti-sense); bcl-2 (716 bp) 5' GGAAATATGGCGCACGCT 3' (sense); 5' TCACTTGTGGCCCAGAT 3' (anti-sense); bax (508 bp) 5' CCAGCTCTGAGCAGATCAT 3' (sense), 5' TATCAGCCCATCTTCTTCC 3' (anti-sense). Polymerse chain reactions were performed in a 50 μL reaction volume. RT-PCR reaction was run in the following conditions: at 94 ℃ for 7 min, 1 circle; at 94 ℃ for 1 min, at 72 ℃ for 1min, 30 circle; at 72 ℃ for 7 min, 1 circle. Ten μL PCR products was placed onto 15 g/L agarose gel and observed by EB staining using the Gel-Pro analyzer.

Statistical analysis

Data were analyzed by analysis of variance, and $P<0.05$ was considered statistically significant.

RESULTS

Inhibitory rate of tumor growth

An inhibitory effect was observed in all therapeutic groups and the inhibition rate of resveratrol at the dose of 500 mg/kg, 1 000 mg/kg and 1 500 mg/kg was 10.58%, 29.68% and 39.14% respectively ($P<0.05$ *vs* the control group, Table 1).

Table 1 Inhibitory effect of resveratrol on implanted tumors in nude mice (mean±SD)

Group	Number of animals		Volume of tumors (mm^3)		Inhibition rate
	Beginning	Ending	Beginning	Ending	%
Control group					
0.2 mL saline	5	5	20.49±0.99	498.73±10.74	
DMSO					
1 500 mg/kg	5	5	20.07±1.24	506.17±8.70	
Resveratrol					
500 mg/kg	5	5	20.44±1.76	448.04±6.32[a]	10.58
1 000 mg/kg	5	5	21.27±1.73	357.55±6.34[a]	29.68
1 500 mg/kg	5	5	21.32±1.72	312.39±9.93[a]	39.14

[a]$P<0.05$ *vs* control group.

Morphological changes

The cells in control groups had normal structures, but some cells in therapeutic groups had apoptotic characteristics including chromatin condensation, chromatin crescent, nucleus fragmentation (Figure 1A, B).

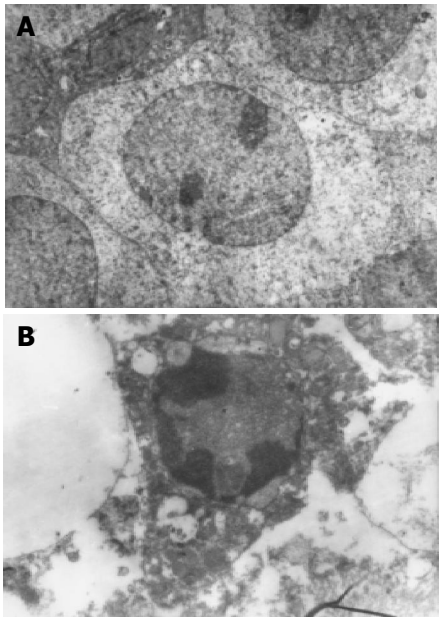

Figure 1 Ultra-microscopic structures of transplanted tumor cells and apoptotic transplanted tumor cells induced by resveratrol. A: Ultra-microscopic structure of transplanted tumor cells (Original magnification: ×4 800); B: Ultra-microscopic structure of apoptotic transplanted tumor cells induced by resveratrol (Original magnification: ×4 800).

TUNEL assay

Positive staining was located in nuclei (Figure 2). The apoptosis index of 0.2 mL normal saline solution, 1 500 mg/kg DMSO, 500 mg/kg resveratrol, 1 000 mg/kg resveratrol, and 1 500 mg/kg resveratrol was 13.68±0.37%, 13.8±0.43%, 48.7±1.07%, 56.44±1.39% and 67±0.96%, respectively (P<0.001 *vs* the control group Table 2).

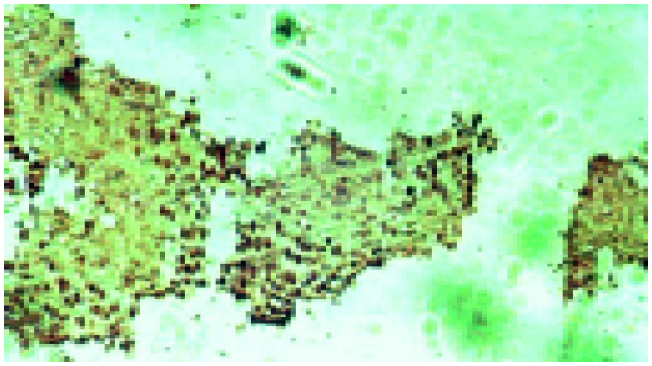

Figure 2 TUNEL assay of apoptotic transplanted tumor cells induced by resveratrol (Original magnification: ×200).

Table 2 Apoptotic index (AI) of implanted tumors in nude mice

	Control	DMSO	500 mg/kg	1 000 mg/kg	1 500 mg/kg
AI (%)	13.68±0.37	13.80±0.43	48.70±1.07	56.44±1.39	67±0.96
F		0.13	1344.25[b]	2651.16[b]	7984.02[b]
P		>0.05	<0.001	<0.001	<0.001

[b]P<0.001 *vs* control group.

Expression of bcl-2 proteins

Positive staining was located in cytoplasm. The positive rate of bcl-2 protein of 0.2 mL normal saline solution, 1 500 mg/kg DMSO, 500 mg/kg resveratrol, 1 000 mg/kg resveratrol, and 1 500 mg/kg resveratrol was 29.48±0.51%, 27.56±1.40%, 11.86±0.97%, 5.7±0.84% and 3.92±0.85% respectively by immunohistochemical staining (P<0.001 *vs* the control group Table 3).

Table 3 Positive rate of bcl-2 proteins of implanted tumors in nude mice

	Control	DMSO	500 mg/kg	1 000 mg/kg	1 500 mg/kg
PT(%)	29.48±0.51	27.56±1.40	11.86±0.93	5.70±0.84	3.92±0.85
F		4.98	775.51[b]	1879.11[b]	1994.65[b]
P		>0.05	<0.001	<0.001	<0.001

[b]P<0.001 *vs* control group.

Expression of bax proteins

Positive staining was located in cytoplasm. The positive rate of bax protein of 0.2 mL normal saline solution, 1 500 mg/kg DMSO, 500 mg/kg resveratrol, 1 000 mg/kg resveratrol, and 1 500 mg/kg resveratrol was 19.34±0.35%, 20.88±0.91%, 40.02±1.20%, 45.72±0.88% and 52.3±1.54% respectively (P<0.001 *vs* the control group Table 4).

RT-PCR

The density of bcl-2 mRNA in 0.2 mL normal saline solution, 1 500 mg/kg DMSO, 500 mg/kg resveratrol, 1 000 mg/kg resveratrol, and 1 500 mg/kg resveratrol decreased progressively and the density of bax mRNA in 0.2 mL normal saline solution, 1 500 mg/kg DMSO, 500 mg/kg resveratrol, 1 000 mg/kg resveratrol, and 1 500 mg/kg increased progressively with elongation of time by RT-PCR (Figure 3A, B).

Table 4 Positive rate of bax proteins of implanted tumors in nude mice

	Control	DMSO	500 mg/kg	1 000 mg/kg	1 500 mg/kg
PT(%)	19.34±0.35	20.88±0.91	40.02±1.20	45.72±0.88	52.3±1.54
F		7.48	821.11[b]	2327.70[b]	1298.41[b]
P		>0.05	<0.001	<0.001	<0.001

[b]P<0.001 *vs* control group.

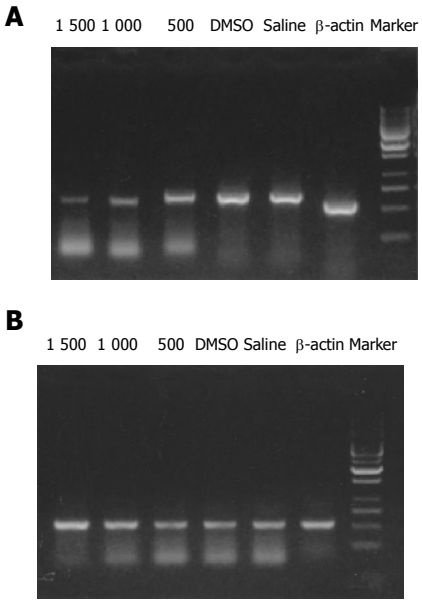

Figure 3 Expression of bcl-2 mRNA and bax mRNA in apoptotic transplanted tumor cells induced by resveratrol. A: Expression of bcl-2 mRNA in apoptotic transplanted tumor cells induced by resveratrol; B: Expression of bax mRNA in apoptotic transplanted tumor cells induced by resveratrol.

DISCUSSION

Currently, only few chemotherapeutic drugs are effective in the treatment of human primary gastric carcinoma and it is necessary to look for new anti-gastric carcinoma drugs. Resveratrol, a polyphenol has been found in various fruits and vegetables and grapes. The root extract from the weed *Polygonum cuspidatum*, an important constituent of Chinese folk medicine, is also an ample source of resveratrol[1,2]. Several studys in the past several years have shown that resveratrol has cardioprotective and chemopreventive effects[3-5]. This constituent might account for the reduced risk of coronary heart disease in humans which could be achieved by a moderate wine consumption[6]. Resveratrol was able to inhibit the growth of a wide variety of tumor cells, including leukemic, prostate, breast and hepatic cells[7-11]. The anti-tumor activity of resveratrol might be related to the induction of tumor apoptosis of tumor cells[12-22].

Bcl-2 family plays a crucial role in the control of apoptosis.

It has been found that the family includes a number of proteins which have homologous amino acid sequences, including anti-apoptotic members such as bcl-2 and bcl-x_L, as well as pro-apoptotic members including bax and bad[23-26]. Overexpression of bax could promote the cell death[27-31]. Conversely, overexpression of antiapoptotic proteins such as Bcl-2 could repress the function of bax[32-36]. Thus, the ratio of bcl-2 /bax was a critical determinant of a cell's threshold for undergoing apoptosis[37].

We found that resveratrol was able to induce apoptosis in primary gastric cancer in *in vitro* experiments. This apoptosis might be mediated by down-regulating the expression of apoptosis-regulated gene *bcl-2* and up-regulating the expression of apoptosis-regulated gene *bax*. In this study, we evaluated the effectiveness of apoptosis of gastric cacinoma induced by resveratrol *in vivo*, investigate the molecular mechanisms further and provide the theoretical and methodological basis for the clinical application of resveratrol.

We observed the inhibitory effect of resveratrol in all therapeutic groups. Cells in control groups had normal structures, but some cells in therapeutic groups had apoptotic characteristics. The apoptosis index of resveratrol at the dose of 500, 1 000, and 1 500 mg/kg was increased. Expression of bcl-2 of resveratrol at the dose of 500, 1 000, and 1 500 mg/kg was decreased, but expression of bax was increased. The density of bcl-2 mRNA induced by resveratrol at the dose of 500, 1 000, and 1 500 mg/kg decreased progressively and the density of bax mRNA increased progressively. The ratio of bcl-2/bax was decreased and triggered the apoptosis of transplanted tumor cells.

Our results demonstrated resveratrol was able to induce the apoptosis of transplanted tumor cells in nude mice. The apoptosis may be mediated by down-regulating the expression of apoptosis-regulated gene *bcl-2* and up-regulating the expression of apoptosis-regulated gene *bax*. Resveratrol may be potentially used as a chemotherapeutic drug in anti-gastric carcinoma chemotherapy.

REFERENCES

1 **Yoon SH,** Kim YS, Ghim SY, Song BH, Bae YS. Inhibition of protein kinase CKII activity by resveratrol, a natural compound in red wine and grapes. *Life Sci* 2002; **71**: 2145-2152
2 **Gao X,** Xu YX, Divine G, Janakiraman N, Chapman RA, Gautam SC. Disparate *in vitro* and *in vivo* antileukemic effects of resveratrol, a natural polyphenolic compound found in grapes. *J Nutr* 2002; **132**: 2076-2081
3 **Bhat KP,** Pezzuto JM. Cancer chemopreventive activity of resveratrol. *Ann N Y Acad Sci* 2002; **957**: 210-229
4 **Kuwajerwala N,** Cifuentes E, Gautam S, Menon M, Barrack ER, Reddy GP. Resveratrol induces prostate cancer cell entry into s phase and inhibits DNA synthesis. *Cancer Res* 2002; **62**: 2488-2492
5 **Joe AK,** Liu H, Suzui M, Vural ME, Xiao D, Weinstein IB. Resveratrol induces growth inhibition, S-phase arrest, apoptosis, and changes in biomarker expression in several human cancer cell lines. *Clin Cancer Res* 2002; **8**: 893-903
6 **Wang Z,** Zou J, Huang Y, Cao K, Xu Y, Wu JM. Effect of resveratrol on platelet aggregation *in vivo* and *in vitro*. *Chin Med J (Engl)* 2002; **115**: 378-380
7 **Ferry-Dumazet H,** Garnier O, Mamani-Matsuda M, Vercauteren J, Belloc F, Billiard C, Dupouy M, Thiolat D, Kolb JP, Marit G, Reiffers J, Mossalayi MD. Resveratrol inhibits the growth and induces the apoptosis of both normal and leukemic hematopoietic cells. *Carcinogenesis* 2002; **23**: 1327-1333
8 **Kampa M,** Hatzoglou A, Notas G, Damianaki A, Bakogeorgou E, Gemetzi C, Kouroumalis E, Martin PM, Castanas E. Wine antioxidant polyphenols inhibit the proliferation of human prostate cancer cell lines. *Nutr Cancer* 2000; **37**: 223-233
9 **Bove K,** Lincoln DW, Tsan MF. Effect of resveratrol on growth of 4T1 breast cancer cells *in vitro* and *in vivo*. *Biochem Biophys Res Commun* 2002; **291**: 1001-1005
10 **Tian XM,** Zhang ZX. The anticancer activity of resveratrol on implanted tumor of HepG2 in nude mice. *Shijie Huaren Xiaohua Zazhi* 2001; **9**: 161-164
11 **Sun ZJ,** Pan CE, Liu HS, Wang GJ. Anti-hepatoma activity of resveratrol *in vitro*. *World J Gastroenterol* 2002; **8**: 79-81
12 **Pervaiz S.** Resveratrol-from the bottle to the bedside? *Leuk Lymphoma* 2001; **40**: 491-498
13 **Dorrie J,** Gerauer H, Wachter Y, Zunino SJ. Resveratrol induces extensive apoptosis by depolarizing mitochondrial membranes and activating caspase-9 in acute lymphoblastic leukemia cells. *Cancer Res* 2001; **61**: 4731-4739
14 **She QB,** Bode AM, Ma WY, Chen NY, Dong Z. Resveratrol-induced activation of p53 and apoptosis is mediated by extracellular-signal-regulated protein kinases and p38 kinase. *Cancer Res* 2001; **61**: 1604-1610
15 **Tsan MF,** White JE, Maheshwari JG, Bremner TA, Sacco J. Resveratrol induces Fas signalling-independent apoptosis in THP-1 human monocytic leukaemia cells. *Br J Haematol* 2000; **109**: 405-412
16 **Szende B,** Tyihak E, Kiraly-Veghely Z. Dose-dependent effect of resveratrol on proliferation and apoptosis in endothelial and tumor cell cultures. *Exp Mol Med* 2000; **32**: 88-92
17 **Bernhard D,** Tinhofer I, Tonko M, Hubl H, Ausserlechner MJ, Greil R, Kofler R, Csordas A. Resveratrol causes arrest in the S-phase prior to Fas-independent apoptosis in CEM-C7H2 acute leukemia cells. *Cell Death Differ* 2000; **7**: 834-842
18 **Mouria M,** Gukovskaya AS, Jung Y, Buechler P, Hines OJ, Reber HA, Pandol SJ. Food-derived polyphenols inhibit pancreatic cancer growth through mitochondrial cytochrome C release and apoptosis. *Int J Cancer* 2002; **98**: 761-769
19 **Shih A,** Davis FB, Lin HY, Davis PJ. Resveratrol induces apoptosis in thyroid cancer cell lines via a MAPK- and p53-dependent mechanism. *J Clin Endocrinol Metab* 2002; **87**: 1223-1232
20 **Mahyar-Roemer M,** Katsen A, Mestres P, Roemer K. Resveratrol induces colon tumor cell apoptosis independently of p53 and precede by epithelial differentiation, mitochondrial proliferation and membrane potential collapse. *Int J Cancer* 2001; **94**: 615-622
21 **Lin HY,** Shih A, Davis FB, Tang HY, Martino LJ, Bennett JA, Davis PJ. Resveratrol induced serine phosphorylation of p53 causes apoptosis in a mutant p53 prostate cancer cell line. *J Urol* 2002; **168**: 748-755
22 **She QB,** Huang C, Zhang Y, Dong Z. Involvement of c-jun NH (2)-terminal kinases in resveratrol-induced activation of p53 and apoptosis. *Mol Carcinog* 2002; **33**: 244-250
23 **Konopleva M,** Konoplev S, Hu W, Zaritskey AY, Afanasiev BV, Andreeff M. Stromal cells prevent apoptosis of AML cells by up-regulation of anti-apoptotic proteins. *Leukemia* 2002; **16**: 1713-1724
24 **van der Woude CJ,** Jansen PL, Tiebosch AT, Beuving A, Homan M, Kleibeuker JH, Moshage H. Expression of apoptosis-related proteins in Barrett's metaplasia-dysplasia-carcinoma sequence: a switch to a more resistant phenotype. *Hum Pathol* 2002; **33**: 686-692
25 **Panaretakis T,** Pokrovskaja K, Shoshan MC, Grander D. Activation of Bak, Bax, and BH3-only proteins in the apoptotic response to doxorubicin. *J Biol Chem* 2002; **277**: 44317-44326
26 **Bellosillo B,** Villamor N, Lopez-Guillermo A, Marce S, Bosch F, Campo E, Montserrat E, Colomer D. Spontaneous and drug-induced apoptosis is mediated by conformational changes of Bax and Bak in B-cell chronic lymphocytic leukemia. *Blood* 2002; **100**: 1810-1816
27 **Matter-Reissmann UB,** Forte P, Schneider MK, Filgueira L, Groscurth P, Seebach JD. Xenogeneic human NK cytotoxicity against porcine endothelial cells is perforin/granzyme B dependent and not inhibited by Bcl-2 overexpression. *Xenotransplantation* 2002; **9**: 325-337
28 **Lanzi C,** Cassinelli G, Cuccuru G, Supino R, Zuco V, Ferlini C, Scambia G, Zunino F. Cell cycle checkpoint efficiency and cellular response to paclitaxel in prostate cancer cells. *Prostate*

2001; **48**: 254-264
29 **Mertens HJ,** Heineman MJ, Evers JL. The expression of apoptosis-related proteins Bcl-2 and Ki67 in endometrium of ovulatory menstrual cycles. *Gynecol Obstet Invest* 2002; **53**: 224-230
30 **Mehta U,** Kang BP, Bansal G, Bansal MP. Studies of apoptosis and bcl-2 in experimental atherosclerosis in rabbit and influence of selenium supplementation. *Gen Physiol Biophys* 2002; **21**: 15-29
31 **Chang WK,** Yang KD, Chuang H, Jan JT, Shaio MF. Glutamine protects activated human T cells from apoptosis by up-regulating glutathione and Bcl-2 levels. *Clin Immunol* 2002; **104**: 151-160
32 **Chen GG,** Lai PB, Hu X, Lam IK, Chak EC, Chun YS, Lau WY. Negative correlation between the ratio of Bax to Bcl-2 and the size of tumor treated by culture supernatants from Kupffer cells. *Clin Exp Metastasis* 2002; **19**: 457-464
33 **Usuda J,** Chiu SM, Azizuddin K, Xue LY, Lam M, Nieminen AL, Oleinick NL. Promotion of photodynamic therapy-induced apoptosis by the mitochondrial protein Smac/DIABLO: dependence on Bax. *Photochem Photobiol* 2002; **76**: 217-223
34 **Sun F,** Akazawa S, Sugahara K, Kamihira S, Kawasaki E, Eguchi K, Koji T. Apoptosis in normal rat embryo tissues during early organogenesis: the possible involvement of Bax and Bcl-2. *Arch Histol Cytol* 2002; **65**: 145-157
35 **Jang MH,** Shin MC, Shin HS, Kim KH, Park HJ, Kim EH, Kim CJ. Alcohol induces apoptosis in TM3 mouse Leydig cells via bax-dependent caspase-3 activation. *Eur J Pharmacol* 2002; **449**: 39-45
36 **Tilli CM,** Stavast-Koey AJ, Ramaekers FC, Neumann HA. Bax expression and growth behavior of basal cell carcinomas. *J Cutan Pathol* 2002; **29**: 79-87
37 **Pettersson F,** Dalgleish AG, Bissonnette RP, Colston KW. Retinoids cause apoptosis in pancreatic cancer cells via activation of RAR-gamma and altered expression of Bcl-2/Bax. *Br J Cancer* 2002; **87**: 555-561

Edited by Wang XL **Proofread by** Chen WW

PO Box 2345, Beijing 100023, China
Fax: +86-10-85381893
E-mail: wjg@wjgnet.com www.wjgnet.com

ELSEVIER

World J Gastroenterol 2005;11(2):285-288
World Journal of Gastroenterology ISSN 1007-9327

• BRIEF REPORTS •

Loss of heterozygosity on 10q23.3 and mutation of tumor suppressor gene PTEN in gastric cancer and precancerous lesions

Yi-Ling Li, Zhong Tian, Dong-Ying Wu, Bao-Yu Fu, Yan Xin

Yi-Ling Li, Bao-Yu Fu, Department of Gastroenterology, First Hospital of China Medical University, Shenyang 110001, Liaoning Province, China
Zhong Tian, Department of Surgery, Second Hospital of China Medical University, Shenyang 110003, Liaoning Province, China
Dong-Ying Wu, Yan Xin, The Fourth Laboratory, Cancer Institute, First Hospital of China Medical University, Shenyang 110001, Liaoning Province, China
Supported by the National Natural Science Foundation of China, No. 30070845
Correspondence to: Professor Yan Xin, The Fourth Laboratory, Cancer Institute, First Hospital of China Medical University, Shenyang 110001, Liaoning Province, China. yxin@mail.cmu.edu.cn
Telephone: +86-24-23256666 Ext. 6351 **Fax:** +86-24-23253443
Received: 2004-04-07 **Accepted:** 2004-05-24

Abstract

AIM: To investigate the loss of heterozygosity (LOH) and mutation of tumor suppressor gene PTEN in gastric cancer and precancerous lesions.

METHODS: Thirty cases of normal gastric mucosa, advanced and early stage gastric cancer, intestinal metaplasia, atrophic gastritis, and atypical hyperplasia were analyzed for PTEN LOH and mutations within the entire coding region of PTEN gene by PCR-SSCP denaturing PAGE gel electrophoresis, and PTEN mutation was detected by PCR-SSCP sequencing followed by silver staining.

RESULTS: LOH rate found in respectively atrophic gastritis was 10% (3/30), intestinal metaplasia 10% (3/30), atypical hyperplasia 13.3% (4/30), early stage gastric cancer 20% (6/30), and advanced stage gastric cancer 33.3% (9/30), None of the precancerous lesions and early stage gastric cancer showed PTEN mutations, but 10% (3/30) of the advanced stage gastric cancers, which were all positive for LOH, showed PTEN mutation.

CONCLUSION: LOH of PTEN gene appears in precancerous lesions, and PTEN mutations are restricted to advanced gastric cancer, LOH and mutation of PTEN gene are closely related to the infiltration and metastasis of gastric cancer.

Key words: Gastric cancer; Precancerous lesions; PTEN gene; Loss of heterozygosity; Mutation

Li YL, Tian Z, Wu DY, Fu BY, Xin Y. Loss of heterozygosity on 10q23.3 and mutation of tumor suppressor gene PTEN in gastric cancer and precancerous lesions. *World J Gastroenterol* 2005; 11(2): 285-288
http://www.wjgnet.com/1007-9327/11/285.asp

INTRODUCTION

A candidate tumor suppressor gene PTEN (also known as MMAC1 or TEP1) has recently been isolated from chromosome 10q23.3[1-3]. They are found mutated in several cancer types that display LOH in this region[4,5]. The PTEN gene encodes a 403 amino acid protein homologous to some protein phosphatases, and the protein has been shown to possess protein phosphatase activity *in vitro*[6-8]. It is thought that PTEN protein dephosphorylates the 3 positions of phosphatidylinositol 3,4,5-triphosphate (PIP3), a well-known intracellular messenger of certain cell-growth stimulators[9,10]. The molecular mechanisms of PTEN have been elucidated recently, and it is considered that PTEN belongs to a class of tumor suppressor genes together with p^{53}, Rb, and APC. Gastric cancer is the most common digestive tract cancer diagnosed in China. In spite of its impact on human health, the molecular mechanisms involved in the pathogenesis of gastric cancer remain relatively unknown. PTEN is expressed in normal gastric mucosa, implying that loss of function may have some consequences in gastric cancer. We examined patients of advanced stage gastric cancer, especially the precancerous lesions for LOH at the loci, and observed the PTEN gene and its mutation from different visual aspects. We found the frequent presence of LOHs at 10q23.3 in gastric cancer and the precancerous lesions and mutations of PTEN gene in patients with advanced stage gastric cancer, suggesting that the inactivation of PTEN gene might be more closely related to the infiltration and metastasis of gastric cancer than previous observations.

MATERIALS AND METHODS

Tissue samples

Thirty cases of normal gastric mucosa, atrophic gastritis, intestinal metaplasia, atypical hyperplasia, and the early and advanced stage gastric cancer were obtained from the Endoscopic Center and operation rooms of China Medical University from 2000 to 2002. The tissues were extracted 5 cm away from the lesion for the control group. All the specimens were embedded in OCT rather then snap-frozen in the liquid nitrogen, and kept frozen at -70 ℃. The cryostat sections from each tumor specimen were examined histologically, and only those blocks of tumor tissues composed of more than 70% neoplastic cells were selected for subsequent DNA isolation. DNA was from gastric cancers, precancerous lesions, and the corresponding normal tissues following the saturated sodium chloride method.

LOH analysis

Three microsatellite markers (D10S215, D10S541 and D10S 2491) were used to evaluate LOH on 10q23.3[11]. All the primers used in this study were obtained from AoKe Corporation, Beijing. The sequences of the primers are shown in Table 1. Each of the PCR mixtures contained 20 ng of genomic DNA, 2 μL of 10×PCR buffer, 0.4 μmol/L of each primer, 1.5 mmol/L Mg^{2+}, 200 mmol/L of dNTPs, and 1 unit of Taq DNA polymerase (Takara, Dalian). PCR was carried out over 35 amplification cycles for 45 s at 94 ℃, 45 s at 55 ℃, 60 s at 72 ℃. The PCR mixture was subjected to predegeneration for 5 min at 95 ℃ and a further extension for 10 min at 72 ℃. After the amplification, PCR products were resolved on 160 g/L denaturing polyacrylamide gel and sliver staining was performed for analysis.

PTEN mutations

Exons 5 and 8 of PTEN were amplified separately using the primer sets described by Risinger *et al*[12]. The primer sequences of exons 5 and 8 are shown in Table 1. Genomic DNA was subjected to PCR amplification in 20 μL of the reaction mixture, which contained 20 ng of genomic DNA, 2.5 mol/L of each primer, 2 μL of 10× PCR buffer, 2.0 mmol/L Mg^{2+}, 200 mmol/L dNTP, and 1 unit of TaqDNA polymerase (Takara, Dalian). PCR was carried out over 35 amplification cycles for 45 s at 94 ℃, 30 s at 58 ℃, 60 s at 72 ℃. The PCR mixture was subjected to predenaturation at 95 ℃ for 5 min and a final extension at 72 ℃ for 10 min. After completion of PCR, the ratio of 1:5 volume of sequencing-stop-solution was added, heated at 95 ℃ and rapidly cooled on ice, and 1-5 μL of resulting mixtures was loaded on 120 g/L non-denaturing polyacrylamide gel and silver stained, then the shifted bands were sequenced.

DNA sequencing

After the electrophoresis, shifted SSCP bands were excised from the gel. We extracted the DNA from the gel with distilled water, then reamplified it using the original PCR primers. The reamplified PCR products were sequenced with an ABI PRISM310 dye terminator cycle sequencing ready reaction kit.

RESULTS

LOH analysis

We examined the genotypes of gastric cancer and precancerous lesions at three highly polymorphic loci distributed at 10q23.3 (D10S215, D10S541 and D10S 2491). In our study, 10% of atrophic gastritis and intestinal metaplasia and 13.3% of atypical hyperplasia demonstrated LOH in the 10q23.3 region (Figure 1 and Table 1). To examine whether the LOH found frequently in this region was also present in gastric cancer, we further studied 30 early stage and 30 advanced stage cancers (Table 2 and Figure 1). We found that 20% of the early stage gastric cancers and 30% of the advanced stage gastric cancers demonstrated LOH at 10q23.3, while none of the normal gastric mucosa showed LOH at D10S215, D10S54, or D10S 2491.

Table 1 Primers of PTEN microsatellite loci and exons

Loci	Position	Primer sequence
D10S215	$10q^{22-23}$	P_1 TGGCATCATTCTGGGGA
		P_2 TTACGTTTCTTCACATGGT
D10S541	$10q^{22-23}$	P_1 AAGCAAGTGAAGTCTTAGAACCACC
		P_2 CCACAAGTAACAGAAAGCCTGTCTC
D10S2491	$10q^{23-23}$	P_1 TTATAAGGACTGAGTGAGGGA
		P_2 GTTAGATAGAGTACCTGCACTC
Exon 5		P_1 CTTATTCTGAGGTTATCTTTTTTACC
		P_2 CTCAGAATCCAGGAAGAGGA
Exon 8		P_1 ACACATCACATACATACAAGTC
		P_2 GTGCAGATAATGACAAGGAATA

SSCP and sequencing

SSCP analysis of the PTEN gene was performed on gastric cancer and precancerous lesions. We screened the exons 5 and 8 of PTEN coding region, and no mutation was detected in early stage gastric cancer or precancerous lesions. However, one mutation in exon 5, and two mutations in exon 8 of PTEN coding region were detected in advanced gastric cancer (Table 3 and Figure 1)

Table 2 PTEN LOH in gastric cancer and precancerous lesion

Lesions	D10S215 % (*n*)	D10S541 % (*n*)	D10S2491 % (*n*)	Total %
AG	3.3 (1/30)	3.3 (1/30)	6.7 (2/30)	10
IM	3.3 (1/30)	3.3 (1/30)	3.3 (1/30)	10
AH	6.7 (2/30)	3.3 (1/30)	6.7 (2/30)	13.3
Gastric cancer				
Early stage	6.7 (2/30)	10 (3/30)	6.7 (2/30)	20
Advanced stage	13.3 (4/30)	6.7 (2/30)	13.3 (4/30)	30

AG: atrophic gastritis; IM: intestinal metaplasia; AH: atypical hyperplasia.

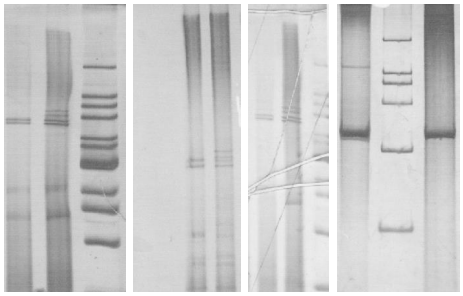

Figure 1 Representative silver staining showing allelic losses at markers near or within PTEN and mutation of PTEN (T: tumor; N: normal;).

DISCUSSION

PTEN/MMAC1 was originally isolated from a region homozygously deleted in several cancer cell lines, including glioma and cancers of the breast and prostate. Mutations in this gene have been reported as glioma, endometrial carcinoma, breast tumors, and malignant melanoma[13-16]. Germ-line mutation of PTEN/MMAC1 is also associated with two autosomal dominant disorders belonging to the family of hamartomatous polyposis syndrome[17,18]. Thus some cancers seem devoid of PTEN/MMAC1 alterations (e.g., serous carcinoma of endometrium and cervical cancer)[19]. Genetic changes of PTEN/MMAC1 occur in multiple types of cancer, suggesting that inactivation of PTEN/MMAC1 may play an important but perhaps somewhat general role in the pathogenesis of a variety of human malignancies.

There is strong circumstantial evidence that allelic loss of PTEN is found in a large variety of human cancers. The inactivation of PTEN gene may be due to mutation and LOH or decreasing expression of PTEN mRNA or protein[20-22]. The earliest research done on PTEN gene was for experimentation of glioma. The

Table 3 Mutation of PTEN in gastric cancer

Case	Exon	LOH	Coden	Base change	Stage	Pathology
11	5	+	91	GAA to CAA	III_a	Signet-ring cell cancer
19	8	+	335	CGA to TGA	II	Hypodifferentiated adenocarcinoma
22	8	+	329	Del 4 bp	III_b	Undifferentiated gastric cancer

result showed that LOH rate was 70-80%, while the mutation rate was 27-30% for the PTEN gene in glioma[23]. In prostate cancer, PTEN LOH was reported to be 32-63% while PTEN mutation rate was 12-25%[24,25]. In endometrial carcinoma, PTEN mutation rate was 19%[26], and ovary cancer showed 27.3-42.1% of PTEN LOH with a mutation rate of 8.3-21%[27]. In the benign lesion of ovary cyst, the PTEN LOH rate was 56.3%, and PTEN mutation rate was 20.6%[28]. It has been speculated that PTEN mutation and its relation to gastrointestinal tumor often occur in the colorectal tumor with hereditary tendency such as familial polyposis[29]. The mutation rate is low in sporadic colorectal cancers[30]. Taniyama *et al*[31] studied 32 cases of sporadic colon cancer, but observed a bi-allelic genomic alteration that caused loss of function of the gene only in one case. Wang *et al*[32] found only one somatic mutation of PTEN gene out of 72 colon cancer cases. Regarding the relationship between PTEN mutation and gastric cancer, Zheng *et al*[33] found PTEN was closely related to the infiltration and metastasis of gastric cancer. Our previous study showed PTEN inactivation was also related to the precancerous lesion of gastric cancer. In this study, the rates of PTEN LOH in atrophic gastritis, intestinal metaplasia, and atypical hyperplasia were 10, 10, and 13.3%, respectively. In early stage gastric cancer, PTEN LOH rate was 20%, while it was 30% in the advanced gastric cancer. There were no PTEN mutations in precancerous lesions or in any early stage gastric cancer. The PTEN mutation rate was observed in 10% of advanced gastric cancers, showing that the loss or inactivation of PTEN gene is related to the tumor genesis of gastric cancer, especially to the invasion and metastasis of gastric cancer. For the three cases of PTEN showing mutations, one tumor located in the anus prolonged and spread to the lower part of esophagus, and the pathology showed signet cancer. One case showing the tumor located in the corpus without penetrating the seroma, with the lymph node metastasis around the artery, pathology showed Undifferentiated cancer. Another case showing the tumor located in the sinus was able to infiltrate to muscular layer, with the metastasis of lymph node within 5 cm of the tumor margin. The pathology for this particular case was regarded as poorly-differentiated adenocarcinoma.

Li *et al* has previously studied the expression of PTEN encoding products in gastric cancer and precancerous lesions by immunohistochemistry. The result showed PTEN was down-regulated in the tumorigenesis of gastric cancer.

Based on the findings from this study, we conclude that PTEN LOH and the mutation rates are lower in gastric cancer compared with that in the other tumors (10 -33.3% for PTEN LOH and 0-10% for the mutation rate). This further supports that the pathogenesis of gastric cancer is a complicated molecular mechanism closely associated with genes, such as oncogene, tumor suppressor gene, mismatch repair gene, telomere and telomerase, cellular adhesive factors, *etc*.

REFERENCES

1 **Kim S,** Domon-Dell C, Wang Q, Chung DH, Di Cristofano A, Pandolfi PP, Freund JN, Evers BM. PTEN and TNF-alpha regulation of the intestinal-specific Cdx-2 homeobox gene through a PI3K,PKB/Akt, and NF-kappaB-dependent pathway. *Gastroenterology* 2002; **123**: 1163-1178

2 **McConnachie G,** Pass I, Walker SM, Downes CP. Interfacial kinetic analysis of the tumour suppressor phosphatase, PTEN: evidence for activation by anionic phospholipids. *Biochem J* 2003; **371**: 947-955

3 **Li J,** Yen C, Liaw D, Podsypanina K, Bose S, Wang SI, Puc J, Miliaresis C, Rodgers L, McCombie R, Bigner SH, Giovanella BC, Ittmann M, Tycko B, Hibshoosh H, Wigler MH, Parsons R. PTEN, a putative protein tyrosine phosphatase gene mutated in human brain, breast, and prostate cancer. *Science* 1997; **275**: 1943-1947

4 **Zhao H,** Dupont J, Yakar S, Karas M, LeRoith D. PTEN inhibits cell proliferation and induces apoptosis by downregulating cell surface IGF-IR expression in prostate cancer cells. *Oncogene* 2004; **23**: 786-794

5 **Konopka B,** Janiec-Jankowska A, Paszko Z, Goluda M. The coexistence of ERBB2, INT2, and CMYC oncogene amplifications and PTEN gene mutations in endometrial carcinoma. *J Cancer Res Clin Oncol* 2004; **130**: 114-121

6 **Brown KS,** Blair D, Reid SD, Nicholson EK, Harnett MM. FcgammaRIIb-mediated negative regulation of BCR signalling is associated with the recruitment of the MAPkinase-phosphatase, Pac-1, and the 3'-inositol phosphatase, PTEN. *Cell Signal* 2004; **16**: 71-80

7 **Cho SH,** Lee CH, Ahn Y, Kim H, Kim H, Ahn CY, Yang KS, Lee SR. Redox regulation of PTEN and protein tyrosine phosphatases in H(2)O(2) mediated cell signaling. *FEBS Lett* 2004; **560**: 7-13

8 **Wishart MJ,** Dixon JE. PTEN and myotubularin phosphatases: from 3-phosphoinositide dephosphorylation to disease. *Trends Cell Biol* 2002; **12**: 579-585

9 **Mills GB,** Kohn E, Lu Y, Eder A, Fang X, Wang H, Bast RC, Gray J, Jaffe R, Hortobagyi G. Linking molecular diagnostics to molecular therapeutics: targeting the PI3K pathway in breast cancer. *Semin Oncol* 2003; **30**: 93-104

10 **Orchiston EA,** Bennett D, Leslie NR, Clarke RG, Winward L, Downes CP, Safrany ST. PTEN M-CBR3, a versatile and selective regulator of inositol 1,3,4,5,6-pentakisphosphate (Ins (1,3, 4,5,6) P5). Evidence for Ins (1,3,4,5,6)P5 as a proliferative signal. *J Biol Chem* 2004; **279**: 1116-1122

11 **Whang YE,** Wu X, Suzuki H, Reiter RE, Tran C, Vessella RL, Said JW, Isaacs WB, Sawyers CL. Inactivation of the tumor suppressor PTEN/MMAC1 in advanced human prostate cancer through loss of expression. *Proc Natl Acad Sci USA* 1998; **95**: 5246-5250

12 **Risinger JI,** Hayes AK, Berchuck A, Barrett JC. PTEN/MMAC1 mutations in endometrial cancers. *Cancer Res* 1997; **57**: 4736-4738

13 **Ding X,** Endo S, Zhang SJ, Saito T, Kouno M, Kuroiwa T, Washiyama K, Kumanishi T. Primary malignant lymphoma of the brain: analysis of MMAC1 (PTEN) tumor suppressor gene. *Brain Tumor Pathol* 2001; **18**: 139-143

14 **Kanamori Y,** Kigawa J, Itamochi H, Sultana H, Suzuki M, Ohwada M, Kamura T, Sugiyama T, Kikuchi Y, Kita T, Fujiwara K, Terakawa N. PTEN expression is associated with prognosis for patients with advanced endometrial carcinoma undergoing postoperative chemotherapy. *Int J Cancer* 2002; **100**: 686-689

15 **Chung MJ,** Jung SH, Lee BJ, Kang MJ, Lee DG. Inactivation of the PTEN gene protein product is associated with the invasiveness and metastasis, but not angiogenesis, of breast cancer. *Pathol Int* 2004; **54**: 10-15

16 **Tsao H,** Goel V, Wu H, Yang G, Haluska FG. Genetic interaction between NRAS and BRAF mutations and PTEN/MMAC1 inactivation in melanoma. *J Invest Dermatol* 2004; **122**: 337-341

17 **Vega A,** Torres J, Torres M, Cameselle-Teijeiro J, Macia M, Carracedo A, Pulido R. A novel loss-of-function mutation (N48K) in the PTEN gene in a Spanish patient with Cowden disease. *J Invest Dermatol* 2003; **121**: 1356-1359

18 **Huang SC,** Chen CR, Lavine JE, Taylor SF, Newbury RO, Pham TT, Ricciardiello L, Carethers JM. Genetic heterogeneity in familial juvenile polyposis. *Cancer Res* 2000; **60**: 6882-6885

19 **Martini M,** Ciccarone M, Garganese G, Maggiore C, Evangelista A, Rahimi S, Zannoni G, Vittori G, Larocca LM. Possible involvement of hMLH1, p16 (INK4a) and PTEN in the malignant transformation of endometriosis. *Int J Cancer* 2002; **102**: 398-406

20 **Ning K,** Pei L, Liao M, Liu B, Zhang Y, Jiang W, Mielke JG, Li L, Chen Y, El-Hayek YH, Fehlings MG, Zhang X, Liu F, Eubanks J, Wan Q. Dual neuroprotective signaling mediated by downregulating two distinct phosphatase activities of PTEN. *J Neurosci* 2004; **24**: 4052-4060

21 **Hlobilkova A,** Knillova J, Bartek J, Lukas J, Kolar Z. The mechanism of action of the tumour suppressor gene PTEN. *Biomed Pap Med Fac Univ Palacky Olomouc Czech Repub* 2003; **147**: 19-25

22 **Mahimainathan L,** Choudhury GG. Inactivation of platelet-derived growth factor receptor by the tumor suppressor PTEN

provides a novel mechanism of action of the phosphatase. *J Biol Chem* 2004; **279**: 15258-15268

23 **Sano T,** Lin H, Chen X, Langford LA, Koul D, Bondy ML, Hess KR, Myers JN, Hong YK, Yung WK, Steck PA. Differential expression of MMAC/PTEN in glioblastoma multiforme: relationship to localization and prognosis. *Cancer Res* 1999; **59**: 1820-1824

24 **Whang YE,** Wu X, Suzuki H, Reiter RE, Tran C, Vessella RL, Said JW, Isaacs WB, Sawyers CL. Inactivation of the tumor suppressor PTEN/MMAC1 in advanced human prostate cancer through loss of expression. *Proc Natl Acad Sci USA* 1998; **95**: 5246-5250

25 **Zhao H,** Dupont J, Yakar S, Karas M, LeRoith D. PTEN inhibits cell proliferation and induces apoptosis by downregulating cell surface IGF-IR expression in prostate cancer cells. *Oncogene* 2004; **23**: 786-94

26 **Salvesen HB,** Stefansson I, Kalvenes MB, Das S, Akslen LA. Loss of PTEN expression is associated with metastatic disease in patients with endometrial carcinoma. *Cancer* 2002; 94: 2185-2191

27 **Obata K,** Hoshiai H. Common genetic changes between endometriosis and ovarian cancer. *Gynecol Obstet Invest* 2000; **50** Suppl 1: 39-43

28 **Sato N,** Tsunoda H, Nishida M, Morishita Y, Takimoto Y, Kubo T, Noguchi M. Loss of heterozygosity on 10q23.3 and mutation of the tumor suppressor gene PTEN in benign endometrial cyst of the ovary: possible sequence progression from benign endometrial cyst to endometrioid carcinoma and clear cell carcinoma of the ovary. *Cancer Res* 2000; **60**: 7052-7056

29 **Negoro K,** Takahashi S, Kinouchi Y, Takagi S, Hiwatashi N, Ichinohasama R, Shimosegawa T, Toyota T. Analysis of the PTEN gene mutation in polyposis syndromes and sporadic gastrointestinal tumors in Japanese patients. *Dis Colon Rectum* 2000; **43**: S29-S33

30 **Guanti G,** Resta N, Simone C, Cariola F, Demma I, Fiorente P, Gentile M. Involvement of PTEN mutations in the genetic pathways of colorectal cancerogenesis. *Hum Mol Genet* 2000; **9**: 283-287

31 **Taniyama K,** Goodison S, Ito R, Bookstein R, Miyoshi N, Tahara E, Tarin D, Urquidi V. PTEN expression is maintained in sporadic colorectal tumours. *J Pathol* 2001; **194**: 341-348

32 **Wang Q,** Wang X, Hernandez A, Hellmich MR, Gatalica Z, Evers BM. Regulation of TRAIL expression by the phosphatidylinositol 3-kinase/Akt/GSK-3 pathway in human colon cancer cells. *J Biol Chem* 2002; **277**: 36602-36610

33 **Zheng HC,** Chen Y, Kuang LG, Yang L, Li JY, Wu DY, Zhang SM, Xin Y. Expression of PTEN-encoding product in different stages of carcinogenesis and progression of gastric carcinoma. *Zhonghua Zhongliu Zazhi* 2003; **25**: 13-16

Edited by Kumar M and Ma JY

PO Box 2345, Beijing 100023, China
Fax: +86-10-85381893
E-mail: wjg@wjgnet.com www.wjgnet.com

ELSEVIER

World J Gastroenterol 2005;11(2):289-292
World Journal of Gastroenterology ISSN 1007-9327

• BRIEF REPORTS •

Homozygosity for Pro of p53 Arg72Pro as a potential risk factor for hepatocellular carcinoma in Chinese population

Zhong-Zheng Zhu, Wen-Ming Cong, Shu-Fang Liu, Hui Dong, Guan-Shan Zhu, Meng-Chao Wu

Zhong-Zheng Zhu, Wen-Ming Cong, Hui Dong, Meng-Chao Wu, Department of Pathology, Eastern Hepatobiliary Surgery Hospital, Second Military Medical University, Shanghai 200438, China
Shu-Fang Liu, HealthDigit Company Limited, Shanghai 200233, China
Guan-Shan Zhu, Department of Infectious Diseases, Changhai Hospital, Second Military Medical University, Shanghai 200433, China, and National Institute on Alcohol Abuse and Alcoholism, National Institutes of Health, Rockville, Maryland 20852, USA
Supported by the National Natural Science Foundation of China, No. 30370645, and by the Hundred Leading Scientists Program of the Public Health Sector of Shanghai, No. 98BR007
Correspondence to: Professor Wen-Ming Cong, Department of Pathology, Eastern Hepatobiliary Surgery Hospital, Second Military Medical University, Shanghai 200438, China. wmcong@smmu.edu.cn
Telephone: +86-21-25070860
Received: 2004-03-15 **Accepted:** 2004-04-05

Abstract

AIM: Codon 72 exon 4 polymorphism (Arg72Pro) of the p53 gene has been implicated in cancer risk. Our objective was to investigate the possible association between p53 Arg72Pro polymorphism and susceptibility to hepatocellular carcinoma (HCC) among Chinese population.

METHODS: The p53 Arg72Pro genotypes were determined by PCR-based restriction fragment length polymorphism (RFLP) analysis in 507 HCC cases and 541 controls. Odds ratios (ORs) for HCC and 95% confidence intervals (CIs) from unconditional logistic regression models were used to evaluate relative risks. Potential risk factors were included in the logistic regression models as covariates in the multivariate analyses on genotype and HCC.

RESULTS: The frequencies for Pro and Arg alleles were 44.5%, 55.5% in HCC cases, and 40.3% and 59.7% in controls, respectively. The Pro allele was significantly associated with the presence of HCC ($P = 0.05$) and had a higher risk for HCC (OR = 1.19, 95% CI 1.00-1.41) as compared with the Arg allele. After adjusted for potential risk factors, Arg/Pro heterozygotes had an 1.21-fold increased risk (95% CI 0.82-1.78, $P = 0.34$) of HCC compared with Arg homozygotes, whereas the risk for Pro homozygotes was 1.79 (95% CI 1.06-3.01, $P = 0.03$) times higher than that for Arg homozygotes. Pro-allele carriers had a higher relative risk of HCC than the Arg-only carriers (adjusted OR = 1.33, 95% CI 0.92-1.92, $P = 0.13$), although the difference was not statistically significant.

CONCLUSION: Homozygosity for Pro of p53 Arg72Pro is potentially one of the genetic risk factors for HCC in Chinese population. The p53 Arg72Pro polymorphism may be used as a stratification marker in screening individuals at a high risk of HCC.

Key words: Hepatocellular carcinoma; p53 gene; Arg72Pro

Zhu ZZ, Cong WM, Liu SF, Dong H, Zhu GS, Wu MC. Homozygosity for Pro of p53 Arg72Pro as a potential risk factor for hepatocellular carcinoma in Chinese population. *World J Gastroenterol* 2005; 11(2): 289-292
http://www.wjgnet.com/1007-9327/11/289.asp

INTRODUCTION

Hepatocellular carcinoma (HCC) is one of the most common malignant neoplasms worldwide with most cases exhibited in southeast Asia and tropical Africa[1]. In mainland China, the mortality rate of HCC is 337 for men and 123 for women per million people and both rank top in the world[2]. Furthermore, the age-adjusted death rate of HCC is still increasing in both rural and urban areas of mainland China[3].

Etiologically, HCC is a complex and multifactorial disease that is linked to both viral and chemical carcinogens. Major etiologic factors include infection with HBV and HCV, cigarette smoking, alcohol drinking and AFB_1 exposure[4-9]. However, not all individuals with exposure to risk factors develop cancer even after a long-term follow-up indicating that susceptibility to HCC is mediated by genetically determined differences. Germline polymorphisms of several genes, most of which encode for xenobiotic metabolizing enzymes (cytochrome P450, glutathione *S*-transferase, *N*-acetyltransferase 2, microsomal epoxide hydrolase, and uridine 5'-diphosphate-glucuronosyltransferases)[10-14], have been studied as potential risk factors for HCC. However, the pathogenesis of human HCC is a multistage process with the involvement of a series of genes, including oncogenes and tumor suppressor genes. Germline polymorphisms of these genes may also determine individual susceptibility to HCC.

The p53 tumor suppressor gene is of critical importance for the regulation of cell cycle and maintenance of genomic integrity. Loss of p53 function has been suggested to be a critical step in multistage hepatocarcinogenesis[15]. The wild-type p53 gene exhibits a polymorphism at codon 72 in exon 4, with a single nucleotide change that causes a substitution of proline for arginine (Arg72Pro)[16]. The Arg72Pro polymorphism is located in a proline-rich region (residues 64-92) of the p53 protein, where the 72Pro amino acid constitutes one of five PXXP motifs resembling a SH3 binding domain. The region is required for the growth suppression and apoptosis mediated by p53 but not for cell cycle arrest. The two polymorphic variants of wild-type p53 have been shown to have some different biochemical and biological properties[17]. Since Storey *et al* (1998) established an association of p53 Arg72Pro with cervical cancer, the p53 polymorphism has been studied as a risk factor in various cancers with inconsistent results[18-29].

To investigate the possible association between p53 Arg72Pro polymorphism and susceptibility to HCC, we conducted a hospital-based case-control study in a large-size sample of Chinese population.

MATERIALS AND METHODS

Patients

Five hundred and seven cases of HCC and 541 controls were

recruited from the Eastern Hepatobiliary Surgery Hospital, Shanghai, China, during the period from February 1999 to May 2003. Controls were subjects with intrahepatic stones ($n = 207$), cavernous hemangioma ($n = 238$), and other benign liver diseases ($n = 96$). Informed consent was obtained from all study subjects. All individuals received surgeries on liver and liver tissues were available, including formalin-fixed and paraffin-embedded archival samples (193 HCC and 291 controls) and formalin-fixed samples (314 HCC and 250 controls), for DNA isolation. For each formalin-fixed and paraffin-embedded archival sample, five 7-μm-thick sections were obtained for microdissection-based extraction of genomic DNA. Two flanking sections, 4 μm, hematoxylin and eosin-stained, were prepared to ensure the composition of histological components. One pathologist (Dr. WM Cong) assessed all patients and assigned non-tumor and tumor areas on 4-μm slides (non-tumor areas were used in analyses). For each formalin-fixed sample, non-tumor liver tissues were obtained within one week after operation, and stored at -80 ℃ until examination. All pathological diagnoses were reviewed by the same pathologist. Genomic DNA was isolated from the liver tissues using standard phenol-chloroform methods.

Information on age, sex, cigarette smoking, alcohol drinking, HBsAg status, anti-HCV status and family history of HCC in first-degree relatives was obtained from the hospital registration.

Genotyping of p53 Arg72Pro polymorphism

The genotypes of p53 Arg72Pro were determined using PCR-based restriction fragment length polymorphism (RFLP) method. The PCR primers used for amplifying the polymorphism region were: forward, 5'-TTGCCGTCCCAAGCAATGGATGA-3'; reverse, 5'-TCTGGGAAGGGACAGAAGATGAC-3'. PCR condition was 2 min at 94 ℃, followed by 35 cycles of 30 s at 94 ℃, 30 s at 60 ℃, and 30 s at 72 ℃, and with a final extension at 72 ℃ for 7 min. A 10-μL aliquot of PCR product was digested overnight at 60 ℃ in a 15-μL reaction volume containing 10 units of *BstU I* (New England BioLabs). After overnight digestion, the fragments were separated by electrophoresis on a vertical 90 g/L non-denaturing polyacrylamide gel at 120 V for 45 min, stained with ethidium bromide. Homozygotes for Pro were represented by a DNA band with the size of 199 bp, whereas Arg homozygotes were represented by DNA bands with sizes of 113 bp and 86 bp. Heterozygotes displayed a combination of both alleles (199, 113, and 86 bp) (Figure 1). Negative and positive controls were assessed during analysis to ensure that PCR products were not contaminated and that the enzyme digestion worked correctly. In addition, laboratory personnel were kept blind as to group status, and the extent of random misclassification was controlled through randomly genotyping 100 samples twice.

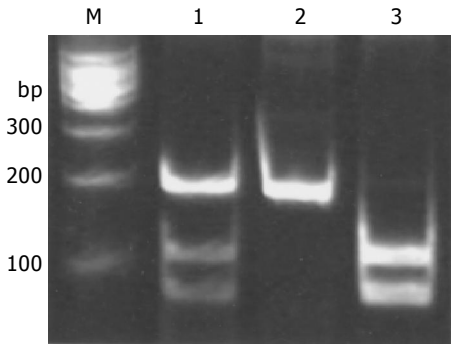

Figure 1 Non-denaturing polyacrylamide gel electrophoresis of p53 Arg72Pro region PCR products digested with *BstU I*. M: 100-bp DNA ladder, 1: Arg/Pro heterozygote, 2: Pro homozygote, 3: Arg homozygote.

Statistical analysis

Odds ratios (ORs) for HCC and 95% confidence intervals (CIs) from unconditional logistic regression models were used to evaluate relative risks. *t*-test was used to evaluate the age difference between groups. In the multivariate analyses on genotype and HCC, potential risk factors including sex, age, cigarette smoking, alcohol drinking, HBsAg status, anti-HCV status and family history of HCC in first-degree relatives were included in the logistic regression models as covariates. All the above analyses were performed using SPSS 10.0 software (SPSS, Chicago, IL). Hardy-Weinberg equilibrium (HWE) tests and allele-specific OR were performed using website-based software at http://ihg.gsf.de/ihg/snps.html.

RESULTS

There were a total of 507 HCC cases and 541 controls in this study. The distribution of the p53 Arg72Pro genotypes in HCC cases and controls, and the genotype- and allele-specific ORs for HCC are shown in Table 1. Male, cigarette smoking, HBsAg-

Table 1 Frequency distributions and odds ratios of multiple risk factors in 507 HCC cases and 541 controls

Risk factor	Variable	HCC case	Control	Crude	Adjusted	*P*
		n (%)	*n* (%)	OR (95% CI)	OR (95% CI)[1]	
p53 Arg72Pro	Arg	563 (55.5)	646 (59.7)	1.0		
	Pro	451 (44.5)	436 (40.3)	1.19 (1.00-1.41)		0.05
	Arg/Arg	145 (28.6)	188 (34.8)	1.0	1.0	
	Arg/Pro	273 (53.8)	270 (49.9)	1.31 (1.00-1.73)	1.21 (0.82-1.78)	0.34
	Pro/Pro	89 (17.6)	83 (15.3)	1.39 (0.96-2.01)	1.79 (1.06-3.01)	0.03
Sex	Female	73 (14.4)	278 (51.4)	1.0	1.0	
	Male	434 (85.6)	263 (48.6)	6.28 (4.66-8.48)	4.97 (3.28-7.52)	<0.001
Cigarette smoking	No	288 (56.8)	437 (80.8)	1.0	1.0	
	Yes	219 (43.2)	104 (19.2)	3.20 (2.42-4.21)	1.90 (1.19-3.02)	<0.01
Alcohol drinking	No	304 (60.0)	446 (82.4)	1.0	1.0	
	Yes	203 (40.0)	95 (17.6)	3.13 (2.36-4.16)	1.20 (0.75-1.93)	0.44
HBsAg	Negative	137 (27.0)	445 (82.3)	1.0	1.0	
	Positive	370 (73.0)	96 (17.7)	12.52 (9.32-16.82)	16.83 (11.53-24.56)	<0.001
Anti-HCV	Negative	469 (92.5)	527 (97.4)	1.0	1.0	
	Positive	38 (7.5)	14 (2.6)	3.05 (1.63-5.69)	7.29 (3.17-16.80)	<0.001
Family history[2]	No	433 (85.4)	532 (98.3)	1.0	1.0	
	Yes	74 (14.6)	9 (1.7)	10.07 (5.00-20.33)	9.47 (3.92-22.90)	<0.001

[1]All the variables in the table and age were included in the logistic regression model; [2]Family history of HCC in first-degree relatives.

positive, anti-HCV-positive and family history of HCC in first-degree relatives were also significant risk factors for developing HCC. No significant association with HCC was found for alcohol drinking. The age (mean±SD) of HCC cases and controls were 50.3±11.6 and 44.7±10.8 years respectively (P<0.001). We have randomly genotyped 100 samples twice and got concordant results.

The frequencies of the three genotypes were as follows: Arg/Arg 34.8%, Arg/Pro 49.9% and Pro/Pro 15.3% in controls and Arg/Arg 28.6%, Arg/Pro 53.8% and Pro/Pro 17.6% in HCC cases respectively. Based on these data, the frequencies for Pro and Arg alleles were 44.5%, 55.5% in HCC cases, and 40.3% and 59.7% in controls, respectively. The Pro allele was significantly associated with the presence of HCC (P = 0.05) and had a higher risk for HCC (OR = 1.19, 95% CI 1.00-1.41) as compared to the Arg allele. Genotype distributions were in HWE for controls, but not for HCC cases (P = 0.04) with marginally statistical significance. The genotype frequencies in our control group were similar to those reported by other authors in Chinese population[22,30].

No overall association between p53 Arg72Pro genotypes and HCC was observed. However, particular genotypic frequencies were different in HCC cases and controls. After adjusted for potential risk factors, Arg/Pro heterozygotes had an 1.21-fold increased risk of HCC compared to Arg homozygotes, whereas the risk for Pro homozygotes was 1.79 (95% CI 1.06-3.01, P= 0.03) times higher than that for Arg homozygotes. Pro-allele carriers had a higher relative risk of HCC compared to Arg-only carriers, although the difference was not statistically significant.

It is also important to elucidate the frequency of loss of heterozygosity (LOH) in HCC using tissues out of the liver as referencing materials since the surrounding non-cancerous liver tissues used as referencing materials might have already accumulated genetic alterations. Thus, we also examined genotypes of p53 Arg72Pro in blood DNA of a part of our HCC patients homozygous for the Arg or the Pro allele (33 and 21 cases, respectively). No LOH was detected in this locus.

DISCUSSION

The p53 gene is one of the most extensively studied human genes because of its role as a tumor suppressor gene. Its diverse functions include DNA binding, cell cycle control, DNA repair, differentiation, genomic plasticity, and apoptosis[31]. Thus, the overall function of p53 is to maintain genomic integrity as a whole, providing a protective effect against tumorigenesis. Wild type p53 is polymorphic at codon 72 in human populations and it has been reported that homozygosity for Pro of p53 Arg72Pro is potentially a risk factor for cancers of the lung, esophagus, stomach, breast, nasopharynx, urothelium, and prostate[23-29]. In this study, we used PCR-based RFLP method to analyze the p53 Arg72Pro polymorphism in HCC among the Chinese population.

We found that the Pro allele was significantly associated with the presence of HCC and that carriers of the Pro, or the "risk allele", had an 1.33-fold increased risk of HCC compared to Arg-only carriers, without statistical significance. Arg/Pro heterozygotes of the p53 polymorphism had an 1.21-fold increased risk of HCC compared to Arg homozygotes. Pro homozygotes had an 1.79-fold increased risk of HCC with statistical significance. This large epidemiological study suggests that homozygosity for Pro of p53 Arg72Pro is potentially one of the genetic risk factors for HCC in Chinese population. The p53 Arg72Pro polymorphism may be used as a stratification marker in screening individuals at a high risk of HCC.

There have been two case-control studies conducted to examine the association between p53 Arg72Pro and HCC[32,33]. A significant association between Pro allele and HCC in HBsAg-positive males with chronic liver diseases or family history of HCC was reported in a Taiwanese case-control study conducted by Yu *et al*[32]. However, no overall increased frequency of the Pro allele was observed in HCC cases in that study. One possible explanation is that the effect of Pro allele of p53 Arg72Pro polymorphism might be masked by the stronger tumorigenic effect of chronic HBV infection. A recent case-control study performed in Spain by Anzola *et al*[33] failed to observe any association between p53 Arg72Pro and HCC. The inconsistency in the association could be attributable to ethnic difference, since the study by Anzola *et al* was performed in a Caucasian population, while the study by Yu *et al*, as well as the current study, were performed in an Asian population.

The hypothesized relationship of the p53 polymorphism to cancer susceptibility has been unclear. It was reported that these two polymorphic variants of wild type p53 differ in E6-mediated degradation, transcription activation and induction of apoptosis[17]. Recent studies indicated that the Arg allele is preferentially mutated and retained in various human cancers arising in Pro/Arg heterozygotes, and that the p53 mutant is a more potent inhibitor of p73 when p53 has Arg in codon 72 rather than Pro[33-36]. These findings suggest that this polymorphism acts as an intragenic modifier of mutant p53 behavior and has an effect on the biological activity of p53. However, results of other studies show that the polymorphism does not influence protein-protein interaction (p53mut-p53WT or p53mut-p73βWT)[37,38]. Thus, the implications of the p53 polymorphism in cancer development require further study. We must also consider the possibility that the p53 Arg72Pro is simply in a state of linkage disequilibrium (LD) with an as-yet-unidentified functional locus. The highest cancer risk figures have been reported in intronic polymorphisms (MspI RFLPs in intron 6 and a 16-bp duplication in intron 3) in p53 gene suggesting that the mechanism underlying these associations might be a locus which is in LD with p53 Arg72Pro polymorphism rather than direct functional involvement of the Arg/Pro substitution itself[20,21].

The p53 Arg72Pro polymorphism displays a similar association pattern in HCC compared with previously examined esophageal and lung cancer patients from the Chinese population, in which the risk of Pro homozygotes for cancer was about 2 times against Arg homozygotes[22,24,39]. Taken together, there might be, at least in Chinese population, a common genetic basis for the pathogenesis of these different cancers.

In summary, homozygosity for Pro of p53 Arg72Pro is potentially one of the genetic risk factors for HCC in Chinese population. The p53 Arg72Pro polymorphism may be used as a stratification marker in screening individuals at a high risk of HCC.

REFERENCES

1 **Bosch FX,** Ribes J, Borras J. Epidemiology of primary liver cancer. *Semin Liver Dis* 1999; **19**: 271-285
2 **Zhang S,** Li L, Lu F. Mortality of primary liver cancer in China from 1990 through 1992. *Zhonghua Zhongliu Zazhi* 1999; **21**: 245-249
3 **Li L,** Lu F, Zhang S. Analyses of variation trend and short-term detection of Chinese malignant tumor mortality during twenty years. *Zhonghua Zhongliu Zazhi* 1997; **19**: 3-9
4 **Tang ZY.** Hepatocellular carcinoma-cause, treatment and metastasis. *World J Gastroenterol* 2001; **7**: 445-454
5 **Zhu ZZ,** Cong WM. Roles of hepatitis B virus and hepatitis C virus in hepato-carcinogenesis. *Zhonghua Ganzangbing Zazhi* 2003; **11**: 574-576
6 **Kuper H,** Tzonou A, Kaklamani E, Hsieh CC, Lagiou P, Adami HO, Trichopoulos D, Stuver SO. Tobacco smoking, alcohol consumption and their interaction in the causation of hepato-

cellular carcinoma. *Int J Cancer* 2000; **85**: 498-502
7 **Chen CJ,** Wang LY, Lu SN, Wu MH, You SL, Zhang YJ, Wang LW, Santella RM. Elevated aflatoxin exposure and increased risk of hepatocellular carcinoma. *Hepatology* 1996; **24**: 38-42
8 **Ross RK,** Yuan JM, Yu MC, Wogan GN, Qian GS, Tu JT, Groopman JD, Gao YT, Henderson BE. Urinary aflatoxin biomarkers and risk of hepatocellular carcinoma. *Lancet* 1992; **339**: 943-946
9 **Qian GS,** Ross RK, Yu MC, Yuan JM, Gao YT, Henderson BE, Wogan GN, Groopman JD. A follow-up study of urinary markers of aflatoxin exposure and liver cancer risk in Shanghai, People's Republic of China. *Cancer Epidemiol Biomarkers Prev* 1994; **3**: 3-10
10 **Silvestri L,** Sonzogni L, De Silvestri A, Gritti C, Foti L, Zavaglia C, Leveri M, Cividini A, Mondelli MU, Civardi E, Silini EM. CYP enzyme polymorphisms and susceptibility to HCV-related chronic liver disease and liver cancer. *Int J Cancer* 2003; **104**: 310-317
11 **Sun CA,** Wang LY, Chen CJ, Lu SN, You SL, Wang LW, Wang Q, Wu DM, Santella RM. Genetic polymorphisms of glutathione *S*-transferases M1 and T1 associated with susceptibility to aflatoxin-related hepatocarcinogenesis among chronic hepatitis B carriers: a nested case-control study in Taiwan. *Carcinogenesis* 2001; **22**: 1289-1294
12 **Huang YS,** Chern HD, Wu JC, Chao Y, Huang YH, Chang FY, Lee SD. Polymorphism of the *N*-acetyltransferase 2 gene, red meat intake, and the susceptibility of hepatocellular carcinoma. *Am J Gastroenterol* 2003; **98**: 1417-1422
13 **Sonzogni L,** Silvestri L, De Silvestri A, Gritti C, Foti L, Zavaglia C, Bottelli R, Mondelli MU, Civardi E, Silini EM. Polymorphisms of microsomal epoxide hydrolase gene and severity of HCV-related liver disease. *Hepatology* 2002; **36**: 195-201
14 **Vogel A,** Kneip S, Barut A, Ehmer U, Tukey RH, Manns MP, Strassburg CP. Genetic link of hepatocellular carcinoma with polymorphisms of the UDP-glucuronosyltransferase UGT1A7 gene. *Gastroenterology* 2001; **121**: 1136-1144
15 **Staib F,** Hussain SP, Hofseth LJ, Wang XW, Harris CC. TP53 and liver carcinogenesis. *Hum Mutat* 2003; **21**: 201-216
16 **Buchman VL,** Chumakov PM, Ninkina NN, Samarina OP, Georgiev GP. A variation in the structure of the protein-coding region of the human p53 gene. *Gene* 1988; **70**: 245-252
17 **Thomas M,** Kalita A, Labrecque S, Pim D, Banks L, Matlashewski G. Two polymorphic variants of wild-type p53 differ biochemically and biologically. *Mol Cell Biol* 1999; **19**: 1092-1100
18 **Storey A,** Thomas M, Kalita A, Harwood C, Gardiol D, Mantovani F, Breuer J, Leigh IM, Matlashewski G, Banks L. Role of a p53 polymorphism in the development of human papillomavirus-associated cancer. *Nature* 1998; **393**: 229-234
19 **Minaguchi T,** Kanamori Y, Matsushima M, Yoshikawa H, Taketani Y, Nakamura Y. No evidence of correlation between polymorphism at codon 72 of p53 and risk of cervical cancer in Japanese patients with human papillomavirus 16/18 infection. *Cancer Res* 1998; **58**: 4585-4586
20 **Birgander R,** Sjalander A, Rannug A, Alexandrie AK, Sundberg MI, Seidegard J, Tornling G, Beckman G, Beckman L. P53 polymorphisms and haplotypes in lung cancer. *Carcinogenesis* 1995; **16**: 2233-2236
21 **Birgander R,** Sjalander A, Zhou Z, Fan C, Beckman L, Beckman G. p53 polymorphisms and haplotypes in nasopharyngeal cancer. *Hum Hered* 1996; **46**: 49-54
22 **Zhang JH,** Li Y, Wang R, Wen DG, Wu ML, He M. p53 gene polymorphism with susceptibility to esophageal cancer and lung cancer in Chinese population. *Zhonghua Zhongliu Zazhi* 2003; **25**: 365-367
23 **Irarrazabal CE,** Rojas C, Aracena R, Marquez C, Gil L. Chilean pilot study on the risk of lung cancer associated with codon 72 polymorphism in the gene of protein p53. *Toxicol Lett* 2003; **144**: 69-76
24 **Lee JM,** Lee YC, Yang SY, Shi WL, Lee CJ, Luh SP, Chen CJ, Hsieh CY, Wu MT. Genetic polymorphisms of p53 and GSTP1, but not NAT2, are associated with susceptibility to squamous-cell carcinoma of the esophagus. *Int J Cancer* 2000; **89**: 458-464
25 **Hiyama T,** Tanaka S, Kitadai Y, Ito M, Sumii M, Yoshihara M, Shimamoto F, Haruma K, Chayama K. p53 Codon 72 polymorphism in gastric cancer susceptibility in patients with *Helicobacter pylori*-associated chronic gastritis. *Int J Cancer* 2002; **100**: 304-308
26 **Sjalander A,** Birgander R, Hallmans G, Cajander S, Lenner P, Athlin L, Beckman G, Beckman L. p53 polymorphisms and haplotypes in breast cancer. *Carcinogenesis* 1996; **17**: 1313-1316
27 **Tsai MH,** Lin CD, Hsieh YY, Chang FC, Tsai FJ, Chen WC, Tsai CH. Prognostic significance of the proline form of p53 codon 72 polymorphism in nasopharyngeal carcinoma. *Laryngoscope* 2002; **112**: 116-119
28 **Kuroda Y,** Tsukino H, Nakao H, Imai H, Katoh T. p53 Codon 72 polymorphism and urothelial cancer risk. *Cancer Lett* 2003; **189**: 77-83
29 **Suzuki K,** Matsui H, Ohtake N, Nakata S, Takei T, Nakazato H, Okugi H, Koike H, Ono Y, Ito K, Kurokawa K, Yamanaka H. A p53 codon 72 polymorphism associated with prostate cancer development and progression in Japanese. *J Biomed Sci* 2003; **10**: 430-435
30 **Beckman G,** Birgander R, Sjalander A, Saha N, Holmberg PA, Kivela A, Beckman L. Is p53 polymorphism maintained by natural selection? *Hum Hered* 1994; **44**: 266-270
31 **Hofseth LJ,** Hussain SP, Harris CC. p53: 25 years after its discovery. *Trends Pharmacol Sci* 2004; **25**: 177-181
32 **Yu MW,** Yang SY, Chiu YH, Chiang YC, Liaw YF, Chen CJ. A p53 genetic polymorphism as a modulator of hepatocellular carcinoma risk in relation to chronic liver disease, familial tendency, and cigarette smoking in hepatitis B carriers. *Hepatology* 1999; **29**: 697-702
33 **Anzola M,** Cuevas N, Lopez-Martinez M, Saiz A, Burgos JJ, de Pancorbo MM. Frequent loss of p53 codon 72 Pro variant in hepatitis C virus-positive carriers with hepatocellular carcinoma. *Cancer Lett* 2003; **193**: 199-205
34 **Marin MC,** Jost CA, Brooks LA, Irwin MS, O'Nions J, Tidy JA, James N, McGregor JM, Harwood CA, Yulug IG, Vousden KH, Allday MJ, Gusterson B, Ikawa S, Hinds PW, Crook T, Kaelin WG. A common polymorphism acts as an intragenic modifier of mutant p53 behaviour. *Nat Genet* 2000; **25**: 47-54
35 **Tada M,** Furuuchi K, Kaneda M, Matsumoto J, Takahashi M, Hirai A, Mitsumoto Y, Iggo RD, Moriuchi T. Inactivate the remaining p53 allele or the alternate p73 ? Preferential selection of the Arg72 polymorphism in cancers with recessive p53 mutants but not transdominant mutants. *Carcinogenesis* 2001; **22**: 515-517
36 **Papadakis ED,** Soulitzis N, Spandidos DA. Association of p53 codon 72 polymorphism with advanced lung cancer: the Arg allele is preferentially retained in tumours arising in Arg/Pro germline heterozygotes. *Br J Cancer* 2002; **87**: 1013-1018
37 **Monti P,** Campomenosi P, Ciribilli Y, Iannone R, Aprile A, Inga A, Tada M, Menichini P, Abbondandolo A, Fronza G. Characterization of the p53 mutants ability to inhibit p73 beta transactivation using a yeast-based functional assay. *Oncogene* 2003; **22**: 5252-5260
38 **Gaiddon C,** Lokshin M, Ahn J, Zhang T, Prives C. A subset of tumor-derived mutant forms of p53 down-regulate p63 and p73 through a direct interaction with the p53 core domain. *Mol Cell Biol* 2001; **21**: 1874-1887
39 **Zhang L,** Xing D, He Z, Lin D. p53 gene codon 72 polymorphism and susceptibility to esophageal squamous cell carcinoma in a Chinese population. *Zhonghua Yixue Yichuanxue Zazhi* 2002; **19**: 10-13

Assistant Editor Guo SY **Edited by** Zhang JZ and Ma JY

PO Box 2345, Beijing 100023, China
Fax: +86-10-85381893
E-mail: wjg@wjgnet.com www.wjgnet.com

ELSEVIER

World J Gastroenterol 2005;11(2):293-295
World Journal of Gastroenterology ISSN 1007-9327

• BRIEF REPORTS •

Mechanism of benign biliary stricture: A morphological and immunohistochemical study

Zhi-Min Geng, Ying-Min Yao, Qing-Guang Liu, Xin-Jie Niu, Xiao-Gong Liu

Zhi-Min Geng, Ying-Min Yao, Qing-Guang Liu, Xin-Jie Niu, Xiao-Gong Liu, Department of Hepatobiliary Surgery, First Hospital of Xi'an Jiaotong University, Xi'an 710061, Shaanxi Province, China
Correspondence to: Dr. Zhi-Min Geng, Department of Hepatobiliary Surgery, First Hospital of Xi'an Jiaotong University, Xi'an 710061, Shaanxi Province, China. zhimin@pub.xaonline.com
Telephone: +86-29-85324009 **Fax:** +86-29-85324009
Received: 2003-03-02 **Accepted:** 2003-04-03

Abstract

AIM: To explore the mechanism of benign biliary stricture.

METHODS: A model of trauma of bile duct was established in 28 dogs. The anastomosed tissues were resected and examined by light and electron microscopes on day 3, in wk 1, 3 and mo 3, 6 after operation. CD68, TGF-β1 and α-SMA were examined by immunohistochemical staining, respectively.

RESULTS: The mucosal epithelium of the bile duct was slowly recovered, chronic inflammation lasted for a long time, fibroblasts proliferated actively, extracellular matrix was over-deposited. Myofibroblasts functioned actively and lasted through the whole process. The expression of macrophages in lamina propria under mucosa, TGF-β1 in granulation tissue, fibroblasts and endothelial cells of blood vessels, α-SMA in myofiroblasts were rather strong from the 1st wk to the 6th mo after operation.

CONCLUSION: The type of healing occurring in bile duct belongs to overhealing. Myofibroblasts are the main cause for scar contracture and stricture of bile duct. High expressions of CD68, TGF-β1 and α-SMA are closely related to the active proliferation of fibroblasts, extracellular matrix over-deposition and scar contracture of bile duct.

Key words: Benign biliary stricture; Immunohistochemistry

Geng ZM, Yao YM, Liu QG, Niu XJ, Liu XG. Mechanism of benign biliary stricture: A morphological and immunohistochemical study. *World J Gastroenterol* 2005; 11(2): 293-295
http://www.wjgnet.com/1007-9327/11/293.asp

INTRODUCTION

It is difficult to cope with benign biliary stricture in biliary surgery. Its postoperative manifestations are scar contracture and stenosis of bile duct, especially in hepatic porta or above[1,2]. We established an animal model of trauma-repair in bile duct in this experiment in order to explore the formation mechanism of benign biliary stricture. Changes of histology and ultrastructure during the process of trauma and repair in the bile duct were observed during tissue healing. Expression intensity, positive cells counts and distribution of macrophage, TGF-β1 and α-SMA were dynamically examined by immunohistochemical staining in different stages of healing.

MATERIALS AND METHODS

Animal model

Twenty-eight hybrid dogs with an average weight of 15.3 kg were anesthetized with an intraperitoneal injection of 2.5% sodium thiopental (1 mL/kg). An incision across rectus of the right upper abdomen was made and common bile duct (CBD) was separated at the point of 2 cm away from the superior margin of duodenum (the range of separation was within 1 cm). Then an incision of the anterior wall of CBD was made transversally with the length of about one third of its circumference between the vertical axes of both sides. Then the incision of CBD was anastomosed by microsurgical technology with non-invasive Dexon sutures, with the pinhole distance of 0.5-0.6 mm, and edge distance of 0.3-0.4 mm. After making sure that there was no bile leakage at the anastomotic stoma, an abdominal drainage-tube was placed at the site. Then the abdomen was closed. Postoperative anti-infection treatment was administered for 3 d, and the drainage-tube was then removed.

General condition of animals

General condition and behavior of the animals were observed, including diet, activities, reaction, drainage and postoperative complications.

Histological observation

Pathological examinations as follows were applied to specimens that were obtained on the 3rd d, in the 1st and 3rd wk, and the 3rd, 6th mo after operation, and 5 dogs were randomly selected each time.

Anastomotic stoma and tissues about 2 cm around the stoma were removed and fixed in 10% formaldehyde solution. Specimens were observed by a microscope with HE stain, Masson stain and Verhoeff stain respectively. Percentage of collagen area was calculated with VIDAS image analysis system to observe changes of collagen content. A piece of tissue around the stoma where the scar was obvious was selected and trimmed into a small piece of 1 mm^3 at low temperature, followed by immediate fixation in 2.5% glutaraldehyde solution. It was observed with TEM (HITCH-600) and photographed. The piece of tissue was plated with gold by using an ion coater of EIKO-IB-3 type and observed with a scanning electron microscope (KYKY-2000) and photographed. To measure the content change of extracellular collagen, each photograph of TEM was analyzed with VIDAS image analysis system, and the change of relative extracellular volume density (ECVD) was calculated based on three-dimensional analysis principles.

Immunohistochemical observation

Rat anti-human macrophage (CD68) monoclonal antibody and rat anti-human smooth muscle actin (actin 1A4) monoclonal antibodies were purchased from Zhongshan Biotechnology Incorporation. Rabbit anti-human TGF-β1 polyclonal antibody

was purchased from Santa Cruz Biotechnology Incorporation. Second antibodies, goat anti-rat IgG marked biotin and goat anti-rabbit IgG marked biotin were the product of ZYMED Incorporation. SP test kit was the product of ZYMED Incorporation.

The expressions of CD68, TGF-β1 and α-SMA were detected by immunohistochemical SP method with positive and negative controls. The quantity of positive cells in unit area of the section in each group was analyzed by VIDAS image analysis system and positive cells were stained as brownish yellow granules in cytoplasm.

Statistical analysis

All data were expressed as mean±SD. Analysis of variance was used to analyze the difference, and analysis linear correlation was used to analyze the expression of CD68, TGF-β1 and α-SMA.

RESULTS

General condition of animals after operation

One dog died of bile fistula 12 d after operation, 2 dogs died of obstructive jaundice 4 and 5 mo after operation and 25 dogs survived. Appetite, activity and reaction of the dogs in the early stage were normal, but in the later stage, 4 of 8 dogs developed obstructive jaundice with declined appetite, weight loss, dark urine and Kaolin stool 3 mo after operation. An average of 30-40 mL blood-bile mixture was drained from abdominal cavity.

Histological changes

Mucosa in anastomotic stoma of the bile duct became necrotic, and was exfoliated 3 d after operation and had acute inflammatory reactions. Surface exudation from stoma deceased one week after operation, and proliferation of granulation tissue could be observed under mucosa. Wall of the bile duct became thicker. Collagenous fibers were disorderly arranged, elastic fibers under mucosa ruptured into segments, and irregularly arranged capillary-like collagens could be found with Masson stain and Verhoeff stain. Mucosa of the stoma had chronic inflammatory reactions 3 wk after operation and mucosa partly recovered. Wall of the stoma that was proliferative with cicatricial tissue obviously thickened, the part of fiberous tissue had hyaline degeneration and capillaries were proliferated, dilated, and engorged. In Masson and Verhoeff stains neocollagenous fibers were massively proliferated and arranged densely in nodule or annual ring. Neocollagenous nodes that were circled with microvessels contained high-dense fibroblasts, and radiated neocollagenous fibers were arranged densely. Region of neocollagenous nodes was short of elastic fibers. During the 3rd-6th mo after operation mucosa of the stoma was infiltrated with chronic inflammatory cells and had a small quantity of mucous gland in lamina propria. Though the mucosa was almost completely repaired, it was arranged in disorder and became thinner. Proliferated blood capillaries here were degenerated more than before. Wall of the stoma was thinner, collagenous fibers were arranged more disorderly and densely than before. Specimens of the liver demonstrated hepatic congestion and bile stasis.

Ultrastructural changes

TEM One week after operation, the proliferation of fibroblasts could be observed in the scar tissue at stoma. The cells were active and in synthesis condition. Many collagenous fibers outside the cells could be observed, with a diameter of 40-80 nm. They were thinner than normal cells, and arranged densely in bundle, and scattered around without directivity. Meanwhile, a certain amount of larger, flat and spindle-shaped myofibroblasts could be observed. Well-developed microfilaments and dense body that paralleled to the long axis existed near the cytomembrane, besides the rich roughly surfaced endoplasmic reticulum and developed Golgi body. In addition, infiltration of inflammatory cells and transudatory erythrocytes could be observed in scar tissue. Three week after operation, the functions of fibroblasts and myofibroblasts in the scar tissue were more active. The percentage of myofibroblasts was increased. Microfilament and dense body could be observed more easily. Roughly surfaced endoplasmic reticulum was expanded, and the number of neutrophilic granulocytes and erythrocytes was reduced. Macrophagocytes and lymphocytes became the main inflammatory cells at this stage. Extracellular collagenous fibers were oversedimentated in whirlpool or annual ring shape and arranged densely in a scattering manner. Three months after operation, the cells in scar tissue still kept active, and the number of myofibroblasts reached the highest. The extracellular collagenous fibers were still arranged without directivity, part of which melted into irregular lumps. Six mo after operation, fibrocytes appeared though they were still comparatively quiet in function. The number of myofibroblasts was decreased. Collagenous fibers began to show certain directivity and were arranged in a wave-shape manner.

SEM One week after operation, necrosis and exfoliation of mucosa epithelia in the stoma and non-repair could be observed. Three weeks after operation, mucosa was partly repaired, but thinner than normal one and its villus was low and plat. Three mo after operation, repair of the mucosa was nearly complete, but mucosa epithelia were arranged disorderly, papilla was low and flat and interspace was increased.

Percentages of collagenous fiber area and ECVD

The percentages of collagenous fiber area and ECVD of the stoma in different stages after operation are shown in Table 1.

Table 1 Percentages of collagenous fiber area and EVCD in different groups after operation (%) (n = 5, mean±SD)

Group	Percentage of collagenous fiber area	EVCD
1st wk	54.38±3.86	58.23±4.56
3rd wk	69.26±5.24	70.67±3.32
3rd mo	78.06±4.13	81.42±3.74
6th mo	72.48±4.52	75.48±4.36

Significant difference between all groups (P<0.05).

Immunohistochemical observation

CD68 was expressed in mucosa lamina propria of the bile duct but weak in submucosa. In normal control the expression of CD68 was negative. TGF-β1 was expressed in granulation tissue, fibroblasts, macrophages, cytoplasm and cytomembrane of endothelial cells of blood vessel. The expression of TGF-β1 was weak in fibrous tissue of normal bile duct wall. α-SMA was expressed in cytoplasm of myofibroblasts and smooth muscle tissue. In normal wall of bile duct, α-SMA was just expressed in a small amount of smooth muscle tissue (Table 2).

Table 2 Expression of CD68, TGF-β1, α-SMA in healing of bile duct (n = 5, mean±SD)

Group	CD68	Positive cells (%)	TGF-β1	Positive cells (%)	α-SMA	Positive cells (%)
Normal	-	3.7±0.6	-~+	12.3±3.5	+	14.4±5.3
1st wk	++~+++	65.3±5.3[a]	+++	68.3±5.2[a]	++~+++	54.6±6.4[a]
3rd wk	++	42.2±4.2[ab]	+++	65.3±4.2[a]	+++	63.1±5.7[a]
3rd mo	++	45.1±6.2[ab]	++~+++	59.4±5.0[a]	+++	68.9±4.2[a]
6th mo	++	39.3±4.4[ab]	++	55.1±6.4[a]	++	51.4±5.7[a]

[a]P<0.05, *vs* 1st wk. [b]P<0.01, *vs* Normal.

DISCUSSION

Formation of cicatrix is the inevitable result of wound healing which is inevitably accompanied with formation of cicatrix in different degrees. Over-deposition of collagens in lesion region could lead to over-proliferation of cicatrix[3-6]. The main manifestations of benign biliary stricture after operation are scar contracture and stenosis of bile duct, but the mechanism underlying stricture formation remains unclear. We found that epithelial cells of the bile duct recovered poorly, chronic inflammation existed continuously, fibroblasts proliferated actively, collagens were over-deposited in submucosa, and reconstruction was poor after the healing. All these result in proliferation of cicatrix and high incidence rate of stenosis of anastomotic stoma.

In recent years, it has gradually become clear that myofibroblasts are closely related to scar contracture[7,8]. Myofibroblasts are atypical fibroblasts, which have the characteristics of both fibroblasts and smooth muscle cells in ultrastructure. In this experiment, a large number of myofibroblasts were observed in the scar tissue. One week after operation, myofibroblasts appeared and three week after operation, they reached the peak and maintained it for a longer period. Cyclogeny of the cells and hyperplastic contraction of granulation tissue were almost consistent, suggesting that myofibroblasts are significant in the healing process and are the important cause of cicatrical contracture in bile duct and biliary stenosis after operation. As a marker of differentiation, α-SMA could differentiate myofibroblasts from fibroblasts[9,10]. Our study has confirmed that myofibroblasts were the important cause of benign biliary stenosis.

The foundation of wound healing is a series of interactions between inflammatory cells and repairing cells. As one kind of major inflammatory cells and immunologic cells, macrophages have been regarded as the "instructor" of tissue repair, which not only takes part in tissue inflammatory and immunologic reactions, but also influences tissue angiogenesis and fibrosis by releasing a variety of media in a direct or indirect, sole or synergic manner[11,12]. TGF-β is the most reprehensible growth factor closely related to the formation of scar and is a kind of strong mitogens that play an important role in cell division, multiplication and migration. This is why TGF-β1 induces formation of granulation tissue. If this function became too strong, TGF-β1 would cause formation of scar[13-16].

Our study not only confirmed autocrine of TGF-β1 but also demonstrated high expression of CD68 and TGF-β1 which is closely related to proliferation of biliary cicatrix. As an important substance of signal conduction, macrophages and TGF-β1 solely or synergically, directly or indirectly play an important role in the interaction between cells and extracellular matrix, and cause dysfunction of inflammatory cells and repairing cells as well as disorder of collagen metabolism, which might cause prolonged healing of bile duct trauma, over-deposition of extracellular matrix, cicatrix contracture, stenosis of anastomotic stoma.

Our study indicates that high expression of CD68 and TGF-β1 might be related to chronic inflammation of bile duct wall, which is caused by stimulation of bile. Continuous inflammatory reaction results in massive gathering of macrophages, which synthesize and secrete polypeptide growth factors such as MDGF, TGF-β1, *etc*. Polypeptide growth factor could cause high proliferation of fibroblasts, over-synthesis of collagen, and cicatrix stenosis of bile duct. Thus reducing bile-stimulated inflammation, shortening time of healing and inhibiting over-infiltration and over-function of macrophages can reduce proliferation of cicatrix of bile duct.

REFERENCES

1 **Huang ZQ,** Huang XQ. Changing patterns of traumatic bile duct injuries: a review of forty years experience. *World J Gastroenterol* 2002; **8**: 5-12

2 **Geng ZM,** Xiang GA, Han Q, Liu XG, Su BS, Liu QG, Pan CE. An experimental study on mechanism of benign biliary stricture. *Zhonghua Gandan Waike Zazhi* 2001; **7**: 618-619

3 **Alster TS,** Tanzi EL. Hypertrophic scars and keloids: etiology and management. *Am J Clin Dermatol* 2003; **4**: 235-243

4 **Urioste SS,** Arndt KA, Dover JS. Keloids and hypertrophic scars: review and treatment strategies. *Semin Cutan Med Surg* 1999; **18**: 159-171

5 **Haverstock BD.** Hypertrophic scars and keloids. *Clin Podiatr Med Surg* 2001; **18**: 147-159

6 **Brissett AE,** Sherris DA. Scar contractures, hypertrophic scars, and keloids. *Facial Plast Surg* 2001; **17**: 263-272

7 **Nedelec B,** Ghahary A, Scott PG, Tredget EE. Control of wound contraction. Basic and clinical features. *Hand Clin* 2000; **16**: 289-302

8 **Ramtani S,** Fernandes-Morin E, Geiger D. Remodeled-matrix contraction by fibroblasts: numerical investigations. *Comput Biol Med* 2002; **32**: 283-296

9 **Chipev CC,** Simman R, Hatch G, Katz AE, Siegel DM, Simon M. Myofibroblast phenotype and apoptosis in keloid and palmar fibroblasts *in vitro*. *Cell Death Differ* 2000; **7**: 166-176

10 **Badid C,** Mounier N, Costa AM, Desmouliere A. Role of myofibroblasts during normal tissue repair and excessive scarring: interest of their assessment in nephropathies. *Histol Histopathol* 2000; **15**: 269-280

11 **Ashcroft GS,** Mills SJ, Lei K, Gibbons L, Jeong MJ, Taniguchi M, Burow M, Horan MA, Wahl SM, Nakayama T. Estrogen modulates cutaneous wound healing by downregulating macrophage migration inhibitory factor. *J Clin Invest* 2003; **111**: 1309-1318

12 **Eroglu E,** Sari A, Altuntas I, Delibas N, Candir C, Agalar F. The effect of GM-CSF (granulocyte macrophage colony stimulating factor) on doxorubicin induced tissue necrosis and wound healing. *Indian J Cancer* 2000; **37**: 153-157

13 **Tian Y,** Tang S, Luo S. A study on the expressions and the correlation of TGF-beta and alpha-SMA in scars. *Zhonghua Zhengxing Waike Zazhi* 2000; **16**: 75-77

14 **Tang S,** Pang S, Cao Y. Changes in TGF-beta 1 and type I, III procollagen gene expression in keloid and hypertrophic scar. *Zhonghua Zhengxing Shaoshang Waike Zazhi* 1999; **15**: 283-285

15 **Chen W,** Fu X, Sun T, Sun X, Zhao Z, Sheng Z. Change of gene expression of transforming growth factor-beta1, Smad 2 and Smad 3 in hypertrophic scars skins. *Zhonghua Waike Zazhi* 2002; **40**: 17-19

16 **Lu Y,** Luo S, Liu J. The influence of transforming growth factor beta 1 (TGF beta 1) on fibroblast proliferation and collagen synthesis. *Zhonghua Shaoshang Zazhi* 2001; **17**: 345-347

Edited by Qiu WS and Wang XL **Proofread by** Chen WW

PO Box 2345, Beijing 100023, China
Fax: +86-10-85381893
E-mail: wjg@wjgnet.com www.wjgnet.com

ELSEVIER

World J Gastroenterol 2005;11(2):296-298
World Journal of Gastroenterology ISSN 1007-9327

• BRIEF REPORTS •

Heart-shaped anastomosis for Hirschsprung's disease: Operative technique and long-term follow-up

Guo Wang, Xiao-Yi Sun, Ming-Fa Wei, Yi-Zhen Weng

Guo Wang, Xiao-Yi Sun, Ming-Fa Wei, Yi-Zhen Weng, Department of Pediatric Surgery, Tongji Hospital Affiliated Tongji Medical College, Huazhong University of Science and Technology, Wuhan 430030, Hubei Province, China
Supported by the National Natural Science Foundation of China, No.39670746
Correspondence to: Guo Wang, Department of Pediatric Surgery, Tongji Hospital, 1095 Jiefang Avenue, Wuhan 430030, Hubei Province, China. gwang@tjh.tjmu.edu.cn
Telephone: +86-27-83662146
Received: 2004-04-22 **Accepted:** 2004-05-09

Abstract

AIM: To study the long-term therapeutic effect of "heart-shaped" anastomosis for Hirschsprung's disease.

METHODS: From January 1986 to October 1997, we performed one-stage "heart-shaped" anastomosis for 193 patients with Hirschsprung's disease (HD). One hundred and fifty-two patients were followed up patients (follow-up rate 79%). The operative outcome and postoperative complications were retrospectively analyzed.

RESULTS: Early complications included urine retention in 2 patients, enteritis in 10, anastomotic stricture in 1, and intestinal obstruction in 2. No infection of abdominal cavity or wound and anastomotic leakage or death occurred in any patients. Late complications were present in 22 cases, including adhesive intestinal obstruction in 2, longer anal in 5, incision hernia in 2, enteritis in 6, occasional stool stains in 7 and 6 related with improper diet. No constipation or incontinence occurred in any patient.

CONCLUSION: The early and late postoperative complication rates were 7.8% and 11.4% respectively in our "heart-shaped anastomosis" procedure. "Heart-shaped" anastomosis procedure for Hirschsprung's disease provides a better therapeutic effect compared to classic procedures.

Key words: Hirschsprung's disease; Heart-shaped anastomosis; Follow-up studies

Wang G, Sun XY, Wei MF, Weng YZ. Heart-shaped anastomosis for Hirschsprung's disease: Operative technique and long-term follow-up. *World J Gastroenterol* 2005; 11 (2): 296-298
http://www.wjgnet.com/1007-9327/11/296.asp

INTRODUCTION

During the period from 1955 to 1985, more than 400 children received classic operations, including modified Duhamel, Soave, and Ikeda operations, *etc*, for Hirschsprung's disease (HD) in our hospital. Because of a high incidence of complications following these methods[1], we have changed to use a "heart-shaped anastomosis" designed by ourselves since January 1986. During the ten years from 1986 to 1997, we performed this procedure for 193 patients with HD. This procedure could not only effectively prevent the occurrence of postoperative complications, such as infection in wound or abdominal cavity, anastomotic leakage and stricture, but also significantly decrease the incidence of incontinence or soiling and recurrence of constipation after surgery. This article reports the outcome of "heart-shaped anastomosis" procedure in HD.

MATERIALS AND METHODS

Patients

All the 193 cases (155 boys and 38 girls) were diagnosed on the basis of clinical history, radiological studies, rectoanal manometry, and pathologic examination after surgery. The mean age of the patients was 25 mo (range from 9 d to 10 years). Among these patients, short-segment aganglionosis was found in 172 cases and long-segment aganglionosis was found in 21 cases. The descending colon was pulled down for anastomosis in 130 cases, the ascending colon was pulled down for anastomosis in 63 cases, including 21 with intestinal neuronal dysplasia (IND).

Operation methods

The operation was performed as previously described[1]. A low left transverse incision was made extending slightly to the right of the midline. The peritoneal reflection from the rectum was dissected on both the left and right sides down to just above the level of the dentate line. To protect the pelvic autonomic nervous system, the upper third of the lateral rectal ligaments was dissected as close as possible to the rectal wall. Hemostasis was achieved with a sponge pressed into the posterior cavity behind the rectum. The proximal ganglionic bowel was identified with operative biopsies and frozen section. Aganglionic bowel was then dissected and mobilized up to the splenic flexure to allow a tension-free anastomosis with an adequate blood supply.

Attention was then paid to the perineum. The anus was dilated. An olive-shaped dilator was inserted via the anus into the lumen of rectosigmoid and aganglionic rectum was fastened to the dilator at the transition level. The bowel was then prolapsed out of the rectum, and everted (Figure 1). The rectum was transected and the ganglionic bowel was pulled through the anal canal. The most dilated distal portion of aganglionic bowel was resected at this point. The posterior wall of aganglionic anorectum was split longitudinally to the level of the dentate line (Figure 2). The tips of the two halves were trimmed so that the remaining rectal wall, whose anterior aspect was longer than the posterior one, had the shape of a heart. A point of anastomosis in anterior wall was marked at 2 cm above the anal verge and the proximal bowel opposite to this point was shortened about 2.5 cm for avoiding the formation of a valve. The point of anastomosis in posterior wall was marked at 0.5 cm above the dentate line (Figure 3). Interrupted sutures were placed circumferentially at each quadrant through the seromuscular coats of the proximal bowel and the full-thickness

edge of the transected rectum. Each suture was tied and grasped with clamps to prevent retraction. Subsequent sutures were added to each quadrant as full-thickness bites to complete the anastomosis. In order to prevent leakage, the posterior wall was meticulously sutured. At completion of the procedure, the anterior anastomosis was 4 cm above the anal verge and the posterior anastomosis was 2 cm above the anodermal junction.

Among the 193 patients, 152 patients received complete follow-up (follow-up rate 79%). The follow-up time ranged from 24 mo to 140 mo (mean 80 mo).

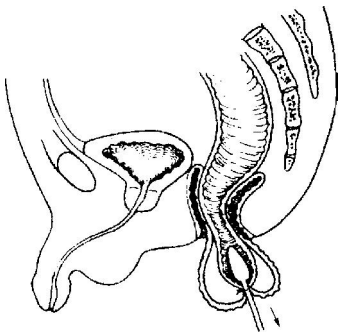

Figure 1 Transrectal dilator tied around ganglionic bowel at transition zone, and pulled through rectum. Bowel was everted until mucocutaneous line was exposed posteriorly, but not anteriorly.

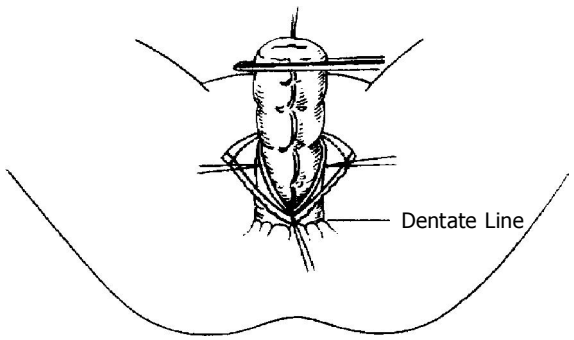

Figure 2 Ganglionic bowel exposed by resection of most dilated bowel. The posterior wall of the aganglionic anorectum was longitudinally split in posterior wall of anorectal canal to dentate line.

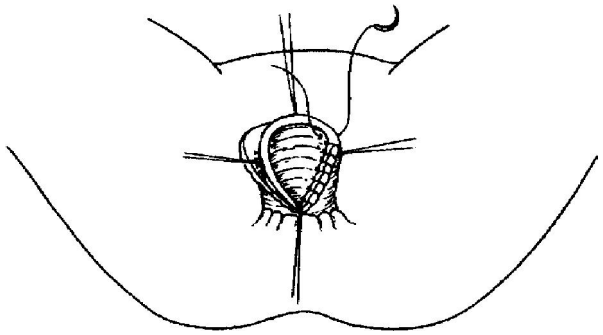

Figure 3 Suturing of seromuscular coats of rectum and colon. The bowel was everted and exteriorized out of the anus.

RESULTS

Early postoperative complications occurred in 15 (7.8%) patients, including urine retention in 2 who recovered following the insertion of a urethral catheter 1wk after operation, enteritis in 1, anastomotic stricture in 1, and intestinal obstruction in 2 who were cured with Chinese herbals. No infection in celiac/pelvic cavity or wound, and anastomotic leakage or death occurred in any patient.

Late complications occurred in 22 (11.4%) patients, such as adhesive intestinal obstruction in 2 who were treated with adhesive bowel resection, constipation due to longer remaining anal canal in 5 who were treated with a strip of internal sphincter cut, incision hernia in 2, enteritis in 6, occasional soiling in 7 and 6 related with improper diet. No incontinence or recurrence of constipation was found in any patient.

DISCUSSION

A number of operating procedures have been reported for treating HD. Previous studies have shown that the incidence of early postoperative complications in these procedures is over 25%, and the late complication rate is approximately 40%[2-4]. However, these two complication rates in our "heart-shaped anastomosis" procedure were 7.8 and 11.4%, respectively.

The incidence of infection in celiac/pelvic cavity or wound was approximately 7 to 17% in our study. Unlike other operations in which resection and anastomosis of the colon are performed in abdominal cavity, they were performed outside the abdominal cavity in our study and contamination or infection could be avoided.

Anastomotic leakage is usually the most severe complication in HD, and the incidence is 3 to 15.5%[2]. It often causes septic infection in the abdominal or pelvic cavity and needs colostomy to save the patient's life. In some patients, anastomotic leakage can result in multi-fistulae in pelvic cavity, frozen pelvis or constipation, and even lifelong artificial anus. In our procedure, the splenic flexure and left transverse colon are mobilized sufficiently, so that the colon could be pulled-through easily for a tension-free anastomosis outside the anus. On the other hand, a clear field of vision and reliable manipulation also allow us to avoid the occurrence of anastomotic leakage.

The occurrence of anastomotic stricture is related to ring-stricture at anastomosis, necrosis due to clamping of the bowel and its incidence is about 10%[2]. The "oblique anastomosis" procedure could prevent ring-stricture at the anastomosis and avoid anal dilatation within 3-5 mo after operation[1]. In our patients, valvular stricture in anterior wall was found in one patient due to reservation of anterior coloanal wall and cured by dilating anus.

Because more than half of the internal sphincter is resected in most operations, the incidence of soiling or constipation is approximately 10 to 20%[2,5]. However, our procedure could retain almost all the internal sphincter, so that it prevents recurrence of constipation and decreases the incidence of soiling. On the other hand, this procedure cut off the internal sphincter in the posterior wall, thus preventing spasm of the internal sphincter after operation.

It has been reported that recurrence of incontinence is related to insufficient resection of pathologic colon or/and too much reservation of aganglionic rectum[4]. In our operation, the splenic flexure and transverse colon were regularly mobilized and aganglionic colon was removed sufficiently, therefore recurrence of incontinence was avoided. In our study, a longer rectum was preserved in 5 patients, who were managed by resection of internal sphincter.

This procedure cannot prevent the occurrence of enterocolitis, which is about 8 to 25%. Further studies are needed to elucidate the reason for the occurrence of enterocolitis.

In summary, "heart-shaped" anastomosis for HD provides a clear field of vision, follows simplified steps of operation, there

is no need for a colostomy, minimal mobilization of pelvic cavity, and placement of urethral catheter is not needed. Colon can be resected outside the anus, and oblique colorectal anastomosis is performed end-to-end, thus minimizing the chance of contamination in abdominal/pelvic cavity. Rectal blind pouch, septum, infection or rupture of anastomosis are also avoided. There is no need to dilate anus after operation. No special clamps or stapling devices are required and complications resulting from them are avoided and nursing work is simplified. Not only the internal sphincter is persevered to a maximum degree but also the internal sphincter spasm syndrome is avoided, thereby solving the problems of soiling, incontinence and recurrence of constipation. Currently, this procedure has been widely used in many hospitals in China[6-9].

REFERENCES

1 **Wang G,** Yuan J, Zhou X, Qi B, Teitelbaum DH. A modified operation for Hirschsprung's disease: Posterior longitudinal anorectal split with a "heart-shaped" anastomosis. *Pediatr Surg Int* 1996; **11**: 243-245

2 **Shono K,** Hutson JM. The treatment and postoperative complications. *Pediatr Surg Int* 1994; **9**: 362-365

3 **Reding R,** de Ville de Goyet J, Gosseye S, Clapuyt P, Sokal E, Buts JP, Gibbs P, Otte JB. Hirschsprung's disease: a 20-year experience. *J Pediatr Surg* 1997; **32**: 1221-1225

4 **Skaba R,** Dudorkinova D, Lojda Zd, Dvorakova H, Pycha K, Kabelka M. Kasai's rectoplasty in the treatment Hirschsprung's disease and other types of colorectal dysganlionosis of in children. *Pediatr Surg Int* 1994; **9**: 503-506

5 **Kobayashi H,** Hirakawa H, Surana R, O'Briain DS, Puri P. Intestinal neuronal dysplasia is a possible cause of persistent bowel symptoms after pull-through operation for Hirschsprung's disease. *J Pediatr Surg* 1995; **30**: 253-257; discussion 257-259

6 **Wang ZL,** Li P, Zhang YN, Niu XY, Shi SN. Long-term results of pull-through heart-shape colorectotomy to treat Hirschsprung's disease. *Zhonghua Xiaoer Waike Zazhi* 2003; **24**: 127-128

7 **Li SC,** Wu BY, Zheng HM, Dai YJ, Ye T, Wang YJ. Stump anorectal longitudinal incision and colorectal heart-shape anastomosis for the treatment of Hirschsprung's disease. *Zhonghua Putong Waike Zazhi* 2001; **15**: 651-652

8 **Yi J,** Jiang JP, Li T, Jiang B, Chen YD, Liu DL, Liu JY, Gu XL. Trans-anal colonic pull-through for Hirschsprung's disease. *Zhonghua Xiaoer Waike Zazhi* 2001; **22**: 265-266

9 **Wang GB,** Tang ST, Lu XM, Yuan QL, Guo XL, Tao KX, Liu CP. Primary laparoscopic-assisted pull-through for hirschsprung's disease in infants and children. *Zhonghua Xiaoer Waike Zazhi* 2001; **22**: 136-137

Edited by Wang XL and Kumar M

PO Box 2345, Beijing 100023, China
Fax: +86-10-85381893
E-mail: wjg@wjgnet.com www.wjgnet.com

ELSEVIER

World J Gastroenterol 2005;11(2):299-302
World Journal of Gastroenterology ISSN 1007-9327

• BRIEF REPORTS •

Incidence of HBV variants with a mutation at nt551 among hepatitis B patients in Nanjing and its neighbourhood

Chun-Ling Ma, De-Xing Fang, Kun Yao, Fa-Qing Li, Hui-Ying Jin, Su-Qin Li, Wei-Guo Tan

Chun-Ling Ma, De-Xing Fang, Fa-Qing Li, Hui-Ying Jin, Su-Qin Li, Wei-Guo Tan, Huadong Research Institute for Medical Biotechnics, Nanjing 210002, Jiangsu Province, China
Kun Yao, Microbiology and Immunology Department, Nanjing Medical University, Nanjing 210029, Jiangsu Province, China
Supported by the Natural Science Foundation of Jiangsu Province, No. BJ2000039
Correspondence to: Chun-Ling Ma, Microbiology and Immunology Department, Nanjing Medical University, Nanjing 210029, Jiangsu Province, China. mchunling@hotmail.com
Telephone: +86-25-84542419 **Fax:** +86-25-84541183
Received: 2004-03-19 **Accepted:** 2004-04-21

Abstract

AIM: To investigate the epidemiology of hepatitis B virus (HBV) strains with a mutation at nt551 in surface gene among hepatitis B patients in Nanjing and its neighbourhood.

METHODS: By using mutation-specific polymerase chain reaction (msPCR) established by our laboratory for amplifying HBV DNAs with a mutation at nt551, 117 serum samples taken from hepatitis B patients were detected.

RESULTS: The results showed that 112 samples were positive for nt551A, 4 samples were positive for nt551G. One sample was positive for nt551T. No nt551C of HBV DNA was found. The incidence of HBsAg mutants with G, C, T, A at nt551 among 117 samples was 3.42%, 0%, 0.85%, 95.73%, respectively.

CONCLUSION: In Nanjing and its neighbourhood, hepatitis B patients are mainly infected with wild genotype HBV. The incidence of mutants with a mutation at nt551 in HBV genome is significantly lower than that in wild genotype HBV DNA ($P<0.01$). The necessity of adding components of HBsAg mutants to HBV vaccine needs further investigation.

Key words: Hepatitis B; Hepatitis B virus; nt551; Mutation

Ma CL, Fang DX,Yao K, Li FQ, Jin HY, Li SQ, Tan WG. Incidence of HBV variants with a mutation at nt551 among hepatitis B patients in Nanjing and its neighbourhood. *World J Gastroenterol* 2005; 11(2): 299-302
http://www.wjgnet.com/1007-9327/11/299.asp

INTRODUCTION

Hepatitis B surface antigen (HBsAg) is considered to be one of the best markers for the diagnosis of acute and chronic HBV infection. But in some patients, this antigen cannot be detected by routine serological assays despite the presence of virus. One of the most important explanations for the lack of detectable HBsAg is that mutations which occur within the "a" determinant of HBV S gene can alter expression of HBsAg and lead to changes of antigenicity and immunogenicity of HBsAg accordingly. As a result, these mutants cannot be detected by diagnostic assays. Thus, it is essential to find specific and sensitive methods to detect the new mutants and further investigate their distribution[1,2].

HBV is a hepatotrophic DNA virus. In the reverse transcription process of DNA replication, HBV DNA template is transcribed by cellular RNA polymerase to pregenomic RNA, which is reversely transcribed to DNA by viral polymerase, and a consequence of the unique way of HBV replication is a significant tendency of mutation[1-3]. Substitution, deletion and frame-shift by insertion or deletion of short sequences have been found in four open reading frames[4-7]. The diversity is also shown in different serological subtypes such as adr, adw, ayr and ayw, which have a common "a" determinant. It is well known that "a" determinant is the common antigenic epitope of all subtypes of HBsAg. A large antigenic area of "a" determinant is now called the major hydrophilic region (MHR). Mutations within MHR of HBsAg have been considered to be associated with vaccine failure and chronic infection[1,2,6,8]. These mutations have been reported repeatedly since Carman *et al*[9] found the first case of immune escape mutants in 1990. The point mutation reported most commonly in immunized children causes a substitution from Arg to Gly at position 145 of HBsAg[1,3,8,9]. Other reports about substitutions in HBsAg such as 120, 121, 126, 129, 131, 133, 141, 144 are found repeatedly[8-12]. These findings of HBV immune escape mutants have caused attention of scientists all over the world in recent years. Immune escape of HBV mutants is best known to be associated with HBV genome itself, but the immune pressure is considered to be one of the most important factors that result in escape mutants[12-16].

The immune escape variants could influence the effect of HBV vaccine, it is argued that the components of mutant HBsAg should be added into the HBV vaccine in the future[3,12,16,17]. However, in order to achieve this aim, it is necessary to confirm firstly the mutants that are the big problems among hepatitis B patients. At present, it is very important to find new immune escape mutants and further investigate their distribution. Specific and sensitive assays are essential for investigating the distribution of mutants. To detect the mutant HBV DNA, msPCR is a potential method. Our laboratory has discovered a mutation of A-to-G at nt551 of HBV genome, which can result in the alteration of Met to Val at 133aa of HBsAg. To investigate the distribution of mutants with a mutation at nt551 among hepatitis B patients in Nanjing and its neighbourhood in China, we collected 326 serum samples from hepatitis B patients in different hospitals in Nanjing. One hundred and seventeen positive samples for HBV surface gene were detected by using msPCR which is sensitive and specific to the mutation at nt551 in HBV genome.

MATERIALS AND METHODS

Collection of serum samples

Three hundred and twenty-six serum samples from hepatitis B

patients were provided by Nanjing Jinling Hospital, Bayi Hospital and Nanjing Children's Hospital. Viral markers were tested by using the enzyme immune assay (EIA). ALT levels of all the samples were abnormal. Diagnosis of hepatitis B was made according to the revised standard of hepatitis B diagnosis established at the Tenth National Symposium on Viral Hepatitis in Xi'an in 2000.

Extraction of HBV genome DNAs

By using the HBV DNA extraction method, all the 326 serum samples were prepared and stored at -20 ℃.

Amplification of HBV S DNAs

After nested PCR amplification, we achieved 101 HBV S DNAs. Thirty-five samples were positive for HBsAg and anti-HBs, and the other 66 samples were negative for HBsAg and positive for anti-HBs.

Primers for nested PCR to amplify HBV S DNA were designed according to the known HBV genome sequences and the main popular subtypes, adr and adw in China.

Primers for the first-round: P1': 5'ACATCATCTGT GGAAGGC 3', nt2756-nt2773; the upstream primer; P6': 5'TATCCCATGAAGTTAAGG 3', nt884-nt867, the downstream primer.

Primers for the second-round: PEC: 5'CGGAATTCACC ATATTCTTGGGAACAAG 3', nt2 823-nt2 844, the upstream primer; PPS: 5'GCTGCAGGTTTAAATGTATACCCAAAGAC 3', nt838-nt816, the downstream primer.

An *Eco*RI or a *Pst* I site was originally added at 5'-end respectively for cloning purpose.

Amplification of HBV DNA fragments for control

To achieve HBV DNA fragments with an A at nt551, the wild genotype HBV S DNA as template was amplified by using the primer pair P551A-PPS under the condition of regular PCR. The HBsAg mutant with G at nt551 as template was amplified by using the primer pair P551G-PPS to achieve the HBV DNA fragments with a G at nt551. HBV DNA fragments with C or T at nt551 were achieved by introducing mutation in a PCR. The PCR primer sequences were as follows: P551A: 5'TCCTGCTCA AGGAACCTCTA 3', nt532-nt551, upstream primer; P551G: 5'TCCTGCTCAAGGAACCTCTG 3', nt532-nt551, upstream primer; P551C: 5'TCCTGCTCAAGGAACCTCTC 3', nt532-nt551, upstream primer; P551T: 5'TCCTGCTCAAGGAACC TCTT 3', nt532-nt551, upstream primer; PPS: See the above. P551C-PPS and P551T-PPS were used respectively to amplify HBV DNA fragments with C or T at nt551, which were 314 bp in length. Additionally, two upstream primers were designed respectively by introducing mutation to achieve the controls of HBV DNA with C or T at nt551. P551CM: TCCTGCTCAAG GAACCTCTCTGTTTC, nt532-nt557; P551TM: TCCTGCTC AAGGAACCTCTTTGTTTC, nt532-nt557.

Detection by using msPCR

In order to amplify HBV DNA specifically, 101 serum samples were amplified by primer pair P551A-PPS using msPCR method. The annealing temperature of PCR was at 71 ℃ and the concentration of primers was at 0.8 nmol/mL in 25 μL reaction volume. Thirty cycles of amplification were performed, each at 94 ℃ for 30 s, at 71 ℃ for 30 s, and at 72 ℃ for 1 min. Then the negative samples were amplified by primer pairs P551G-PPS, P551C-PPS and P551T-PPS respectively. For primer pairs P551C-PPS and P551T-PPS, the annealing temperature was at 72 ℃ and the concentration of primers was at 0.2 nmol/mL in 25 μL reaction volume, and other conditions were similar to the amplification by P551A-PPS and P551G-PPS.

Statistical analysis

χ^2-test was used to assess the statistical significance of differences. $P<0.01$ was considered statistically significant.

RESULTS

HBV DNA fragments for control

The HBV S DNA with A, G, C or T at nt551 was amplified respectively for control. The amplified DNA fragments were 314 bp in length. This result is shown in Figure 1.

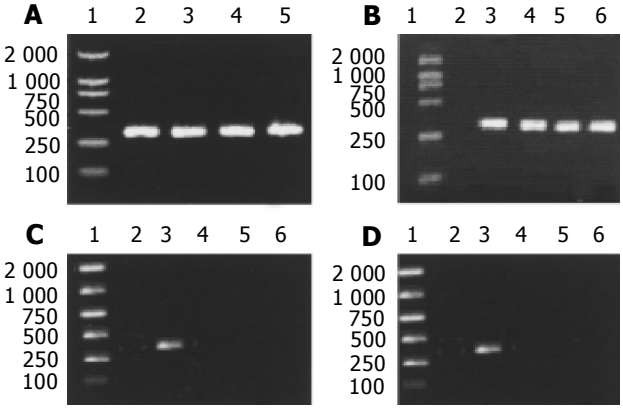

Figure 1 Amplification results of msPCR. A: Amplification of control HBV DNA. Lane 1: DNA marker; lane 2: HBV DNA with an A at nt551; lane 3: HBV DNA with G at nt551; lane 4: HBV DNA with C at nt551; lane 5: HBV DNA with T at nt551. B: The msPCR amplification for No.127, No.210 and No.216 by using P551G-PPS. Lane 1: DNA marker; lanes 2-6: No.8 of nt551A (negative control), No.57 (positive control), No.127, No.210 and No.216 were amplified by P551G-PPS respectively. C: The msPCR amplification for No.127, No.210 and No.216 by using P551C-PPS. Lane 1: DNA marker; lanes 2-6: No.8 of nt551A (negative control), HBV DNA of nt551C (positive control), No.127, No.210 and No.216 were amplified by P551C-PPS respectively. D: The msPCR amplification for No.127, No.210 and No.216 by using P551T-PPS. Lane 1: DNA marker; lanes 2-6: No.8 of nt551A (negative control), No.2 of nt551T (positive control), No.127, No.210 and No.216 were amplified by P551T-PPS respectively.

Detection by using msPCR

One hundred and one serum samples positive for HBV S DNA were detected. After gel electrophoresis, 35 samples (positive for HBsAg and anti-HBs) were positive for P551A-PPS amplification, that is to say, each of these 35 samples was a wild genotype HBV genome with an A at nt551. Among the 66 samples negative for HBsAg and positive for anti-HBs, 3 samples were negative for amplification by P551A-PPS. They were samples of No.127, No.210 and No.216.Then, these 3 samples were amplified by using P551G-PPS, P551C-PPS and P551T-PPS. The electrophoresis results of them were as follows.

As positive and negative controls, No.2, No.8 and No.57 previously sequenced were known to have A, G and T at nt551 respectively. These results confirmed that No.127, No.210 and No.216 all had a G at nt551.

Investigating results

By using msPCR, 101 serum samples positive for HBV S DNA were detected and the other 16 samples were taken from the result we detected before. The results showed that 112 samples were positive for nt551A, 4 samples were positive for nt551G (one of them was taken from the previous DNA sequence). One sample was positive for nt551T. No nt551C of HBV DNA was

found. Thus, the incidence of HBsAg nt551G mutant, nt551C mutants, nt551T mutants, and nt551A of wild genotype HBV DNAs was 3.42%, 0%, 0.85% and 95.73% respectively among the 117 samples. The statistical analysis results are summarized in Tables 1-3.

Table 1 Incidence of nt551 A and nt551 G (%)

	nt551 A	nt551 G
Number of case	112	4
Incidence	112/117 (95.37)	4/117 (3.42)[b]

[b]$P<0.01$ *vs* wild-type HBV DNA (nt551 A).

Table 2 Incidence of nt551 A and nt55 C (%)

	nt551 A	nt551 C
Number of case	112	0
Incidence	112/117 (95.37)	0/117 (0)[b]

[b]$P<0.01$ *vs* wild-type HBV DNA (nt551A).

Table 3 Incidence of nt551 A and nt551 T (%)

	nt551 A	nt551 T
Number of case	112	1
Incidence	112/117 (95.37)	1/117 (0.85)[b]

[b]$P<0.01$ *vs* wild-type HBV DNA (nt551A).

DISCUSSION

It is well known that mutants of HBsAg are able to cause infection and horizontal transmission despite the presence of anti-HBs[18-22]. It has been found that increasing use of HBV vaccine has an overwhelming positive influence on the prevention of hepatitis B viral infection, but has no effective impact on those mutants[23]. Mutations in the coding region of "a" determinant of HBsAg could not be detected in some routine assays[24,25]. In our laboratory a specific and sensitive method for monitoring the HBsAg mutant with a mutation at nt551 has been established. The method of msPCR is different from immunoassays based on the antigen-antibody reaction[26,27]. To detect the mutant HBsAg, unique specific monoclonal antibodies are required. But these kinds of antibodies are limited or not available commercially. Because HBV is a double-stranded DNA virus, its genome is fairly stable in blood and tissues, PCR amplification of HBV DNA is relatively easy. msPCR is a practical method to detect the specific site mutation. This method was firstly developed to detect point mutation of allele-special genes of β-globin genome DNA for sickle cell anemia[28]. Then it is used in virological studies. The feasibility of msPCR has been confirmed by DNA sequence analysis, that is to say, the result of msPCR is accordant with that of DNA sequencing. After msPCR establishment, we have found that the annealing temperature is the key factor to msPCR method. Additionally, the concentration of primers is also an important factor for this msPCR. In short, different primers amplify HBV DNA specifically under different conditions.

In our study, all serum samples detected were taken from hepatitis B patients in Nanjing and its neighbourhood and four mutants of nt551G were found. Their detailed clinical data were as follows: No.57 taken from a man was negative for HBsAg and positive for anti-HBs. His ALT level was considered to be abnormal. No.127 taken from a 3-year-old boy was negative for HBsAg and positive for anti-HBs and HBeAg. His ALT level was higher than normal value. His mother was a HBsAg carrier and the boy was injected with HBV vaccine and HBIg when he was born. No. 210 taken from a 9-year-old boy, was negative for HBsAg and positive for anti-HBs and his ALT level was considered to be abnormal. No. 216 taken from an old male chronic hepatitis B patient, was negative for HBsAg and positive for anti-HBs and his ALT level was considered to be abnormal.

The reason why all these four samples were negative for HBsAg and positive for anti-HBs might be that the mutations of A→G at nt551 could cause a change from Met to Val at 133aa of HBsAg and the structure of HBsAg was altered accordingly. The affinity between HBsAg and anti-HBs might diminish subsequently. The alteration of Met to Val at 133aa of HbsAg can reduce the combination ability between HBsAg and mAb of anti-HBs.

The detection results of these four samples have shown that the anti-HBs loses its protection against HBsAg as usual. On the contrary, they may form immune pressure by recognizing and combining with wild genotype HBV strains, but those mutants having no epitopes can survive and multiply. Therefore, a specific and sensitive method should be used to find those mutants of HBsAg and provide theoretical data for clinical diagnosis and treatment of hepatitis B.

In conclusion, most HBV infections are caused by wild genotype HBV strains. Whether it is necessary to add the component of HBsAg mutants to HBV vaccine needs further study and investigation.

REFERENCES

1 **Koyanagi T**, Nakamuta M, Sakai H, Sugimoto R, Enjoji M, Koto K, Iwamoto H, Kumazawa T, Mukaide M, Nawata H. Analysis of HBs antigen negative variant of hepatitis B virus: unique substitutions, Glu129 to Asp and Gly145 to Ala in the surface antigen gene. *Med Sci Monit* 2000; **6**: 1165-1169

2 **Brunetto MR**, Rodriguez UA, Bonino F. Hepatitis B virus mutants. *Intervirology* 1999; **42**: 69-80

3 **Kfoury Baz EM**, Zheng J, Mazuruk K, Van Le A, Peterson DL. Characterization of a novel hepatitis B virus mutant: demonstration of mutation-induced hepatitis B virus surface antigen group specific "a" determinant conformation change and its application in diagnostic assays. *Transfus Med* 2001; **11**: 355-362

4 **Dong J**, Cheng J, Wang Q, Huangfu J, Shi S, Zhang G, Hong Y, Li L, Si C. The study on heterogeneity of hepatitis B virus DNA. *Zhonghua Yixue Zazhi* 2002; **82**: 81-85

5 **Kreutz C**. Molecular, immunological and clinical properties of mutated hepatitis B viruses. *J Cell Mol Med* 2002; **6**: 113-143

6 **Zhong S**, Chan JY, Yeo W, Tam JS, Johnson PJ. Hepatitis B envelope protein mutants in human hepatocellular carcinoma tissues. *J Viral Hepat* 1999; **6**: 195-202

7 **Weinberger KM,** Zoulek G, Bauer T, Bohm S, Jilg W. A novel deletion mutant of hepatitis B virus surface antigen. *J Med Virol* 1999; **58**: 105-110

8 **Yukimasa N,** Ohkushi H, Fukasawa K, Fukuchi K, Takagi Y, Gomi K. Hepatitis B virus gene mutations in the sera of three patients with coexisting hepatitis B surface antigen and anti-surface antibody. *Rinsho Byori* 2000; **48**: 184-188

9 **Carman WF**, Zanetti AR, Karayiannis P, Waters J, Manzillo G, Tanzi E, Zuckerman AJ, Thomas HC. Vaccine-induced escape mutant of hepatitis B virus. *Lancet* 1990; **336**: 325-329

10 **Yang X,** Lei J, Zhang Y, Luo H, Huang L, Zheng Y, Tang X, Li L. A novel stop codon mutation in S gene: the molecular basis of a patient with cryptogenic cirrhosis. *Zhonghua Yixue Zazhi* 2002; **82**: 400-402

11 **Zhu Q**, Lu Q, Xiong S, Yu H, Duan S. Hepatitis B virus S gene mutants in infants infected despite immunoprophylaxis. *Chin Med J (Engl)* 2001; **114**: 352-354

12 **Santantonio T**, Gunther S, Sterneck M, Rendina M, Messner M, Launois B, Francavilla A, Pastore G, Will H. Liver graft infec-

tion by HBV S-gene mutants in transplant patients receiving long-term HBIg prophylaxis. *Hepatogastroenterology* 1999; **46**: 1848-1854

13 **Rodriguez-Frias F**, Buti M, Jardi R, Vargas V, Quer J, Cotrina M, Martell M, Esteban R, Guardia J. Genetic alterations in the S gene of hepatitis B virus in patients with acute hepatitis B, chronic hepatitis B and hepatitis B liver cirrhosis before and after liver transplantation. *Liver* 1999; **19**: 177-182

14 **He C**, Nomura F, Itoga S, Isobe K, Nakai T. Prevalence of vaccine-induced escape mutants of hepatitis B virus in the adult population in China: a prospective study in 176 restaurant employees. *J Gastroenterol Hepatol* 2001; **16**: 1373-1377

15 **Cooreman MP**, Leroux-Roels G, Paulij WP. Vaccine-and hepatitis B immune globulin-induced escape mutations of hepatitis B virus surface antigen. *J Biomed Sci* 2001; **8**: 237-247

16 **Cooreman MP,** Leroux-Roels G, Paulij WP. Vaccine- and hepatitis B immune globulin-induced escape mutations of hepatitis B virus surface antigen. *J Biomed Sci* 2001; **8**: 237-247

17 **Komatsu H**, Fujisawa T, Sogo T, Isozaki A, Inui A, Sekine I, Kobata M, Ogawa Y. Acute self-limiting hepatitis B after immunoprophylaxis failure in an infant. *J Med Virol* 2002; **66**: 28-33

18 **Heijtink RA**, van Bergen P, van Roosmalen MH, Surmen CM, Paulij WP, Schalm SW, Osterhaus AD. Anti-HBs after hepatitis B immunization with plasma-derived and recombinant DNA-derived vaccines: binding to mutant HBsAg. *Vaccine* 2001; **19**: 3671-3680

19 **Banerjee K**, Guptan RC, Bisht R, Sarin SK, Khandekar P. Identification of a novel surface mutant of hepatitis B virus in a seronegative chronic liver disease patient. *Virus Res* 1999; **65**: 103-109

20 **Chen WN**, Oon CJ. Hepatitis B virus surface antigen (HBsAg) mutants in Singapore adults and vaccinated children with high anti-hepatitis B virus antibody levels but negative for HBsAg. *J Clin Microbiol* 2000; **38**: 2793-2794

21 **Oon CJ**, Chen WN, Goo KS, Goh KT. Intra-familial evidence of horizontal transmission of hepatitis B virus surface antigen mutant G145R. *J Infect* 2000; **41**: 260-264

22 **Chen WN**, Oon CJ, Koh S. Horizontal transmission of a hepatitis B virus surface antigen mutant. *J Clin Microbiol* 2000; **38**: 938-939

23 **Schories M**, Peters T, Rasenack J. Isolation, characterization and biological significance of hepatitis B virus mutants from serum of a patient with immunologically negative HBV infection. *J Hepatol* 2000; **33**: 799-811

24 **Weinberger KM**, Bauer T, Bohm S, Jilg W. High genetic variability of the group-specific a-determinant of hepatitis B virus surface antigen (HBsAg) and the corresponding fragment of the viral polymerase in chronic virus carriers lacking detectable HBsAg in serum. *J Gen Virol* 2000; **81**: 1165-1174

25 **Chen WN**, Oon CJ, Moh MC. Detection of hepatitis B virus surface antigen mutants in paraffin-embedded hepatocellular carcinoma tissues. *Virus Genes* 2000; **20**: 263-267

26 **Ijaz S**, Torre F, Tedder RS, Williams R, Naoumov NV. Novel immunoassay for the detection of hepatitis B surface 'escape' mutants and its application in liver transplant recipients. *J Med Virol* 2001; **63**: 210-216

27 **Jolivet-Reynaud C**, Lesenechal M, O'Donnell B, Becquart L, Foussadier A, Forge F, Battail-Poirot N, Lacoux X, Carman W, Jolivet M. Localization of hepatitis B surface antigen epitopes present on variants and specifically recognised by anti-hepatitis B surface antigen monoclonal antibodies. *J Med Virol* 2001; **65**: 241-249

28 **Wu DY**, Ugozzoli L, Pal BK, Wallace RB. Allele-specific enzymatic amplification of beta-globin genomic DNA for diagnosis of sickle cell anemia. *Proc Natl Acad Sci USA* 1989; **86**: 2757-2760

Edited by Wang XL and Zhu LH

PO Box 2345, Beijing 100023, China
Fax: +86-10-85381893
E-mail: wjg@wjgnet.com www.wjgnet.com

ELSEVIER

World J Gastroenterol 2005;11(2):303-304
World Journal of Gastroenterology ISSN 1007-9327

• CASE REPORT •

Acute hepatitis induced by an Aloe vera preparation: A case report

Christian Rabe, Annemarie Musch, Peter Schirmacher, Wolfgang Kruis, Robert Hoffmann

Christian Rabe, Annemarie Musch, Wolfgang Kruis, Robert Hoffmann, Department of Medicine, Evangelisches Krankenhaus Koeln Kalk, Cologne, Germany
Peter Schirmacher, Institute of Pathology, University of Cologne, Cologne, Germany
Correspondence to: Christian Rabe, M.D., Department of Medicine I, University of Bonn, Sigmund-Freud-Str. 25, D-53105 Bonn, Germany. rabe@uni-bonn.de
Telephone: +49-228-287-5511 **Fax:** +49-228-287-4698
Received: 2004-04-07 **Accepted:** 2004-05-25

Abstract

AIM: Aloe vera, plant extracts of *Aloe barbadensis miller*, is widely used in phytomedicine. The first case of acute hepatitis due to this compound was described.

METHODS: Description of a clinical case.

RESULTS: Hepatitis in a 57-year old female could be linked to the ingestion of Aloe barbadensis miller compounds. The patient´s hepatitis resolved completely after discontinuing this medication.

CONCLUSION: The case emphasizes the importance of considering phytopharmaceutical over-the-counter drugs as causative agents of hepatitis.

Key words: Hepatitis; Aloe vera; Acute diseases

Rabe C, Musch A, Schirmacher P, Kruis W, Hoffmann R. Acute hepatitis induced by an Aloe vera preparation: A case report. *World J Gastroenterol* 2005; 11(2): 303-304
http://www.wjgnet.com/1007-9327/11/303.asp

INTRODUCTION

Aloe vera is a chemically ill-defined extract of the *Aloe barbadensis miller* plant. There is no doubt that this compound is bioactive[1]. Phytomedicine ascribes anti-inflammatory, analgetic, liver-protective, anti-proliferative, anti-carcinogenic, anti-aging, and laxative effects to this plant[2-5]. These effects are thought to be the result of radical scavenging, inhibition of COX-2, and immuno-modulatory mechanisms. The drug is widely used as a self-prescribed anti-aging drug in Western European countries as well as in the USA. Even though it is in widespread use as an over-the-counter drug, its toxicology has not been systematically examined. Here, we describe the first case of liver damage associated with Aloe vera ingestion.

CASE REPORT

Medical history and physical examination

A 57-year old female patient presented to our department with an 1 wk history of progressive jaundice, pruritus, acholic bowel movements, and right-upper quadrant abdominal discomfort. Past medical history did not reveal any preexisting liver disease. There was no history of illicit drug use and no sexual promiscuity. In the hope to delay aging, the patient had begun using Aloe vera tablets containing 500 mg of an extract of *Aloe barbadensis miller* about 4 wk before admission. She also used zinc and vitamin C supplements as directed by the manufacturers. The Aloe vera tablets had been purchased in Spain as they were less expensive there than in Germany.

Clinical examination revealed a mildly overweight (70 kg bodyweight, 167 cm height) jaundiced patient with right-upper quadrant discomfort on deep palpation. Liver and spleen sizes were normal. There was no lymphadenopathy. The remainder of the physical examination was unremarkable.

Laboratory and technical examinations

On abdominal ultrasound examination, a reduced echogenicity of a normal sized liver was noted. Dilatation of intra- or extrahepatic bile ducts was absent. Patency of the hepatic artery, portal vein, and hepatic veins was ascertained using Doppler ultrasound. Splenic size was normal, the examination of kidneys, pancreas and retroperitoneal space was normal as well.

Laboratory abnormalities included a bilirubin concentration of 8.9 mg/dL (normal: <1.1mg/dL), ALAT 1480 U/L (normal: <22 U/L), ASAT 711 U/L (normal: <15 U/L), LDH 506 U/L (normal <240 U/L), alkaline phosphatase 265 U/L (normal: <160 U/L), GGTP 244 U/L (normal: <18 U/L). Creatinine, serum electrolytes, amylase, total protein, electrophoresis, serum concentrations of IgG, IgA, and IgM, white blood cell count, hemoglobin concentration, platelet count, and differential blood cell count were all within the normal range. Coeruloplasmin concentration was normal as was the alpha-1-antitrypsin concentration.

Serologic examinations for hepatitis A, C, and E infection were negative. HCV-PCR was negative. Anti-HBc-IgG and anti-HBs-IgG were positive, while HBsAg and anti-HBc-IgM were negative. There was no serologic evidence for recent infections with cytomegalovirus, Epstein-Barr-virus, or herpes virus. Autoimmune markers showed negative titers for antimitochondrial and borderline titers for antinuclear antibodies (1:40; normal titer defined as <1:40).

Liver biopsy was performed and revealed severe acute hepatitis with portal and acinar infiltrates predominantly consisting of lymphocytes, plasma cells, and eosinophilic granulocytes along with bridging necrosis and bilirubinostasis (Figure 1).

Clinical course

All medications were withheld and aminotransferases as well as the bilirubin concentration gradually returned to normal levels over the course of several months. Two weeks after admission, ALAT concentration was 226 U/L, 5 mo after discharge ALAT concentration was 180 U/L, and 1 year after discharge ALAT concentration decreased to 40 U/L. The patient became completely asymptomatic within a week and has remained so ever since.

DISCUSSION

To our knowledge, this is the first case of toxic hepatitis that can be ascribed to an Aloe vera preparation. The Aloe vera preparation was the only active compound ingested during the period preceding the occurrence of toxic hepatitis. This, the exclusion of common alternative diagnoses, and the rapid improvement and resolution of liver damage following

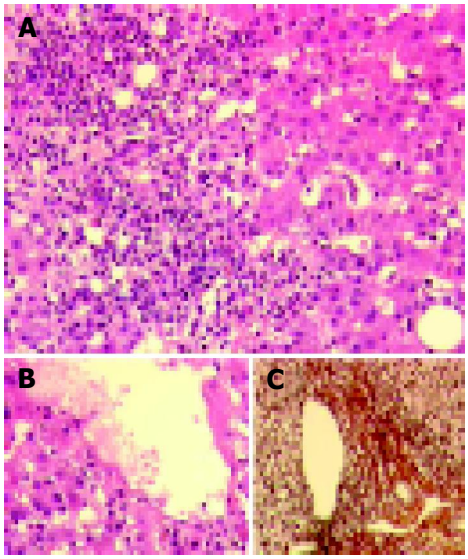

Figure 1 Severe acute hepatitis with portal and acinar inflammatory infiltrates mainly composed of lymphocytes, plasma cells, and eosinophilic granulocytes revealed in liver biopsy. A: Disseminated single-cell and group-cell necroses as well as parenchymal regeneration (H&E). B: Perivenular parenchyma with single cell necroses, regeneration and bilirubinostasis (H&E). C: Largely preserved architecture and only minimally increased fiber deposition in a representative portal tract shown by connective tissue stain (mo. Gomori).

discontinuation of Aloe vera provide strong evidence that the Aloe vera preparation has caused the acute hepatitis.

It is very unlikely that the ongoing concomitant medication with vitamin C and zinc supplements may have been involved, as these substances are not allergenic and hepatotoxic.

Aloe vera, the dried extract from the leaves of *Aloe barbadenis miller* plants, contains several alkaloids that may induce or block hepatic enzyme systems such as cytochrome P450 as well as the enzymes of ethanol metabolism[6]. This interference with detoxification processes leading to dose-related liver damage or direct cytotoxic effects of Aloe[7] or biotransformed constituents[8] are probably not important mechanisms in our case as the resolution of liver damage occurred much too slowly. It is more likely that an idiosyncratic immunological mechanism (hypersensitivity) is responsible for the hepatitis. A role for hypersensitivity is further supported by the presence of eosinophilic granulocytes in the periportal fields seen in the liver biopsy. As there was no evidence for the presence of an autoimmune hepatitis, especially no hypergammaglobinemia or markedly elevated autoantibody titers, we propose that this liver damage was triggered by the Aloe vera preparation. Hypersensitivity to Aloe - which may have a delayed presentation - has been described in humans[9]. Several compounds present in Aloe vera may interact with the host's immune system[10]. This activation of the immune system was also discussed as a possible mechanism for a reported anti-tumor activity of Aloe vera[11]. The interactions with the immune system may inhibit the release or cause the rapid detoxification of reactive oxygen species[12]. This antioxidant effect of Aloe vera is also implicated in the potential anti-hepatocarcinogenic and hepatoprotective properties of the drug[13-17]. Conversely, some constituents of Aloe vera have been reported to be biotransformed to mutagenic compounds with equivocal evidence for *in vivo* carcinogenicity. The growth-inhibiting effect of Aloe vera is mediated through pro-apoptotic pathways. One could speculate that this effect may also be present in normal liver cells and leads to liver damage or to the triggering of an immune response directed toward intracellular antigens. A similar mechanism may be present in kidney damage associated with other Aloe species.

Herbal medicines are widely used in almost all segments of the population. A variety of herbal medicines can cause liver damage. Again, our case emphasizes that phytotherapeutic drugs should be subjected to the same toxicologic studies and pharmacovigilance that synthetic drugs are subjected to.

ACKNOWLEDGEMENTS

We thank Mrs. U. Moser, University of Bonn, for online reference acquisition.

REFERENCES

1 **Logarto Parra A**, Silva Yhebra R, Guerra Sardinas I, Iglesias Buela L. Comparative study of the assay of Artemia salina L. and the estimate of the medium lethal dose (LD50 value) in mice, to determine oral acute toxicity of plant extracts. *Phytomedicine* 2001; **8**: 395-400
2 **Swanson LN**. Therapeutic value of Aloe Vera. *US Pharmacist* 1995: 26-35
3 **Fischer JM**. Medical use of aloe products. *US Pharmacist* 1982; **7**: 37-45
4 **Syed TA**, Ahmad SA, Holt AH, Ahmad SA, Ahmad SH, Afzal M. Management of psoriasis with Aloe vera extract in a hydrophilic cream: a placebo-controlled, double-blind study. *Trop Med Int Health* 1996; **1**: 505-509
5 **Ikeno Y**, Hubbard GB, Lee S, Yu BP, Herlihy JT. The influence of long-term Aloe vera ingestion on age-related disease in male Fischer 344 rats. *Phytother Res* 2002; **16**: 712-718
6 **Chung JH**, Cheong JC, Lee JY, Roh HK, Cha YN. Acceleration of the alcohol oxidation rate in rats with aloin, a quinone derivative of Aloe. *Biochem Pharmacol* 1996; **52**: 1461-1468
7 **Avila H**, Rivero J, Herrera F, Fraile G. Cytotoxicity of a low molecular weight fraction from Aloe vera (Aloe barbadensis Miller) gel. *Toxicon* 1997; **35**: 1423-1430
8 **Mueller SO**, Stopper H, Dekant W. Biotransformation of the anthraquinones emodin and chrysophanol by cytochrome P450 enzymes. Bioactivation to genotoxic metabolites. *Drug Metab Dispos* 1998; **26**: 540-546
9 **Morrow DM**, Rapaport MJ, Strick RA. Hypersensitivity to aloe. *Arch Dermatol* 1980; **116**: 1064-1065
10 **Hart LA**, van Enckevort PH, van Dijk H, Zaat R, de Silva KT, Labadie RP. Two functionally and chemically distinct immunomodulatory compounds in the gel of Aloe vera. *J Ethnopharmacol* 1988; **23**: 61-71
11 **Corsi MM**, Bertelli AA, Gaja G, Fulgenzi A, Ferrero ME. The therapeutic potential of Aloe Vera in tumor-bearing rats. *Int J Tissue React* 1998; **20**: 115-118
12 **Singh RP**, Dhanalakshmi S, Rao AR. Chemomodulatory action of Aloe vera on the profiles of enzymes associated with carcinogen metabolism and antioxidant status regulation in mice. *Phytomedicine* 2000; **7**: 209-219
13 **Shamaan NA**, Kadir KA, Rahmat A, Ngah WZ. Vitamin C and aloe vera supplementation protects from chemical hepatocarcinogenesis in the rat. *Nutrition* 1998; **14**: 846-852
14 **Kim HS**, Kacew S, Lee BM. *In vitro* chemopreventive effects of plant polysaccharides (Aloe barbadensis miller, Lentinus edodes, Ganoderma lucidum and Coriolus versicolor). *Carcinogenesis* 1999; **20**: 1637-1640
15 **Arosio B**, Gagliano N, Fusaro LM, Parmeggiani L, Tagliabue J, Galetti P, De Castri D, Moscheni C, Annoni G. Aloe-Emodin quinone pretreatment reduces acute liver injury induced by carbon tetrachloride. *Pharmacol Toxicol* 2000; **87**: 229-233
16 **Yagi A**, Kabash A, Okamura N, Haraguchi H, Moustafa SM, Khalifa TI. Antioxidant, free radical scavenging and anti-inflammatory effects of aloesin derivatives in Aloe vera. *Planta Med* 2002; **68**: 957-960
17 **Yagi A**, Kabash A, Mizuno K, Moustafa SM, Khalifa TI, Tsuji H. Radical scavenging glycoprotein inhibiting cyclooxygenase-2 and thromboxane A2 synthase from aloe vera gel. *Planta Med* 2003; **69**: 269-271

Edited by Wang XL

PO Box 2345, Beijing 100023, China
Fax: +86-10-85381893
E-mail: wjg@wjgnet.com www.wjgnet.com

ELSEVIER

World J Gastroenterol 2005;11(2):305-307
World Journal of Gastroenterology ISSN 1007-9327

• CASE REPORT •

Gallbladder polyp as a manifestation of hemobilia caused by arterial-portal fistula after percutaneous liver biopsy: A case report

Chih-Lang Lin, Jia-Jang Chang, Tsung-Shih Lee, Kar-Wai Lui, Cho-Li Yen

Chih-Lang Lin, Jia-Jang Chang, Tsung-Shih Lee, Kar-Wai Lui, Cho-Li Yen, Division of Gastroenterology, Department of Internal Medicine, Chang-Gung Memorial Hospital and University, Keelung, Taiwan, China
Correspondence to: Cho-Li Yen, Division of Gastroenterology, Department of Internal Medicine Chang Gung Memorial Hospital, Keelung 222 Mai-Chin Road, Keelung, Taiwan, China. wn49792000@yahoo.com.tw
Telephone: +886-2-24313131-2627 **Fax:** +886-2-24335342
Received: 2004-06-24 **Accepted:** 2004-07-17

Abstract

Outpatient percutaneous liver biopsy is a common practice in the differential diagnosis and treatment of chronic liver disease. The major complication and mortality rate were about 2-4% and 0.01-0.33% respectively. Arterio-portal fistula as a complication of percutaneous liver biopsy was infrequently seen and normally asymptomatic. Hemobilia, which accounted for about 3% of overall major percutaneous liver biopsy complications, resulted rarely from arterio-portal fistula We report a hemobilia case of 68 years old woman who was admitted for abdominal pain after liver biopsy. The initial ultrasonography revealed a gallbladder polypoid tumor and common bile duct (CBD) dilatation. Blood clot was extracted as endoscopic retrograde cholangiopancreatography (ERCP) showed hemobilia. The patient was shortly readmitted because of recurrence of symptoms. A celiac angiography showed an intrahepatic arterio-portal fistula. After superselective embolization of the feeding artery, the patient was discharged uneventfully. Most cases of hemobilia caused by percutaneous liver biopsy resolved spontaneously. Selective angiography embolization or surgical intervention is reserved for patients who failed to respond to conservative treatment.

Key words: Gallbladder polyp; Hemobilia; Arterial-portal fistula; Percutaneous liver biopsy

Lin CL, Chang JJ, Lee TS, Lui KW, Yen CL. Gallbladder polyp as a manifestation of hemobilia caused by arterial-portal fistula after percutaneous liver biopsy: A case report. *World J Gastroenterol* 2005; 11(2): 305-307
http://www.wjgnet.com/1007-9327/11/305.asp

INTRODUCTION

After the first report of liver biopsy by Paul Ehrlich in 1883[1], percutaneous liver biopsy has become a crucial diagnostic tool in liver diseases. Ultrasonography-guided percutaneous liver biopsy has been shown to increase the diagnostic yield and significantly decrease complications even on outpatients[2-6]. The incidence of hemobilia after percutaneous liver biopsy was reported to be 0.023% among 12 750 patients in a liver transplantation center in 1993[7] accounting for 11.5% of all major complications. In a retrospective study of greater case number, the overall major complication rate of percutaneous liver biopsy was about 2.2%[8], of which hemobilia accounted for 2.7% of all complications (4 cases out of 68 276 patients). Arterio-portal fistula as a cause of liver- biopsy related hemobilia was even less frequent. Arterio-portal fistula was seen in only one case in Van Thiel's report[7]. Here, we report a case of hemobilia caused by arterio-portal fistula after percutaneous liver biopsy with an initial presentation of abdominal pain and ultrasound finding of gallbladder polypoid mass.

CASE REPORT

A 68 year-old female patient suffered from chronic C hepatitis for years. She received a percutaneous liver biopsy to evaluate the pathologic change after combination treatment of interferon alfa-2a plus ribavirin therapy. The initial physical examination before liver biopsy was unremarkable. The hemoglobin, prothrombin time, and bleeding time were normal. Percutaneous liver biopsy was conducted under ultrasonography guidance with a 2.8-mm Menghini-type aspiration needle. After liver biopsy, transient hypotension was noted during the first two hours of in-hospital observation. The patient was discharged 6 h later.

Two days later, however, the patient complained of epigastric and right subcostal pain without nausea, melena, hematemesis, or hematochezia. She visited our emergency room where an ultrasonography revealed a polypoid echogenic mass in the gallbladder wall and a mild dilatation of the common bile duct (Figure 1A) An endoscopic retrograde cholangiopancreatography was performed showing blood emanating from the edematous ampullar vater (Figure 2A). The intrahepatic ducts and common bile duct were partially opacified which is consistent with blood impaction of bile ducts (Figure 2B). An endoscopic sphincterotomy was conducted removing blood clot from the common bile duct. The symptoms were alleviated as ultrasonography showed disappearance of gallbladder sludge and polypoid mass. She was discharged seven days later.

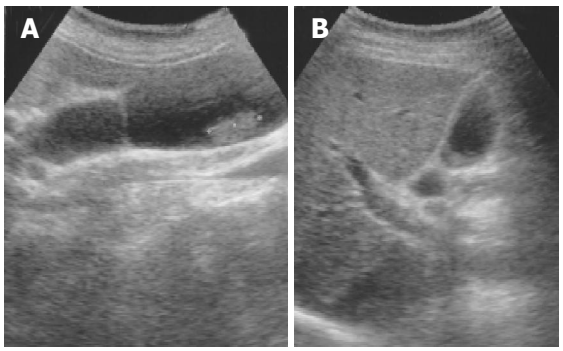

Figure 1 depicted A polypoid mass in the gallbladder wall depicted by ultrasonography (A). and A blood clot resolved between 3-7 days after selective arterial embolization. (B).

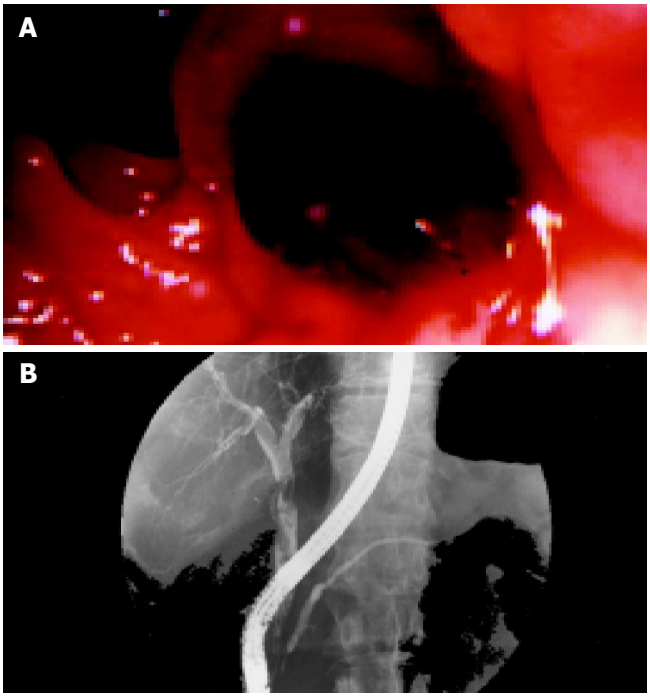

Figure 2 Emanation of fresh blood clots from the ampullar vater (A) and non-homogenous visualization of dilated common bile duct and incomplete visualization of the intrahepatic ducts (B) on endoscopic retrograde cholangiopancreatography.

The patient was shortly readmitted for recurrence of right upper quadrant pain. Arteriography was conducted demonstrating an arterio-portal fistula in segment VII of the liver between a branch of right hepatic artery and right portal vein (Figure 3). After superselective catheterization of the feeding artery, embolization was performed with gel-foam. A repeat angiography demonstrated occlusion of the arterio-portal fistula. The patient was uneventful afterward and discharged fiver days after the procedure. No recurrence of bleeding was observed during the following 6 mo.

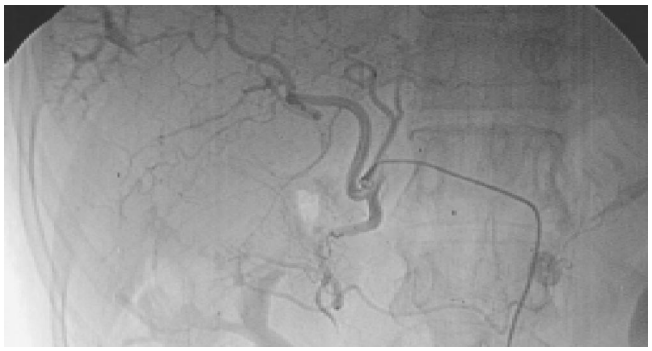

Figure 3 Shunting between a branch of right hepatic artery and right portal vein in segment VII of the liver on arterio-portal fistula on angiography revealing.

DISCUSSION

Hemobilia was first described by Glisson in 1654[9] in a postmortem diagnosis of a young adult stabbed by a sword in the liver. Sandblom in 1948[10] used hemobilia[11,12] as a term of hemorrhage arising from trauma in the biliary tract. With increasing practice of percutaneous liver biopsy, pure ethanol injection, radiofrequency ablation and percutaneous biliary drainage, iatrogenic trauma of biliary tract has been responsible for up to 60% of the hemobilia[13-20] whereas accidental abdominal injury was previously dominant[21].

Ultrasound guided liver biopsy was aimed to decrease complications following percutaneous liver biopsy[4]. However, a controversial report by Van thiel in 1993[7] demonstrated a higher complication rate (3.6%) using an ultrasound-guided cutting needle in 2 of 55 patients who were mostly with a hepatic neoplasm. The underlying disease, coagulative status, the type and the diameter of biopsy needles used[8], and the numbers of needle passes[22] seemed to determine the rate of complications rather than if ultrasonography guided[23], although ultrasound assisted biopsy helped to avoid undesired puncture of surrounding organs.

Classical clinical features of hemobilia include right upper quadrant pain, jaundice, and gastrointestinal hemorrhage[22,24] with less than 50% patients showing full triads[25]. The interval between percutaneous liver biopsy and the symptom onset may be as early as the same day on biopsy up to 21 d after percutaneous liver biopsy with a mean of 5 days[22,26]. The findings of hemobilia on ultrasonography varied depending on the rapidity and severity of the bleeding. Acute intracholecystic bleeding typically manifested as echogenic, non-acoustic polypoid mass[27,28]. The echo texture became reticular, stranding sludge as the clot began to lyse. The border of the clot became concave. The appearance of gallbladder polypoid mass as seen in this case underscored the importance of a high index of suspicion of hemobilia in patients undergoing percutaneous liver biopsy with previously normal ultrasonography. After treatment with arterial embolizaton, the echogenic sludge disappeared between 3-7 d as demonstrated in this case (Figure 1B).

Endoscopic retrograde cholangiopancreatography as well as endoscopy were confirmative in the diagnosis of hemobilia in 40-60% of the cases[13], when showing blood emanating from the ampulla or within the biliary trees[22]. Sphincterectomy and blood clot extraction could release the tension of the biliary trees and alleviate the pain caused by distension of the ducts[29].

Angiographic findings of hemobilia included arterio-portal fistula, arterio-biliary fistula and pseudoaneurysm. Arterio-portal fistula as a complication of percutaneous liver biopsy (PLB) was seen in only one of 3 hemobilia cases in Van's series[7]. Okuda *et al*[30] estimated the incidence of arterio-portal fistula after PLB was approximately 5%, but normally asymptomatic. The actual incidence of arterio-portal fistula induced hemobilia has not been well documented as it was mostly case reported.

Hemobilia recovered spontaneously in most of the cases depending on the severity of the bleeding[30]. Selective arterial embolization for hemobilia was first reported in 1976[31]. The success rate was more than 90-95% using gel-foam or histoacryl with a low morbidity[8,17,22,31,32] Laparotomy for hepatic arterial ligation or hepatectomy was reserved for cases that failed to respond to conservative treatment and hepatic arterial embolization[11,12,33].

In conclusion, arterio-portal fistula after percutaneous liver biopsy is usually asymptomatic. Hemobilia resulting from arterio-portal fistula remains mostly case - reported. Selective arterial embolization provides a successful modality of treatment if conservative treatment fails. Surgical treatment is reserved for selective cases that do not respond to the angiographic embolization.

REFERENCES

1 **Sherlock S,** Dooley J. Disease of the liver and biliary system. 11th ed. Oxford: *Blackwell sci pub* 2002: 37

2 **Caturelli E,** Giacobbe A, Facciorusso D, Bisceglia M, Villani MR, Siena DA, Fusilli S, Squillante MM, Andriulli A. Percutaneous biopsy in diffuse liver disease: increasing diagnostic yield

and decreasing complication rate by routine ultrasound assessment of puncture site. *Am J Gastroenterol* 1996; **91**: 1318-1321
3 **Younossi ZM,** Teran JC, Ganiats TG, Carey WD. Ultrasound-guided liver biopsy for parenchymal liver disease: an economic analysis. *Dig Dis Sci* 1998; **43**: 46-50
4 **Rossi P,** Sileri P, Gentileschi P, Sica GS, Forlini A, Stolfi VM, De Majo A, Coscarella G, Canale S, Gaspari AL. Percutaneous liver biopsy using an ultrasound-guided subcostal route. *Dig Dis Sci* 2001; **46**: 128-132
5 **Farrell RJ,** Smiddy PF, Pilkington RM, Tobin AA, Mooney EE, Temperley IJ, McDonald GS, Bowmer HA, Wilson GF, Kelleher D. Guided versus blind liver biopsy for chronic hepatitis C: clinical benefits and costs. *J Hepatol* 1999; **30**: 580-587
6 **Garcia-Tsao G,** Boyer JL. Outpatient liver biopsy: how safe is it ? *Ann Intern Med* 1993; **118**: 150-153
7 **Van Thiel DH,** Gavaler JS, Wright H, Tzakis A. Liver biopsy. Its safety and complications as seen at a liver transplant center. *Transplantation* 1993; **55**; 1087-1090
8 **Piccinino F,** Sagnelli E, Pasquale G, Giusti G. Complications following percutaneous liver biopsy: a multicentre retrospective study on 68 276 biopsies. *J Hepatol* 1986; **2**: 165-173
9 **Rossi P,** Sileri P, Gentileschi P, Sica GS, Ercoli L, Coscarella G, De Majo A, Gaspari AL. Delayed symptomatic hemobilia after ultrasound-guided liver biopsy: a case report. *Hepatogastroenterology* 2002; **49**: 1659-1662
10 **Sandblom P.** Hemorrhage into the biliary tract following trauma-"traumatic hemobilia". *Surgery* 1948; **24**: 571-586
11 **Merrel SW,** Schneider PD. Hemobilia–evolution of current diagnosis and treatment. *West J Med* 1991; **155**; 621-625
12 **Bloechle C,** Izbicki JR, Rashed MY, el-Sefi T, Hosch SB, Knoefel WT, Rogiers X, Broelsch CE. Hemobilia: presentation, diagnosis, and management. *Am J Gastroenterol* 1994; **89**: 1537-1540
13 **Curet P,** Baumer R, Roche A, Grellet J, Mercadier M. Hepatic hemobilia of traumatic or iatrogenic origin: recent advances in diagnosis and therapy, review of the literature from 1976 to 1981. *World J Surg* 1984; **8**: 2-8
14 **Yoshida J,** Donahue PE, Nyhus LM. Hemobilia: review of recent experience with a worldwide problem. *Am J Gastroenterol* 1987; **82**: 448-453
15 **Rossi P,** Sileri P, Gentileschi P, Sica GS, Erocoli L, Coscarella G, De Majo A, Gaspari AL. Delayed symptomatic hemobilia after ultrasound-guided liver biopsy: a case report. *Hepatogastroenterology* 2002; **49**: 1659-1662
16 **Obi S,** Shiratori Y, Shiina S, Hamamura K, Kato N, Imamura M, Teratani T, Sato S, Komatsu Y, Kawabe T, Omata M. Early detection of haemobilia associated with percutaneous ethanol injection for hepatocellular carcinoma. *Eur J Gastroentrol Hepatol* 2000; **12**: 285-290
17 **Croutch KL,** Gordon RL, Ring EJ, Kerlan RK, LaBerge JM, Roberta JP. Superselective arterial embolization in the liver transplant recipient: a safe treatment for hemobilia caused by percutanous transhepatic biiary drainage. *Liver Transpl Surg* 1996; **2**: 118-123
18 **Francica G,** Marone G, Solbiati L, D'Angelo V, Siani A. Hemobilia, intrahepatic hematoma and acute thrombosis with cavernomatous transformation of the portal vein after percutenous termoalbation of a liver metastasis. *Eur Radiol* 2000; **10**: 926-929
19 **Livraghi T,** Goldberg SN, Lazzaroni S, Meloni F, Solbiati L, Gazelle GS. Small hepatocellular carcinoma: treatment with radio-frequency ablation versus ethanol injection. *Radiology* 1999; **210**: 655-661
20 **Machicao VI,** Lukens FJ, Lange SM, Scolapio JS. Aterioportal fistula causing acute pancreatitis and hemobilia after liver biopsy. *J Clin Gastroenterol* 2002; **34**: 481-484
21 **Sandblom P,** Mirkovitch V. Minor hemobilia. Clinical significance and pathophysiological background. *Ann Surg* 1979; **190**: 254-264
22 **Lichtenstein DR,** Kim D, Chopra S. Delayed massive hemobilia following percutaneous liver biopsy: treatment by embolotherapy. *Am J Gastroenterol* 1992; **87**; 1833-1838
23 **McGill DB,** Rakela J, Zinsmeister AR, Ott BJ. A 21-year experience with major hemorrhage after percutaneous liver biopsy. *Gastroentrology* 1990; **99**: 1396-1400
24 **Lee SP,** Tasman-Jones C, Wattie WJ. Traumatic hemobilia: a complication of percutaneous liver biopsy. *Gasroenterology* 1977; **72**; 941-944
25 **Richardson SC,** Young TL. Liver biopsy-associated hemobilia treated conservatively. *Tenn Med* 1998; **91**: 141-142
26 **Taylor JD,** Carr-Locke DL, Fossard DP. Bile peritonitis and hemobilia after percutaneous liver biopsy: endoscopic retrograde cholangiopancreatography demonstration of bile leak. *Am J Gastroenterol* 1987; **82**: 262-264
27 **Laing FC,** Frates MC, Feldstein VA, Goldstein RB, Mondro S. Hemobilia: sonographic appearance in the gallbladder and biliary tree with emphasis on intracholecystic blood. *J Ultrasound Med* 1997; **16**: 537-543
28 **Grant EG,** Smirniotopoulos JG. Intraluminal gallbladder hematoma: sonographic evidence of hemobilia. *J Clin Ultasound* 1983; **11**: 507-509
29 **Jornod P,** Wiesel PH, Pescatore P, Gonvers JJ. Hemobilia, a rare cause of acute pancreatitis after percutaneous liver biopsy: diagnosis and treatment by endoscopic retrograde cholangiopancreatography. *Am J Gastroenterol* 1999; **94**: 3051-3054
30 **Okuda K,** Musha H, Nakajima Y, Takayasu K, Suzuki Y, Morita M, Yamasaki T. Frequency of intrahepatic arteriovenous fistula as a sequela to percutaneous needle puncture of the liver. *Gastroenterology* 1978; **74**; 1204-1207
31 **Walter JF,** Paaso BT, Cannon WB. Successful transcatheter embolic control of massive hematobilia secondary to liver biopsy *Am J Roentgenol* 1976; **127**: 847-849
32 **Wagner WH,** Lundell CJ, Donovan AJ. Percutaneous angiographic embolization for hepatic arterial hemorrhage. *Arch Surg* 1985; **120**: 1241-1249
33 **Dousset B,** Sauvant A, Bardou M, legmann P, Vilgrain V, Belghiti J. Selective surgical indications for iatrogenic hemobilia. *Surgery* 1997; **121**: 37-41

Assistant Editor Guo SY **Edited by** Wang XL

PO Box 2345, Beijing 100023, China
Fax: +86-10-85381893
E-mail: wjg@wjgnet.com www.wjgnet.com

ELSEVIER

World J Gastroenterol 2005;11(2):308
World Journal of Gastroenterology ISSN 1007-9327

Acknowledgements to Reviewers of *World Journal of Gastroenterology*

Many reviewers have contributed their expertise and time to the peer review, a critical process to ensure the quality of *World Journal of Gastroenterology*. The editors and authors of the articles submitted to the journal are grateful to the following reviewers for evaluating the articles (including those were published and those were rejected in this issue) during the last editing period of time.

Sujit Kumar Bhattacharya, Director
National Institute of Cholera and Enteric Diseases, P-33, CIT Road, Scheme XM, Beliaghata ,Kolkata - 700 010, India

Wolfgang Helmut Caselmann, M.D.
Professor of Medicine and Medical Director of Bavarian Ministry of the Environment, Public Health and Consumer Protection, Schellingstr. 155, D-80797 Munich, Germany

Dai-Ming Fan, Professor
Director of Department of Gastroenterology, Xijing Hospital, Fourth Military Medical University, Xi'an 710032, China

Xue-Gong Fan, Professor
Xiangya Hospital, Changsha 410008, China

Jin Gu, Professor
Peking University School of Oncology, Beijing Cancer Hospital, Beijing 100036, China

Gan-Sheng Feng, M.D.
Huazhong University of Science and Technology, Tongji Medical College,Union Hospital , Wuhan 430032 ,Hubei Province, China

De-Wu Han, M.D.
Director of Institute of Hepatic Diseases, Shanxi Medical University, 86 South Xinjian Road, Taiyuan 030001, Shanxi Province, China

Shao-Heng He, M.D.
Shantou University Medical College, 22 Xinling Road, Shantou 515031, Guangdong Province, China

Bow Ho, M.D.
Associate Professor, Department of Microbiology, National University of Singapore, 5 Science Drive 2, 117597, Singapore

Dusan Jovanovic, M.D.
President of Serbia and Montenegro Gastroenterology Association, Associate Professor of Novi Sad, General Manager of the Institute of Oncology in Sremska Kamenica, Serbia and Montenegro, Institute of Oncology, Institutskl put 4, 21204 Sremska Kamenlca, Serbia and Montenegro, Yugoslavia

Peter James Kahrilas, M.D.
Gilbert H. Marquardt Professor of Medicine, Chief of Division of Gastroenterology, Northwestern University, The Feinberg School of Medicine, 676 N. St. Clair St., Suite 1400, Chicago, IL 60611-2951, United States

Sasa Markovic, Professor
Head, Department of Gastroenterology, Univercity Clinical Center Ljubljana, 2 Japljeva 1525 Ljubljana, Slovenia

Janos Papp, Professor
1st Department of Medicine. Semmelweis University, Korányi Sándor u. 2/a., Budapest 1083, Hungary

Christian Rabe, M.D.
Resident, Department of Medicine 1, University of Bonn Sigumund-Freud-Strasse, 25 D 53105 Bonn, Germany

Tilman Sauerbruch, M.D.
Professor of Medicine, Head of Department of Medicine 1, University of Bonn, Sigmund-Freud-Strasse 25 D-53105 Bonn, Germany

Peng Shang, Ph.D.
Department of Cell Biology, Cell Engineering Research Center, Fourth Military Medical University, 17 Western Changle Road, Xi'an 710032, Shaanxi Province, China

Chun-Yang Wen, M.D.
Assistant Professor, Department of Molecular Pathology, Atomic Bomb Disease Institute, Nagasaki University Graduate School of Biomedical Sciences. 1-12-4 Sakamoto, Nagasaki 852-8523, Japan

E Wisse, M.D.
Laboratory for Cell Biology and Histology, Free University of Brussels, Laarbeeklaan 103, 1090 Brussels, Jette, Belgium

Zhi-Rong Zhang, M.D.
West China School of Pharmacy,Sichuan University, No.17,3 section, Renmin south road, Chengdu 610041, Sichuan Province, China

Mu-Jun Zhao, M.D.
Institute of Biochemistry and Cell Biology, Chinese Academy of Sciences, 320 Yueyang Road, Shanghai 200031, China

Xiao-Hang Zhao, M.D.
National Laboratory of Molecular Oncology, Cancer Institute and Hospital, Chinese Academy of Medical Sciences and Peking Union Medical College, Beijing 100021, China

Shu Zheng, M.D.
Cancer Institute, Zhejiang University, 88 Jiefang Road, Hangzhou 310009, Zhejiang Province, China

PO Box 2345, Beijing 100023, China
Fax: +86-10-85381893
E-mail: wjg@wjgnet.com www.wjgnet.com

ELSEVIER

World J Gastroenterol 2005;11(2):Appendix 1
World Journal of Gastroenterology ISSN 1007-9327

Meetings

Major meetings coming up

Digestive Disease Week
106th Annual Meeting of AGA, The American Gastroenterology Association
May 14-19, 2005
www.ddw.org/
Chicago, Illinois

13th World Congress of Gastroenterology
September 10-14, 2005
www.wcog2005.org/
Montreal, Canada

13th United European Gastroenterology Week, UEGW
October 15-20, 2005
www.uegf.org/
Copenhagen, Denmark

American College of Gastroenterology Annual Scientific Meeting
October 28-November 2, 2005
www.acg.gi.org/
Honolulu Convention Center, Honolulu, Hawaii

Events and Meetings in the upcoming 6 months

Canadian Digestive Disease Week Conference
February 26-March 6, 2005
www.cag-acg.org
Banff, AB

International Colorectal Disease Symposium 2005
February 3–5, 2005
info@icds-hk.org
Hong Kong

EASL 2005 the 40th annual meeting
April 13–17, 2005
www.easl.ch/easl2005/
Paris, France

Pediatric Gastroenterology, Hepatology and Nutrition
March 13, 2005
Jakarta, Indonesia

21st annual international congress ***of Pakistan society of Gastroenterology & GI Endoscopy***
March 25–27, 2005
www.psgc2005.com
Peshawar

8th Congress of the Asian Society of HepatoBiliary Pancreatic Surgery
February 10–13, 2005
Mandaluyong, Philippines

World Congress on Gastrointestinal Cancer
June 15–18, 2005
Barcelona

British Society of Gastroenterology Conference (BSG)
March 14–17, 2005
www.bsg.org.uk
Birmingham

Digestive Disease Week ***DDW 106th Annual Meeting***
May 15–18, 2005
www.ddw.org
Chicago, Illinois

Events and meetings in 2005

Canadian Digestive Disease Week Conference
February 26-March 6, 2005
www.cag-acg.org
Banff, AB

2005 World Congress of Gastroenterology
September 12–14, 2005
Montreal, Canada

International Colorectal Disease Symposium 2005
February 3–5, 2005
Hong Kong

13th UEGW meeting ***United European Gastroenterology Week***
October 15–20, 2005
www.webasistent.cz/guarant/uegw2005/
Copenhagen-Malmoe

7th International Workshop on Therapeutic Endoscopy
September 10–12, 2005
www.alfamedical.com
Theodor Bilharz Research Institute

EASL 2005 the 40th annual meeting
April 13–17, 2005
www.easl.ch/easl2005/
Paris, France

Pediatric Gastroenterology, Hepatology and Nutrition
March 13, 2005
Jakarta, Indonesia

21st annual international congress ***of Pakistan society of Gastroenterology & GI Endoscopy***
March 25–27, 2005
www.psgc2005.com
Peshawar

8th Congress of the Asian Society of HepatoBiliary Pancreatic Surgery
February 10–13, 2005
Mandaluyong, Philippines

APDW 2005 - Asia Pacific Digestive Week 2005
September 25–28, 2005
www.apdw2005.org
Seoul, Korea

World Congress on Gastrointestinal Cancer
June 15–18, 2005
Barcelona

British Society of Gastroenterology Conference (BSG)
March 14–17, 2005
www.bsg.org.uk
Birmingham

Digestive Disease Week ***DDW 106th Annual Meeting***
May 15–18, 2005
www.ddw.org
Chicago, Illinois

70th ACG Annual Scientific Meeting and Postgraduate Course
October 28-November 2, 2005
Honolulu Convention Center, Honolulu, Hawaii

Events and Meetings in 2006

EASL 2006 - THE 41ST ANNUAL MEETING
April 26–30, 2006
Vienna, Austria

Canadian Digestive Disease Week Conference
March 4–12, 2006
www.cag-acg.org
Quebec City

XXX pan-american congress of digestive diseases ***XXX congreso panamericano de anfermedades digestivas***
November 25-December 1, 2006
www.gastro.org.mx
Cancun

World Congress on Gastrointestinal Cancer
June 14–17, 2006
Barcelona, Spain

7th World Congress of the International Hepato-Pancreato-Biliary Association
September 3–7, 2006
www.edinburgh.org/conference
Edinburgh

71st ACG Annual Scientific Meeting and Postgraduate Course
October 20–25, 2006
Venetian Hotel, Las Vegas, Neveda

PO Box 2345, Beijing 100023, China
Fax: +86-10-85381893
E-mail: wjg@wjgnet.com www.wjgnet.com

ELSEVIER

World J Gastroenterol 2005;11(2):Appendix 2-3
World Journal of Gastroenterology ISSN 1007-9327

Instructions to authors

GENERAL INFORMATION

World Journal of Gastroenterology (*WJG,* ISSN 1007-9327) is a weekly journal of more than 48 000 circulation, published on the 7th, 14th, 21st and 28th of every month.

Original Research, Clinical Trials, Reviews, Comments, and Case Reports in esophageal cancer, gastric cancer, colon cancer, liver cancer, viral liver diseases, *etc*., from all over the world are welcome on the condition that they have not been published previously and have not been submitted simultaneously elsewhere.

Published jointly by

The WJG Press and Elsevier Inc.

SUBMISSION OF MANUSCRIPTS

Manuscripts should be typed double-spaced on A4 (297×210 mm) white paper with outer margins of 2.5 cm. Number all pages consecutively, and start each of the following sections on a new page: Title Page , Abstract, Introduction, Materials and Methods, Results, Discussion, Acknowledgements, References, Tables, Figures and Figure Legends. Neither the Editors nor the Publisher is responsible for the opinions expressed by contributors. Manuscripts formally accepted for publication become the permanent property of The WJG Press and Elsevier Inc., and may not be reproduced by any means, in whole or in part without the written permission of both the Authors and the Publisher. We reserve the right to put onto our website and copy-edit accepted manuscripts. Authors should also follow the guidelines for the care and use of laboratory animals of their institution or national animal welfare committee.

Authors should retain one copy of the text, tables, photographs and illustrations, as rejected manuscripts will not be returned to the author(s) and the editors will not be responsible for the loss or damage to photographs and illustrations.

Online submission

Online submission is strongly advised. Manuscripts should be submitted through the Online Submission System at: http://www.wjgnet.com/index.jsp. Authors are highly recommended to consult the ONLINE INSTRUCTIONS TO AUTHORS (http://www.wjgnet.com/wjg/help/instructions.jsp) before attempting to submit online. Authors encountering problems with the Online Submission System may send an email describing the problem to wjg@wjgnet.com for assistance. If you submit manuscript online, do not make a postal contribution. A repeated online submission for the same manuscript is strictly prohibited.

Postal submission

Send 3 duplicate hard copies of the full-text manuscript typed double-spaced on A4(297×210 mm) white paper together with any original photographs or illustrations and a 3.5 inch computer diskette or CD-ROM containing an electronic copy of the manuscript including all the figures, graphs and tables in native Microsoft Word format or *.rtf format to:

World Journal of Gastroenterology
Room 1066, Yishou Garden,
No.58, North Langxinzhuang Road,
PO Box 2345, Beijing 100023, China
E-mail: wjg@wjgnet.com
http: //www.wjgnet.com

MANUSCRIPT PREPARATION

All contributions should be written in English. All articles must be submitted using a word-processing software. All submissions must be typed in 1.5 line spacing and in word size 12 with ample margins. The letter font is Tahoma. For authors originating from China, one copy of the Chinese translation of the manuscript is also required (excluding references). Style should conform to our house format. Required information for each of the manuscript sections is as follows:

Title page

Full manuscript title, running title, all author(s) name(s), affiliations, institution(s) and/or department(s) where the work was accomplished, disclosure of any financial support for the research, and the name, full address, telephone and fax numbers and email address of the corresponding author should be involved. Titles should be concise and informative (removing all unnecessary words), emphasize what is NEW, and avoid abbreviations. A short running title of less than 40 letters should be provided. List the author(s)' name(s) as follows: initials and/or first name, middle name or initial(s) and full family name.

Abstract

An informative, structured abstract of no more than 250 words should accompany each manuscript. Abstracts for original contributions should be structured into the following sections: AIM: Only the purpose should be included. METHODS: The materials, techniques, instruments and equipments, and the experimental procedures should be included. RESULTS: The observatory and experimental results, including data, effects, outcome, *etc*. should be included. Authors should present *P* value where necessary, and the significant data should accompany. CONCLUSION: Accurate view and the value of the results should be included.

The format of structured abstracts is at: http://www.wjgnet.com/wjg/help/11.doc

Key words

Please list 3-10 key words that could reflect content of the study.

Text

For most article types, the main text should be structured into the following sections: INTRODUCTION, MATERIALS AND METHODS, RESULTS and DISCUSSION, and should include appropriate Figures and Tables. Data should be presented in the body text or Figures and Tables, not both.

Illustrations

Figures should be numbered as 1, 2, 3 and so on, and mentioned clearly in the main text. Provide a brief title for each figure on a separate page. No detailed legend should be involved under the figures. This part should add into the text where the figures are applicable. Digital images: black and white photographs should be scanned and saved in TIFF format at a resolution of 300 dpi; color images should be saved as CMYK (print files) and not RGB (screen-viewing files). Place each photograph in a separate file. Print images: supply images of size no smaller than 126×76 mm printed on smooth surface paper; label the image by writing the Figure number and orientation using an arrow. Photomicrographs: indicate the original magnification and stain in the legend. Digital Drawings: supply files in EPS if created by Freehand and Illustrator, or TIFF from Photoshop. EPS files must be accompanied by a version in native file format for editing purposes. Scans of existing line drawings should be scanned at a resolution of 1200 dpi and as close as possible to the size at which they will appear when printed, not smaller. Please use uniform legends for the same subjects. For example: Figure 1 Pathological changes of atrophic gastritis after treatment. A: ...; B: ...;C: ...; D: ...; E: ...; F: ...; G: ...

Tables

Three-line tables should be numbered as 1, 2, 3 and so on, and mentioned clearly in the main text. Provide a brief title for each table. No detailed legend should be involved under the tables. This part should add into the text where the tables are applicable. The information should complement but not duplicate that contained in the text. Use one horizontal line under the title, a second under the column heads, and a third below the Table, above any footnotes. Vertical and italic lines should be omitted.

Notes in tables and illustrations

Data which is not statistically significant should not be noted. $^{a}P<0.05$, $^{b}P<0.01$ ($P>0.05$ should not be noted). If there are other series of *P* values, $^{c}P<0.05$ and $^{d}P<0.01$ are used; Third series of *P* values can be expressed as $^{e}P<0.05$ and $^{f}P<0.01$. Other notes in tables or under illustrations should be expressed as ^{1}F, ^{2}F, ^{3}F; or some other symbols with a superscript (Arabic numerals) in the upper left corner. In a multi-curve illustration, each curve should be labeled with ●, ○, ■, □, ▲, △, *etc*. in a certain sequence.

Acknowledgments

Brief acknowledgments of persons who have made genuine contributions to the manuscripts and who endorse the data and conclusions are included. Authors are responsible for obtaining written permission to use any copyrighted text and/or illustrations.

References

Cited references should mainly be drawn from journals covered in the Science Citation Index (http://www.isinet.com) and/or Index Medicus (http://www.ncbi.nlm.nih.gov/PubMed) databases. Mention all references in the text, tables and figure legends, and set off by consecutive, superscripted Arabic numerals. References should be numbered consecutively in the order in which they appear in the text. Abbreviate journal title names according to the Index Medicus style (http://www.ncbi.nlm.nih.gov/entrez/query.fcgi?db=journals). Unpublished observations and personal communications are not listed as references. The style and punctuation of the references conform to ISO standard and the Vancouver style (5th edition); see examples below. Reference lists not conforming to this style could lead to delayed or even rejected publication status. Examples:

Standard jounal article (list all authors and include the PubMed ID [PMID] where applicable)

1 **Das KM,** Farag SA. Current medical therapy of inflammatory bowel disease. *World J Gastroenterol* 2000; 6: 483-489 [PMID: 11819634]

2 **Pan BR**, Hodgson HJF, Kalsi J. Hyperglobulinemia in chronic liver disease: Relationships between in vitro immunoglobulin synthesis, short lived suppressor cell activity and serum immunoglobulin levels. *Clin Exp Immunol* 1984; 55: 546-551 [PMID: 6231144]

3 **Lin GZ,** Wang XZ, Wang P, Lin J, Yang FD. Immunologic effect of Jianpi Yishen decoction in treatment of Pixu-diarrhoea. *Shijie Huaren Xiaohua Zazhi* 1999; 7: 285-287 [CMFAID:1082371101835979]

Books and other monographs (list all authors)

4 **Sherlock S,** Dooley J. Diseases of the liver and billiary system. 9th ed. Oxford: Blackwell Sci Pub, 1993: 258-296

Chapter in a book (list all authors)

5 **Lam SK.** Academic investigator's perspectives of medical treatment for peptic ulcer. In: Swabb EA, Azabo S. Ulcer disease: investigation and basis for therapy. New York: Marcel Dekker, 1991: 431-450

Electronic journal (list all authors)

6 **Morse SS.** Factors in the emergence of infectious diseases. Emerg Infect Dis serial online, 1995-01-03, cited 1996-06-05; 1(1):24 screens. Available from: URL: http//www.cdc.gov/ncidod/EID/eid.htm

PMID requirement

From the full reference list, please submit a separate list of those references embodied in PubMed, keeping the same order as in the full reference list, with the following information only: (1) abbreviated journal name and citation (e.g. *World J Gastroenterol* 2003;9(11):2400-2403; (2) article title (e.g. Epidemiology of gastroenterologic cancer in Henan Province, China; (3) full author list (e.g. Lu JB, Sun XB, Dai DX, Zhu SK, Chang QL, Liu SZ, Duan WJ; (4) PMID (e.g. 14606064). Provide the full abstracts of these references, as quoted from PubMed on a 3.5 inch disk or CD-ROM in Microsoft Word format and send by post to the *WJG* Press. For those references taken from journals not indexed by *Index Medicus*, a printed copy of the first page of the full reference should be submitted. Attach these references to the end of the manuscript in their order of appearance in the text.

Inappropriate references

Authors should always cite references that are relevant to their article, and avoid any inappropriate references. Inappropriate references include those that are linked with a hyphen and the difference between the two numbers at two sides of the hyphen is more than 5. For example, [1-6], [2-14] and [1,3,4-10,22] are all considered as inappropriate references. Authors should not cite their own unrelated published articles.

Statistical data

Present as mean±SD and mean±SE.

Statistical expression

Express *t* test as *t*(in italics), *F* test as *F*(in italics), chi square test as χ^2(in Greek), related coefficient as *r*(in italics), degree of freedom as γ (in Greek), sample number as *n*(in italics), and probability as *P*(in italics).

Units

Use SI units. For example: body mass, m(B) = 78 kg; blood pressure, p(B) =16.2/12.3 kPa; incubation time, t(incubation)=96 h, blood glucose concentration, c(glucose) 6.4±2.1 mmol/L; blood CEA mass concentration, p(CEA) = 8.6 24.5 μg/L; CO_2 volume fraction, 50 mL/L CO_2 not 5% CO_2; likewise for 40 g/L formaldehyde, not 10% formalin; and mass fraction, 8 ng/g, *etc*. Arabic numerals such as 23,243,641 should be read 23 243 641.

The format about how to accurately write common units and quantum is at: http://www.wjgnet.com/wjg/help/15.doc

Abbreviations

Standard abbreviations should be defined in the abstract and on first mention in the text. In general, terms should not be abbreviated unless they are used repeatedly and the abbreviation is helpful to the reader. Permissible abbreviations are listed in Units, Symbols and Abbreviations: A Guide for Biological and Medical Editors and Authors (Ed. Baron DN, 1988) published by The Royal Society of Medicine, London. Certain commonly used abbreviations, such as DNA, RNA, HIV, LD50, PCR, HBV, ECG, WBC, RBC, CT, ESR, CSF, IgG, ELISA, PBS, ATP, EDTA, mAb, can be used directly without further mention.

Italicization

Quantities: *t* time or temperature, *c* concentration, *A* area, *l* length, *m* mass, *V* volume.
Genotypes: *gyr*A, *arg* 1, *c myc*, *c fos*, *etc*.
Restriction enzymes: *Eco*RI, *Hin*dI, *Bam*HI, *Kbo* I, *Kpn* I, *etc*.
Biology: *Helicobacter pylori, H pylori, E coli, etc*.

SUBMISSION OF THE REVISED MANUSCRIPTS AFTER ACCEPTED

Please revise your article according to the revision policies of *WJG*. The revised version including manuscript and high-resolution image figures (if any) should be copied on a floppy or compact disk. Author should send the revised manuscript, along with printed high-resolution color or black and white photos, copyright transfer letter, the final check list for authors, and responses to reviewers by a courier (such as EMS) (submission of revised manuscript by e-mail or on the WJG Editorial Office Online System is NOT available at present).

Language evaluation

The language of a manuscript will be graded before sending for revision. (1) Grade A: priority publishing; (2) Grade B: minor language polishing; (3) Grade C: a great deal of language polishing; (4) Grade D: rejected. The revised articles should be in grade B or grade A.

Copyright assignment form

It is the policy of WJG to acquire copyright in all contributions. Papers accepted for publication become the copyright of WJG and authors will be asked to sign a transfer of copyright form. All authors must read and agree to the conditions outlined in the Copyright Assignment Form (which can be downloaded from http://www.wjgnet.com/wjg/help/9.doc).

Final check list for authors

The format is at: http://www.wjgnet.com/wjg/help/13.doc

Responses to reviewers

Please revise your article according to the comments/suggestions of reviewers. The format for responses to the reviewers' comments is at: http://www.wjgnet.com/wjg/help/10.doc

Proof of financial support

For paper supported by a foundation, authors should provide a copy of the document and serial number of the foundation.

Publication fee

Authors of accepted articles must pay publication fee.

PO Box 2345, Beijing 100023, China
Fax: +86-10-85381893
E-mail: wjg@wjgnet.com www.wjgnet.com

ELSEVIER

World J Gastroenterol 2005;11(2):Appendix 4
World Journal of Gastroenterology ISSN 1007-9327

World Journal of Gastroenterology standard of quantities and units

Number	Nonstandard	Standard	Notice
1	4 days	4 d	In figures, tables and numerical narration
2	4 days	four days	In text narration
3	day	d	After Arabic numerals
4	Four d	Four days	At the beginning of a sentence
5	2 hours	2 h	After Arabic numerals
6	2 hs	2 h	After Arabic numerals
7	hr, hrs,	h	After Arabic numerals
8	10 seconds	10 s	After Arabic numerals
9	10 year	10 years	In text narration
10	Ten yr	Ten years	At the beginning of a sentence
11	0,1,2 years	0,1,2 yr	In figures and tables
12	0,1,2 year	0,1,2 yr	In figures and tables
13	4 weeks	4 wk	
14	Four wk	Four weeks	At the beginning of a sentence
15	2 months	2 mo	In figures and tables
16	Two mo	Two months	At the beginning of a sentence
17	10 minutes	10 min	
18	Ten min	Ten minutes	At the beginning of a sentence
19	50% (*V/V*)	500 mL/L	
20	50% (m/*V*)	500 g/L	
21	1 M	1 mol/L	
22	10 μM	10 μmol/L	
23	1N HCl	1 mol/L HCl	
24	1N H_2SO_4	0.5 mol/L H_2SO_4	
25	4rd edition	4th edition	
26	15 year experience	15- year experience	
27	18.5 kDa	18.5 ku,18 500u or M_r18 500	
28	25 g.kg^{-1}/d^{-1}	25 g/(kg·d) or 25 g/kg per day	
29	6900	6 900	
30	1000 rpm	1 000 r/min	
31	sec	s	After Arabic numerals
32	1 pg·L^{-1}	1 pg/L	
33	10 kilograms	10 kg	
34	13 000 rpm	13 000 *g*	High speed; *g* should be in italic and suitable conversion.
35	1000 *g*	1 000 r/min	Low speed. *g* cannot be used.
36	Gene bank	GenBank	International classified genetic materials collection bank
37	Ten L	Ten liters	At the beginning of a sentence
38	Ten mL	Ten milliliters	At the beginning of a sentence
39	umol	μmol	
40	30 sec	30 s	
41	1 g/dl	10 g/L	10-fold conversion
42	OD_{260}	A_{260}	"OD" has been abandoned.
43	One g/L	One microgram per liter	At the beginning of a sentence
44	*A*260 nm	$A_{260\,nm}$	*A* should be in italic.
	^{b}P<0.05	^{a}P<0.05	In Table, no note is needed if there is no significance in statistics: ^{a}P<0.05, ^{b}P<0.01 (no note if P>0.05). If there is a second set of P value in the same table, ^{c}P<0.05 and ^{d}P<0.01 are used for a third set: ^{e}P<0.05, ^{f}P<0.01.
45	**F*=9.87, §*F*=25.9, #*F*=67.4	^{1}F=9.87,^{2}F=25.9, ^{3}F=67.4	Notices in or under a table
46	KM	km	kilometer
47	CM	cm	centimeter
48	MM	mm	millimeter
49	Kg, KG	kg	kilogram
50	Gm, gr	g	gram
51	nt	N	newton
52	l	L	liter
53	db	dB	decibel
54	rpm	r/min	rotation per minute
55	bq	Bq	becquerel, a unit symbol
56	amp	A	ampere
57	coul	C	coulomb
57	HZ	Hz	
59	w	W	watt
60	KPa	kPa	kilo-pascal
61	p	Pa	pascal
62	ev	EV	volt (electronic unit)
63	Jonle	J	joule
64	J/mmol	kJ/mol	kilojoule per mole
65	10×10×10cm^3	10 cm×10 cm×10 cm	
66	N·km	KN·m	moment
67	$\bar{x}$±s	mean±SD	In figures, tables or text narration
68	Mean±SEM	mean±SE	In figures, tables or text narration
69	*im*	im	intramuscular injection
70	*iv* iv	intravenous	injection
71	Wang et al	Wang *et al*	
72	EcoRI	*Eco*RI	*Eco* in italic and RI in positive. Restriction endonuclease has its prescript form of writing.
73	Ecoli	*E.coli*	Bacteria and other biologic terms have their specific expression.
74	Hp	*H pylori*	
75	Iga	*Iga*	writing form of genes
76	*igA*	IgA	writing form of proteins
77	-70 kDa	~70 ku	